



Large-Degree Asymptotics of Rational Painlevé-IV Solutions by the Isomonodromy Method

Robert J. Buckingham¹ · Peter D. Miller²

Received: 2 August 2020 / Revised: 2 August 2021 / Accepted: 15 April 2022

© The Author(s), under exclusive licence to Springer Science+Business Media, LLC, part of Springer Nature 2022

Abstract

The Painlevé-IV equation has two families of rational solutions generated, respectively, by the generalized Hermite polynomials and the generalized Okamoto polynomials. We apply the isomonodromy method to represent all of these rational solutions by means of two related Riemann-Hilbert problems, each of which involves two integervalued parameters related to the two parameters in the Painlevé-IV equation. We then use the steepest-descent method to analyze the rational solutions in the limit that at least one of the parameters is large. Our analysis provides rigorous justification for formal asymptotic arguments that suggest that in general solutions of Painlevé-IV with large parameters behave either as an algebraic function or an elliptic function. Moreover, the results show that the elliptic approximation holds on the union of a curvilinear rectangle and, in the case of the generalized Okamoto rational solutions, four curvilinear triangles each of which shares an edge with the rectangle; the algebraic approximation is valid in the complementary unbounded domain. We compare the theoretical predictions for the locations of the poles and zeros with numerical plots of the actual poles and zeros obtained from the generating polynomials, and find excellent agreement.

Communicated by Walter Van Assche.

Peter D. Miller millerpd@umich.edu http://www.math.lsa.umich.edu/ millerpd/

Robert J. Buckingham buckinrt@uc.edu http://homepages.uc.edu/ buckinrt/

Published online: 22 October 2022

- Department of Mathematical Sciences, University of Cincinnati, PO Box 210025, Cincinnati, OH 45221, USA
- Department of Mathematics, University of Michigan, East Hall 530 Church St., Ann Arbor, MI 48109, USA



 $\label{lem:keywords} \textbf{Keywords} \ \ Painlev\'e-IV \ \ equation \cdot Rational \ \ solutions \cdot Generalized \ \ Hermite \ \ and \ \ Okamoto \ \ polynomials \cdot Isomonodromy \ \ method \cdot Riemann-Hilbert \ \ problem \cdot Steepest-descent \ \ method$

Mathematics Subject Classification Primary 34M55; Secondary $34M50 \cdot 33E17 \cdot 34E05 \cdot 34M56 \cdot 34M60$

Contents

1	ntroduction	4
	1 Overview	4
	2 Rational Solutions of Painlevé-IV	6
	1.2.1 Generalized Hermite Polynomials and Rational Solutions of Painlevé-IV	7
	1.2.2 Generalized Okamoto Polynomials and Rational Solutions of Painlevé-IV	9
	1.2.3 The Total Parameter Space for Rational Solutions of Painlevé-IV	12
	1.2.4 Observed Properties of Roots of gH and gO Polynomials	12
	3 Scaling Formalism	13
	1.3.1 Equilibrium Solutions of the Autonomous Approximating Equation and Their Branch	
	Points	14
	1.3.2 Nonequilibrium Solutions of the Autonomous Approximating Equation	16
	4 Results	17
	1.4.1 Boundary Curves	18
	1.4.2 Equilibrium Asymptotics of Painlevé-IV Rational Solutions	20
	1.4.3 Nonequilibrium Asymptotics of Painlevé-IV Rational Solutions	23
	5 Notation	33
	äcklund Transformations and Symmetries	34
3	omonodromy Theory for Rational Solutions of Painlevé-IV	36
	1 Riemann–Hilbert Representations of Rational Painlevé-IV Solutions	37
	2 General Isomonodromy Theory for the Painlevé-IV Equation	40
	3.2.1 A Lax Pair for Painlevé-IV	40
	3.2.2 The Direct Problem for the Lax Pair	40
	3.2.3 The Inverse Problem for the Lax Pair	42
	3 Isomonodromic Schlesinger Transformations	46
	3.3.1 Basic Schlesinger Transformations	47
	3.3.2 Corresponding Bäcklund Transformations	51
	4 The Isomonodromy Approach to Rational Solutions	54
	5 Riemann–Hilbert Representation of gO Rationals	55
	3.5.1 Sowing the Seed: Solving the Direct Monodromy Problem and Formulating the Inverse	
	Monodromy Problem	55
	The Solution $\Psi_1^{(\infty)}(\lambda, x)$	
	The Solution $\Psi_2^{(\infty)}(\lambda, x)$	59
	The Solution $\Psi_3^{(\infty)}(\lambda, x)$	60
	The Solution $\Psi_4^{(\infty)}(\lambda,x)$	61
	The Solution $\Psi^{(0)}(\lambda, x)$	61
	3.5.2 Reaping the Harvest: Use of Schlesinger Transformations to Span the gO Parameter Lattic	e 62
	6 Riemann–Hilbert Representation of gH Rationals	63
	3.6.1 Sowing the Seed: Solving the Direct Monodromy Problem and Formulating the Inverse	
	Monodromy Problem	64
	3.6.2 Reaping the Harvest: Use of Schlesinger Transformations to Span $\Lambda_{gH}^{[3]+}$	65
	3.6.3 Connection to a Riemann–Hilbert Problem for Pseudo-Orthogonal Polynomials	67
4	symptotic Analysis of $\mathbf{Y}(\lambda; x)$ for $(\Theta_0, \Theta_\infty)$ Large: Basic Principles	68
	1 Scaling of Riemann–Hilbert Problem 1	



	4.2	Trivially Equivalent Riemann–Hilbert Problems for $\mathbf{M}(z)$	71
		4.2.1 The gO Case	71
		4.2.2 The gH Case	73
	4.3	Spectral Curve and <i>g</i> -Function	74
	4.4	Boutroux Curves	78
		4.4.1 Boutroux Curves of Class {1111}	78
		4.4.2 Continuation of Boutroux Curves	79
		4.4.3 Boutroux Curves for μ on the Real or Imaginary Axes	80
		4.4.4 Boutroux Domains on the Real and Imaginary Axes	83
	Δος	Improving Analysis of $\mathbf{M}(z)$ for Sufficiently Large $ \mu $: gO Case	83
•		Analysis of the Exponent $h(z)$	84
	3.1	5.1.1 The Zero-Level Set of $Re(h(z))$	84
		5.1.2 Defining $h(z)$ as a Single-Valued Function	89
	5.2	Introduction of $g(z)$ and Steepest Descent	91
			96
	3.3	Parametrix Construction	96
		5.3.1 Outer Parametrix	
		5.3.2 Inner Parametrices	98
	٠.	5.3.3 Global Parametrix and Error Estimation	100
	5.4	Conditionally Valid Asymptotic Formulæ for the gO Rational Solutions of Painlevé-IV	100
	5.5	Bifurcation Points and Conditions for Validity	104
		5.5.1 Harmless Bifurcation Points	105
		5.5.2 Catastrophic Bifurcation Points	105
		Uniformity of Estimates	107
)		mptotic Analysis of $\mathbf{M}(z)$ for Sufficiently Large $ \mu $: gH Case	108
	6.1	Analysis of the Exponent $h(z)$	108
		6.1.1 The Zero-Level Set of $Re(h(z))$	108
		6.1.2 Defining $h(z)$ as a Single-Valued Function	110
		Introduction of $g(z)$ and Steepest Descent	111
	6.3	Parametrix Construction	113
		6.3.1 Outer Parametrix	113
		6.3.2 Inner Parametrices	114
		6.3.3 Global Parametrix and Error Estimation	114
		Conditionally Valid Asymptotic Formulæ for the gH Rational Solutions of Painlevé-IV	115
	6.5	Bifurcation Points and Conditions for Validity	115
		6.5.1 Harmless Bifurcation Points	116
		6.5.2 Catastrophic Bifurcation Points	116
	6.6	Uniformity of Estimates	117
7	Asy	emptotic Analysis of $\mathbf{M}(z)$ in Boutroux Domains for the gO and gH Cases	117
		Stokes Graphs for Boutroux Spectral Curves of Class {1111} and Abstract Stokes Graphs for	
		Boutroux Domains	117
	7.2	Hypotheses Concerning Boutroux Domains	119
		Basic Setup	120
		Steepest Descent	122
		Specification of $h(z)$	124
		Parametrix Construction	126
		7.6.1 Outer Parametrix	126
		7.6.2 Inner Parametrices	136
		7.6.3 Global Parametrix and Error Estimation	137
	7.7	Asymptotic Formulæ for the Rational Solutions of Painlevé-IV on Boutroux Domains	138
		Differential Equations Satisfied by the Approximations	141
	, .0	7.8.1 Derivation of the Differential Equation for $\check{U}_{\rm E}^{[3]}(\zeta;\mu)$	141
		7.8.2 Derivation of the Differential Equation for $\check{U}_{\rm F}^{[1]}(\zeta;\mu)$	143
		7.8.3 Relation Between the Corresponding Spectral Curves	145
	7.9	Zeros and Poles of the Approximations	148
	7.10	Residues of the Approximations at the Malgrange Divisor	149
		7.10.1 Molgrange Pasidues of $\check{U}^{[3]}$	



	7.10.2 Malgrange Residues of $\check{U}_{\rm F}^{[1]}$ and $\check{U}_{\rm F}^{[2]}$	151
	7.10.3 Removal of the Condition $(\mu, \zeta, T) \in \mathcal{S}(\epsilon)$	151
	7.10.4 Accurate Approximation of Poles and Zeros of Rational Painlevé-IV Solutions. Zeros	
	of the gH and gO Polynomials	153
8	Boundary Curves and Maximal Boutroux Domains	154
	8.1 Universal Condition for Phase Transitions	154
	8.2 Curves in an Auxiliary Coordinate Plane	154
	8.2.1 Rational Parametrization of Γ	155
	8.2.2 Relating the Condition $Re(h(\gamma)) = 0$ to the v-Trajectories of a Rational Quadratic	
	Differential	155
	8.2.3 Critical Points of $\Phi'(t)^2 dt^2$ and the Role of the Critical v-Trajectories	158
	8.2.4 Local Structure of the Critical v-Trajectories	159
	8.2.5 Global Structure of the Critical v-Trajectories	159
	8.3 Abstract Stokes Graphs for Degenerate Boutroux Curves	162
	8.4 The Domains S_0 , S_{∞} , and S_{\pm} in the Auxiliary Plane	164
	8.5 The Exterior Domain $\mathcal{E}_{gH}(\kappa)$ as the Image of S_{∞}	165
	8.6 The Boutroux Domain $\mathring{\mathcal{B}}_{\square}(\kappa)$	168
	8.7 Aside: Asymptotic Analysis of gO Rationals at Points of $\partial \mathcal{E}_{gH}(\kappa)$	168
	8.8 The Exterior Domain $\mathcal{E}_{gO}(\kappa)$ as the Image of S_0	170
	8.9 The Boutroux Domains $\mathcal{B}_{\triangleright}(\kappa)$ and $\mathcal{B}_{\triangle}(\kappa)$	173
	8.10 Proofs of Proposition 2 and Theorems 1 and 2	176
	8.11 Proofs of Proposition 3 and Theorems 3 and 4	177
A	ppendix A. Selected Plots of Poles and Zeros	178
A	ppendix B. Branch Points of Equilibria	179
A	ppendix C. Formal Painlevé-I Approximation Near Branch Points	181
A	ppendix D. Rational Painlevé-IV Solutions Near the Origin	183
A	ppendix E. Diagrams and Tables for Steepest-Descent Analysis on Boutroux Domains	187
	E.1. The gO Case with $\mu \in \mathcal{B}_{\square}(\kappa)$ and $s = 1 \dots \dots \dots \dots \dots \dots \dots \dots \dots$	187
	E.2. The gH Case with $\mu \in \mathcal{B}_{\square}(\kappa)$ and $s = 1 \dots \dots \dots \dots \dots \dots \dots \dots \dots$	190
	E.3. The gO Case with $\mu \in \mathcal{B}_{\square}(\kappa)$ and $s = -1$	192
	E.4. The gO Case with $\mu \in \mathcal{B}_{\triangleright}(\kappa)$ and $s = 1 \dots \dots \dots \dots \dots \dots \dots \dots \dots$	194
	E.5. The gO Case with $\mu \in \mathcal{B}_{\triangleright}(\kappa)$ and $s = -1 \dots \dots \dots \dots \dots \dots \dots \dots$	196
	E.6. The gO Case with $\mu \in \mathcal{B}_{\Delta}(\kappa)$ and $s = 1 \dots \dots \dots \dots \dots \dots \dots \dots \dots$	198
	E.7. The gO Case with $\mu \in \mathcal{B}_{\Delta}(\kappa)$ and $s = -1$	200
A	ppendix F. User's Guide: Approximating Rational Solutions on Boutroux Domains	202
A	ppendix G.User's Guide: Practical Computation of Boundary Curves	204
	ppendix H. Alternate Approach to Rational Solutions of Types 1 and 2	205
	H.1. Monodromy Data for gH Rational Solutions of Types 1 and 2	205
	H.2. Critical v-Trajectories of $h'(z)^2 dz^2$ for $ \kappa > 1$	207
R	eferences	208

1 Introduction

1.1 Overview

The Painlevé-IV equation 1

$$u'' = \frac{(u')^2}{2u} + \frac{3}{2}u^3 + 4xu^2 + 2(x^2 + 1 - 2\Theta_{\infty})u - \frac{8\Theta_0^2}{u},$$

$$v' = \frac{d}{dx}, \quad u : \mathbb{C} \to \mathbb{C} \text{ with parameters } \Theta_0, \Theta_{\infty} \in \mathbb{C},$$

$$(1.1)$$

¹ We use the Jimbo–Miwa notation [40] for the parameters. The parameters $(\alpha, \beta) = (2\Theta_{\infty} - 1, -8\Theta_0^2)$ are also considered standard and used in many references; see [53, Eqn. 32.2.4].



for a function u = u(x) is a fundamental equation of mathematical physics with applications ranging from nonlinear wave equations [6] and quantum gravity [34] to orthogonal polynomials [28] and random matrix theory [20, 36, 59]. Equation (1.1) is well known to have a (unique) rational solution if Θ_0 and Θ_∞ belong to certain real discrete sets described precisely in Sect. 1.2 [37, 43, 52, 54, 57]. These rational solutions have attracted attention in a wide number of applications including rational-oscillatory solutions of the defocusing nonlinear Schrödinger equation [22], rational solutions of the Boussinesq equation [24] and the classical Boussinesq system [25], rational-logarithmic solutions of the dispersive water wave equation and the modified Boussinesq equation [27], the point vortex equations with quadrupole background flow [26], the steady-state distribution of electric charges in a parabolic potential [44], and rational extensions of the harmonic oscillator and related exceptional orthogonal polynomials [45]. They also exhibit intriguing patterns of their zeros and poles [15, 21, 23, 46, 47, 54].

There are two distinct families of rational solutions: those that can be expressed via generalized Hermite polynomials (the gH family), and those that can be expressed via generalized Okamoto polynomials (the gO family). In the complex x-plane, the zeros and poles of a gH solution appear to form a quasi-rectangular grid (see Fig. 3). The aspect ratio of the quasi-rectangle depends on the angle in the real $(\Theta_0, \Theta_{\infty})$ -plane, while the number of zeros and poles grows with $|\Theta_0|$ and $|\Theta_\infty|$. The gH solutions are naturally divided into types j = 1, 2, and 3 depending on the angle in the $(\Theta_0, \Theta_\infty)$ plane. The microstructure of zeros and poles is different for each type. We label the gH solutions $u_{gH}^{[j]}(x; m, n)$, where m and n are non-negative integers. The zeros and poles of the gO solutions are more complicated, appearing to form a quasi-rectangle with quasi-triangles attached to each edge (see Fig. 4). We also (somewhat artificially) divide the gO solutions into types 1, 2, and 3, and label solutions as $u_{gO}^{[j]}(x; m, n)$. An important difference is that for a given type the gH solutions occupy one sector in the $(\Theta_0, \Theta_\infty)$ -plane while the gO solutions occupy two opposite sectors. Using our conventions, for the gO solutions the integers m and n will both be nonnegative in one of these sectors and both nonpositive in the other.

For either family, if one fixes an angle in the $(\Theta_0, \Theta_\infty)$ -plane and writes $T := |\Theta_0|$ and $\mu := T^{-1/2}x$, the region in which zeros and poles lie becomes more clearly defined in the μ -plane as $T \to \infty$. In this work, we analytically determine the boundaries of the quasi-rectangles and (for the gO family) the quasi-triangles in the μ -plane. We prove that in the exterior of the rectangular and triangular regions, the scaled rational Painlevé-IV functions $T^{-1/2}u_{\rm F}^{[j]}(T^{1/2}\mu;m,n)$ are asymptotically approximated by algebraic equilibrium solutions of the autonomous approximating equation (derived in Sect. 1.3) for a function $\tilde{U} = \tilde{U}(\zeta)$

$$\frac{\mathrm{d}^2 \breve{U}}{\mathrm{d}\zeta^2} = \frac{1}{2\breve{U}} \left(\frac{\mathrm{d}\breve{U}}{\mathrm{d}\zeta} \right)^2 + \frac{3}{2} \breve{U}^3 + 4\mu \breve{U}^2 + (2\mu^2 + 4\kappa) \breve{U} - \frac{8}{\breve{U}}$$
(1.2)



² Throughout this paper, we use a breve accent to indicate an approximation.

(see Theorems 1 and 2). Furthermore, for each μ in the rectangular and triangular domains, we show that, as a function of ζ , $T^{-1/2}u_{\rm F}^{[j]}(T^{1/2}\mu+T^{-1/2}\zeta;m,n)$ is asymptotically approximated by a classical elliptic function solution of (1.2) (see Theorems 3 and 4). All of these results are new, with the exception of the exterior asymptotics for the gH family, which were obtained in [15]. Our results assume that μ does not lie on the boundaries of the rectangular or triangular regions. We furthermore exclude the angles $\pm \frac{1}{4}\pi$, $\pm \pi$, and $\pm \frac{3}{4}\pi$ in the $(\Theta_0, \Theta_\infty)$ -plane, i.e., those angles for which the zero/pole region collapses to a line segment (for gH solutions) or two triangles (for gO solutions).

In the remainder of the introduction, we properly define the rational Painlevé-IV solutions (Sect. 1.2), introduce our scaling conventions and formally derive the approximating equation (1.2) and describe its solutions (Sect. 1.3), and formulate our results (Sect. 1.4). To prove our theorems, we first recall in Sect. 2 some symmetries of (1.1) that allow us to focus on the sectors of parameter space for rational solutions of type 3 only. Then in Sect. 3 we use the isomonodromy method to derive two versions of a Riemann-Hilbert problem encoding the gO and gH solutions, respectively; the reader interested more in the statement of these problems than in their derivation can find the results in Sect. 3.1. In Sect. 4, we perform the preliminary steps of the Riemann-Hilbert analysis that are common to both families. In particular, both families of rational solutions are related to the same spectral curves (see Sects. 4.3–4.4). In Sects. 5 and 6, we use the steepest descent method to analyze the gO and gH solutions, respectively, in the exterior of the corresponding zero/pole region. In Sect. 7, we do the same to study both families within the zero/pole regions. The analysis in Sects. 5–7 produces results that hold under precisely specified conditions that are settled in Sect. 8. In particular, the asymptotic boundaries of the pole/zero regions are determined at this final stage. In a series of appendices, we display larger versions of certain subplots from Figs. 3 and 4 (Appendix A), prove a simple result about the vertices of the quasirectangles and quasi-triangles (Appendix B), present a formal asymptotic analysis of (1.1) near the vertices (Appendix C), give some results on the rational solutions near the origin (Appendix D), compile the diagrams and tables needed to fill in the details of the analysis in Sect. 7 (Appendix E), give two "user's guides" to implementing the approximations of the rational solutions in their zero/pole regions (Appendix F) and to computing the boundary curves between the rectangular and triangular regions and the exterior domain (Appendix G), and briefly discuss an alternate method of analyzing the rational solutions of types 1 and 2 (Appendix H).

1.2 Rational Solutions of Painlevé-IV

Rational solutions of Painlevé-IV have been studied by many authors, including [2, 3, 21, 23, 37, 43, 52, 54, 57]. See also [61, Sect. 6.1.3] and references therein. One important fact [37, 43, 52] is that there is at most one rational solution of (1.1) for given coefficients $\Theta_0^2 \in \mathbb{C}$ and $\Theta_\infty \in \mathbb{C}$. If $\Theta_0 = 0$, then there are no rational solutions that do not vanish identically and (1.1) is indeterminate for $u(x) \equiv 0$, although if one multiplies through first by u(x) one may consider $u(x) \equiv 0$ as a rational solution for $\Theta_0 = 0$ and all $\Theta_\infty \in \mathbb{C}$. Therefore, we restrict attention to $\Theta_0 \neq 0$ for the



rest of the paper.³ It is also known that the rational solutions come in two *families*, one associated with generalized Hermite polynomials and another associated with generalized Okamoto polynomials.

If the Painlevé-IV equation (1.1) admits a rational solution for a given values of $\Theta_0^2 \in \mathbb{C}$ and $\Theta_\infty \in \mathbb{C}$, then one can attempt to generate other rational solutions by applying or iterating elementary Bäcklund transformations [22, 37, 43, 54] such as those described at the beginning of Sect. 2 (see also Sect. 3.3). These transformations can change the parameters and when they are determinate, they preserve rationality and hence produce the rational solution at another point in the parameter space. Therefore, it is not surprising that when acting on rational solutions, the iterated Bäcklund transformations induce recurrence relations for certain special polynomial factors (the generalized Hermite and generalized Okamoto polynomials). Although it is the square Θ_0^2 of the parameter Θ_0 that appears in (1.1), the effect of Bäcklund transformations on the pair $(\Theta_0, \Theta_\infty)$ is easiest to understand.

1.2.1 Generalized Hermite Polynomials and Rational Solutions of Painlevé-IV

The *generalized Hermite* (*gH*) *polynomials* $\{H_{m,n}(x)\}_{(m,n)\in\mathbb{Z}_{\geq 0}\times\mathbb{Z}_{\geq 0}}$ can be defined via the recurrence relations [54]

$$2mH_{m+1,n}(x)H_{m-1,n}(x) = H_{m,n}(x)H''_{m,n}(x) - H'_{m,n}(x)^2 + 2mH_{m,n}(x)^2$$

$$2nH_{m,n+1}(x)H_{m,n-1}(x) = -H_{m,n}(x)H''_{m,n}(x) + H'_{m,n}(x)^2 + 2nH_{m,n}(x)^2$$
(1.3)

with initial conditions $H_{0,0}(x) = H_{1,0}(x) = H_{0,1}(x) = 1$ and $H_{1,1}(x) = 2x$. As was apparently first shown in [42], the gH polynomials also have expressions as Wronskians of classical Hermite polynomials; see also [22]. The gH polynomials can be used to construct rational solutions of (1.1) in the gH family of three distinct *types* j = 1, 2, 3. Adapting the notation of [22] to the $(\Theta_0, \Theta_\infty)$ parameter space, we define three disjoint sets of parameters indexed by pairs of integers as follows:

$$\begin{split} & \Lambda_{\mathrm{gH}}^{[1]-} := \left\{ (\Theta_{0}, \Theta_{\infty}) = (\Theta_{0,\mathrm{gH}}^{[1]}(m,n), \Theta_{\infty,\mathrm{gH}}^{[1]}(m,n)) : (m,n) \in \mathbb{Z}_{\geq 0} \times \mathbb{Z}_{> 0} \right\} \\ & \Lambda_{\mathrm{gH}}^{[2]-} := \left\{ (\Theta_{0}, \Theta_{\infty}) = (\Theta_{0,\mathrm{gH}}^{[2]}(m,n), \Theta_{\infty,\mathrm{gH}}^{[2]}(m,n)) : (m,n) \in \mathbb{Z}_{> 0} \times \mathbb{Z}_{\geq 0} \right\}, \\ & \Lambda_{\mathrm{gH}}^{[3]+} := \left\{ (\Theta_{0}, \Theta_{\infty}) = (\Theta_{0,\mathrm{gH}}^{[3]}(m,n), \Theta_{\infty,\mathrm{gH}}^{[3]}(m,n)) : (m,n) \in \mathbb{Z}_{\geq 0} \times \mathbb{Z}_{\geq 0} \right\}, \end{split}$$

in which the parameters $(\Theta_{0,\mathrm{gH}}^{[j]}(m,n), \Theta_{\infty,\mathrm{gH}}^{[j]}(m,n))$ for each type are as indicated in Table 1.

$$\Theta_0^2 = \left[N - \frac{1}{2}(M - 1)\right]^2$$
 or $\Theta_0^2 = \left[N - \frac{1}{2}M + \frac{1}{6}\right]^2$

where M and N are arbitrary integers. However, this parametrization incorrectly suggests that when $\Theta_0 = 0$ there is a rational solution exactly when $\Theta_{\infty} \in \mathbb{Z}$.



In the literature, the necessary and sufficient condition for existence of a rational solution of (1.1) is usually phrased as (using our notation) $\Theta_{\infty} = \frac{1}{2}(M+1)$ and either

Type j	$\Theta_{0,\mathrm{gH}}^{[j]}(m,n)$	$\Theta^{[j]}_{\infty,\mathrm{gH}}(m,n)$	$\tau_{\rm gH}^{[j]}(x;m,n)$	$u_{\mathrm{gH}}^{[j]}(x;m,n)$
1	$-\frac{1}{2}n$	$1+m+\frac{1}{2}n$	$\frac{H_{m+1,n}(x)}{H_{m,n}(x)}$	$2n\frac{H_{m,n+1}(x)H_{m+1,n-1}(x)}{H_{m,n}(x)H_{m+1,n}(x)}$
2	$-\frac{1}{2}m$	$-\frac{1}{2}m-n$	$\frac{H_{m,n}(x)}{H_{m,n+1}(x)}$	$-2m\frac{H_{m-1,n+1}(x)H_{m+1,n}(x)}{H_{m,n}(x)H_{m,n+1}(x)}$
3	$\frac{1}{2} + \frac{1}{2}(m+n)$	$\frac{1}{2} + \frac{1}{2}(n-m)$	$e^{-x^2} \frac{H_{m,n+1}(x)}{H_{m+1,n}(x)}$	$-\frac{H_{m,n}(x)H_{m+1,n+1}(x)}{H_{m,n+1}(x)H_{m+1,n}(x)}$

Table 1 Representation of gH solutions of Painlevé-IV in terms of gH polynomials

In terms of these definitions, the unique rational solution $u(x) = u_{\rm gH}^{[j]}(x; m, n)$ of (1.1) associated to the parameters $(\Theta_0, \Theta_\infty) = (\Theta_{0,\rm gH}^{[j]}(m, n), \Theta_{\infty,\rm gH}^{[j]}(m, n))$ can be written in logarithmic derivative form

$$u_{\text{gH}}^{[j]}(x; m, n) = \frac{d}{dx} \log \left(\tau_{\text{gH}}^{[j]}(x; m, n) \right)$$
 (1.5)

for a suitable function $\tau_{\rm gH}^{[j]}(x;m,n)$ expressed in terms of a ratio of two gH polynomials, or equivalently $u_{\rm gH}^{[j]}(x;m,n)$ can be written as a ratio of four gH polynomials, as shown in Table 1. $H_{m,n}(x)$ has degree mn, so it follows from (1.5) (and Proposition 4 in Sect. 2) that

$$\begin{split} u_{\mathrm{gH}}^{[1]}(x;m,n) &= \frac{n}{x}(1 + \mathcal{O}(x^{-2})) = -\frac{2\Theta_0}{x}(1 + \mathcal{O}(x^{-2})), \quad x \to \infty, \quad \Theta_0 = \Theta_{0,\mathrm{gH}}^{[1]}(m,n), \\ u_{\mathrm{gH}}^{[2]}(x;m,n) &= -\frac{m}{x}(1 + \mathcal{O}(x^{-2})) = \frac{2\Theta_0}{x}(1 + \mathcal{O}(x^{-2})), \quad x \to \infty, \quad \Theta_0 = \Theta_{0,\mathrm{gH}}^{[2]}(m,n), \\ u_{\mathrm{gH}}^{[3]}(x;m,n) &= -2x(1 + \mathcal{O}(x^{-2})), \quad x \to \infty. \end{split}$$

See [15, 21, 54] for more details. The functions $u(x) = u_{gH}^{[j]}(x; m, n)$ constitute the *gH family* of rational solutions of (1.1).

The parameter pairs in the disjoint union

$$\Lambda_{gH} := \Lambda_{gH}^{[1]-} \sqcup \Lambda_{gH}^{[2]-} \sqcup \Lambda_{gH}^{[3]+}$$
 (1.7)

are shown as unfilled dots in Fig. 1. Because the Painlevé-IV equation (1.1) only involves Θ_0^2 while the components of Λ_{gH} consist of points with a fixed sign of Θ_0 indicated by the superscript \pm , we could in principle also plot the reflections of all of these points in the vertical Θ_∞ -axis. However, there is no need to do so since each reflected point corresponds to the same solution of (1.1) for the same effective parameters $(\Theta_0^2, \Theta_\infty)$. Displaying only the points in the three sets (1.4) also emphasizes that these sets have boundaries that cannot be stepped over; in Sects. 3.3 and 3.6, we will see that at a boundary point any Bäcklund transformation that might access a "virtual" lattice point beyond the boundary is indeterminate.



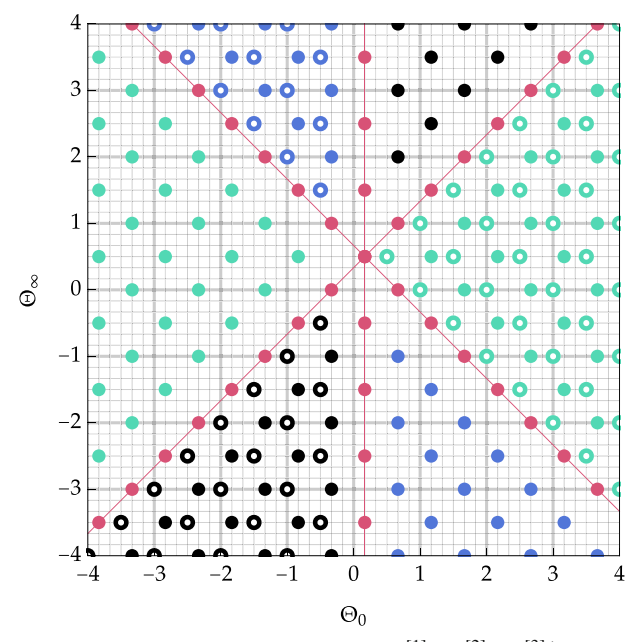


Fig. 1 Unfilled blue/black/green dots: the points in the set $\Lambda_{gH}^{[1]-}/\Lambda_{gH}^{[2]-}/\Lambda_{gH}^{[3]+}$. Filled blue/black/green dots: the points in the set $\Lambda_{gO}^{[1]\pm}/\Lambda_{gO}^{[2]\pm}/\Lambda_{gO}^{[3]\pm}$. Filled red dots: the points of $\Lambda_{gO}\cap L$. Points in $\Lambda_{F}^{[j]\pm}$ for F=gH or F=gO have $\pm\Theta_0>0$ (Color figure online)

1.2.2 Generalized Okamoto Polynomials and Rational Solutions of Painlevé-IV

The *generalized Okamoto* (gO) *polynomials* $\{Q_{m,n}(x)\}_{(m,n)\in\mathbb{Z}^2}$ can be defined⁴ by the recurrence relations [54]

$$Q_{m+1,n}(x)Q_{m-1,n}(x) = \frac{9}{2} [Q_{m,n}(x)Q''_{m,n}(x) - Q'_{m,n}(x)^{2}]$$

$$+ [2x^{2} + 3(2m + n - 1)]Q_{m,n}(x)^{2}$$

$$Q_{m,n+1}(x)Q_{m,n-1}(x) = \frac{9}{2} [Q_{m,n}(x)Q''_{m,n}(x) - Q'_{m,n}(x)^{2}]$$

$$+ [2x^{2} + 3(1 - m - 2n)]Q_{m,n}(x)^{2}$$

$$(1.8)$$

with the initial conditions $Q_{0,0}(x) = Q_{1,0}(x) = Q_{0,1}(x) = 1$ and $Q_{1,1}(x) = \sqrt{2}x$. Determinantal representations of the gO polynomials were first obtained in [54], and in [3] it was shown that the gO polynomials can be expressed as Wronskians of certain classical Hermite polynomials. We emphasize that while the gH polynomials $H_{m,n}(x)$ are defined by (1.3) for nonnegative indices m, n only, the gO polynomials $Q_{m,n}(x)$ are well defined by (1.8) also for negative m and/or n. If both indices are positive, $Q_{m,n}(x)$ has degree mn + m(m-1) + n(n-1) which exceeds the degree of $H_{m,n}(x)$ by twice the sum of two triangular numbers. From the recurrence relations (1.8), it

⁴ There are different definitions for the gO polynomials in the literature. Our definition of $Q_{m,n}(x)$ follows [21] and differs from the original definition in [54].



Type j	$\Theta_{0,gO}^{[j]}(m,n)$	$\Theta_{\infty,\mathrm{gO}}^{[j]}(m,n)$	$\tau_{\mathrm{gO}}^{[j]}(x;m,n)$	$u_{gO}^{[j]}(x;m,n)$
1	$\frac{1}{6} - \frac{1}{2}n$	$\frac{1}{2} + m + \frac{1}{2}n$	$e^{-\frac{1}{3}x^2} \frac{Q_{m+1,n}(x)}{Q_{m,n}(x)}$	$-\frac{\sqrt{2}}{3}\frac{Q_{m,n+1}(x)Q_{m+1,n-1}(x)}{Q_{m,n}(x)Q_{m+1,n}(x)}$
2	$\frac{1}{6} - \frac{1}{2}m$	$\frac{1}{2} - \frac{1}{2}m - n$	$e^{-\frac{1}{3}x^2} \frac{Q_{m,n}(x)}{Q_{m,n+1}(x)}$	$-\frac{\sqrt{2}}{3}\frac{Q_{m-1,n+1}(x)Q_{m+1,n}(x)}{Q_{m,n}(x)Q_{m,n+1}(x)}$
3	$\frac{1}{6} + \frac{1}{2}(m+n)$	$\frac{1}{2} + \frac{1}{2}(n-m)$	$e^{-\frac{1}{3}x^2} \frac{Q_{m,n+1}(x)}{Q_{m+1,n}(x)}$	$-\frac{\sqrt{2}}{3}\frac{Q_{m,n}(x)Q_{m+1,n+1}(x)}{Q_{m,n+1}(x)Q_{m+1,n}(x)}$

Table 2 Representation of gO solutions of Painlevé-IV in terms of gO polynomials

follows easily that [21]

$$Q_{m,n}(x) = Q_{n,1-m-n}(x) = Q_{1-m-n,m}(x), \quad (m,n) \in \mathbb{Z}^2.$$

In particular, gO polynomials with indices of opposite signs can be easily identified with gO polynomials with either both nonnegative or both nonpositive indices. The gO polynomials were first studied⁵ by Noumi and Yamada [54].

In explaining how to construct rational solutions of (1.1) from gO polynomials, a subdivision of the parameter space into sectors by type j=1,2,3 is somewhat artificial. Nonetheless we begin by following a similar indexing scheme as for the components of $\Lambda_{\rm gH}$. First define

$$\Lambda_{gO}^{[1]-} = \left\{ (\Theta_{0}, \Theta_{\infty}) = (\Theta_{0,gO}^{[1]}(m,n), \Theta_{\infty,gO}^{[1]}(m,n)) : (m,n) \in \mathbb{Z}_{>0} \times \mathbb{Z}_{>0} \right\},
\Lambda_{gO}^{[2]-} = \left\{ (\Theta_{0}, \Theta_{\infty}) = (\Theta_{0,gO}^{[2]}(m,n), \Theta_{\infty,gO}^{[2]}(m,n)) : (m,n) \in \mathbb{Z}_{>0} \times \mathbb{Z}_{>0} \right\},
\Lambda_{gO}^{[3]+} = \left\{ (\Theta_{0}, \Theta_{\infty}) = (\Theta_{0,gO}^{[3]}(m,n), \Theta_{\infty,gO}^{[3]}(m,n)) : (m,n) \in \mathbb{Z}_{>0} \times \mathbb{Z}_{>0} \right\},$$
(1.9)

in which $(\Theta_{0,gO}^{[j]}(m,n), \Theta_{\infty,gO}^{[j]}(m,n)$ are given in Table 2.

The unique rational solution $u(x) = u_{gO}^{[j]}(x; m, n)$ of (1.1) for parameters $(\Theta_0, \Theta_\infty) \in \Lambda_{gO}^{[1]} \sqcup \Lambda_{gO}^{[2]} \sqcup \Lambda_{gO}^{[3]}$ can then be expressed in terms of the gO polynomials either by a logarithmic derivative formula analogous to (1.5), i.e.

$$u_{gO}^{[j]}(x; m, n) = \frac{d}{dx} \log \left(\tau_{gO}^{[j]}(x; m, n) \right),$$
 (1.10)

$$f_0'(x) + f_0(x)(f_1(x) - f_2(x)) = \alpha_0$$

$$f_1'(x) + f_1(x)(f_2(x) - f_0(x)) = \alpha_1$$

$$f_2'(x) + f_2(x)(f_0(x) - f_1(x)) = \alpha_2$$

where α_k are constants satisfying $\alpha_0 + \alpha_1 + \alpha_2 = -2$ and subject to the constraint that $f_0(x) + f_1(x) + f_2(x) = -2x$. For details of the connection with rational solutions, see [23, Eqn. 4.7].



⁵ Noumi and Yamada derived their results using a symmetric form of Painlevé-IV introduced by Adler [1] for functions $f_k(x)$, k = 0, 1, 2:

or directly as a ratio of four polynomials as shown in Table 2.

The division into types j=1,2,3 is artificial for the gO family of rational solutions because the gO polynomials are defined for arbitrary integer indices. Therefore, each row in Table 2 actually defines a rational solution of (1.1) at the indicated parameters for all $(m,n) \in \mathbb{Z}^2$. It is easy to see that letting (m,n) range over \mathbb{Z}^2 in the three formulæ $(\Theta_0,\Theta_\infty)=(\Theta_{0,\mathrm{gO}}^{[j]}(m,n),\Theta_{\infty,\mathrm{gO}}^{[j]}(m,n))$ produces exactly the same lattice of parameter values regardless of j=1,2,3, namely

$$\Lambda_{gO} := \left\{ (\Theta_0, \Theta_\infty) \in \mathbb{C}^2 : (\Theta_0 + \Theta_\infty - \frac{2}{3}, \Theta_0 - \Theta_\infty + \frac{1}{3}) \in \mathbb{Z}^2 \right\}. \tag{1.11}$$

The points of Λ_{gO} are shown with filled dots in Fig. 1. We say that any rational solution of (1.1) for parameters $(\Theta_0, \Theta_\infty) \in \Lambda_{gO}$ is a solution in the gO family. It follows from uniqueness of the rational solution for given $(\Theta_0, \Theta_\infty)$ that there are three different ways to express every rational solution in the gO family, each in terms of different gO polynomials. Note that although Λ_{gO} contains points $(\Theta_0, \Theta_\infty)$ with both signs of Θ_0 for a given value of Θ_∞ , no two points of Λ_{gO} yield the same effective parameters $(\Theta_0^2, \Theta_\infty)$ of the Painlevé-IV equation (1.1).

The disjoint sets of parameters defined in (1.9) are all contained in Λ_{gO} but they do not exhaust it. However, if we define similar sets with negative indices by setting

$$\begin{split} & \Lambda_{\mathrm{gO}}^{[1]+} = \left\{ (\Theta_0, \Theta_\infty) = (\Theta_{0,\mathrm{gO}}^{[1]}(m,n), \Theta_{\infty,\mathrm{gO}}^{[1]}(m,n)) : (m,n) \in \mathbb{Z}_{<0} \times \mathbb{Z}_{<0} \right\}, \\ & \Lambda_{\mathrm{gO}}^{[2]+} = \left\{ (\Theta_0, \Theta_\infty) = (\Theta_{0,\mathrm{gO}}^{[2]}(m,n), \Theta_{\infty,\mathrm{gO}}^{[2]}(m,n)) : (m,n) \in \mathbb{Z}_{<0} \times \mathbb{Z}_{<0} \right\}, \\ & \Lambda_{\mathrm{gO}}^{[3]-} = \left\{ (\Theta_0, \Theta_\infty) = (\Theta_{0,\mathrm{gO}}^{[3]}(m,n), \Theta_{\infty,\mathrm{gO}}^{[3]}(m,n)) : (m,n) \in \mathbb{Z}_{<0} \times \mathbb{Z}_{<0} \right\}, \end{split}$$

then the disjoint union $\Lambda_{gO}^{[1]+} \sqcup \Lambda_{gO}^{[1]-} \sqcup \Lambda_{gO}^{[2]+} \sqcup \Lambda_{gO}^{[2]-} \sqcup \Lambda_{gO}^{[3]+} \sqcup \Lambda_{gO}^{[3]-}$ omits from Λ_{gO} only those points for which m=0 and/or n=0 in $(\Theta_{0,gO}^{[j]}(m,n),\Theta_{\infty,gO}^{[j]}(m,n))$ for any j. It is awkward to index them explicitly by integers without overlaps, but it is easy to see that these are the lattice points of Λ_{gO} that lie on the union L of three lines through the point $(\frac{1}{6},\frac{1}{2})\colon\Theta_{\infty}-\frac{1}{2}=\pm(\Theta_0-\frac{1}{6})$ and $\Theta_0=\frac{1}{6}$. The point $(\Theta_0,\Theta_\infty)=(\frac{1}{6},\frac{1}{2})\in\Lambda_{gO}$ gives the parameters for which the Painlevé-IV equation (1.1) admits the simplest rational solution $u(x)=-\frac{2}{3}x$ in the gO family. The lattice points in $\Lambda_{gO}\cap L$ are shown with red dots in Fig. 1. When $(\Theta_0,\Theta_\infty)\in\Lambda_{gO}\cap L$, the rational solution given by any of the formulæ in Table 2 necessarily involves either $Q_{0,n}(x)$ or $Q_{m,0}(x)$, special cases of $Q_{m,n}(x)$ that are simply called Okamoto polynomials and were first studied in [57] (likewise $H_{n,1}(x)=i^nH_{1,n}(-ix)=H_n(x),$ $n=0,1,2,\ldots$, are the classical Hermite polynomials while $H_{n,0}(x)$ and $H_{0,n}(x)$ are constants, see [22]).

Unlike for the gH family of rational solutions, boundary points of the sub-lattices $\Lambda_{gO}^{[j]\pm}$ are in no way special when it comes to the action of Bäcklund transformations. These transformations can be used to move with full freedom throughout the entire lattice Λ_{gO} . See Sects. 3.3 and 3.5 for more details. Even though there is not as much of a distinction between different components of Λ_{gO} as in the case of Λ_{gH} , still we



follow the literature and say that points of $\Lambda_{gO}^{[j]\pm}$ correspond to gO rational solutions of type j. Rational solutions for points in $\Lambda_{gO} \cap L$ can be considered as being of two different types simultaneously, or in the case of the intersection point $(\frac{1}{6},\frac{1}{2})$, three different types.

Remark 1 The formulæ (1.5) and (1.10) expressing u(x) in terms of logarithmic derivatives of ratios of special polynomials are common in the literature (see, e.g., [22]) and they lead quickly to the asymptotic relations (1.6) and likewise show that

$$u(x) = -\frac{2}{3}x(1 + \mathcal{O}(x^{-2})), \quad x \to \infty,$$

 $u(x)$ a rational solution of (1.1) for $(\Theta_0, \Theta_\infty) \in \Lambda_{gO}$. (1.12)

On the other hand, the alternate formulæ for u(x) as ratios of four special polynomials are not as well-known (although, see for example [23]) but can be obtained by combining the implied large-x asymptotics with the zero and pole locations for rational solutions tabulated in [46, Table 2] and the known leading coefficients of the four polynomial factors. These alternate formulæ can (informally) help explain the patterns of zeros and poles of rational Painlevé solutions. Each of the four factors corresponds to a different color of zero or pole in Figs. 3 and 4.

1.2.3 The Total Parameter Space for Rational Solutions of Painlevé-IV

Other than the special case of $\Theta_0 = 0$ which must be handled separately, it is known that all parameters for which the Painlevé-IV equation (1.1) has a (unique) rational solution are covered by the parameters for the gH and gO families. Recalling the definitions (1.7) and (1.11), we summarize the above discussion with the following Lemma.

Lemma 1 (See [22, 37, 43, 52]) Neglecting the case $\Theta_0 = 0$, the Painlevé-IV equation in the form (1.1) has a unique rational solution if and only if the parameters satisfy either $(\pm\Theta_0,\Theta_\infty)\in\Lambda_{gH}$ (the generalized Hermite family) or $(\pm\Theta_0,\Theta_\infty)\in\Lambda_{gO}$ (the generalized Okamoto family). Note that $\Lambda_{gH}\cap\Lambda_{gO}=\emptyset$ and no two points of $\Lambda_{gH}\sqcup\Lambda_{gO}$ yield the same set of effective parameters $(\Theta_0^2,\Theta_\infty)$ of (1.1).

The sets Λ_{gH} and Λ_{gO} are shown in Fig. 1.

1.2.4 Observed Properties of Roots of gH and gO Polynomials

From plots [21, 54], one can see that the mn zeros of the gH polynomial $H_{m,n}(x)$ are arranged in the complex x-plane in a quasi-rectangular $m \times n$ grid. Likewise, if both m and n are positive, the zeros of the gO polynomial $Q_{m,n}(x)$ are arranged in a quasi-rectangular $m \times n$ grid, two quasi-triangular grids with a base of m-1 zeros, and two quasi-triangular grids with a base of n-1 zeros. If both m and n are negative, then one has instead a $|n| \times |m|$ quasi-rectangular grid, two quasi-triangular grids with a base of |n| zeros, and two quasi-triangular grids with a base of |m| zeros. See Fig. 2. Note that, despite appearance of a qualitatively similar quasi-rectangular grid of the



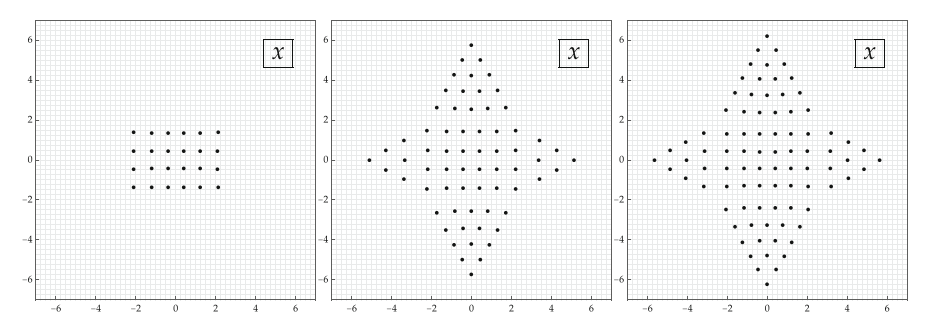


Fig. 2 Left: the roots of $H_{6,4}(x)$ in the complex x-plane. Center: the roots of $Q_{6,4}(x)$ in the complex x-plane. Right: the roots of $Q_{-4,-6}(x)$ in the complex x-plane

same dimensions in all three cases, in general $H_{m,n}(x)$ is not a factor of either $Q_{m,n}(x)$ or $Q_{-n,-m}(x)$.

Since $H_{m,1}(x)$ is a classical Hermite polynomial of degree m, in this case the roots are exactly real and the quasi-rectangle degenerates to a line. Likewise for $Q_{m,1}(x)$ one has a (non-generalized) Okamoto polynomial for which the quasi-rectangle again degenerates to a line and two of the quasi-triangles degenerate to points, while two quasi-triangles of base m remain.

Assembling the rational solutions from the gH polynomials using Table 1, one can easily display the interaction between the poles and zeros contributed by different gH polynomial factors, and illustrate how the organization of the poles and zeros varies with the parameters in Λ_{gH} , as shown in Fig. 3.

The analogous information for the gO case is shown in Fig. 4.

1.3 Scaling Formalism

We consider the parameters Θ_0 and Θ_∞ to be large, of proportional magnitude. Therefore, we take T>0 to be a large parameter, and we assume that for $s=\mathrm{sgn}(\Theta_0)=\pm 1$ and $\kappa\in\mathbb{R}$ fixed,

$$\Theta_0 = sT$$
 and $\Theta_{\infty} = -\kappa T$, $T > 0$, $\kappa \in \mathbb{R}$. (1.13)

With this scaling, we formally analyze the Painlevé-IV equation (1.1) in the limit $T \to +\infty$. To obtain a dominant balance, we will also scale u and x as follows:

$$u = T^{1/2}U$$
 and, for fixed $\mu \in \mathbb{C}$, $x = T^{1/2}\mu + T^{-1/2}\zeta$ (1.14)

where we view U and ζ as the new dependent and independent variables, respectively. Then it is easy to see that the Painlevé-IV equation takes the form

$$\frac{\mathrm{d}^2 U}{\mathrm{d} \zeta^2} = \frac{1}{2 U} \left(\frac{\mathrm{d} U}{\mathrm{d} \zeta} \right)^2 + \frac{3}{2} U^3 + 4 \mu U^2 + (2 \mu^2 + 4 \kappa) U - \frac{8}{U} + \mathcal{O}(T^{-1}).$$



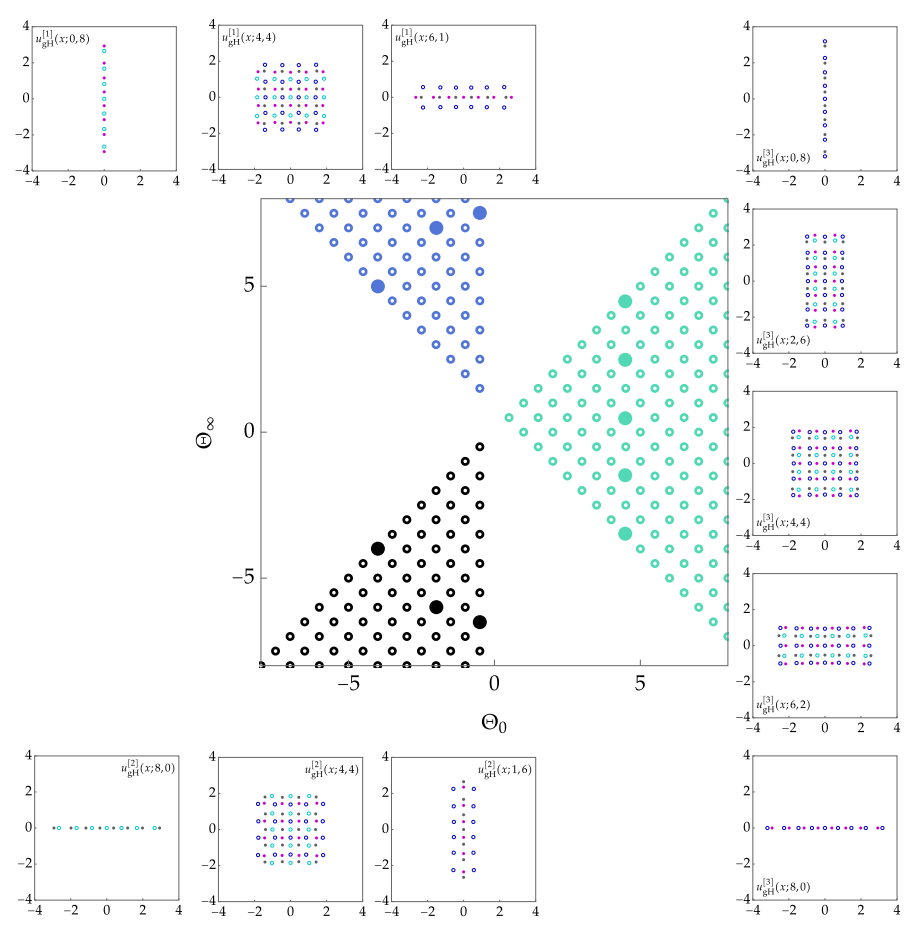


Fig. 3 Representative plots of poles (dots; magenta for residue +1 and gray for residue -1) and zeros (circles; cyan for positive derivative and blue for negative derivative) of the three types of rational solutions in the gH family. The large dots in the central plot show the location of the corresponding parameters in the $(\Theta_0, \Theta_\infty)$ -plane; as in Fig. 1, blue, black, and green dots indicate type-1, type-2, and type-3, respectively. Selected subplots are reproduced larger in Fig. 33 in Appendix A (Color figure online)

Letting $T \to \infty$, we formally obtain the autonomous equation (1.2) governing an approximation $\check{U}(\zeta)$ of $U(\zeta)$, in which $\mu \in \mathbb{C}$ and $\kappa \in \mathbb{R} \setminus \{-1, 1\}$ appear as parameters.

1.3.1 Equilibrium Solutions of the Autonomous Approximating Equation and Their Branch Points

The approximating equation (1.2) has equilibrium solutions $\check{U}(\zeta) = U_0$ (independent of ζ) that are roots of the quartic equation

$$\frac{3}{2}U_0^4 + 4\mu U_0^3 + (2\mu^2 + 4\kappa)U_0^2 - 8 = 0.$$
 (1.15)



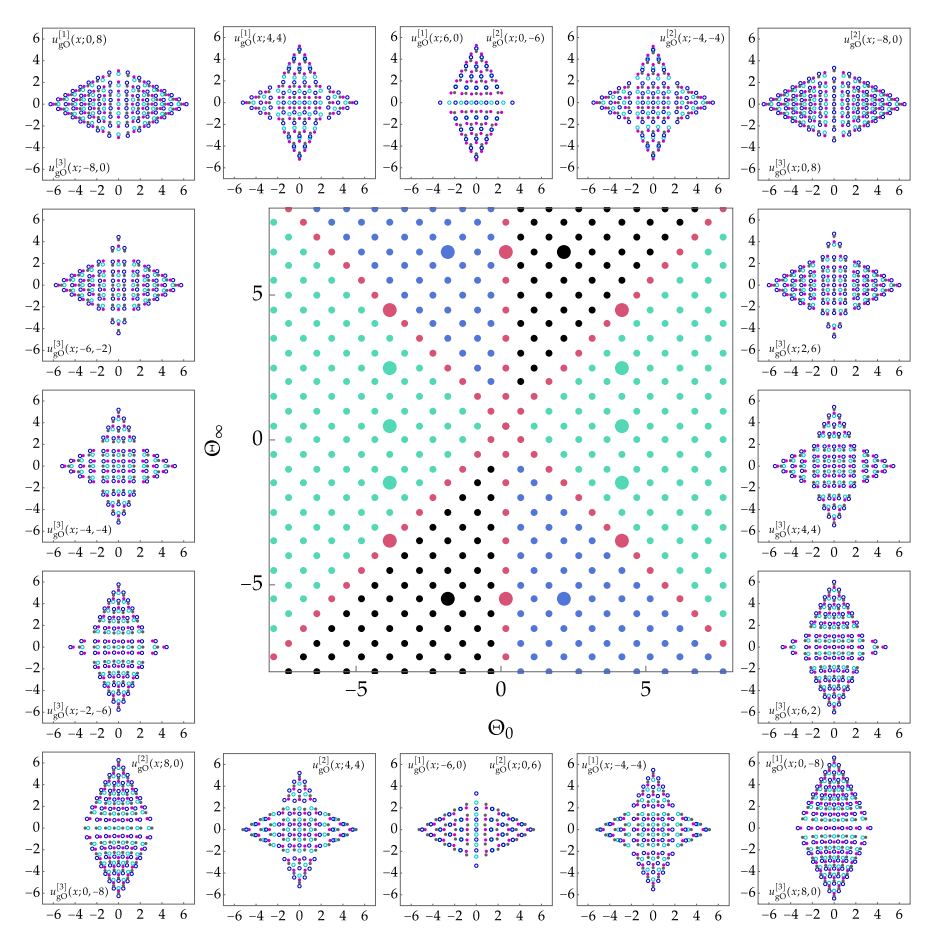


Fig. 4 As in Fig. 3 but for the gO family of rational solutions. Note that rational solutions corresponding to red dots in the central plot hence have two equivalent representations as functions of different types in the indexing scheme in Table 2, for instance in the top left subplot, both types 1 and 3. Selected subplots are reproduced larger in Fig. 34 in Appendix A (Color figure online)

When μ is large, there are four distinct roots which we denote by $U_0 = U_{0,\text{gH}}^{[j]}(\mu;\kappa)$, j=1,2,3, and $U_0 = U_{0,\text{gO}}(\mu;\kappa)$. These are all analytic functions of μ large with asymptotic behavior

$$\begin{split} U_{0,\mathrm{gH}}^{[1]}(\mu;\kappa) &= 2\mu^{-1}(1+\mathcal{O}(\mu^{-2})), \\ U_{0,\mathrm{gH}}^{[2]}(\mu;\kappa) &= -2\mu^{-1}(1+\mathcal{O}(\mu^{-2})), \\ U_{0,\mathrm{gH}}^{[3]}(\mu;\kappa) &= -2\mu(1+\mathcal{O}(\mu^{-2})), \quad \text{and} \\ U_{0,\mathrm{gO}}(\mu;\kappa) &= -\frac{2}{3}\mu(1+\mathcal{O}(\mu^{-2})), \quad \mu \to \infty. \end{split} \tag{1.16}$$

If we select any of the equilibria and try to analytically continue the solution to finite values of μ , we will only encounter any obstruction at branch points of U_0 ; these



are precisely the values of μ for which there are double roots U_0 of (1.15). These points are the solutions of

$$B(\mu; \kappa) := \mu^8 - 24(\kappa^2 + 3)\mu^4 - 64\kappa(\kappa + 3)(\kappa - 3)\mu^2 - 48(\kappa^2 + 3)^2 = 0$$
 for branch points μ of equilibria. (1.17)

The most important properties of the branch points are summarized as follows.

Proposition 1 Let $\kappa \in \mathbb{R} \setminus \{-1, 1\}$. Then (i) the set of roots of $B(\mu; \kappa) = 0$ is symmetric in reflection through the real and imaginary axes, (ii) the eight roots are all simple, and (iii) each coordinate half-plane (i.e., $\pm \text{Re}(\mu) > 0$ or $\pm \text{Im}(\mu) > 0$) contains exactly three roots forming the vertices of an equilateral triangle.

We give the proof in Appendix B.

1.3.2 Nonequilibrium Solutions of the Autonomous Approximating Equation

More generally we may consider nonequilibrium solutions of the model differential equation (1.2). Using the integrating factor $\check{U}'(\zeta)/\check{U}(\zeta)$, (1.2) implies

$$0 = \frac{1}{\check{U}} \frac{d\check{U}}{d\zeta} \frac{d^2 \check{U}}{d\zeta^2} - \frac{1}{2\check{U}^2} \left(\frac{d\check{U}}{d\zeta} \right)^3 - \frac{3}{2} \check{U}^2 \frac{d\check{U}}{d\zeta} - 4\mu \check{U} \frac{d\check{U}}{d\zeta} - (2\mu^2 + 4\kappa) \frac{d\check{U}}{d\zeta} + \frac{8}{\check{U}^2} \frac{d\check{U}}{d\zeta}$$
$$= \frac{d}{d\zeta} \left[\frac{1}{2\check{U}} \left(\frac{d\check{U}}{d\zeta} \right)^2 - \frac{1}{2} \check{U}^3 - 2\mu \check{U}^2 - (2\mu^2 + 4\kappa) \check{U} - \frac{8}{\check{U}} \right].$$

Therefore, if E denotes an integration constant, then $\check{U} = f(\zeta)$ is a solution of the first-order second-degree equation

$$\left(\frac{\mathrm{d}f}{\mathrm{d}\zeta}\right)^2 = P(f), \text{ where}$$

$$P(f) = P(f; \mu, \kappa, E) := f^4 + 4\mu f^3 + 4(\mu^2 + 2\kappa) f^2 + 2Ef + 16.$$
(1.18)

Since P(f) is a quartic polynomial, the nonequilibrium solutions $U = f(\zeta)$ are clearly elliptic functions with modulus depending on μ , κ , and E, having two fundamental periods

$$Z_{\mathfrak{a}} := \oint_{\mathfrak{a}} \frac{\mathrm{d}f}{\sqrt{P(f)}} \quad \text{and} \quad Z_{\mathfrak{b}} := \oint_{\mathfrak{b}} \frac{\mathrm{d}f}{\sqrt{P(f)}}$$
 (1.19)

where \mathfrak{a} and \mathfrak{b} are independent cycles on the genus-1 Riemann surface of the equation $w^2 = P(z)$, forming a basis for its homology group. In other words, $f(\zeta + Z_{\mathfrak{a}}) = f(\zeta + Z_{\mathfrak{b}}) = f(\zeta)$, and $Z_{\mathfrak{a}}$ and $Z_{\mathfrak{b}}$ are linearly independent over the real numbers. It is easy to see that every nonconstant solution (1.18) is an elliptic function with only simple zeros (with derivative ± 4) and at worst simple poles (with residue ± 1). Moreover, every solution has one zero with each sign of derivative and one pole of



each residue within each period parallelogram. Since (1.18) is a first-order second-degree autonomous equation, if $f(\zeta)$ denotes the unique solution of the differential equation (1.18) satisfying the initial conditions f(0) = 0 and f'(0) = 4, then every non-constant solution of (1.18) can be written in the form $f(\zeta - \zeta_0)$ for a uniquely determined constant phase shift $\zeta_0 \in \mathbb{C}$ that one may specify modulo integer linear combinations of the periods $Z_{\mathfrak{q}}$ and $Z_{\mathfrak{b}}$.

Remark 2 The quartic polynomial $P(f) = P(f; \mu, \kappa, E)$ has been motivated here by formal asymptotic analysis of the Painlevé-IV equation and hence f plays the role of the dependent variable. However, as will be seen in Sect. 4.3 it also defines a *spectral curve* in which f plays instead the role of a rescaled auxiliary spectral parameter z from the Lax pair representation of the Painlevé-IV equation, see (4.17). The same polynomial again appears in the anharmonic quantum oscillator theory of Masoero and Roffelsen [46, 47], in which the leading term $V(\lambda)$ in the anharmonic potential is proportional to $\lambda^{-2}P(\lambda)$. Here again the variable λ plays an auxiliary role not directly tied to an approximate solution of the Painlevé-IV equation.

Remark 3 Constant solutions of (1.18) corresponding to simple roots of P(f) are not equilibrium solutions of (1.2). However, the equilibrium condition (1.15) can be rederived by insisting that P(f) have a double root $f = U_0$ and hence eliminating E between $P(U_0) = 0$ and $P'(U_0) = 0$, leading to

$$E = -2U_0^3 - 6\mu U_0^2 - 4(\mu^2 + 2\kappa)U_0. \tag{1.20}$$

Another way of putting this is: if $U_0 = U_0(\mu; \kappa)$ is a function of $\mu \in \mathbb{C}$ and $\kappa \in \mathbb{R} \setminus \{-1, 1\}$ that solves (1.15), and E is expressed in terms of μ and κ by (1.20), then P(f) has a double root that persists over the whole domain of definition of $U_0(\mu; \kappa)$, namely $f = U_0(\mu; \kappa)$. With E determined by (1.20), the remaining simple roots solve a quadratic equation with known coefficients:

$$f^2 + (4\mu + 2\gamma)f + 16\gamma^{-2} = 0, \quad \gamma = U_0(\mu; \kappa).$$
 (1.21)

1.4 Results

Our objective is to use the integrable structure of (1.1) to analytically prove many of these qualitative observations by computing the leading-order asymptotic behavior of the rational Painlevé functions built from both the generalized Hermite and the generalized Okamoto polynomials. Specifically, we use the isomonodromy approach adapted to a Lax pair representation of (1.1) first found in [40]. An outline of how this method leads to Riemann–Hilbert representations of all rational solutions of (1.1) can be found in Sect. 3.4. With these representations in hand, we apply elements of the Deift–Zhou steepest-descent method [30] (in particular, we use the important mechanism of the so-called g-function first introduced in [29]). This rigorous method of asymptotic analysis, carefully adapted to various cases depending on the region of parameter space illustrated in Fig. 1 and the region of the μ -plane under consideration, allows the desired asymptotic formulæ to be proved. Families of rational solutions



to other Painlevé equations have recently been analyzed asymptotically, including rational solutions of the Painlevé-II equation [7, 18, 19], rational solutions of the Painlevé-II hierarchy [4], and rational solutions of the Painlevé-III equation [12, 13]. All of these works use some sort of Riemann–Hilbert representation and the steepestdescent method. However, in the papers [4, 7] the representation used comes from a Hankel determinant identity and the Fokas-Its-Kitaev theory of pseudo-orthogonal polynomials [34], while the papers [12, 13, 18, 19] follow more the approach described in Sect. 3.4. As for the Painlevé-IV equation, the gH family of rational solutions has been studied in [15] using the Hankel determinant approach, but so far the gO family has resisted any representation convenient for that method. The isomonodromy method has been applied to the gO family of rational solutions by Novokshenov and Shchelkonogov [55], but only in the special case that m = 0, i.e., the rational solutions $u_{\sigma\Omega}^{[j]}(x;0,n)$ were analyzed for large n. An attempt was made in [56] to use similar methods for the gH family, but that paper has been shown to contain errors that invalidate its results. An explicit connection between the Hankel determinant approach and the isomonodromy method (for a suitable Lax pair) was explained for the Painlevé-II equation in [50]. We make a similar connection in this paper for the gH family for Painlevé-IV (see (3.73) in Sect. 3.6). From the point of view of isomonodromy theory, it seems that it is the absence of nontrivial Stokes phenomenon in the Lax pair that is correlated with the existence of a Hankel determinant identity suitable for further asymptotic analysis.

We also want to mention here a third approach available to study the roots of the gH and gO polynomials themselves. It is possible to encode the condition that a gH or gO polynomial vanish at a given point in a kind of eigenvalue condition on a quantum anharmonic oscillator equation in one dimension [46]; see also Remark 2. This method has been used to obtain detailed information about the roots of the gH polynomials [47], and work is underway to do the same for the gO polynomials [48].

1.4.1 Boundary Curves

Central to the asymptotic description of rational Painlevé-IV solutions are two particular families of Jordan curves that we denote $\partial \mathcal{E}_{gH}(\kappa)$ and $\partial \mathcal{E}_{gO}(\kappa)$, respectively, with the families being parametrized by $\kappa \in \mathbb{R} \setminus \{-1,1\}$. Given κ , the curves $\partial \mathcal{E}_{gH}(\kappa)$ and $\partial \mathcal{E}_{gO}(\kappa)$ are finite unions of analytic arcs that can be described as follows. Let $U_0(\mu;\kappa)$ be a solution of the equilibrium equation (1.15) analytic for μ in some domain \mathcal{D} , and define $E = E(\mu;\kappa)$ in turn by (1.20). Then by Remark 3, for all $\mu \in \mathcal{D}$ the polynomial P(f) in (1.18) has a double root $f = \gamma(\mu;\kappa) := U_0(\mu;\kappa)$ and two simple roots, $f = \alpha(\mu;\kappa)$, $\beta(\mu;\kappa)$ solving the quadratic equation (1.21). It follows that the equation



$$\operatorname{Re}\left(\int_{\alpha(\mu;\kappa)}^{\gamma(\mu;\kappa)} \frac{\sqrt{P(f)}}{f} \, \mathrm{d}f\right)$$

$$= \operatorname{Re}\left(\int_{\alpha(\mu;\kappa)}^{\gamma(\mu;\kappa)} \frac{(f - \gamma(\mu;\kappa))\sqrt{(f - \alpha(\mu;\kappa))(f - \beta(\mu;\kappa))}}{f} \, \mathrm{d}f\right) = 0$$
(1.22)

defines an analytic arc (possibly empty) in \mathcal{D} . On a given domain \mathcal{D} , there may be up to four analytic equilibria, and each choice of equilibrium (near $\mu = \infty$ these are distinguished by the asymptotic behavior (1.16)) gives different arcs on \mathcal{D} .

In principle, the boundary curves can be expressed via (1.22) as arcs of the indicated level curve of an explicit multivalued analytic function, because (i) since $P(f) = (f - \gamma)^2 (f - \alpha) (f - \beta)$ has a double root, the integral in (1.22) can be evaluated by quadratures in terms of elementary functions, and (ii) the quartic equation (1.15) for the double root can be solved by radicals. The resulting formula is unwieldy but can be used to make plots such as Fig. 5. An explicit implementation of (i) is given in Appendix G, and a similar formula can be found in [15, Eqn. 18]; that step is the same for arcs of both curves $\partial \mathcal{E}_{gH}(\kappa)$ and $\partial \mathcal{E}_{gO}(\kappa)$. This method does not clarify which arcs satisfying (1.22) must be selected, and there are some extraneous arcs generated by (1.22) that are not contained within either $\partial \mathcal{E}_{gH}(\kappa)$ or $\partial \mathcal{E}_{gO}(\kappa)$, but the fact that the curves $\partial \mathcal{E}_{gH}(\kappa)$ and $\partial \mathcal{E}_{gO}(\kappa)$ are both obtained from exactly the same equation (1.22) is worth noting.

A description of $\partial \mathcal{E}_{gH}(\kappa)$ and $\partial \mathcal{E}_{gO}(\kappa)$ that makes precise exactly which arcs produced by (1.22) are needed in each case will be given in Sect. 8, where it is also shown that the arcs arise by conformal mapping from the trajectories of a certain rational quadratic differential (see (8.8) in Sect. 8.2; plots showing a uniform parametrization of all possible arcs arising from (1.22) are shown in Fig. 29). The curves are then properly defined as boundaries of domains $\mathcal{E}_{gH}(\kappa)$ and $\mathcal{E}_{gO}(\kappa)$ in Definitions 7 and 8, respectively, of Sects. 8.5 and 8.8. The most important properties of the Jordan curves $\partial \mathcal{E}_{gH}(\kappa)$ and $\partial \mathcal{E}_{gO}(\kappa)$ are the following.

Proposition 2 The families of curves $\partial \mathcal{E}_{gH}(\kappa)$ and $\partial \mathcal{E}_{gO}(\kappa)$ have the following properties.

- (1) For each $\kappa \in \mathbb{R} \setminus \{-1, 1\}$:
 - (a) $\partial \mathcal{E}_{gH}(\kappa)$ and $\partial \mathcal{E}_{gO}(\kappa)$ are Jordan curves enjoying Schwarz reflection symmetry in both the real and imaginary axes.
 - (b) $\partial \mathcal{E}_{gH}(\kappa)$ consists of four analytic arcs joining in pairs the four branch points $B(\mu;\kappa)=0$ lying in the four open quadrants of the μ -plane, traversed in the direction of increasing $\arg(\mu)$.
 - (c) $\partial \mathcal{E}_{gO}(\kappa)$ consists of eight analytic arcs joining in pairs all eight branch points $B(\mu; \kappa) = 0$, traversed in the direction of increasing $\arg(\mu)$.
 - (d) Except for the four common vertices of $\partial \mathcal{E}_{gH}(\kappa)$ and $\partial \mathcal{E}_{gO}(\kappa)$, $\partial \mathcal{E}_{gO}(\kappa)$ lies in the exterior of $\partial \mathcal{E}_{gH}(\kappa)$.
- (2) The curves in a given family, $\partial \mathcal{E}_F(\kappa)$, F = gH, gO, $\kappa \in \mathbb{R} \setminus \{-1, 1\}$, are related to one another by a finite symmetry group of geometric transformations with the



following three generators:

$$\begin{split} \partial \mathcal{E}_{\mathrm{F}}(-\kappa) &= \mathrm{i} \partial \mathcal{E}_{\mathrm{F}}(\kappa), \quad (\textit{rotation by} \quad \frac{1}{2}\pi), \\ \partial \mathcal{E}_{\mathrm{F}}(I^{\pm}(\kappa)) &= \sqrt{\frac{2}{1 \pm \kappa}} \partial \mathcal{E}_{\mathrm{F}}(\kappa), \quad I^{\pm}(\kappa) := -\frac{\kappa \mp 3}{1 \pm \kappa}, \quad (\textit{homothetic dilation}), \end{split}$$

$$(1.23)$$

all defined for $\kappa \in (-1,1)$. In particular, since $I^+:(-1,1) \to (1,+\infty)$ and $I^-:(-1,1) \to (-\infty,-1)$, the curves $\partial \mathcal{E}_F(\kappa)$ are determined for all $\kappa \in \mathbb{R} \setminus \{-1,1\}$ as dilations of those curves with $\kappa \in (-1,1)$. Also, the curves for $\kappa = -3,0,3$ have additional symmetry, being invariant under rotation about the origin by $\frac{1}{2}\pi$ radians.

- (3) Letting $\mathcal{E}_{gH}(\kappa)$ and $\mathcal{E}_{gO}(\kappa)$ denote the exterior of $\partial \mathcal{E}_{gH}(\kappa)$ and $\partial \mathcal{E}_{gO}(\kappa)$, respectively,
 - (a) for all $\kappa < -1$, the equilibrium $U_{0,gH}^{[1]}(\mu;\kappa)$ is an analytic function of $\mu \in \mathcal{E}_{gH}(\kappa)$;
 - (b) for all $\kappa > 1$, the equilibrium $U_{0,\mathrm{gH}}^{[2]}(\mu;\kappa)$ is an analytic function of $\mu \in \mathcal{E}_{\mathrm{gH}}(\kappa)$;
 - (c) for all $\kappa \in (-1, 1)$, the equilibrium $U_{0,gH}^{[3]}(\mu; \kappa)$ is an analytic function of $\mu \in \mathcal{E}_{gH}(\kappa)$;
 - (d) for all $\kappa \in \mathbb{R} \setminus \{-1, 1\}$, the equilibrium $U_{0,gO}(\mu; \kappa)$ is an analytic function of $\mu \in \mathcal{E}_{gO}(\kappa)$ that satisfies $U_{0,gO}(\mu; \kappa) \neq U_{0,gH}^{[1]}(\mu; \kappa)$ for $\kappa < -1$, $U_{0,gO}(\mu; \kappa) \neq U_{0,gH}^{[2]}(\mu; \kappa)$ for $\kappa > 1$, and $U_{0,gO}(\mu; \kappa) \neq U_{0,gH}^{[3]}(\mu; \kappa)$ for $\kappa \in (-1, 1)$.

We give the proof in Sect. 8.10. Note that by composing the symmetry generators in (1.23) or their inverses several other interesting relations emerge. For instance, the rotation symmetry $\partial \mathcal{E}_F(-\kappa) = \mathrm{i}\partial \mathcal{E}_F(\kappa)$ also holds for $\kappa < -1$ and $\kappa > 1$, trivially relating the curves for these ranges of κ by inversion of aspect ratio. There is also a map relating two curves with $\kappa > 1$ (or two curves with $\kappa < -1$) by a combination of dilation and rotation, and a pure dilation map relating curves with $\kappa > 1$ to curves with $\kappa < -1$. In deriving these implied relations, it is useful to note that the Möbius transformations $I^{\pm}(\kappa)$ are both involutions of the Riemann sphere: $I^{\pm}(I^{\pm}(\kappa)) = \kappa$. Qualitatively, $\partial \mathcal{E}_{\mathrm{gH}}(\kappa)$ is a curvilinear rectangle symmetric in reflection through both real and imaginary axes, while for the same κ , $\partial \mathcal{E}_{\mathrm{gO}}(\kappa)$ replaces each edge of $\partial \mathcal{E}_{\mathrm{gH}}(\kappa)$ with two curvilinear edges having a common vertex in the exterior $\mathcal{E}_{\mathrm{gH}}(\kappa)$ on the axis ray bisecting the original edge. See Fig. 5.

1.4.2 Equilibrium Asymptotics of Painlevé-IV Rational Solutions

Our first results assert that the rational solutions are accurately approximated by equilibrium solutions of the formal approximating equation (1.2) (roots of the quartic (1.15)), provided that μ lies in the exterior of the relevant Jordan curve. The following result was first proved in [15] using a Hankel determinant identity and techniques from the theory of pseudo-orthogonal polynomials. We give a new proof in this paper based



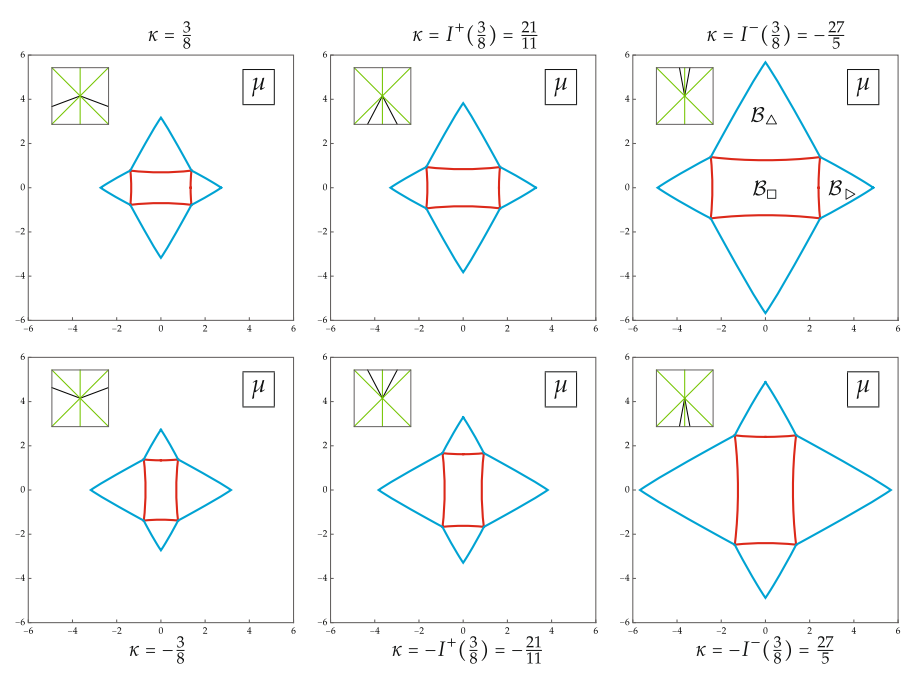


Fig. 5 The curves $\partial \mathcal{E}_{gH}(\kappa)$ (red) and $\partial \mathcal{E}_{gO}(\kappa)$ (cyan) for six values of κ related by the transformations generated by (1.23), with insets showing the corresponding rays $\Theta_{\infty} = -\kappa |\Theta_0|$ (black) in the $(\Theta_0, \Theta_{\infty})$ plane divided into sectors with green lines. On the upper right-hand panel are also shown the domains $\mathcal{B}_{\square} = \mathcal{B}_{\square}(\kappa)$, $\mathcal{B}_{\triangleright} = \mathcal{B}_{\triangleright}(\kappa)$, and $\mathcal{B}_{\triangle} = \mathcal{B}_{\triangle}(\kappa)$ defined in Sect. 1.4.3. The curves were plotted using (1.22) (see also Appendix G) (Color figure online)

on the isomonodromy method. For $\rho > 0$, set

$$\begin{split} \kappa_{\infty}^{[1]}(\rho) &:= -1 - 2\rho^{-1} < -1, \quad \kappa_{\infty}^{[2]}(\rho) := 1 + 2\rho > 1, \\ \text{and} \quad \kappa_{\infty}^{[3]}(\rho) &:= \frac{1 - \rho}{1 + \rho} \in (-1, 1). \end{split}$$

Theorem 1 (Equilibrium asymptotics of gH rationals) Let $\rho > 0$ be a fixed rational aspect ratio, and recall that $\mathcal{E}_{gH}(\kappa)$ denotes the unbounded exterior of the Jordan curve $\partial \mathcal{E}_{gH}(\kappa)$. Then for j = 1, 2, 3, as $m, n \to +\infty$ with $n = \rho m$,

$$u_{gH}^{[j]}(x; m, n) = T^{1/2} \left(\check{U} + \mathcal{O}(T^{-1}) \right), \quad \check{U} = U_{0,gH}^{[j]}(\mu; \kappa),$$

$$x = T^{1/2} \mu, \quad T = |\Theta_{0,gH}^{[j]}(m, n)|,$$

$$\mu \in \mathcal{E}_{gH}(\kappa), \quad \kappa = -\frac{\Theta_{\infty,gH}^{[j]}(m, n)}{T} \to \kappa_{\infty} = \kappa_{\infty}^{[j]}(\rho).$$
(1.24)

In each case (type j=1,2,3), the error estimate holds uniformly for μ in any fixed closed (possibly unbounded) subset of $\mathcal{E}_{gH}(\kappa_{\infty})$, and the error tends to zero as $\mu \to \infty$.



The pseudo-orthogonal polynomial method has not yet been successfully applied to the gO family of rational solutions, but the isomonodromy approach applies just as well, yielding the following result.

Theorem 2 (Equilibrium asymptotics of gO rationals) Let $\rho > 0$ be a fixed rational aspect ratio, and recall that $\mathcal{E}_{gO}(\kappa)$ denotes the unbounded exterior of the Jordan curve $\partial \mathcal{E}_{gO}(\kappa)$. Then for j = 1, 2, 3, as $m, n \to \pm \infty$ with $n = \rho m$,

$$u_{gO}^{[j]}(x; m, n) = T^{1/2} \left(\check{U} + \mathcal{O}(T^{-1}) \right), \quad \check{U} = U_{0,gO} (\mu; \kappa),$$

$$x = T^{1/2} \mu, \quad T = |\Theta_{0,gO}^{[j]}(m, n)|,$$

$$\mu \in \mathcal{E}_{gO}(\kappa), \quad \kappa = -\frac{\Theta_{\infty,gO}^{[j]}(m, n)}{T} \to \kappa_{\infty} = \pm \kappa_{\infty}^{[j]}(\rho).$$
(1.25)

In each case (type j=1,2,3), the error estimate holds uniformly for μ in any fixed closed (possibly unbounded) subset of $\mathcal{E}_{gO}(\kappa_{\infty})$, and the error tends to zero as $\mu \to \infty$.

An elementary corollary of these results is the following, in which F = gH or F = gO, and type j = 1, 2, 3 is arbitrary.

Corollary 1 (Pole- and zero-free regions for Painlevé-IV rational solutions) *Let* $C \subset \mathcal{E}_F(\kappa_\infty)$ *be closed (note that* κ_∞ *is a different function of aspect ratio* ρ *for different types* j=1,2,3). Then $u_F^{[j]}(x;m,n)$ has no poles or zeros for $\mu \in C$ if m,n are sufficiently large and $n=\rho m$.

Proof For the gO family, the uniform convergence on C to an analytic equilibrium guaranteed by Theorem 2 proves the absence of poles. Then the argument principle implies the absence of zeros, since the equilibrium $U_{0,\mathrm{gO}}(\mu;\kappa)$ is analytic and bounded away from zero on C according to (1.15) and the asymptotic $U_{0,\mathrm{gO}}(\mu;\kappa) \sim -\frac{2}{3}\mu$ as $\mu \to \infty$.

For the gH family, the proof is similar, except that the equilibria $U_{0,\mathrm{gH}}^{[1]}(\mu;\kappa)$ and $U_{0,\mathrm{gH}}^{[2]}(\mu;\kappa)$ vanish as $\mu\to\infty$, being proportional to μ^{-1} . In these cases, however, the fact that the error term vanishes as $\mu\to\infty$ shows that the simple zero of the equilibrium at infinity cannot be perturbed into the finite μ -plane should C be taken to be unbounded.

The fact that the error terms in Theorems 1 and 2 vanish as $\mu \to \infty$ follows by comparing the known large-x asymptotic behavior of the rational solution (see (1.6) and (1.12)) with the large- μ behavior of the leading terms (see (1.16)). Note that combining the symmetries (2.2) and (2.3) in Sect. 2 with the fact following from Proposition 2 that $\mathcal{E}_{gH}(-\kappa) = i\mathcal{E}_{gH}(\kappa)$ and $\mathcal{E}_{gO}(-\kappa) = i\mathcal{E}_{gO}(\kappa)$ holds for all $\kappa \in \mathbb{R} \setminus \{-1, 1\}$, formulæ (1.24) and (1.25) for j = 2 follow from the same formulæ with j = 1. For rational functions of types j = 1, 3, the asymptotic formulæ in Theorems 1 and 2 are proved without first specifying the domains of validity in Sects. 5–6. The domains of validity of these formulæ are then obtained in Sects. 8.5 and 8.8 by determining exactly which arcs generated by (1.22) are relevant. Uniformity of convergence is



discussed in Sects. 5.6 and 6.6. Based on these intermediate results, the proofs of Theorems 1 and 2 are completed in Sect. 8.10.

1.4.3 Nonequilibrium Asymptotics of Painlevé-IV Rational Solutions

The interior of $\partial \mathcal{E}_{gH}(\kappa)$ is a domain that we call $\mathcal{B}_{\square}(\kappa)$, and according to item (1d) from Proposition 2 the intersection of $\mathcal{E}_{gH}(\kappa)$ with the interior of $\partial \mathcal{E}_{gO}(\kappa)$ is a disjoint union of four domains, each of which intersects just one of the four coordinate axes in the μ -plane. We call the domain intersecting the positive real (resp., imaginary) axis $\mathcal{B}_{\rhd}(\kappa)$ (resp., $\mathcal{B}_{\vartriangle}(\kappa)$). The domain $\mathcal{B}_{\square}(\kappa)$ is a curvilinear rectangle, while the domains $\mathcal{B}_{\rhd}(\kappa)$ and $\mathcal{B}_{\vartriangle}(\kappa)$ are curvilinear triangles. Note that although Proposition 1 asserts that the vertices of $\mathcal{B}_{\rhd}(\kappa)$ and $\mathcal{B}_{\vartriangle}(\kappa)$ are those of exact equilateral triangles, their edges are analytic arcs that neither are straight-line segments, nor are symmetric under rotation about the center by $\frac{2}{3}\pi$ radians. See the upper right-hand panel of Fig. 5. The remaining two domains are then $-\mathcal{B}_{\rhd}(\kappa)$ and $-\mathcal{B}_{\vartriangle}(\kappa)$ (reflections through the origin). We now describe the gH rational solutions of Painlevé-IV for values of κ corresponding to κ corresponding to a neighborhood of the curve κ corresponding to a neighborhood of the curve κ corresponding only) of the curve κ corresponding only) of the curve κ

Recall the quartic polynomial $P(f) = P(f; \mu, \kappa, E)$ defined in (1.18). Given $\kappa \in \mathbb{R} \setminus \{-1, 1\}$ and $\mu \in \mathcal{B}_{\square}(\kappa) \cup \mathcal{B}_{\triangleright}(\kappa) \cup \mathcal{B}_{\triangle}(\kappa)$, there is a specific value of $E \in \mathbb{C}$ such that the conditions (compare with (1.22))

$$\operatorname{Re}\left(\oint_{\mathfrak{a}} \frac{\sqrt{P(f)}}{f} \, \mathrm{d}f\right) = \operatorname{Re}\left(\oint_{\mathfrak{b}} \frac{\sqrt{P(f)}}{f} \, \mathrm{d}f\right) = 0 \tag{1.26}$$

both hold. The conditions (1.26) also appear in the Masoero–Roffelsen theory of zeros of gH polynomials, where they serve to define a mapping S (see [47, Eqn. 11]) used to localize the zeros. Note that these integrals are independent of path on the Riemann surface of $w^2 = P(z)$ because the differential in the integrand, while singular over z = 0, ∞ , has purely real residues. Taken together, they are also independent of specific choice of basis of cycles $\mathfrak a$ and $\mathfrak b$. The specific value we use is denoted $E = E(\mu; \kappa)$ and is properly defined in Definition 10 of Sect. 8.9. The most important properties of $E(\mu; \kappa)$ are the following.

Proposition 3 For each $\kappa \in \mathbb{R} \setminus \{-1, 1\}$ and $\mu \in \mathcal{B}_{\square}(\kappa) \cup \mathcal{B}_{\triangleright}(\kappa) \cup \mathcal{B}_{\triangle}(\kappa)$, the quartic $P(f; \mu, \kappa, E(\mu; \kappa))$ satisfies the conditions (1.26). If κ is fixed, the function $\mu \mapsto E$ is smooth but not analytic on each component of its domain, and it extends continuously to $\partial \mathcal{E}_{gH}(\kappa) \cup \partial \mathcal{E}_{gO}(\kappa)$. The functions $\mu \mapsto E$ are related for different κ by the following symmetries:



$$E(\mu; I^{\pm}(\kappa)) = \left(\frac{2}{1 \pm \kappa}\right)^{3/2} \left[E\left(\sqrt{\frac{1}{2}(1 \pm \kappa)}\mu; \kappa\right) - 4(\kappa \mp 1)\sqrt{\frac{1}{2}(1 \pm \kappa)}\mu \right], I^{\pm}(\kappa) := -\frac{\kappa \mp 3}{1 \pm \kappa},$$

$$(1.27)$$

$$E(\mu; -\kappa) = iE(i\mu; \kappa).$$

$$(1.28)$$

In particular, the latter symmetry implies that $E(-\mu; \kappa) = -E(\mu; \kappa)$, i.e., E is an odd function of μ for each $\kappa \in \mathbb{R} \setminus \{-1, 1\}$.

The proof is given in Sect. 8.11. Setting $E = E(\mu; \kappa)$ in the differential equation (1.18), let $f(\zeta) = f(\zeta; \mu, \kappa)$ denote the unique solution of this equation satisfying f(0) = 0 and f'(0) = 4. The next results concern the approximation of the rational Painlevé-IV solutions by suitable phase shifts of the elliptic function f. Define an exponent by

$$\chi(\zeta) := \begin{cases} 1, & |f(\zeta)| \le 1 \\ -1, & |f(\zeta)| > 1. \end{cases}$$

The purpose of $\chi(\zeta)$ is to allow a streamlined asymptotic description of rational functions near both zeros and poles.

Theorem 3 (Elliptic asymptotics of gH rationals) Let $\rho > 0$ be a fixed rational aspect ratio. Then for j = 1, 2, 3 there is a well-defined family of smooth but not analytic maps $\mu \mapsto \zeta_0 = \zeta_{0,\text{gH}}^{[j]}(\mu; m, n)$, $\mathcal{B}_{\square}(\kappa) \to \mathbb{C}$, such that as $m, n \to +\infty$ with $n = \rho m$,

$$u_{gH}^{[j]}(x; m, n) = T^{1/2} \left(\check{U}^{\chi} + \mathcal{O}(T^{-1}) \right)^{\chi}, \quad \check{U} = f(\zeta - \zeta_0),$$

$$x = T^{1/2} \mu + T^{-1/2} \zeta, \quad T = |\Theta_{0,gH}^{[j]}(m, n)|,$$

$$\mu \in \mathcal{B}_{\square}(\kappa), \quad \kappa = -\frac{\Theta_{\infty, gH}^{[j]}(m, n)}{T} \to \kappa_{\infty} = \kappa_{\infty}^{[j]}(\rho),$$
(1.29)

where $\chi = \chi(\zeta - \zeta_0)$, and where the error estimate holds uniformly for μ in any fixed compact subset of $\mathcal{B}_{\square}(\kappa_{\infty})$ and for ζ bounded. The phase ζ_0 is defined implicitly by (1.31).

Theorem 4 (Elliptic asymptotics of gO rationals) Let $\rho > 0$ be a fixed rational aspect ratio, and let $\mathcal{B}(\kappa)$ denote either $\mathcal{B}_{\square}(\kappa)$, $\pm \mathcal{B}_{\triangleright}(\kappa)$, or $\pm \mathcal{B}_{\triangle}(\kappa)$. Then for j=1,2,3 there is a well-defined family of smooth but not analytic maps $\mu \mapsto \zeta_0 = \zeta_{0,\mathrm{gO}}^{[j]}(\mu;m,n)$, $\mathcal{B}(\kappa) \to \mathbb{C}$, such that as $m,n \to \pm \infty$ with $n=\rho m$,

$$u_{gO}^{[j]}(x; m, n) = T^{1/2} \left(\check{U}^{\chi} + \mathcal{O}(T^{-1}) \right)^{\chi}, \quad \check{U} = f(\zeta - \zeta_0),$$

$$x = T^{1/2} \mu + T^{-1/2} \zeta, \quad T = |\Theta_{0, gO}^{[j]}(m, n)|,$$

$$\mu \in \mathcal{B}(\kappa), \quad \kappa = -\frac{\Theta_{\infty, gO}^{[j]}(m, n)}{T} \to \kappa_{\infty} = \pm \kappa_{\infty}^{[j]}(\rho),$$
(1.30)



where $\chi = \chi(\zeta - \zeta_0)$, and where the error estimate holds uniformly for μ in any fixed compact subset of $\mathcal{B}(\kappa_{\infty})$ and for ζ bounded. The phase ζ_0 is defined implicitly by (1.31).

Remark 4 The approximation formulæ (1.29) and (1.30) in Theorems 3 and 4, respectively, assert that $T^{-1/2}u_{\rm F}^{[j]}(x;m,n)$ and \check{U} are $\mathcal{O}(T^{-1})$ -close as functions with values on the Riemann sphere. Therefore, in terms of the chordal metric

$$d(w,z) := \frac{2|w-z|}{\sqrt{1+|w|^2}\sqrt{1+|z|^2}}$$

the results can be written without the device of $\chi(\zeta)$ as $d(T^{-1/2}u_F^{[j]}(x; m, n), \check{U}) = \mathcal{O}(T^{-1})$.

These results therefore assert the existence of the phase shift ζ_0 as a function of μ and large parameters (m,n) for which the elliptic approximation formally described in Sect. 1.3.2, but with a specific value $E=E(\mu;\kappa)$ of the integration constant, is accurate to the indicated order. We will not give formulæ for the phase shift (but see Appendix D for the special case of $\mu=0$), because in our proofs of these results we actually use a different representation of $f(\zeta-\zeta_0)$ in terms of theta functions. This representation has the advantage of isolating the two different lattices of poles and zeros of $f(\zeta-\zeta_0)$, allowing for comparison with the roots of the four different polynomial factors in each exact rational solution according to the representations shown in the right-most columns of Tables 1 and 2. Specifically, we prove that, for a suitable canonical homology basis underlying the periods $Z_{\mathfrak{a}}$ and $Z_{\mathfrak{b}}$ defined in (1.19) (see Fig. 28 in Sect. 7.6), the leading term $f(\zeta-\zeta_0)$ in Theorems 3 and 4 can be written as

$$f(\zeta - \zeta_0) = \psi(\mu) \frac{\vartheta(\frac{2\pi \mathrm{i}}{Z_a}\zeta + \mathrm{i}\xi(\mu; m, n) + \mathrm{i}\mathfrak{z}_1(\mu) + \mathcal{K})\vartheta(\frac{2\pi \mathrm{i}}{Z_a}\zeta + \mathrm{i}\xi(\mu; m, n) + \mathrm{i}\mathfrak{z}_2(\mu) + \mathcal{K})}{\vartheta(\frac{2\pi \mathrm{i}}{Z_a}\zeta + \mathrm{i}\xi(\mu; m, n) + \mathrm{i}\mathfrak{p}_1(\mu) + \mathcal{K})\vartheta(\frac{2\pi \mathrm{i}}{Z_a}\zeta + \mathrm{i}\xi(\mu; m, n) + \mathrm{i}\mathfrak{p}_2(\mu) + \mathcal{K})},$$

$$(1.31)$$

where only the common phase $\xi(\mu; m, n)$ contains terms proportional to the large parameters (m, n), $\mathcal{K} := \mathrm{i}\pi(1 + Z_{\mathfrak{b}}/Z_{\mathfrak{a}})$, and $\vartheta(z)$ is the Riemann theta function (see (7.22) in Sect. 7.6) for the homology basis $(\mathfrak{a}, \mathfrak{b})$ of the elliptic curve $w^2 = P(z)$. The latter is an entire function of z with simple zeros only at the points $z = \mathcal{K} + 2\pi \mathrm{i}k + 2\pi \mathrm{i}\ell Z_{\mathfrak{b}}/Z_{\mathfrak{a}}$ for $(k, \ell) \in \mathbb{Z} \times \mathbb{Z}$. The bounded and nonvanishing factor $\psi(\mu)$ (see (7.43) and (7.49) in Sect. 7.7) and the phases $\xi(\mu; m, n)$ (see (7.26) in Sect. 7.6), $\mathfrak{z}_{1,2}(\mu)$, and $\mathfrak{p}_{1,2}(\mu)$ (see (7.41) and (7.47) in Sect. 7.7) are different for each family and type of rational solution and, in the case of the gO family, for each of the regions $\mathcal{B}_{\square}(\kappa)$, $\pm \mathcal{B}_{\triangleright}(\kappa)$, and $\pm \mathcal{B}_{\triangle}(\kappa)$. While the various ingredients in the formula (1.31) appear naturally as part of the proof of accuracy, for the reader's convenience we summarize in Appendix F how these ingredients are effectively computed for each family (gH or



gO), type (j=1,2,3), and region $\mathcal{B}(\kappa)$. Although it is not hard to see that (1.31) defines an elliptic function of ζ , it is far less obvious that it is a solution of the specific differential equation (1.18). In fact, our proof derives both the formula (1.31) and the differential equation (1.18) independently from the same model Riemann–Hilbert problem. While the knowledge that $f(\zeta - \zeta_0)$ solves (1.18) is satisfying from the point of view of the formal asymptotic analysis described in Sect. 1.3, the formula (1.31) is more convenient to use in practice; it is how we made the plots in Figs. 6–12.

The basic asymptotic formulæ (1.29) and (1.30) are established in the form (1.31) in Sect. 7.7, and are then related to the differential equation (1.18) in Sect. 7.8. The fact that these formulæ are valid on the indicated domains complementary to $\mathcal{E}_{gH}(\kappa)$ or $\mathcal{E}_{gO}(\kappa)$ is then shown in Sect. 8.6 (for both families of rational solutions on $\mathcal{B}_{\square}(\kappa)$) and in Sect. 8.9 (for the gO rational solutions on $\mathcal{B}_{\triangleright}(\kappa)$ and $\mathcal{B}_{\triangle}(\kappa)$). The proofs of Theorems 3 and 4 are completed in Sect. 8.11.

A characteristic feature of the approximation formulæ in Theorems 3 and 4 is that while the rational function approximated depends on only one variable x = $T^{1/2}\mu + T^{-1/2}\zeta$, the approximation $T^{1/2}f(\zeta - \zeta_0)$ essentially involves μ and ζ as independent variables, and while it is certainly meromorphic in ζ , it has a nonzero $\overline{\partial}$ derivative with respect to μ . This means that for a given value of $T^{-1/2}x$, the approximation formula in each of these theorems offers a one-parameter family of different approximations of the same rational function. Two particularly useful ways to make use of this freedom are (i) to fix ζ and vary μ within one of the regions $\mathcal{B}_{\square}(\kappa)$ or $\mathcal{B}_{\triangleright}(\kappa)$ or $\mathcal{B}_{\triangle}(\kappa)$ or (ii) to fix μ and instead allow ζ to vary in a bounded set. The approach (i) yields an approximation that is uniformly accurate over a given compact set in μ that corresponds to a large region of size $T^{1/2}$ in the x-plane, but the approximation fails to be meromorphic in μ (its $\bar{\partial}$ derivative is of course exactly cancelled by that of the error term, although that term is not known in any detail). On the other hand, the approach (ii) yields an approximation that is an exact elliptic function, hence meromorphic, but the approximation is only accurate for bounded ζ , which corresponds to a small region of size $T^{-1/2}$ in the x-plane. Putting the two approaches together, one can think of (μ, ζ) as coordinates on the complex tangent bundle over $\mathcal{B}_{\square}(\kappa)$, $\mathcal{B}_{\triangleright}(\kappa)$, or $\mathcal{B}_{\triangle}(\kappa)$. These two interpretations of the asymptotic formulæ in Theorems 3 and 4 are consistent with the simple idea that in a given region the rational Painlevé-IV functions are approximated by an elliptic function whose modulus and phase shift vary slowly on scales that are large compared to the periods $Z_{\mathfrak{a}}$ and $Z_{\mathfrak{b}}$. This is a familiar notion in the asymptotic analysis of Painlevé equations; in the setting of large-x asymptotics this goes back to Boutroux [14]. See also [41] for a recent review. For modulated elliptic approximations in the large-parameter regime, see [4, 7, 12, 13, 18, 46, 47, 50].

Using the approach (i) allows one to combine the equilibrium asymptotics of Theorems 1–2 with the elliptic asymptotics of Theorems 3–4 and obtain an approximation \check{U} of $U=T^{-1/2}u_{\rm F}^{[j]}(T^{1/2}\mu;m,n)$, defined piecewise in the complex μ -plane, the accuracy of which is guaranteed for all $\mu\in\mathbb{C}$ except for values near the Jordan curves $\partial\mathcal{E}_{\rm gH}(\kappa)$ and $\partial\mathcal{E}_{\rm gO}(\kappa)$. These approximations are remarkably accurate even for (m,n) not too large, as can be seen in Figs. 6–8.



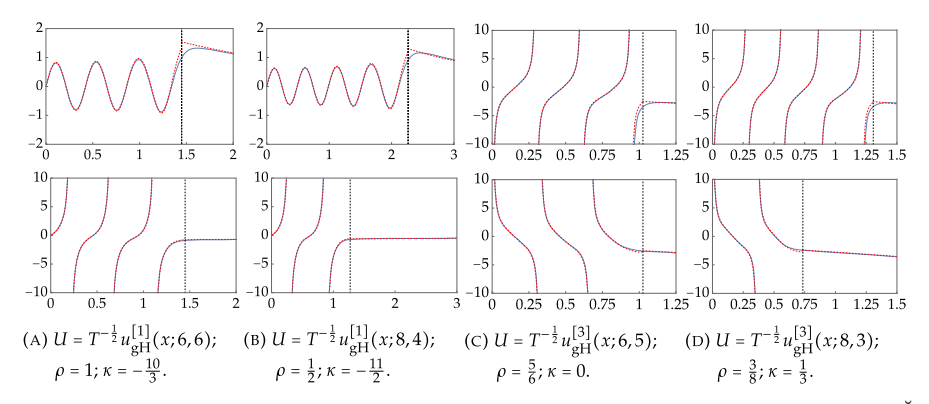


Fig. 6 Quantitative comparison of scaled gH rational solutions U (blue curves) with the leading terms \check{U} (dashed red curves) in Theorems 1 and 3 for $x=T^{1/2}\mu$ (taking $\zeta=0$ fixed in the latter case). Axes for top row of plots: U and \check{U} versus μ . Axes for bottom row of plots: -iU and $-i\check{U}$ versus $-i\mu$. Dotted vertical lines indicate the intersection points of $\partial \mathcal{E}_{gH}(\kappa)$ with the coordinate axes, near which neither Theorem 1 nor 3 provides a uniformly accurate approximation (Color figure online)

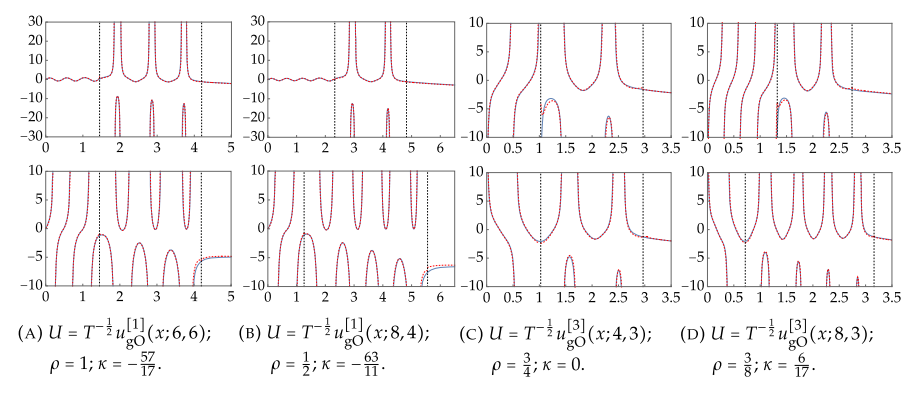


Fig. 7 Quantitative comparison of scaled gO rational solutions U (blue curves) for positive indices (m,n) with the leading terms \check{U} (dashed red curves) in Theorems 2 and 4 for $x=T^{1/2}\mu$ (taking $\zeta=0$ fixed in the latter case). Axes for top row of plots: U and \check{U} versus μ . Axes for bottom row of plots: -iU and $-i\check{U}$ versus $-i\mu$. Dotted vertical lines indicate the intersection points of $\partial \mathcal{E}_{gH}(\kappa)$ and $\partial \mathcal{E}_{gO}(\kappa)$ with the coordinate axes, near which neither Theorem 2 nor 4 provides a uniformly accurate approximation (Color figure online)

On the other hand, the approach (ii) allows one to accurately compare $U=T^{-1/2}u_{\rm F}^{[j]}(T^{1/2}\mu+T^{-1/2}\zeta;m,n)$ with an exact elliptic function $\check{U}=f(\zeta-\zeta_0)$ of ζ , by fixing a point μ . Theorems 3–4 predict the accuracy of such an approximation provided that ζ remains bounded. Figure 9 illustrates the nature of convergence to such an exact elliptic approximation. For given (m,n), the approach (ii) approximation fails as ζ increases, just as the tangent space fails to approximate a curved base



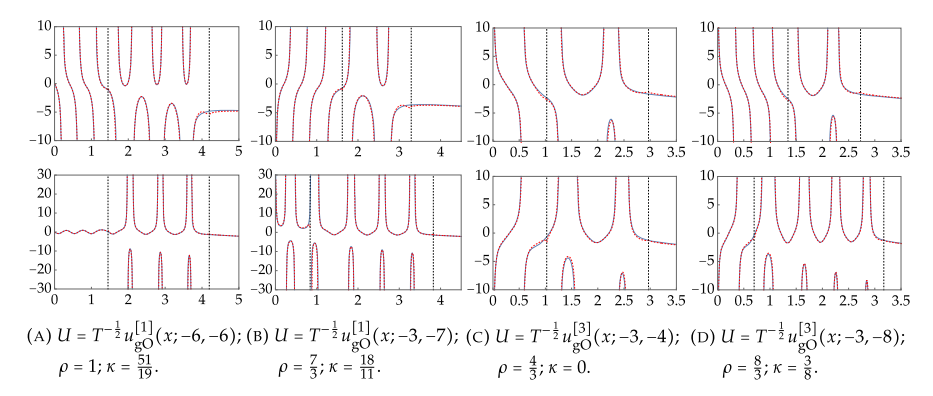


Fig. 8 As in Fig. 7 but for negative indices (m, n) (Color figure online)

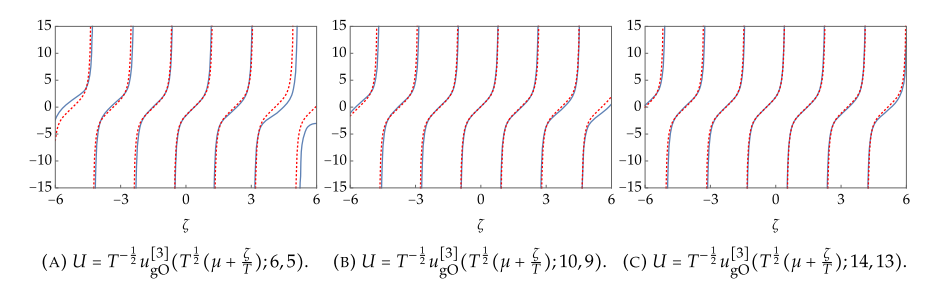


Fig. 9 Exact elliptic function approximations $\check{U}=f(\zeta-\zeta_0)$ (dashed red curves) and the rational solutions U they approximate (blue curves) near $\mu=\frac{1}{10}\in\mathcal{B}_{\square}(\kappa)\cap\mathbb{R}$ as functions of $\zeta\in\mathbb{R}$. For all three plots, $\kappa=0$ (Color figure online)

manifold except near the given base point. For another application of approach (ii), see Appendix D.

A good application of switching back and forth between the base manifold and its tangent space at a point is the proof of the following corollary of Theorems 3 and 4 (and of their proof, which specifies the various phases in (1.31)). Note that according to (1.31), the zeros of $f(\zeta - \zeta_0)$ are given by, for k = 1 or k = 2, the quantization conditions (the superscript * denotes complex conjugation)

$$\frac{\operatorname{Im}(Z_{\mathfrak{b}}^{*} \cdot (\zeta + \frac{Z_{\mathfrak{a}}}{2\pi}(\xi(\mu; m, n) + \mathfrak{z}_{k}(\mu))))}{\operatorname{Im}(Z_{\mathfrak{a}}^{*}Z_{\mathfrak{b}})} \in \mathbb{Z} \text{ and}$$

$$-\frac{\operatorname{Im}(Z_{\mathfrak{a}}^{*} \cdot (\zeta + \frac{Z_{\mathfrak{a}}}{2\pi}(\xi(\mu; m, n) + \mathfrak{z}_{k}(\mu))))}{\operatorname{Im}(Z_{\mathfrak{a}}^{*}Z_{\mathfrak{b}})} \in \mathbb{Z}. \tag{1.32}$$



Likewise, the poles of $f(\zeta - \zeta_0)$ are given by, for k = 1 or k = 2, the quantization conditions

$$\frac{\operatorname{Im}(Z_{\mathfrak{b}}^{*} \cdot (\zeta + \frac{Z_{\mathfrak{a}}}{2\pi}(\xi(\mu; m, n) + \mathfrak{p}_{k}(\mu))))}{\operatorname{Im}(Z_{\mathfrak{a}}^{*}Z_{\mathfrak{b}})} \in \mathbb{Z} \quad \text{and} \quad \\ -\frac{\operatorname{Im}(Z_{\mathfrak{a}}^{*} \cdot (\zeta + \frac{Z_{\mathfrak{a}}}{2\pi}(\xi(\mu; m, n) + \mathfrak{p}_{k}(\mu))))}{\operatorname{Im}(Z_{\mathfrak{a}}^{*}Z_{\mathfrak{b}})} \in \mathbb{Z}. \tag{1.33}$$

The phase $\xi(\mu; m, n)$ is given in (7.26) of Sect. 7.6, in which the dependence on the family (gH or gO), domain $\mathcal{B}_{\square}(\kappa)$, $\mathcal{B}_{\triangleright}(\kappa)$, or $\mathcal{B}_{\triangle}(\kappa)$, and a sign s ($s = -\mathrm{sgn}(\Theta_0)$ for type-1 solutions and $s = \mathrm{sgn}(\Theta_0)$ for type-3 solutions) enters via the data in Table 6 of that same section. In particular, $\xi(\mu; m, n)$ contains terms proportional via $T \gg 1$ to real quantities R_1 and R_2 (see (7.1) in Sect. 7.3) that are essentially the imaginary parts of the integrals whose real parts vanish in (1.26). The phase shifts $\mathfrak{z}_k(\mu)$ and $\mathfrak{p}_k(\mu)$ depend on μ as well as the type of the rational solution. They are written in Sect. 7.7 for type-1 solutions in (7.47) and for type-3 solutions in (7.41). Define, for either family F = gH or F = gO, and types j = 1, 2, 3,

$$\begin{split} \mathcal{Z}_{\mathrm{F}}^{[j]}(m,n) &:= \{ \mu \in \mathbb{C} : u_{\mathrm{F}}^{[j]}(|\Theta_{0,\mathrm{F}}^{[j]}(m,n)|^{1/2}\mu;m,n) = 0 \} \\ \mathcal{P}_{\mathrm{F}}^{[j]}(m,n) &:= \{ \mu \in \mathbb{C} : u_{\mathrm{F}}^{[j]}(|\Theta_{0,\mathrm{F}}^{[j]}(m,n)|^{1/2}\mu;m,n) = \infty \} \end{split}$$

as the sets of rescaled zeros and poles of the indicated rational solution. Likewise, set

$$\check{\mathcal{Z}}_{\mathrm{F}}^{[j]}(m,n):=\{\mu\in\mathbb{C}:f(-\zeta_0)=0\}\quad\text{and}\quad \check{\mathcal{P}}_{\mathrm{F}}^{[j]}(m,n):=\{\mu\in\mathbb{C}:f(-\zeta_0)=\infty\}$$

where $f(\zeta - \zeta_0)$ is the approximation of the corresponding rational solution via Theorem 3 or 4. In other words, $\check{Z}_F^{[j]}(m,n)$ (resp., $\check{\mathcal{P}}_F^{[j]}(m,n)$) is the set of all points μ satisfying both conditions in (1.32) (resp., in (1.33)) with $\zeta = 0$ fixed for either k = 1 or k = 2 and phases determined for the family, type, and region of interest.

Corollary 2 (Poles and zeros of Painlevé-IV rational solutions) *Fix a rational aspect* ratio $\rho > 0$ and a compact set C within one of the domains $\mathcal{B}_{\square}(\kappa)$, $\mathcal{B}_{\triangleright}(\kappa)$, or $\mathcal{B}_{\triangle}(\kappa)$ (the latter two for the gO family only). Then, there is a constant r > 0 (depending on C and ρ) such that for m, n sufficiently large with $n = \rho m$ the following statements hold with $T = |\Theta_{0}^{[j]}(m, n)|$.

- For each point $\check{\mu} \in \check{\mathcal{Z}}_F^{[j]}(m,n) \cap C$, there is a unique point $\mu \in \mathcal{Z}_F^{[j]}(m,n)$ that satisfies $|\mu \check{\mu}| \leq rT^{-2}$. Likewise for each point $\mu \in \mathcal{Z}_F^{[j]}(m,n) \cap C$, there is a unique point $\check{\mu} \in \check{\mathcal{Z}}_F^{[j]}(m,n)$ that satisfies $|\check{\mu} \mu| \leq rT^{-2}$.
- For each point $\check{\mu} \in \check{\mathcal{P}}_{F}^{[j]}(m,n) \cap C$, there is a unique point $\mu \in \mathcal{P}_{F}^{[j]}(m,n)$ that satisfies $|\mu \check{\mu}| \leq rT^{-2}$. Likewise for each point $\mu \in \mathcal{P}_{F}^{[j]}(m,n) \cap C$, there is a unique point $\check{\mu} \in \check{\mathcal{P}}_{F}^{[j]}(m,n)$ that satisfies $|\check{\mu} \mu| \leq rT^{-2}$.



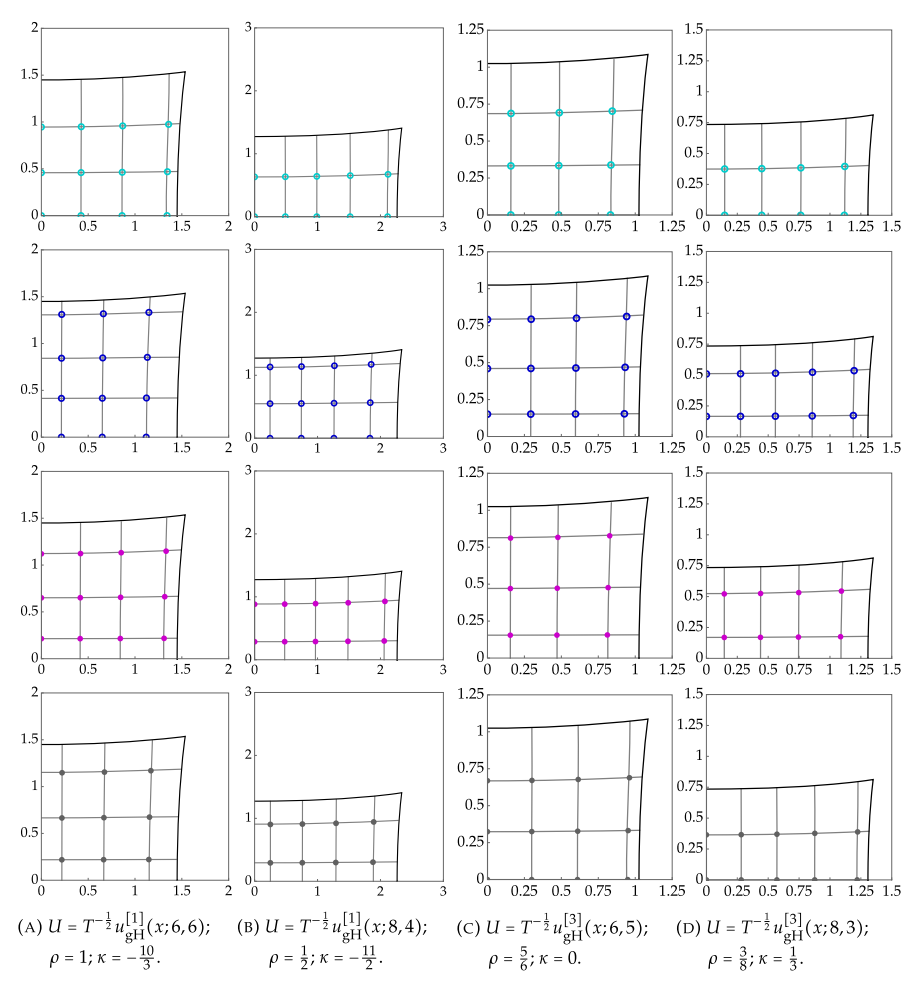


Fig. 10 Quantitative comparison of zeros (circles, cyan for positive derivative and blue for negative derivative, top two rows of plots) and poles (dots, magenta for positive residue and gray for negative residue, bottom two rows of plots) of scaled gH rational solutions U with the approximations given according to Corollary 2 by the intersection points of integer level curves (gray) of the two conditions in (1.32) or (1.33) plotted in the $\mu = T^{-1/2}x$ -plane (Color figure online)

The proof of Corollary 2 is given in Sect. 7.10. The accuracy of approximation of poles and zeros of the rational Painlevé-IV solutions $u_F^{[j]}(x;m,n)$ for both families F = gH and F = gO and types j = 1 and j = 3 is shown in Figs. 10–12 for μ in the closed first quadrant $0 \le \arg(\mu) \le \frac{1}{2}\pi$. Again, the accuracy is remarkable even for (m,n) not very large. We do not show analogous plots for type j = 2 since these can be immediately obtained from (2.2) and Proposition 4 in Sect. 2.

With just a bit more work, the analysis behind Corollary 2 allows one to extract the asymptotic behavior of the zeros of the special gH and gO polynomials themselves. For a uniform treatment of both families of polynomials, set $Q_{gH}(x; m, n) := H_{m,n}(x)$



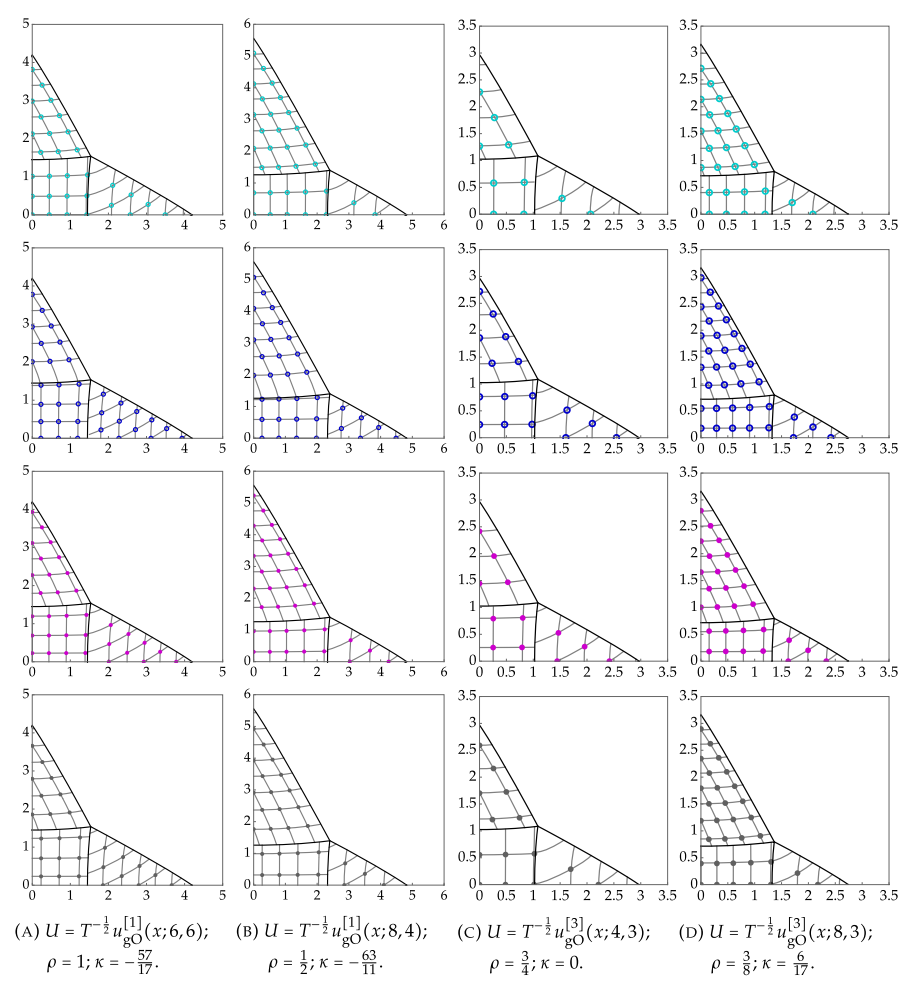


Fig. 11 Quantitative comparison of zeros (circles, cyan for positive derivative and blue for negative derivative, top two rows of plots) and poles (dots, magenta for positive residue and gray for negative residue, bottom two rows of plots) of scaled gO rational solutions U with the approximations given according to Corollary 2 by the intersection points of integer level curves (gray) of the two conditions in (1.32) or (1.33) plotted in the $\mu = T^{-1/2}x$ -plane (Color figure online)

and $Q_{gO}(x; m, n) := Q_{m,n}(x)$. Then define

$$\mathcal{D}_{\mathbf{F}}(m,n) := \{ \mu \in \mathbb{C} : Q_{\mathbf{F}}(|\Theta_{0,\mathbf{F}}^{[1]}(m,n)|^{1/2}\mu; m,n) = 0 \}, \quad \mathbf{F} = \mathbf{gH}, \mathbf{gO}$$

as the set of all roots of the indicated polynomial, suitably rescaled. Similarly, let $\mathcal{D}_F(m,n)$ denote the set of values of μ for which both conditions in (1.33) hold with $\zeta=0$ fixed for type j=1 and k=2. The selection of k=2 turns out to correspond to $\zeta=0$ being a pole of $f(\zeta-\zeta_0)$ of residue -1. The following result was first proved in the gH case by Masoero and Roffelsen using the theory of a family of quantum



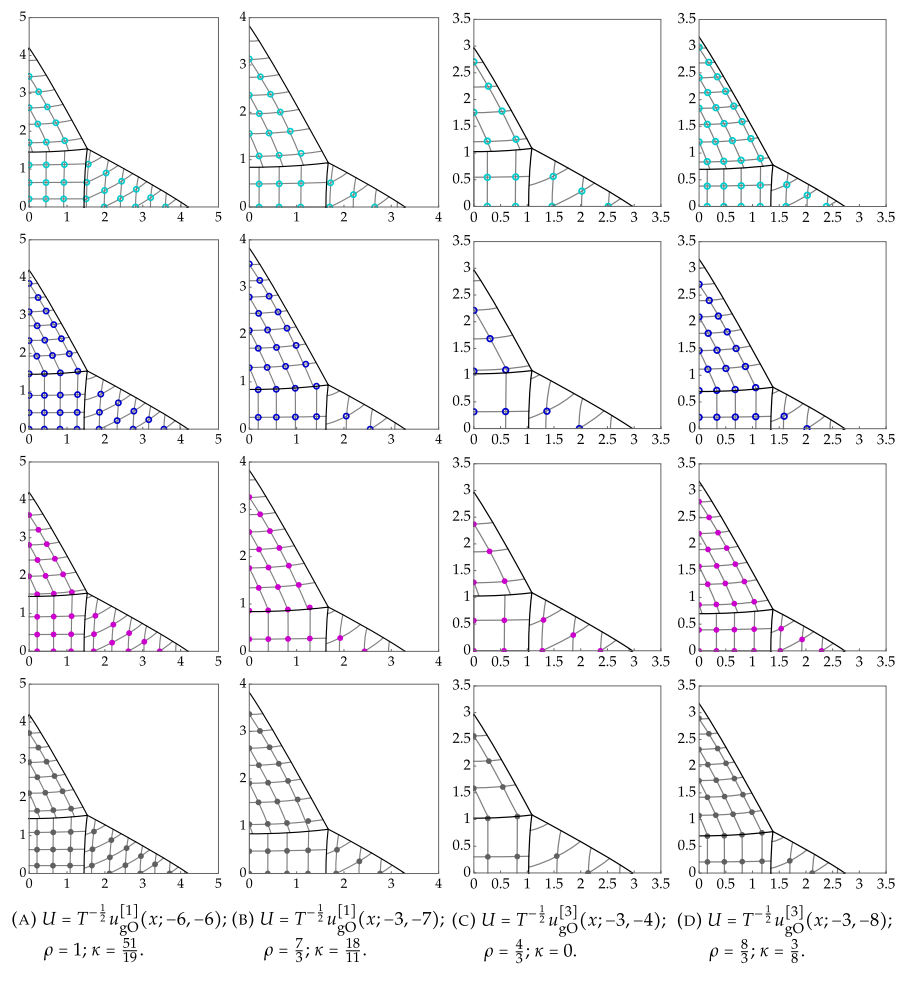


Fig. 12 As in Fig. 7 but for negative indices (m, n)

oscillators with anharmonic potentials. The same authors are currently working on an analogous result for the gO polynomials [48]. Our proof is a consequence of the isomonodromy method and hence applies equally well in the gH and gO cases.

Corollary 3 (Roots of gH and gO polynomials; cf. [47, Theorem 2] for the gH case) Fix a rational aspect ratio $\rho > 0$ and a compact set C within one of the domains $\mathcal{B}_{\square}(\kappa)$, $\mathcal{B}_{\triangleright}(\kappa)$, or $\mathcal{B}_{\triangle}(\kappa)$ (the latter two for the gO family only). Then, there is a constant r > 0 (depending on C and ρ) such that for m, n sufficiently large with $n = \rho m$ the following statements hold with $T = |\Theta_{0,F}^{[1]}(m,n)|$. For each point $\check{\mu} \in \check{\mathcal{D}}_F(m,n) \cap C$, there is a unique point $\mu \in \mathcal{D}_F(m,n)$ that satisfies $|\mu - \check{\mu}| \leq rT^{-2}$. Likewise for each point $\mu \in \mathcal{D}_F(m,n) \cap C$, there is a unique point $\check{\mu} \in \check{\mathcal{D}}_F(m,n)$ that satisfies $|\check{\mu} - \mu| \leq rT^{-2}$.



The proof is given in Sect. 7.10, and it is based on the fact that, according to Tables 1 and 2, the gH and gO polynomials $H_{m,n}(x)$ and $Q_{m,n}(x)$ give rise to poles of residue -1 of $u_{\rm gH}^{[1]}(x;m,n)$ and $u_{\rm gO}^{[1]}(x;m,n)$, respectively. Therefore, the accuracy of the approximation of roots of the gH and gO polynomials given in Corollary 3 can also be seen in the bottom row of the first two columns of Figs. 10–12.

The σ -form of the Painlevé-IV equation [40, 57] also admits rational solutions, each of which can be expressed in terms of just one gH or gO polynomial (see, for example, [23]). Results for the polynomials themselves such as Corollary 3 or the theorems of Masoero and Roffelsen [47] can therefore be used to write asymptotic approximations for rational solutions of the σ -Painlevé-IV equation.

1.5 Notation

We define the three Pauli matrices

$$\sigma_1 := \begin{pmatrix} 0 & 1 \\ 1 & 0 \end{pmatrix}, \quad \sigma_2 := \begin{pmatrix} 0 & -i \\ i & 0 \end{pmatrix}, \quad \sigma_3 := \begin{pmatrix} 1 & 0 \\ 0 & -1 \end{pmatrix}.$$

It will be convenient to have some compact notation for 2×2 matrices having certain structure; thus, given a complex number a we define unit determinant lower triangular, upper triangular, diagonal, and "twist" matrices by

$$\mathbf{L}(a) := \begin{pmatrix} 1 & 0 \\ a & 1 \end{pmatrix}, \quad \mathbf{U}(a) := \begin{pmatrix} 1 & a \\ 0 & 1 \end{pmatrix}, \quad \mathbf{D}(a) := a^{\sigma_3} = \begin{pmatrix} a & 0 \\ 0 & a^{-1} \end{pmatrix}, \quad \mathbf{T}(a) := \begin{pmatrix} 0 & -a^{-1} \\ a & 0 \end{pmatrix}. \tag{1.34}$$

In terms of these elementary matrices, we will frequently use the following factorizations, which assume ad - bc = 1:

$$\begin{pmatrix} a & b \\ c & d \end{pmatrix} = \mathbf{L}(ca^{-1})\mathbf{D}(a)\mathbf{U}(ba^{-1}), \quad a \neq 0, \quad \text{("LDU")},$$

$$= \mathbf{L}(db^{-1})\mathbf{T}(-b^{-1})\mathbf{L}(ab^{-1}), \quad b \neq 0, \quad \text{("LTL")},$$

$$= \mathbf{U}(bd^{-1})\mathbf{D}(d^{-1})\mathbf{L}(cd^{-1}), \quad d \neq 0, \quad \text{("UDL")},$$

$$= \mathbf{U}(ac^{-1})\mathbf{T}(c)\mathbf{U}(dc^{-1}), \quad c \neq 0, \quad \text{("UTU")}.$$

$$(1.35)$$

For a function f defined on the complement of an oriented arc in the complex plane, we use subscripts "+" (resp., "-") to denote the boundary value taken at a given point on the arc from the left (resp., right): f_{\pm} . We sometimes abbreviate the average and difference of these boundary values by writing

$$\langle f \rangle := \frac{1}{2}(f_+ + f_-)$$
 and $\Delta f := f_+ - f_-$.

Throughout this paper, we use * to denote complex conjugation, and for a quantity Q we use a breve (Q) to indicate a corresponding approximation. Finally, for expressions applicable to either family, gH or gO, we frequently use a generic subscript F (for "family").



2 Bäcklund Transformations and Symmetries

Transformations among the rational solutions of (1.1) play a crucial role in our work, and in this section we briefly describe their most important properties. We refer the reader to [23, 35, 37, 43, 51] for background and more information. Each of the four parameter sets $\Lambda_{\rm gH}^{[1]-}$, $\Lambda_{\rm gH}^{[2]-}$, $\Lambda_{\rm gH}^{[3]+}$, and $\Lambda_{\rm gO}$, along with its corresponding rational solutions of (1.1), can be generated from a "seed" triple $(\Theta_0,\Theta_\infty,u(x))$ by iteratively applying certain Bäcklund transformations in order to increment or decrement the parameters $(\Theta_0, \Theta_\infty)$ by a basis (over \mathbb{Z}) of lattice vectors. The basis can be chosen to correspond to integer increments of m and n. Such Bäcklund transformations are isomonodromic and they lift to Schlesinger transformations of corresponding simultaneous solutions of the Lax pair for Painlevé-IV; see Sect. 3.3 for details. For each type of rational solution in the gH family, a basic isomonodromic Bäcklund transformation becomes indeterminate (i.e., producing an identically vanishing denominator) for the transformed rational solution if it is applied at a lattice point on the boundary of the parameter sector and would yield transformed parameters one step outside the sector. For example, at the points $(\Theta_0, \Theta_\infty) = (\frac{1}{2} + \frac{1}{2}n, \frac{1}{2} + \frac{1}{2}n), n = 0, 1, 2, \dots$, that make up part of the boundary of $\Lambda_{gH}^{[3]+}$, the isomonodromic Bäcklund transformation $(\Theta_0, \Theta_\infty, u(x)) \mapsto (\Theta_0 + \frac{1}{2}, \Theta_\infty - \frac{1}{2}, u_{\setminus}(x))$ (see (3.49)) is indeterminate as it leads to negative values of m. The same transformation is however valid at all other points of $\Lambda_{gH}^{[3]+}$. The reason this occurs is that the three sets of monodromy data consisting of Stokes and connection matrices for the three types of gH rational solutions of (1.1) are all different. This phenomenon does not occur for the gO family, each point of which yields the same monodromy data (but different again from that of all three gH types).

Therefore, if it is desired to generate one type of rational solution of (1.1) in the gH family from another type of solution in the same family, one must apply a Bäcklund transformation that is *not* isomonodromic. We will find useful two such transformations, both of which can correspond to large leaps in the $(\Theta_0, \Theta_\infty)$ -plane rather than incremental steps, and hence might be thought of as global symmetries of the Painlevé-IV equation. Firstly, there is an elementary symmetry $\mathcal{S}_{\updownarrow}$ of (1.1)

$$S_{\updownarrow}(\Theta_0, \Theta_{\infty}, u(x)) = (\Theta_{0, \updownarrow}, \Theta_{\infty, \updownarrow}, u_{\updownarrow}(x)) := (\Theta_0, 1 - \Theta_{\infty}, iu(-ix))$$
 (2.1)

due to Boiti and Pempinelli [11]. The action of $\mathcal{S}_{\updownarrow}$ in the parameter space is merely a reflection through the horizontal line $\Theta_{\infty}=\frac{1}{2}$, which obviously preserves both lattices Λ_{gH} and Λ_{gO} . In particular, note that for either family F=gH or F=gO,

$$\begin{split} (\Theta_0,\Theta_\infty) &= (\Theta_{0,\mathsf{F}}^{[1]}(m,n),\Theta_{\infty,\mathsf{F}}^{[1]}(m,n)) & \Longrightarrow & (\Theta_{0,\updownarrow},\Theta_{\infty,\updownarrow}) = (\Theta_{0,\mathsf{F}}^{[2]}(n,m),\Theta_{\infty,\mathsf{F}}^{[2]}(n,m)) \\ (\Theta_0,\Theta_\infty) &= (\Theta_{0,\mathsf{F}}^{[3]}(m,n),\Theta_{\infty,\mathsf{F}}^{[3]}(m,n)) & \Longrightarrow & (\Theta_{0,\updownarrow},\Theta_{\infty,\updownarrow}) = (\Theta_{0,\mathsf{F}}^{[3]}(n,m),\Theta_{\infty,\mathsf{F}}^{[3]}(n,m)). \end{split}$$

⁶ The seed triples we use are $(-\frac{1}{2}, \frac{3}{2}, \frac{1}{x})$ for $\Lambda_{gH}^{[1]-}$, $(-\frac{1}{2}, -\frac{3}{2}, -\frac{1}{x})$ for $\Lambda_{gH}^{[2]-}$, $(\frac{1}{2}, \frac{1}{2}, -2x)$ for $\Lambda_{gH}^{[3]+}$, and $(\frac{1}{6}, \frac{1}{2}, -\frac{2}{3}x)$ for Λ_{gO} .



Therefore, as the rational solution of (1.1) for given parameters is unique, (2.1) implies that

$$u_{\rm F}^{[2]}(x;m,n) = iu_{\rm F}^{[1]}(-ix;n,m) u_{\rm F}^{[3]}(x;m,n) = iu_{\rm F}^{[3]}(-ix;n,m).$$
 (2.2)

Since this shows that the rational solutions $u_{\rm gH}^{[2]}(x;m,n)$ and $u_{\rm gO}^{[2]}(x;m,n)$ are trivially related to $u_{\rm gH}^{[1]}(x;n,m)$ and $u_{\rm gO}^{[1]}(x;n,m)$, respectively, it is sufficient to prove results for the rational solutions of types 1 and 3 in the gH and gO families.

Remark 5 The equilibrium relation (1.15) is invariant under an analogue of the Boiti–Pempenelli symmetry S_{\updownarrow} with action $S_{\updownarrow}(\kappa, \mu, U_0) \mapsto (-\kappa, i\mu, iU_0)$. Since the equilibria as defined for large μ in (1.15)–(1.16) are all distinct, S_{\updownarrow} acts on them by

$$\begin{split} \mathcal{S}_{\updownarrow}U_{0,\mathrm{gH}}^{[1]}(\mu;\kappa) &:= \mathrm{i}U_{0,\mathrm{gH}}^{[1]}(-\mathrm{i}\mu;-\kappa) = U_{0,\mathrm{gH}}^{[2]}(\mu;\kappa) \\ \mathcal{S}_{\updownarrow}U_{0,\mathrm{gH}}^{[2]}(\mu;\kappa) &:= \mathrm{i}U_{0,\mathrm{gH}}^{[2]}(-\mathrm{i}\mu;-\kappa) = U_{0,\mathrm{gH}}^{[1]}(\mu;\kappa) \\ \mathcal{S}_{\updownarrow}U_{0,\mathrm{gH}}^{[3]}(\mu;\kappa) &:= \mathrm{i}U_{0,\mathrm{gH}}^{[3]}(-\mathrm{i}\mu;-\kappa) = U_{0,\mathrm{gH}}^{[3]}(\mu;\kappa) \\ \mathcal{S}_{\updownarrow}U_{0,\mathrm{gO}}(\mu;\kappa) &:= \mathrm{i}U_{0,\mathrm{gO}}(-\mathrm{i}\mu;-\kappa) = U_{0,\mathrm{gO}}(\mu;\kappa). \end{split} \tag{2.3}$$

These relations also imply that, for fixed $\kappa \in \mathbb{R} \setminus \{-1, 1\}$, all four equilibrium branches are odd functions of μ .

The rational solutions of type 1 and 3 are in turn related by a more complicated nonisomonodromic Bäcklund transformation that we denote by $\mathcal{S}_{\mathbb{Q}}$ with action

$$S_{\uparrow}(\Theta_0, \Theta_\infty, u(x)) = (\Theta_{0,\uparrow}, \Theta_{\infty,\uparrow}, u_{\uparrow}(x))$$

$$:= \left(-\frac{1}{2}(\Theta_0 + \Theta_\infty), \frac{3}{2}\Theta_0 - \frac{1}{2}\Theta_\infty + 1, \frac{u'(x)}{2u(x)} - \frac{2\Theta_0}{u(x)} - x - \frac{1}{2}u(x)\right). \tag{2.4}$$

This is a version of the transformation of Lukashevich [43] and Gromak [37] denoted by \widetilde{W} in [22, Sect. 2] and by \mathscr{T}_1^{\pm} in [53, §32.7(iv)]. It is interesting to note that the induced action on the $(\Theta_0, \Theta_{\infty})$ -plane has unit Jacobian; hence, area and orientation are preserved. In fact, setting

$$\mathbf{D}(3^{1/4}) := \begin{pmatrix} 3^{1/4} & 0 \\ 0 & 3^{-1/4} \end{pmatrix} \quad \text{and} \quad \mathbf{R}(\varphi) := \begin{pmatrix} \cos(\varphi) - \sin(\varphi) \\ \sin(\varphi) & \cos(\varphi) \end{pmatrix}$$

(so $\mathbf{D}(3^{1/4})$ is the matrix of stretching by $3^{1/4}$ along the Θ_0 axis and compression by $3^{-1/4}$ along the Θ_{∞} axis, and $\mathbf{R}(\varphi)$ is the matrix of rigid rotation about the origin by φ radians), we have

$$\mathcal{S}_{\mathbb{t}}: \left[\begin{pmatrix}\Theta_0\\\Theta_\infty\end{pmatrix} - \begin{pmatrix}\frac{1}{6}\\\frac{1}{2}\end{pmatrix}\right] \mapsto \begin{pmatrix}-\frac{1}{2}\\\frac{1}{2}\end{pmatrix} + \mathbf{D}(3^{1/4})^{-1}\mathbf{R}(\frac{2}{3}\pi)\mathbf{D}(3^{1/4}) \left[\begin{pmatrix}\Theta_0\\\Theta_\infty\end{pmatrix} - \begin{pmatrix}\frac{1}{6}\\\frac{1}{2}\end{pmatrix}\right].$$



This shows that $\mathcal{S}_{\mathbb{Q}}$ is an isomorphism of $\Lambda_{gH}^{[3]+}$ onto $\Lambda_{gH}^{[1]-}$, as well as an isomorphism of Λ_{gO} onto itself. For either family F=gH or F=gO,

$$(\Theta_0, \Theta_\infty) = (\Theta_{0,F}^{[3]}(m, n), \Theta_{\infty,F}^{[3]}(m, n)) \Longrightarrow$$

$$(\Theta_0, \widehat{\gamma}, \Theta_{\infty, \widehat{\gamma}}) = (\Theta_{0,F}^{[1]}(m, n+1), \Theta_{\infty,F}^{[1]}(m, n+1))$$

so again by uniqueness of the rational solution of (1.1) for given parameters,

$$u(x) = u_F^{[3]}(x; m, n) \implies u_{\uparrow}(x) = u_F^{[1]}(x; m, n+1).$$
 (2.5)

Although the rational solutions of types 1 and 3 in each family are therefore related explicitly by S_{\uparrow} , the explicit expression for $u_{\uparrow}(x)$ in terms of u(x) written in (2.4) is not convenient for the study of $u_{\uparrow}(x)$ when the parameters are large, even if u(x) is understood with some detail (estimates of derivatives of error terms would be required, for instance). Therefore, we will not use S_{\uparrow} directly; however, we will use it indirectly to show that one may extract u(x) and $u_{\uparrow}(x)$ from the same Riemann–Hilbert problem by formulæ of comparable complexity, neither of which requires differentiation (see (3.2)).

Another useful but elementary symmetry of (1.1) is the Schwarz symmetry S_* defined by

$$\mathcal{S}_*(\Theta_0, \Theta_\infty, u(x)) := (\Theta_0^*, \Theta_\infty^*, u(x^*)^*),$$

where * denotes complex conjugation. This symmetry combines with iteration of the Boiti–Pempinelli symmetry $\mathcal{S}_{\updownarrow}$ to yield the following.

Proposition 4 Every rational solution u(x) of the Painlevé-IV equation (1.1) satisfies

$$u(-x) = -u(x), \quad u(x^*) = u(x)^*, \quad and \quad u(-x^*) = -u(x)^*.$$
 (2.6)

In particular, every rational solution u(x) has either a pole or a zero at x=0, is real for real x and imaginary for imaginary x, and is determined by its values in the closed first quadrant $0 \le \arg(x) \le \frac{1}{2}\pi$.

Proof Noting that S_{\updownarrow} is an involution on the parameter space that preserves rationality of u(x), and using uniqueness of the rational solution for each $(\Theta_0, \Theta_\infty) \in \Lambda_{\rm gH} \sqcup \Lambda_{\rm gO}$ we deduce that every rational solution u(x) of (1.1) is odd: u(-x) = -u(x). On the other hand, S_* fixes the (real) parameters $(\Theta_0, \Theta_\infty)$ of any rational solution and preserves rationality so by uniqueness every rational solution is Schwarz-symmetric: $u(x^*) = u(x)^*$; the relation $u(-x^*) = -u(x)^*$ then follows from odd symmetry. \square

3 Isomonodromy Theory for Rational Solutions of Painlevé-IV

We now use the isomonodromy approach to derive Riemann–Hilbert problems for the gH and gO rational solutions. We state the Riemann–Hilbert problems in Sect. 3.1.



The reader who is primarily interested in the asymptotic analysis of these Riemann–Hilbert problems can proceed directly from the end of Sect. 3.1 to Sect. 4 without loss of continuity. In Sects. 3.2 and 3.3, we develop the background we will need regarding the general Painlevé-IV Riemann–Hilbert Problem 1 and associated isomonodromic Schlesinger transformations. While much of this theory is in the literature (see, for instance, [33, Sects. 5.1 and 6.3] and [35]), to deal with the rational solutions we will add some important details by

- implementing the isomonodromy method for resonant Fuchsian singular points such as for the gH solutions because $\Theta_0 \in \frac{1}{2}\mathbb{Z}$;
- identifying non-differential formulæ for the solution u(x);
- identifying a formula for the related solution $u_{\uparrow}(x)$;
- determining conditions where various discrete isomonodromic transformations are well defined.

Then, in Sects. 3.5 and 3.6 we apply the method described in Sect. 3.4, using the *x*-equation in the Lax pair to compute monodromy data and then applying Schlesinger transformations to prove Theorems 5 and 6 from Sect. 3.1.

3.1 Riemann-Hilbert Representations of Rational Painlevé-IV Solutions

The following Riemann–Hilbert problem associated to general Painlevé-IV functions can be found, for example, in [33].

Riemann-Hilbert Problem 1 (Painlevé-IV Inverse Monodromy Problem) Fix $(\Theta_0, \Theta_\infty) \in \mathbb{C}^2$. Let Stokes matrices $\mathbf{V}_{j,k}$, (j,k)=(2,1), (2,3), (4,3), (4,1), and connection matrices \mathbf{V}_j , $j=1,\ldots,4$ be given, and assume that they all have unit determinant, that $\mathbf{V}_{2,1}$ and $\mathbf{V}_{4,3}$ are lower triangular and $\mathbf{V}_{2,3}$ and $\mathbf{V}_{4,1}$ are upper triangular, and that the matrices are related by (3.20). Seek a 2×2 matrix function $\lambda \mapsto \mathbf{Y}(\lambda; x)$ with the following properties:

- Analyticity: the function $\lambda \mapsto \mathbf{Y}(\lambda; x)$ is analytic for $\lambda \in \mathbb{C} \setminus \Sigma$.
- **Jump conditions:** $\mathbf{Y}(\lambda; x)$ assumes continuous boundary values on Σ from each component of $\mathbb{C} \setminus \Sigma$, except at the origin. Using a subscript + (resp., -) to indicate a boundary value taken from the left (resp., right) by orientation, the boundary values are related on each arc of Σ by the jump condition

$$\mathbf{Y}_{+}(\lambda; x) = \mathbf{Y}_{-}(\lambda; x) \exp\left(\left(\frac{1}{2}\lambda^{2} + x\lambda\right)\sigma_{3}\right) \mathbf{V} \exp\left(-\left(\frac{1}{2}\lambda^{2} + x\lambda\right)\sigma_{3}\right)$$

where **V** is the arcwise-constant function defined on Σ as follows:

$$\mathbf{V} := \mathbf{V}_{j,k}, \quad \lambda \in \Sigma_{j,k}, \quad (j,k) = (2,1), (2,3), (4,3), (4,1),$$

$$\mathbf{V} := \mathbf{V}_{j}, \quad \lambda \in \Sigma_{j}, \quad j = 1, \dots, 4,$$

and

$$\mathbf{V}:=\mathbf{V}_0=e^{2\pi\,\mathrm{i}\Theta_0\sigma_3},\quad \lambda\in\Sigma_0.$$



- **Behavior near the origin:** $\mathbf{Y}(\lambda; x) \lambda^{-\Theta_0 \sigma_3}$ is bounded as $\lambda \to 0$.
- Normalization: $\mathbf{Y}(\lambda; x) \lambda^{\Theta_{\infty} \sigma_3} \to \mathbb{I} \text{ as } \lambda \to \infty.$

From a solution $\mathbf{Y}(\lambda; x)$ of Riemann–Hilbert Problem 1, we can try to define two matrix functions of $x \in \mathbb{C}$ by

$$\mathbf{Y}_0^0(x) := \lim_{\lambda \to 0} \mathbf{Y}(\lambda; x) \lambda^{-\Theta_0 \sigma_3} \quad \text{and} \quad \mathbf{Y}_1^{\infty}(x) := \lim_{\lambda \to \infty} \lambda(\mathbf{Y}(\lambda; x) \lambda^{\Theta_\infty \sigma_3} - \mathbb{I}) \quad (3.1)$$

and related scalar functions given by

$$u(x) := -2\Theta_0 \frac{Y_{0,11}^0(x)Y_{0,12}^0(x)}{Y_{0,12}^\infty(x)} \quad \text{and} \quad u_{\uparrow}(x) := -2\frac{Y_{0,21}^0(x)Y_{1,12}^\infty(x)}{Y_{0,11}^0(x)}, \tag{3.2}$$

wherever these definitions make sense. The following theorem is proved in Sect. 3.5.

Theorem 5 (Riemann–Hilbert representation of gO rational solutions) $Fix(\Theta_0, \Theta_\infty) \in \Lambda_{gO}$. Let Stokes matrices $V_{j,k}$ be defined by

$$\begin{split} \mathbf{V}_{2,1} &= \begin{pmatrix} 1 & 0 \\ 2i & 1 \end{pmatrix}, \quad \mathbf{V}_{2,3} = \begin{pmatrix} 1 & -\frac{1}{2}i \\ 0 & 1 \end{pmatrix}, \quad \mathbf{V}_{4,3} = e^{2\pi i \Theta_{\infty}} \begin{pmatrix} 1 & 0 \\ 2i & 1 \end{pmatrix}, \quad and \\ \mathbf{V}_{4,1} &= \begin{pmatrix} 1 & -\frac{1}{2}i \\ 0 & 1 \end{pmatrix}, \end{split} \tag{3.3}$$

and let connection matrices V_i be defined by

$$\begin{split} \mathbf{V}_{1} &= \begin{pmatrix} \frac{1}{\sqrt{3}} & -\frac{1}{2} \\ \frac{2}{\sqrt{3}} e^{\frac{i\pi}{6}} & e^{-\frac{i\pi}{6}} \end{pmatrix}, \quad \mathbf{V}_{2} = \begin{pmatrix} e^{\frac{i\pi}{6}} & \frac{1}{2} \\ \frac{2}{\sqrt{3}} e^{\frac{5i\pi}{6}} & \frac{1}{\sqrt{3}} \end{pmatrix}, \quad \mathbf{V}_{3} = \begin{pmatrix} \frac{1}{\sqrt{3}} e^{-\frac{i\pi}{3}} & \frac{1}{2} e^{-\frac{2i\pi}{3}} \\ \frac{2}{\sqrt{3}} e^{-\frac{i\pi}{6}} & e^{\frac{i\pi}{6}} \end{pmatrix}, \quad and \\ \mathbf{V}_{4} &= \begin{pmatrix} e^{-\frac{i\pi}{6}} & \frac{1}{2} e^{-\frac{i\pi}{3}} \\ \frac{2}{\sqrt{3}} e^{-\frac{5i\pi}{6}} & \frac{1}{\sqrt{3}} e^{\frac{i\pi}{3}} \end{pmatrix}, \end{split} \tag{3.4}$$

which satisfy the consistency conditions (3.20). Then Riemann–Hilbert Problem 1 has a unique solution for all but finitely many values of $x \in \mathbb{C}$, and the functions u(x) and $u_{\uparrow}(x)$ defined by (3.2) are the unique (gO) rational solutions of the Painlevé-IV equation (1.1) for parameters $(\Theta_0, \Theta_{\infty})$ and for $(\Theta_0, \uparrow, \Theta_{\infty}, \uparrow) \in \Lambda_{gO}$ defined in (2.4), respectively.

Similarly, the following theorem is proved in Sect. 3.6.

Theorem 6 (Riemann–Hilbert representation of gH rational solutions) $Fix(\Theta_0, \Theta_\infty) \in \Lambda_{gH}^{[3]+}$. Let Stokes matrices $\mathbf{V}_{j,k}$ be defined by

$$\mathbf{V}_{2,1} = \mathbf{V}_{2,3} = \mathbf{V}_{4,1} = \mathbb{I}, \quad \mathbf{V}_{4,3} = e^{2\pi i \Theta_{\infty}} \mathbb{I},$$
 (3.5)



Fig. 13 The oriented contour Σ consists of four rays, the oriented segment $\Sigma_0 = (-1,0)$, and four oriented arcs of the unit circle in the λ -plane

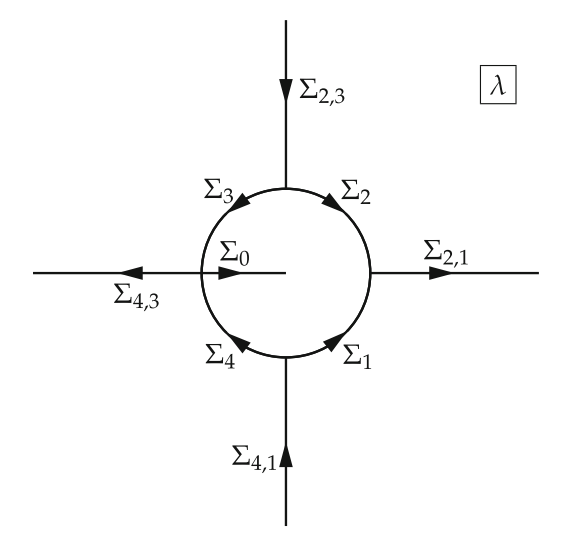
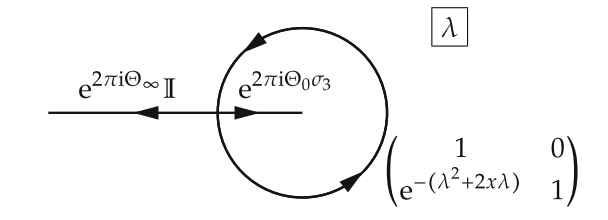


Fig. 14 The oriented contour $\Sigma_{\mathrm{gH}} = S^1 \cup \Sigma_0 \cup \Sigma_{4,3}$ and the jump matrix $\mathbf{Y}_-(\lambda;x)^{-1}\mathbf{Y}_+(\lambda;x)$ for gH rational solutions with $(\Theta_0,\Theta_\infty) \in \Lambda_{\mathrm{gH}}^{[3]+}$



and let connection matrices V_i be defined by

$$\mathbf{V}_1 = \mathbf{V}_3 = \begin{pmatrix} 1 & 0 \\ 1 & 1 \end{pmatrix}$$
 and $\mathbf{V}_2 = \mathbf{V}_4 = \begin{pmatrix} 1 & 0 \\ -1 & 1 \end{pmatrix}$, (3.6)

which satisfy the consistency conditions (3.20). Then Riemann–Hilbert Problem 1 has a unique solution for all but finitely many values of $x \in \mathbb{C}$, and the functions u(x) and $u_{\uparrow}(x)$ defined by (3.2) are the unique (gH) rational solutions of the Painlevé-IV equation (1.1) for parameters $(\Theta_0, \Theta_\infty) \in \Lambda_{gH}^{[3]+}$ and for $(\Theta_0, \uparrow, \Theta_\infty, \uparrow) \in \Lambda_{gH}^{[1]-}$ defined in (2.4), respectively.

Remark 6 Since three of the Stokes matrices in (3.5) are trivial and since the connection matrices in (3.6) are either identical or related by matrix inversion on oppositely oriented arcs of the unit circle $|\lambda|=1$, in the case of gH rationals for $(\Theta_0,\Theta_\infty)\in\Lambda_{gH}^{[3]+}$ we can use a simplified jump contour $\Sigma=\Sigma_{gH}=S^1\cup\Sigma_0\cup\Sigma_{4,3}$ and jump matrix $\mathbf{Y}_-(\lambda;x)^{-1}\mathbf{Y}_+(\lambda;x)$ as shown in Fig. 14.



3.2 General Isomonodromy Theory for the Painlevé-IV Equation

We now develop the isomonodromy theory for the Painlevé-IV equation starting from the Lax pair. For a good overview of this theory, we also refer the reader to [33].

3.2.1 A Lax Pair for Painlevé-IV

If y(x) is a nonzero solution of

$$y'(x) = -(u(x) + 2x)y(x)$$
(3.7)

and z is defined uniquely in terms of u by

$$4z(x) = -u'(x) + u(x)^{2} + 2xu(x) + 4\Theta_{0},$$
(3.8)

then the differential equations (1.1) and (3.7) for u and y are the compatibility conditions for the Garnier–Jimbo–Miwa Lax pair [33, 40]

$$\Psi_{\lambda} = \Lambda \Psi, \quad \Psi_{x} = \mathbf{X} \Psi, \tag{3.9}$$

with coefficient matrices

$$\Lambda := \lambda \sigma_{3} + \Lambda_{0}(x) + \lambda^{-1} \Lambda_{1}(x), \quad \Lambda_{0}(x) := \begin{pmatrix} x & y(x) \\ 2y(x)^{-1}(z(x) - \Theta_{0} - \Theta_{\infty}) & -x \end{pmatrix},
\Lambda_{1}(x) := \begin{pmatrix} \Theta_{0} - z(x) & -\frac{1}{2}u(x)y(x) \\ 2y(x)^{-1}u(x)^{-1}z(x)(z(x) - 2\Theta_{0}) & z(x) - \Theta_{0} \end{pmatrix}$$
(3.10)

and

$$\mathbf{X} := \lambda \sigma_3 + \mathbf{X}_0(x), \quad \mathbf{X}_0(x) := \begin{pmatrix} 0 & y(x) \\ 2y(x)^{-1} (z(x) - \Theta_0 - \Theta_\infty) & 0 \end{pmatrix} = \mathbf{\Lambda}_0(x) - x\sigma_3.$$
(3.11)

Note that $\lambda=0$ is a Fuchsian (regular singular) point for the equation $\Psi_{\lambda}=\Lambda\Psi$, with exponents $\pm\Theta_0$. The only other singularity of $\Psi_{\lambda}=\Lambda\Psi$ is $\lambda=\infty$, an irregular singular point. Formal expansions of solutions about $\lambda=\infty$ include a single-valued exponential factor and a sub-dominant factor proportional to $\lambda^{\pm\Theta_{\infty}}$. Hence the utility of the Jimbo–Miwa parameters $(\Theta_0,\Theta_{\infty})$ over other parameters common in the literature such as $(\alpha,\beta)=(2\Theta_{\infty}-1,-8\Theta_0^2)$ (see [53, Eqn. 32.2.4]) is that they explicitly encode the formal monodromy about $\lambda=0$ and $\lambda=\infty$ in the solution Ψ of the Lax system (3.9).

3.2.2 The Direct Problem for the Lax Pair

Let u(x) and y(x) solve (1.1) and (3.7) for given parameters Θ_0 and Θ_{∞} . Then for generic $x \in \mathbb{C}$, the spectral equation $\Psi_{\lambda} = \Lambda \Psi$ has an irregular singular point at $\lambda = \infty$ and a regular singular point at $\lambda = 0$ with Frobenius exponents $\pm \Theta_0$. The



irregular singular point has four Stokes sectors that we will label as (following the subscript notation of [33]):

$$S_1 := \{\lambda \in \mathbb{C}, \ \lambda \neq 0, \ -\frac{1}{2}\pi \leq \arg(\lambda) \leq 0\}$$

$$S_2 := \{\lambda \in \mathbb{C}, \ \lambda \neq 0, \ 0 \leq \arg(\lambda) \leq \frac{1}{2}\pi\}$$

$$S_3 := \{\lambda \in \mathbb{C}, \ \lambda \neq 0, \ \frac{1}{2}\pi \leq \arg(\lambda) \leq \pi\}$$

$$S_4 := \{\lambda \in \mathbb{C}, \ \lambda \neq 0, \ -\pi \leq \arg(\lambda) \leq -\frac{1}{2}\pi\}.$$

Associated with each Stokes sector S_j , there is a simultaneous fundamental solution matrix $\Psi = \Psi_j^{(\infty)}(\lambda, x)$ of both equations of the Lax pair (3.9) determined by the normalization condition

$$\Psi_j^{(\infty)}(\lambda, x) \lambda^{\Theta_{\infty} \sigma_3} \exp(-(\frac{1}{2}\lambda^2 + x\lambda)\sigma_3) = \mathbb{I} + \mathcal{O}(\lambda^{-1}), \quad \lambda \to \infty, \quad \lambda \in S_j,$$

$$j = 1, 2, 3, 4,$$
(3.12)

where the power functions $\lambda^{\pm\Theta_{\infty}}$ refer to the principal branches. Applying Abel's Theorem to the simultaneous equations (3.9) noting that $\operatorname{tr}(\mathbf{\Lambda}) = \operatorname{tr}(\mathbf{X}) = 0$, it follows that the four solutions satisfy $\det(\Psi_j^{(\infty)}(\lambda,x)) = 1, j = 1,\ldots,4$. For simultaneous solutions of (3.9) near $\lambda = 0$, observe that whenever $(\Theta_0,\Theta_{\infty}) \in$

For simultaneous solutions of (3.9) near $\lambda=0$, observe that whenever $(\Theta_0,\Theta_\infty)\in\Lambda_{gO}$, the Frobenius exponents $\pm\Theta_0$ are unequal mod \mathbb{Z} , making the regular singular point *nonresonant* and guaranteeing the existence of a basis of convergent Puiseux series solutions that can be found by the method of Frobenius. On the other hand, when $(\Theta_0,\Theta_\infty)\in\Lambda_{gH}$, the exponents always differ by integers making the singular point *resonant*. In general, the method of Frobenius fails to produce a basis of solutions near a resonant regular singular point, however we will see that such a basis indeed exists nonetheless when $(\Theta_0,\Theta_\infty)\in\Lambda_{gH}$ and the coefficients in the Lax pair refer to the corresponding rational solution, making the resonant singular point an *apparent singularity*. Whether the singularity is nonresonant, or resonant but apparent, there exists a fundamental simultaneous solution matrix $\Psi=\Psi^{(0)}(\lambda,x)$ defined for λ on a neighborhood of $\lambda=0$ with a branch cut on the negative real line omitted, such that

$$\Psi^{(0)}(\lambda, x)\lambda^{-\Theta_0\sigma_3}$$
 is analytic at $\lambda = 0$ (3.13)

(and hence entire, since there are no other finite singular points) where the power functions $\lambda^{\pm\Theta_0}$ indicate principal branches. In the nonresonant case, $\Psi^{(0)}(\lambda,x)$ is unique up to multiplication on the right by a constant invertible diagonal matrix, while in the resonant but apparent case there is additional freedom that enters via the ambiguity of adding an arbitrary multiple of the subdominant solution to the dominant solution. Since Abel's Theorem implies that $\Psi^{(0)}(\lambda,x)$ has constant determinant, we agree to partly resolve the ambiguity in this solution by insisting that $\det(\Psi^{(0)}(\lambda,x))=1$

The five simultaneous fundamental solutions are necessarily related pairwise on certain overlap domains by right-multiplication by constant matrices. In particular,



the following constant matrices are well defined and have unit determinants:

$$\mathbf{V}_{2,1} := \mathbf{\Psi}_{1}^{(\infty)}(\lambda, x)^{-1} \mathbf{\Psi}_{2}^{(\infty)}(\lambda, x), \quad \arg(\lambda) = 0, \tag{3.14}$$

$$\mathbf{V}_{2,3} := \mathbf{\Psi}_3^{(\infty)}(\lambda, x)^{-1} \mathbf{\Psi}_2^{(\infty)}(\lambda, x), \quad \arg(\lambda) = \frac{1}{2}\pi, \tag{3.15}$$

$$\mathbf{V}_{4,3} := \mathbf{\Psi}_3^{(\infty)}(\lambda, x)^{-1} \mathbf{\Psi}_4^{(\infty)}(\lambda, x), \quad \arg(-\lambda) = 0, \tag{3.16}$$

$$\mathbf{V}_{4,1} := \mathbf{\Psi}_{1}^{(\infty)}(\lambda, x)^{-1} \mathbf{\Psi}_{4}^{(\infty)}(\lambda, x), \quad \arg(\lambda) = -\frac{1}{2}\pi, \tag{3.17}$$

$$\mathbf{V}_{j} := \mathbf{\Psi}_{j}^{(\infty)}(\lambda, x)^{-1} \mathbf{\Psi}^{(0)}(\lambda, x), \quad \lambda \in S_{j}, \quad j = 1, 3, \tag{3.18}$$

and

$$\mathbf{V}_{j} := \mathbf{\Psi}^{(0)}(\lambda, x)^{-1} \mathbf{\Psi}_{j}^{(\infty)}(\lambda, x), \quad \lambda \in S_{j}, \quad j = 2, 4.$$
 (3.19)

The *Stokes matrices* $V_{j,k}$ are necessarily triangular (upper for $V_{2,3}$ and $V_{4,1}$, lower for $V_{2,1}$ and $V_{4,3}$), and their off-diagonal elements are *Stokes multipliers* measuring the Stokes phenomenon associated with the irregular singular point of $\Psi_{\lambda} = \Lambda \Psi$ at $\lambda = \infty$. The remaining four matrices V_j are called *connection matrices*. These matrices are always related by the following identities:

$$\begin{aligned} \mathbf{V}_{2,1} &= \mathbf{V}_1 \mathbf{V}_2, \quad \mathbf{V}_{2,3} &= \mathbf{V}_3 \mathbf{V}_2, \quad \mathbf{V}_{4,1} &= \mathbf{V}_1 \mathbf{V}_4, \\ \mathbf{V}_{4,3} &= \mathbf{V}_3 e^{-2\pi i \Theta_0 \sigma_3} \mathbf{V}_4, \quad \mathbf{V}_{2,3} \mathbf{V}_{2,1}^{-1} \mathbf{V}_{4,1} \mathbf{V}_{4,3}^{-1} &= e^{2\pi i \Theta_\infty \sigma_3}. \end{aligned} \tag{3.20}$$

Modulo these identities, the Stokes and connection matrices constitute the *monodromy* data for the solution u(x) of (1.1). It turns out that the monodromy data is the same for all rational solutions in the gO family, and is the same for each type of rational solution in the gH family.

Assuming existence of all five particular simultaneous solutions for a given value of $x \in \mathbb{C}$, and assuming that the Fuchsian singularity at $\lambda = 0$ is either nonresonant, or resonant but apparent, the matrix function $\mathbf{Y}(\lambda; x)$ defined as follows:

$$\mathbf{Y}(\lambda; x) := \begin{cases} \mathbf{\Psi}_{j}^{(\infty)}(\lambda, x) \exp(-(\frac{1}{2}\lambda^{2} + x\lambda)\sigma_{3}), & \lambda \in S_{j}, \quad |\lambda| > 1, \quad j = 1, 2, 3, 4, \\ \mathbf{\Psi}^{(0)}(\lambda, x) \exp(-(\frac{1}{2}\lambda^{2} + x\lambda)\sigma_{3}), & |\lambda| < 1, \end{cases}$$
(3.21)

solves Riemann–Hilbert Problem 1 relative to the jump contour Σ shown in Fig. 13.

3.2.3 The Inverse Problem for the Lax Pair

We now present several useful facts about Riemann–Hilbert Problem 1.

Proposition 5 *The following statements are true:*

- Given $x \in \mathbb{C}$, every solution of Riemann–Hilbert Problem 1 satisfies $\det(\mathbf{Y}(\lambda; x))$ = 1 for all $\lambda \in \mathbb{C} \setminus \Sigma$.
- There exists at most one solution of Riemann–Hilbert Problem 1 for each $x \in \mathbb{C}$.
- Either
 - Riemann-Hilbert Problem 1 has no solution for any $x \in \mathbb{C}$, or



- Riemann-Hilbert Problem 1 has a solution for $x \in \mathbb{C} \setminus \mathcal{D}$, where $\mathcal{D} \subset \mathbb{C}$ is a discrete set, for each $\lambda \in \mathbb{C} \setminus \Sigma$ the solution is an analytic function of $x \in \mathbb{C} \setminus \mathcal{D}$, and the solution admits an asymptotic expansion to all orders as $\lambda \to \infty$ in the sense that

$$\mathbf{Y}(\lambda; x) \lambda^{\Theta_{\infty} \sigma_3} \sim \mathbb{I} + \sum_{k=1}^{\infty} \mathbf{Y}_k^{\infty}(x) \lambda^{-k}, \quad \lambda \to \infty,$$
 (3.22)

and a convergent expansion in a neighborhood of $\lambda = 0$ of the form

$$\mathbf{Y}(\lambda; x)\lambda^{-\Theta_0\sigma_3} = \sum_{k=0}^{\infty} \mathbf{Y}_k^0(x)\lambda^k$$
 (3.23)

in which all matrix coefficients $\mathbf{Y}_k^{\infty}(x)$ for $k \in \mathbb{Z}_{>0}$ and $\mathbf{Y}_k^0(x)$ for $k \in \mathbb{Z}_{\geq 0}$ are meromorphic functions of x with poles in \mathcal{D} . Both expansions (3.22) and (3.23) are differentiable term-by-term with respect to both λ and x.

Proof The first and second statements are both simple consequences of Liouville's Theorem. In light of the identities (3.20), the third statement is a consequence of the Analytic Fredholm Theorem applied to a system of singular integral equations equivalent to Riemann–Hilbert Problem 1. See [33] for details.

From the uniqueness, one easily obtains the following.

Corollary 4 Suppose that the arcwise-constant matrix $\mathbf{V}(\lambda)$ satisfies $\mathbf{V}(\lambda^*)^* = \mathbf{V}(\lambda)^{-1}$, where \mathbf{V}^* denotes elementwise complex conjugation. If Riemann–Hilbert Problem 1 has a solution $\mathbf{Y}(\lambda; x)$ for some $x \in \mathbb{C}$, then it does also for x^* , and $\mathbf{Y}(\lambda^*; x^*) = \mathbf{Y}(\lambda; x)^*$.

The next result shows that simultaneous differential equations of the form (3.9) can be deduced directly from the conditions of Riemann–Hilbert Problem 1.

Proposition 6 Suppose that Riemann–Hilbert Problem 1 has a solution for $x \in \mathbb{C} \setminus \mathcal{D}$, where \mathcal{D} is a discrete set. Then $\Psi(\lambda, x) := \mathbf{Y}(\lambda; x) \exp((\frac{1}{2}\lambda^2 + x\lambda)\sigma_3)$ satisfies the Lax equations

$$\frac{\partial \Psi}{\partial x}(\lambda, x) = (\lambda \sigma_3 + [\mathbf{Y}_1^{\infty}(x), \sigma_3]) \Psi(\lambda, x)$$
 (3.24)

and

$$\frac{\partial \Psi}{\partial \lambda}(\lambda, x) = \left(\lambda \sigma_3 + x \sigma_3 + [\mathbf{Y}_1^{\infty}(x), \sigma_3] + \lambda^{-1} \mathbf{\Lambda}_1(x)\right) \Psi(\lambda, x) \tag{3.25}$$

for each $(\lambda, x) \in (\mathbb{C} \setminus \Sigma) \times (\mathbb{C} \setminus \mathcal{D})$, where the coefficient matrix $\Lambda_1(x)$ has two equivalent representations:

$$\mathbf{\Lambda}_{1}(x) = x[\mathbf{Y}_{1}^{\infty}(x), \sigma_{3}] + [\mathbf{Y}_{2}^{\infty}(x), \sigma_{3}] - [\mathbf{Y}_{1}^{\infty}(x), \sigma_{3}]\mathbf{Y}_{1}^{\infty}(x) - \Theta_{\infty}\sigma_{3}
= \Theta_{0}\mathbf{Y}_{0}^{0}(x)\sigma_{3}\mathbf{Y}_{0}^{0}(x)^{-1}.$$
(3.26)



Proof The function $\Psi(\lambda, x)$ is analytic in both variables (λ, x) exactly where $\mathbf{Y}(\lambda; x)$ is, and it satisfies jump conditions analogous to those satisfied by $\mathbf{Y}(\lambda; x)$ but with the exponential factors omitted. These jump conditions are independent of both λ and x, so the partial derivatives on the left-hand sides of (3.24) and (3.25) satisfy the same jump conditions as does $\Psi(\lambda, x)$ itself. Taking into account the classical nature of the boundary values on the jump contour Σ and the unit determinant of $\Psi(\lambda, x)$ guaranteed by the first property of Proposition 5, it then follows easily that $\mathbf{X}(\lambda, x) := \partial_x \Psi(\lambda, x) \cdot \Psi(\lambda, x)^{-1}$ and $\mathbf{A}(\lambda, x) := \partial_\lambda \Psi(\lambda, x) \cdot \Psi(\lambda, x)^{-1}$ are both analytic functions of $\lambda \in \mathbb{C} \setminus \{0\}$ for every $x \in \mathcal{D}$. Using (3.22) and its derivatives with respect to x and λ shows that

$$\mathbf{X}(\lambda, x) = \lambda \sigma_3 + [\mathbf{Y}_1^{\infty}(x), \sigma_3] + \mathcal{O}(\lambda^{-1}), \quad \lambda \to \infty$$
 (3.27)

and

$$\mathbf{\Lambda}(\lambda, x) = \lambda \sigma_3 + x \sigma_3 + [\mathbf{Y}_1^{\infty}(x), \sigma_3] + \lambda^{-1} \mathbf{\Lambda}_1(x) + \mathcal{O}(\lambda^{-2}), \quad \lambda \to \infty$$
 (3.28)

where $\Lambda_1(x)$ is given by the first line of (3.26). Likewise, using (3.23) and its derivatives with respect to x and λ shows that

$$\mathbf{X}(\lambda, x) = \mathcal{O}(1), \quad \lambda \to 0$$

and

$$\mathbf{\Lambda}(\lambda, x) = \lambda^{-1} \Theta_0 \mathbf{Y}_0^0(x) \sigma_3 \mathbf{Y}_0^0(x)^{-1} + \mathcal{O}(1), \quad \lambda \to 0.$$
 (3.29)

Note that $\det(\mathbf{Y}_0^0(x)) = 1$ according to the first statement of Proposition 5. Hence, by Liouville's Theorem, $\mathbf{X}(\lambda, x)$ is a linear function of λ given by the two explicit terms on the right-hand side of (3.27), while $\mathbf{\Lambda}(\lambda, x)$ is a Laurent polynomial of degree (1, 1) given by the four explicit terms on the right-hand side of (3.28). Comparing the latter with (3.29) then gives the second equality in (3.26) and completes the proof. \square

Proposition 7 Suppose that Riemann–Hilbert Problem 1 has a solution for $x \in \mathbb{C} \setminus \mathcal{D}$, where \mathcal{D} is a discrete set. Set

$$y(x) := -2Y_{1,12}^{\infty}(x)$$

$$z(x) := \Theta_0 + \Theta_{\infty} - 2Y_{1,12}^{\infty}(x)Y_{1,21}^{\infty}(x) = -2\Theta_0Y_{0,12}^0(x)Y_{0,21}^0(x)$$

$$u(x) := 2Y_{1,22}^{\infty}(x) - 2x - 2\frac{Y_{2,12}^{\infty}(x)}{Y_{1,12}^{\infty}(x)} = -2\Theta_0\frac{Y_{0,11}^0(x)Y_{0,12}^0(x)}{Y_{1,12}^{\infty}(x)}.$$
(3.30)

The definition of u(x) is determinate if and only if $Y_{1,12}^{\infty}(x)$ does not vanish identically. In this case, y(x), z(x), and u(x) are meromorphic on $\mathbb{C} \setminus \mathcal{D}$; more precisely y(x) is analytic and not identically vanishing, z(x) is analytic, and u(x) has a discrete set of poles in $\mathbb{C} \setminus \mathcal{D}$ corresponding to the necessarily isolated zeros of the analytic function $Y_{1,12}^{\infty}(x)$ proportional to y(x). Assuming furthermore that u(x) does not



vanish identically, the Lax equations (3.24) and (3.25) take exactly the form (3.9) subject to (3.10)–(3.11). Furthermore, the differential identities

$$y' = -(2x + u)y$$

$$z' = (\Theta_0 + \Theta_\infty)u + 4\Theta_0 \frac{z}{u} - uz - 2\frac{z^2}{u}$$

$$u' = 4\Theta_0 + 2xu + u^2 - 4z$$
(3.31)

hold for every $x \in \mathbb{C} \setminus \mathcal{D}$ that is not a pole or zero of u(x), and u(x) is a meromorphic solution of the Painlevé-IV equation in the form (1.1).

Proof The definitions (3.30) amount to nothing more than a parametrization of the coefficients in the Lax equations (3.24) and (3.25) from Proposition 6, subject to the condition following from the second line of (3.26) that $\Lambda_1(x)$ has trace zero and determinant $-\Theta_0^2$; the alternate forms of z(x) and u(x) then follow from comparing the two different representations of $\Lambda_{1,11}(x)$ and $\Lambda_{1,12}(x)$ given on the two lines of (3.26). The relation between the basic analyticity properties of these functions and the statement that $Y_{1,12}^{\infty}(x)$ is an analytic function on $\mathbb{C} \setminus \mathcal{D}$ that does not vanish identically then follow from Proposition 5. The three equations (3.31) are exactly those arising from the zero-curvature compatibility condition $\Lambda_x - \mathbf{X}_{\lambda} + [\Lambda, \mathbf{X}] = \mathbf{0}$ upon separating out the coefficients of the different powers of λ that appear, and these make sense provided neither y(x) nor u(x) vanishes identically. Finally, elimination of z in favor of u by using the third equation of (3.31) in the second yields the Painlevé-IV equation (1.1) on u(x).

Remark 7 The formulæ for u(x) given in (3.30) are particularly useful to us because they do not require differentiation; however a more compact formula obtained by combining the definition of y(x) in (3.30) with the first differential equation in (3.31) is simply (see [33, Eqn. 5.1.13])

$$u(x) = -2x - \frac{d}{dx} \log(Y_{1,12}^{\infty}(x)).$$

Note also that up to a constant factor, the alternate representation of u(x) given in (3.30) (see also (3.2)) is the reciprocal of the formula for extracting the solution of the Painlevé-III equation from its Riemann–Hilbert problem (see [13, Eqn. 18], which corrects a corresponding formula in [33, Theorem 5.4]).

An apparently new result that is extremely useful to us is that Riemann–Hilbert Problem 1 contains also the solution of *another* Painlevé-IV equation:

Proposition 8 Suppose that $\Theta_0 \neq 0$, that Riemann–Hilbert Problem 1 has a solution for $x \in \mathbb{C} \setminus \mathcal{D}$, where \mathcal{D} is a discrete set, and that the function u(x) given by (3.30) is well defined as a meromorphic function on $\mathbb{C} \setminus \mathcal{D}$. Let $u_{\mathbb{C}}(x)$ be defined in terms of $\mathbf{Y}(\lambda; x)$ by (3.2). Then $u_{\mathbb{C}}(x)$ is a meromorphic solution of the Painlevé-IV equation (1.1) with modified parameters $(\Theta_0, \mathbb{C}, \Theta_\infty, \mathbb{C})$ given in (2.4), and $u_{\mathbb{C}}(x)$ is explicitly related to u(x) by the Bäcklund transformation indicated also in (2.4). Thus the same



Riemann–Hilbert problem encodes explicitly a solution $(\Theta_0, \Theta_\infty, u(x))$ and its image under the symmetry $S_{\mathbb{N}}$.

Proof Without the hypothesis that $\Theta_0 \neq 0$, by Proposition 7, the function u(x) given by the alternate expression in (3.30) is a meromorphic solution of the Painlevé-IV equation (1.1). However, since $\Theta_0 \neq 0$, it follows easily that (1.1) does not admit the identically vanishing solution, so it follows in particular that $Y_{0,11}^0(x)$ does not vanish identically. Therefore, $u_{\uparrow}(x)$ is indeed a meromorphic function, and comparing with the alternate definitions of z(x) and u(x) in (3.30) one sees that $u_{\uparrow}(x) = -2z(x)/u(x)$. Eliminating z(x) using the last equation in the system (3.31) yields the Bäcklund transformation formula given in (2.4). It is then straightforward to deduce the Painlevé-IV equation satisfied by $u_{\uparrow}(x)$ from that satisfied by u(x).

Corollary 5 *Under the same additional conditions as in Corollary 4, it follows that* $y(x^*) = y(x)^*$, $z(x^*) = z(x)^*$, $u(x^*) = u(x)^*$, and $u_{\uparrow}(x^*) = u_{\uparrow}(x)^*$.

Remark 8 The Painlevé-IV equation involves the parameter Θ_0 only in the form of its square Θ_0^2 , but the Lax pair and Riemann–Hilbert problem break the symmetry of $\Theta_0 \mapsto -\Theta_0$. However, symmetry in the Lax pair is easily restored with the use of the quantity $\widehat{z}(x) := z(x) - \Theta_0$ in place of z(x). Then the matrices \mathbf{X} and $\mathbf{\Lambda}$ are written in terms of $u, y, \widehat{z}, \Theta_\infty$, and Θ_0^2 , but Θ_0 alone does not appear. From (3.30) one sees that the value of Θ_0 is not required to express $\widehat{z}(x)$ in terms of the solution of the Riemann–Hilbert problem, and making the substitution $z(x) = \Theta_0 + \widehat{z}(x)$ shows that the first order system on y, \widehat{z} , and u implied by (3.31) only involves Θ_0 via its square. Finally, the substitution $\mathbf{Y}(\lambda; x) \mapsto \mathbf{Y}(\lambda; x) \exp((\frac{1}{2}\lambda^2 + x\lambda)\sigma_3) \mathrm{i}\sigma_1 \exp(-(\frac{1}{2}\lambda^2 + x\lambda)\sigma_3)$ for $|\lambda| < 1$ gives an equivalent Riemann–Hilbert problem in which Θ_0 is replaced by $-\Theta_0$, while $Y_{0,11}^0(x)Y_{0,12}^0(x) \mapsto -Y_{0,12}^0(x)Y_{0,11}^0(x)$ leaving the alternate expression for u(x) in (3.30) (see also (3.2)) invariant as well. However, the expression for u(x) in (3.2) is *not* invariant, and indeed the target parameters $\Theta_{0, \uparrow}^2$ and $\Theta_{\infty, \uparrow}$ for which $u_{\uparrow}(x)$ solves (1.1) depend on Θ_0 and not its square.

Note that making the substitution $\Psi(\lambda, x) = \mathbf{Y}(\lambda; x) \exp((\frac{1}{2}\lambda^2 + x\lambda)\sigma_3)$ with either the expansion (3.22) or (3.23) into the Lax equation $\Psi_{\lambda} = \mathbf{\Lambda}\Psi$ with coefficient matrix given by (3.10), and separating out the powers of λ yields from each expansion an infinite hierarchy of algebraic identities such as (from (3.23)):

$$\mathbf{Y}_{1}^{0}(x) + \Theta_{0}\mathbf{Y}_{1}^{0}(x)\sigma_{3} - \mathbf{\Lambda}_{1}(x)\mathbf{Y}_{1}^{0}(x) + x\mathbf{Y}_{0}^{0}(x)\sigma_{3} - \mathbf{\Lambda}_{0}(x)\mathbf{Y}_{0}^{0}(x) = \mathbf{0}.$$
 (3.32)

3.3 Isomonodromic Schlesinger Transformations

The parameter lattices $\Lambda_{gH}^{[3]+}$ and Λ_{gO} are both generated from a given point by linear combinations over integers of diagonal lattice vectors $(\frac{1}{2},\pm\frac{1}{2})$. If we think of fixing the monodromy data V in Riemann–Hilbert Problem 1 from Sect. 3.1 (up to a sign for $V_{4,3}$) and letting the parameters (Θ_0,Θ_∞) vary, then it is possible to explicitly relate the solutions for two instances of this problem when the parameters differ by $(\frac{1}{2},\pm\frac{1}{2})$, via a certain left-multiplier (i.e., gauge transformation of the Lax pair) called



a *Schlesinger transformation*. Since the monodromy data are unchanged, these transformations are *isomonodromic*. When we use formulæ such as (3.2) to extract u(x) and $u_{\uparrow}(x)$ from these related problems, we obtain explicit relations between these functions for related parameter values, which are *isomonodromic Bäcklund transformations*. For more on Schlesinger and Bäcklund transformations for the Painlevé-IV equation see, for example, [5, 35].

3.3.1 Basic Schlesinger Transformations

Suppose $\mathbf{Y}(\lambda; x)$ is the solution of Riemann–Hilbert Problem 1 for parameters $(\Theta_0, \Theta_\infty)$. There are four basic transformations \mathcal{T} of $\mathbf{Y}(\lambda; x)$ we will develop, all of which are based on the same kind of gauge transformation formula:

$$T\mathbf{Y}(\lambda; x) := \mathbf{G}(\lambda; x)\mathbf{Y}(\lambda; x), \quad \mathbf{G}(\lambda; x) = \mathbf{G}^{+}(x)\lambda^{1/2} + \mathbf{G}^{-}(x)\lambda^{-1/2}, \quad (3.33)$$

where the power functions refer to the principal branches, cut along $\lambda < 0$, and the matrix coefficients $\mathbf{G}^{\pm}(x)$ are to be determined so that $T\mathbf{Y}(\lambda;x)$ solves a Riemann–Hilbert problem closely related to Riemann–Hilbert Problem 1. Indeed, from (3.33) it is straightforward to check that domains of analyticity of $\mathbf{Y}(\lambda;x)$ and $T\mathbf{Y}(\lambda;x)$ agree, and that the jump conditions are preserved except on Σ_0 and $\Sigma_{4,3}$ where signs change across the branch cut of $\lambda^{\pm 1/2}$ in (3.33). So $\mathbf{G}^{\pm}(x)$ are to be chosen so that the conditions specifying the behavior of the solution at $\lambda = \infty$ and $\lambda = 0$ hold in some form.

To replace $(\Theta_0, \Theta_\infty)$ by $(\Theta_0 + \frac{1}{2}, \Theta_\infty + \frac{1}{2})$, we require that $\mathbf{Y}_{\nearrow}(\lambda; x) = \mathcal{T}\mathbf{Y}(\lambda; x)$ satisfy the conditions

$$\mathbf{Y}_{\nearrow}(\lambda; x)\lambda^{(\Theta_{\infty} + \frac{1}{2})\sigma_{3}} = \mathbb{I} + \mathbf{Y}_{\nearrow, 1}^{\infty}(x)\lambda^{-1} + \mathcal{O}(\lambda^{-2}), \quad \lambda \to \infty$$

$$\mathbf{Y}_{\nearrow}(\lambda; x)\lambda^{-(\Theta_{0} + \frac{1}{2})\sigma_{3}} = \mathbf{Y}_{\nearrow, 0}^{0}(x) + \mathcal{O}(\lambda), \quad \lambda \to 0$$
(3.34)

for some matrices $\mathbf{Y}_{\nearrow,1}^{\infty}(x)$ and $\mathbf{Y}_{\nearrow,0}^{0}(x)$. Using the expansions (3.22) and (3.23) it is straightforward to see that, assuming the matrix element $Y_{0,21}^{0}(x)$ in (3.23) is a meromorphic function that does not vanish identically, these relations will hold if and only if

$$\mathbf{G}^{+}(x) = \mathbf{G}_{\nearrow}^{+} := \begin{pmatrix} 0 & 0 \\ 0 & 1 \end{pmatrix} \text{ and}$$

$$\mathbf{G}^{-}(x) = \mathbf{G}_{\nearrow}^{-}(x) := \begin{pmatrix} 1 & -Y_{0,21}^{0}(x)^{-1}Y_{0,11}^{0}(x) \\ -Y_{1,21}^{\infty}(x) & Y_{1,21}^{\infty}(x)Y_{0,21}^{0}(x)^{-1}Y_{0,11}^{0}(x) \end{pmatrix}, \quad (3.35)$$

defining $\mathcal{T} = \mathcal{T}_{\nearrow}$ as a gauge transformation that exists except at the isolated zeros of $Y^0_{0,21}(x)$. Note that, using (3.30), we may write $\mathbf{G}_{\nearrow}(x)$ in the form

$$\mathbf{G}_{\nearrow}^{-}(x) = \begin{pmatrix} 1 & \frac{1}{2}u(x)y(x)z(x)^{-1} \\ (\Theta_0 + \Theta_{\infty} - z(x))y(x)^{-1} & \frac{1}{2}(\Theta_0 + \Theta_{\infty} - z(x))u(x)z(x)^{-1} \end{pmatrix}. (3.36)$$



It is straightforward to check that subject to (3.35), $det(\mathbf{G}(\lambda; x)) = 1$, so this transformation preserves determinants. The gauge matrix $\mathbf{G}(\lambda; x)$ in this case is denoted \mathbf{R}_3 in [35]. See also [5, Sect. 2.1].

To replace $(\Theta_0, \Theta_\infty)$ by $(\Theta_0 - \frac{1}{2}, \Theta_\infty - \frac{1}{2})$, we require that $\mathbf{Y}_{\swarrow}(\lambda; x) = \mathcal{T}\mathbf{Y}(\lambda; x)$ satisfy

$$\mathbf{Y}_{\swarrow}(\lambda; x)\lambda^{(\Theta_{\infty} - \frac{1}{2})\sigma_{3}} = \mathbb{I} + \mathbf{Y}_{\swarrow, 1}^{\infty}(x)\lambda^{-1} + \mathcal{O}(\lambda^{-2}), \quad \lambda \to \infty$$

$$\mathbf{Y}_{\swarrow}(\lambda; x)\lambda^{-(\Theta_{0} - \frac{1}{2})\sigma_{3}} = \mathbf{Y}_{\swarrow, 0}^{0}(x) + \mathcal{O}(\lambda), \quad \lambda \to 0$$
(3.37)

for some matrices $\mathbf{Y}^{\infty}_{\checkmark,1}(x)$ and $\mathbf{Y}^{0}_{\checkmark,0}(x)$. Again using the expansions (3.22) and (3.23), assuming now that $Y^{0}_{0,12}(x)$ does not vanish identically, the above conditions will hold if and only if

$$\mathbf{G}^{+}(x) = \mathbf{G}_{\swarrow}^{+} := \begin{pmatrix} 1 & 0 \\ 0 & 0 \end{pmatrix} \text{ and}$$

$$\mathbf{G}^{-}(x) = \mathbf{G}_{\swarrow}^{-}(x) := \begin{pmatrix} Y_{1,12}^{\infty}(x)Y_{0,12}^{0}(x)^{-1}Y_{0,22}^{0}(x) & -Y_{1,12}^{\infty}(x) \\ -Y_{0,12}^{0}(x)^{-1}Y_{0,22}^{0}(x) & 1 \end{pmatrix}, (3.38)$$

defining $\mathcal{T}=\mathcal{T}_{\swarrow}$ as a gauge transformation that exists except at the isolated zeros of $Y^0_{0.12}(x)$ and preserves determinants. Using (3.30) we can also write

$$\mathbf{G}_{\swarrow}^{-}(x) = \begin{pmatrix} (z(x) - 2\Theta_0)u(x)^{-1} & \frac{1}{2}y(x) \\ 2(z(x) - 2\Theta_0)u(x)^{-1}y(x)^{-1} & 1 \end{pmatrix}. \tag{3.39}$$

The gauge matrix $G(\lambda; x)$ in this case is denoted R_4 in [35].

To replace $(\Theta_0, \Theta_\infty)$ with $(\Theta_0 + \frac{1}{2}, \Theta_\infty - \frac{1}{2})$ we insist that $\mathbf{Y}_{\searrow}(\lambda; x) = \mathcal{T}\mathbf{Y}(\lambda; x)$ satisfy the conditions

$$\mathbf{Y}_{\searrow}(\lambda; x) \lambda^{(\Theta_{\infty} - \frac{1}{2})\sigma_{3}} = \mathbb{I} + \mathbf{Y}_{\searrow, 1}^{\infty}(x) \lambda^{-1} + \mathcal{O}(\lambda^{-2}), \quad \lambda \to \infty$$

$$\mathbf{Y}_{\searrow}(\lambda; x) \lambda^{-(\Theta_{0} + \frac{1}{2})\sigma_{3}} = \mathbf{Y}_{\searrow, 0}^{0}(x) + \mathcal{O}(\lambda), \quad \lambda \to 0$$
(3.40)

for some matrices $\mathbf{Y}^{\infty}_{\searrow,1}(x)$ and $\mathbf{Y}^{0}_{\searrow,0}(x)$. Assuming that $Y^{0}_{0,11}(x)$ does not vanish identically, these conditions hold if and only if

$$\mathbf{G}^{+}(x) = \mathbf{G}_{\searrow}^{+} := \begin{pmatrix} 1 & 0 \\ 0 & 0 \end{pmatrix} \text{ and }$$

$$\mathbf{G}^{-}(x) = \mathbf{G}_{\searrow}^{-} := \begin{pmatrix} Y_{1,12}^{\infty}(x)Y_{0,11}^{0}(x)^{-1}Y_{0,21}^{0}(x) & -Y_{1,12}^{\infty}(x) \\ -Y_{0,11}^{0}(x)^{-1}Y_{0,21}^{0}(x) & 1 \end{pmatrix}, \tag{3.41}$$



defining $\mathcal{T} = \mathcal{T}_{\searrow}$ as a gauge transformation existing except at the isolated zeros of $Y_{0.11}^0(x)$ and preserving determinants. From (3.30) we also have

$$\mathbf{G}_{\searrow}^{-}(x) = \begin{pmatrix} z(x)u(x)^{-1} & \frac{1}{2}y(x) \\ 2z(x)u(x)^{-1}y(x)^{-1} & 1 \end{pmatrix}.$$
(3.42)

The gauge matrix $G(\lambda; x)$ for this case is denoted R_2 in [35].

Finally, to replace $(\Theta_0, \Theta_\infty)$ with $(\Theta_0 - \frac{1}{2}, \Theta_\infty + \frac{1}{2})$ we insist that $\mathbf{Y}_{\kappa}(\lambda; x) = \mathcal{T}\mathbf{Y}(\lambda; x)$ satisfy the conditions

$$\mathbf{Y}_{\nwarrow}(\lambda; x)\lambda^{(\Theta_{\infty} + \frac{1}{2})\sigma_{3}} = \mathbb{I} + \mathbf{Y}_{\nwarrow, 1}^{\infty}(x)\lambda^{-1} + \mathcal{O}(\lambda^{-2}), \quad \lambda \to \infty$$

$$\mathbf{Y}_{\nwarrow}(\lambda; x)\lambda^{-(\Theta_{0} - \frac{1}{2})\sigma_{3}} = \mathbf{Y}_{\nwarrow, 0}^{0}(x) + \mathcal{O}(\lambda), \quad \lambda \to 0$$
(3.43)

for some matrices $\mathbf{Y}_{\nwarrow,1}^{\infty}(x)$ and $\mathbf{Y}_{\nwarrow,0}^{0}(x)$. Assuming that $Y_{0,22}^{0}(x)$ does not vanish identically, these conditions hold if and only if

$$\mathbf{G}^{+}(x) = \mathbf{G}_{\setminus}^{+} = \begin{pmatrix} 0 & 0 \\ 0 & 1 \end{pmatrix} \text{ and}$$

$$\mathbf{G}^{-}(x) = \mathbf{G}_{\setminus}^{-}(x) = \begin{pmatrix} 1 & -Y_{0,22}^{0}(x)^{-1}Y_{0,12}^{0}(x) \\ -Y_{1,21}^{\infty}(x) & Y_{1,21}^{\infty}(x)Y_{0,22}^{0}(x)^{-1}Y_{0,12}^{0}(x) \end{pmatrix}, (3.44)$$

defining $\mathcal{T} = \mathcal{T}_{\setminus}$ as a gauge transformation existing except at the isolated zeros of $Y^0_{0.22}(x)$ and preserving determinants. From (3.30) we can write

$$\mathbf{G}_{\mathbb{N}}^{-}(x) = \begin{pmatrix} 1 & \frac{1}{2}u(x)y(x)(z(x) - 2\Theta_{0})^{-1} \\ (\Theta_{0} + \Theta_{\infty} - z(x))y(x)^{-1} & \frac{1}{2}u(x)(\Theta_{0} + \Theta_{\infty} - z(x))(z(x) - 2\Theta_{0})^{-1} \end{pmatrix}.$$
(3.45)

The gauge matrix $G(\lambda; x)$ for this case is denoted R_1 in [35].

We have therefore established the following:

Proposition 9 Suppose that $\mathbf{Y}(\lambda; x)$ is the solution of Riemann–Hilbert Problem 1.

- If $Y_{0,21}^0(x)$ does not vanish identically, then $\mathbf{Y}_{\nearrow}(\lambda;x)$ defined by (3.33) with (3.35) solves an analogous Riemann–Hilbert problem in which parameters (Θ_0,Θ_∞) are replaced with $(\Theta_0+\frac{1}{2},\Theta_\infty+\frac{1}{2})$ and the sign of the matrix $\mathbf{V}_{4,3}$ is changed.
- If $Y_{0,12}^0(x)$ does not vanish identically, then $\mathbf{Y}_{\swarrow}(\lambda;x)$ defined by (3.33) with (3.38) solves an analogous Riemann–Hilbert problem in which parameters (Θ_0,Θ_∞) are replaced by $(\Theta_0-\frac{1}{2},\Theta_\infty-\frac{1}{2})$ and the sign of the matrix $\mathbf{V}_{4,3}$ is changed.
- If $Y_{0,11}^0(x)$ does not vanish identically, then $\mathbf{Y}_{\searrow}(\lambda;x)$ defined by (3.33) with (3.41) solves an analogous Riemann–Hilbert problem in which parameters (Θ_0,Θ_∞) are replaced by $(\Theta_0+\frac{1}{2},\Theta_\infty-\frac{1}{2})$ and the sign of the matrix $\mathbf{V}_{4,3}$ is changed.
- If $Y_{0,22}^0(x)$ does not vanish identically, then $\mathbf{Y}_{\nwarrow}(\lambda;x)$ defined by (3.33) with (3.44) solves an analogous Riemann–Hilbert problem in which parameters (Θ_0,Θ_∞) are replaced by $(\Theta_0 \frac{1}{2},\Theta_\infty + \frac{1}{2})$ and the sign of the matrix $\mathbf{V}_{4,3}$ is changed.



We can easily give conditions on the parameters $(\Theta_0, \Theta_\infty)$ sufficient to guarantee existence of the transformation in each case:

Proposition 10 Suppose that Riemann–Hilbert Problem 1 has a solution for $x \in \mathbb{C} \setminus \mathcal{D}$, where \mathcal{D} is a discrete set.

- The Schlesinger transformations $\mathbf{Y}(\lambda; x) \mapsto \mathbf{Y}_{\nearrow}(\lambda; x)$ and $\mathbf{Y}(\lambda; x) \mapsto \mathbf{Y}_{\swarrow}(\lambda; x)$ are well defined provided that $\Theta_0(\Theta_{\infty} + \Theta_0) \neq 0$.
- The Schlesinger transformations $\mathbf{Y}(\lambda; x) \mapsto \mathbf{Y}_{\searrow}(\lambda; x)$ and $\mathbf{Y}(\lambda; x) \mapsto \mathbf{Y}_{\nwarrow}(\lambda; x)$ are well defined provided that $\Theta_0(\Theta_{\infty} \Theta_0) \neq 0$.

Remark 9 The conditions on $(\Theta_0, \Theta_\infty)$ in Proposition 10 imply the corresponding conditions on the elements of $\mathbf{Y}_0^0(x)$ in Proposition 9 but not necessarily vice-versa. We will encounter a situation in which $\Theta_\infty = \Theta_0$ but the Schlesinger transformation $\mathbf{Y}(\lambda;x) \mapsto \mathbf{Y}_{\searrow}(\lambda;x)$ exists nonetheless, because $Y_{0,11}^0(x)$ does not vanish identically. The utility of Proposition 10 lies in the simplicity of its conditions, which do not depend on the choice of solution of Painlevé-IV for the given parameters $(\Theta_0, \Theta_\infty)$.

Proof Suppose first that the transformation $\mathbf{Y}(\lambda; x) \mapsto \mathbf{Y}_{\swarrow}(\lambda; x)$ is undefined. Therefore, by Proposition 9 $Y_{0,12}^0(x) \equiv 0$ on some open subset of $(\lambda, x) \in (\mathbb{C} \setminus \Sigma) \times (\mathbb{C} \setminus \mathcal{D})$. Since $\det(\mathbf{Y}_0^0(x)) \equiv 1$ by the first statement of Proposition 5 in Sect. 3.2, it then follows that also $Y_{0,11}^0(x)Y_{0,22}^0(x) \equiv 1$ so the matrix $\mathbf{\Lambda}_1(x)$ as given by the second line of (3.26) can be written in the form

$$\mathbf{\Lambda}_1(x) = \begin{pmatrix} \Theta_0 & 0 \\ V(x) & -\Theta_0 \end{pmatrix}$$

for some analytic function V(x). Therefore, the Lax equation (3.24) takes the form

$$\frac{\partial \Psi}{\partial x}(\lambda, x) = \begin{pmatrix} \lambda & U(x) \\ W(x) & -\lambda \end{pmatrix} \Psi(\lambda, x) \tag{3.46}$$

for some analytic functions U(x) and W(x), while the Lax equation (3.25) becomes

$$\frac{\partial \Psi}{\partial \lambda}(\lambda, x) = \begin{pmatrix} \lambda + x + \lambda^{-1}\Theta_0 & U(x) \\ W(x) + \lambda^{-1}V(x) - \lambda - x - \lambda^{-1}\Theta_0 \end{pmatrix} \Psi(\lambda, x). \tag{3.47}$$

Compatibility of the equations (3.46) and (3.47) implies that either $\Theta_0 = 0$ or $U(x) \equiv 0$. If $\Theta_0 \neq 0$, the alternative $U(x) \equiv 0$ implies, via (3.46) and (3.47) that

$$\Psi_{11}(\lambda, x) = c \exp(\frac{1}{2}\lambda^2 + x\lambda)\lambda^{\Theta_0},$$

where c is a constant that can take different values in each of the five components of $\mathbb{C}\setminus\Sigma$. Consider letting $\lambda\to\infty$ in any one of the four unbounded components of $\mathbb{C}\setminus\Sigma$. Then from the normalization condition in Riemann–Hilbert Problem 1 and the relation $\Psi(\lambda,x)=Y(\lambda;x)\exp((\frac{1}{2}\lambda^2+x\lambda)\sigma_3)$ we arrive at a contradiction unless $\Theta_0+\Theta_\infty=0$.



Now suppose instead that the Schlesinger transformation $\mathbf{Y}(\lambda;x) \mapsto \mathbf{Y}_{\nearrow}(\lambda;x)$ is undefined, which by Proposition 9 means that $Y_{0,21}^0(x) \equiv 0$. Following similar reasoning as above, we then arrive at (3.46) and (3.47) in which the coefficient matrices are replaced by their transposes; compatibility implies again either $\Theta_0 = 0$ or $U(x) \equiv 0$, which in turn implies that $\Psi_{22}(\lambda,x) = c \exp(-(\frac{1}{2}\lambda^2 + x\lambda))\lambda^{-\Theta_0}$ for a different constant c in each component of $\mathbb{C} \setminus \Sigma$. Once again, consistency with the normalization condition in Riemann–Hilbert Problem 1 leads to a contradiction unless $\Theta_0 + \Theta_{\infty} = 0$.

To obtain the corresponding results for the Schlesinger transformations $\mathbf{Y}(\lambda; x) \mapsto \mathbf{Y}_{\setminus}(\lambda; x)$ and $\mathbf{Y}(\lambda; x) \mapsto \mathbf{Y}_{\setminus}(\lambda; x)$, we can apply similar reasoning as in Remark 8 in Sect. 3.2 to first replace Θ_0 with $-\Theta_0$ at the cost of essentially swapping the columns of the matrix $\mathbf{Y}_0^0(x)$. It then follows from the above arguments that these transformations will be defined unless either $\Theta_0 = 0$ or $\Theta_{\infty} - \Theta_0 = 0$.

3.3.2 Corresponding Bäcklund Transformations

Now we suppose that $\mathbf{Y}(\lambda; x)$ solves Riemann–Hilbert Problem 1 and that u(x) given in terms of the solution by (3.30) is well defined. According to Proposition 7 in Sect. 3.2, u(x) is a meromorphic solution of the Painlevé-IV equation in the form (1.1) for parameters $(\Theta_0, \Theta_\infty)$. We now deduce from the Schlesinger transformations summarized in Proposition 9 the corresponding solutions $u_{\nearrow}(x), u_{\swarrow}(x), u_{\searrow}(x)$, and $u_{\nwarrow}(x)$ of (1.1) for the modified parameters indicated in Proposition 9.

If $Y_{0,21}^0(x)$ is not identically zero, then $\mathbf{Y}_{\nearrow}(\lambda; x)$ exists, and it generates a solution of (1.1) for parameters $(\Theta_0 + \frac{1}{2}, \Theta_{\infty} + \frac{1}{2})$ given by (cf. (3.30))

$$u_{\mathcal{I}}(x) := -2(\Theta_0 + \frac{1}{2}) \frac{Y^0_{\mathcal{I},0,11}(x) Y^0_{\mathcal{I},0,12}(x)}{Y^\infty_{\mathcal{I},1,12}(x)}$$

provided the latter expression is determinate. The formulæ for the matrices $\mathbf{Y}^{\infty}_{7,1}(x)$ and $\mathbf{Y}^{0}_{7,0}(x)$ appearing in (3.34) are

$$\begin{split} \mathbf{Y}^{\infty}_{\mathcal{I},1}(x) &= \mathbf{G}^{+}_{\mathcal{I}} \mathbf{Y}^{\infty}_{2}(x) \begin{pmatrix} 1 & 0 \\ 0 & 0 \end{pmatrix} + \mathbf{G}^{+}_{\mathcal{I}} \mathbf{Y}^{\infty}_{1}(x) \begin{pmatrix} 0 & 0 \\ 0 & 1 \end{pmatrix} + \mathbf{G}^{-}_{\mathcal{I}}(x) \mathbf{Y}^{\infty}_{1}(x) \begin{pmatrix} 1 & 0 \\ 0 & 0 \end{pmatrix} \\ &+ \mathbf{G}^{-}_{\mathcal{I}}(x) \begin{pmatrix} 0 & 0 \\ 0 & 1 \end{pmatrix}, \\ \mathbf{Y}^{0}_{\mathcal{I},0}(x) &= \mathbf{G}^{+}_{\mathcal{I}} \mathbf{Y}^{0}_{0}(x) \begin{pmatrix} 1 & 0 \\ 0 & 0 \end{pmatrix} + \mathbf{G}^{-}_{\mathcal{I}}(x) \mathbf{Y}^{0}_{1}(x) \begin{pmatrix} 1 & 0 \\ 0 & 0 \end{pmatrix} + \mathbf{G}^{-}_{\mathcal{I}}(x) \mathbf{Y}^{0}_{0}(x) \begin{pmatrix} 0 & 0 \\ 0 & 1 \end{pmatrix}. \end{split}$$

Using (3.35)–(3.36) in these, along with the identity (3.32) to eliminate elements of the matrix $\mathbf{Y}_1^0(x)$ and the definitions (3.30) as well as the first-order system (3.31), we may express $u_{\mathcal{T}}(x)$ explicitly in terms of u(x) and u'(x) as:

$$u_{\nearrow}(x) = \frac{16\Theta_0^2 + 8(\Theta_0 + \Theta_\infty)u(x)^2 - 4x^2u(x)^2 - 4xu(x)^3 - u(x)^4 - 8\Theta_0u'(x) + u'(x)^2}{2u(x)(4\Theta_0 + 2xu(x) + u(x)^2 - u'(x))}. \tag{3.48}$$



If $Y_{0,12}^0(x)$ does not vanish identically, we can apply similar reasoning to extract a solution $u_{\swarrow}(x)$ of Painlevé-IV (1.1) for parameters $(\Theta_0 - \frac{1}{2}, \Theta_{\infty} - \frac{1}{2})$ from u(x). The starting point is

$$u_{\swarrow}(x) := -2(\Theta_0 - \frac{1}{2}) \frac{Y_{\swarrow,0,11}^0(x) Y_{\swarrow,0,12}^0(x)}{Y_{\swarrow,1,12}^\infty(x)},$$

assuming this expression is determinate, where the matrices $\mathbf{Y}_{\checkmark,1}^{\infty}(x)$ and $\mathbf{Y}_{\checkmark,0}^{0}(x)$ in (3.37) are given by

$$\begin{aligned} \mathbf{Y}_{\checkmark,1}^{\infty}(x) &= \mathbf{G}_{\checkmark}^{+} \mathbf{Y}_{2}^{\infty}(x) \begin{pmatrix} 0 & 0 \\ 0 & 1 \end{pmatrix} + \mathbf{G}_{\checkmark}^{+} \mathbf{Y}_{1}^{\infty}(x) \begin{pmatrix} 1 & 0 \\ 0 & 0 \end{pmatrix} + \mathbf{G}_{\checkmark}^{-}(x) \mathbf{Y}_{1}^{\infty}(x) \begin{pmatrix} 0 & 0 \\ 0 & 1 \end{pmatrix} \\ &+ \mathbf{G}_{\checkmark}^{-}(x) \begin{pmatrix} 1 & 0 \\ 0 & 0 \end{pmatrix}, \\ \mathbf{Y}_{\checkmark,0}^{0}(x) &= \mathbf{G}_{\checkmark}^{+} \mathbf{Y}_{0}^{0}(x) \begin{pmatrix} 0 & 0 \\ 0 & 1 \end{pmatrix} + \mathbf{G}_{\checkmark}^{-}(x) \mathbf{Y}_{1}^{0}(x) \begin{pmatrix} 0 & 0 \\ 0 & 1 \end{pmatrix} + \mathbf{G}_{\checkmark}^{-}(x) \mathbf{Y}_{0}^{0}(x) \begin{pmatrix} 1 & 0 \\ 0 & 0 \end{pmatrix}. \end{aligned}$$

Using (3.38)–(3.39) in these, together with (3.30), (3.31), and (3.32), we find

$$u_{\swarrow}(x) = \frac{16\Theta_0^2 + 8(\Theta_0 + \Theta_\infty - 1)u(x)^2 - 4x^2u(x)^2 - 4xu(x)^3 - u(x)^4 + 8\Theta_0u'(x) + u'(x)^2}{2u(x)(4\Theta_0 + 2xu(x) + u(x)^2 + u'(x))}.$$

$$(3.49)$$

If $Y_{0,11}^0(x)$ does not vanish identically, then we can extract from $\mathbf{Y}_{\searrow}(\lambda; x)$ a solution $u_{\searrow}(x)$ of (1.1) for parameters $(\Theta_0 + \frac{1}{2}, \Theta_{\infty} - \frac{1}{2})$ by starting from the expression

$$u_{\searrow}(x) := -2(\Theta_0 + \frac{1}{2}) \frac{Y_{\searrow,0,11}^0(x) Y_{\searrow,0,12}^0(x)}{Y_{\searrow,1,12}^\infty(x)}$$

provided it is determinate. The matrices $\mathbf{Y}_{\searrow,1}^{\infty}(x)$ and $\mathbf{Y}_{\searrow,0}^{0}(x)$ from (3.40) are given by

$$\begin{split} \mathbf{Y}_{\searrow,1}^{\infty}(x) &= \mathbf{G}_{\searrow}^{+} \mathbf{Y}_{2}^{\infty}(x) \begin{pmatrix} 0 & 0 \\ 0 & 1 \end{pmatrix} + \mathbf{G}_{\searrow}^{+} \mathbf{Y}_{1}^{\infty}(x) \begin{pmatrix} 1 & 0 \\ 0 & 0 \end{pmatrix} + \mathbf{G}_{\searrow}^{-}(x) \mathbf{Y}_{1}^{\infty}(x) \begin{pmatrix} 0 & 0 \\ 0 & 1 \end{pmatrix} \\ &+ \mathbf{G}_{\searrow}^{-}(x) \begin{pmatrix} 1 & 0 \\ 0 & 0 \end{pmatrix}, \\ \mathbf{Y}_{\searrow,0}^{0}(x) &= \mathbf{G}_{\searrow}^{+} \mathbf{Y}_{0}^{0}(x) \begin{pmatrix} 1 & 0 \\ 0 & 0 \end{pmatrix} + \mathbf{G}_{\searrow}^{-}(x) \mathbf{Y}_{1}^{0}(x) \begin{pmatrix} 1 & 0 \\ 0 & 0 \end{pmatrix} + \mathbf{G}_{\searrow}^{-}(x) \mathbf{Y}_{0}^{0}(x) \begin{pmatrix} 0 & 0 \\ 0 & 1 \end{pmatrix}. \end{split}$$

Recalling (3.41)–(3.42), eliminating the elements of the first column of $\mathbf{Y}_1^0(x)$ using (3.32), and then using the definitions (3.30) and the differential equations (3.31), we obtain

$$u_{\searrow}(x) = \frac{16\Theta_0^2 + 8(\Theta_\infty - \Theta_0 - 1)u(x)^2 - 4x^2u(x)^2 - 4xu(x)^3 - u(x)^4 - 8\Theta_0u'(x) + u'(x)^2}{2u(x)(-4\Theta_0 + 2xu(x) + u(x)^2 + u'(x))}.$$
(3.50)



Finally, if $Y_{0,22}^0(x)$ does not vanish identically, we can extract from $\mathbf{Y}_{\nwarrow}(\lambda;x)$ a solution $u_{\nwarrow}(x)$ of the Painlevé-IV equation (1.1) for parameters $(\Theta_0 - \frac{1}{2}, \Theta_{\infty} + \frac{1}{2})$ in the form

$$u_{\nwarrow}(x) := -2(\Theta_0 - \frac{1}{2}) \frac{Y_{\nwarrow,0,11}^0(x) Y_{\nwarrow,0,12}^0(x)}{Y_{\nwarrow,1,12}^\infty(x)}$$

provided it is determinate. Here the matrices $\mathbf{Y}^{\infty}_{\mathbb{N},1}(x)$ and $\mathbf{Y}^{0}_{\mathbb{N},0}(x)$ from (3.43) are given by

$$\begin{split} \mathbf{Y}_{\nwarrow,1}^{\infty}(x) &= \mathbf{G}_{\nwarrow}^{+} \mathbf{Y}_{2}^{\infty}(x) \begin{pmatrix} 1 & 0 \\ 0 & 0 \end{pmatrix} + \mathbf{G}_{\nwarrow}^{+} \mathbf{Y}_{1}^{\infty}(x) \begin{pmatrix} 0 & 0 \\ 0 & 1 \end{pmatrix} + \mathbf{G}_{\nwarrow}^{-}(x) \mathbf{Y}_{1}^{\infty}(x) \begin{pmatrix} 1 & 0 \\ 0 & 0 \end{pmatrix} \\ &+ \mathbf{G}_{\nwarrow}^{-}(x) \begin{pmatrix} 0 & 0 \\ 0 & 1 \end{pmatrix}, \\ \mathbf{Y}_{\nwarrow,0}^{0}(x) &= \mathbf{G}_{\nwarrow}^{+} \mathbf{Y}_{0}^{0}(x) \begin{pmatrix} 0 & 0 \\ 0 & 1 \end{pmatrix} + \mathbf{G}_{\nwarrow}^{-}(x) \mathbf{Y}_{1}^{0}(x) \begin{pmatrix} 0 & 0 \\ 0 & 1 \end{pmatrix} + \mathbf{G}_{\nwarrow}^{-}(x) \mathbf{Y}_{0}^{0}(x) \begin{pmatrix} 1 & 0 \\ 0 & 0 \end{pmatrix}. \end{split}$$

Recalling (3.44)–(3.45), using (3.32) to eliminate the second column of $\mathbf{Y}_1^0(x)$, and appealing to the definitions (3.30) and the differential system (3.31) yields

$$u_{\mathcal{N}}(x) = \frac{16\Theta_0^2 + 8(\Theta_\infty - \Theta_0)u(x)^2 - 4x^2u(x)^2 - 4xu(x)^3 - u(x)^4 + 8\Theta_0u'(x) + u'(x)^2}{2u(x)(-4\Theta_0 + 2xu(x) + u(x)^2 - u'(x))}.$$
(3.51)

Even if the Schlesinger transformation exists and is applied to a solution $\mathbf{Y}(\lambda;x)$ of Riemann–Hilbert Problem 1 for which u(x) is well defined, the corresponding Bäcklund transformation formula may be indeterminate. To detect the latter issue, we may observe first that if $\Theta_0 \neq 0$, the Painlevé-IV equation (1.1) does not admit the vanishing solution $u(x) \equiv 0$, so the problem reduces question of the existence of simultaneous solutions u(x) of (1.1) and of the Riccati equation obtained by setting to zero the other factor in the denominator of each of the formulæ (3.48), (3.49), (3.50), and (3.51). In each case, this amounts to a condition on the parameters $(\Theta_0, \Theta_\infty)$, as summarized in the following proposition.

Proposition 11 Let u(x) be a solution of the Painlevé-IV equation (1.1) for parameters $(\Theta_0, \Theta_\infty)$.

- The Bäcklund transformation (3.48) taking u(x) to $u_{\nearrow}(x)$ solving (1.1) for shifted parameters $(\Theta_0 + \frac{1}{2}, \Theta_\infty + \frac{1}{2})$ is determinate provided that $\Theta_0(\Theta_\infty + \Theta_0) \neq 0$.
- The Bäcklund transformation (3.49) taking u(x) to $u_{\swarrow}(x)$ solving (1.1) for shifted parameters $(\Theta_0 \frac{1}{2}, \Theta_\infty \frac{1}{2})$ is determinate provided that $\Theta_0(\Theta_\infty + \Theta_0 1) \neq 0$.
- The Bäcklund transformation (3.50) taking u(x) to $u_{\searrow}(x)$ solving (1.1) for shifted parameters $(\Theta_0 + \frac{1}{2}, \Theta_\infty \frac{1}{2})$ is determinate provided that $\Theta_0(\Theta_\infty \Theta_0 1) \neq 0$.
- The Bäcklund transformation (3.51) taking u(x) to $u_{\nwarrow}(x)$ solving (1.1) for shifted parameters $(\Theta_0 \frac{1}{2}, \Theta_{\infty} + \frac{1}{2})$ is determinate provided that $\Theta_0(\Theta_{\infty} \Theta_0) \neq 0$.



As is well-known, the four lines in the parameter space $\Theta_{\infty} \pm \Theta_0 = 0$ and $\Theta_{\infty} \pm \Theta_0 = 1$ give precisely the parameter values where the Painlevé-IV equation (1.1) admits solutions in terms of classical special functions, namely those solving the linear second-order equation related in the usual way to the Riccati equation consistent with (1.1).

3.4 The Isomonodromy Approach to Rational Solutions

Our approach to representing the rational solutions of (1.1) in a form convenient for asymptotic analysis in the limit that the parameters $(\Theta_0, \Theta_\infty)$ are large consists of the following steps:

- (1) Select a family of rational solutions and isolate within that family a distinguished parameter pair $(\Theta_0, \Theta_\infty)$ and its corresponding unique rational solution to serve as a "seed". Using the seed in the matrices defined by (3.10)–(3.11), the Lax pair equations (3.9) become compatible and admit simultaneous solutions.
- (2) Sow the seed, i.e.,
 - (a) Find simultaneous fundamental solution matrices $\Psi(\lambda, x)$ of the Lax pair suitably normalized for λ in the different Stokes sectors near each irregular singular point of the "spectral equation" $\Psi_{\lambda} = \Lambda \Psi$ and in a full neighborhood of each regular singular point (Fuchsian singularity) of the same equation. Compute explicitly the constants expressing the columns of each of these fundamental matrices as suitable linear combinations of the columns of the fundamental matrices for neighboring regions of the λ -plane (direct monodromy problem).
 - (b) Use this information to recast the fundamental matrices equivalently in terms of the solution of a matrix Riemann–Hilbert problem (inverse monodromy problem).

In this step, we take full advantage of choice of seed solution to simplify the equation $\Psi_x = X\Psi$ and leverage this to obtain simultaneous solutions of (3.9). This is in contrast to the usual approach in using the Lax pair (3.9) to solve the initial-value problem for Painlevé equations, where only initial values are available and therefore one must instead start by solving the more complicated spectral equation $\Psi_\lambda = \Lambda \Psi$.

- (3) Reap the harvest, i.e.,
 - (a) Apply isomonodromic Schlesinger transformations to increment/decrement the integer parameters of $(\Theta_0, \Theta_\infty)$, and hence obtain a Riemann–Hilbert problem for each pair $(\Theta_0, \Theta_\infty)$ in a certain lattice (for which the Schlesinger transformations are well defined).
 - (b) Show that the resulting lattice matches the full family of parameters for the rational solution family from which the seed was selected, and that the Riemann–Hilbert problem for given parameters in the family encodes a rational solution of the Painlevé equation at hand.

This method is general, and it has been applied before to characterize the rational solutions of the Painlevé-II equation [16, 50], the rational solutions of the Painlevé-III



equation [13], and the gO rational solutions for the Painlevé-IV equation [55] (although the Riemann–Hilbert problem reported in that paper differs from the one we shall develop below). The isomonodromy approach avoids completely the need for special determinantal representations of rational solutions having suitable analytic structure as has been used to study the rational solutions of Painlevé-II [7] and the gH rational solutions of Painlevé-IV [15]. Hence it is useful in the study of rational solutions that are not known to have such representations, such as the rational solutions of Painlevé-III and the gO rational solutions of Painlevé-IV. Even though such a determinantal representation is available for the gH rational solutions, the isomonodromy approach allows the gH and gO rational solutions of Painlevé-IV to be analyzed more-or-less on the same footing, which is a main point of our paper.

3.5 Riemann-Hilbert Representation of gO Rationals

Now we carry out the program outlined in Sect. 3.4 to arrive at a Riemann–Hilbert representation of the rational solutions of the Painlevé-IV equation (1.1) in the gO family. The procedure begins with the selection of a seed solution for the family, which we take to correspond to the special point $(\Theta_0, \Theta_\infty) = (\frac{1}{6}, \frac{1}{2}) \in \Lambda_{gO}$. The rational solution of (1.1) may be obtained equivalently from any row of Table 2 in Sect. 1.2 for m = n = 0, which gives simply $u(x) = -\frac{2}{3}x$.

3.5.1 Sowing the Seed: Solving the Direct Monodromy Problem and Formulating the Inverse Monodromy Problem

The Lax pair equations (3.9) for the seed solution involve $\Theta_0 = \frac{1}{6}$, $\Theta_\infty = \frac{1}{2}$, $u(x) = -\frac{2}{3}x$, a nontrivial solution y(x) of the first-order linear equation (3.7) that we take without loss of generality to be $y(x) = \exp(-\frac{2}{3}x^2)$, and $z(x) = \frac{1}{4}(-u'(x) + u(x)^2 + 2xu(x) + 4\Theta_0) = \frac{1}{3} - \frac{2}{9}x^2$ (see (3.8)). In particular, the x-equation $\Psi_x = \mathbf{X}\Psi$ in the Lax pair (3.9) takes the form

$$\Psi_x = \begin{pmatrix} \lambda & \exp(-\frac{2}{3}x^2) \\ (-\frac{2}{3} - \frac{4}{0}x^2) \exp(\frac{2}{3}x^2) & -\lambda \end{pmatrix} \Psi.$$

The exponential factors in the coefficient matrix are easily removed with the help of a gauge transformation: $\Psi = \exp(-\frac{1}{3}x^2\sigma_3)\Psi^{\{1\}}$, which leads to the equivalent system

$$\Psi_x^{\{1\}} = \begin{pmatrix} \lambda + \frac{2}{3}x & 1\\ -\frac{2}{3} - \frac{4}{9}x^2 & -\lambda - \frac{2}{3}x \end{pmatrix} \Psi^{\{1\}}.$$
 (3.52)

Using the first equation in this system to explicitly eliminate the second row yields a closed equation on elements $\Psi_{1k}^{\{1\}}$ of the first row:

$$\Psi_{1k,xx}^{\{1\}} = \left(\lambda^2 + \frac{4}{3}\lambda x\right)\Psi_{1k}^{\{1\}}, \quad k = 1, 2.$$



This is easily transformed into Airy's equation. Indeed, by a linear transformation $x \mapsto X$ for fixed λ we arrive at

$$\Psi_{1k,XX}^{\{1\}} = X\Psi_{1k}^{\{1\}}, \quad k = 1, 2, \quad X := (\frac{4}{3}\lambda)^{1/3}(x + \frac{3}{4}\lambda).$$
 (3.53)

Once the first row is determined, the elements of the second row follow from the relation

$$\Psi_{2k}^{\{1\}} = \Psi_{1k,x}^{\{1\}} - \left(\lambda + \frac{2}{3}x\right)\Psi_{1k}^{\{1\}}, \quad k = 1, 2. \tag{3.54}$$

Note that in terms of $\Psi^{\{1\}}$, the λ -equation in the Lax pair (3.9) for the gO seed solution takes the form

$$\Psi_{\lambda}^{\{1\}} = \begin{pmatrix} \lambda + x + \lambda^{-1}(\frac{2}{9}x^2 - \frac{1}{6}) & 1 + \frac{1}{3}\lambda^{-1}x \\ -\frac{4}{9}x^2 - \frac{2}{3} + \lambda^{-1}x(\frac{2}{9} - \frac{4}{27}x^2) - \lambda - x - \lambda^{-1}(\frac{2}{9}x^2 - \frac{1}{6}) \end{pmatrix} \Psi^{\{1\}}. \quad (3.55)$$

The above calculations suggest the utility of the independent variables X and $\Lambda := \lambda$ in place of (x, λ) . The differentiation formulæ needed to effect the change of variables are

$$\frac{\partial}{\partial x} = \left(\frac{4}{3}\Lambda\right)^{1/3} \frac{\partial}{\partial X} \quad \text{and} \quad \frac{\partial}{\partial \lambda} = \frac{\partial}{\partial \Lambda} + \left(\frac{1}{3}\frac{X}{\Lambda} + \frac{3}{4}\left(\frac{4}{3}\Lambda\right)^{1/3}\right) \frac{\partial}{\partial X}. \tag{3.56}$$

Next, it is convenient to introduce a subsequent gauge transformation in order to arrive at a X-equation for which the second row can be solved in terms of functions of X alone (rather than also involving Λ). Noting that the relation (3.54) implies that also

$$\Psi_{2k}^{\{1\}} = \left(\frac{4}{3}\Lambda\right)^{1/3} \Psi_{1k,X}^{\{1\}} - \left(\frac{1}{2}\Lambda + \frac{2}{3}\left(\frac{4}{3}\Lambda\right)^{-1/3}X\right) \Psi_{1k}^{\{1\}}, \quad k = 1, 2,$$

we introduce the "shearing" transformation

$$\Psi^{\{1\}} = \mathbf{S}(X, \Lambda) \Psi^{\{2\}}, \quad \mathbf{S}(X, \Lambda) := \left(-\left(\frac{1}{2}\Lambda + \frac{2}{3} \left(\frac{4}{3}\Lambda\right)^{-1/3} X\right) \left(\frac{4}{3}\Lambda\right)^{1/3} \right). \tag{3.57}$$

After some computation, it then follows from (3.52), (3.56), and (3.57) that

$$\Psi_X^{\{2\}} = \begin{pmatrix} 0 & 1 \\ X & 0 \end{pmatrix} \Psi^{\{2\}}.$$
 (3.58)

Similarly, combining this result with (3.55), (3.56), and (3.57),

$$\Psi_{\Lambda}^{\{2\}} = -\frac{1}{6\Lambda} \Psi^{\{2\}}.$$
 (3.59)



After this simplification, it is completely clear that every simultaneous fundamental solution matrix of (3.58) and (3.59) has the form

$$\Psi^{\{2\}} = \Lambda^{-1/6} \begin{pmatrix} f_1(X) & f_2(X) \\ f'_1(X) & f'_2(X) \end{pmatrix} \mathbf{C}$$

where \mathbb{C} is a matrix independent of both X and Λ with $\det(\mathbb{C}) \neq 0$ and $f_j(X)$, j = 1, 2 form a fundamental pair of solutions of Airy's equation f''(X) = Xf(X). Putting the pieces together we find the following result.

Lemma 2 Fix a fundamental pair $f_1(\cdot)$, $f_2(\cdot)$ of solutions of Airy's equation, a simply connected domain $D \subset \mathbb{C} \setminus \{0\}$ and arbitrary branches of $\lambda^{4/3}$ and $\lambda^{-1/6}$ analytic on D. For $\lambda \in D$ and $x \in \mathbb{C}$, define the matrix function

$$\mathbf{F}(\lambda, x) := \lambda^{-\frac{1}{6}} \exp(-\frac{1}{3}x^{2}\sigma_{3}) \begin{pmatrix} 1 & 0 \\ -\lambda - \frac{2}{3}x & (\frac{4}{3}\lambda)^{\frac{1}{3}} \end{pmatrix} \cdot \begin{pmatrix} f_{1}((\frac{3}{4})^{\frac{2}{3}}\lambda^{\frac{4}{3}}(1 + \frac{4}{3}\lambda^{-1}x)) & f_{2}((\frac{3}{4})^{\frac{2}{3}}\lambda^{\frac{4}{3}}(1 + \frac{4}{3}\lambda^{-1}x)) \\ f'_{1}((\frac{3}{4})^{\frac{2}{3}}\lambda^{\frac{4}{3}}(1 + \frac{4}{3}\lambda^{-1}x)) & f'_{2}((\frac{3}{4})^{\frac{2}{3}}\lambda^{\frac{4}{3}}(1 + \frac{4}{3}\lambda^{-1}x)) \end{pmatrix}.$$
(3.60)

Let $\Theta_0 = \frac{1}{6}$, $\Theta_\infty = \frac{1}{2}$, and consider the exact solution $u(x) = -\frac{2}{3}x$ of the corresponding Painlevé-IV equation (1.1). If $y(x) = \exp(-\frac{2}{3}x^2)$, then the Lax pair equations (3.9) are simultaneously solvable for all $(\lambda, x) \in D \times \mathbb{C}$, and every simultaneous solution matrix has the form

$$\Psi(\lambda, x) = \mathbf{F}(\lambda, x)\mathbf{C}, \quad (\lambda, x) \in D \times \mathbb{C}, \tag{3.61}$$

where \mathbf{C} is a matrix independent of both x and λ .

Remark 10 In [55, Sect. 3], the authors obtain analogues of these results by a different method. Namely, they observe that by fixing x = 0, the equation $\Psi_{\lambda} = \Lambda \Psi$ (cf. (3.9)–(3.10)), which is usually intractable from the point of view of classical special functions, reduces for the gO seed to a specific confluent hypergeometric equation solvable in terms of Whittaker functions. For the specific parameters involved, the Whittaker functions reduce to Airy functions, see [53, Eqn. 13.18.10]. This results in a computation of the Stokes matrices that agrees with our calculations written in (3.3) (and derived below) up to a constant diagonal conjugation. No attempt is made in [55] to calculate any connection matrices.

With this result in hand, we now consider how to choose the matrices $\mathbf{C} = \mathbf{C}_j^{(\infty)}$, j=1,2,3,4, corresponding to the four solutions $\Psi = \Psi_j^{(\infty)}(\lambda;x)$ to achieve the normalization condition (3.12) for each Stokes sector abutting the irregular singular point at $\lambda = \infty$. To make this calculation precise, we interpret all fractional powers of λ appearing in (3.61) as principal branches: $\lambda^p = \mathrm{e}^{p\log(\lambda)}$, $-\pi < \mathrm{Im}(\log(\lambda)) < \pi$. This means in particular that λ^p has in general a different meaning on the common boundary of S_3 and S_4 , depending on which of those two sectors is under consideration.



For each sector S_j in turn, we shall choose first for f_1 and f_2 a specific fundamental pair of solutions of f''(X) = Xf(X) that exhibits no Stokes phenomenon as $\lambda \to \infty$ in the sector. Then we use well-known asymptotic formulæ for Airy functions of large argument to determine the corresponding matrix $\mathbf{C}_j^{(\infty)}$. Once $\Psi_j^{(\infty)}(\lambda, x)$ has been determined for $j = 1, \ldots, 4$, we will build a solution $\Psi^{(0)}(\lambda, x)$ that satisfies the condition (3.13).

The Solution $\Psi_1^{(\infty)}(\lambda, x)$

If λ is large in the sector S_1 , then X defined in (3.53) is also large, and $-\frac{\pi}{2} \leq \arg(\lambda) \leq 0$ implies that $-\frac{2\pi}{3} - \epsilon \leq \arg(X) \leq \epsilon$ holds for every $\epsilon > 0$ if λ is large enough given ϵ . The solutions $f_1(X) = \operatorname{Ai}(X)$ and $f_2(X) = \operatorname{Ai}(e^{2i\pi/3}X)$ do not exhibit Stokes phenomenon in this sector as $w \to \infty$ for ϵ small enough. Using [53, Eqns. 9.7.5 & 9.7.6] and composing with the definition of X in (3.53) gives

$$f_{1}(X) = \frac{\exp\left(-\frac{1}{3}x^{2}\right)}{2\sqrt{\pi}} \left(\frac{4}{3}\right)^{\frac{1}{6}} \lambda^{-\frac{1}{3}} \exp\left(-\left(\frac{1}{2}\lambda^{2} + x\lambda\right)\right) \left(1 + \left(\frac{2}{27}x^{3} - \frac{1}{3}x\right)\lambda^{-1} + \mathcal{O}(\lambda^{-2})\right),$$

$$\lambda \to \infty, \quad \lambda \in S_{1},$$
(3.62)

$$f_1'(X) = -\frac{\exp\left(-\frac{1}{3}x^2\right)}{2\sqrt{\pi}} \left(\frac{3}{4}\right)^{\frac{1}{6}} \lambda^{\frac{1}{3}} \exp\left(-\left(\frac{1}{2}\lambda^2 + x\lambda\right)\right) \left(1 + \left(\frac{2}{27}x^3 + \frac{1}{3}x\right)\lambda^{-1} + \mathcal{O}(\lambda^{-2})\right),$$

$$\lambda \to \infty, \quad \lambda \in S_1,$$

$$(3.63)$$

$$\begin{split} f_2(X) &= \mathrm{e}^{-\frac{\mathrm{i}\pi}{6}} \frac{\exp\left(\frac{1}{3}x^2\right)}{2\sqrt{\pi}} \left(\frac{4}{3}\right)^{\frac{1}{6}} \lambda^{-\frac{1}{3}} \exp\left(\frac{1}{2}\lambda^2 + x\lambda\right) \left(1 - \left(\frac{2}{27}x^3 + \frac{1}{3}x\right)\lambda^{-1} + \mathcal{O}(\lambda^{-2})\right), \\ \lambda &\to \infty, \quad \lambda \in S_1, \end{split}$$

and

$$\begin{split} f_2'(X) &= \mathrm{e}^{-\frac{\mathrm{i}\pi}{6}} \frac{\exp\left(\frac{1}{3}x^2\right)}{2\sqrt{\pi}} \left(\frac{3}{4}\right)^{\frac{1}{6}} \lambda^{\frac{1}{3}} \exp\left(\frac{1}{2}\lambda^2 + x\lambda\right) \left(1 - \left(\frac{2}{27}x^3 - \frac{1}{3}x\right)\lambda^{-1} + \mathcal{O}(\lambda^{-2})\right), \\ \lambda &\to \infty, \quad \lambda \in S_1. \end{split}$$

A straightforward computation then shows that if $\Psi_1^{(\infty)}(\lambda, x)$ has the form (3.61) with the above choices for $f_1(X)$ and $f_2(X)$, and with the constant matrix $\mathbf{C} = \mathbf{C}_1^{(\infty)}$, then



using $\Theta_{\infty} = \frac{1}{2}$,

$$\begin{split} & \Psi_{1}^{(\infty)}(\lambda, x) \lambda^{\Theta_{\infty}\sigma_{3}} \exp\left(-\left(\frac{1}{2}\lambda^{2} + x\lambda\right)\sigma_{3}\right) \\ & = \begin{pmatrix} \mathcal{O}(\lambda^{-1}) & \frac{1}{2\sqrt{\pi}} \left(\frac{4}{3}\right)^{1/6} e^{-i\pi/6} + \mathcal{O}(\lambda^{-1}) \\ -\frac{1}{\sqrt{\pi}} \left(\frac{4}{3}\right)^{1/6} + \mathcal{O}(\lambda^{-1}) & \mathcal{O}(\lambda^{-1}) \end{pmatrix} \\ & \cdot \lambda^{\sigma_{3}/2} \exp\left(-\left(\frac{1}{2}\lambda^{2} + x\lambda\right)\sigma_{3}\right) \mathbf{C}_{1}^{(\infty)} \exp\left(-\left(\frac{1}{2}\lambda^{2} + x\lambda\right)\sigma_{3}\right) \lambda^{\sigma_{3}/2}, \\ & \lambda \to \infty, \quad \lambda \in S_{1}. \end{split}$$

Therefore to achieve the desired asymptotic normalization condition (3.12) for j = 1, we must take

$$\mathbf{C}_{1}^{(\infty)} := \begin{pmatrix} 0 & -\sqrt{\pi} \left(\frac{3}{4}\right)^{1/6} \\ 2\sqrt{\pi} \left(\frac{3}{4}\right)^{1/6} e^{i\pi/6} & 0 \end{pmatrix}.$$

This completes the determination of the normalized simultaneous fundamental solution matrix $\Psi_1^{(\infty)}(\lambda, x)$.

The Solution $\Psi_2^{(\infty)}(\lambda,x)$

When $\lambda \in S_2$, we have $-\epsilon \leq \arg(X) \leq \frac{2\pi}{3} + \epsilon$ as $\lambda \to \infty$ and hence also $w \to \infty$. In this case, to avoid Stokes phenomenon we choose solutions $f_1(X) = \operatorname{Ai}(X)$ and $f_2(X) = \operatorname{Ai}(e^{-2\mathrm{i}\pi/3}X)$. Thus, again composing the definition of X in (3.53) with [53, Eqns. 9.7.5 & 9.7.6], the expansions (3.62)–(3.63) are also valid as $\lambda \to \infty$ for $\lambda \in S_2$ and we have

$$f_2(X) = e^{\frac{i\pi}{6}} \frac{\exp(\frac{1}{3}x^2)}{2\sqrt{\pi}} \left(\frac{4}{3}\right)^{\frac{1}{6}} \lambda^{-\frac{1}{3}} \exp\left(\frac{1}{2}\lambda^2 + x\lambda\right) \left(1 - \left(\frac{2}{27}x^3 + \frac{1}{3}x\right)\lambda^{-1} + \mathcal{O}(\lambda^{-2})\right),$$

$$\lambda \to \infty, \quad \lambda \in S_2$$
(3.64)

and

$$f_2'(X) = e^{\frac{i\pi}{6}} \frac{\exp\left(\frac{1}{3}x^2\right)}{2\sqrt{\pi}} \left(\frac{3}{4}\right)^{\frac{1}{6}} \lambda^{\frac{1}{3}} \exp\left(\frac{1}{2}\lambda^2 + x\lambda\right) \left(1 - \left(\frac{2}{27}x^3 - \frac{1}{3}x\right)\lambda^{-1} + \mathcal{O}(\lambda^{-2})\right),$$

$$\lambda \to \infty, \quad \lambda \in S_7. \tag{3.65}$$



Taking these choices for $f_1(X)$ and $f_2(X)$ in (3.61) with $\Psi = \Psi_2^{(\infty)}(\lambda, x)$ and $\mathbf{C} = \mathbf{C}_2^{(\infty)}$, for $\Theta_{\infty} = \frac{1}{2}$,

$$\begin{split} & \Psi_{2}^{(\infty)}(\lambda, x) \lambda^{\Theta_{\infty}\sigma_{3}} \exp\left(-\left(\frac{1}{2}\lambda^{2} + x\lambda\right)\sigma_{3}\right) \\ &= \begin{pmatrix} \mathcal{O}(\lambda^{-1}) & \frac{1}{2\sqrt{\pi}} \left(\frac{4}{3}\right)^{1/6} e^{i\pi/6} + \mathcal{O}(\lambda^{-1}) \\ -\frac{1}{\sqrt{\pi}} \left(\frac{4}{3}\right)^{1/6} + \mathcal{O}(\lambda^{-1}) & \mathcal{O}(\lambda^{-1}) \end{pmatrix} \\ & \cdot \lambda^{\sigma_{3}/2} \exp\left(-\left(\frac{1}{2}\lambda^{2} + x\lambda\right)\sigma_{3}\right) \mathbf{C}_{2}^{(\infty)} \exp\left(-\left(\frac{1}{2}\lambda^{2} + x\lambda\right)\sigma_{3}\right) \lambda^{\sigma_{3}/2}, \\ & \lambda \to \infty, \quad \lambda \in S_{2}. \end{split}$$

Therefore, to achieve the desired normalization condition (3.12) we must take

$$\mathbf{C}_{2}^{(\infty)} := \begin{pmatrix} 0 & -\sqrt{\pi} \left(\frac{3}{4}\right)^{1/6} \\ 2\sqrt{\pi} \left(\frac{3}{4}\right)^{1/6} e^{-\mathrm{i}\pi/6} & 0 \end{pmatrix},$$

which completes the construction of $\Psi_2^{(\infty)}(\lambda,x)$. We observe here that $\mathbf{C}_2^{(\infty)}=\mathbf{C}_1^{(\infty)*}$ (element-wise complex conjugation), which is consistent with the fact that for $\Psi_2^{(\infty)}$ we selected a basis $(f_1(X), f_2(X))$ whose elements are the Schwarz reflections of the basis elements selected to construct $\Psi_1^{(\infty)}$.

The Solution $\Psi_3^{(\infty)}(\lambda,x)$

The sector S_3 corresponds to $\frac{2\pi}{3} - \epsilon \leq \arg(X) \leq \frac{4\pi}{3} + \epsilon$ as $\lambda \to \infty$. We hence choose the basis $f_1(X) := \operatorname{Ai}(\mathrm{e}^{-2\mathrm{i}\pi/3}X)$ and $f_2(X) := \operatorname{Ai}(\mathrm{e}^{-4\mathrm{i}\pi/3}X) = \operatorname{Ai}(\mathrm{e}^{2\mathrm{i}\pi/3}X)$ to avoid Stokes phenomenon. It follows that the expansions (3.64)–(3.65) are also valid (for $f_1(X)$ and $f_1'(X)$ in place of $f_2(X)$ and $f_2'(X)$ on the left-hand sides) as $\lambda \to \infty$ for $\lambda \in S_3$, and that

$$f_2(X) = e^{\frac{i\pi}{3}} \frac{\exp\left(-\frac{1}{3}x^2\right)}{2\sqrt{\pi}} \left(\frac{4}{3}\right)^{\frac{1}{6}} \lambda^{-\frac{1}{3}} \exp\left(-\left(\frac{1}{2}\lambda^2 + x\lambda\right)\right) \left(1 + \left(\frac{2}{27}x^3 - \frac{1}{3}x\right)\lambda^{-1} + \mathcal{O}(\lambda^{-2})\right),$$

$$\lambda \to \infty, \quad \lambda \in S_3$$

and

$$f_2'(X) = -e^{\frac{i\pi}{3}} \frac{\exp\left(-\frac{1}{3}x^2\right)}{2\sqrt{\pi}} \left(\frac{3}{4}\right)^{\frac{1}{6}} \lambda^{\frac{1}{3}} \exp\left(-\left(\frac{1}{2}\lambda^2 + x\lambda\right)\right) \left(1 + \left(\frac{2}{27}x^3 + \frac{1}{3}x\right)\lambda^{-1} + \mathcal{O}(\lambda^{-2})\right),$$

$$\lambda \to \infty, \quad \lambda \in S_3.$$



With these choices for $f_1(X)$ and $f_2(X)$ in (3.61) with $\Psi = \Psi_3^{(\infty)}(\lambda, x)$ and $\mathbb{C} = \mathbb{C}_3^{(\infty)}$, we find that

$$\begin{split} &\Psi_{3}^{(\infty)}(\lambda,x)\lambda^{\Theta_{\infty}\sigma_{3}}\exp\left(-\left(\frac{1}{2}\lambda^{2}+x\lambda\right)\sigma_{3}\right) \\ &= \begin{pmatrix} \frac{1}{2\sqrt{\pi}}\left(\frac{4}{3}\right)^{1/6}e^{i\pi/6}+\mathcal{O}(\lambda^{-1}) & \mathcal{O}(\lambda^{-1}) \\ \mathcal{O}(\lambda^{-1}) & \frac{1}{\sqrt{\pi}}\left(\frac{4}{3}\right)^{1/6}e^{-2i\pi/3}+\mathcal{O}(\lambda^{-1}) \end{pmatrix} \\ &\cdot \lambda^{-\sigma_{3}/2}\exp\left(\left(\frac{1}{2}\lambda^{2}+x\lambda\right)\sigma_{3}\right)\mathbf{C}_{3}^{(\infty)}\exp\left(-\left(\frac{1}{2}\lambda^{2}+x\lambda\right)\sigma_{3}\right)\lambda^{\sigma_{3}/2}, \quad \lambda \to \infty, \quad \lambda \in S_{3}. \end{split}$$

Therefore, to achieve the desired normalization condition (3.12) for j = 3 we must take

$$\mathbf{C}_{3}^{(\infty)} := \begin{pmatrix} 2\sqrt{\pi} \left(\frac{3}{4}\right)^{1/6} e^{-i\pi/6} & 0\\ 0 & \sqrt{\pi} \left(\frac{3}{4}\right)^{1/6} e^{2i\pi/3} \end{pmatrix}.$$

This completes the construction of $\Psi_3^{(\infty)}(\lambda, x)$.

The Solution $\Psi_4^{(\infty)}(\lambda, x)$

The sector S_4 corresponds to $-\frac{4\pi}{3} - \epsilon \leq \arg(X) \leq -\frac{2\pi}{3} + \epsilon$ as $\lambda \to \infty$. We choose the basis $f_1(X) := \operatorname{Ai}(e^{2i\pi/3}X)$ and $f_2(X) := \operatorname{Ai}(e^{4i\pi/3}X) = \operatorname{Ai}(e^{-2i\pi/3}X)$ to avoid Stokes phenomenon. Observing that these basis functions are the Schwarz reflections of those selected to construct $\Psi_3^{(\infty)}$, one can check that taking $\Psi = \Psi_4^{(\infty)}(\lambda, x)$ and $\mathbf{C} = \mathbf{C}_4^{(\infty)}$ in (3.61), the normalization condition (3.12) holds provided that

$$\mathbf{C}_{4}^{(\infty)} := \mathbf{C}_{3}^{(\infty)*} = \begin{pmatrix} 2\sqrt{\pi} \left(\frac{3}{4}\right)^{1/6} e^{i\pi/6} & 0\\ 0 & \sqrt{\pi} \left(\frac{3}{4}\right)^{1/6} e^{-2i\pi/3} \end{pmatrix}.$$

This completes the construction of $\Psi_4^{(\infty)}(\lambda, x)$.

The Solution $\Psi^{(0)}(\lambda, x)$.

Finally, we determine the constant matrix $\mathbf{C} = \mathbf{C}^{(0)}$ in (3.61) so that with $\mathbf{\Psi} = \mathbf{\Psi}^{(0)}(\lambda, x)$ and $\Theta_0 = \frac{1}{6}$ the condition (3.13) holds. This is possible because the Fuchsian singularity at $\lambda = 0$ of $\mathbf{\Psi}_{\lambda} = \mathbf{\Lambda}\mathbf{\Psi}$ is nonresonant for $\Theta_0 = \frac{1}{6}$. For this calculation we may choose any basis of solutions of Airy's equation, so we select the same basis as in the definition of $\mathbf{\Psi}_1^{(\infty)}(\lambda, x)$, namely $f_1(X) = \mathrm{Ai}(X)$ and $f_2(X) = \mathrm{Ai}(e^{2i\pi/3}X)$. This will make it easiest to relate $\mathbf{\Psi}^{(0)}(\lambda, x)$ explicitly to $\mathbf{\Psi}_1^{(\infty)}(\lambda, x)$. We begin with the following elementary observation: it can be shown that with the above definitions,

$$\tilde{f}_1(X) := f_1(X) - f_2(X)$$



is a nontrivial solution of Airy's equation whose Taylor expansion at the origin contains only terms proportional to X^{3n+1} , $n = 0, 1, 2, \dots$ Likewise

$$\tilde{f}_2(X) := f_1(X) - e^{-2i\pi/3} f_2(X)$$

is a nontrivial solution of Airy's equation whose Taylor expansion at the origin contains only terms proportional to X^{3n} , $n=0,1,2,\ldots$. Composing with the definition of X in (3.53) shows that $\lambda^{-1/3}\tilde{f}_1(X)$ and $\tilde{f}_2(X)$ are both analytic functions of λ at $\lambda=0$. Taking into account that $\Theta_0=\frac{1}{6}$ then shows that $\Psi^{(0)}(\lambda,x)\lambda^{-\Theta_0\sigma_3}$ will be analytic at $\lambda=0$ if we take $\Psi=\Psi^{(0)}(\lambda,x)$ in the form (3.61) with the above choice of basis $f_1(X)$ and $f_2(X)$ and insist that $\mathbf{C}=\mathbf{C}^{(0)}$ has the form

$$\mathbf{C}^{(0)} := \begin{pmatrix} 1 & 1 \\ -1 & e^{\mathrm{i}\pi/3} \end{pmatrix} \mathbf{D}$$

where **D** is any constant invertible diagonal matrix. Modulo the choice of **D**, which we will make concrete below (see (3.66)), this completes the construction of $\Psi^{(0)}(\lambda, x)$.

The last step of sowing the seed is to formulate the inverse monodromy problem, which simply amounts to the calculation of the constant matrices relating the five simultaneous fundamental solution matrices of the Lax pair (3.9). For the Stokes matrices $\mathbf{V}_{2,1}$, $\mathbf{V}_{2,3}$, $\mathbf{V}_{4,3}$, and $\mathbf{V}_{4,1}$ defined by (3.14)–(3.17), we use the identity $\mathrm{Ai}(X) + \mathrm{e}^{2\mathrm{i}\pi/3}\mathrm{Ai}(\mathrm{e}^{2\mathrm{i}\pi/3}X) + \mathrm{e}^{-2\mathrm{i}\pi/3}\mathrm{Ai}(\mathrm{e}^{-2\mathrm{i}\pi/3}X) = 0$ (see [53, Eqn. 9.2.12]) to explicitly relate the simultaneous solutions $\Psi_j^{(\infty)}(\lambda,x)$, $j=1,\ldots,4$, leading to (3.3) in which $\Theta_\infty = \frac{1}{2}$. The computation of the Stokes matrix $\mathbf{V}_{4,3}$ requires more care than the others, because one must take into account the jump in the principal branch of λ^p across the negative real axis. For the connection matrices defined by (3.18)–(3.19), first note that since the basis of Airy functions $f_1(X)$ and $f_2(X)$ in the formula (3.61) is exactly the same for $\Psi = \Psi_1^{(\infty)}(\lambda,x)$ and $\Psi = \Psi^{(0)}(\lambda,x)$, (3.18) gives $\mathbf{V}_1 = \mathbf{C}_1^{(\infty)-1}\mathbf{C}_1^{(0)}$. Therefore, choosing without loss of generality that

$$\mathbf{D} := \begin{pmatrix} -\frac{2}{\sqrt{3}} (\frac{3}{4})^{1/6} \sqrt{\pi} & 0\\ 0 & -(\frac{3}{4})^{1/6} \sqrt{\pi} \end{pmatrix} e^{i\pi\sigma_3/6} = -(\frac{4}{3})^{1/12} \sqrt{\pi} ((\frac{4}{3})^{1/4} e^{i\pi/6})^{\sigma_3},$$
(3.66)

we obtain the unimodular connection matrix \mathbf{V}_1 from (3.18), after which it is easiest to obtain \mathbf{V}_2 , \mathbf{V}_3 , and \mathbf{V}_4 by combining the Stokes matrices (3.3) with the first three identities in (3.20). In this way, we obtain the connection matrices given in (3.4). From these formulæ one can observe that $\mathbf{V}_1^* = \mathbf{V}_2^{-1}$ and $\mathbf{V}_3^* = \mathbf{V}_4^{-1}$, a useful symmetry in light of Corollary 4 from Sect. 3.2 that explains our choice of the diagonal constant matrix \mathbf{D} in (3.66).

3.5.2 Reaping the Harvest: Use of Schlesinger Transformations to Span the gO Parameter Lattice

The above arguments have shown that Riemann–Hilbert Problem 1 obviously has a solution when $(\Theta_0, \Theta_\infty) = (\frac{1}{6}, \frac{1}{2})$ and the piecewise-constant matrix **V** is defined



on the jump contour Σ in terms of the Stokes matrices (3.3) and the connection matrices (3.4), namely the solution given by the formula (3.21). One can check that the function u(x) returned from this solution via the formula (3.30) is well defined and coincides with the seed $u(x) = -\frac{2}{3}x$ from which we began. Noting that the gO rational solution parameter lattice Λ_{gO} may be written as the set of points $(\Theta_0, \Theta_\infty)$ of the form $(\Theta_0, \Theta_\infty) = (\frac{1}{6}, \frac{1}{2}) + \mathbb{Z}(\frac{1}{2}, \frac{1}{2}) + \mathbb{Z}(\frac{1}{2}, -\frac{1}{2})$, none of which satisfy any of the conditions $\Theta_0 = 0$, $\Theta_\infty \pm \Theta_0 = 0$, or $\Theta_\infty \pm \Theta_0 = 1$, arbitrary iterations of the four Schlesinger transformations developed in Sect. 3.3.1 and their coincident Bäcklund transformations from Sect. 3.3.2 can be applied to the seed to reach any point of Λ_{gO} . Since the only effect on the jump conditions of these Schlesinger transformations is to change the sign of $\mathbf{V}_{4,3}$ with each iteration, and since the Bäcklund transformations obviously map rational solutions to rational solutions, which are necessarily unique for given parameter values, we have arrived at the Riemann–Hilbert representation of the gO rational solutions of Painlevé-IV given in Theorem 5 in Sect. 3.5, the proof of which we now complete.

Proof of Theorem 5 If $(\Theta_0, \Theta_\infty) = (\frac{1}{6}, \frac{1}{2})$, then the statement is true with $u(x) = -\frac{2}{3}x$ and $u_{\zeta}(x) = x^{-1} - \frac{2}{3}x$, the latter solving (1.1) for parameters $(\Theta_{0,\zeta}, \Theta_{\infty,\zeta}) =$ $(-\frac{1}{3}, 1)$. By Proposition 10 in Sect. 3.3 we can apply the four Schlesinger transformations $\mathbf{Y}(\lambda; x) \mapsto \mathbf{Y}_{\nearrow}(\lambda; x), \mathbf{Y}(\lambda; x) \mapsto \mathbf{Y}_{\nearrow}(\lambda; x), \mathbf{Y}(\lambda; x) \mapsto \mathbf{Y}_{\searrow}(\lambda; x), \text{ and/or}$ $\mathbf{Y}(\lambda; x) \mapsto \mathbf{Y}_{\nabla}(\lambda; x)$ to increment and/or decrement Θ_0 and Θ_{∞} by half-integers iteratively to reach any point in Λ_{gO} (any path from $(\frac{1}{6},\frac{1}{2})$ to $(\Theta_0,\Theta_\infty)\in\Lambda_{gO}$ through Λ_{gO} suffices, because each path produces a solution of the same Riemann-Hilbert problem, which must be unique by Proposition 5 from Sect. 3.2). Each step in the lattice introduces a sign change in $V_{4,3}$, which is automatically taken into account in the definition (see (3.3)). Next, we observe that the corresponding Bäcklund transformations $u(x) \mapsto u_{\nearrow}(x)$, $u(x) \mapsto u_{\nearrow}(x)$, $u(x) \mapsto u_{\searrow}(x)$, and $u(x) \mapsto u_{\nwarrow}(x)$ induced by the Schlesinger transformations all map rational functions to rational functions. By uniqueness of rational solutions for Painlevé-IV it follows that u(x) extracted from Riemann–Hilbert Problem 1 is the unique rational solution of (1.1) with arbitrary parameters $(\Theta_0, \Theta_\infty) \in \Lambda_{gO}$. Since $u_{\gamma}(x)$ is related to the rational function u(x)by the Bäcklund transformation in (2.4), it is well defined (since u(x) cannot vanish identically as $\Theta_0 \neq 0$ in the gO parameter lattice) and rational. Hence it is the unique rational solution of (1.1) for parameters $(\Theta_{0,\uparrow},\Theta_{\infty,\uparrow})$ defined by (2.4) (these also lie in Λ_{gO}).

3.6 Riemann-Hilbert Representation of gH Rationals

It is straightforward to check that if $\Theta_0 = \Theta_\infty = \frac{1}{2}$ in (1.1), then u(x) = -2x is an exact solution; this corresponds to taking m = n = 0 in the type-3 row of Table 1 in Sect. 1.2. We shall use it as a seed in the same way that $u(x) = -\frac{2}{3}x$ was used in Sect. 3.5 to derive a Riemann–Hilbert representation of the generalized Hermite rational solutions of Painlevé-IV.



3.6.1 Sowing the Seed: Solving the Direct Monodromy Problem and Formulating the Inverse Monodromy Problem

When $(\Theta_0, \Theta_\infty, u(x)) = (\frac{1}{2}, \frac{1}{2}, -2x)$, the differential equation (3.7) has the general solution $y(x) = y_0$, a constant (assumed nonzero), and the quantity z(x) defined in (3.8) is $z(x) \equiv 1$. Without loss of generality, we take $y_0 = 2$. Therefore the Lax pair equations (3.9) take a particularly simple form in this case, because the coefficient matrices defined generally in (3.10)–(3.11) are now upper triangular:

$$(\Theta_0, \Theta_\infty, u(x)) = \left(\frac{1}{2}, \frac{1}{2}, -2x\right)$$

$$\implies \mathbf{\Lambda} = \begin{pmatrix} \lambda + x - \frac{1}{2}\lambda^{-1} & 2 + 2x\lambda^{-1} \\ 0 & -\lambda - x + \frac{1}{2}\lambda^{-1} \end{pmatrix}, \mathbf{X} = \begin{pmatrix} \lambda & 2 \\ 0 & -\lambda \end{pmatrix}.$$

Therefore, the second row elements of a simultaneous matrix solution Ψ satisfy a compatible first-order scalar system, whose general solution is easily seen to be $\Psi_{2j} = c \exp(-(\frac{1}{2}\lambda^2 + x\lambda))\lambda^{1/2}$, where c is an integration constant (independent of both x and λ). Using this result, the first row elements Ψ_{1j} then satisfy their own compatible scalar system, which can be solved with the help of an integrating factor proportional to Ψ_{2j} . The result of these completely elementary calculations is the following.

Lemma 3 Fix a simply connected domain $D \subset \mathbb{C} \setminus \{0\}$ and a branch of $\lambda^{1/2}$ analytic on D. Let $\Theta_0 = \Theta_\infty = \frac{1}{2}$, and consider the exact solution u(x) = -2x of the corresponding Painlevé-IV equation (1.1). If y(x) = 2, then the Lax pair equations (3.9) are simultaneously solvable for all $(\lambda, x) \in D \times \mathbb{C}$, and every simultaneous solution matrix has the form

$$\Psi(\lambda, x) = \begin{pmatrix} \lambda^{-1/2} \exp(\frac{1}{2}\lambda^2 + x\lambda) & -\lambda^{-1/2} \exp(-(\frac{1}{2}\lambda^2 + x\lambda)) \\ 0 & \lambda^{1/2} \exp(-(\frac{1}{2}\lambda^2 + x\lambda)) \end{pmatrix} \mathbf{C}, \quad (\lambda, x) \in D \times \mathbb{C},$$
(3.67)

where \mathbf{C} is a matrix independent of both x and λ .

The simplest invertible choice for C is simply $C = \mathbb{I}$. Assuming this and also taking the principal branch for $\lambda^{1/2}$, consider imposing the condition (3.12) in one of the Stokes sectors near $\lambda = \infty$. Using $\Theta_{\infty} = \frac{1}{2}$ we find that

$$\mathbf{C} = \mathbb{I} \implies \Psi(\lambda, x) \lambda^{\Theta_{\infty} \sigma_3} \exp(-(\frac{1}{2}\lambda^2 + x\lambda)\sigma_3) = \begin{pmatrix} 1 - \lambda^{-1} \\ 0 & 1 \end{pmatrix}$$

which tends to \mathbb{I} as $\lambda \to \infty$ regardless of choice of Stokes sector. Therefore, there is no Stokes phenomenon about the irregular singular point $\lambda = \infty$ in this case, and the normalized solutions associated with the four Stokes sectors are all the same:

$$\Psi_{j}^{(\infty)}(\lambda, x) = \Psi^{(\infty)}(\lambda, x) := \begin{pmatrix} \lambda^{-1/2} \exp(\frac{1}{2}\lambda^{2} + x\lambda) & -\lambda^{-1/2} \exp(-(\frac{1}{2}\lambda^{2} + x\lambda)) \\ 0 & \lambda^{1/2} \exp(-(\frac{1}{2}\lambda^{2} + x\lambda)) \end{pmatrix},$$

$$j = 1, \dots, 4, \quad \arg(\lambda) \in (-\pi, \pi).$$
(3.68)



The Fuchsian singular point $\lambda=0$ is resonant in the case $\Theta_0=\frac{1}{2}$ under consideration, but the singularity is also apparent as is clear from the absence of logarithms in the general solution (3.67). Therefore it is possible to choose the matrix $\mathbf{C}=\mathbf{C}^{(0)}$ to define a solution $\Psi=\Psi^{(0)}(\lambda,x)$ so that the condition (3.13) for $\Theta_0=\frac{1}{2}$ holds. This condition requires analyticity of the following expression, which generally has a simple pole at $\lambda=0$:

$$\Psi^{(0)}(\lambda, x)\lambda^{-\Theta_0\sigma_3} = \begin{pmatrix} C_{11}^{(0)} - C_{21}^{(0)} & 0\\ 0 & 0 \end{pmatrix} \lambda^{-1} + \text{holomorphic.}$$

Therefore, the only condition imposed on $\mathbf{C} = \mathbf{C}^{(0)}$ by (3.13) is that $C_{11}^{(0)} = C_{21}^{(0)}$. Compared with the nonresonant case discussed in Sect. 3.5.1, the resonant but apparent case here allows for an additional degree of freedom. It is also convenient to assume that $\det(\mathbf{C}^{(0)}) = 1$ which in turn guarantees that $\det(\mathbf{\Psi}^{(0)}(\lambda, x)) = 1$. Therefore, we will take $\mathbf{C}^{(0)}$ to be a matrix of the form $\begin{pmatrix} a & b \\ a & b + a^{-1} \end{pmatrix}$ with $a \neq 0$ so that

$$\Psi^{(0)}(\lambda, x) = \begin{pmatrix} \lambda^{-1/2} \exp(\frac{1}{2}\lambda^2 + x\lambda) & -\lambda^{-1/2} \exp(-(\frac{1}{2}\lambda^2 + x\lambda)) \\ 0 & \lambda^{1/2} \exp(-(\frac{1}{2}\lambda^2 + x\lambda)) \end{pmatrix} \begin{pmatrix} a & b \\ a & b + a^{-1} \end{pmatrix}.$$
(3.69)

For convenience we pick a=1 and b=0, which completes the construction of the five canonical simultaneous solutions of the Lax pair for $(\Theta_0, \Theta_\infty) = (\frac{1}{2}, \frac{1}{2})$ and u(x) = -2x.

It is now straightforward to compute the Stokes matrices for the irregular singular point at $\lambda = \infty$ by using (3.14)–(3.17) and (3.68), and the results are trivial except for the contribution of the branch cut of $\lambda^{1/2}$ along the negative real line, leading directly to (3.5) in which $\Theta_{\infty} = \frac{1}{2}$. Likewise, we compute the connection matrices using (3.18)–(3.19), (3.68), and (3.69) with a = 1 and b = 0 to arrive at (3.6).

3.6.2 Reaping the Harvest: Use of Schlesinger Transformations to Span $\Lambda_{gH}^{[3]+}$

The formula (3.21) clearly gives a solution of Riemann–Hilbert Problem 1 from Sect. 3.1 for $(\Theta_0, \Theta_\infty) = (\frac{1}{2}, \frac{1}{2})$ when the piecewise-constant matrix **V** is defined on the jump contour Σ with the use of the Stokes matrices (3.5) and the connection matrices (3.6), and this solution returns the rational solution u(x) = -2x of Painlevé-IV that started the calculation. We also observe that, using (3.69) in (3.21) and referring to the expansion (3.23), we have

$$\mathbf{Y}_0^0(x) = \begin{pmatrix} 2x & -1\\ 1 & 0 \end{pmatrix} \text{ for } (\Theta_0, \Theta_\infty) = (\frac{1}{2}, \frac{1}{2}).$$
 (3.70)

The component $\Lambda_{gH}^{[3]+}$ of the gH parameter lattice contains the point $(\Theta_0,\Theta_\infty)=(\frac{1}{2},\frac{1}{2})$ and can be viewed as the set of points (Θ_0,Θ_∞) of the form $(\Theta_0,\Theta_\infty)=(\frac{1}{2},\frac{1}{2})+\mathbb{Z}_{\geq 0}(\frac{1}{2},\frac{1}{2})+\mathbb{Z}_{\geq 0}(\frac{1}{2},-\frac{1}{2})$. Using Proposition 9 from Sect. 3.3, we see from (3.70) that the only basic Schlesinger transformation that is possibly undefined at



 $(\Theta_0, \Theta_\infty) = (\frac{1}{2}, \frac{1}{2}) \in \Lambda_{gH}^{[3]+}$ is $\mathbf{Y}(\lambda; x) \mapsto \mathbf{Y}_{\nwarrow}(\lambda; x)$, and from Proposition 11 (also from Sect. 3.3) we see that of the three that are certainly defined, only $\mathbf{Y}(\lambda; x) \mapsto \mathbf{Y}_{\nearrow}(\lambda; x)$ and $\mathbf{Y}(\lambda; x) \mapsto \mathbf{Y}_{\searrow}(\lambda; x)$ are guaranteed to give determinate Bäcklund transformations of u(x). So, from $(\frac{1}{2}, \frac{1}{2}) \in \Lambda_{gH}^{[3]+}$ we may certainly step to the nearest neighbor points (1, 1) and (1, 0) in the same lattice. Without using specific information such as (3.70), from Propositions 10 and 11, we observe that

- The Schlesinger transformation Y(λ; x) → Y_Z(λ; x) is defined and yields a determinate Bäcklund transformation u(x) → u_Z(x) at each point of Λ^{[3]+}_{gH}.
 The Schlesinger transformation Y(λ; x) → Y_Z(λ; x) is defined at each point of
- The Schlesinger transformation $\mathbf{Y}(\lambda; x) \mapsto \mathbf{Y}_{\swarrow}(\lambda; x)$ is defined at each point of $\Lambda_{\mathrm{gH}}^{[3]+}$. Furthermore it is guaranteed to yield a determinate Bäcklund transformation $u(x) \mapsto u_{\swarrow}(x)$ except possibly at those points of the form $(\Theta_0, \Theta_\infty) = (\frac{1}{2}, \frac{1}{2}) + \mathbb{Z}_{\geq 0}(\frac{1}{2}, -\frac{1}{2})$, which satisfy $\Theta_\infty + \Theta_0 = 1$.
- The Schlesinger transformation $\mathbf{Y}(\lambda; x) \mapsto \mathbf{Y}_{\searrow}(\lambda; x)$ is defined at each point of $\Lambda_{\mathrm{gH}}^{[3]+}$ except possibly at those points of the form $(\Theta_0, \Theta_\infty) = (\frac{1}{2}, \frac{1}{2}) + \mathbb{Z}_{\geq 0}(\frac{1}{2}, \frac{1}{2})$ where $\Theta_\infty \Theta_0 = 0$. The corresponding Bäcklund transformation $u(x) \mapsto u_{\searrow}(x)$ is determinate at every point of $\Lambda_{\mathrm{gH}}^{[3]+}$, including those points at which the Schlesinger transformation from which it is derived is not guaranteed by Proposition 10 to be defined.
- The Schlesinger transformation $\mathbf{Y}(\lambda; x) \mapsto \mathbf{Y}_{\nwarrow}(\lambda; x)$ is defined at each point of $\Lambda_{\mathrm{gH}}^{[3]+}$ except possibly at those points of the form $(\Theta_0, \Theta_\infty) = (\frac{1}{2}, \frac{1}{2}) + \mathbb{Z}_{\geq 0}(\frac{1}{2}, \frac{1}{2})$ where $\Theta_\infty \Theta_0 = 0$. The corresponding Bäcklund transformation $u(x) \mapsto u_{\nwarrow}(x)$ is guaranteed to be determinate except possibly at the same excluded points.

Therefore, starting from the seed $(\Theta_0, \Theta_\infty) = (\frac{1}{2}, \frac{1}{2})$, we may arrive at an arbitrary point in $\Lambda_{gH}^{[3]+}$ by iteratively applying Schlesinger transformations resulting in determinate Bäcklund transformations according to the following principles.

- To reach a point of the form $(\Theta_0, \Theta_\infty) = (n+1)(\frac{1}{2}, \frac{1}{2}) \in \Lambda_{gH}^{[3]+}, n = 0, 1, 2, \dots$, we apply $\mathbf{Y}(\lambda; x) \mapsto \mathbf{Y}_{\nearrow}(\lambda; x) n$ times.
- To reach any other point of $\Lambda_{gH}^{[3]+}$, we first step from $(\frac{1}{2}, \frac{1}{2})$ to (1,0) using $\mathbf{Y}(\lambda; x) \mapsto \mathbf{Y}_{\searrow}(\lambda; x)$. Then we choose any path in $\Lambda_{gH}^{[3]+}$ from (1,0) to the target point that contains only points with $\Theta_{\infty} < \Theta_0$, and iteratively apply the Schlesinger transformations associated with the steps in the selected path.

We have thus arrived at the Riemann–Hilbert representation in Theorem 6 from Sect. 3.1 of the gH rational solutions of Painlevé-IV for parameters in $\Lambda_{\rm gH}^{[3]+}$, and via the non-isomonodromic Bäcklund transformation $u(x) \mapsto u_{\uparrow}(x)$, in $\Lambda_{\rm gH}^{[1]-}$. The rest of its proof is nearly the same as the proof in Sect. 3.5 of Theorem 5 except that the Schlesinger transformation steps should be taken to follow the above principles.

In contrast with the gO case, it is not possible to access the other lattice components $\Lambda_{gH}^{[1]-}$ or $\Lambda_{gH}^{[2]-}$ via Schlesinger transformations from the sector $\Lambda_{gH}^{[3]+}$. Our approach is to obtain the rational gH solutions of types 1 and 2 from the type 3 function using the symmetries $\mathcal{S}_{\mathbb{Q}}$ and $\mathcal{S}_{\mathbb{Q}}$ described in Sect. 2. It is possible to directly formulate a version of Riemann–Hilbert Problem 1 for which the type 1 and type 2 rational



solutions are encoded as the function u(x), but the results are quite different from Theorem 6. See Appendix H.

3.6.3 Connection to a Riemann-Hilbert Problem for Pseudo-Orthogonal Polynomials

The simplification observed in Remark 6 in Sect. 3.1 suggests a connection between the gH rational solutions of Painlevé-IV and pseudo-orthogonal polynomials via the Riemann–Hilbert approach of Fokas, Its, and Kitaev [34]. Setting $\mathbf{W}(\lambda;x) := \sigma_1 \mathbf{Y}(\lambda;x) \lambda^{-\Theta_0 \sigma_3} \sigma_1$ and taking the parameters (Θ_0,Θ_∞) to be given by $(\Theta_{0,\mathrm{gH}}^{[3]}(m,n),\Theta_{\infty,\mathrm{gH}}^{[3]}(m,n))$ as defined in Table 1 in Sect. 1.2, it is easy to see that $\mathbf{W}(\lambda;x)$ is analytic for $|\lambda| \neq 1$, obeys the jump condition

$$\mathbf{W}_{+}(\lambda; x) = \mathbf{W}_{-}(\lambda; x) \begin{pmatrix} 1 & w_{M}(\lambda; x) \\ 0 & 1 \end{pmatrix}, \quad |\lambda| = 1,$$

$$w_{M}(\lambda; x) := \lambda^{-M} \exp(-(\lambda^{2} + 2x\lambda)), \quad M := 2\Theta_{0}, \tag{3.71}$$

where the jump contour is given counterclockwise orientation, and satisfies the normalization condition

$$\lim_{\lambda \to \infty} \mathbf{W}(\lambda; x) \lambda^{-N\sigma_3} = \mathbb{I}, \quad N := \Theta_{\infty} + \Theta_0.$$
 (3.72)

Noting that M and N are integers, this is the Fokas-Its-Kitaev Riemann–Hilbert problem. If $\mathbf{W}(\lambda; x)$ exists, then $\det(\mathbf{W}(\lambda; x)) = 1$. It is well-known and easy to see that solvability requires N > 0, because otherwise the fact that the first column of $\mathbf{W}(\lambda; x)$ is entire, which follows from the jump condition (3.71), together with the normalization condition (3.72) implies that the first column of W vanishes identically by Liouville's Theorem; but this is inconsistent with $det(\mathbf{W}) = 1$. If the solution $\mathbf{W}(\lambda; x)$ exists for N = 0, 1, 2, ..., the matrix element $W_{11}(\lambda; x)$ is the monic pseudo-orthogonal polynomial⁷ of degree N with respect to the weight $w_M(\lambda; x)$ on the unit circle. However such a polynomial can only exist if M > 0 because otherwise the weight is analytic for $|\lambda| < 1$ and hence every polynomial is pseudo-orthogonal to every monomial by Cauchy's Theorem. Likewise, the matrix element $W_{21}(\lambda; x)$ is a polynomial in λ of degree at most N-1 in terms of which the matrix element $W_{22}(\lambda; x)$ is expressed as a Cauchy integral against the weight; the condition (3.72) then requires that $W_{22}(\lambda; x) = \lambda^{-N} + \mathcal{O}(\lambda^{-(N+1)})$ as $\lambda \to \infty$ which leads to a contradiction unless N < M + 1 (in other words, given M = 1, 2, 3, ... there can only be finitely many pseudo-orthogonal polynomials of degrees N = 0, 1, ..., M). In terms of $(\Theta_0, \Theta_\infty)$, the conditions $M = 1, 2, 3, \dots$ and $N = 1, 2, \dots, M$ correspond precisely to the

$$\oint_{|\lambda|=1} \pi_m(\lambda; x) \pi_n(\lambda; x) w_M(\lambda; x) d\lambda = h_n \delta_{mn},$$

which is not proper orthogonality because the left-hand side does not define a Hermitian inner product.



⁷ Pseudo-orthogonality of monic polynomials $\pi_m(\lambda; x)$ and $\pi_n(\lambda; x)$ of degrees m and n respectively means that for some norming constants h_n ,

points of $\Lambda_{\rm gH}^{[3]+}$. While $\mathbf{W}(\lambda;x)$ and hence $\mathbf{Y}(\lambda;x)$ can also exist for N=0 and $M=1,2,3,\ldots$, these additional values do not yield a solution u(x) of the Painlevé-IV equation via the formula (3.2) because $\mathbf{W}(\lambda;x)$ is upper-triangular for N=0, so $\mathbf{Y}(\lambda;x)$ is lower-triangular, and hence $Y_{1,12}^{\infty}(x)\equiv 0$.

In [15], the gH rational solutions of Painlevé-IV were studied by means of another system of pseudo-orthogonal polynomials obtained by further developing the method of Bertola and Bothner [7]. It is easy to relate the Riemann–Hilbert representation used in [15] to the gH Riemann–Hilbert problem for $\mathbf{Y}(\lambda; x)$. Indeed, from the solution $\mathbf{Y}(\lambda; x)$ of Riemann–Hilbert Problem 1 in the gH type-3 case, set

$$\mathbf{M}(\zeta; y) := \left(\frac{\exp\left(\frac{1}{4}i\pi(2\Theta_{\infty} - 1)\right)}{\sqrt{2\pi}}\right)^{\sigma_{3}} i^{(\Theta_{\infty} + \Theta_{0})\sigma_{3}} \sigma_{1} \mathbf{Y}_{0}^{0} (iy)^{-1} \mathbf{Y}\left(-\frac{i}{\zeta}; iy\right) \left(-\frac{i}{\zeta}\right)^{\Theta_{\infty}\sigma_{3}} \cdot \sigma_{1} \left(\frac{\exp(\frac{1}{4}i\pi(2\Theta_{\infty} - 1))}{\sqrt{2\pi}}\right)^{-\sigma_{3}}.$$
(3.73)

It is straightforward to check that $\mathbf{M}(\zeta; y)$ solves [15, Riemann–Hilbert Problem 1] with parameters $m = 1 - 2\Theta_{\infty}$ and $n = \Theta_{\infty} + \Theta_0$, both integers. In light of the variable transformation $\lambda = -\mathrm{i}\zeta^{-1}$, the pseudo-orthogonal polynomials in [15] are related to the *reciprocal* pseudo-orthogonal polynomials encoded in the matrix $\mathbf{W}(\lambda; x)$. The connection between $\mathbf{Y}(\lambda; x)$ and $\mathbf{M}(\zeta; y)$ is analogous to an observation made in [50], namely that the Riemann–Hilbert problem encoding the Yablonskii-Vorob'ev polynomials found by Bertola and Bothner [7] is explicitly related to the inverse monodromy problem for the Flaschka-Newell Lax pair for the Painlevé-II rational solutions built from those polynomials.

Note also that these arguments connecting Riemann–Hilbert Problem 1 in the gH case with pseudo-orthogonal polynomials explain why Schlesinger transformations do not allow one to escape from the set $\Lambda_{gH}^{[3]+}$ into any larger lattice spanned by the same lattice vectors. This is a special phenomenon of the gH rational solutions, since we have seen that the entire $\mathbb{Z}\times\mathbb{Z}$ gO lattice is accessible by Schlesinger transformations from any given lattice point.

4 Asymptotic Analysis of $Y(\lambda; x)$ for $(\Theta_0, \Theta_\infty)$ Large: Basic Principles

In light of the explicit and trivial relation (2.2) between $u_{\rm F}^{[2]}(x;m,n)$ and $u_{\rm F}^{[1]}(x;m,n)$ for both families F=gH and F=gO, to prove our results it will be sufficient to consider only rational solutions of types 1 and 3. Moreover, since (2.5) and (3.2) together imply that the rational solutions of both types 1 and 3 are simultaneously encoded in Riemann–Hilbert Problem 1, it is only necessary to study the latter problem in the situation that the parameters $(\Theta_0, \Theta_\infty)$ correspond to a rational solution of type 3 in either family.

We therefore assume that the parameters $(\Theta_0, \Theta_\infty)$ are large in either $\Lambda_{gO} \cap (W^{[3]+} \cup W^{[3]-})$ or $\Lambda_{gH}^{[3]+}$ for the gO and gH families, respectively. This implies that, in terms of the parameters T, s, κ from (1.13), T > 0 will be the large parameter and $\kappa \in (-1, 1)$. For the gO family we allow both signs $s = \pm 1$ for Θ_0 to access



both sectors $W^{[3]\pm}$, while for the gH family it is enough to consider only s=1 since $\Lambda_{\rm gH}^{[3]+}\subset W^{[3]+}$. In this section we introduce the basic principles underpinning the asymptotic analysis of rational Painlevé-IV solutions using Riemann–Hilbert Problem 1 together with Theorems 5 and 6. We bring the scalings from Sect. 1.3 into the Riemann–Hilbert problem in Sect. 4.1, introduce the key contour deformations in Sect. 4.2, and explain the key notion of spectral curves in Sects. 4.3–4.4.

4.1 Scaling of Riemann-Hilbert Problem 1

Recalling the parametrization (1.13) of $(\Theta_0, \Theta_\infty)$ by T, s, κ , it is convenient to introduce the following scalings into the solution $\mathbf{Y}(\lambda; x)$ of Riemann–Hilbert Problem 1:

$$x = T^{1/2}X$$
, $X = \mu + T^{-1}\zeta$, and $\lambda = \frac{1}{2}T^{1/2}z$. (4.1)

We set $\mathbf{M}^{(T,s,\kappa)}(z;X) := (\frac{1}{2}T^{1/2})^{-\kappa T\sigma_3}\mathbf{Y}(\lambda;x)$, and we write $\mathbf{M}(z) = \mathbf{M}^{(T,s,\kappa)}(z;X)$ when we wish to suppress the dependence on parameters. Then under the scalings (4.1) the exponent in the jump conditions of Riemann–Hilbert Problem 1 becomes

$$\lambda^2 + 2x\lambda = 2T\phi(z;\mu) + \zeta z, \quad \phi(z;\mu) := \frac{1}{8}z^2 + \frac{1}{2}\mu z, \tag{4.2}$$

and $\mathbf{M}(z)z^{-sT\sigma_3}$ is bounded as $z\to 0$ while $\mathbf{M}(z)z^{-\kappa T\sigma_3}\to \mathbb{I}$ as $z\to \infty$. Because the jump matrices on all arcs of Σ are all entire functions of λ and are cyclically consistent at all self-intersection points in $\mathbb{C}\setminus\{0\}$ due to the consistency relations (3.20), by elementary substitutions in the four sectors between the circles of radius $|z|=\frac{1}{2}T^{1/2}$ and |z|=1 we may simply take the jump contour for $\mathbf{M}(z)$ to again be the original unscaled jump contour Σ , now in the z-plane. Since the constant pre-factor $(\frac{1}{2}T^{1/2})^{-\kappa T\sigma_3}$ does not affect any jump conditions, the jump matrices for $\mathbf{M}(z)$ are precisely the same as those of $\mathbf{Y}(\lambda;x)$ on the same arcs of Σ except that the exponents are replaced in each case according to (4.2), and Θ_0 and Θ_∞ are replaced with sT and $-\kappa T$, respectively.

Remark 11 Given a family F = gO or F = gH, the parameters T, s, κ , and the auxiliary variable X appearing in $\mathbf{M}(z) = \mathbf{M}^{(T,s,\kappa)}(z;X)$ are naturally related to the function $u(x) = u_F^{[3]}(x;m,n)$ solving the Painlevé-IV equation (1.1) for parameters $(\Theta_0,\Theta_\infty) = (\Theta_{0,F}^{[3]}(m,n),\Theta_{\infty,F}^{[3]}(m,n))$. To study the function $u_{gH}^{[3]}(x;m,n)$, we therefore relate these quantities to the integer parameters $(m,n) \in \mathbb{Z}_{>0}^2$ by

$$T := \frac{1}{2} + \frac{1}{2}(m+n), \quad s := +1, \quad \kappa := -\frac{1+n-m}{1+m+n},$$

$$x = \sqrt{\frac{1+m+n}{2}}\mu + \sqrt{\frac{2}{1+m+n}}\zeta,$$
(4.3)

and observe that as $m, n \to +\infty$ with $n = \rho m$ for a fixed aspect ratio $\rho > 0, T \to \infty$ and $\kappa \to (1 - \rho)/(1 + \rho) \in (-1, 1)$. Likewise, to study the function $u_{\sigma O}^{[3]}(x; m, n)$,



for integer parameters $(m, n) \in \mathbb{Z}_{>0}^2$ with mn > 0 we use instead

$$T := \left| \frac{1}{6} + \frac{1}{2}(m+n) \right|, \quad s := \operatorname{sgn}(m+n), \quad \kappa := -\frac{3+3n-3m}{|1+3m+3n|},$$

$$x = \sqrt{\frac{|1+3m+3n|}{6}} \mu + \sqrt{\frac{6}{|1+3m+3n|}} \zeta, \tag{4.4}$$

and observe that as $m, n \to \infty$ with $n = \rho m$ for a fixed aspect ratio $\rho > 0, T \to \infty$ and $\kappa \to \operatorname{sgn}(m+n)(1-\rho)/(1+\rho) \in (-1,1)$.

However, the function $u_{\rm F}^{[1]}(x;m,n)$ satisfies (1.1) for different parameters, namely for $(\Theta_0, \uparrow, \Theta_{\infty}, \uparrow) = (\Theta_{0,{\rm F}}^{[1]}(m,n), \Theta_{\infty,{\rm F}}^{[1]}(m,n))$ related to $(\Theta_0, \Theta_{\infty})$ via the symmetry \mathcal{S}_{\uparrow} defined in (2.4). Writing $(\Theta_0, \Theta_{\infty})$ in terms of the integer indices (m,n) for this function therefore requires inverting the mapping \mathcal{S}_{\uparrow} on the parameters as follows. For the function $u_{\uparrow}(x) = u_{\rm gH}^{[1]}(x;m,n)$, the parameters in Riemann–Hilbert Problem 1 become

$$(\Theta_0, \Theta_{\infty}) = \mathcal{S}_{\mathbb{Q}}^{-1} \circ (\Theta_{0, gH}^{[1]}(m, n), \Theta_{\infty, gH}^{[1]}(m, n)) = (\frac{1}{2}m + \frac{1}{2}n, -\frac{1}{2}m + \frac{1}{2}n), (4.5)$$

yielding for M(z) the parameters

$$T := \frac{1}{2}(m+n), \quad s = +1, \quad \kappa := \frac{m-n}{m+n},$$
 (4.6)

in which $T \to +\infty$ and $\kappa = (1-\rho)/(1+\rho) \in (-1,1)$ as $m,n \to +\infty$ with $n=\rho m$, while for the function $u \in (x) = u_{\mathrm{gO}}^{[1]}(x;m,n)$, we have instead

$$(\Theta_0, \Theta_\infty) = \mathcal{S}_{\mathbb{Q}}^{-1} \circ (\Theta_{0, gO}^{[1]}(m, n), \Theta_{\infty, gO}^{[1]}(m, n)) = (-\frac{1}{3} + \frac{1}{2}m + \frac{1}{2}n, -\frac{1}{2}m + \frac{1}{2}n),$$

$$(4.7)$$

yielding

$$T := \frac{1}{2}|m+n-\frac{2}{3}|, \quad s = \operatorname{sgn}(m+n), \quad \kappa := \frac{m-n}{|m+n-\frac{2}{3}|}$$
 (4.8)

in which $T \to +\infty$ and $\kappa \to \text{sgn}(m+n)(1-\rho)/(1+\rho)$ as $m, n \to \infty$ with mn > 0 and $n = \rho m$. We emphasize that in this case, $(\Theta_0, \Theta_\infty)$ are *not* the parameters in (1.1) for which the indicated type-1 function satisfies the Painlevé-IV equation, but they are the parameters in Riemann–Hilbert Problem 1 for which this function is encoded as $u_{\hat{\tau}}(x)$ given by (3.2).

The analysis we present in the rest of this section and in Sects. 5–7 will refer to the quantities T, s, and κ defined as above depending on which family and type of rational function is being considered. A remaining issue in interpreting the results of a large-T asymptotic analysis of $\mathbf{M}(z)$ is that while it is natural in light of the scalings (1.13) to write x in the form $x = T^{1/2}\mu + T^{-1/2}\zeta$ as indicated above for the type-3 rational solutions, for the type-1 rational functions in the family F we need to use $|\Theta_{0,F}^{[1]}(m,n)|$



in place of $|\Theta_0|$ in defining μ and ζ . This amounts to replacing

$$\mu \text{ with } \sqrt{\frac{|\Theta_{0,F}^{[1]}(m,n)|}{|\Theta_{0}|}} \mu \text{ and } \zeta \text{ with } \sqrt{\frac{|\Theta_{0}|}{|\Theta_{0,F}^{[1]}(m,n)|}} \zeta$$
 (4.9)

in all final formulæ. Note that using Tables 1 and 2, and taking Θ_0 to be given by (4.5) or (4.7) respectively,

$$\frac{|\Theta_{0,gH}^{[1]}(m,n)|}{|\Theta_0|} = \frac{n}{m+n} \quad \text{and} \quad \frac{|\Theta_{0,gO}^{[1]}(m,n)|}{|\Theta_0|} = \frac{n-\frac{1}{3}}{m+n-\frac{2}{3}}.$$
 (4.10)

Equivalently, since $\Theta_{0,F}^{[1]}(m,n) = \Theta_{0,\uparrow}$, in terms of the parameters s and κ related to the indices (m,n) for the F=gH and F=gO families by (4.6) and (4.8) respectively,

$$\frac{|\Theta_{0,F}^{[1]}(m,n)|}{|\Theta_{0}|} = \frac{1}{2}(1 - s\kappa). \tag{4.11}$$

4.2 Trivially Equivalent Riemann–Hilbert Problems for M(z)

Here we describe how the jump contour for $\mathbf{M}(z) = \mathbf{M}^{(T,s,\kappa)}(z;X)$ with $X = \mu + T^{-1}\zeta$ can be usefully modified beyond mere rescaling, depending on the values of the parameters s, κ , and μ . Importantly, we will assume that the modified contour, also denoted Σ , is independent of both the large parameter $T \gg 1$ and the value of ζ .

4.2.1 The gO Case

To study M(z) in the case that the monodromy data corresponds to the family of gO rational solutions of Painlevé-IV (see Theorem 5 in Sect. 3.1), by a similar argument using analyticity of jump matrices and cyclic consistency at nonzero self-intersection points, the jump contour Σ can be replaced by a qualitatively similar jump contour consisting of

- an arbitrary Jordan curve C enclosing the origin and divided into arcs Σ_j , j = 1, 2, 3, 4 (the indicated sub-arcs are homeomorphic in $\mathbb{C} \setminus \{0\}$ with the corresponding curves on the unit circle shown in Fig. 13),
- an arbitrary simple arc Σ_0 in the interior of C that connects the junction point of Σ_3 and Σ_4 to the origin, and
- four arbitrary disjoint simple arcs $\Sigma_{j,k}$, unbounded in one direction and connecting $z = \infty$ with the junction point of Σ_j and Σ_k such that the approach to $z = \infty$ is in the (vertical or horizontal) direction shown in Fig. 13.

In general, the union of Σ_0 and $\Sigma_{4,3}$ should be taken as the branch cut for the functions $z^{-sT\sigma_3}$ and $z^{-\kappa T\sigma_3}$, and the branches of these functions remain principal for sufficiently



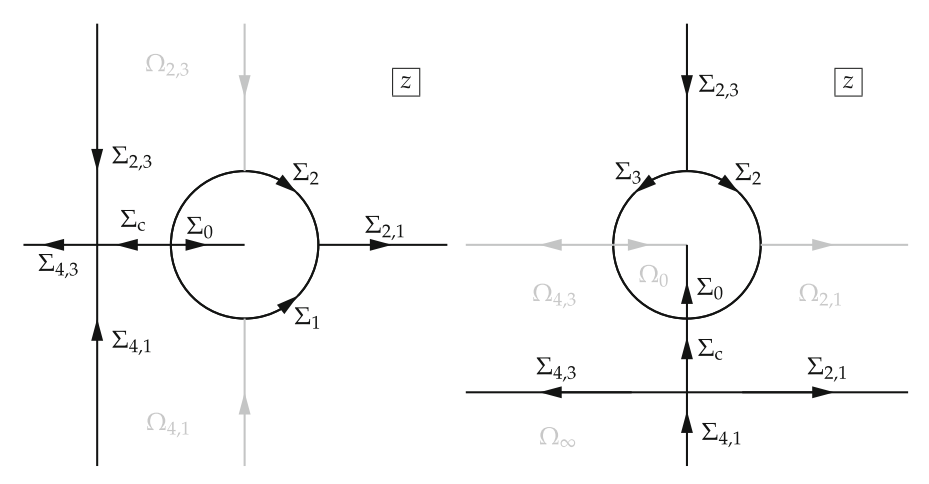


Fig. 15 Left: the jump contour for the "leftward" deformation of M(z). Right: the jump contour for the "downward" deformation of M(z)

large |z|. The formula for the jump matrix on each arc of Σ after the deformation is exactly the same in each case as before the deformation.

It will be useful to introduce two modifications of the Riemann–Hilbert conditions for $\mathbf{M}(z)$ that do not preserve the topology of Σ .

Beginning with the jump contour shown in Fig. 13 and referring to the left-hand panel of Fig. 15 we define a "leftward" deformation of the jump contour for $\mathbf{M}(z)$ by making the following piecewise-analytic substitution in the domains $\Omega_{2,3}$ and $\Omega_{4,1}$ exterior to the unit circle in the *z*-plane (recall the notation (1.34)):

$$\begin{split} \mathbf{M}(z) &\mapsto \mathbf{M}(z)\mathbf{U}(-\tfrac{1}{2}\mathrm{i}\mathrm{e}^{2T\phi(z;\mu)+\zeta z}), \quad z \in \Omega_{2,3}, \\ \mathbf{M}(z) &\mapsto \mathbf{M}(z)\mathbf{U}(\tfrac{1}{2}\mathrm{i}\mathrm{e}^{2T\phi(z;\mu)+\zeta z}), \quad z \in \Omega_{4,1}, \end{split}$$

and elsewhere we leave $\mathbf{M}(z)$ unchanged. This results in the same jump conditions as indicated in Riemann–Hilbert Problem 1 with monodromy data taken from (3.3)–(3.4) on the corresponding labeled arcs (but in the *z*-plane, and with the exponents modified as indicated in (4.2)), and a new jump condition on the arc labeled Σ_c in the left-hand panel of Fig. 15, namely

$$\mathbf{M}_{+}(z) = \mathbf{M}_{-}(z)e^{-2\pi i T\kappa}\mathbf{T}(2ie^{-2T\phi(z;\mu)-\zeta z}), \quad z \in \Sigma_{c}.$$

Likewise, referring to the right-hand panel of Fig. 15 we can define a "downward" deformation of the jump contour for $\mathbf{M}(z)$ by making the following analytic substitutions in the indicated domains:

$$\begin{split} \mathbf{M}(z) &\mapsto \mathbf{M}(z) \mathrm{e}^{2\pi \mathrm{i} s T \sigma_3}, \quad z \in \Omega_0, \\ \mathbf{M}(z) &\mapsto \mathbf{M}(z) \mathrm{e}^{2\pi \mathrm{i} T \kappa} \mathbf{L}(-2\mathrm{i} \mathrm{e}^{-2T\phi(z;\mu)-\zeta z}), \quad z \in \Omega_{4,3}, \\ \mathbf{M}(z) &\mapsto \mathbf{M}(z) \mathbf{L}(2\mathrm{i} \mathrm{e}^{-2T\phi(z;\mu)-\zeta z}), \quad z \in \Omega_{2,1}, \end{split}$$



and

$$\mathbf{M}(z) \mapsto \mathbf{M}(z)e^{2\pi i T\kappa}, \quad z \in \Omega_{\infty}.$$
 (4.12)

Once again, the resulting jump conditions on the arcs labeled as in Fig. 13 correspond to those in Riemann–Hilbert Problem 1 with monodromy data given in (3.3)–(3.4), except on the arcs $\Sigma_{4,3}$ and $\Sigma_{4,1}$ where we have instead

$$\begin{aligned} \mathbf{M}_{+}(z) &= \mathbf{M}_{-}(z)\mathbf{L}(2i\mathrm{e}^{-2T\phi(z;\mu)-\zeta z}), \quad z \in \Sigma_{4,3}, \\ \mathbf{M}_{+}(z) &= \mathbf{M}_{-}(z)\mathrm{e}^{2\pi\mathrm{i}T\kappa}\mathbf{U}(-\frac{1}{2}\mathrm{i}\mathrm{e}^{2T\phi(z;\mu)+\zeta z}), \quad z \in \Sigma_{4,1}, \end{aligned}$$

(as the substitution (4.12) effectively moves the scalar factor $e^{-2\pi i T \kappa}$ from the jump across $\Sigma_{4,3}$ to that across $\Sigma_{4,1}$) and there is a new jump condition across the arc labeled Σ_c in the right-hand panel of Fig. 15 that reads

$$\mathbf{M}_{+}(z) = \mathbf{M}_{-}(z)e^{2\pi i T\kappa}\mathbf{T}(-2ie^{-2T\phi(z;\mu)+\zeta z}), \quad z \in \Sigma_{c}.$$

In interpreting the conditions on $\mathbf{M}(z)$ as z tends to 0 and ∞ , one should now replace the principal branch power functions $z^{-sT\sigma_3}$ and $z^{-T\kappa\sigma_3}$ by branches with $\arg(z) \in (-\frac{\pi}{2}, \frac{3\pi}{2})$.

In the case of both deformations, one can subsequently replace the unit circle in the z-plane by any Jordan curve enclosing the origin, and employ similar contour deformations that respect the topology and direction of approach to $z=\infty$. In the case of the leftward deformation, the union of the deformations of Σ_0 , Σ_c , and $\Sigma_{4,3}$ should be taken as the branch cut of $z^{-sT\sigma_3}$ and $z^{-T\kappa\sigma_3}$, which should then be interpreted via $\arg(z)\in(-\pi,\pi)$ near $z=\infty$. In the case of the downward deformation, the union of the deformations of Σ_0 , Σ_c , and $\Sigma_{4,1}$ form the branch cut of these functions, which are to be interpreted via $\arg(z)\in(-\frac{\pi}{2},\frac{3\pi}{2})$ near $z=\infty$.

4.2.2 The gH Case

When we consider the matrix $\mathbf{M}(z)$ connected to the solution of Riemann–Hilbert Problem 1 with gH monodromy data given in Theorem 6 of Sect. 3.1, there is a corresponding dramatic simplification of the rescaled jump contour as described in Remark 6 from the same section. Indeed, the rescaled version of Σ can be taken to appear exactly as shown in Fig. 14, but now in the z-plane. Here there will be no need for deformations that change the topology of the jump contour, but as in the gO case we may always replace the unit circle in the z-plane with any Jordan curve C enclosing the origin, and we may replace the contour arcs lying on the negative real line with arcs still denoted Σ_0 and $\Sigma_{4,3}$ making up any simple curve that connects z=0 with $z=-\infty$ and that intersects C only at one point. The branch cuts of $z^{-sT\sigma_3}$ and $z^{-\kappa T\sigma_3}$ are then taken to coincide with the latter curve, and the branches are chosen to be principal for large |z|.



4.3 Spectral Curve and g-Function

The analysis in this section applies equally to the matrix M(z) in all configurations of Σ , regardless of whether Riemann–Hilbert Problem 1 from Sect. 3.1 describes gO or gH rational solutions of Painlevé-IV. Indeed, the fact that one can use the same theory of spectral curves to study both families of rational solutions is one of the main advantages of putting both families on the same footing via Riemann–Hilbert Problem 1.

Let $g: \mathbb{C} \setminus \Sigma \to \mathbb{C}$ be analytic with continuous boundary values such that g'(z) is also such a function, and moreover, for some constants g_0 and g_∞ ,

$$g(z) = \begin{cases} -s \log(z) + g_0 + \mathcal{O}(z), & z \to 0, \\ -\kappa \log(z) + g_\infty + \mathcal{O}(z^{-1}), & z \to \infty \end{cases}$$

$$\implies g'(z) = \begin{cases} -sz^{-1} + \mathcal{O}(1), & z \to 0, \\ -\kappa z^{-1} + \mathcal{O}(z^{-2}), & z \to \infty. \end{cases}$$
(4.13)

Here the branch of $\log(z)$ corresponds to the definition of the power functions $z^{-sT\sigma_3}$ and $z^{-T\kappa\sigma_3}$ as indicated in Sect. 4.2. We assume that, like the jump contour Σ , g may depend parametrically on s, κ , and μ , but not on $T \gg 1$ or ζ .

Given such a function, from $\mathbf{M}^{(T,s,\kappa)}(z;X)$ with $X = \mu + T^{-1}\zeta$ we define a new unknown denoted $\mathbf{N}(z) = \mathbf{N}^{(T,s,\kappa)}(z;\mu,\zeta)$ by the substitution

$$\mathbf{N}(z) := e^{-Tg_{\infty}\sigma_3} \mathbf{M}(z) e^{Tg(z)\sigma_3}, \quad z \in \mathbb{C} \setminus \Sigma.$$
 (4.14)

Note that from (4.13), $\mathbf{N}(z) \to \mathbb{I}$ as $z \to \infty$. The induced jump conditions for $\mathbf{N}(z)$ will involve exponentials on the diagonal elements with exponents $\pm T \Delta g(z)$ and on the off-diagonal elements with exponents $\pm 2T(\langle g \rangle(z) - \phi(z; \mu)) \mp \zeta z$ where $\Delta g(z)$ and $\langle g \rangle(z)$ are defined in terms of the boundary values $g_{\pm}(z)$ taken on an arc of Σ as in Sect. 1.5. Assuming that Σ is partitioned into arcs independent of both $T \gg 1$ and ζ in which either $\Delta g(z) = g_{+}(z) - g_{-}(z)$ or $2(\langle g \rangle(z) - \phi(z; \mu)) = g_{+}(z) + g_{-}(z) - 2\phi(z; \mu)$ is independent of z, we easily see that the function $(g'(z) - \phi'(z; \mu))^2$ has no jump across any of the arcs of Σ and hence is a function analytic for $z \in \mathbb{C} \setminus \{0\}$. To identify this function, we use (4.2) and (4.13) to examine its behavior near z = 0:

$$(g'(z) - \phi'(z; \mu))^2 = (-sz^{-1} + \mathcal{O}(1))^2 = z^{-2} + \mathcal{O}(z^{-1}), \quad z \to 0,$$
 (4.15)

and near $z = \infty$:

$$(g'(z) - \phi'(z; \mu))^{2} = \left(-\frac{1}{4}z - \frac{1}{2}\mu - \kappa z^{-1} + \mathcal{O}(z^{-2})\right)^{2}$$
$$= \frac{1}{16}z^{2} + \frac{1}{4}\mu z + \left(\frac{1}{4}\mu^{2} + \frac{1}{2}\kappa\right) + \mathcal{O}(z^{-1}), \quad z \to \infty.$$
(4.16)



By Liouville's Theorem it therefore follows that if $\frac{1}{8}E$ denotes the common coefficient of z^{-1} in (4.15) and (4.16), then

$$(g'(z) - \phi'(z; \mu))^2 = \frac{1}{16}z^2 + \frac{1}{4}\mu z + \left(\frac{1}{4}\mu^2 + \frac{1}{2}\kappa\right) + \frac{1}{8}Ez^{-1} + z^{-2}$$

$$= \frac{1}{16z^2}P(z),$$
(4.17)

where $P(\cdot)$ is exactly the same quartic polynomial defined in (1.18). Replacing the left-hand side by v^2 , (4.17) is said to define the spectral curve relating $(z, v) \in \mathbb{C}^2$.

There are, in principle, five possible configurations for the quartic P(z), only three of which are consistent with our assumptions:

- {31}: Two distinct roots, one of multiplicity 3 and one simple. Suppose that $P(z) = (z \alpha)^3 (z \beta)$ for some $\alpha \neq \beta$. Comparing the coefficients and eliminating α and β shows that given $\kappa \approx \kappa_{\infty}$ with $\kappa_{\infty} \in (-1, 1)$, μ must be a root of the 8th degree polynomial (1.17) defining the branch points of equilibrium solutions U_0 (see (1.15) and Proposition 1 in Sect. 1.3; these are precisely the vertices visible in the plots in Fig. 5 from the same section). Given κ , for each of these eight points, the values of α , β , and E are uniquely determined.
- {211}: Three distinct roots, one double and two simple. Suppose that $P(z) = (z \alpha)(z \beta)(z \gamma)^2$ for distinct values α , β , and γ . Comparing the coefficients yields the system of equations

$$\alpha + \beta + 2\gamma = -4\mu$$

$$\alpha\beta + 2(\alpha + \beta)\gamma + \gamma^2 = 4(\mu^2 + 2\kappa)$$

$$2\alpha\beta\gamma + (\alpha + \beta)\gamma^2 = -2E$$

$$\alpha\beta\gamma^2 = 16.$$
(4.18)

Eliminating α and β between the first, second, and fourth equations gives the following quartic equation for γ :

$$Q(\gamma, \mu; \kappa) := \gamma^4 + \frac{8}{3}\mu\gamma^3 + \frac{4}{3}(\mu^2 + 2\kappa)\gamma^2 - \frac{16}{3} = 0.$$
 (4.19)

This is precisely the same as the equation (1.15) under the substitution $\gamma \mapsto U_0$, and hence the discriminant defining the branch points for γ is (1.17). From (1.16) we see that there are four distinct values of γ when μ is large, namely

$$\begin{split} \gamma &= 2\mu^{-1} + \mathcal{O}(\mu^{-2}), \quad \gamma = -2\mu^{-1} + \mathcal{O}(\mu^{-2}), \quad \gamma = -2\mu + \mathcal{O}(1), \quad \text{and} \\ \gamma &= -\frac{2}{3}\mu + \mathcal{O}(1), \quad \mu \to \infty. \end{split}$$



Given $\mu \in \mathbb{C}$, $\kappa \approx \kappa_{\infty}$ with $\kappa_{\infty} \in (-1, 1)$, and any root γ of (4.19), the values of E, α , and β (the latter up to permutation) are determined from

$$E = -16\gamma^{-1} + 2\mu\gamma^2 + \gamma^3$$
, $\alpha\beta = 16\gamma^{-2}$, $\alpha + \beta = -4\mu - 2\gamma$. (4.20)

According to Theorems 1–2 in light of Remark 3 from Sect. 1.3, this configuration will turn out to be relevant for $\mu \in \mathcal{E}_F(\kappa)$ depending on the family F = gH or F = gO.

- {1111}: Four distinct roots, all simple. Suppose that $P(z) = (z-\alpha)(z-\beta)(z-\gamma)(z-\delta)$ for distinct values α , β , γ , δ . This configuration again places no conditions on μ or κ , but now the constant E is also free, and some additional conditions need to be specified to relate it to μ and κ . These will be the *Boutroux conditions* to be introduced in Sect. 4.4 (see also (1.26)). This configuration will turn out to be relevant for μ in the bounded regions $\mathcal{B}_{\square}(\kappa)$, $\pm \mathcal{B}_{\triangleright}(\kappa)$, $\pm \mathcal{B}_{\triangle}(\kappa)$ introduced in Sect. 1.4.3.
 - {4}: One root of multiplicity 4. Suppose that $P(z) = (z \alpha)^4$ for some α . Comparing the coefficients and eliminating α shows easily that this form is consistent only if $\mu^4 = 16$ and $\kappa = \frac{1}{4}\mu^2$. But further eliminating $\mu^2 = \pm 4$ gives $\kappa = \pm 1$ which is inconsistent in the limit with $\kappa \to \kappa_\infty$ with $\kappa_\infty \in (-1, 1)$.
 - {22}: Two distinct double roots. Suppose that $P(z) = (z \alpha)^2 (z \beta)^2$ for some $\alpha \neq \beta$. Comparing the coefficients then yields, as in the case of a single root of multiplicity 4, that $\kappa = \pm 1$ which is inconsistent for large T with $\kappa_{\infty} \in (-1, 1)$.

Therefore, only cases $\{31\}$, $\{211\}$, and $\{1111\}$ will be relevant to our study going forward, and we will say that the spectral curve is of *class* $\{31\}$, $\{211\}$, or $\{1111\}$. In any of these cases, we can solve for g'(z) by introducing suitable bounded branch cuts between pairs of distinct roots of the quartic P(z) and defining a function R(z) analytic except on these cuts that satisfies

$$R(z)^{2} = P(z)$$
 and $R(z) = z^{2} + \mathcal{O}(z), z \to \infty.$ (4.21)

Then, in order to satisfy the necessary condition $g'(z) \to 0$ as $z \to \infty$ we need to take the square root in (4.17) precisely as follows:

$$g'(z) = \phi'(z; \mu) - \frac{1}{4}z^{-1}R(z).$$

That this formula also gives $g'(z) = -sz^{-1} + \mathcal{O}(1)$ as $z \to 0$ then requires in addition that R(0) = 4s, which we interpret as a condition on how the branch cuts of R(z) must be placed relative to the origin in order to achieve the correct sign of R(0). When it is necessary to emphasize the parameter dependence we will write $g(z) = g^{(s,\kappa)}(z;\mu)$ going forward. It will be convenient to define the related function $h(z) = h^{(s,\kappa)}(z;\mu)$ by

$$h^{(s,\kappa)}(z;\mu) := g^{(s,\kappa)}(z;\mu) - \phi(z;\mu) \implies h^{(s,\kappa)'}(z;\mu) = -\frac{R(z)}{4z}. \quad (4.22)$$



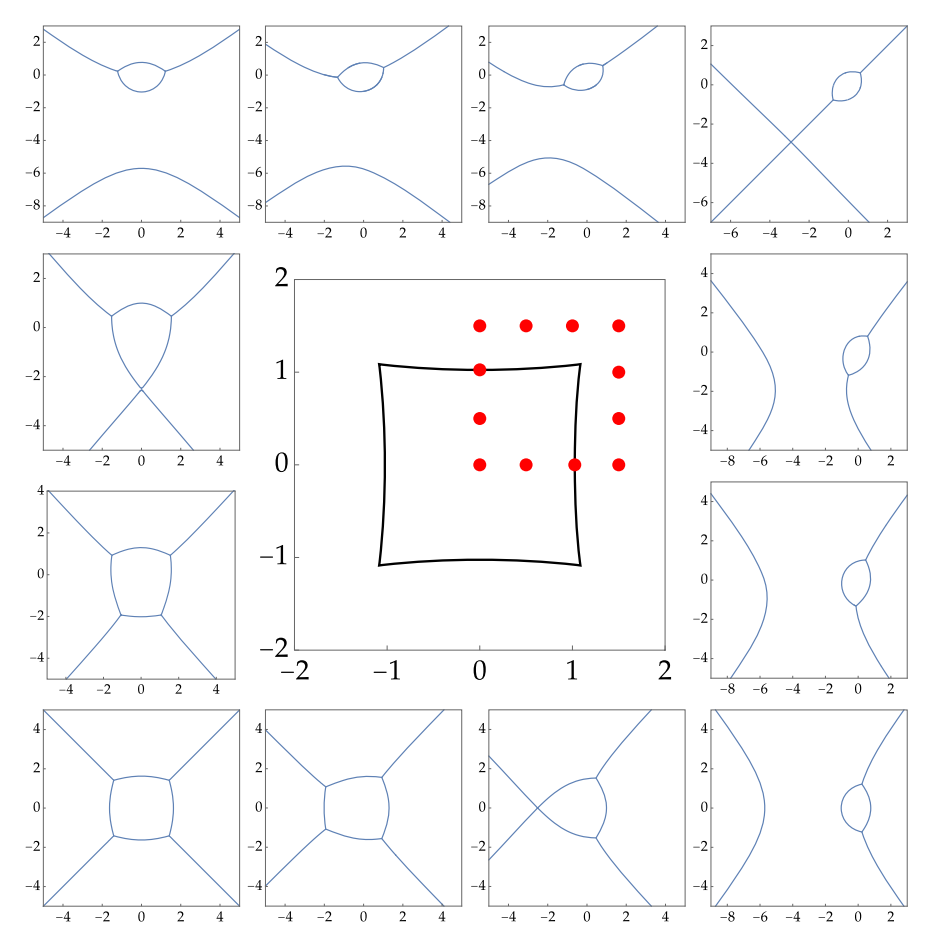


Fig. 16 Critical v-trajectories of $h'(z)^2$ d z^2 emanating from (for generic μ) simple roots of P(z) for $\kappa=0$ for the gH family. The same topological structure holds for $-1 < \kappa < 1$. Counterclockwise from top left: $\mu=1.5$ i, $\mu\approx1.0253$ i, $\mu=0.5$ i, $\mu=0.5$ i, $\mu=0.5$, $\mu\approx1.0253$, $\mu=1.5$, $\mu=1.5+0.5$ i, $\mu=1.5+i$, $\mu=1.5+1.5$ i, $\mu=1.5+1.5$ i, $\mu=0.5+1.5$ i. Inset: Boundary of $\mathcal{B}_{\square}(0)$ in the μ -plane. The μ -values corresponding to different trajectory plots are indicated by red dots (Color figure online)

A key role in our analysis will be played by certain trajectories of the quadratic differential $h'(z)^2 dz^2$, and how they depend on μ once the coefficient E is suitably determined as a function of μ for given κ and the family (gH or gO) of interest. We will deduce all of the needed properties theoretically below, but it is also easy to compute them numerically, so as a preview of what will come, we present plots of the trajectories connected to simple roots of P(z) (as well as trajectories connected to roots of higher multiplicity when those are also connected to simple roots) in Figs. 16 and 17.



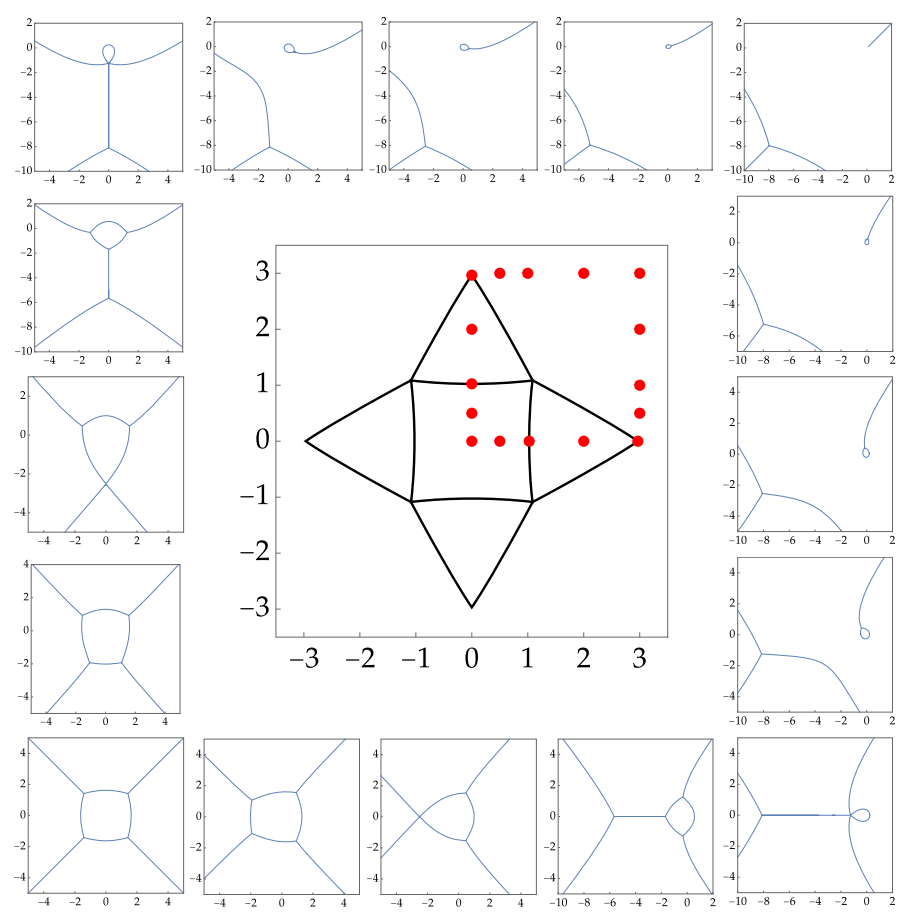


Fig. 17 Critical v-trajectories of $h'(z)^2\,\mathrm{d}z^2$ emanating from (for generic μ) simple roots of P(z) for $\kappa=0$ for the gO family. The same topological structure holds for $-1<\kappa<1$. Counterclockwise from top left: $\mu\approx2.96773$ i, $\mu=2$ i, $\mu\approx1.0253$ i, $\mu=0.5$ i, $\mu=0$, $\mu=0.5$, $\mu\approx1.0253$, $\mu=2$, $\mu\approx2.96773$, $\mu=3+1$, $\mu=3+1$, $\mu=3+2$ i, $\mu=3+3$ i, $\mu=2+3$ i, $\mu=1+3$ i, $\mu=0.5+3$ i. Inset: Boundaries of the regions $\mathcal{B}_{\square}(0)$, $\pm\mathcal{B}_{\triangleright}(0)$, and $\pm\mathcal{B}_{\triangle}(0)$ in the μ -plane. The μ -values corresponding to different trajectory plots are indicated by red dots. Note that the μ -values within the quasi-rectangle are the same as those in Fig. 16, and the corresponding trajectory plots also match exactly. This is one reason why the gO and gH rational solutions can be treated on the same footing (Color figure online)

4.4 Boutroux Curves

4.4.1 Boutroux Curves of Class {1111}

If the quartic P(z) is in the most general case {1111}, then comparing with (4.22), the rational equation $v^2 = h'(z)^2 = P(z)/(16z^2)$ defines the spectral curve \mathcal{R} as an elliptic curve (genus 1) parametrized by $\mu \in \mathbb{C}$, $\kappa \in (-1, 1)$, and $E \in \mathbb{C}$ (cf. (4.17)).



We will be interested in spectral curves satisfying the *Boutroux conditions* (cf. (1.26))

$$\operatorname{Re}\left(\oint_{\mathfrak{a}}v\,\mathrm{d}z\right)=0$$
 and $\operatorname{Re}\left(\oint_{\mathfrak{b}}v\,\mathrm{d}z\right)=0$ (4.23)

where $\mathfrak a$ and $\mathfrak b$ are representatives of a canonical basis of homology cycles on $\mathcal R$ chosen not to pass through any poles of v (at the two points each over $z=0,\infty$). Note that although the differential v dz has residues at these four points, they are all purely real (± 1 for the points over z=0 and $\pm \kappa$ for the points over $z=\infty$) so the Boutroux conditions depend only on the homology classes of the cycles $\mathfrak a$ and $\mathfrak b$. Moreover, since ($\mathfrak a$, $\mathfrak b$) is a basis for the homology group of $\mathcal R$, the conditions (4.23) taken together depend intrinsically on $\mathcal R$ itself. We will determine E as a function of μ and κ such that $\mathcal R$ satisfies (4.23), making it a *Boutroux curve*.

4.4.2 Continuation of Boutroux Curves

If a homology basis $(\mathfrak{a}, \mathfrak{b})$ is specified on a given curve \mathcal{R} , then letting $E_R := \text{Re}(E)$ and $E_I := \text{Im}(E)$, the following functions are locally defined:

$$f_{\mathfrak{a},\mathfrak{b}}(E_{\mathbf{R}}, E_{\mathbf{I}}; \mu, \kappa) := \operatorname{Re}\left(\oint_{\mathfrak{a},\mathfrak{b}} v \,\mathrm{d}z\right).$$

The Boutroux conditions (4.23) then read $f_{\mathfrak{a}}(E_{R}, E_{I}; \mu, \kappa) = f_{\mathfrak{b}}(E_{R}, E_{I}; \mu, \kappa) = 0$. A direct calculation then shows that

$$\frac{\partial f_{\mathfrak{a},\mathfrak{b}}}{\partial E_{\mathbf{R}}} = \frac{1}{4} \operatorname{Re} \left(\oint_{\mathfrak{a},\mathfrak{b}} \frac{\mathrm{d}z}{4zv} \right) \quad \text{and} \quad \frac{\partial f_{\mathfrak{a},\mathfrak{b}}}{\partial E_{\mathbf{I}}} = -\frac{1}{4} \operatorname{Im} \left(\oint_{\mathfrak{a},\mathfrak{b}} \frac{\mathrm{d}z}{4zv} \right).$$

It follows that the Jacobian of (f_a, f_b) with respect to (E_R, E_I) is

$$\frac{\partial (f_{\mathfrak{a}},\,f_{\mathfrak{b}})}{\partial (E_{\mathsf{R}},\,E_{\mathsf{I}})} = \frac{1}{16} \mathrm{Im}(Z_{\mathfrak{a}}Z_{\mathfrak{b}}^{*}), \quad Z_{\mathfrak{a}} := \oint_{\mathfrak{a}} \frac{\mathrm{d}z}{4zv} \quad Z_{\mathfrak{b}} := \oint_{\mathfrak{b}} \frac{\mathrm{d}z}{4zv}.$$

Since $\mathrm{d}z/(4zv)$ is up to scaling the unique nonzero holomorphic differential on the elliptic curve \mathcal{R} , it follows from [31, Corollary 1] that $\partial(f_\mathfrak{a}, f_\mathfrak{b})/\partial(E_R, E_I)$ is finite and nonzero whenever \mathcal{R} is a smooth elliptic curve, i.e., whenever the quartic polynomial P(z) is in case {1111}, having four distinct roots. Therefore, starting from a known solution $(E_R, E_I) = (E_R^\#, E_I^\#)$ of the Boutroux equations (4.23) for $\mu = \mu^\#$ and $-1 < \kappa < 1$ such that \mathcal{R} is a nonsingular curve, the Implicit Function Theorem guarantees that we may uniquely continue this solution along a path in the μ -plane emanating from $\mu = \mu^\#$ until \mathcal{R} degenerates from class {1111} to either class {31} or {211} under continuation. A spectral curve that lies at the terminal endpoint of such a maximal path is called a *degenerate Boutroux curve*.

⁸ The Jacobian is proportional to the area of a fundamental period parallogram formed by the complex periods $Z_{a,b}$.



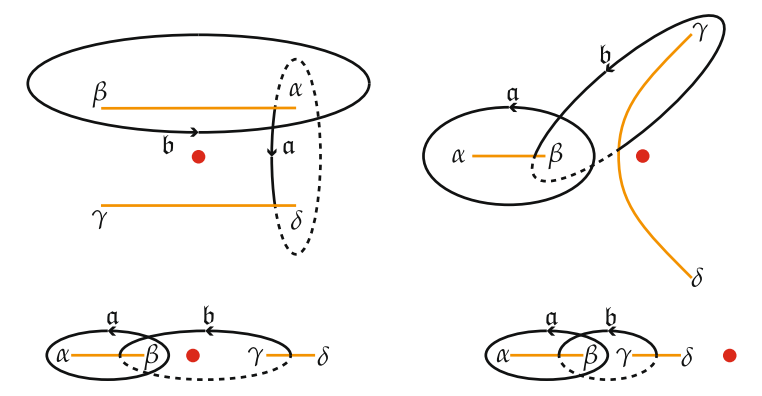


Fig. 18 Four configurations of branch points and homology cycles for spectral curves with $\mu=\mu_R$ and $E=E_R$ real. The canonical $\mathfrak a$ and $\mathfrak b$ cycles (solid black curves) on the sheet of $\mathcal R$ on which v is a single-valued analytic function of z with branch cuts (orange) connecting the branch points in pairs, and such that $v\sim\frac14z$ as $z\to\infty$. Part of the $\mathfrak a$ cycle (dashed) is on the other sheet, on which v has the opposite sign. The red dot is the origin (Color figure online)

4.4.3 Boutroux Curves for μ on the Real or Imaginary Axes

Given $\kappa \in (-1, 1)$, we claim that whenever $\mu = \mu_R \in \mathbb{R}$ there is a unique (possibly degenerate) Boutroux curve \mathcal{R} for which E is real, i.e., $E_I = 0$. Indeed, if both μ and E are real it follows easily that the quartic polynomial P(z) is Schwarz symmetric: $P(z^*) = P(z)^*$. Let us assume for the moment that the spectral curve for such μ and E is of class {1111} so that P(z) has four distinct roots. These roots necessarily come in complex-conjugate or real pairs.

We first simplify the Boutroux conditions (4.23) under the additional assumption that there are no real roots, and without loss of generality we let α and β denote the roots in the upper half-plane, and assume that $\gamma = \beta^*$ and that $\delta = \alpha^*$. We define v(z) as a function satisfying $v^2 = P(z)/(16z^2)$ that is analytic apart from z = 0 and a Schwarz-symmetric system of two branch cuts, one of which lies in the upper half-plane joining α and β , and that satisfies $v(z) = \frac{1}{4}z + \frac{1}{2}\mu_R + \kappa z^{-1} + \mathcal{O}(z^{-2})$ as $z \to \infty$. Then we select a homology basis $(\mathfrak{a},\mathfrak{b})$ compatible with the canonical intersection condition $\mathfrak{a} \circ \mathfrak{b} = 1$ that topologically matches the diagram in the upper left-hand panel of Fig. 18.

Taking \mathfrak{a} to be Schwarz-symmetric up to orientation we easily see from $v(z^*) = v(z)^*$ that $\oint_{\mathfrak{a}} v \, dz$ is purely imaginary, i.e., $f_{\mathfrak{a}}(E_{\mathrm{R}}, 0; \mu_{\mathrm{R}}, \kappa) = 0$ holds automatically. To simplify the remaining Boutroux condition, we first apply Cauchy's Theorem to write

$$\oint_{b} v(z) dz = \oint_{b} \left[v(z) - \frac{1}{4}z - \frac{1}{2}\mu_{R} \right] dz.$$
 (4.24)

The integrand satisfies $v(z) - \frac{1}{4}z - \frac{1}{2}\mu_R = \kappa z^{-1} + \mathcal{O}(z^{-2})$ as $z \to \infty$ and has a simple pole at z=0 with real residue, so by enlarging the loop $\mathfrak b$ to consist of a path from z=-L to z=L indented above the pole at the origin together with a semicircular path from z=L to z=L in the upper half-plane, and letting $L\to +\infty$ we find



that

$$f_{\mathfrak{b}}(E_{R}, 0; \mu_{R}, \kappa) = P.V. \int_{\mathbb{R}} \left[v(z) - \frac{1}{4}z - \frac{1}{2}\mu_{R} \right] dz$$

$$= P.V. \int_{\mathbb{R}} \left[\frac{\sqrt{P(z)}}{4z} - \frac{1}{4}z - \frac{1}{2}\mu_{R} \right] dz$$
(4.25)

where the positive square root is meant, and the principal value exclusions occur both at z = 0 and $z = \infty$.

Next suppose that P(z) has exactly two real roots. Then it follows from the fact that $P(0) = 16 \neq 0$ that both real roots have the same sign. We define a single-valued function v(z) by $v(z)^2 = P(z)/(16z^2)$, $v(z) = \frac{1}{4}z + \frac{1}{2}\mu_R + \mathcal{O}(z^{-1})$ as $z \to \infty$ with v(z) analytic except for a branch cut chosen to connect the two real roots of P(z)and another connecting the conjugate pair of roots of P(z), symmetric with respect to Schwarz reflection, and crossing the real axis vertically at a unique point between the origin and the real pair of roots. Then we equip R with a canonical homology basis (a, b) with representatives taken as in the upper right-hand panel of Fig. 18. Since $v(z) = v(z^*)^*$ takes imaginary boundary values on the real branch cut $[\alpha, \beta]$, $\oint_{\mathfrak{a}} v \, dz$ is purely imaginary so once again the condition $f_{\mathfrak{a}}(E_{\mathbb{R}}, 0; \mu_{\mathbb{R}}, \kappa)$ is satisfied automatically. Again using the identity (4.24), we deform the cycle b partly toward $z = \infty$ in the upper half-plane and partly toward the real axis from the upper half-plane. Using that the residues at z = 0 and $z = \infty$ are purely real, upon taking the real part of $\oint_{b} v \, dz$ we deduce the expression on the second line of (4.25) for $f_{b}(E_{R}, 0; \mu_{R}, \kappa)$ in which the square root $\sqrt{P(z)}$ is multiplied by the characteristic function of $\mathbb{R} \setminus [\alpha, \beta]$, i.e., the real intervals over which P(z) > 0 holds.

Finally, suppose that P(z) has four real roots. Then since P(0)=16>0 there are either two roots of each sign, or all roots have the same sign; we take the branch cuts of v(z) and homology basis representatives as shown in the lower left-hand and lower right-hand panels of Fig. 18 respectively. In both cases the fact that the boundary values of $v(z)=v(z^*)^*$ on the branch cut $[\alpha,\beta]$ are imaginary implies that the condition $f_{\mathfrak{a}}(E_R,0;\mu_R,\kappa)=0$ holds automatically. And in both cases the use of (4.24) admits a deformation of \mathfrak{b} toward $z=\infty$ in the upper half-plane and toward the real axis elsewhere. Using reality of the residues at $z=0,\infty$ we arrive again at the expression in the second line of (4.25) for $f_{\mathfrak{b}}(E_R,0;\mu_R,\kappa)$ in which the square root $\sqrt{P(z)}$ is multiplied by the characteristic function of the union of intervals $(-\infty,\alpha) \cup (\beta,\gamma) \cup (\delta,+\infty)$, i.e., where P(z)>0 holds on the real line.

We conclude that in all cases that \mathcal{R} is a class {1111} spectral curve corresponding to real μ and E, the Boutroux conditions (4.23) are satisfied provided only that $E = E_R \in \mathbb{R}$ satisfies the real equation

$$f_{\mathfrak{b}}(E_{\mathrm{R}}, 0; \mu_{\mathrm{R}}, \kappa) = \text{P.V.} \int_{\mathbb{R}} \left[\chi_{P(z) > 0}(z) \frac{\sqrt{P(z)}}{4z} - \frac{1}{4}z - \frac{1}{2}\mu_{\mathrm{R}} \right] dz = 0.$$
 (4.26)

Considering various limits in which a class {1111} curve degenerates to class {31} or class {211}, we see that (4.26) is also necessary for the degeneration to satisfy the Boutroux conditions when $P(z) = P(z^*)^*$ has fewer than four distinct roots.



Given $\kappa \in (-1, 1)$ and $\mu = \mu_R \in \mathbb{R}$, $f_b(E_R, 0; \mu_R, \kappa)$ is a continuous function of $E_R \in \mathbb{R}$, in which the dependence on $E = E_R$ in the integrand enters via P(z) in the form (1.18). Moreover, it follows from (4.26) that $f_b(E_R, 0; \mu_R, \kappa)$ is differentiable with respect to E_R whenever the roots of P are distinct, and that for such E_R ,

$$\frac{\partial f_{\mathfrak{b}}}{\partial E_{\mathbf{R}}}(E_{\mathbf{R}}, 0; \mu_{\mathbf{R}}, \kappa) = \frac{1}{4} \int_{\mathbb{R}} \chi_{P(z) > 0}(z) \frac{\mathrm{d}z}{\sqrt{P(z)}},\tag{4.27}$$

where the integral is absolutely convergent and positive. A simple discriminant calculation shows that points $E=E_{\rm R}\in\mathbb{R}$ for which the polynomial P(z) has fewer than four distinct roots are isolated. It is then clear that as $E_{\rm R}$ approaches any value that makes \mathcal{R} degenerate, the derivative (4.27) diverges to $+\infty$. Thus for each and $\kappa\in(-1,1)$ and $\mu=\mu_{\rm R}\in\mathbb{R}$, the function $E_{\rm R}\mapsto f_{\mathfrak b}$ is continuous and strictly monotone increasing on \mathbb{R} . Moreover, we have the following asymptotic behavior:

$$f_{\mathfrak{b}}(E_{\mathbf{R}}, 0; \mu_{\mathbf{R}}, \kappa) = \pm C|E_{\mathbf{R}}|^{2/3} + o(|E_{\mathbf{R}}|^{2/3}), \quad E_{\mathbf{R}} \to \pm \infty,$$

for all fixed real μ_R and κ , where the constant C is given by (taking the square roots to be positive)

$$C := \int_{-\infty}^{-2^{1/3}} \left(-\sqrt{\frac{w^4 + 2w}{16w^2}} - \frac{w}{4} \right) dw + \int_{-2^{1/3}}^{0} \left(-\frac{w}{4} \right) dw + \int_{0}^{+\infty} \left(\sqrt{\frac{w^4 + 2w}{16w^2}} - \frac{w}{4} \right) dw$$

$$\approx 1.25203 > 0.$$

Hence, by strict monotonicity and the Intermediate Value Theorem, there exists exactly one root $E_R = E_R(\mu_R, \kappa) \in \mathbb{R}$ for which $f_{\mathfrak{b}}(E_R, 0; \mu_R, \kappa) = 0$.

If $\mu=\mu_R=0$ and also $E_R=0$, then it is easy to see that for any $\kappa\in(-1,1)$ the integrand in (4.26) is odd and hence $E=E_R=0$ is the unique real solution of the Boutroux equations (4.23) for $\mu=0$. In this special case, $P(z)=z^4+8\kappa z^2+16$, the roots of which satisfy $z^2=-4\kappa\pm4\mathrm{i}\sqrt{1-\kappa^2}$, forming a complex-conjugate pair on the circle of radius $|z^2|=4$. Therefore, the four roots of P(z) form a quartet in the complex z-plane like in the configuration shown in the upper left-hand panel of Fig. 18 but with additional reflection symmetry in the imaginary axis, and lying on the circle of radius |z|=2. Introducing the parametrization

$$\kappa = \sin(\frac{1}{2}\varphi), \quad \varphi \in (-\pi, \pi),$$
(4.28)

so that also $\sqrt{1-\kappa^2}=\cos(\frac{1}{2}\varphi)>0$, the roots of P(z) are exactly $z=\alpha,\beta,\gamma,\delta,$ where

$$\begin{split} \alpha &= 2\mathrm{e}^{\mathrm{i}\varpi}, \quad \beta = -2\mathrm{e}^{-\mathrm{i}\varpi}, \quad \gamma = -2\mathrm{e}^{\mathrm{i}\varpi}, \quad \text{and} \quad \delta = 2\mathrm{e}^{-\mathrm{i}\varpi}, \\ \varpi &:= \frac{1}{4}(\varphi + \pi) \in (0, \frac{\pi}{2}). \end{split} \tag{4.29}$$



These are arranged in counterclockwise order about the origin.

We can just as easily obtain a unique Boutroux curve with E purely imaginary for every purely imaginary value of μ . Let $\mu=\mathrm{i}\mu_\mathrm{I}$ and $E=\mathrm{i}E_\mathrm{I}$ both be purely imaginary. Then it is clear that the polynomial P(z) has Schwarz reflection symmetry about the imaginary axis in the z-plane: $P(-z^*)=P(z)^*$. Following a similar approach as in the case of $\mu\in\mathbb{R}$, we find that one of the Boutroux conditions in (4.23) is trivially satisfied, while the other gives a real relation between $\mu_\mathrm{I}\in\mathbb{R}$ and $E_\mathrm{I}\in\mathbb{R}$ that can be solved uniquely for E_I by the Intermediate Value Theorem, yielding a continuous real map $\mu_\mathrm{I}\mapsto E_\mathrm{I}$. Moreover, it is not difficult to check that the Boutroux equations (4.23) are consistent with the symmetry

$$(\mu, \kappa, E) \mapsto (i\mu, -\kappa, -iE)$$
 (4.30)

which implies that whenever $E = E_R(\eta, \kappa) \in \mathbb{R}$ corresponds to $\mu = \eta \in \mathbb{R}$ and $\kappa \in (-1, 1), E = -iE_R(\eta, \kappa)$ corresponds to $\mu = i\eta \in i\mathbb{R}$ and the *opposite* parameter $-\kappa$.

4.4.4 Boutroux Domains on the Real and Imaginary Axes

Starting from the real and imaginary axes in the μ -plane, we may now try to follow the continuation procedure described in Sect. 4.4.2. Hence, for given $\kappa \in (-1,1)$, each point μ on the real (resp., imaginary) axis for which the unique Boutroux curve \mathcal{R} with real (resp., imaginary) E is of class {1111} has a simply connected neighborhood on which is defined a unique solution of the Boutroux equations (4.23) extending the on-axis curve \mathcal{R} . This immediately shows that the nondegenerate Boutroux curves appear on the axes in open intervals, each of which bisects a simply connected open region of the μ -plane supporting a smooth solution (Re(μ), Im(μ)) \mapsto (E_R , E_I) of (4.23). We call such a region a *Boutroux domain*. In particular, the origin $\mu=0$ is contained in a Boutroux domain for which E=0 at $\mu=0$. The mapping $\mu\mapsto E$ on a given Boutroux domain is decidedly non-analytic as can be seen by a direct calculation of the Cauchy-Riemann $\overline{\partial}$ derivative of E with respect to μ via implicit differentiation of (4.23) using a Riemann bilinear identity.

5 Asymptotic Analysis of M(z) for Sufficiently Large $|\mu|$: gO Case

In this section, we start to analyze the rational solutions of (1.1) for μ in the exterior domain. Although in Sect. 1.4 we presented the result for the gH family first, we begin here with the gO case which is more complicated. Then in Sect. 6 we will re-use much of this material to study the simpler gH case.

Fix $\kappa_{\infty} \in (-1,1)$, so that also κ is bounded away from ± 1 for T sufficiently large. To analyze $\mathbf{M}(z)$ for large $|\mu|$ with $-\epsilon < \arg(\mu) < \frac{\pi}{2} + \epsilon$ for some small $\epsilon > 0$, it suffices to take a polynomial P(z) in case {211}, and for the gO case we select the solution of the quartic (4.19) that satisfies $\gamma = U_{0,\mathrm{gO}}(\mu;\kappa) = -\frac{2}{3}\mu + \mathcal{O}(\mu^{-1})$ as $\mu \to \infty$ (see Sect. 1.3).



Definition 1 Let $\kappa \in (-1, 1)$. We denote by $\Gamma = \Gamma(\kappa)$ the Riemann surface of the quartic (4.19), i.e., the set of ordered pairs $(\mu, \gamma) \in \mathbb{C}^2$ satisfying $Q(\gamma, \mu; \kappa) = 0$.

The solution $\gamma=-\frac{2}{3}\mu+\mathcal{O}(\mu^{-1})$ can be analytically continued to finite values of μ on Γ along any path that avoids the branch points solving $B(\mu;\kappa)=0$. Corresponding to the asymptotic $\gamma=-\frac{2}{3}\mu+\mathcal{O}(\mu^{-1})$, from (4.18) we have (breaking permutation symmetry) $\alpha=-\frac{8}{3}\mu+\mathcal{O}(1)$ and $\beta=-\frac{27}{2}\mu^{-3}+\mathcal{O}(\mu^{-4})$ as $\mu\to\infty$.

Remark 12 In Sects. 5 and 6 we will set $\zeta = 0$. The parameter ζ is a tool useful for capturing rapid variations in the rational solutions that do not occur in the exterior domain studied in Sects. 5 and 6. Dependence on ζ is however useful in the analysis of rational solutions on Boutroux domains; see Sect. 7.

5.1 Analysis of the Exponent h(z)

The function $z\mapsto h'(z)=h^{(s,\kappa)'}(z;\mu)$ is well defined for $z\neq 0$ up to a sign, and moreover the formula $\varrho(z):=h'(z)^2=\frac{1}{16}z^{-2}P(z)=\frac{1}{16}z^{-2}(z-\gamma)^2(z-\alpha)(z-\beta)$ shows that h'(z) is meromorphic on a two-sheeted Riemann surface $\mathcal R$ over the z-plane having genus zero (a single branch cut connects α and β), with simple poles over z=0 and triple poles over $z=\infty$. It is easily checked that since $\kappa\in\mathbb R$, the residues at all four poles are purely real, so since $\mathcal R$ has genus zero it follows that by integration that $\operatorname{Re}(h(z))$ is single valued on $\mathcal R$ and harmonic away from the poles. It is determined up to a real integration constant which we choose so that $\operatorname{Re}(h(\alpha))=0$. Then $\operatorname{Re}(h(z))$ takes opposite signs on the two sheets of $\mathcal R$ at points corresponding to the same value of z and so also $\operatorname{Re}(h(\beta))=0$ as α and β are the only two points common to both sheets.

5.1.1 The Zero-Level Set of Re(h(z))

The zero-level curves of Re(h(z)) effectively lie on the z-plane by choice of integration constant. To determine their structure, and for other purposes throughout our paper, we use some theory of trajectories of rational quadratic differentials [39, 60], for which we give the following definition.

Definition 2 (*Trajectories of rational quadratic differentials*) Given a rational function $z\mapsto \varrho(z)$, a maximal smooth curve $\mathbb{R}\ni s\mapsto z(s)\in\mathbb{C}, |z'(s)|=1$, along which $\varrho(z(s))z'(s)^2<0$ (resp., $\varrho(z(s))z'(s)^2>0$) is called a *vertical* (resp., *horizontal*) *trajectory* of the quadratic differential $\varrho(z)\,\mathrm{d} z^2$. Vertical (resp., horizontal) trajectories are mapped by the primitive $z\mapsto w=\int^z\sqrt{\varrho(z')}\,\mathrm{d} z'$ to vertical (resp., horizontal) lines in the *w*-plane. However these curves are rarely vertical (resp., horizontal) in the native *z*-plane, so we will call them *v-trajectories* (resp., *h-trajectories*) to avoid any potential confusion. A *trajectory* is either a *v-trajectory* or an h-trajectory. A trajectory that is neither a closed curve nor terminates in both directions at zeros or poles of $\varrho(z)\,\mathrm{d} z^2$ is called *divergent*. A trajectory with either a zero or simple pole of $\varrho(z)$ as an endpoint, or an unbounded trajectory if $\varrho(z)=\mathcal{O}(z^{-3})$ as $z\to\infty$, is called *critical*.



Some of the level curves therefore coincide with the three v-trajectories of the quadratic differential $\varrho(z)$ d z^2 , that by local analysis emanate from each of the branch points z= α and $z = \beta$ at equal angles of $\frac{2\pi}{3}$. Since all level curves of Re(h(z)) are projections $\mathcal{R} \to \mathbb{C}$ of v-trajectories of $\rho(z) dz^2$ on \mathcal{R} , and since this function is not identically constant on \mathcal{R} , there can be no divergent v-trajectories on \mathcal{R} . Indeed, according to [60, Theorem 11.1, pg. 48], any such v-trajectory is also "recurrent", and then by [60, Corollary (1), pg. 51], the limit set of the recurrent v-trajectory has a non-empty connected interior, i.e., a domain on \mathcal{R} on which Re(h(z)) is necessarily constant, yielding a contradiction as Re(h(z)) is nonconstant and harmonic on $\mathcal{R} \setminus \{poles\}$. Clearly any divergent v-trajectory of $\rho(z) dz^2$ on \mathbb{C} is the projection under $\mathcal{R} \to \mathbb{C}$ of a divergent v-trajectory on \mathcal{R} , so there can be no such v-trajectories in the complex z-plane either. In this situation, the Basic Structure Theorem (see [39, pg. 37]) asserts that the closure K_z of the union of critical v-trajectories, here the three v-trajectories emanating from each of α and β together with the four v-trajectories emanating from the double zero $z = \gamma$, has an empty interior and divides the z-sphere $\overline{\mathbb{C}}$ into finitely many domains, each of which is foliated by non-critical v-trajectories. Each component of $\overline{\mathbb{C}} \setminus K_z$ has at least one of the critical points $z = \alpha, \beta, \gamma$ on its boundary, and on each component that has either α or β on its boundary the strict inequality |Re(h(z))| > 0holds. In this paper, we will refer to the following kinds of domains (see [39, Definitions 3.7-3.10).

Definition 3 (Circle, end, strip, and ring domains of rational quadratic differentials) Let $\varrho(z)\,\mathrm{d}z^2$ be a rational quadratic differential. Every double pole z_0 of $\varrho(z)$ with real and positive leading coefficient lies in a circle domain D with the property that $D\setminus\{z_0\}$ is foliated by noncritical v-trajectories that are all Jordan curves enclosing the pole. An end domain is a region mapped conformally by the primitive $z\mapsto w=\int^z\sqrt{\varrho(z')}\,\mathrm{d}z'$ onto a half-plane with a vertical boundary. A strip domain is a region mapped conformally by $z\mapsto w$ onto a vertical strip in the w-plane. Circle, end, and strip domains are simply connected. A ring domain is a multiply-connected domain foliated by noncritical v-trajectories that are all Jordan curves and that is mapped conformally by $z\mapsto e^w$ onto an annulus. The boundary of each circle, end, strip, or ring domain consists of critical v-trajectories and their endpoints.

Since z=0 is a simple pole of h'(z) with real residue, the component of $\overline{\mathbb{C}}\setminus K_z$ containing the origin is a circle domain \mathcal{D}_\circ foliated by noncritical v-trajectories that are all Jordan curves enclosing the origin, and having at least one of α , β , or γ on its boundary. Under the scaling $z=\beta Z$, we find that $\varrho(z)\,\mathrm{d} z^2=[(1-Z)Z^{-2}+\mathcal{O}(\mu^{-4})]\,\mathrm{d} Z^2$ where we have used $\alpha\beta\gamma^2=16$ (cf. (4.18)) and where the error term is uniform for bounded Z. The simplified quadratic differential has only one critical point, Z=1 corresponding to $z=\beta$, so the latter critical point alone lies on the boundary of the circle domain containing the origin in the z-plane. When $|\mu|$ is sufficiently large, this boundary therefore consists of a single v-trajectory that terminates at $z=\beta$ in both directions, leaving only one v-trajectory emanating from $z=\beta$ yet to be accounted for.

We temporarily make the stronger assumption that $0 < \epsilon \le \arg(\mu) \le \frac{\pi}{2} - \epsilon$; the weaker assumption that $-\epsilon < \arg(\mu) < \frac{\pi}{2} + \epsilon$ will be restored in Sect. 5.5.1. Then for $|\mu|$ sufficiently large there can be no critical v-trajectory connecting $z = \gamma$ with



either $z = \alpha$ or $z = \beta$. Indeed if there were such a v-trajectory, then it would follow that $Re(h(\gamma)) = 0$. However, a calculation shows that

$$\operatorname{Re}(h(\gamma)) = \operatorname{Re}\left(\int_{\alpha}^{\gamma} h'(z) \, \mathrm{d}z\right) = \pm \frac{\operatorname{Re}(\mu)\operatorname{Im}(\mu)}{\sqrt{3}} + o(\mu^2), \quad \mu \to \infty, \quad (5.1)$$

which cannot vanish under the indicated condition on $\arg(\mu)$. Therefore, the v-trajectory emanating from $z=\beta$ that does not return to β either terminates at $z=\alpha$ or escapes to $z=\infty$. Likewise, the three v-trajectories emanating from $z=\alpha$ either return to $z=\alpha$, terminate at $z=\beta$, or escape to $z=\infty$. All four v-trajectories emanating from $z=\gamma$ return to $z=\gamma$ or escape to $z=\infty$. We may rule out the scenarios in which a v-trajectory from $z=\alpha$ or $z=\gamma$ returns to the same point by using Teichmüller's Lemma (see [60, pg. 71]). This is an index identity that applies to Jordan curves $\mathcal J$ that are the unions of trajectories and junction points that can be poles or zeros of $\varrho(z)$ and that equates a left-hand side $\mathcal L$ computed from data involving the orders of ϱ at the junction points and the interior angles of $\mathcal J$ at those points with a right-hand side $\mathcal L$ computed from the orders of poles and zeros of $\varrho(z)$ in the interior of $\mathcal J$. The precise statement is the following.

Lemma 4 (Teichmüller's Lemma) Let \mathcal{J} be a Jordan curve that is the closure of the union of finitely many trajectories of a rational quadratic differential $\varrho(z) \, \mathrm{d} z^2$, the endpoints of each of which are poles or zeros of $\varrho(z)$ forming the vertices of \mathcal{J} . Define indices L and R by

$$L := \sum_{\text{vertices } j} \left(1 - \theta_j \frac{n_j + 2}{2\pi} \right) \tag{5.2}$$

where θ_j is the interior angle of \mathcal{J} at the vertex and n_j is the order of the rational function $\varrho(z)$ at the vertex (positive for zeros, negative for poles), and

$$R := 2 + \sum_{\text{interior points } z} n(z) \tag{5.3}$$

where n(z) is the order of $\varrho(z)$ at a point z (n(z) = 0 if z is not a zero or pole of $\varrho(z)$, hence the sum is finite). Then L = R.

To apply this result in the present context, note that if $\mathcal J$ is the closure of a single trajectory that terminates at the same zero of $\varrho(z)$ in both directions, then $L\leq 0$. Since the only pole of $\varrho(z)$ in the finite z-plane is a double pole at the origin, $R\geq 0$ with equality if and only if $\mathcal J$ encloses the origin but none of the zeros of $\varrho(z)$. However this equality forces the closure of $\mathcal J$ to be the boundary of the circle domain which we have shown contains $z=\beta$ but not $z=\alpha$ or $z=\gamma$. Therefore, all four v-trajectories emanating from $z=\gamma$ escape to $z=\infty$, and either (a) the remaining v-trajectory emanating from $z=\beta$ terminates at $z=\alpha$ leaving two additional v-trajectories emanating from $z=\alpha$ that must escape to $z=\infty$ or (b) the remaining v-trajectory emanating from $z=\beta$ and all three v-trajectories emanating from $z=\alpha$ escape to $z=\infty$. Note that a v-trajectory that escapes to $z=\infty$ must do so asymptotically in one of the four directions $\arg(z)=\pm\frac{\pi}{4},\pm\frac{3\pi}{4}$.



To determine whether (a) or (b) holds, and also to determine the manner that the four v-trajectories emanating from $z=\gamma$ tend to infinity, let us further restrict attention to the case that $\arg(\mu)=\frac{\pi}{4}$. Then rescaling z by $z=\mu Z$, we find that $\varrho(z)\,\mathrm{d}z^2=[\frac{1}{16}\mu^4(Z+\frac{8}{3})(Z+\frac{2}{3})^2Z^{-1}+\mathcal{O}(\mu^3)]\,\mathrm{d}Z^2$, where the error term is uniform for Z and Z^{-1} bounded. Since $\arg(\mu)=\frac{1}{4}\pi$ implies that $\mu^4<0$, we see that to leading order as $|\mu|\to\infty$, the v-trajectories are Schwarz symmetric in the Z-plane, and the rays $Z<-\frac{8}{3}$ and Z>0 are themselves v-trajectories. In the z-plane, this corresponds to reflection symmetry to leading order about the diagonal $\mathrm{Re}(z)=\mathrm{Im}(z)$. In the case that also $\kappa=0$, this symmetry is exact for all $|\mu|>0$. For $|\mu|$ large then, the remaining v-trajectory emanating from $z=\beta$ escapes to $z=\infty$ in the direction $\arg(z)=\frac{\pi}{4}$, so (b) holds.

The same asymptotic symmetry shows that for large $|\mu|$ one v-trajectory emanating from $z = \alpha$ escapes to $z = \infty$ in the direction $\arg(z) = -\frac{3\pi}{4}$. In the large- $|\mu|$ limit the two other v-trajectories emanating from $z = \alpha$ and escaping to $z = \infty$ are reflections of each other through the diagonal and are therefore confined to the two half-planes separated by that diagonal because v-trajectories cannot intersect. The last thing to determine is the direction of escape for these two v-trajectories. In fact, the v-trajectory lying below (resp., above) the diagonal must escape in the direction $\arg(z) = -\frac{\pi}{4}$ (resp., $\arg(z) = \frac{3\pi}{4}$). Indeed, if we suppose to the contrary that the v-trajectory below the diagonal escapes in the direction $\arg(z) = -\frac{3\pi}{4}$, then applying Teichmüller's Lemma on the z-sphere to the curve \mathcal{J} made up of this v-trajectory and the v-trajectory emanating from $z = \alpha$ and trapped along the diagonal in the direction $\arg(z) = -\frac{3\pi}{4}$ with interior angles $\theta = \frac{2\pi}{3}$ at α and $\theta = 0$ at ∞ , the lefthand side is L=1, but as there are no poles or zeros in the interior of \mathcal{J} , R=2, a contradiction. Likewise, if we suppose that the v-trajectory below the diagonal escapes in the direction $arg(z) = \frac{\pi}{4}$, then again taking \mathcal{J} to consist of the same v-trajectories making an interior angle of $\theta = \frac{2\pi}{3}$ at α and $\theta = \pi$ at ∞ , we calculate that L = 3while again R = 2, again a contradiction (here we need to use the fact that in the local coordinate $k = z^{-1}$ at $z = \infty$, ϱ has a pole of order 6 at k = 0). Therefore the only remaining direction of approach to infinity for the v-trajectory emanating from $z = \alpha$ into the half-plane below the diagonal is $\arg(z) = -\frac{\pi}{4}$. By reflection through the diagonal, the v-trajectory exiting α into the half-plane above the diagonal escapes in the direction $\arg(z)=\frac{3\pi}{4}$. This settles the behavior of the critical v-trajectories emanating from $z=\alpha,\beta$ for $\arg(\mu)=\frac{\pi}{4}$ and $|\mu|$ large. Similar analysis applied to the v-trajectories emanating from $z = \gamma$, which lies asymptotically on the diagonal between $z = \alpha$ and z = 0 shows that one v-trajectory escapes in the direction $\arg(z) = -\frac{\pi}{4}$, another escapes in the direction $\arg(z) = \frac{3\pi}{4}$, and the remaining two escape in the same direction, $arg(z) = \frac{\pi}{4}$, but on either side of the circle domain containing z = 0 and having $z = \beta$ on its boundary.

It follows that for large μ with $\arg(\mu) = \frac{\pi}{4}$ there are seven components of $\overline{\mathbb{C}} \setminus K_z$:

- One circle domain \mathcal{D}_{\circ} containing z=0 with $z=\beta$ on its boundary and excluding $z=\alpha, \gamma$. The inequality $|\operatorname{Re}(h(z))|>0$ holds strictly on the interior and $\operatorname{Re}(h(z))=0$ on the boundary. The boundary $\partial \mathcal{D}_{\circ}$ is a Jordan curve.
- Four end domains abutting the point at $z = \infty$:



- one bounded by the critical v-trajectories emanating from $z = \alpha$ and escaping to $z = \infty$ in the directions $\arg(z) = \frac{3\pi}{4}$ and $\arg(z) = -\frac{3\pi}{4}$ and containing the direction $\arg(-z) = 0$ for large z,
- one bounded by the critical v-trajectories emanating from $z = \alpha$ and escaping to $z = \infty$ in the directions $\arg(z) = -\frac{\pi}{4}$ and $\arg(z) = -\frac{3\pi}{4}$ and containing the direction $\arg(z) = -\frac{\pi}{2}$ for large z,
- one bounded by the two critical v-trajectories emanating from $z=\gamma$ into the half-plane above the diagonal and containing the direction $\arg(z)=\frac{\pi}{2}$ for large z, and
- one bounded by the two critical v-trajectories emanating from $z = \gamma$ into the half-plane below the diagonal and containing the direction $\arg(z) = 0$ for large z.

The former two end domains are each mapped by an analytic branch of h(z) onto the open right or left half-plane, and hence |Re(h(z))| > 0 holds strictly on each while Re(h(z)) = 0 on the boundary. However, the latter two end domains are each mapped onto a horizontal translation of the left or right half-plane, since $\text{Re}(h(\gamma)) \neq 0$.

- Two strip domains:
 - one with $z = \alpha$ and $z = \gamma$ on its boundary, foliated by v-trajectories escaping to $z = \infty$ in opposite directions $\arg(z) = -\frac{\pi}{4}$ and $\arg(z) = \frac{3\pi}{4}$, and
 - one with $z = \gamma$ and $z = \beta$ on its boundary (the latter actually being two points of the boundary), foliated by v-trajectories escaping in both directions to $z = \infty$ in the same direction $\arg(z) = \frac{\pi}{4}$ and wrapping around the circle domain.

The strip domains are each mapped by an analytic branch of h(z) to a vertical strip with the imaginary axis as one boundary. Hence |Re(h(z))| > 0 holds on the interior of each domain and Re(h(z)) = 0 holds on the part of the boundary mapped to the imaginary axis.

Therefore, the only components of $\overline{\mathbb{C}} \setminus K_z$ that might contain points with $\mathrm{Re}(h(z)) = 0$ are the two end domains with $z = \gamma$ on their boundaries. However, one can see that neither of these end domains is mapped by h(z) onto a half-plane containing the imaginary axis, because $z = \gamma$ is a simple saddle point of $\mathrm{Re}(h(z))$ at which these end domains dovetail with the two strip domains at a common boundary where $\mathrm{Re}(h(z)) \neq 0$. It finally follows that the zero-level set of $\mathrm{Re}(h(z))$ consists precisely of the two disjoint components of K_z that contain $z = \alpha$ and $z = \beta$ respectively. (The remaining component containing $z = \gamma$ necessarily lies on a different level of $\mathrm{Re}(h(z))$.) See Fig. 19.

Having understood the global v-trajectory structure for large $|\mu|$ with $\arg(\mu) = \frac{\pi}{4}$, by working on the Riemann surface Γ of Definition 1 we can analytically continue α , β , and γ as functions of μ along any path that avoids all eight branch points (roots μ of $B(\mu; \kappa)$ defined by (1.17)), and these three points will remain distinct. Under such continuation, the global structure will remain topologically identical as long as $\operatorname{Re}(h(\gamma)) = \operatorname{Re}(h^{(s,\kappa)}(\gamma;\mu)) \neq 0$ for $\gamma = U_{0,gO}(\mu;\kappa)$. Note that while $\operatorname{Re}(h(z))$ is



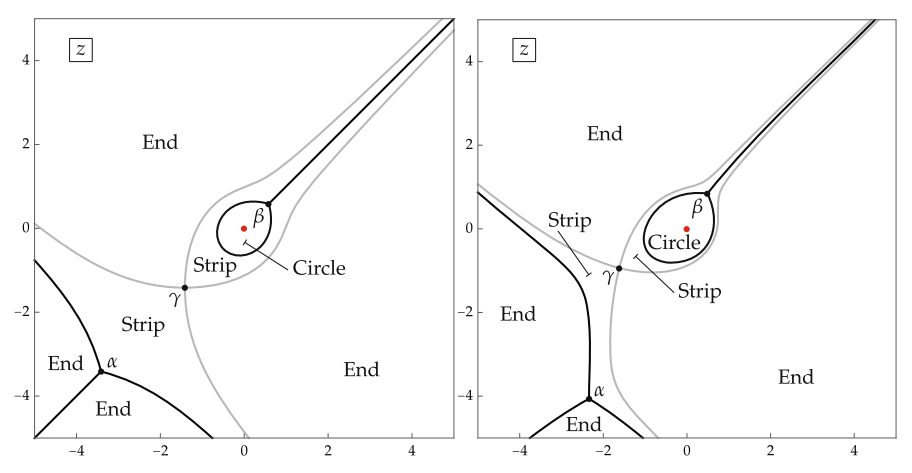


Fig. 19 The critical v-trajectories of $\varrho(z) \, \mathrm{d}z^2$ and the seven domains into which they separate the z-sphere. Left: $\kappa = 0$ and $\mu = 2\mathrm{e}^{\mathrm{i}\pi/4}$ (exact symmetry through the diagonal). Right: $\kappa = 0.5$ and $\mu = 1.8\mathrm{e}^{\mathrm{i}\pi/4}$. The closure of the union of the black trajectories is the zero-level set of $\mathrm{Re}(h(z))$ (Color figure online)

only determined up to a sign until a specific branch is selected (see Sect. 5.1.2), the condition $Re(h(\gamma)) \neq 0$ is unambiguous.

5.1.2 Defining h(z) as a Single-Valued Function

To properly define h(z) as an analytic function in the z-plane, we first choose branch cuts for R(z) (defined in terms of the case {211} polynomial P(z) in (4.21)) as illustrated in one of the two cases shown in Fig. 20.

Then, with R(z) well defined and analytic in the complement of its branch cut, we obtain h'(z) from (4.22) as a function analytic in the same domain except for a simple pole at z=0. We then choose a simple curve Σ_0 in the circle domain \mathcal{D}_{\circ} connecting the origin with $z=\beta$ and a point $z_+\in\partial\mathcal{D}_{\circ}\setminus\{\beta\}$ such that for any simple arc $L\subset\mathcal{D}_{\circ}$ from z_+ to β via z=0,

P.V.
$$\int_{I} h'(z) dz = 0.$$
 (5.4)

The existence of such a point follows from the Intermediate Value Theorem. Then:

- In the configuration shown in the left-hand panel of Fig. 20, we choose a continuation $\Sigma_{4,3}$ of Σ_c tangent to Σ_c at $z=\alpha$ and connecting $z=\alpha$ to $z=\infty$ in the shaded region with asymptotic angle $\arg(-z)=0$. Then we define Σ_h as $\Sigma_h:=\Sigma_0\cup\Sigma_c\cup\Sigma_{4,3}$ if s=+1 or $\Sigma_h:=\Sigma_0\cup\Sigma_c\cup\Sigma_{4,3}\cup\partial\mathcal{D}_\circ$ if s=-1.
- In the configuration shown in the right-hand panel of Fig. 20, we choose a continuation $\Sigma_{4,1}$ of Σ_c tangent to Σ_c at $z=\alpha$ and connecting $z=\alpha$ to $z=\infty$ in the unshaded region with asymptotic angle $\arg(z)=-\frac{\pi}{2}$. Then we define Σ_h as $\Sigma_h:=\Sigma_0\cup\Sigma_c\cup\Sigma_{4,1}$ if s=-1 or $\Sigma_h:=\Sigma_0\cup\Sigma_c\cup\Sigma_{4,1}\cup\partial\mathcal{D}_\circ$ if s=+1.

⁹ We allow this choice of two alternatives to be able to sidestep difficulties arising from certain unimportant topological changes in the level set topology; see Sect. 5.5.1 for details.



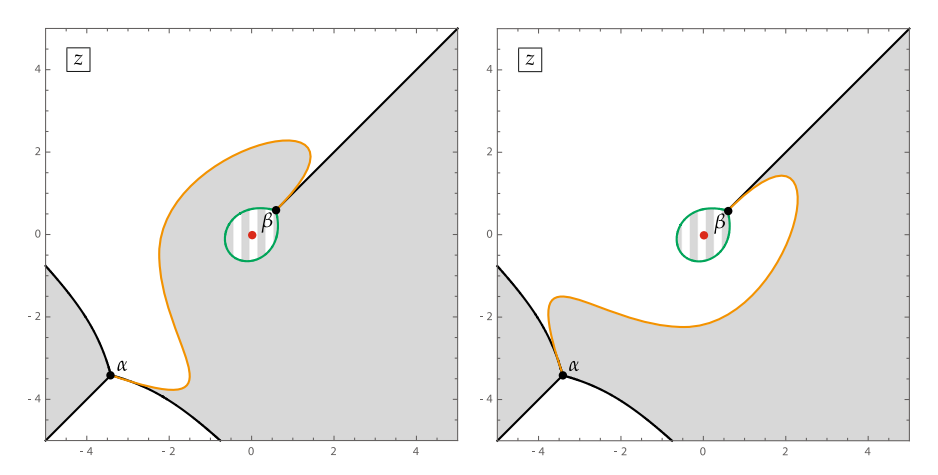


Fig. 20 Two ways to choose the branch cuts of R(z) in the z-plane so that h'(z) becomes an analytic function on the complement leading to Re(h(z)) > 0 (resp., Re(h(z)) < 0) in the unshaded (resp., shaded) regions, and sgn(Re(h(z))) = s in the circle domain \mathcal{D}_{\circ} indicated with stripes. In both cases the orange arc denoted Σ_c is included in the branch cut, and in the case illustrated in the left-hand (resp., right-hand) panel the closed component $\partial \mathcal{D}_{\circ}$ of the level curve surrounding the origin is also part of the branch cut if and only if s = -1 (resp., s = +1). The arc Σ_c lies in the interior of the closure of the union of end and strip domains that abut $z = \gamma$, and is tangent to the v-trajectories emanating from α and β as indicated (Color figure online)

Finally, we define $h(z) = h^{(s,\kappa)}(z;\mu)$ for $z \in \mathbb{C} \setminus \overline{\Sigma_h}$ by integration of h'(z) from $z = z_+$ along an arbitrary path in the same domain. Then it follows that $\operatorname{Re}(h(z))$ is well defined and continuous for $z \in \mathbb{C} \setminus (\{0\} \cup \Sigma_c)$, vanishing only along the black and green curves and elsewhere having the signs shown in Fig. 20. It is harmonic in the same domain except for the closed curve $\partial \mathcal{D}_{\circ}$ (but only if the sign is the same in the interior and exterior; otherwise it is also harmonic on $\partial \mathcal{D}_{\circ}$).

The boundary values $h_+(z)$ and $h_-(z)$ taken by $h(z) = h^{(s,\kappa)}(z;\mu)$ on the arcs of its jump contour Σ_h from the left and right, respectively, (according to the orientations shown in Fig. 21) are related as follows, recalling the notation in Sect. 1.5.

• A residue calculation for the pole of h'(z) at z=0 shows that

$$\Delta h(z) = -2\pi i s, \quad z \in \Sigma_0. \tag{5.5}$$

• The condition (5.4) guarantees that the sum of boundary values taken by h(z) across Σ_c vanishes at the endpoint $z = \beta$. Since R(z) changes sign across Σ_c it then follows that

$$\langle h \rangle(z) = 0, \quad z \in \Sigma_c.$$
 (5.6)

- Calculating a residue of h'(z) at $z = \infty$ shows that
 - In the configuration shown in the left-hand panel of Fig. 20,

$$\Delta h(z) = 2\pi i \kappa, \quad z \in \Sigma_{4,3}.$$



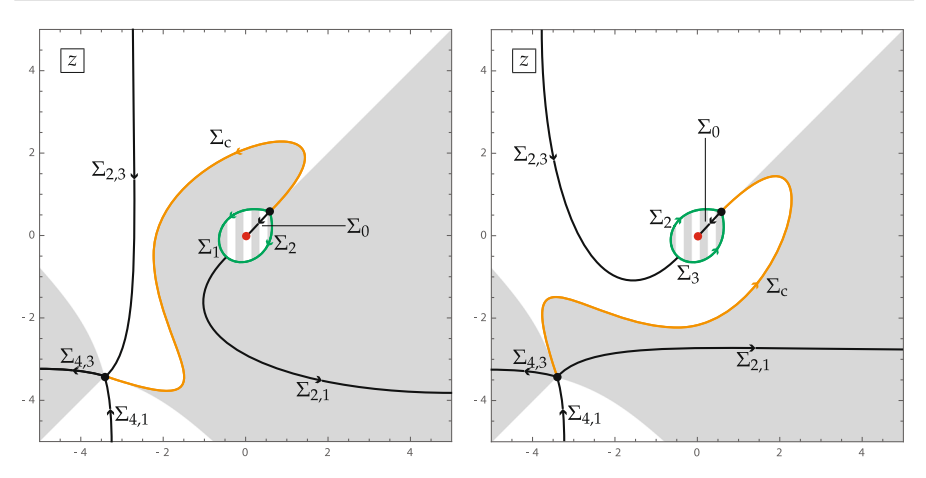


Fig. 21 Left: the use of the "leftward" deformation of the jump contours for M(z). Right: the use of the "downward" deformation. The self-intersection points of Σ lying on $C = \partial \mathcal{D}_0$ are $z = \beta$ and $z = z_+$. The sign of Re(h(z)) is indicated by shading as in Fig. 20 (Color figure online)

- In the configuration shown in the right-hand panel of Fig. 20,

$$\Delta h(z) = -2\pi i \kappa, \quad z \in \Sigma_{4.1}.$$

• If $\partial \mathcal{D}_{\circ} \subset \Sigma_h$, then R(z) changes sign across $\partial \mathcal{D}_{\circ}$ while $h(z_+) = 0$ unambiguously, so

$$\langle h \rangle(z) = 0, \quad z \in \partial \mathcal{D}_{\circ} \subset \Sigma_h.$$
 (5.7)

Otherwise, h(z) is analytic on $\partial \mathcal{D}_{\circ} \setminus \{\beta\}$, across which curve Re(h(z)) changes sign.

5.2 Introduction of g(z) and Steepest Descent

Next, depending upon which of the two configurations of branch cuts is selected, we choose either the "leftward" or "downward" deformation of the jump contour for $\mathbf{M}(z)$ and lay the jump contour over the sign chart for $\mathrm{Re}(h(z))$ as shown in the two panels of Fig. 21. In particular, we take the closed contour $C \subset \Sigma$ to coincide with $\partial \mathcal{D}_{\circ}$.

Then, we introduce $g(z) = g^{(s,\kappa)}(z;\mu) = \phi(z;\mu) + h^{(s,\kappa)}(z;\mu)$ via (4.14), in which the constant g_{∞} is determined from the precise definition of h(z); we will not need to know its exact value. Using (5.5), it is easy to check that $\mathbf{N}(z) = \mathbf{N}^{(T,s,\kappa)}(z;\mu,0)$ has no jump discontinuity across Σ_0 ; then since the residue of g'(z) at z=0 is -s, the condition that $\mathbf{M}(z)z^{-sT\sigma_3}$ is bounded near the origin implies that $\mathbf{N}(z)$ has a removable singularity at z=0 and hence is analytic in the interior of C. Also $\mathbf{N}(z) \to \mathbb{I}$ as $z \to \infty$. The matrix function $z \mapsto \mathbf{N}(z)$ is analytic except on the arcs of $\Sigma \setminus \Sigma_0$, is normalized to the identity as $z \to \infty$, and is continuous up to the jump contour in each component of its complement. Using (5.6)–(5.7), the jump



conditions satisfied by N(z) take the following forms.

$$\mathbf{N}_{+}(z) = \mathbf{N}_{-}(z)\mathbf{U}(-\frac{1}{2}i\mathrm{e}^{-2Th(z)}), \quad z \in \Sigma_{2,3}.$$

 $\mathbf{N}_{+}(z) = \mathbf{N}_{-}(z)\mathbf{L}(2i\mathrm{e}^{2Th(z)}), \quad z \in \Sigma_{2,1}.$

In the "leftward" configuration where h(z) has a jump across $\Sigma_{4,3}$,

$$\mathbf{N}_{+}(z) = \mathbf{N}_{-}(z)\mathbf{L}(2\mathrm{i}\mathrm{e}^{-2\pi\mathrm{i}T\kappa}\mathrm{e}^{2T\langle h\rangle(z)}), \quad z \in \Sigma_{4,3},$$
 "leftward" configuration,

while

$$\mathbf{N}_{+}(z) = \mathbf{N}_{-}(z)\mathbf{L}(2\mathrm{i}\mathrm{e}^{2Th(z)}), \quad z \in \Sigma_{4,3},$$
 "downward" configuration.

Similarly,

$$\mathbf{N}_{+}(z) = \mathbf{N}_{-}(z)\mathbf{U}(-\frac{1}{2}\mathrm{i}\mathrm{e}^{-2Th(z)}), \quad z \in \Sigma_{4,1},$$
 "leftward" configuration,

while as there is a jump for h(z) across $\Sigma_{4,1}$ in the "downward" configuration,

$$\mathbf{N}_+(z) = \mathbf{N}_-(z)\mathbf{U}(-\tfrac{1}{2}\mathrm{i}\mathrm{e}^{-2\pi\mathrm{i}T\kappa}\mathrm{e}^{-2T\langle h\rangle(z)}), \quad z \in \Sigma_{4,1}, \quad \text{``downward'' configuration}.$$

In both configurations h(z) has a jump across Σ_c , and we find that

$$\mathbf{N}_{+}(z) = \mathbf{N}_{-}(z)e^{-2\pi i T_{\kappa}}\mathbf{T}(2i), \quad z \in \Sigma_{c}, \quad \text{``leftward'' configuration},$$
 (5.8)

while

$$\mathbf{N}_{+}(z) = \mathbf{N}_{-}(z)e^{2\pi i T\kappa}\mathbf{T}(-2i), \quad z \in \Sigma_{c},$$
 "downward" configuration. (5.9)

Remark 13 Note that (5.8)–(5.9) are essentially the same jump condition since in both cases Σ_c is a contour connecting the same points α and β but with opposite orientations in the two configurations. Also, the jump matrices in (5.8)–(5.9) both have unit determinant, because the scalar factor satisfies $e^{2\pi i T \kappa} = e^{-2\pi i T \kappa}$ since $\Theta_{\infty} = -T\kappa$ and $2\Theta_{\infty} \in \mathbb{Z}$ holds for $(\Theta_0, \Theta_{\infty}) \in \Lambda_{gO}$.

On the arcs of C it appears at first that one should get different jump conditions for $\mathbf{N}(z)$ depending on whether or not $C \subset \Sigma_h$, but if one uses the fact that $\Delta g(z) = \Delta h(z)$ and observes the dichotomy that either $\Delta h(z) = 0$ or $\langle h \rangle(z) = 0$, one can write the jump conditions in the same form for both cases:

$$\mathbf{N}_{+}(z) = \mathbf{N}_{-}(z)e^{-Th_{-}(z)\sigma_{3}}\mathbf{V}_{k}e^{Th_{+}(z)\sigma_{3}}, \quad z \in \Sigma_{k}, \quad k = 1, 2, 3,$$

where V_k , k = 1, 2, 3 are the gO connection matrices defined in (3.4).



To deal with the jump conditions on the arcs of C, we use the following factorizations, all of which are special cases of (1.35) with two of the three factors combined:

$$V_{1} = \mathbf{L}(2e^{i\pi/6}) \begin{pmatrix} \frac{1}{\sqrt{3}} - \frac{1}{2} \\ 0 \sqrt{3} \end{pmatrix} \quad \text{("L(DU)")}$$

$$= \mathbf{L}(-2e^{-i\pi/6}) \begin{pmatrix} \frac{1}{\sqrt{3}} - \frac{1}{2} \\ 2 & 0 \end{pmatrix} \quad \text{("L(TL)")},$$

$$V_{2} = \begin{pmatrix} \sqrt{3} & \frac{1}{2} \\ 0 & \frac{1}{\sqrt{3}} \end{pmatrix} \mathbf{L}(-2e^{-i\pi/6}) \quad \text{("(UD)L")}$$

$$= \begin{pmatrix} 0 & \frac{1}{2} \\ -2 & \frac{1}{\sqrt{3}} \end{pmatrix} \mathbf{L}(2e^{i\pi/6}) \quad \text{("(LT)L")}$$

$$= \begin{pmatrix} e^{i\pi/6} & 0 \\ -\frac{2}{\sqrt{3}}e^{-i\pi/6} & e^{-i\pi/6} \end{pmatrix} \mathbf{U}(\frac{1}{2}e^{-i\pi/6}) \quad \text{("(LD)U")}$$

$$= \begin{pmatrix} e^{i\pi/6} & \frac{\sqrt{3}}{2}e^{i\pi/6} \\ -\frac{2}{\sqrt{3}}e^{-i\pi/6} & 0 \end{pmatrix} \mathbf{U}(-\frac{1}{2}e^{i\pi/6}) \quad \text{("(UT)U")},$$

$$V_{3} = \mathbf{U}(\frac{1}{2}e^{-5i\pi/6}) \begin{pmatrix} e^{-i\pi/6} & 0 \\ \frac{2}{\sqrt{3}}e^{-i\pi/6} & e^{i\pi/6} \end{pmatrix} \quad \text{("U(DL)")}$$

$$= \mathbf{U}(\frac{1}{2}e^{-i\pi/6}) \begin{pmatrix} 0 & -\frac{\sqrt{3}}{2}e^{i\pi/6} \\ e^{i\pi/6} & e^{i\pi/6} \end{pmatrix} \quad \text{("U(TU)")}.$$
(5.12)

Based on these, we transform N(z) into $O(z) = O^{(T,s,\kappa)}(z;\mu)$ by making the following explicit substitutions in the "lens" domains Λ_1 and Λ_2 (in case we are using the "leftward" configuration) or Λ_2 and Λ_3 (in case we are using the "downward" configuration) shown in Fig. 22 as well as in the interior of C.

- For the "leftward" configuration:
 - If $C \not\subset \Sigma_h$ (i.e., s = +1), we combine the factorizations on the first lines of (5.10) and (5.11) to set

$$\mathbf{O}(z) := \mathbf{N}(z)\mathbf{L}(2e^{i\pi/6}e^{2Th(z)}), \quad z \in \Lambda_1,$$

$$\mathbf{O}(z) := \mathbf{N}(z)\mathbf{L}(2e^{-i\pi/6}e^{2Th(z)}), \quad z \in \Lambda_2,$$

$$\mathbf{O}(z) := \mathbf{N}(z)\begin{pmatrix} \sqrt{3} & \frac{1}{2}e^{-2Th(z)} \\ 0 & \frac{1}{\sqrt{3}} \end{pmatrix}, \quad z \text{ in the interior of } C. \quad (5.13)$$



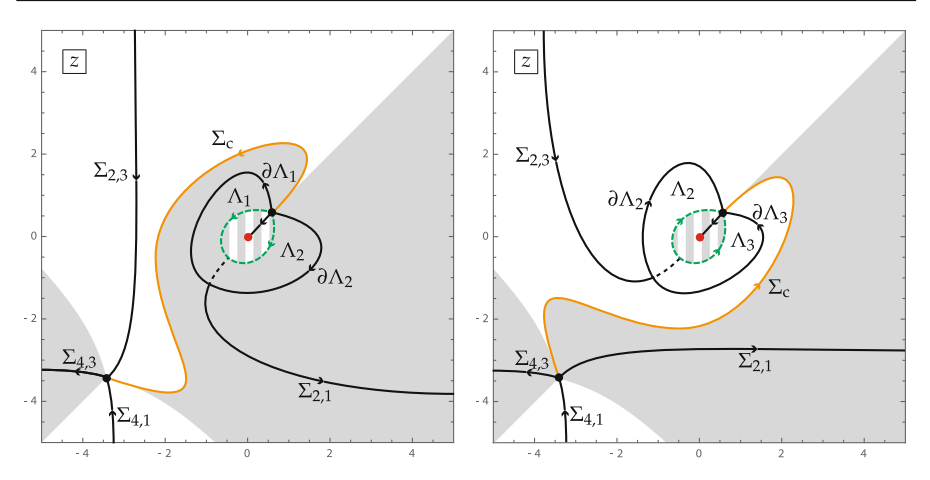


Fig. 22 The "lens" domains Λ_j , j=1,2,3 and their boundaries in the "leftward" configuration (left) and the "downward" configuration (right). The indicated solid black and orange arcs form the final jump contour for $\mathbf{O}(z)$ (the dashed arcs have been removed by the transformation $\mathbf{N}(z) \mapsto \mathbf{O}(z)$). Shading indicates the sign of $\mathrm{Re}(h(z))$ as in Figs. 20 and 21 (Color figure online)

- If $C \subset \Sigma_h$ (i.e., s = -1), we combine the factorizations on the second lines of (5.10) and (5.11) to set

$$\mathbf{O}(z) := \mathbf{N}(z)\mathbf{L}(-2e^{-i\pi/6}e^{2Th(z)}), \quad z \in \Lambda_1,$$

$$\mathbf{O}(z) := \mathbf{N}(z)\mathbf{L}(-2e^{i\pi/6}e^{2Th(z)}), \quad z \in \Lambda_2,$$

$$\mathbf{O}(z) := \mathbf{N}(z)\begin{pmatrix} 0 & \frac{1}{2} \\ -2 & \frac{1}{\sqrt{3}}e^{2Th(z)} \end{pmatrix}, \quad z \text{ in the interior of } C. \quad (5.14)$$

- For the "downward" configuration:
 - If $C \not\subset \Sigma_h$ (i.e., s = -1), we combine the factorizations on the third line of (5.11) and the first line of (5.12) to set

$$\mathbf{O}(z) := \mathbf{N}(z)\mathbf{U}(-\frac{1}{2}e^{-i\pi/6}e^{-2Th(z)}), \quad z \in \Lambda_{2},
\mathbf{O}(z) := \mathbf{N}(z)\mathbf{U}(\frac{1}{2}e^{-5i\pi/6}e^{-2Th(z)}), \quad z \in \Lambda_{3},
\mathbf{O}(z) := \mathbf{N}(z)\begin{pmatrix} e^{i\pi/6} & 0 \\ -\frac{2}{\sqrt{3}}e^{-i\pi/6}e^{2Th(z)} & e^{-i\pi/6} \end{pmatrix}, \quad z \text{ in the interior of } C.$$
(5.15)



- If $C \subset \Sigma_h$ (i.e., s = +1), we combine the factorizations on the fourth line of (5.11) and the second line of (5.12) to set

$$\begin{aligned} \mathbf{O}(z) &:= \mathbf{N}(z) \mathbf{U}(\frac{1}{2} \mathrm{e}^{\mathrm{i}\pi/6} \mathrm{e}^{-2Th(z)}), \quad z \in \Lambda_2, \\ \mathbf{O}(z) &:= \mathbf{N}(z) \mathbf{U}(\frac{1}{2} \mathrm{e}^{-\mathrm{i}\pi/6} \mathrm{e}^{-2Th(z)}), \quad z \in \Lambda_3, \\ \mathbf{O}(z) &:= \mathbf{N}(z) \begin{pmatrix} \mathrm{e}^{\mathrm{i}\pi/6} \mathrm{e}^{-2Th(z)} & \frac{\sqrt{3}}{2} \mathrm{e}^{\mathrm{i}\pi/6} \\ -\frac{2}{\sqrt{3}} \mathrm{e}^{-\mathrm{i}\pi/6} & 0 \end{pmatrix}, \quad z \text{ in the interior of } C. \end{aligned}$$

$$(5.16)$$

In all cases, elsewhere that $\mathbf{N}(z)$ has a definite value we set $\mathbf{O}(z) := \mathbf{N}(z)$. Then $\mathbf{O}(z)$ no longer has any jump discontinuity across the arcs of C, and the jump across the arc of $\Sigma_{2,1}$ common to the boundary of the lens domains Λ_1 and Λ_2 is also removed in the "leftward" configuration, while the jump across the arc of $\Sigma_{2,3}$ common to the boundary of the lens domains Λ_2 and Λ_3 is also removed in the "downward" configuration. The domain of analyticity of $\mathbf{O}(z) = \mathbf{O}^{(T,s,\kappa)}(z;\mu)$ is the complement of the jump contour shown with solid black and orange curves in the two panels of Fig. 22, and the jump conditions satisfied by $\mathbf{O}(z)$ on the arcs $\Sigma_{2,3}$, $\Sigma_{4,3}$, $\Sigma_{4,1}$, Σ_c , and the rest of $\Sigma_{2,1}$ (resp., $\Sigma_{2,1}$, $\Sigma_{4,3}$, $\Sigma_{4,1}$, Σ_c , and the rest of $\Sigma_{2,3}$) for the "leftward" (resp., "downward") configuration are exactly the same as for $\mathbf{N}(z)$. New jump conditions for $\mathbf{O}(z)$ appear on the lens boundaries and on Σ_0 :

• For the "leftward" configuration, we have

$$\mathbf{O}_{+}(z) = \mathbf{O}_{-}(z)\mathbf{L}(2se^{si\pi/6}e^{2Th(z)}), \quad z \in \partial \Lambda_{1},$$

$$\mathbf{O}_{+}(z) = \mathbf{O}_{-}(z)\mathbf{L}(-2se^{-si\pi/6}e^{2Th(z)}), \quad z \in \partial \Lambda_{2},$$
(5.17)

and

$$\mathbf{O}_{+}(z) = \mathbf{O}_{-}(z)\mathbf{U}(\frac{1}{2\sqrt{3}}s(e^{-2Tsh_{+}(z)} - e^{-2Tsh_{-}(z)})),$$

= $\mathbf{O}_{-}(z)\mathbf{U}(-\frac{1}{2}ie^{-2\pi iT\kappa}e^{-2sT\langle h\rangle(z)}), \quad z \in \Sigma_{0}.$ (5.18)

• For the "downward" configuration, we have

$$\mathbf{O}_{+}(z) = \mathbf{O}_{-}(z)\mathbf{U}(-\frac{1}{2}se^{si\pi/6}e^{-2Th(z)}), \quad z \in \partial \Lambda_{2},
\mathbf{O}_{+}(z) = \mathbf{O}_{-}(z)\mathbf{U}(\frac{1}{2}se^{-si\pi/6}e^{-2Th(z)}), \quad z \in \partial \Lambda_{3},$$
(5.19)

and

$$\mathbf{O}_{+}(z) = \mathbf{O}_{-}(z)\mathbf{L}(\frac{2}{\sqrt{3}}s(e^{-2Tsh_{+}(z)} - e^{-2Tsh_{-}(z)}))$$

$$= \mathbf{O}_{-}(z)\mathbf{L}(-2ie^{-2\pi iT\kappa}e^{-2sT\langle h\rangle\langle z\rangle}), \quad z \in \Sigma_{0}.$$
(5.20)

To go from the first to the second line in (5.18) and (5.20), we use the identity $s(e^{-2Tsh_+(z)} - e^{-2Tsh_-(z)}) = -i\sqrt{3}e^{-2\pi iT\kappa}e^{-2Ts\langle h\rangle(z)}$ which follows from $h_{\pm}(z) = \langle h\rangle(z) \pm \frac{1}{2}\Delta h(z)$, the jump condition (5.5), the parametrization $(\Theta_0, \Theta_{\infty}) = (sT, -\kappa T)$, and the gO lattice conditions (1.11). As $\mathbf{O}(z) = \mathbf{N}(z)$ for large |z|, the normalization condition reads $\mathbf{O}(z) \to \mathbb{I}$ as $z \to \infty$.



5.3 Parametrix Construction

Comparing the jump contours shown in Fig. 22 with the sign charts for Re(h(z)) shown in Fig. 20, it is now clear that under the working assumption that the sign chart has the structure established in Sect. 5.1.1 for large μ in the first quadrant, the jump matrix for $\mathbf{O}(z)$ decays exponentially to \mathbb{I} as $T \to +\infty$ except on the arc Σ_c and neighborhoods of its endpoints α and β . To deal with these, we construct outer and inner parametrices for $\mathbf{O}(z)$.

5.3.1 Outer Parametrix

The outer parametrix $\check{\mathbf{O}}^{\text{out}}(z)$ is defined by the properties that

- it is analytic for $z \in \mathbb{C} \setminus \Sigma_c$,
- it takes continuous boundary values on Σ_c except at $z = \alpha, \beta$, where negative one-fourth power singularities are admitted,
- the boundary values satisfy exactly the same jump condition on Σ_c as do those of O(z), and
- it tends to \mathbb{I} as $z \to \infty$.

Since the jump conditions for O(z) on Σ_c match those for N(z) given in (5.8) or (5.9), by Remark 13 of Sect. 5.2 we may diagonalize the constant jump matrix and hence see that the unique matrix function satisfying the above conditions can be written in the same form for both "leftward" and "downward" configurations:

$$\check{\mathbf{O}}^{\text{out}}(z) = \mathbf{S}_{\text{gO}} j(z)^{\sigma_3} \mathbf{S}_{\text{gO}}^{-1}, \quad \mathbf{S}_{\text{gO}} := \begin{pmatrix} \frac{1}{2} e^{-2\pi i T \kappa} & -\frac{1}{2} e^{-2\pi i T \kappa} \\ 1 & 1 \end{pmatrix}, \tag{5.21}$$

where j(z) is the unique function analytic for $z \in \mathbb{C} \setminus \Sigma_c$ with the properties that $j(z)^4 = (z - \alpha)/(z - \beta)$ and $j(z) \to 1$ as $z \to \infty$. By expanding j(z) for large z, it is easy to see that

$$\check{\mathbf{O}}^{\text{out}}(z) = \mathbb{I} + z^{-1} \check{\mathbf{O}}_{1}^{\text{out}} + \mathcal{O}(z^{-2}), \quad z \to \infty, \tag{5.22}$$

where

$$\check{O}_{1,12}^{\text{out}} = \frac{1}{8} (\beta - \alpha) e^{-2\pi i T \kappa}.$$
(5.23)

We may also unambiguously evaluate $\check{\mathbf{O}}^{\mathrm{out}}(z)$ at z=0, because the branch cut Σ_{c} for j(z) lies in the exterior of the Jordan curve C enclosing z=0. From the formula



(5.21) we get

$$\check{O}_{11}^{\text{out}}(0) \, \check{O}_{12}^{\text{out}}(0) = \frac{1}{8} e^{-2\pi i T \kappa} \left[j(0)^2 - j(0)^{-2} \right],
\frac{\check{O}_{11}^{\text{out}}(0)}{\check{O}_{21}^{\text{out}}(0)} = \frac{1}{2} e^{-2\pi i T \kappa} \frac{j(0) + j(0)^{-1}}{j(0) - j(0)^{-1}} = \frac{1}{2} e^{-2\pi i T \kappa} \frac{j(0)^2 + j(0)^{-2} + 2}{j(0)^2 - j(0)^{-2}},
\frac{\check{O}_{12}^{\text{out}}(0)}{\check{O}_{22}^{\text{out}}(0)} = \frac{1}{2} e^{-2\pi i T \kappa} \frac{j(0) - j(0)^{-1}}{j(0) + j(0)^{-1}} = \frac{1}{2} e^{-2\pi i T \kappa} \frac{j(0)^2 + j(0)^{-2} - 2}{j(0)^2 - j(0)^{-2}}.$$
(5.24)

To simplify the expressions (5.24) further, note that using the definition of j(z) and the final identity in (4.18),

$$\left(j(0)^2 \pm j(0)^{-2}\right)^2 = j(0)^4 + j(0)^{-4} \pm 2 = \frac{\alpha}{\beta} + \frac{\beta}{\alpha} \pm 2 = \frac{(\alpha \pm \beta)^2}{\alpha\beta} = \frac{\gamma^2(\alpha \pm \beta)^2}{16}.$$
(5.25)

Now from the identity $j(0)^4 = \alpha/\beta$ we get the asymptotic expansion $j(0)^4 = \frac{16}{81}\mu^4 + \mathcal{O}(\mu^3)$ as $\mu \to \infty$ with $0 < \arg(\mu) < \frac{\pi}{2}$. From the plots in Fig. 21 or 22 which show the case of $\arg(\mu) = \frac{\pi}{4}$, we see that the correct branch of the square root to take to calculate $j(0)^2$ depends on the configuration:

$$j(0)^2 = \begin{cases} \frac{4}{9}\mu^2 + \mathcal{O}(\mu), & \text{in the "leftward" configuration} \\ -\frac{4}{9}\mu^2 + \mathcal{O}(\mu), & \text{in the "downward" configuration} \end{cases}$$

in the limit $\mu \to \infty$. So, since we also have the asymptotic expansion $\frac{1}{4}\gamma(\alpha \pm \beta) = \frac{4}{9}\mu^2 + \mathcal{O}(\mu)$ as $\mu \to \infty$, we find the exact identity

$$j(0)^{2} \pm j(0)^{-2} = \begin{cases} \frac{1}{4}\gamma(\alpha \pm \beta), & \text{in the "leftward" configuration} \\ -\frac{1}{4}\gamma(\alpha \pm \beta), & \text{in the "downward" configuration.} \end{cases}$$
(5.26)

Using this result in (5.24) and combining with (5.23) and the identities in (4.18) gives the following combinations that will be used in Sect. 5.4:

$$\frac{\breve{O}_{11}^{\text{out}}(0)\breve{O}_{12}^{\text{out}}(0)}{\breve{O}_{1,12}^{\text{out}}} = \begin{cases} -\frac{1}{4}\gamma, & \text{in the "leftward" configuration} \\ \frac{1}{4}\gamma, & \text{in the "downward" configuration;} \end{cases}$$
(5.27)

$$\frac{\check{O}_{1,12}^{\text{out}}\check{O}_{21}^{\text{out}}(0)}{\check{O}_{11}^{\text{out}}(0)} = \begin{cases} \mu + \frac{1}{2}\gamma + 2\gamma^{-1}, & \text{in the "leftward" configuration} \\ \mu + \frac{1}{2}\gamma - 2\gamma^{-1}, & \text{in the "downward" configuration;} \end{cases}$$
(5.28)

$$\frac{\check{O}_{1,12}^{\text{out}} \check{O}_{22}^{\text{out}}(0)}{\check{O}_{01}^{\text{out}}(0)} = \begin{cases} \mu + \frac{1}{2}\gamma - 2\gamma^{-1}, & \text{in the "leftward" configuration} \\ \mu + \frac{1}{2}\gamma + 2\gamma^{-1}, & \text{in the "downward" configuration.} \end{cases}$$
(5.29)



To finish our discussion of the outer parametrix, we observe that $\check{\mathbf{O}}^{\text{out}}(z)$ has unit determinant and for z bounded away from $z=\alpha$ and $z=\beta$, $\check{\mathbf{O}}^{\text{out}}(z)$ is uniformly bounded as $T\to +\infty$.

5.3.2 Inner Parametrices

Inner parametrices are to be used in place of the outer parametrix in T-independent neighborhoods D_{α} and D_{β} of $z=\alpha$ and $z=\beta$ respectively. These are defined in terms of a 2×2 matrix function $\mathbf{A}(\xi)$ satisfying the following Riemann–Hilbert conditions:

- $\mathbf{A}(\xi)$ is analytic in the four sectors complementary to the four rays $\arg(\xi) = 0$, $\arg(\xi) = \frac{2\pi}{3}$, $\arg(\xi) = -\frac{2\pi}{3}$, and $\arg(-\xi) = 0$.
- A(ξ) takes continuous boundary values from each sector of analyticity on the union of rays forming the sector boundary. Assuming the four rays are oriented in the direction away from the origin, the boundary values are related by the jump conditions

$$\mathbf{A}_{+}(\xi) = \mathbf{A}_{-}(\xi)\mathbf{L}(i\exp(-\xi^{3/2})), \quad \arg(\xi) = 0,$$
 (5.30)

$$\mathbf{A}_{+}(\xi) = \mathbf{A}_{-}(\xi)\mathbf{U}(\mathrm{i}\exp(\xi^{3/2})), \quad \arg(\xi) = \pm \frac{2\pi}{3},$$
 (5.31)

and

$$\mathbf{A}_{+}(\xi) = \mathbf{A}_{-}(\xi)\mathbf{T}(-i), \quad \arg(-\xi) = 0.$$
 (5.32)

• $A(\xi)$ is normalized by the condition

$$\mathbf{A}(\xi) \frac{1}{\sqrt{2}} \begin{pmatrix} 1 & -1 \\ 1 & 1 \end{pmatrix} \xi^{-\sigma_3/4} = \begin{pmatrix} 1 + \mathcal{O}(\xi^{-3}) & \mathcal{O}(\xi^{-1}) \\ \mathcal{O}(\xi^{-2}) & 1 + \mathcal{O}(\xi^{-3}) \end{pmatrix}, \quad \xi \to \infty. \quad (5.33)$$

It is well known that there is a unique solution of these conditions, and the matrix $A(\xi)$ can be explicitly written in terms of the Airy function $Ai(\cdot)$ and its derivative [53]. We will not need this formula, however. The inner parametrices are defined as follows. Referring to the appropriate entry of Table 3 corresponding to the disk D_p ($p=\alpha,\beta$) and the "leftward" or "downward" configuration, we first fix the contour arc associated with arg(W)=0 within D_p so that a function W(z) is well defined as indicated on that arc by taking the $\frac{2}{3}$ power of a positive quantity. This function can be analytically continued to the whole disk as a conformal mapping because $h'(z)^2$ has simple zeros at $z=\alpha,\beta$ and $\langle h\rangle(\alpha)=\langle h\rangle(\beta)=0$. Once the conformal mapping W is defined, we fix the remaining arcs of the jump contour within D_p so that they are mapped by W to the rays indicated in the table.

Next, noting the value of the constant matrix \mathbf{C} defined in the same table, we then define a matrix $\mathbf{H}(z)$ by writing the outer parametrix in the form

$$\check{\mathbf{O}}^{\text{out}}(z) = \mathbf{H}(z)W(z)^{\sigma_3/4} \frac{1}{\sqrt{2}} \begin{pmatrix} 1 & 1 \\ -1 & 1 \end{pmatrix} \mathbf{C}, \quad z \in D_p \setminus \Sigma_{\mathbf{c}}.$$
 (5.34)

It is easy to see that $\mathbf{H}(z)$ has no jump across $\Sigma_{\mathbf{c}} \cap D_p$ and that any singularity at W = 0 is removable. Therefore $\mathbf{H}(z)$ is a holomorphic matrix function on D_p with



p	Configuration	Conformal map $W:$ $D_p \to \mathbb{C}$	Ray Preimages in D_p		Constant matrix C
			arg(W)	Preimage	
α	"leftward"	$(-2\langle h \rangle(z))^{2/3}$, continued from $\Sigma_{4,3}$	0	$\Sigma_{4,3}$	$e^{-i\pi T\kappa\sigma_3}2^{\sigma_3/2}$
			$\frac{2\pi}{3}$	$\Sigma_{4,1}$	
			$-\frac{2\pi}{3}$	$\Sigma_{2,3}$	
			$\pm\pi$	$\Sigma_{ m c}$	
α	"downward"	$(2\langle h \rangle(z))^{2/3}$, continued from $\Sigma_{4,1}$	0	$\Sigma_{4,1}$	$i\sigma_1 e^{i\pi T \kappa \sigma_3} 2^{\sigma_3/2}$
			$\frac{2\pi}{3}$	$\Sigma_{2,1}$	
			$-\frac{2\pi}{3}$	$\Sigma_{4,3}$	
			$\pm\pi$	$\Sigma_{ m c}$	
β	"leftward"	$(2s\langle h\rangle(z))^{2/3}$, continued from Σ_0	0	Σ_0	$i\sigma_1 i^{\sigma_3} e^{i\pi T \kappa \sigma_3} 2^{\sigma_3/2}$
			$\frac{2\pi}{3}$	$\partial \Lambda_2$	
			$-\frac{2\pi}{3}$	$\partial \Lambda_1$	
			$\pm\pi$	$\Sigma_{ m c}$	
β	"downward"	$(2s\langle h\rangle(z))^{2/3}$, continued from Σ_0	0	Σ_0	$i^{\sigma_3}e^{-i\pi T\kappa\sigma_3}2^{\sigma_3/2}$
			$\frac{2\pi}{3}$	$\partial \Lambda_3$	
			$-\frac{2\pi}{3}$	$\partial \Lambda_2$	
			$\pm\pi$	$\Sigma_{ m c}$	

Table 3 Data for defining the inner parametrices in D_{α} and D_{β}

unit determinant, and it follows from the formula (5.21) that the elements of $\mathbf{H}(z)$ are bounded on D_p uniformly with respect to the large parameter T. Using $\mathbf{H}(z)$ and $\mathbf{A}(\xi)$ we define an inner parametrix on D_p by setting

$$\mathbf{\check{O}}^{\text{in},p}(z) := \mathbf{H}(z)T^{-\sigma_3/6}\mathbf{A}(T^{2/3}W(z))\mathbf{C}, \quad z \in D_p \setminus \{\arg(W(z)) \in \{0, \pm \frac{2\pi}{3}, \pm \pi\}\}.$$
(5.35)

Recalling the parametrization $(\Theta_0, \Theta_\infty) = (sT, -s\kappa)$ and the gO lattice conditions (1.11), in all four cases it follows from the sectorial analyticity of $\mathbf{A}(\xi)$ and the jump conditions (5.30)–(5.32) that $\check{\mathbf{O}}^{\mathrm{in},\alpha}(z)$ (resp., $\check{\mathbf{O}}^{\mathrm{in},\beta}(z)$) is analytic within D_α (resp., D_β) exactly where $\mathbf{O}(z)$ is, and satisfies exactly the same jump conditions. To show this it is helpful to recall the jump conditions satisfied by h(z) (see (5.5)–(5.7)) and that, depending on the value of s, analytic continuation of h across C can introduce a change of sign. Therefore, the inner parametrices are *exact local solutions* of the Riemann–Hilbert conditions characterizing $\mathbf{O}(z)$. Moreover, it follows from (5.33) and the fact that $z \in \partial D_{\alpha,\beta}$ bounds the conformal coordinate W(z) away from zero that the following estimates hold uniformly with respect to z on the indicated contours:

$$\check{\mathbf{O}}^{\text{in},\alpha}(z)\check{\mathbf{O}}^{\text{out}}(z)^{-1} = \mathbb{I} + \mathcal{O}(T^{-1}), \quad z \in \partial D_{\alpha},
\check{\mathbf{O}}^{\text{in},\beta}(z)\check{\mathbf{O}}^{\text{out}}(z)^{-1} = \mathbb{I} + \mathcal{O}(T^{-1}), \quad z \in \partial D_{\beta}.$$
(5.36)



5.3.3 Global Parametrix and Error Estimation

The *global parametrix* for $\mathbf{O}(z) = \mathbf{O}^{(T,s,\kappa)}(z;\mu)$ is then defined as follows:

$$\check{\mathbf{O}}(z) := \begin{cases}
\check{\mathbf{O}}^{\text{in},p}(z), & z \in D_p, \quad p \in \{\alpha,\beta\}, \\
\check{\mathbf{O}}^{\text{out}}(z), & \text{elsewhere that } \check{\mathbf{O}}^{\text{out}}(z) \text{ is analytic.}
\end{cases}$$
(5.37)

The corresponding error in modeling $\mathbf{O}(z)$ with the global parametrix is the error $\mathbf{E}(z) = \mathbf{E}^{(T,s,\kappa)}(z;\mu)$ defined by

$$\mathbf{E}(z) := \mathbf{O}(z)\check{\mathbf{O}}(z)^{-1}. \tag{5.38}$$

Since both $\mathbf{O}(z)$ and its parametrix satisfy exactly the same jump conditions within D_{α} and D_{β} , and also along Σ_c , $\mathbf{E}(z)$ can be viewed as an analytic function in the complex z-plane, with only the parts lying outside of the neighborhoods D_{α} and D_{β} of the black arcs of the jump contour shown in the panels of Fig. 22 in Sect. 5.2 and the boundaries $\partial D_{\alpha,\beta}$ of the neighborhoods excluded. We take the latter to have clockwise orientation. Since $\check{\mathbf{O}}^{\text{out}}(z)$ and its inverse are uniformly bounded for $z \in \mathbb{C} \setminus (D_{\alpha} \cup D_{\beta})$ and T sufficiently large, it is easy to check that due to the exponentially rapid convergence to the identity of the jump matrices for $\mathbf{O}(z)$ on the parts of the jump contour for $\mathbf{E}(z)$ lying outside the closure of $D_{\alpha} \cup D_{\beta}$, we have also $\mathbf{E}_{+}(z) = \mathbf{E}_{-}(z)(\mathbb{I} + \text{exponentially small})$ as $T \to +\infty$ on those arcs. For the closed curves $\partial D_{\alpha,\beta}$ it is easy to see from (5.36) that $\mathbf{E}_{+}(z) = \mathbf{E}_{-}(z)(\mathbb{I} + \mathcal{O}(T^{-1}))$ holds uniformly on $\partial D_{\alpha,\beta}$ as $T \to +\infty$. Since it also follows from (5.38) that $\mathbf{E}(z) \to \mathbb{I}$ as $z \to \infty$, we may apply small norm theory in the L^2 setting as described, for instance, in [18, Appendix B] to conclude that

$$\mathbf{E}(z) = \mathbb{I} + z^{-1}\mathbf{E}_1 + \mathcal{O}(z^{-2}), \quad z \to \infty,$$
 (5.39)

where $\mathbf{E}_1 = \mathbf{E}_1^{(T,s,\kappa)}(\mu) = \mathcal{O}(T^{-1})$ and that $\mathbf{E}(0) = \mathbb{I} + \mathcal{O}(T^{-1})$ as $T \to +\infty$.

5.4 Conditionally Valid Asymptotic Formulæ for the gO Rational Solutions of Painlevé-IV

Recalling the scaling relationships between x and μ and between λ and z given in (4.1) (for $\zeta = 0$) we see that for |z| sufficiently large,

$$\mathbf{Y}(\lambda; x) = \left(\frac{1}{2}T^{1/2}\right)^{\kappa T \sigma_3} \mathbf{M}(z)$$

$$= \left(\frac{1}{2}T^{1/2}\right)^{\kappa T \sigma_3} e^{Tg_{\infty}\sigma_3} \mathbf{N}(z) e^{-Tg(z)\sigma_3}$$

$$= \left(\frac{1}{2}T^{1/2}\right)^{\kappa T \sigma_3} e^{Tg_{\infty}\sigma_3} \mathbf{O}(z) e^{-Tg(z)\sigma_3}$$

$$= \left(\frac{1}{2}T^{1/2}\right)^{\kappa T \sigma_3} e^{Tg_{\infty}\sigma_3} \mathbf{E}(z) \check{\mathbf{O}}(z) e^{-Tg(z)\sigma_3}$$

$$= \left(\frac{1}{2}T^{1/2}\right)^{\kappa T \sigma_3} e^{Tg_{\infty}\sigma_3} \mathbf{E}(z) \check{\mathbf{O}}^{\text{out}}(z) e^{-Tg(z)\sigma_3}.$$
(5.40)



Now using the expansions (5.39), (5.22), and $g(z) = -\kappa \log(z) + g_{\infty} + g_1 z^{-1} + \mathcal{O}(z^{-2})$ as $z \to \infty$, which implies that also

$$\mathrm{e}^{-Tg(z)\sigma_3} = \left(\mathbb{I} - Tg_1z^{-1}\sigma_3 + \mathcal{O}(z^{-2})\right) \cdot \mathrm{e}^{-Tg_\infty\sigma_3}z^{T\kappa\sigma_3}, \quad z \to \infty,$$

upon again taking into account the scaling $\lambda = \frac{1}{2}T^{1/2}z$ one sees that the matrix element $Y_{1,12}^{\infty}(x)$ defined in (3.1) can be written in the form

$$Y_{1,12}^{\infty}(x) = \left(\frac{1}{4}T\right)^{\kappa T} e^{2Tg_{\infty}} \frac{1}{2} T^{1/2} \left(\check{O}_{1,12}^{\text{out}} + E_{1,12} \right)$$

$$= \left(\frac{1}{4}T\right)^{\kappa T} e^{2Tg_{\infty}} \frac{1}{2} T^{1/2} \left(\check{O}_{1,12}^{\text{out}} + \mathcal{O}(T^{-1}) \right), \quad T \to +\infty.$$
(5.41)

Now, the first two lines of (5.40) are also valid for $|\lambda|$ sufficiently small, so using (4.13), the matrix $\mathbf{Y}_0^0(x)$ defined in (3.1) can be written as

$$\mathbf{Y}_{0}^{0}(x) = \lim_{z \to 0} \left(\frac{1}{2}T^{1/2}\right)^{\kappa T \sigma_{3}} e^{Tg_{\infty}\sigma_{3}} \mathbf{N}(z) e^{-Tg(z)\sigma_{3}} z^{-sT\sigma_{3}} \left(\frac{1}{2}T^{1/2}\right)^{-sT\sigma_{3}}$$

$$= \left(\frac{1}{2}T^{1/2}\right)^{\kappa T \sigma_{3}} e^{Tg_{\infty}\sigma_{3}} \mathbf{N}(0) e^{-Tg_{0}\sigma_{3}} \left(\frac{1}{2}T^{1/2}\right)^{-sT\sigma_{3}}.$$
(5.42)

Using (5.13), (5.14), (5.15), and (5.16) in which the exponential factor $e^{\pm 2Th(z)}$ vanishes at the origin z=0 in each case, we have

$$\mathbf{N}(0) = \begin{cases} \mathbf{O}(0)\mathbf{D}(\frac{1}{\sqrt{3}}), & \text{in the "leftward" configuration, for } C \not\subset \Sigma_h \quad \text{(i.e., } s = 1) \\ \mathbf{O}(0)\mathbf{T}(2), & \text{in the "leftward" configuration, for } C \subset \Sigma_h \quad \text{(i.e., } s = -1) \\ \mathbf{O}(0)\mathbf{D}(\exp(-\frac{\mathrm{i}\pi}{6})), & \text{in the "downward" configuration, for } C \not\subset \Sigma_h \quad \text{(i.e., } s = -1) \\ \mathbf{O}(0)\mathbf{T}(\frac{2}{\sqrt{3}}\exp(-\frac{\mathrm{i}\pi}{6})), & \text{in the "downward" configuration, for } C \subset \Sigma_h \quad \text{(i.e., } s = 1), \end{cases}$$

$$(5.43)$$

where we are using the compact notation $\mathbf{D}(a)$ and $\mathbf{T}(a)$ for diagonal and off-diagonal matrix factors defined in (1.34).

Then since $\mathbf{O}(0) = \mathbf{E}(0)\check{\mathbf{O}}(0) = \mathbf{E}(0)\check{\mathbf{O}}^{\text{out}}(0) = (\mathbb{I} + \mathcal{O}(T^{-1}))\check{\mathbf{O}}^{\text{out}}(0)$ and $\check{\mathbf{O}}^{\text{out}}(0)$ is bounded,

$$Y_{0,11}^{0}(x)Y_{0,12}^{0}(x) = \begin{cases} \left(\frac{1}{4}T\right)^{\kappa T} e^{2Tg_{\infty}}(\check{O}_{11}^{\text{out}}(0)\check{O}_{12}^{\text{out}}(0) + \mathcal{O}(T^{-1})), & C \not\subset \Sigma_{h} \\ -\left(\frac{1}{4}T\right)^{\kappa T} e^{2Tg_{\infty}}(\check{O}_{11}^{\text{out}}(0)\check{O}_{12}^{\text{out}}(0) + \mathcal{O}(T^{-1})), & C \subset \Sigma_{h}. \end{cases}$$
(5.44)

Therefore, recalling $\Theta_0 = sT$ and using the definition (3.2) of u(x), we combine (5.41) and (5.44) with (5.27) to obtain, for integers m, n such that $(\Theta_0, \Theta_\infty) = (\Theta_0^{[3]}, \Theta_0^{[3]}, \Theta_0^{[3]})$



$$\Theta_{\infty,\mathrm{gO}}^{[3]}(m,n)),$$

$$u_{gO}^{[3]}(x; m, n) = u(x) = -2sT \frac{Y_{0,11}^{0}(x)Y_{0,12}^{0}(x)}{Y_{1,12}^{\infty}(x)}$$

$$= T^{1/2}(\gamma + \mathcal{O}(T^{-1}))$$

$$= |\Theta_{0}|^{1/2} \left(U_{0,gO}(\mu; \kappa) + \mathcal{O}(|\Theta_{0}|^{-1})\right),$$

$$\mu = \frac{x}{|\Theta_{0}|^{1/2}}, \quad \kappa = -\frac{\Theta_{\infty}}{|\Theta_{0}|}.$$
(5.45)

The fact that the same formula results in all cases comes from the correlation between $s = \pm 1$ and whether or not $C \subset \Sigma_h$ in each configuration.

Likewise, using also the fact that the matrix elements of $\check{\mathbf{O}}^{\text{out}}(0)$ are bounded away from zero,

$$\frac{Y_{0,11}^{0}(x)}{Y_{0,21}^{0}(x)} = \begin{cases}
\left(\frac{1}{4}T\right)^{\kappa T} e^{2Tg_{\infty}} \left(\frac{\breve{O}_{11}^{\text{out}}(0)}{\breve{O}_{21}^{\text{out}}(0)} + \mathcal{O}(T^{-1})\right), & C \not\subset \Sigma_{h} \\
\left(\frac{1}{4}T\right)^{\kappa T} e^{2Tg_{\infty}} \left(\frac{\breve{O}_{12}^{\text{out}}(0)}{\breve{O}_{22}^{\text{out}}(0)} + \mathcal{O}(T^{-1})\right), & C \subset \Sigma_{h}.
\end{cases} (5.46)$$

Therefore, recalling the definition of $u_{\uparrow}(x)$ in (3.2) and combining (5.41) and (5.46) with either (5.28) or (5.29) we obtain, now for integers m, n such that $(\Theta_{0,gO}^{[1]}(m,n), \Theta_{\infty,gO}^{[1]}(m,n)) = (\Theta_{0,\uparrow}, \Theta_{\infty,\uparrow}),$

$$u_{gO}^{[1]}(x; m, n) = u_{\mathbb{Q}}(x) = -2 \frac{Y_{0,21}^{0}(x) Y_{1,12}^{\infty}(x)}{Y_{0,11}^{0}(x)}$$

$$= T^{1/2} \left(-\mu - \frac{1}{2}\gamma - 2s\gamma^{-1} + \mathcal{O}(T^{-1}) \right)$$

$$= |\Theta_{0}|^{1/2} \left(-\mu - \frac{1}{2}U_{0,gO}(\mu; \kappa) - 2sU_{0,gO}(\mu; \kappa)^{-1} + \mathcal{O}(|\Theta_{0}|^{-1}) \right),$$
(5.47)

where μ and κ are exactly as in (5.45). Here, the only evidence of the four-fold origin of this asymptotic formula is the sign $s = \pm 1$.

Now, in both asymptotic formulæ (5.45) and (5.47), $\gamma = U_{0,gO}(\mu;\kappa)$ is the branch of the solution of the quartic (4.19) satisfying $U_{0,gO}(\mu;\kappa) = -\frac{2}{3}\mu + \mathcal{O}(\mu^{-1})$ as $\mu \to \infty$. However, recalling Remark 11 in Sect. 4.1, the parameters $(\Theta_0,\Theta_\infty) \in \Lambda_{gO}$ appearing in these formulæ are those for which u(x) satisfies the Painlevé-IV equation, while $u_{\mathbb{Q}}(x)$ solves the Painlevé-IV equation for different parameters $(\Theta_0,\mathbb{Q},\Theta_\infty,\mathbb{Q})$; see (2.4). Since the latter definition implies that $|\Theta_0,\mathbb{Q}| = \frac{1}{2}|\Theta_0|(1-s\kappa)$ and $1-s\kappa \neq 0$



for $\kappa \in (-1, 1)$, it makes sense to write (5.47) in the form

$$\begin{split} u_{\mathrm{gO}}^{[1]}(x;m,n) &= u_{\mathfrak{J}}(x) = |\Theta_{0,\mathfrak{J}}|^{1/2} \\ \cdot C_{\mathfrak{J}}\left(-\frac{\mu}{C_{\mathfrak{J}}} - \frac{1}{2}U_{0,\mathrm{gO}}\left(\frac{\mu}{C_{\mathfrak{J}}};\kappa\right) - 2sU_{0,\mathrm{gO}}\left(\frac{\mu}{C_{\mathfrak{J}}};\kappa\right)^{-1} + \mathcal{O}(|\Theta_{0,\mathfrak{J}}|^{-1})\right), \end{split}$$

i.e., replacing μ with μ/C_{\uparrow} and using $|\Theta_0|^{1/2} = |\Theta_{0,\uparrow}|^{1/2}C_{\uparrow}$, where now μ is related to x differently:

$$\mu := \frac{x}{|\Theta_0, \gamma|^{1/2}} \text{ and } C_{\gamma} := \sqrt{\frac{2}{1 - s\kappa}}.$$
 (5.48)

Next, we observe the following.

Lemma 5 Given $\kappa \in (-1, 1)$, suppose that $\gamma = \gamma(\mu)$ is a solution of the quartic equation (4.19) analytic on a domain D, i.e., $\mu \mapsto \gamma(\mu)$ is analytic on D and $Q(\gamma(\mu), \mu; \kappa) = 0$ holds identically on D. Set

$$\gamma_{\updownarrow}(\mu) := C_{\updownarrow} \left(-\frac{\mu}{C_{\updownarrow}} - \frac{1}{2}\gamma \left(\frac{\mu}{C_{\updownarrow}} \right) - 2s\gamma \left(\frac{\mu}{C_{\updownarrow}} \right)^{-1} \right). \tag{5.49}$$

Then for $s = \pm 1$,

$$Q\left(\gamma_{\updownarrow}(\mu), \mu; -\frac{\kappa + 3s}{1 - s\kappa}\right) = 0 \tag{5.50}$$

holds for $\mu \in C_{\uparrow} D$ (dilation of the domain D by C_{\uparrow} defined in (5.48)).

Proof This follows from the identity

$$\begin{split} Q\left(C_{\updownarrow}(-\mu-\tfrac{1}{2}\gamma-2s\gamma^{-1}),C_{\updownarrow}\mu;-\frac{\kappa+3s}{1-s\kappa}\right)\\ &=\frac{\gamma^4-4(\mu^2+2\kappa)\gamma^2-32s\mu\gamma-48}{4\gamma^4(1-s\kappa)^2}Q(\gamma,\mu;\kappa). \end{split}$$

One can easily check that if $\gamma(\mu) = -\frac{2}{3}\mu + \mathcal{O}(\mu^{-1})$ in (5.49), then also $\gamma(\mu) = -\frac{2}{3}\mu + \mathcal{O}(\mu^{-1})$. Therefore, using Lemma 5 we can finally express (5.47) in the form

$$u_{gO}^{[1]}(x; m, n) = u_{\updownarrow}(x) = |\Theta_{0, \updownarrow}|^{1/2} \left(U_{0, gO}(\mu; \kappa_{\updownarrow}) + \mathcal{O}(|\Theta_{0, \updownarrow}|^{-1}) \right),$$

$$\mu := \frac{x}{|\Theta_{0, \updownarrow}|^{1/2}}, \quad \kappa_{\updownarrow} = -\frac{\Theta_{\infty, \updownarrow}}{|\Theta_{0, \updownarrow}|},$$

$$(5.51)$$

because $U_{0,gO}(\mu;\kappa)$ is a simple root of the quartic (4.19), and

$$-\frac{\Theta_{\infty, \uparrow}}{|\Theta_{0, \uparrow}|} = -\frac{3\Theta_0 - \Theta_{\infty} + 2}{|\Theta_0 + \Theta_{\infty}|} = -\frac{\kappa + 3s}{1 - s\kappa} + \mathcal{O}(|\Theta_{0, \uparrow}|^{-1}).$$



According to (2.2), the formula (5.51) immediately gives an asymptotic formula for the type-2 rational function $u_{\sigma\Omega}^{[2]}(x;m,n)$.

5.5 Bifurcation Points and Conditions for Validity

The pointwise validity of the asymptotic formulæ (5.45) and (5.51) is guaranteed if (μ, γ) is obtained by analytic continuation from a neighborhood of $\mu = \infty$ on the sheet of Γ (see Definition 1 at the start of Sect. 5) corresponding for large μ to $\gamma = U_{0,gO}(\mu;\kappa)$, throughout which the zero-level set of Re(h(z)) remains topologically equivalent to that described for large μ in Sect. 5.1.1. Topological changes in the zero-level set can only occur if upon analytic continuation the double root $\gamma = \gamma(\mu)$ of P(z) first moves onto the level set, and when this occurs the level set becomes connected and equal to K_z (the strip domains disappear).

Definition 4 (*Bifurcation points*) Given $\kappa \in (-1, 1)$, let (μ, γ) be a point on Γ , and let α and β be determined up to permutation from (μ, γ) by (4.18). Then (μ, γ) is a *bifurcation point* if the closure K_z of the union of critical v-trajectories of $\varrho(z)$ d $z^2 = \frac{1}{16}z^{-2}(z-\gamma)^2(z-\alpha)(z-\beta)$ d z^2 is connected. A bifurcation point that is not a branch point of (4.19) is called a *generic bifurcation point*.

Some bifurcations are harmless in the sense that they cause the proof to fail only in one or the other of the two configurations ("leftward" versus "downward") of branch cuts and jump contours, while others are catastrophic, signaling a genuine change in asymptotic behavior of the rational Painlevé-IV solutions. Starting from the representative pictures of K_z in Fig. 19, the possible generic bifurcations are points (μ, γ) where:

- (i) the v-trajectory emanating from $z=\alpha$ with asymptotic direction $\arg(z)=-\frac{\pi}{4}$ merges with $\gamma(\mu)$ and the v-trajectory emanating from $z=\beta$ on the side with asymptotic direction $\arg(z)=\frac{\pi}{4}+0$,
- (ii) the v-trajectory emanating from $z=\alpha$ with asymptotic direction $\arg(z)=\frac{3\pi}{4}$ merges with $\gamma(\mu)$ and the v-trajectory emanating from $z=\beta$ on the side with asymptotic direction $\arg(z)=\frac{\pi}{4}-0$,
- (iii) the v-trajectory emanating from $z = \alpha$ with asymptotic direction $\arg(z) = -\frac{\pi}{4}$ merges with $\gamma(\mu)$ and $\partial \mathcal{D}_{\circ}$,
- (iv) the v-trajectory emanating from $z = \alpha$ with asymptotic direction $\arg(z) = \frac{3\pi}{4}$ merges with $\gamma(\mu)$ and $\partial \mathcal{D}_{\circ}$,
- (v) the v-trajectory emanating from $z=\alpha$ with asymptotic direction $\arg(z)=-\frac{\pi}{4}$ merges with $\gamma(\mu)$ and the v-trajectory emanating from $z=\beta$ on the side with asymptotic direction $\arg(z)=\frac{\pi}{4}-0$, and
- (vi) the v-trajectory emanating from $z=\alpha$ with asymptotic direction $\arg(z)=\frac{3\pi}{4}$ merges with $\gamma(\mu)$ and the v-trajectory emanating from $z=\beta$ on the side with asymptotic direction $\arg(z)=\frac{\pi}{4}+0$.



5.5.1 Harmless Bifurcation Points

Harmless bifurcations are generic bifurcation points when either (i) or (ii) occurs. These two scenarios occur for large μ in the limits $\arg(\mu) \downarrow 0$ and $\arg(\mu) \uparrow \frac{\pi}{2}$ respectively.

Indeed, the asymptotic behavior of α , β , and γ for large μ described at the beginning of this section shows that as $arg(\mu) \downarrow 0$, α and γ approach the negative real zaxis from below while β approaches the negative real axis from above. Roughly speaking, the connected component of K_7 containing α rotates around the origin in the clockwise direction while the component containing β rotates around the origin in the counterclockwise direction, and these trap the component containing γ ; at the bifurcation point all three components become one with γ on the same level as α and β . This approach to bifurcation resembles the progression of plots in Fig. 17 moving down the right-hand side toward the lower right-hand corner, but is less singular as that sequence of plots arrives at a spectral curve of class {31} (hence a nongeneric bifurcation point). In the "leftward" configuration shown in the left-hand panel of Fig. 22 the only arc of the jump contour for O(z) that becomes constrained by this bifurcation as $arg(\mu) \downarrow 0$ is Σ_c ; however this arc carries a constant (in z) jump condition (5.8) whose analytical properties in the limit $T \to +\infty$ do not depend on the sign chart for Re(h(z)). By contrast, in the "downward" configuration shown in the right-hand panel of Fig. 22, the arcs $\Sigma_{2,3}$ and $\Sigma_{2,1}$ are additional casualties of the bifurcation as $arg(\mu) \downarrow 0$, and unlike Σ_c , these contours carry jump conditions with exponentials whose rapid decay to zero as $T \to +\infty$ is ruined in the limit, near $z = \gamma$ at least.

In a similar way, one can see that as $\arg(\mu)\uparrow\frac{\pi}{2}$ it is the "downward" configuration that preserves the required exponential decay in all jump matrices at the bifurcation point. The corresponding approach to bifurcation is similar to but less singular than the sequence of plots along the top edge of Fig. 17 moving toward the upper left-hand corner. We therefore conclude that as a consequence of making the best choice of contour deformation, the asymptotic formulæ (5.45) and (5.47) remain valid when either bifurcation (i) or (ii) occurs, and even beyond the bifurcation point when γ moves off the level set once again, which then breaks the other way around the saddle point. Since for large $|\mu|$ these harmless bifurcations occur on the real and imaginary axes, the latter observation allows us to weaken the assumption $\epsilon \leq \arg(\mu) \leq \frac{\pi}{2} - \epsilon$ introduced before (5.1) in Sect. 5.1.1 to the original assumption that $-\epsilon < \arg(\mu) < \frac{\pi}{2} + \epsilon$ for some small $\epsilon > 0$.

5.5.2 Catastrophic Bifurcation Points

The remaining four scenarios for generic bifurcation are catastrophic for the asymptotic analysis based on the assumption of a spectral curve of class {211} in that beyond the bifurcation point it is no longer possible to use either the "leftward" or the "downward" configuration; instead one must try to use a Boutroux curve of class {1111}. This approach will be detailed in Sect. 7.

However, exactly at a such a generic catastrophic bifurcation point it remains possible to prove a version of the asymptotic formulæ (5.45) and (5.51) in which only



the rate of decay of the error terms is slower. We explain the necessary modifications in the situation that bifurcation (iv) occurs, in which case we select the "downward" deformation. If (iii) occurs we proceed similarly using instead the "leftward" deformation.

Looking at the right-hand panel of Fig. 22, one can see that the effect of approaching the indicated catastrophe is that the unshaded region where $\operatorname{Re}(h(z)) > 0$ holds is pinched to a narrow isthmus near $z = \gamma$ in the vicinity of the contours $\Sigma_{2,3} \cup \partial \Lambda_2 \cup \partial \Lambda_3$. By cyclic consistency of the jump conditions at the self-intersection point of these three arcs, it is sufficient to assume that it is only $\partial \Lambda_3$ that passes right over the saddle point $z = \gamma$, and hence in the limit the strict inequality on the real part of the exponent in the upper-triangular jump matrix in (5.19) fails at the saddle. To deal with this issue we install a different kind of inner parametrix in a fixed disk D_{γ} centered at $z = \gamma$ by first defining a conformal mapping on D_{γ} via the equation $W(z)^2 = 2(h(z) - h(\gamma))$ and taking the square root in such a way that $\partial \Lambda_3$ is mapped to the real W-axis near the origin in the direction of increasing W. Then we define a matrix function $\xi \mapsto \mathbf{B}(\xi)$ that is analytic for $\xi \in \mathbb{C} \setminus \mathbb{R}$, that satisfies the jump condition

$$\mathbf{B}_{+}(\xi) = \mathbf{B}_{-}(\xi)\mathbf{U}(\exp(-\xi^{2})), \quad \xi \in \mathbb{R},$$

and that satisfies the normalization condition $\mathbf{B}(\xi) \to \mathbb{I}$ as $\xi \to \infty$. This triangular problem with identity normalization is explicitly solved by a Cauchy integral:

$$\mathbf{B}(\xi) = \mathbf{U}\left(\frac{1}{2\pi i} \int_{\mathbb{R}} \frac{\exp(-\lambda^2) \, \mathrm{d}\lambda}{\lambda - \xi}\right), \quad \xi \in \mathbb{C} \setminus \mathbb{R}.$$

Denoting by ω any square root of $\omega^2 = \frac{1}{2}s\mathrm{e}^{-s\mathrm{i}\pi/6}\mathrm{e}^{-2Th(\gamma)}$, we finally define an inner parametrix for $\mathbf{O}(z)$ in D_{γ} by

$$\check{\mathbf{O}}^{\mathrm{in},\gamma}(z) := \check{\mathbf{O}}^{\mathrm{out}}(z)\omega^{\sigma_3}\mathbf{B}(T^{1/2}W(z))\omega^{-\sigma_3}, \quad z \in D_{\gamma}. \tag{5.52}$$

Then because $\check{\mathbf{O}}^{\text{out}}(z)$ is analytic in D_{γ} it is straightforward to check that $\check{\mathbf{O}}^{\text{in},\gamma}(z)$ is an exact local solution of the jump conditions for $\mathbf{O}(z)$ within D_{γ} , and because ω and ω^{-1} are uniformly bounded since $\text{Re}(h(\gamma)) = 0$ holds exactly at the catastrophic value of μ we also find that

$$\check{\mathbf{O}}^{\mathrm{in},\gamma}(z)\check{\mathbf{O}}^{\mathrm{out}}(z)^{-1} = \mathbb{I} + \mathcal{O}(T^{-1/2}), \quad T \to +\infty$$

holds uniformly for $z \in \partial D_{\gamma}$. Modifying the global parametrix defined in (5.37) in the obvious way and using the fact that neither z = 0 nor $z = \infty$ are contained in D_{γ} , we draw exactly the same conclusions, namely (5.45) and (5.51) only replacing the error estimates with their square roots.

If scenario (v) (resp., (vi)) occurs we use the "leftward" (resp., "downward") deformation and apply a similar procedure to the triangular jump carried by $\Sigma_{2,1}$ (resp., $\Sigma_{2,3}$), and we obtain the same result.

The Riemann–Hilbert problem defining the matrix $\mathbf{B}(\xi)$ is a special case of the Fokas-Its-Kitaev problem encoding the Hermite polynomial of degree n [34]; here we



simply have the n=0 case. To penetrate beyond the bifurcation point one can increase the index n in an effort to compensate for the fact that $Re(h(\gamma))$ becomes negative, also making a suitable modification of the outer parametrix. This generalized method has been successfully used to capture asymptotic behavior slightly beyond a phase transition boundary; see [8, 9, 19].

Although the proof will only be given in Sect. 8.3, only generic bifurcations (i)–(iv) actually occur as (μ, γ) is brought in from $\mu = \infty$ along the designated branch of Γ following a path that avoids the eight branch points that satisfy $B(\mu; \kappa) = 0$. Also, while we have only introduced the harmless and catastrophic bifurcation points in the context of the sector $-\epsilon < \arg(\mu) < \frac{\pi}{2} + \epsilon$, we can easily use the symmetries $(\mu, \gamma) \mapsto (-\mu, -\gamma)$ and $(\mu, \gamma) \mapsto (\mu^*, \gamma^*)$ of Γ to extend the definitions to all of Γ .

Definition 5 (*gO paths*) Let $\kappa \in (-1, 1)$. A gO path is an oriented contour P on Γ originating at $\mu = \infty$ on the gO sheet $\gamma = U_{0,gO}(\mu;\kappa) = -\frac{2}{3}\mu + \mathcal{O}(\mu^{-1})$ such that no point or endpoint of P is a branch point (necessarily lying above a solution of $B(\mu;\kappa) = 0$), and such that no interior point of P is a catastrophic bifurcation point.

A condition under which the asymptotic formulæ (5.45) and (5.51) are valid can then be formulated as follows.

Lemma 6 (Pointwise validity of gO exterior asymptotics) Let $\kappa \in (-1, 1)$. Suppose that $\mu \in \mathbb{C}$ is the sheet projection to \mathbb{C} from the Riemann surface Γ of the endpoint (μ, γ) of a gO path. If (μ, γ) is not a catastrophic bifurcation point, then the asymptotic formula (5.45) is valid with $U_{0,gO}(\mu; \kappa) = \gamma$, and (5.51) holds as well with the indicated rescaling of μ and modification of κ . If (μ, γ) is a catastrophic bifurcation point, the same is true but the relative error terms $\mathcal{O}(|\Theta_0|^{-1})$ and $\mathcal{O}(|\Theta_0, \gamma|^{-1})$ are replaced with $\mathcal{O}(|\Theta_0|^{-1/2})$ and $\mathcal{O}(|\Theta_0, \gamma|^{-1/2})$ respectively.

If $-\epsilon < \arg(\mu) < \frac{\pi}{2} + \epsilon$, then this is a consequence of the steepest-descent analysis presented above. To extend the result to arbitrary values of $\arg(\mu)$, we combine the holomorphic and antiholomorphic symmetries of Γ with Proposition 4 in Sect. 2. In particular, the hypotheses hold for sufficiently large $|\mu|$. Also, note that the condition that the terminal endpoint (μ, γ) is not a catastrophic bifurcation point is open with respect to μ .

5.6 Uniformity of Estimates

It is a minor technical matter to strengthen the pointwise convergence result of Lemma 6 to uniformity on closed subsets of the unbounded region $\mathcal{E}_{gO}(\kappa)$ in the μ -plane where the hypotheses hold with (μ, γ) not a catastrophic bifurcation point. It is not difficult to see that the estimate $\mathbf{E}_+(z) = \mathbf{E}_-(z)(\mathbb{I} + \mathcal{O}(T^{-1}))$, with the error term interpreted in the sup-norm sense over the jump contour Σ_E , holds uniformly on any such closed subset. The analytical issue is that in the small-norm theory of Riemann–Hilbert problems this error estimate is amplified by the $L^2(\Sigma_E)$ operator norm of the Cauchy projection operator with respect to Σ_E . That norm generally depends on the underlying jump contour, and as explained in Sect. 5.3 the contour



 $\Sigma_{\rm E}$ in turn varies with μ through h(z) and α , β , γ . The strategy one takes in controlling the Cauchy operator norm uniformly is to notice that the local dependence of $\Sigma_{\rm E}$ on μ is artificial. Indeed, by cyclic compatibility of the jump matrices for ${\rm E}(z)$ at self-intersection points the jump contour for one value of μ may be deformed into that for another value of μ sufficiently close, and this deformation will not affect the uniform estimates on the jump matrix because those estimates are implied by strict inequalities on the real parts of exponents. So, covering a compact subset of $\mathcal{E}_{\rm gO}(\kappa)$ with a union of open sets on each of which the jump contour $\Sigma_{\rm E}$ can be taken to be fixed, we extract a finite subcover and take the maximum of a finite number of Cauchy operator norms to obtain a uniform error estimate. For uniformity as $\mu \to \infty$, one has to first perform a rescaling of the z-plane to fix the roots $z = \alpha$ and $z = \beta$ in the limit; however since the Cauchy integral operators commute with scaling it is then easy to adapt the uniform convergence argument to a neighborhood of $\mu = \infty$. For details of these arguments in a similar context, see [18, pp. 2519–2520].

This proves the following.

Lemma 7 Let $\kappa \in (-1, 1)$, and suppose that $D \subset \mathbb{C}$ is an unbounded domain consisting of points μ where the hypotheses of Lemma 6 hold with (μ, γ) not a catastrophic bifurcation point. If $F \subset D$ is closed, then (5.45) and (5.51) hold uniformly on F.

To complete the proof of Theorem 2 from Sect. 1.4 it therefore remains only to specify the region in the μ -plane where (5.45) and (5.51) are valid respectively. This will be done in Sect. 8.8.

6 Asymptotic Analysis of M(z) for Sufficiently Large $|\mu|$: gH Case

Now we develop a simplified version of the analysis from Sect. 5 applicable to the gH family. We take $(\Theta_0, \Theta_\infty) \in \Lambda_{\rm gH}^{[3]+}$ so that $s = {\rm sgn}(\Theta_0) = 1$ and $\kappa = -\Theta_\infty/|\Theta_0| \in (-1,1)$, and we assume that for $|\mu|$ sufficiently large with $-\epsilon < {\rm arg}(\mu) < \frac{\pi}{2} + \epsilon$ for some small $\epsilon > 0$, the polynomial P(z) is again in case {211}. However, now we select the solution of the quartic (4.19) that satisfies $\gamma = U_{0,{\rm gH}}^{[3]}(\mu;\kappa) = -2\mu + \mathcal{O}(\mu^{-1})$ as $\mu \to \infty$ (see Sect. 1.3.1). Solving for α and β from (4.20) gives (breaking permutation symmetry) $\alpha = (-2\kappa + 2\mathrm{i}\sqrt{1-\kappa^2})\mu^{-1} + \mathcal{O}(\mu^{-2})$ and $\beta = (-2\kappa - 2\mathrm{i}\sqrt{1-\kappa^2})\mu^{-1} + \mathcal{O}(\mu^{-2})$ as $\mu \to \infty$. Recalling the parametrization of κ by (4.28), we have $\alpha = 2\mathrm{i}\mathrm{e}^{\mathrm{i}\varphi/2}\mu^{-1} + \mathcal{O}(\mu^{-2})$ and $\beta = -2\mathrm{i}\mathrm{e}^{-\mathrm{i}\varphi/2}\mu^{-1} + \mathcal{O}(\mu^{-2})$ as $\mu \to \infty$.

6.1 Analysis of the Exponent h(z)

6.1.1 The Zero-Level Set of Re(h(z))

We remind the reader of the terminology introduced in Sect. 5.1, and of Definitions 2 and 3 in particular. For large $|\mu|$, the quadratic differential $\varrho(z)\,\mathrm{d}z^2$ for $\varrho(z)=\frac{1}{16}z^{-2}(z-\gamma)^2(z-\alpha)(z-\beta)$ can be written under the rescaling $Z=\mu z$ as $\varrho(z)\,\mathrm{d}z^2=\frac{1}{4}Z^{-2}((Z+2\kappa)^2+4(1-\kappa^2))(1+\mathcal{O}(\mu^{-1}))\,\mathrm{d}Z^2$, where the error term is uniform for bounded Z. Neglecting the error term yields a quadratic differential in



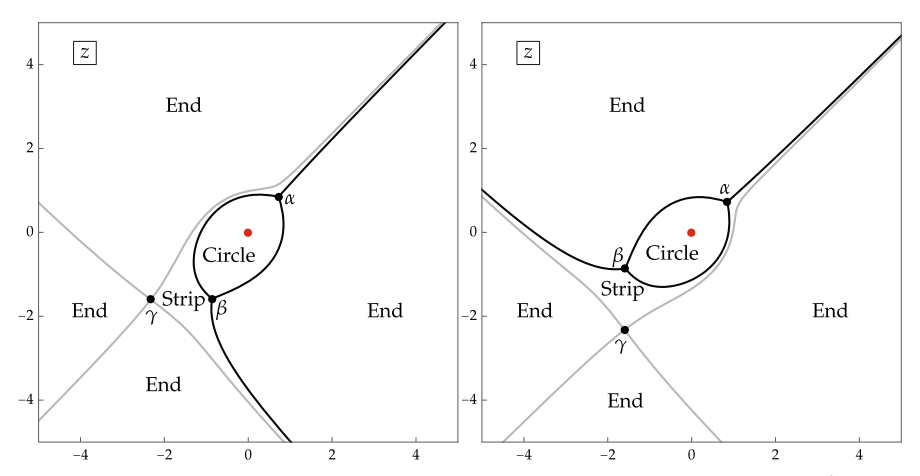


Fig. 23 For $\kappa=0$ and $\mu=1.198+0.983$ i (left) and $\mu=0.983+1.198$ i (right) ($\gamma=U_{0,\mathrm{gH}}^{[3]}(\mu;\kappa)$ analytically continued from large μ), situations in which $\mathrm{Re}(h(\gamma))$ has opposite signs. In both cases the critical v-trajectories divide the plane into four end domains, one strip domain, and one circle domain (Color figure online)

the Z-plane that has Schwarz symmetry and only two finite critical points; hence both finite critical points necessarily lie on the boundary of the circle domain \mathcal{D}_{\circ} containing Z=0. This leading-order model resolves the limiting v-trajectories in the part of the z-plane that asymptotically contains z=0, $z=\alpha$, and $z=\beta$, while $z=\gamma$ is out of the picture. Restoring the error term, one can show that for large $|\mu|$ this structure is preserved and hence both α and β lie on $\partial \mathcal{D}_{\circ}$ while $\gamma \in \mathbb{C} \setminus \overline{\mathcal{D}_{\circ}}$. Therefore, $\partial \mathcal{D}_{\circ}$ is the closure of the union of two v-trajectories, each with endpoints $z=\alpha$, β . From each of the latter critical points, exactly one additional v-trajectory emanates into the exterior of $\partial \mathcal{D}_{\circ}$, and since there can be no divergent v-trajectories by the same argument as in Sect. 5.1, these two v-trajectories can either coincide, terminate at $z=\gamma$, or tend to $z=\infty$. The scenario of coincidence would imply a closed loop formed of v-trajectories that can be easily ruled out by Lemma 4 of Sect. 5.1. Without loss of generality, we assume that $\mathrm{Re}(h(\alpha))=0$.

Suppose that $\operatorname{Re}(h(\gamma)) \neq 0$. It then follows that the v-trajectories emanating from $z = \alpha$, β into the exterior of the circle domain both tend to $z = \infty$, and the exterior of $\partial \mathcal{D}_{\circ}$ is divided by these trajectories into two disjoint components, exactly one of which must contain $z = \gamma$ and the four critical v-trajectories emanating from it. Therefore, the complement of the closure K_z of the union of critical v-trajectories of $\varrho(z) \, \mathrm{d} z^2$ is the disjoint union of four end domains, one strip domain, and one circle domain, as shown in Fig. 23.

One important distinction from the gO case discussed in Sect. 5.1 is that here α and β lie in the same connected component of K_z , as can be seen in Fig. 23. Moreover α and β are joined by two v-trajectories, which implies that in this case the component of K_z containing α and β is a strict subset of the level set Re(h(z)) = 0, because the component contains only two unbounded arcs while the level set has four arcs that go to $z = \infty$ parallel to the four directions $\arg(z) = \pm \frac{\pi}{4}, \pm \frac{3\pi}{4}$. Since the two



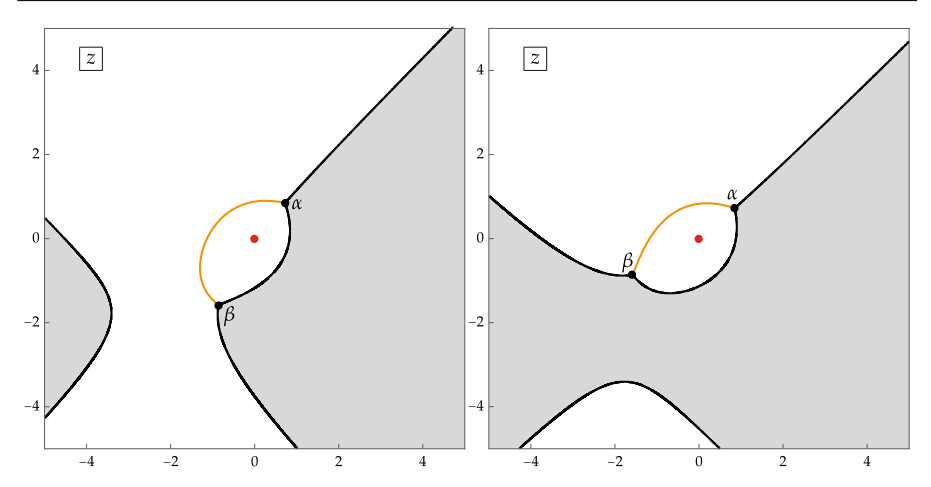


Fig. 24 For the same parameters as in the corresponding panels of Fig. 23, the zero-level set of Re(h(z)) (black and orange curves), the branch cut for h'(z) (orange), and sign of Re(h(z)) (shaded for negative, unshaded for positive) (Color figure online)

missing unbounded arcs of the level set tend to $z=\infty$ in different directions distinct from the direction of the unbounded arcs emanating from α and β and cannot cross the arcs emanating from $z=\gamma$ because $\text{Re}(h(\gamma))\neq 0$ by assumption, it follows that they are trapped within the end domain opposite γ from $z=0\subset\mathcal{D}_{\circ}$. Since the end domain does not contain any critical points, the missing unbounded arcs of the level set actually form the same v-trajectory, which can be seen near the left (resp., bottom) of the left-hand (resp., right-hand) panel of Fig. 24.

The disjoint union of this v-trajectory with the component of K_z containing α and β is precisely the level set Re(h(z)) = 0.

Now we consider the possibility that $Re(h(\gamma)) = 0$. A calculation parallel to (5.1) shows that

$$\operatorname{Re}(h(\gamma)) = \operatorname{Re}\left(\int_{\alpha}^{\gamma} h'(z) \, \mathrm{d}z\right) = \pm \frac{1}{2} \left(\operatorname{Re}(\mu)^2 - \operatorname{Im}(\mu)^2\right) + o(\mu^2), \quad \mu \to \infty,$$

so that $\operatorname{Re}(h(\gamma))$ cannot vanish for large $|\mu|$ unless $\operatorname{arg}(\mu) \approx \frac{\pi}{4} \in (-\epsilon, \frac{\pi}{2} + \epsilon)$. If $\operatorname{Re}(h(\gamma)) = 0$, then the topology of K_z is different. In particular K_z becomes connected and it now coincides with the level set $\operatorname{Re}(h(z)) = 0$. However we observe that if $|\mu|$ is large, then since γ is large while \mathcal{D}_{\circ} is small, the condition $\operatorname{Re}(h(\gamma)) = 0$ can only occur without γ lying on $\partial \mathcal{D}_{\circ}$. Therefore, the topology of the level set $\operatorname{Re}(h(z)) = 0$ in a neighborhood of the circle domain \mathcal{D}_{\circ} is just as if $\operatorname{Re}(h(\gamma)) \neq 0$. We touch on this observation again later in Sect. 6.5.1.

6.1.2 Defining h(z) as a Single-Valued Function

Given the structure of the level set Re(h(z)) = 0 near \mathcal{D}_o as shown in Fig. 24, we now explain how to determine h'(z) and then h(z) precisely. Unlike in the gO case discussed in Sect. 5.1, we can and will take the branch cut Σ_c of R(z) to coincide with



one of the two v-trajectories connecting α and β ; because s=1, we need to select the specific v-trajectory to use so that R(0) = 4s = 4. In the special case that $\kappa = 0$ and $\arg(\mu) = \frac{\pi}{4}$, it is easy to see that for $|\mu|$ sufficiently large α , β , and γ all lie on the diagonal line through the origin, with $\arg(\alpha) = \frac{\pi}{4}$ and $\arg(\beta) = \arg(\gamma) = -\frac{3\pi}{4}$. This implies that $R(z)^2$ is real for z along the same diagonal line, and since by definition $R(z) = z^2 + \mathcal{O}(z)$ as $z \to \infty$, R(z) is positive imaginary for $\arg(z) = \frac{\pi}{4}$ and $|z| > |\alpha|$. It then follows that to have R(0) > 0 we must choose Σ_c to lie in the half-plane above the diagonal line: Im(z) > Re(z). This is the unique v-trajectory on the Jordan curve $\partial \mathcal{D}_{\circ}$ that abuts a region exterior to $\partial \mathcal{D}_{\circ}$ on which Re(h(z)) > 0, and this topological characterization of Σ_c is robust as κ and μ vary. The branch cut Σ_c for R(z) is shown with an orange curve in each panel of Fig. 24. Once R(z) is determined, then so is h'(z) by (4.22). Accounting for the pole of h'(z) at z=0, we choose the point $z=\beta$ to be the common endpoint of the arcs Σ_0 and $\Sigma_{4,3}$ and then we take the jump contour for h(z) to be $\Sigma_h := \Sigma_c \cup \Sigma_0 \cup \Sigma_{4,3}$. Finally, we define $\mathbb{C} \setminus \Sigma_h \ni z \mapsto h(z)$ by integration of $h'(\cdot)$ from α to z over any path lying in $\mathbb{C} \setminus \Sigma_h$. Note that while in the gO case Re(h(z)) exhibits a jump discontinuity across Σ_c , in this case Re(h(z)) extends to Σ_c as a continuous function as a consequence of choosing Σ_c as a zero-level curve of Re(h(z)). The sign of Re(h(z)) is as indicated with shading in Fig. 24.

The analytic function h(z) defined in this way takes continuous boundary values on Σ_h that are related by (with the orientation of the arcs Σ_0 and $\Sigma_{4,3}$ as indicated in Fig. 13 from Sect. 3.1)

$$\Delta h(z) = -2\pi i, \quad z \in \Sigma_0,$$

$$\langle h \rangle (z) = 0, \quad z \in \Sigma_c,$$

$$\Delta h(z) = 2\pi i \kappa, \quad z \in \Sigma_{4,3}.$$
(6.1)

6.2 Introduction of g(z) and Steepest Descent

We proceed to lay the (suitably deformed and fixed in the *z*-plane) jump contour Σ_{gH} from Fig. 14 from Sect. 3.1 over the sign chart of Re(h(z)) as shown in Fig. 25.

In particular, we take $\Sigma_c \subset C \subset \Sigma_{gH}$ and insist that $\operatorname{Re}(h(z)) < 0$ holds on $C \setminus \Sigma_c$. Then we define g(z) from h(z) by (4.22) and use it to define $\mathbf{N}(z)$ from $\mathbf{M}(z)$ by (4.14). Using (6.1) it is easy to check that this transformation removes the jump discontinuities from the arcs $\Sigma_0 \cup \Sigma_{4,3}$, so that $\mathbf{N}(z)$ is analytic for $z \in \mathbb{C} \setminus C$ and $\mathbf{N}(z) \to \mathbb{I}$ as $z \to \infty$. Its jump conditions are

$$\mathbf{N}_{+}(z) = \mathbf{N}_{-}(z) \begin{pmatrix} \mathrm{e}^{T\Delta h(z)} & 0 \\ \mathrm{e}^{2T\langle h\rangle(z)} & \mathrm{e}^{-T\Delta h(z)} \end{pmatrix}, \quad z \in \Sigma_{\mathrm{c}}$$

and

$$\mathbf{N}_{+}(z) = \mathbf{N}_{-}(z)\mathbf{L}(e^{2Th(z)}), \quad z \in C \setminus \Sigma_{c}. \tag{6.2}$$



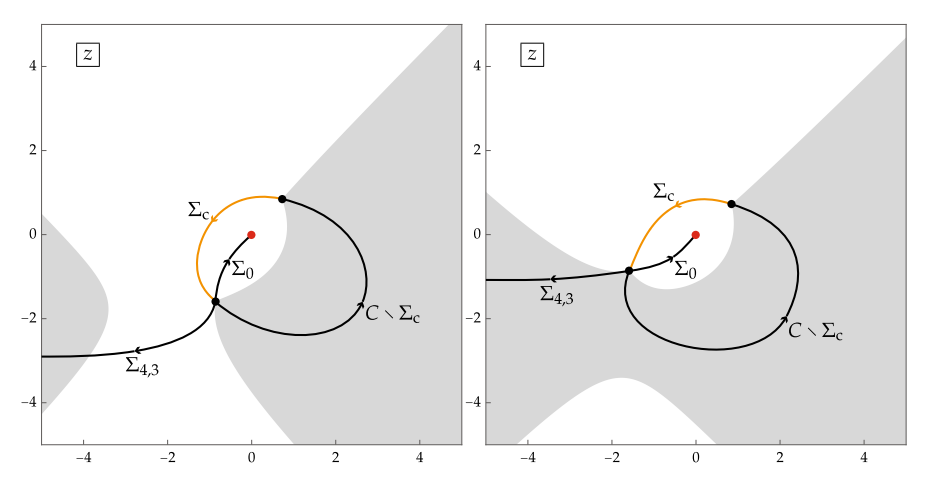


Fig. 25 For the same parameters as in the corresponding panels of Figs. 23 and 24, the jump contour for M(z) (Color figure online)

Applying a "UTU" factorization (see (1.35)) the jump matrix on Σ_c can be written in the form

$$\begin{pmatrix}
\mathbf{e}^{T\Delta h(z)} & 0 \\
\mathbf{e}^{2T\langle h\rangle(z)} & \mathbf{e}^{-T\Delta h(z)}
\end{pmatrix} = \mathbf{e}^{-Th_{-}(z)\sigma_{3}} \begin{pmatrix} 1 & 0 \\
1 & 1 \end{pmatrix} \mathbf{e}^{Th_{+}(z)\sigma_{3}}$$

$$= \mathbf{e}^{-Th_{-}(z)\sigma_{3}} \mathbf{U}(1)\mathbf{T}(1)\mathbf{U}(1)\mathbf{e}^{Th_{+}(z)\sigma_{3}}$$

$$= \mathbf{U}(\mathbf{e}^{-2Th_{-}(z)})\mathbf{T}(\mathbf{e}^{2T\langle h\rangle(z)})\mathbf{U}(\mathbf{e}^{-2Th_{+}(z)})$$

$$= \mathbf{U}(\mathbf{e}^{-2Th_{-}(z)})\mathbf{T}(1)\mathbf{U}(\mathbf{e}^{-2Th_{+}(z)})$$

where in the last step we used (6.1). Based on this factorization, we introduce lens domains Λ^+ and Λ^- on the left and right, respectively, of Σ_c as shown in Fig. 26.

Then we define a new unknown matrix O(z) in terms of N(z) by setting

$$\mathbf{O}(z) := \begin{cases} \mathbf{N}(z)\mathbf{U}(e^{-2Th(z)})^{-1}, & z \in \Lambda^{+} \\ \mathbf{N}(z)\mathbf{U}(e^{-2Th(z)}), & z \in \Lambda^{-} \\ \mathbf{N}(z), & \text{elsewhere,} \end{cases}$$

and it follows that the three factors in the jump of N(z) across Σ_c are split into separate jumps of O(z) across three arcs with the same endpoints:

$$\mathbf{O}_{+}(z) = \mathbf{O}_{-}(z)\mathbf{U}(e^{-2Th(z)}), \quad z \in \partial \Lambda^{\pm}, \tag{6.3}$$

and

$$\mathbf{O}_{+}(z) = \mathbf{O}_{-}(z)\mathbf{T}(1), \quad z \in \Sigma_{c}.$$



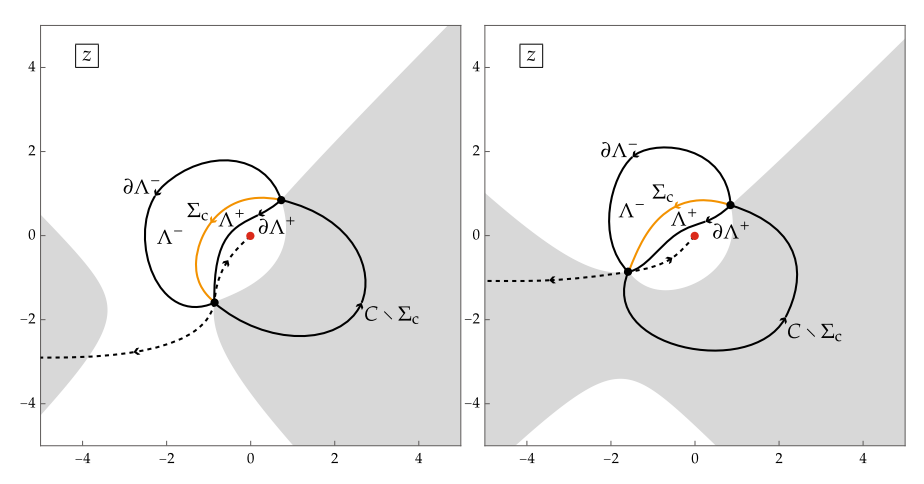


Fig. 26 For the same parameters as in the corresponding panels of Figs. 23–25, the "lens" domains Λ^{\pm} and the modified jump contour for $\mathbf{O}(z)$ (the dashed arcs have been removed by the transformation $\mathbf{M}(z) \mapsto \mathbf{N}(z)$) (Color figure online)

6.3 Parametrix Construction

As in Sect. 5.3, we proceed under the working assumption that as (μ, γ) is analytically continued on the Riemann surface Γ of Definition 1 from the start of Sect. 5 from $\mu = \infty$ along the gH branch $\gamma = U_{0,\mathrm{gH}}^{[3]}(\mu;\kappa)$, the sign chart of $\mathrm{Re}(h(z))$ near the jump contour for $\mathbf{O}(z)$ retains the same structure as established above for sufficiently large $|\mu|$ in the first quadrant.

6.3.1 Outer Parametrix

Because $C \setminus \Sigma_c$ lies in a region where $\operatorname{Re}(h(z)) < 0$ while the lens boundaries $\partial \Lambda^{\pm}$ both lie in regions where $\operatorname{Re}(h(z)) > 0$, it appears reasonable to neglect the jumps on these arcs. We therefore define an outer parametrix $\check{\mathbf{O}}^{\text{out}}(z)$ to be analytic except on Σ_c across which it satisfies the same jump condition as does $\mathbf{O}(z)$, and we insist that $\check{\mathbf{O}}^{\text{out}}(z)$ be bounded except near $z = \alpha$, β where negative one-fourth power divergences are admitted and that $\check{\mathbf{O}}^{\text{out}}(z) \to \mathbb{I}$ as $z \to \infty$. Thus, the outer parametrix is explicitly given by (cf. (5.21))

$$\check{\mathbf{O}}^{\text{out}}(z) = \mathbf{S}_{\text{gH}} j(z)^{\sigma_3} \mathbf{S}_{\text{gH}}^{-1}, \quad \mathbf{S}_{\text{gH}} := \begin{pmatrix} \frac{1}{2} & \mathbf{i} \\ \frac{1}{2} & \mathbf{i} \end{pmatrix}, \tag{6.4}$$

where the function j(z) is defined exactly as in Sect. 5.3. This formula can be obtained from (5.21) using a conjugation by a constant diagonal matrix, and therefore it follows immediately that all four equations in (5.23)–(5.24) are modified only by a common factor. The identity (5.25) holds exactly as written, but it requires a reinterpretation because α , β , and γ are different functions of μ in the gH and gO cases. In the gH case, we have $j(0)^4 = \alpha/\beta = -e^{i\varphi} + \mathcal{O}(\mu^{-1})$ as $\mu \to \infty$. To take the square



p	Conformal map $W:D_p\to\mathbb{C}$	Ray Prein	nages in D_p	Constant matrix C	
		arg(W)	Preimage		
χ	$(-2h(z))^{2/3}$, continued from $C \setminus \Sigma_c$	0	$C \setminus \Sigma_{\mathbf{c}}$	$e^{i\pi\sigma_3/4}$	
		$\frac{2\pi}{3}$	$\partial \Lambda^-$		
		$-\frac{2\pi}{3}$	$\partial \Lambda^+$		
		$\pm\pi$	$\Sigma_{ m c}$		
3	$(-2h(z))^{2/3}$, continued from $C \setminus \Sigma_c$	0	$C\setminus\Sigma_{\mathbf{c}}$	$e^{-i\pi\sigma_3/4}$	
		$\frac{2\pi}{3}$	$\partial \Lambda^+$		
		$-\frac{2\pi}{3}$	$\partial \Lambda^-$		
		$\pm\pi$	$\Sigma_{ m c}$		

Table 4 Data for defining the inner parametrices in D_{α} and D_{β}

root correctly it is easiest to take $\kappa=0$ and $\arg(\mu)=\frac{\pi}{4}$ to arrange α and β along the diagonal with the branch cut for j(z) lying above the diagonal. Then it is easy to see that $j(0)^2=-\mathrm{i}\mathrm{e}^{\mathrm{i}\varphi/2}+\mathcal{O}(\mu^{-1})$ as $\mu\to\infty$. Therefore $j(0)^2\pm j(0)^{-2}=-\mathrm{i}\mathrm{e}^{\mathrm{i}\varphi/2}\pm\mathrm{i}\mathrm{e}^{-\mathrm{i}\varphi/2}+\mathcal{O}(\mu^{-1})$ for large μ . Since also from the large- μ expansions of α , β , and γ in the gH case we have $\frac{1}{4}\gamma(\alpha\pm\beta)=-\mathrm{i}\mathrm{e}^{\mathrm{i}\varphi/2}\pm\mathrm{i}\mathrm{e}^{-\mathrm{i}\varphi/2}+\mathcal{O}(\mu^{-1})$, the exact identity $j(0)^2\pm j(0)^{-2}=\frac{1}{4}\gamma(\alpha\pm\beta)$ holds in place of the more complicated formula (5.26). It follows that both formulæ (5.27)–(5.28) are valid in the gH case as well if we take the first line corresponding to the "leftward" configuration.

6.3.2 Inner Parametrices

Fixing disks D_{α} and D_{β} containing $z=\alpha$ and $z=\beta$ respectively, we can define conformal maps $z\mapsto W(z)$ on each as shown in Table 4. Taking the constant matrix ${\bf C}$ as given in the same table, we again use the formula (5.34) to define from the conformal map W(z) and the outer parametrix (now given by (6.4)) a holomorphic unit determinant matrix ${\bf H}(z)$ on each disk. Then we use (5.35) to define inner parametrices $\check{{\bf O}}^{{\rm in},\alpha}(z)$ and $\check{{\bf O}}^{{\rm in},\beta}(z)$ on D_{α} and D_{β} respectively.

Again, these inner parametrices are exact local solutions within D_{α} and D_{β} of the analyticity and jump conditions to be satisfied by $\mathbf{O}(z)$, and it follows from the construction that the estimates (5.36) are valid in the gH case as well.

6.3.3 Global Parametrix and Error Estimation

We adopt the same definition (5.37) as in the gO case for the global parametrix $\tilde{\mathbf{O}}(z)$ in terms of the (slightly modified) outer and inner parametrices just described. The analysis of the error $\mathbf{E}(z)$ given by (5.38) outlined at the end of Sect. 5.3 is soft and it applies equally well in the present context with the same results; the expansion (5.39) holds with $\mathbf{E}_1 = \mathcal{O}(T^{-1})$ and $\mathbf{E}(0) = \mathbb{I} + \mathcal{O}(T^{-1})$.



6.4 Conditionally Valid Asymptotic Formulæ for the gH Rational Solutions of Painlevé-IV

The relationship between $\mathbf{Y}(\lambda; x)$ and the product $\mathbf{E}(z)\check{\mathbf{O}}^{\text{out}}(z)$ for large λ or large z is exactly as in the gO case, and hence the formula (5.41) for $Y_{1,12}^{\infty}(x)$ holds in the gH case as well. Likewise, the exact formula (5.42) for $\mathbf{Y}_0^0(x)$ is valid; however in the gH case there is substantial simplification in expressing $\mathbf{N}(0)$ in terms of known or estimable quantities. Indeed, in place of (5.43) we have simply $\mathbf{N}(0) = \mathbf{O}(0)$, and then as in the gO case, $\mathbf{O}(0) = (\mathbb{I} + \mathcal{O}(T^{-1}))\check{\mathbf{O}}^{\text{out}}(0)$. Hence the formula for $Y_{0,11}^0(x)Y_{0,12}^0(x)$ matches the first line of (5.44); combining this with (5.41), using the first line of (5.27) and taking into account s = 1 in the definition (3.2) we find

$$u_{\text{gH}}^{[3]}(x; m, n) = u(x) = T^{1/2}(\gamma + \mathcal{O}(T^{-1})) = |\Theta_0|^{1/2} (U_{0,\text{gH}}^{[3]}(\mu; \kappa) + \mathcal{O}(|\Theta_0|^{-1})),$$

$$\mu := \frac{x}{|\Theta_0|^{1/2}}, \quad \kappa := -\frac{\Theta_\infty}{|\Theta_0|}.$$
(6.5)

Likewise, the formula for the fraction $Y_{0,11}^0(x)/Y_{0,21}^0(x)$ matches the first line of (5.46). Combining this with (5.41) and using the first line of (5.28) in the definition (3.2) gives

$$\begin{split} u_{\mathrm{gH}}^{[1]}(x;m,n) &= u_{\mathbb{Q}}(x) = T^{1/2} \left(-\mu - \tfrac{1}{2} \gamma - 2 \gamma^{-1} + \mathcal{O}(T^{-1}) \right) \\ &= |\Theta_0|^{1/2} \left(-\mu - \tfrac{1}{2} U_{0,\mathrm{gH}}^{[3]}(\mu;\kappa) - 2 U_{0,\mathrm{gH}}^{[3]}(\mu;\kappa)^{-1} + \mathcal{O}(|\Theta_0|^{-1}) \right). \end{split}$$

We can apply Lemma 5 from Sect. 5.4 in the case s=1 to write this formula in a more convenient form. Noting that if $\gamma(\mu)$ is the branch of the quartic (4.19) that behaves like $\gamma(\mu) = -2\mu + 2\kappa \mu^{-1} + \mathcal{O}(\mu^{-3})$ then the related function $\gamma_{\mathbb{Q}}(\mu)$ defined by (5.49) obeys $\gamma_{\mathbb{Q}}(\mu) = 2\mu^{-1} + \mathcal{O}(\mu^{-3})$ as $\mu \to \infty$, we arrive at the following:

$$u_{gH}^{[1]}(x; m, n) = u_{\mathbb{Q}}(x) = |\Theta_{0, \mathbb{Q}}|^{1/2} \left(U_{0, gH}^{[1]}(\mu; \kappa_{\mathbb{Q}}) + \mathcal{O}(|\Theta_{0, \mathbb{Q}}|^{-1}) \right),$$

$$\mu := \frac{x}{|\Theta_{0, \mathbb{Q}}|^{1/2}}, \quad \kappa_{\mathbb{Q}} := -\frac{\Theta_{\infty, \mathbb{Q}}}{|\Theta_{0, \mathbb{Q}}|},$$
(6.6)

where $\gamma = U_{0,\mathrm{gH}}^{[1]}(\mu;\kappa)$ is the solution of the quartic (4.19) with asymptotic behavior $U_{0,\mathrm{gH}}^{[1]}(\mu;\kappa) = 2\mu^{-1} + \mathcal{O}(\mu^{-3})$ as $\mu \to \infty$. See Sect. 1.3.

6.5 Bifurcation Points and Conditions for Validity

Looking at the representative plots of K_z in Fig. 23 and recalling Definition 4 of Sect. 5.5, we can describe the possible generic bifurcation scenarios as follows:

- (i) $\gamma(\mu)$ merges with one of the two unbounded v-trajectories emanating from $z = \alpha$, β from either side, or
- (ii) $\gamma(\mu)$ merges with one of the two v-trajectories forming $\partial \mathcal{D}_{\circ}$.



In each of the panels of Fig. 23 two bifurcations described by (i) and one bifurcation described by (ii) are possible. The two diagrams can be connected through a bifurcation point where scenario (i) occurs on the unbounded v-trajectory emanating from $z = \beta$.

6.5.1 Harmless Bifurcation Points

In the gH setting, harmless bifurcations are generic bifurcation points when scenario (i) occurs. When μ is large in the first quadrant with $\gamma = U_{0,\mathrm{gH}}^{[3]}(\mu;\kappa)$, we find such bifurcation points near $\arg(\mu) = \frac{\pi}{4}$. In the special case that $\kappa = 0$, the bifurcation occurs exactly for $\arg(\mu) = \frac{\pi}{4}$ provided that $|\mu|$ is sufficiently large. In this case, setting $\arg(\mu) = \frac{\pi}{4}$ gives the exact result that $\arg(\alpha) = \frac{\pi}{4}$ and $\arg(\gamma) = \arg(\beta) = -\frac{3\pi}{4}$, and by reflection symmetry in the diagonal one can see that γ is connected to β by a critical v-trajectory of $\varrho(z)\,\mathrm{d} z^2$. Harmless bifurcation points are not an obstruction to the steepest descent analysis because the jump contours for $\mathbf{O}(z)$ as shown in Fig. 26 are always localized near the circle domain \mathcal{D}_\circ , while any bifurcation where (i) occurs only affects the topology of the level set $\mathrm{Re}(h(z)) = 0$ outside of some neighborhood of \mathcal{D}_\circ . Therefore the asymptotic formulæ (6.5) and (6.6) remain valid at and beyond any harmless bifurcation points.

6.5.2 Catastrophic Bifurcation Points

The bifurcation points corresponding to scenario (ii) are catastrophic for the steepest descent analysis. Indeed, if (ii) occurs, then the unbounded component of the zero-level curve of Re(h(z)) not containing either $z=\alpha$ or $z=\beta$ merges with γ and the adjacent critical v-trajectory joining α and β and forming part of $\partial \mathcal{D}_{\circ}$. Figure 26 shows that when the isthmus pinches off, either $\partial \Lambda^-$ (left panel) or $C \setminus \Sigma_c$ (right panel) is forced to pass directly over the saddle $z=\gamma$, which at the bifurcation point lies exactly on the zero level of Re(h(z)). According to (6.2) and the fact that $\mathbf{O}(z)=\mathbf{N}(z)$ on $C \setminus \Sigma_c$, the latter contour carries the lower-triangular jump matrix $\mathbf{L}(\mathrm{e}^{2Th(z)})$. Likewise, according to (6.3), the contour $\partial \Lambda^-$ carries the upper-triangular jump matrix $\mathbf{U}(\mathrm{e}^{-2Th(z)})$.

Both of these jump conditions fail to be exponentially small perturbations of the identity jump near the catastrophic bifurcation point. Once the bifurcation point is passed, it becomes necessary to use a spectral curve of class {1111}; however just at the bifurcation point we can reproduce the asymptotic formulæ (6.5) and (6.6) with error terms replaced by their square roots by suitably modifying the procedure described in Sect. 5.5. For instance, approaching the bifurcation point from the configuration in the left panel of Fig. 26, we deal with the upper-triangular jump matrix on $\partial \Lambda^-$ as follows. First we introduce a conformal mapping near $z = \gamma$ by $W(z)^2 = 2(h(z) - h(\gamma))$, then we set $\omega = \mathrm{e}^{-Th(\gamma)}$ (a number with unit modulus), and then we use $\mathbf{B}(T^{1/2}W(z))$ and the relevant outer parametrix given by (6.4) to define an inner parametrix in the disk D_{γ} exactly by (5.52). The inner and outer parametrices match on ∂D_{γ} up to terms of order $\mathcal{O}(T^{-1/2})$, so the desired result follows by small-norm theory. The same idea from Sect. 5.5 of replacing the degree-zero Hermite polynomial parametrix by the degree-n Hermite parametrix allows one to penetrate somewhat beyond the catastrophic bifurcation point, but we will only need the result sketched above.



Appealing to Proposition 4 in Sect. 2 and the symmetries $(\mu, \gamma) \mapsto (-\mu, -\gamma)$ and $(\mu, \gamma) \mapsto (\mu^*, \gamma^*)$ of Γ we may extend the steepest-descent results and the definitions of harmless and catastrophic bifurcation points to allow for arbitrary $\arg(\mu)$. By analogy with Definition 5 and Lemma 6 in Sect. 5.5 we then have the following.

Definition 6 (*gH paths*) Let $\kappa \in (-1, 1)$. A gH path is an oriented contour P on Γ originating at $\mu = \infty$ on the gH sheet $\gamma = U_{0,\text{gH}}^{[3]}(\mu; \kappa) = -2\mu + \mathcal{O}(\mu^{-1})$ such that no point or endpoint of P is a branch point (necessarily lying above a solution of $B(\mu; \kappa) = 0$), and such that no interior point of P is a catastrophic bifurcation point.

Lemma 8 (Pointwise validity of gH exterior asymptotics) Let $\kappa \in (-1,1)$. Suppose that $\mu \in \mathbb{C}$ is the sheet projection to \mathbb{C} from Γ of the endpoint (μ,γ) of a gH path. If (μ,γ) is not a catastrophic bifurcation point, then the asymptotic formula (6.5) is valid with $U_{0,\mathrm{gH}}^{[3]}(\mu;\kappa) = \gamma$, and (6.6) holds as well with γ replaced by $\gamma_{\mathbb{C}}$ and with the indicated rescaling of μ and modification of κ . If (μ,γ) is a catastrophic bifurcation point, the same is true but the relative error terms $\mathcal{O}(|\Theta_0|^{-1})$ and $\mathcal{O}(|\Theta_0,\mathbb{C}|^{-1})$ are replaced with $\mathcal{O}(|\Theta_0|^{-1/2})$ and $\mathcal{O}(|\Theta_0,\mathbb{C}|^{-1/2})$ respectively.

6.6 Uniformity of Estimates

Exactly the same arguments from Sect. 5.6 apply in the gH case as well to yield the following analogue of Lemma 7 from Sect. 5.6.

Lemma 9 Let $\kappa \in (-1, 1)$, and suppose that $D \subset \mathbb{C}$ is an unbounded domain consisting of points μ where the hypotheses of Lemma 8 hold with (μ, γ) not a catastrophic bifurcation point. If $F \subset D$ is closed, then (6.5) and (6.6) hold uniformly on F.

Combining the asymptotic formulæ (6.5) and (6.6) with the symmetry (2.2) then proves Theorem 1 of Sect. 1.4 except for the determination of the region of validity (see Sect. 8.5). But first we study the asymptotic behavior assuming that the spectral curve is of class {1111} and that μ belongs to a suitable Boutroux domain.

7 Asymptotic Analysis of M(z) in Boutroux Domains for the gO and gH Cases

Now we turn to the analysis of the rational solutions of (1.1) in the domains where the solutions have many zeros and poles. Although details are different in several cases (see Appendix E), still a unified treatment of the gH and gO families is possible. A reader mostly interested in the exterior asymptotics and the boundary curves can safely skip ahead to Sect. 8, wherein only the arguments in Sect. 8.7 are motivated by Sects. 7.3–7.5.

7.1 Stokes Graphs for Boutroux Spectral Curves of Class {1111} and Abstract Stokes Graphs for Boutroux Domains

We start by revisiting the relationship between the zero-level curve of Re(h(z)) and the closure of the union of critical trajectories K_z begun in Sects. 5.1 and 6.1, now under the



assumption that the Riemann surface \mathcal{R} is a Boutroux curve of class {1111}. From the formula $\varrho(z) := h'(z)^2 = \frac{1}{16}z^{-2}P(z) = \frac{1}{16}z^{-2}(z-\alpha)(z-\beta)(z-\gamma)(z-\delta)$ we see that h'(z) may be considered to be a meromorphic function on \mathcal{R} with purely real residues at the poles over $z=0,\infty$. Therefore the only possible monodromy of $\operatorname{Re}(h(z))$ on \mathcal{R} arises from the nontrivial homology of \mathcal{R} as a curve of genus one. But since \mathcal{R} is Boutroux, there is no such monodromy and therefore $\operatorname{Re}(h(z))$ is determined up to an integration constant as a single-valued non-constant function on \mathcal{R} that is harmonic away from the poles of h'(z). As in Sect. 5.1, it follows that the quadratic differential $\varrho(z) \, \mathrm{d} z^2$ has no divergent critical v-trajectories (i.e., v-trajectories having a zero of $\varrho(z)$ as an endpoint; see Definition 2 in that section). In the current setting we refer to the closure K_z of the union of the critical v-trajectories of $\varrho(z) \, \mathrm{d} z^2$ as the *Stokes graph* of \mathcal{R} .

The key feature contributed by the condition that \mathcal{R} is Boutroux is that the Stokes graph of \mathcal{R} coincides with the projection from \mathcal{R} to the z-plane of the level curve $\operatorname{Re}(h(z)) = \operatorname{Re}(h(\alpha))$ (or $= \operatorname{Re}(h(\beta)) = \operatorname{Re}(h(\gamma)) = \operatorname{Re}(h(\delta))$ by the Boutroux conditions (4.23)). To see this, we argue as follows. Clearly every point on the Stokes graph of \mathcal{R} is on the level curve. The complement of the Stokes graph is then the disjoint union of a single circle domain \mathcal{D}_o containing the double pole z=0 and finitely many end domains (strip domains and ring domains being excluded because they require any branch of $\operatorname{Re}(h(z))$ to take different values on different parts of their boundaries); see Definition 3 from Sect. 5.1. But each end domain is mapped conformally by a branch of $e^{h(z)}$ onto an open right or left half-plane while the circle domain is mapped conformally by a branch of $e^{h(z)}$ onto the interior or exterior of a circle. Therefore in the interior of each end domain or circle domain, $\operatorname{Re}(h(z))$ is unequal to its constant value on the boundary. So there are no points of the level set of $\operatorname{Re}(h(z)) = \operatorname{Re}(h(\alpha))$ not contained in the Stokes graph of \mathcal{R} .

Since there are no strip domains and $\varrho(z)\,\mathrm{d}z^2$ has a pole of order 6 at $z=\infty$, a neighborhood of the point at infinity is covered by the disjoint union of four end domains and four critical v-trajectories separating them and approaching $z=\infty$ asymptotically in the diagonal directions $\arg(z)=\pm\frac{\pi}{4},\pm\frac{3\pi}{4}$. These four are the only end domains since there are no other poles of $\varrho(z)\,\mathrm{d}z^2$ of order greater than two, and the four end domains are mutually disjoint on the z-sphere (every end domain has exactly one such pole at a unique point on its boundary on the z-sphere). On the z-sphere the Stokes graph is therefore a planar graph bounding exactly five faces (four end domains and one circle domain). The vertices of the graph are the points $z=\alpha$, β , γ , δ , ∞ of degrees $d(\alpha)=d(\beta)=d(\gamma)=d(\delta)=3$ and $d(\infty)=4$. Based on the count of vertices and their degrees and the fact that $z=\infty$ is necessarily connected to a finite vertex, by enumeration it is easy to check that the Stokes graph of $\mathcal R$ is connected, and therefore by Euler's formula there are exactly 8 edges.

Given the Stokes graph K_z of \mathbb{R} , we may assume that h'(z) is an analytic function in $\mathbb{C} \setminus K_z$ by suitably arranging the branch cut locus B of R(z) in the formula (4.22) to lie within K_z . It then follows by integration along contours in $\mathbb{C} \setminus (B \cup \{0\})$ with fixed base point in the same domain that $\operatorname{Re}(h(z))$ becomes a well-defined single-valued function of z that is harmonic on $\mathbb{C} \setminus (B \cup \{0\})$ and that extends continuously to B. By choice of base point (integration constant) we may assume that $\operatorname{Re}(h(z)) = 0$ whenever $z \in K_z$,



and then the sign of Re(h(z)) will be well defined in each component of $\mathbb{C} \setminus K_z$. This essential property of h(z) will play a key role in the steepest descent analysis below.

If we retain only the essential topological information, we associate to the Stokes graph of \mathcal{R} an abstract Stokes graph. This is a kind of connected planar graph (allowing for loops) with four vertices of degree 3 representing $z=\alpha,\beta,\gamma,\delta$ and four special vertices of degree 1 representing the four diagonal directions at $z=\infty$. We place the four latter vertices at the four corners of a bounding square (the edges of which are not considered as part of the graph) and require that all other edges lie within this square. Each abstract Stokes graph has exactly 5 faces on the square representing the four end domains and one circle domain, and by Euler's formula, there are exactly 8 edges. We identify two abstract Stokes graphs that are related by a homeomorphism of the bounding square and its interior that fixes the square.

Now suppose that for given $\kappa \in (-1, 1)$, a suitable smooth function $\mu \mapsto E$ is specified on a Boutroux domain $\mathcal B$ so that the Boutroux curve $\mathcal R$ varies with $\mu \in \mathcal B$. While the Stokes graph of $\mathcal R$ generally also varies with μ , the abstract Stokes graph is an invariant, depending only Boutroux domain $\mathcal B$ and the corresponding solution $\mu \mapsto E$ of the Boutroux equations (4.23). This also implies that the branch points α , β , γ , and δ may be consistently labeled on $\mathcal B$ by labeling them for just one value of $\mu \in \mathcal B$.

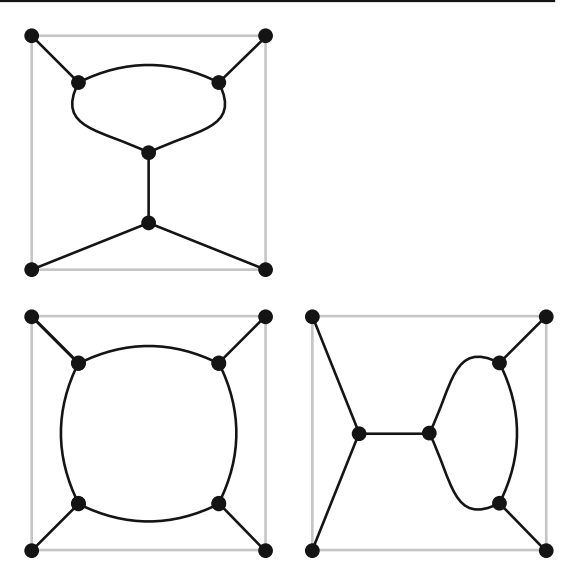
7.2 Hypotheses Concerning Boutroux Domains

Recall from Sect. 4.4 that $\mu=0$ is contained within a Boutroux domain on which E=0 at the origin. Without worrying about its boundary, we denote this domain by \mathcal{B}_{\square} , and we can use the invariance of the abstract Stokes graph for \mathcal{B}_{\square} to deduce it from the special point $(\mu, E)=(0,0)$. The Stokes graph K_z for this point is the closure of the union of the three critical v-trajectories emanating from each of the four zeros $z=\alpha,\beta,\gamma,\delta$ of P(z), which are written explicitly in (4.28)–(4.29). Each of these v-trajectories must either terminate at one of the four zeros (possibly returning to the same zero a priori, although we will shortly rule that out) or escape to $z=\infty$ in one of the four directions $\arg(z)=\pm\frac{\pi}{4},\pm\frac{3\pi}{4}$. Each of the latter directions accepts exactly one critical v-trajectory. Also recall that exactly one of the five maximal connected components of $\overline{\mathbb{C}}\setminus K_z$ is a circle domain \mathcal{D}_{\circ} that has at least one of the four zeros $z=\alpha,\beta,\gamma,\delta$ on its boundary $\partial\mathcal{D}_{\circ}$, a Jordan curve.

Now observe that if $\mu=0$ and E=0, then the quadratic differential $\varrho(z)\,\mathrm{d} z^2$ enjoys Schwarz reflection symmetry in both the real and imaginary z-axes. Since the group of reflection symmetries acts freely on the four roots of P(z) in this case, all four branch points lie on the boundary $\partial \mathcal{D}_o$ of the circle domain \mathcal{D}_o . Thus, there are four critical v-trajectories whose closure is $\partial \mathcal{D}_o$, and that connect the four zeros in pairs. It remains to determine the fate of the remaining critical v-trajectory emanating from each of the four zeros. By Lemma 4 of Sect. 5.1, none of these can coincide with any of the others (necessarily forming, with part of $\partial \mathcal{D}_o$, a Jordan curve of v-trajectories and their endpoints with only regular points in its interior so that referring to (5.2)–(5.3) $L \leq 0$ while R=2), so all four of them must go to $z=\infty$. By symmetry, the v-trajectory emanating from each zero tends to infinity in the same quadrant that



Fig. 27 Abstract Stokes graphs for the Boutroux domains \mathcal{B}_{\square} (lower left), $\mathcal{B}_{\triangleright}$ (right), and \mathcal{B}_{\triangle} (top)



contains the zero. This completes the qualitative description of the Stokes graph for $\mu=0$ with E=0 for all $\kappa\in(-1,1)$. Numerical plots confirm this qualitative description; see the upper left-hand panel of Fig. 39a or Fig. 41a in Appendix E for the Stokes graph for $\mu=0$ and $\kappa=0$. The corresponding abstract Stokes graph for the whole Boutroux domain \mathcal{B}_{\square} is shown in the lower left-hand plot in Fig. 27.

We now hypothesize the existence of two additional Boutroux domains of the type described at the end of Sect. 4.4. These are assumed to be pairwise disjoint and disjoint from \mathcal{B}_{\square} , and they are generated by continuation from class {1111} Boutroux curves based at nonzero points on the positive real and imaginary μ -axes. We denote them by $\mathcal{B}_{\triangleright}$ and \mathcal{B}_{\triangle} respectively, and we further hypothesize that the abstract Stokes graphs for these Boutroux domains are as illustrated in Fig. 27. These hypotheses will be proved in Sect. 8.9.

The asymptotic approximations for the rational Painlevé-IV functions that we will obtain in the rest of this section are conditional on the assumption that $\mu \in \mathcal{B}_{\square} \cup \mathcal{B}_{\triangleright} \cup \mathcal{B}_{\triangle}$ and that the abstract Stokes graphs for the three Boutroux domains are as hypothesized.

7.3 Basic Setup

To study the rational Painlevé-IV functions on Boutroux domains, for $T=|\Theta_0|\gg 1$, $s=\mathrm{sgn}(\Theta_0)=\pm 1$ we represent x in the form (cf. (1.14)) $x=T^{1/2}\mu+T^{-1/2}\zeta$, where we assume that $\mu\in\mathcal{B}_\square\cup\mathcal{B}_\rhd\cup\mathcal{B}_\vartriangle$ and $s=\pm 1$ (gO case) or $\mu\in\mathcal{B}_\square$ and s=1 (gH case), and that $\zeta\in\mathbb{C}$. Recalling from Remark 11 in Sect. 4.1 that the parameters Θ_0 and Θ_∞ are associated with the function $u(x)=u_F^{[3]}(x;m,n)$ for $F=\mathrm{gH}$ or $F=\mathrm{gO}$, we have $\kappa:=-\Theta_\infty/T\in(-1,1)$ differing from a limiting value in the same interval by $\mathcal{O}(T^{-1})$. The matrix $\mathbf{M}(z)=\mathbf{M}^{(T,s,\kappa)}(z;X)=\mathbf{M}^{(T,s,\kappa)}(z;\mu+T^{-1}\zeta)$



depends on (μ, ζ) only through the linear combination $X = \mu + T^{-1}\zeta$, but later (μ, ζ) will admit interpretation as independent variables.

Indeed, the variables (μ, ζ) immediately play distinguished roles, as the first step of our analysis of $\mathbf{M}(z)$ is to make use of the Stokes graph in the z-plane whose abstract version is determined only by the Boutroux domain containing μ . Examples of actual Stokes graphs for representative values of $\mu \in \mathcal{B}_{\square} \cup \mathcal{B}_{\triangleright} \cup \mathcal{B}_{\triangle}$ and κ are shown with black and orange arcs in the left-hand panels of Figs. 39a–45a that can be found in Appendix E. In these plots, the union of black and orange arcs form the same Stokes graph for both signs of $s=\pm 1$. However, the orange arcs are distinguished as the branch cuts for R(z) and hence h'(z), and we choose these to differ for s=1 and s=-1 as indicated. As was shown in Sect. 7.1, the assumption that the spectral curve \mathcal{R} is Boutroux and the choice that the branch cuts of h'(z) are arcs of the Stokes graph together imply that $\text{Re}(h(z)) = \text{Re}(h^{(s,\kappa)}(z;\mu))$ is well defined as a continuous function of $z \in \mathbb{C} \setminus \{0\}$ that is harmonic except on the branch cuts of h'(z) (orange arcs) and that vanishes exactly on the Stokes graph. Hence it has a well-defined sign on each connected component of the complement of the Stokes graph, and these signs are indicated in all plots in Appendix E with white for positive and shading for negative.

Also indicated on the left-hand panels of Figs. 39a–45a are two contours, ℓ_1 and ℓ_2 (in some cases ℓ_2 is a union of two arcs), and invoking the Boutroux conditions (4.23) we use these arcs to define two real constants, R_1 and R_2 , by the formula

$$R_j := -i \int_{\ell_j} h'(z) \, dz = \frac{1}{4} i \int_{\ell_j} \frac{R(z)}{z} \, dz \in \mathbb{R}, \quad j = 1, 2.$$
 (7.1)

The next step is to place the jump contour Σ appropriately relative to the Stokes graph in the *z*-plane. We use

- In the gO case:
 - the basic configuration of Σ (see Fig. 13 from Sect. 3.1, in the *z*-plane instead of the λ -plane) when $\mu \in \mathcal{B}_{\square}$,
 - the "leftward" deformation of Σ (see the left-hand panel of Fig. 15 from Sect. 4.2) when $\mu \in \mathcal{B}_{\triangleright}$, and
 - the "downward" deformation of Σ (see the right-hand panel of the same figure) when $\mu \in \mathcal{B}_{\Delta}$;
- In the gH case: the simplified contour $\Sigma = \Sigma_{\rm gH}$ described in Remark 6 of Sect. 3.1 (see Fig. 14 from that section, in the *z*-plane instead of the λ -plane, and denoting the deformed closed-loop component of $\Sigma_{\rm gH}$ by C).

We then arrange the arcs of the jump contour Σ relative to the Stokes graph as shown in the right-hand panels of Figs. 39a–45a in Appendix E. In these plots, an arc of Σ is frequently split into sub-arcs that belong to different critical v-trajectories in the Stokes graph, in which case we use superscripts to distinguish the different sub-arcs that carry the same jump matrix for $\mathbf{M}(z)$. In particular for the gO case, subarcs Σ_j^k of Σ_j , j=1,2,3,4 will always be placed on $\partial \mathcal{D}_\circ$ and the arc Σ_c will always be placed on another arc of the Stokes graph. In both the gO and gH cases, the arcs of Σ carrying triangular jump matrices satisfy the principle that those carrying lower-



triangular (resp., upper-triangular) matrices should be placed such that the possibly non-strict inequality $\operatorname{Re}(h(z)) \leq 0$ (resp., $\operatorname{Re}(h(z)) \geq 0$) holds, in order to avoid exponential growth of the off-diagonal matrix element. Finally, the arc Σ_0 always carries a diagonal jump matrix, and it may be placed arbitrarily within the circle domain \mathcal{D}_{\circ} once its endpoints have been fixed by prior considerations (one of the endpoints is z=0).

7.4 Steepest Descent

While $\operatorname{Re}(h(z))$ is well defined as a continuous function on the z-plane, h(z) itself has discontinuities along certain cuts due to the monodromy of $\operatorname{Im}(h(z))$ about (i) the branch cuts of h'(z) as measured by the real constants R_j , j=1,2 defined in (7.1), and (ii) the poles of h'(z) at z=0 and $z=\infty$ as measured by the real residues $-\kappa$ and -s, respectively. We will explain how we determine one or more purely imaginary integration constants to fix h(z) later in Sect. 7.5. However, we can say now that h(z) will certainly be analytic except on some arcs of the jump contour Σ for $\mathbf{M}(z)$ as already determined. Therefore $g(z)=g^{(s,\kappa)}(z;\mu):=h^{(s,\kappa)}(z;\mu)+\phi(z;\mu)$ is analytic for $z\in\mathbb{C}\setminus\Sigma$ so we may use the formula (4.14) to transform $\mathbf{M}(z)$ into $\mathbf{N}(z)$. Because $\mathbf{M}(z)=\mathbf{M}^{(T,s,\kappa)}(z;\mu+T^{-1}\zeta)$ depends on $X=\mu+T^{-1}\zeta$ while g is independent of ζ , we write $\mathbf{N}(z)=\mathbf{N}^{(T,s,\kappa)}(z;\mu,\zeta)$ to distinguish the now-independent roles of the parameters $\mu\in\mathcal{B}_\square\cup\mathcal{B}_\triangleright\cup\mathcal{B}_\triangle$ and $\zeta\in\mathbb{C}$.

The jump conditions for M(z) take the form

$$\mathbf{M}_{+}(z) = \mathbf{M}_{-}(z) \exp\left(\left[\frac{1}{2}\zeta z + T\phi(z;\mu)\right]\sigma_{3}\right) \mathbf{V} \exp\left(-\left[\frac{1}{2}\zeta z + T\phi(z;\mu)\right]\sigma_{3}\right),\,$$

where **V** is a different constant matrix on different arcs of Σ . It then follows that the corresponding jump condition for **N**(z) on a given arc $A \subset \Sigma$ can be written as

$$\mathbf{N}_{+}(z) = \mathbf{N}_{-}(z)e^{\zeta z\sigma_{3}/2}e^{-Th_{-}(z)\sigma_{3}}\mathbf{V}e^{Th_{+}(z)\sigma_{3}}e^{-\zeta z\sigma_{3}/2}, \quad z \in A \subset \Sigma.$$

Here $h_{\pm}(z)$ denote the boundary values taken on the arc A by h(z). We then transform $\mathbf{N}(z)$ into $\mathbf{O}(z)$ by the following steepest-descent procedure, in which we "open lenses" of the jump contour about those arcs of Σ lying on the Stokes graph, with the sole exception of Σ_c when $\mu \in \mathcal{B}_{\triangleright} \cup \mathcal{B}_{\triangle}$. We first factor the constant "core" jump matrix \mathbf{V} for each such arc A into a product $\mathbf{V}^-\mathbf{V}^0\mathbf{V}^+$ of three unit-determinant constant factors using an appropriate choice among the identities (1.35). The factor \mathbf{V}^+ (resp., \mathbf{V}^-) will be associated with the region of $\mathbb{C} \setminus \Sigma$ lying immediately to the left (resp., right) of the arc A. We require \mathbf{V}^\pm to be lower (upper) triangular if the inequality $\mathrm{Re}(h(z)) < 0$ ($\mathrm{Re}(h(z)) > 0$) holds on the corresponding region of the z-plane; this criterion then determines exactly which of the identities (1.35) is to be used in each case. For the gO family, we will need to apply this procedure to the four "core" jump matrices $\mathbf{V} = \mathbf{V}_i$, $j = 1, \ldots, 4$, as defined by (3.4) for which the factorizations in



(1.35) take the form

$$\begin{split} \mathbf{V}_1 &= \mathbf{L} \left(2 \exp \left(\frac{\mathrm{i} \pi}{6} \right) \right) \mathbf{D} \left(\frac{1}{\sqrt{3}} \right) \mathbf{U} (-\frac{\sqrt{3}}{2}) \quad \text{("LDU")} \\ &= \mathbf{L} \left(2 \exp \left(\frac{\mathrm{5} \mathrm{i} \pi}{6} \right) \right) \mathbf{T} (2) \mathbf{L} \left(-\frac{2}{\sqrt{3}} \right) \quad \text{("LTL")} \\ &= \mathbf{U} \left(\frac{1}{2} \exp \left(-\frac{\mathrm{5} \mathrm{i} \pi}{6} \right) \right) \mathbf{D} \left(\exp \left(\frac{\mathrm{i} \pi}{6} \right) \right) \mathbf{L} \left(\frac{2}{\sqrt{3}} \exp \left(\frac{\mathrm{i} \pi}{3} \right) \right) \quad \text{("UDL")} \\ &= \mathbf{U} \left(\frac{1}{2} \exp \left(-\frac{\mathrm{i} \pi}{6} \right) \right) \mathbf{T} \left(\frac{2}{\sqrt{3}} \exp \left(\frac{\mathrm{i} \pi}{6} \right) \right) \mathbf{U} \left(\frac{\sqrt{3}}{2} \exp \left(-\frac{\mathrm{i} \pi}{3} \right) \right) \quad \text{("UTU")}, \\ \mathbf{V}_2 &= \mathbf{V}_1^{*-1} = \mathbf{L} \left(\frac{2}{\sqrt{3}} \exp \left(\frac{2\mathrm{i} \pi}{3} \right) \right) \mathbf{D} \left(\exp \left(\frac{\mathrm{i} \pi}{6} \right) \right) \mathbf{U} \left(\frac{1}{2} \exp \left(-\frac{\mathrm{i} \pi}{6} \right) \right) \quad \text{("LDU")} \\ &= \mathbf{L} \left(\frac{2}{\sqrt{3}} \right) \mathbf{T} (-2) \mathbf{L} \left(2 \exp \left(\frac{\mathrm{i} \pi}{6} \right) \right) \quad \text{("LTL")} \\ &= \mathbf{U} \left(\frac{\sqrt{3}}{2} \right) \mathbf{D} (\sqrt{3}) \mathbf{L} \left(2 \exp \left(\frac{\mathrm{i} \pi}{6} \right) \right) \quad \mathbf{U} \left(\frac{1}{2} \exp \left(-\frac{\mathrm{5} \mathrm{i} \pi}{6} \right) \right) \quad \text{("UTU")}, \\ \mathbf{V}_3 &= \mathbf{L} \left(2 \exp \left(\frac{\mathrm{i} \pi}{6} \right) \right) \mathbf{D} \left(\frac{1}{\sqrt{3}} \exp \left(-\frac{\mathrm{i} \pi}{3} \right) \right) \mathbf{U} \left(\frac{\sqrt{3}}{2} \exp \left(-\frac{\mathrm{i} \pi}{3} \right) \right) \quad \text{("LDU")} \\ &= \mathbf{L} \left(2 \exp \left(\frac{\mathrm{5} \mathrm{i} \pi}{6} \right) \right) \mathbf{D} \left(2 \exp \left(-\frac{\mathrm{i} \pi}{3} \right) \right) \mathbf{U} \left(\frac{\sqrt{3}}{2} \exp \left(-\frac{\mathrm{i} \pi}{3} \right) \right) \quad \text{("LDU")} \\ &= \mathbf{U} \left(\frac{1}{2} \exp \left(-\frac{\mathrm{5} \mathrm{i} \pi}{6} \right) \right) \mathbf{D} \left(\exp \left(-\frac{\mathrm{i} \pi}{6} \right) \right) \mathbf{L} \left(\frac{2}{\sqrt{3}} \exp \left(\frac{\mathrm{i} \pi}{3} \right) \right) \quad \text{("UDL")} \\ &= \mathbf{U} \left(\frac{1}{2} \exp \left(-\frac{\mathrm{5} \mathrm{i} \pi}{6} \right) \right) \mathbf{D} \left(\exp \left(-\frac{\mathrm{i} \pi}{6} \right) \right) \mathbf{U} \left(\frac{\sqrt{3}}{2} \exp \left(\frac{\mathrm{i} \pi}{3} \right) \right) \quad \text{("UDL")} \\ &= \mathbf{U} \left(\frac{1}{2} \exp \left(-\frac{\mathrm{i} \pi}{6} \right) \right) \mathbf{D} \left(\exp \left(-\frac{\mathrm{i} \pi}{6} \right) \right) \mathbf{U} \left(\frac{\sqrt{3}}{2} \exp \left(\frac{\mathrm{i} \pi}{3} \right) \right) \quad \text{("UDU")} \\ &= \mathbf{L} \left(\frac{2}{\sqrt{3}} \exp \left(-\frac{2\mathrm{i} \pi}{3} \right) \right) \mathbf{D} \left(\exp \left(-\frac{\mathrm{i} \pi}{6} \right) \right) \mathbf{U} \left(\frac{1}{2} \exp \left(-\frac{\mathrm{i} \pi}{6} \right) \right) \quad \text{("UDU")} \\ &= \mathbf{L} \left(\frac{2}{\sqrt{3}} \exp \left(-\frac{2\mathrm{i} \pi}{3} \right) \right) \mathbf{D} \left(2 \exp \left(-\frac{2\mathrm{i} \pi}{3} \right) \right) \mathbf{L} \left(2 \exp \left(\frac{\mathrm{5} \mathrm{i} \pi}{6} \right) \right) \quad \text{("UDU")} \\ &= \mathbf{U} \left(\frac{\sqrt{3}}{2} \exp \left(-\frac{2\mathrm{i} \pi}{3} \right) \right) \mathbf{D} \left(\sqrt{3} \exp \left(-\frac{\mathrm{i} \pi}{3} \right) \right) \mathbf{L} \left(2 \exp \left(\frac{\mathrm{5} \mathrm{i} \pi}{6} \right) \right) \quad \text{("UDU")} \\ &= \mathbf{U} \left(\frac{\sqrt{3}}{2} \exp \left(-\frac{2\mathrm{i} \pi}{3} \right) \right) \mathbf{D} \left(\frac{\sqrt{3}}{3} \exp \left(-\frac{\mathrm{i$$

For the gH family, the only "core" jump matrix that requires any factoring is the matrix L(1) and just the "UTU" factorization suffices:

$$L(1) = U(1)T(1)U(1).$$

Now let A^+ (resp., A^-) denote an arc with the same endpoints and orientation as A but lying in the region to the left (resp., right) of A; thus A^\pm form a "lens" about the central arc A. Then, we set

$$\mathbf{O}(z) := \mathbf{N}(z) \mathrm{e}^{\zeta z \sigma_3/2} \mathrm{e}^{-Th(z)\sigma_3} (\mathbf{V}^\pm)^{\mp 1} \mathrm{e}^{Th(z)\sigma_3} \mathrm{e}^{-\zeta z \sigma_3/2}, \quad \text{for } z \text{ between } A \text{ and } A^\pm.$$

Repeating this substitution for each arc $A \subset \Sigma$, $A \neq \Sigma_c$, lying on the Stokes graph and elsewhere defining $\mathbf{O}(z) := \mathbf{N}(z)$, we arrive at an equivalent unknown matrix $\mathbf{O}(z) = \mathbf{O}^{(T,s,\kappa)}(z;\mu,\zeta)$. The matrix function $z \mapsto \mathbf{O}(z)$ is analytic except on the



contour Σ augmented with the lens boundaries A^{\pm} and omitting Σ_0 and, in the gH case, $\Sigma_{4,3}$ (the omitted arcs are removed already by the substitution $\mathbf{M}(z) \mapsto \mathbf{N}(z)$). Also $\mathbf{O}(z)$ satisfies the normalization condition $\mathbf{O}(z) \to \mathbb{I}$ as $z \to \infty$. The jump conditions for O(z) are illustrated for each case in Figs. 39b-45b in Appendix E, in which we specify the matrix **W** for each arc such that $\widetilde{\mathbf{O}}_{+}(z) = \widetilde{\mathbf{O}}_{-}(z)\mathbf{W}$, where

$$\widetilde{\mathbf{O}}(z) := \mathbf{O}(z) e^{\zeta z \sigma_3/2} e^{-Th(z)\sigma_3}.$$

Note that **W** is a "core" jump matrix for O(z) on an arc of the modified jump contour in the same way that V is a "core" jump matrix for N(z) on an arc of Σ .

Some further simplification of the jump contour for O(z) is easily performed. Indeed, one may observe that in any situation that two lenses share a common endpoint $z_0 \in \partial \mathcal{D}_0$ that is not one of the four distinguished points $z = \alpha, \beta, \gamma, \delta$, the (two or three) contours approaching z_0 either from within or from without \mathcal{D}_{\circ} can be fused together into a single arc across which O(z) experiences no jump at all. One then checks further that the remaining jumps for O(z) on the two remaining arcs of Σ that meet at z_0 are consistent.

Example 1 In the configuration for the gO family with $\mu \in \mathcal{B}_{\square}$ and s=1 as depicted in Fig. 39a of Appendix E, we can regard the jump contour for O(z) as having just one lens joining the pair of points $z = \alpha$, β and consisting of

- an arc inside \mathcal{D}_{\circ} from α to β carrying the "core" jump matrix $\mathbf{W}=\mathbf{U}(\frac{\sqrt{3}}{2}\exp(\frac{\mathrm{i}\pi}{3}))$, an arc along $\partial\mathcal{D}_{\circ}$ from α to β carrying the "core" jump matrix $\mathbf{W}=\mathbf{T}(\frac{2}{\sqrt{3}}\exp(-\frac{\mathrm{i}\pi}{6}))$, and
- two arcs outside \mathcal{D}_{\circ} from an arbitrary point on $\Sigma_{2,3}$ away from $\partial \mathcal{D}_{\circ}$ to α and to β carrying "core" jump matrices $\mathbf{W} = \mathbf{U}(\frac{1}{2}\exp(-\frac{5i\pi}{6}))$ and $\mathbf{W} = \mathbf{U}(\frac{1}{2}\exp(-\frac{i\pi}{6}))$ respectively.

Completely analogous deformations produce single lenses joining the pairs $z = \alpha$, δ and $z = \gamma$, δ . With the additional use of jump identities for the function h(z) near the junction point between $\Sigma_{4,3}$ and Σ_0 (as shown for the case at hand in the left-hand panel of Fig. 39c), one achieves a similar result and obtains a single lens connecting $z = \beta$, γ , but the simplification occurs only for the matrix $\mathbf{O}(z)$ and not also $\mathbf{O}(z)$, and it hinges on $sT = \Theta_0$, $T\kappa = -\Theta_{\infty}$, and the gO lattice conditions $(\Theta_0, \Theta_{\infty}) \in \Lambda_{gO}$ (see (1.11)).

In each case, the fact that such simplification is possible stems from the fact that the jump conditions of Riemann-Hilbert Problem 1 in Sect. 3.1 are consistent at all selfintersection points. By analyticity of the exponent function $\lambda^2 + 2x\lambda$, this consistency makes the locations of these junction points somewhat arbitrary.

7.5 Specification of h(z)

We now resolve all remaining ambiguity about the function h(z). As mentioned at the beginning of Sect. 7.4, since h'(z) is well defined with branch cuts on the orange arcs of the Stokes graph as shown in the left-hand panels of Figs. 39a–45a in Appendix E,



all that remains to fully specify h(z) is to complete its jump contour with additional arcs to handle the monodromy about the poles and then to give values for one or more integration constants. The real parts of these constants are determined so that the level set $\operatorname{Re}(h(z))=0$ coincides with the Stokes graph. We complete the specification of h(z) first for the following three gO cases: (a) $\mu \in \mathcal{B}_{\square}$ with s=1, (b) $\mu \in \mathcal{B}_{\triangleright}$ with s=1, and (c) $\mu \in \mathcal{B}_{\triangle}$ with s=1. We take additional cuts as shown for cases (a), (b), and (c) respectively in the left-hand panels of Figs. 39c, 42c, and 45c so that h(z) is analytic in a simply connected domain Ω_h , and therefore just one integration constant needs to be determined. We fix it by setting

$$h(z) = \int_{\delta}^{z} h'(w) \, \mathrm{d}w - \frac{1}{2} \mathrm{i}R_1, \quad z \in \Omega_h$$
 (7.2)

where the value of the integral is independent of any path of integration taken in the domain Ω_h , and where $R_1 \in \mathbb{R}$ is defined in (7.1). Using the fact that h'(z) has residues of -s and $-\kappa$ at z=0 and $z=\infty$ respectively, and again taking note of (7.1) referring to the location of the integration contours ℓ_1 and ℓ_2 as shown on the Stokes graph plots in the left-hand panels of Figs. 39a-45a, one checks that the function h(z) defined by (7.2) satisfies the jump conditions on the sum and difference of boundary values as shown in the left-hand panels of Figs. 39c, 42c, and 45c. To define h(z) in the three remaining gO cases, (d) $\mu \in \mathcal{B}_{\square}$ with s = -1, (e) $\mu \in \mathcal{B}_{\triangleright}$ with s = -1, and (f) $\mu \in \mathcal{B}_{\Delta}$ with s = 1, we note that this requires changing the sign of s from cases (a), (b), and (c) respectively, which also means that we change the sign of h'(z) in the circle domain \mathcal{D}_{\circ} while leaving h'(z) unchanged in the exterior of \mathcal{D}_{\circ} . Therefore it seems natural to also define h(z) by starting with the formula (7.2) and simply changing the sign of h(z) within \mathcal{D}_{\circ} . We follow this approach and proceed with the implied choice of integration constants. Finally, for the only gH case ($\mu \in \mathcal{B}_{\square}$ with s = 1), we simply define h(z) exactly as in gO case (a). It is then straightforward to verify the jump conditions satisfied by h(z) in these four remaining cases as shown in the left-hand panels of Figs. 40c, 41c, 43c, and 44c.

In general, the constants R_1 and R_2 defined by (7.1) are independent. However, if $\mu \in (\mathcal{B}_{\square} \cup \mathcal{B}_{\triangleright}) \cap \mathbb{R}$, then with the indicated choice of integration constant we recover a Schwarz symmetry: $h'(z^*) = h'(z)^*$. Considering the difference of loop integrals of h'(z) around z = 0, ∞ computed by residues on one hand and by (7.1) on the other, this symmetry in turn implies the identity

$$R_2 = \frac{1}{2}\pi(1-\kappa), \quad \mu \in \mathcal{B}_{\square} \cap \mathbb{R}, \quad \kappa \in (-1,1), \tag{7.3}$$

and, by a simpler computation,

$$R_2 = 0, \quad \mu \in \mathcal{B}_{\triangleright} \cap \mathbb{R}, \quad \kappa \in (-1, 1).$$

Similarly, if $\mu \in (\mathcal{B}_{\square} \cup \mathcal{B}_{\triangle}) \cap i\mathbb{R}$, then $h'(-z^*) = h'(z)^*$, which implies the identities

$$R_1 = -\frac{1}{2}\pi(1+\kappa), \quad \mu \in \mathcal{B}_{\square} \cap i\mathbb{R}, \quad \kappa \in (-1,1), \quad \text{and}$$
 (7.4)
 $R_2 = 0, \quad \mu \in \mathcal{B}_{\triangle} \cap i\mathbb{R}, \quad \kappa \in (-1,1).$



7.6 Parametrix Construction

We now show how to build an approximation of the matrix function $z \mapsto \mathbf{O}(z)$, the accuracy of which can be controlled. With h(z) defined precisely as described in Sect. 7.5, we observe that due to the position of the jump contour for $\mathbf{O}(z)$ relative to the sign chart of $\mathrm{Re}(h(z))$, the jump matrix for $\mathbf{O}(z)$ is an exponentially small perturbation of the identity matrix for $T \gg 1$ wherever the jump matrix is upper or lower triangular.

7.6.1 Outer Parametrix

If we simply neglect these jumps and use known information about the boundary values of h(z) in the remaining diagonal and off-diagonal jump matrices, we arrive at a modified Riemann–Hilbert problem for the outer parametrix. More precisely, the outer parametrix $\check{\mathbf{O}}^{\text{out}}(z)$ is defined as the matrix analytic in the complement of the jump contour shown in the right-hand panels of Figs. 39(c)–45c in Appendix E, with the indicated jump matrix on each arc, normalized to the identity as $z \to \infty$, and continuous up to the jump contour with the exception of the four points $z = \alpha, \beta, \gamma, \delta$ at each of which a negative one-fourth root divergence is admitted to account for the discontinuity of the jump matrix.

While the details are different in each case, the conditions characterizing the outer parametrix can be easily mapped to a single universal form. Indeed, we will define a new unknown $\check{\mathbf{P}}^{\text{out}}(z)$ in terms of $\check{\mathbf{O}}^{\text{out}}(z)$ in different regions of the z-plane according to Table 5.

The jump contour for $\check{\mathbf{P}}^{\text{out}}(z)$ is a simple curve consisting of three consecutive arcs: an arc B_1 from $z=\alpha$ to $z=\beta$, an arc G from $z=\beta$ to $z=\gamma$, and an arc B_2 from $z=\gamma$ to $z=\delta$. We think of these arcs as two "bands" (B_1 and B_2) separated by a "gap" G (see the left-hand panel of Fig. 28). Defining real phases C_G and C_B as shown for each case in Table 6, it is straightforward to check that $\check{\mathbf{P}}^{\text{out}}(z)$ is the necessarily unique solution of the following Riemann–Hilbert problem.

Riemann-Hilbert Problem 2 (Uniformized Outer Parametrix) Let $\zeta \in \mathbb{C}$ and real constants C_G and C_B be given. Seek a 2×2 matrix function $z \mapsto \check{\mathbf{P}}^{\text{out}}(z; \zeta)$ with the following properties:

- Analyticity: $\check{\mathbf{P}}^{\text{out}}(z; \zeta)$ is an analytic function of z in the domain $z \in \mathbb{C} \setminus (B_1 \cup G \cup B_2)$.
- **Jump conditions:** $\check{\mathbf{P}}^{\text{out}}(z;\zeta)$ assumes continuous boundary values on its jump contour from either side except at the four points $p = \alpha, \beta, \gamma, \delta$, where $(z p)^{1/4}\check{\mathbf{P}}^{\text{out}}(z;\zeta)$ is bounded. The boundary values are related on each arc of $B_1 \cup G \cup B_2$ by the jump conditions

$$\mathbf{\breve{P}}_{+}^{\text{out}}(z;\zeta) = \mathbf{\breve{P}}_{-}^{\text{out}}(z;\zeta)\mathbf{T}(-e^{-\zeta z}), \quad z \in B_{1},$$
(7.5)

$$\check{\mathbf{P}}_{+}^{\text{out}}(z;\zeta) = \check{\mathbf{P}}_{-}^{\text{out}}(z;\zeta)\mathbf{D}(e^{iC_{G}}), \quad z \in G, \quad \text{and}$$
 (7.6)

$$\check{\mathbf{P}}_{+}^{\text{out}}(z;\zeta) = \check{\mathbf{P}}_{-}^{\text{out}}(z;\zeta)\mathbf{T}(-e^{iC_{\text{B}}}e^{-\zeta z}), \quad z \in B_{2}. \tag{7.7}$$



Table 5 The relation between $\check{\mathbf{O}}^{\text{out}}(z)$ and $\check{\mathbf{P}}^{\text{out}}(z)$ in different domains of the z-plane

$\check{\mathbf{p}}^{\mathrm{out}}(z)$	$\mathbf{D}(\sqrt{2}e^{5i\pi/12}e^{iTR_1/2})\tilde{\mathbf{O}}^{\text{out}}(z)\mathbf{D}(\sqrt{\frac{3}{2}}e^{-5i\pi/12}e^{-iTR_1/2})$ $\mathbf{D}(\sqrt{2}e^{5i\pi/12}e^{iTR_1/2})\tilde{\mathbf{O}}^{\text{out}}(z)\mathbf{D}(\frac{1}{\sqrt{2}}e^{-5i\pi/12}e^{-iTR_1/2})$	$\mathbf{D}(\mathbf{e}^{-\mathrm{i}\pi/2}\mathbf{e}^{\mathrm{i}T}R_{1}/2)\tilde{\mathbf{O}}^{\mathrm{out}}(z)\mathbf{D}(\mathbf{e}^{\mathrm{i}\pi/2}\mathbf{e}^{-\mathrm{i}T}R_{1}/2)$ $\mathbf{D}(\zeta_{\rho}^{\mathrm{i}\pi/12}\mathbf{e}^{\mathrm{i}T}R_{1}/2)\tilde{\mathbf{O}}^{\mathrm{out}}(z)\mathbf{T}(\zeta_{\rho}^{\mathrm{out}}/2)\mathbf{D}^{\mathrm{out}}(z)\mathbf{T}(\zeta_{\rho}^{\mathrm{out}}/2)\mathbf{D}^{\mathrm{out}}(z)\mathbf{D}^{\mathrm{out}}($	$\mathbf{D}(\sqrt{2}e^{i\pi/12}e^{iTR_1/2})\tilde{\mathbf{D}}$ out $(z)\mathbf{D}(\frac{1}{\sqrt{2}}e^{-i\pi/12}e^{-iTR_1/2})$	$\mathbf{D}(\sqrt{2}e^{\mathrm{i}\pi/4}e^{-\mathrm{i}\pi\Theta_{\infty}}e^{\mathrm{i}TR_{2}/2})\tilde{\mathbf{O}}^{\mathrm{out}}(z)\mathbf{T}(\sqrt{\frac{2}{3}}e^{11\mathrm{i}\pi/12}e^{-\mathrm{i}T(R_{1}+R_{2}/2)}e^{-\zetaz})$	$\mathbf{D}(\sqrt{2}e^{\mathrm{i}\pi/4}e^{-\mathrm{i}\pi\Theta_{\infty}}e^{\mathrm{i}TR_{2}/2})\check{\mathbf{O}}^{\mathrm{out}}(z)\mathbf{D}(\frac{1}{\sqrt{\beta}}e^{-\mathrm{i}\pi/4}e^{\mathrm{i}\pi\Theta_{\infty}}e^{-\mathrm{i}TR_{2}/2})$	$\mathbf{D}(\sqrt{2}e^{\mathrm{i}\pi/4}e^{-\mathrm{i}\pi\Theta_{\infty}}e^{\mathrm{i}TR_{2}/2})\tilde{\mathbf{O}}^{\mathrm{out}}(z)\mathbf{D}(\tilde{\frac{1}{\sqrt{2}}}e^{-5\mathrm{i}\pi/12}e^{\mathrm{i}\pi\Theta_{\infty}}e^{-\mathrm{i}T(R_{1}+R_{2}/2)})$	$\mathbf{D}(\sqrt{2}\mathrm{e}^{\mathrm{i}\pi/4}\mathrm{e}^{-\mathrm{i}\pi\Theta_{\infty}}\mathrm{e}^{\mathrm{i}TR_{2}/2})\check{\mathbf{O}}^{\mathrm{out}}(_{2})\mathbf{D}(\overset{1}{\sqrt{2}}\mathrm{e}^{-\mathrm{i}\pi/4}\mathrm{e}^{\mathrm{i}\pi\Theta_{\infty}}\mathrm{e}^{-\mathrm{i}TR_{2}/2})$	$\mathbf{D}(\sqrt{2}e^{\mathrm{i}\pi/4}e^{\mathrm{i}\pi\Theta_{\infty}}e^{\mathrm{i}TR_2/2})\check{\mathbf{O}}^{\mathrm{out}}(z)\mathbf{D}(\sqrt{\frac{3}{2}}e^{-\mathrm{i}\pi/4}e^{-\mathrm{i}\pi\Theta_{\infty}}e^{-\mathrm{i}T(R_1+R_2/2)})$	$\mathbf{D}(\sqrt{2}\mathrm{e}^{\mathrm{i}\pi/4}\mathrm{e}^{\mathrm{i}\pi\Theta_{\infty}}\mathrm{e}^{\mathrm{i}T}R_{2}/^{2})\check{\mathbf{O}}^{\mathrm{out}}(z)\mathbf{D}(\frac{1}{\sqrt{2}}\mathrm{e}^{-\mathrm{i}\pi/4}\mathrm{e}^{-\mathrm{i}\pi\Theta_{\infty}}\mathrm{e}^{-\mathrm{i}T}R_{2}/^{2})$	$\mathbf{D}(\sqrt{2}e^{\mathrm{i}\pi/4}e^{\mathrm{i}\pi\Theta_{\infty}}e^{\mathrm{i}TR_2/2})\check{\mathbf{O}}^{\mathrm{out}}(_z)\mathbf{T}(\sqrt{2}e^{3\mathrm{i}\pi/4}e^{-\mathrm{i}\pi\Theta_{\infty}}e^{-\mathrm{i}T(R_1+R_2/2)}e^{-\zeta z})$	$\mathbf{D}(\sqrt{2}e^{i\pi/4}e^{i\pi\Theta\infty}e^{iTR_2/2})\tilde{\mathbf{O}}^{\mathrm{out}}(_{z})\mathbf{D}(\frac{1}{\sqrt{2}}e^{-i\pi/4}e^{-i\pi\Theta\infty}e^{-iTR_2/2})$
Domain	\mathcal{D}_{\circ} $\mathbb{C}\setminus\overline{\mathcal{D}_{\circ}}$		$\mathbb{C}\setminus\overline{\mathcal{D}_o}$	\mathcal{D}_{\circ}	$\mathbb{C}\setminus \overline{\mathcal{D}_{\circ}}$	\mathcal{D}_{\circ}	$\mathbb{C}\setminus\overline{\mathcal{D}_{\circ}}$	\mathcal{D}_{\circ}	$\mathbb{C}\setminus \overline{\mathcal{D}_o}$	\mathcal{D}_{\circ}	$\mathbb{C}\setminus\overline{\mathcal{D}_o}$
S	1		•	_		-1		-		-1	
family	Os	Hg	a a	Og				Og			
В	\mathcal{B}_\square			$\mathcal{B}_{ hd}$				$\mathcal{B}_{ riangle}$			



\mathcal{B}	family	S	$C_{\mathbf{G}} \pmod{2\pi}$	$C_{\mathrm{B}} \pmod{2\pi}$	ν
\mathcal{B}_{\square}	gO	1	$-2TR_2 - \frac{\pi}{3}$	$-2TR_1 + \frac{\pi}{3}$	1
	gH	1	$-2TR_2$	$-2TR_1$	1
	gO	-1	$-2TR_2 + \frac{\pi}{3}$	$-2TR_1 - \frac{\pi}{3}$	-1
\mathcal{B}_{\rhd}	gO	1	$2TR_1 - \frac{\pi}{3}$	$-T(R_1 + R_2) + 2\pi(\Theta_{\infty} + \frac{1}{3})$	-1
		-1	$2TR_1 + \frac{\pi}{3}$	$-T(R_1 + R_2) + 2\pi(\Theta_{\infty} - \frac{1}{3})$	1
${\cal B}_{\triangle}$	gO	1	$2TR_1 + \frac{\pi}{3}$	$-T(R_1 + R_2) - 2\pi(\Theta_{\infty} + \frac{1}{3})$	1
		-1	$2TR_1 - \frac{\pi}{3}$	$-T(R_1+R_2)-2\pi(\Theta_\infty-\tfrac13)$	-1

Table 6 The phases $C_{\rm G}$ and $C_{\rm B}$, and the sign $\nu=\pm 1$

• Normalization: $\check{\mathbf{P}}^{\mathrm{out}}(z;\zeta) \to \mathbb{I}$ as $z \to \infty$.

Given existence of a solution of Riemann–Hilbert Problem 2, uniqueness is straightforward to establish. This is an algebro-geometric problem that can be solved in terms of the function theory of the elliptic spectral curve \mathcal{R} associated with the quartic polynomial $P(z) = (z - \alpha)(z - \beta)(z - \gamma)(z - \delta)$ (cf. (1.18)). To develop the solution in concrete terms, we introduce a branch of $\sqrt{P(z)}$ adapted to the jump contour at hand; let r(z) denote the function analytic for $z \in \mathbb{C} \setminus B_1 \cup B_2$ that satisfies $r(z)^2 = P(z)$ and has asymptotic behavior $r(z) = z^2 + \mathcal{O}(z)$ as $z \to \infty$. Its domain of analyticity is the complement of the orange arcs in the right-hand panel of Fig. 28. Comparing with the orange arcs in the left-hand panels of Figs. 39a–45a in Appendix E we may relate r(z) with R(z) explicitly:

$$r(z) = \begin{cases} vR(z), & z \in \mathcal{D}_{\circ} \\ R(z), & z \in \mathbb{C} \setminus \overline{\mathcal{D}_{\circ}}, \end{cases}$$
(7.8)

where $\nu = \pm 1$ is the sign indicated for each case in Table 6. We then define

$$\begin{split} F(z) := -\frac{1}{2}\zeta z + C_{\mathrm{G}}\frac{r(z)}{2\pi} \int_{G} \frac{\mathrm{d}s}{r(s)(s-z)} + C_{\mathrm{B}}\frac{r(z)}{2\pi} \int_{B_{2}} \frac{\mathrm{d}s}{r_{+}(s)(s-z)}, \\ z \in \mathbb{C} \setminus (B_{1} \cup G \cup B_{2}). \end{split}$$

The function F(z) is analytic and bounded on its domain of definition, and its boundary values satisfy the jump conditions

$$\langle F \rangle(z) = -\frac{1}{2}\zeta z, \quad z \in B_1,$$

$$\Delta F(z) = iC_G, \quad z \in G,$$

$$\langle F \rangle(z) = -\frac{1}{2}\zeta z + \frac{1}{2}iC_B, \quad z \in B_2.$$

$$(7.9)$$

Also, F(z) is analytic for large |z| and has an expansion of the form

$$F(z) = F_1 z + F_0 + \mathcal{O}(z^{-1}), \quad z \to \infty,$$
 (7.10)





Fig. 28 Left: topologically accurate representation of the jump contour of Riemann–Hilbert Problem 2 and of the Abel map a(z). Right: corresponding jump contour for r(z) and for $\check{\mathbf{Q}}^{\text{out}}(z)$, and homology cycles \mathfrak{a} and \mathfrak{b} on \mathcal{R}

where F_1 and F_0 are independent of z. We will not need the explicit form of F_0 , but F_1 is given by

$$F_1 := -\frac{1}{2}\zeta - \frac{C_G}{2\pi} \int_G \frac{dz}{r(z)} - \frac{C_B}{2\pi} \int_{R_2} \frac{dz}{r_+(z)}.$$
 (7.11)

Then define $\mathbf{\check{O}}^{\text{out}}(z)$ via

$$\check{\mathbf{Q}}^{\text{out}}(z) := e^{F_0 \sigma_3} \check{\mathbf{P}}^{\text{out}}(z) e^{-F(z)\sigma_3}, \quad z \in \mathbb{C} \setminus (B_1 \cup G \cup B_2). \tag{7.12}$$

Clearly $\check{\mathbf{Q}}^{\text{out}}(z)$ is analytic at least for $z \in \mathbb{C} \setminus (B_1 \cup G \cup B_2)$, and its boundary values are continuous except at $p = \alpha, \beta, \gamma, \delta$ where $(z - p)^{1/4} \check{\mathbf{Q}}^{\text{out}}(z)$ is bounded. Using (7.9) in (7.6), and applying Morera's Theorem shows that G may be removed from the jump contour, i.e., $\check{\mathbf{Q}}^{\text{out}}(z)$ is analytic for $z \in \mathbb{C} \setminus (B_1 \cup B_2)$. Using (7.9) in (7.5) and (7.7) then shows that $\check{\mathbf{Q}}^{\text{out}}(z)$ satisfies jump conditions on $B_1 \cup B_2$ of a universal form: $\check{\mathbf{Q}}^{\text{out}}(z) = \check{\mathbf{Q}}^{\text{out}}(z)\mathbf{T}(-1)$, where $\mathbf{T}(-1)$ is an elementary "twist" matrix defined in (1.34). Finally, from the normalization condition on $\check{\mathbf{P}}^{\text{out}}(z)$ and the expansion (7.10) one sees that $\check{\mathbf{Q}}^{\text{out}}(z)e^{F_1z\sigma_3} \to \mathbb{I}$ as $z \to \infty$.

These conditions on $\check{\mathbf{Q}}^{\text{out}}(z)$ are standard; for example, they are directly analogous to conditions defining the function $\mathbf{S}(\lambda)$ in [10, Sect. 4]. We now summarize the construction of $\check{\mathbf{Q}}^{\text{out}}(z)$.

Define a basis of homology cycles \mathfrak{a} and \mathfrak{b} as in the right-hand panel of Fig. 28. The basic normalized holomorphic differential on \mathcal{R} is $\omega(z) dz$, where on one sheet of \mathcal{R} modeled as two copies of the complex z-plane cut and identified along $B_1 \cup B_2$,

$$\omega(z) := \frac{1}{c} \cdot \frac{2\pi i}{r(z)} \quad \text{where} \quad c := \oint_{\mathfrak{a}} \frac{ds}{r(s)}$$

$$\implies \oint_{\mathfrak{a}} \omega(z) \, dz = 2\pi i. \tag{7.13}$$

Note that c is a concrete form of the period $Z_{\mathfrak{a}}$ defined in (1.19). A meromorphic differential on \mathcal{R} is $\Omega(z) dz$, where on the same sheet that (7.13) holds,

$$\Omega(z) := \frac{z^2 - \frac{1}{2}(\alpha + \beta + \gamma + \delta)z}{r(z)} - C\omega(z), \quad C := \frac{1}{2\pi i} \oint_{\mathfrak{a}} \frac{z^2 - \frac{1}{2}(\alpha + \beta + \gamma + \delta)z}{r(z)} dz$$

$$\implies \oint_{\mathfrak{a}} \Omega(z) dz = 0. \tag{7.14}$$



Note that $\Omega(z) dz$ has double poles at the points over $z = \infty$ on \mathcal{R} , but no residues. The \mathfrak{b} -period of the \mathfrak{a} -normalized holomorphic differential $\omega(z) dz$ is

$$H_{\omega} := \oint_{\mathfrak{b}} \omega(z) \, \mathrm{d}z = -2 \int_{G} \omega(z) \, \mathrm{d}z, \tag{7.15}$$

and that of the \mathfrak{a} -normalized meromorphic differential $\Omega(z)$ dz is

$$H_{\Omega} := \oint_{\mathfrak{b}} \Omega(z) \, \mathrm{d}z = -2 \int_{G} \Omega(z) \, \mathrm{d}z. \tag{7.16}$$

Here the first formula in each case is a contour integral on the Riemann surface \mathcal{R} , and the second formula is a contour integral over the gap G where the integrand as defined in (7.13) and (7.14) respectively has a definite value. A fundamental fact of the theory is that $\text{Re}(H_{\omega}) < 0$. Note also that H_{ω} is a concrete version of the period ratio $2\pi i Z_{\mathfrak{b}}/Z_{\mathfrak{a}}$; see (1.19). The Abel map a(z) is defined by

$$a(z) := \int_{\alpha}^{z} \omega(s) \, \mathrm{d}s, \quad z \in \mathbb{C} \setminus (B_1 \cup G \cup B_2), \tag{7.17}$$

where the integral is independent of path taken in the indicated domain, on which $z \mapsto a(z)$ is holomorphic. The analogous integral with the meromorphic differential $\Omega(z)$ dz in place of $\omega(z)$ dz is

$$A(z) := \int_{\alpha}^{z} \Omega(s) \, \mathrm{d}s, \quad z \in \mathbb{C} \setminus (B_1 \cup G \cup B_2),$$

again independent of path in the indicated domain (there is no residue at $z=\infty$) and defining an analytic function on that domain. Absence of a residue at $z=\infty$ also implies existence of the limit

$$J := \lim_{z \to \infty} (z - A(z)).$$

It is straightforward to confirm that a(z) and A(z) satisfy the following jump conditions:

$$\langle a \rangle(z) = 0$$
 and $\langle A \rangle(z) = 0$, $z \in B_1$,
 $\Delta a(z) = -2\pi i$ and $\Delta A(z) = 0$, $z \in G$,
 $\langle a \rangle(z) = -\frac{1}{2}H_{\omega}$ and $\langle A \rangle(z) = -\frac{1}{2}H_{\Omega}$, $z \in B_2$.

Note that using (7.13) and (7.15) in (7.11), we can rewrite F_1 equivalently in the form

$$F_{1} = -\frac{\zeta}{2} - \frac{C_{G}c}{4\pi^{2}i} \int_{G} \omega(z) dz - \frac{C_{B}c}{4\pi^{2}i} \int_{B_{2}} \omega_{+}(z) dz$$

$$= -\frac{\zeta}{2} + \frac{C_{G}cH_{\omega}}{8\pi^{2}i} - \frac{C_{B}c}{4\pi}.$$
(7.18)



A further useful identity can be found by integrating the differential $a(z)\Omega(z) dz$ around the boundary of the canonical dissection of \mathcal{R} and expressing the integral alternately via residues at the two poles and via periods occurring on the four edges of the boundary. The result is that H_{Ω} defined in (7.16) can be expressed in terms of c defined in (7.13) as

$$H_{\Omega} = \frac{4\pi i}{c}.\tag{7.19}$$

See [31] or [17, Lemma B.1] for details.

The analogue of the function j(z) from Sect. 5.3 is here defined as the unique function analytic for $z \in \mathbb{C} \setminus (B_1 \cup B_2)$ satisfying the conditions

$$j(z)^4 := \frac{(z-\alpha)(z-\gamma)}{(z-\beta)(z-\delta)}$$
 and $\lim_{z\to\infty} j(z) = 1$.

This function satisfies the jump condition $j_+(z) = -\mathrm{i} j_-(z)$ for $z \in B_1 \cup B_2$. Further define

$$f^{\mathcal{D}}(z) := \frac{j(z) + j(z)^{-1}}{2}, \quad f^{\mathcal{O}\mathcal{D}}(z) := \frac{j(z) - j(z)^{-1}}{2i}$$
 (7.20)

with jump conditions $f_+^D(z) = f_-^{OD}(z)$ and $f_+^{OD}(z) = -f_-^D(z)$ for $z \in B_1 \cup B_2$ and large-z asymptotic expansions $f_-^D(z) = 1 + \mathcal{O}(z^{-1})$ and $f_-^{OD}(z) = \frac{1}{4}i(\alpha - \beta + \gamma - \delta)z^{-1} + \mathcal{O}(z^{-2})$. Clearly the product $r(z)f_-^D(z)f_-^{OD}(z)$ is an entire function with $r(z)f_-^D(z)f_-^{OD}(z) = \mathcal{O}(z)$ as $z \to \infty$ and hence is a linear function. Let $z = z_0$ denote the unique root of this function (possibly $z_0 = \infty$ if and only if $f_-^{OD}(z) = \mathcal{O}(z^{-2})$ as $z \to \infty$). Explicitly,

$$r(z)f^{D}(z)f^{OD}(z) = -\frac{1}{4i}\left([\alpha - \beta + \gamma - \delta]z - [\alpha\gamma - \beta\delta]\right)$$

$$\implies z_0 := \frac{\alpha\gamma - \beta\delta}{\alpha - \beta + \gamma - \delta}.$$
(7.21)

A direct computation shows that z_0 cannot coincide with any of the roots $z = \alpha$, β , γ , δ provided the latter are distinct. Therefore the simple root z_0 belongs to exactly one of the two factors $f^D(z)$ or $f^{OD}(z)$. We assume in what follows that $f^{OD}(z_0) = 0$; the modifications necessary to handle the other case $f^D(z_0) = 0$ are explained in [12, Sect. 4.4.2].

Finally, to construct $\check{\mathbf{Q}}^{\text{out}}(z)$ and hence also $\check{\mathbf{P}}^{\text{out}}(z)$, we introduce the Riemann theta function of the elliptic curve \mathcal{R} for the homology basis $(\mathfrak{a}, \mathfrak{b})$ defined by

$$\vartheta(z) := \sum_{k \in \mathbb{Z}} e^{H_{\omega}k^2/2} e^{kz}. \tag{7.22}$$

This is an entire function of z that satisfies

$$\vartheta(-z) = \vartheta(z), \quad \vartheta(z + 2\pi i) = \vartheta(z), \quad \vartheta(z + H_{\omega}) = e^{-H_{\omega}/2}e^{-z}\vartheta(z)$$
 (7.23)

and has simple zeros only at the points of a \mathbb{Z}^2 -lattice:

$$\vartheta(z) = 0$$
 if and only if $z = \mathcal{K} + 2\pi i k + H_{\omega} \ell$ for $k, \ell \in \mathbb{Z}$, (7.24)

where $\mathcal{K} = \mathcal{K}(H_{\omega}) := i\pi + \frac{1}{2}H_{\omega}$ is one of the zeros. See [53, Chapter 20], which uses Jacobi's notation $\vartheta(z) = \theta_3(w|\tau) = \theta_3(w,q)$ where z = 2iw, $H_{\omega} = 2\pi i \tau$, and $q = e^{i\pi \tau}$.

The final result is that the matrix elements of $\mathbf{\tilde{Q}}^{\text{out}}(z)$ are

$$\begin{split} & \check{Q}_{11}^{\text{out}}(z) := f^{\text{D}}(z) \frac{\vartheta(a(\infty) + a(z_0) + \mathcal{K})\vartheta(a(z) + a(z_0) + \mathcal{K} - F_1 H_{\Omega})}{\vartheta(a(\infty) + a(z_0) + \mathcal{K} - F_1 H_{\Omega})\vartheta(a(z) + a(z_0) + \mathcal{K})} \mathrm{e}^{-F_1[J + A(z)]}, \\ & \check{Q}_{12}^{\text{out}}(z) := -f^{\text{OD}}(z) \frac{\vartheta(a(\infty) + a(z_0) + \mathcal{K})\vartheta(a(z) - a(z_0) - \mathcal{K} + F_1 H_{\Omega})}{\vartheta(a(\infty) + a(z_0) + \mathcal{K} - F_1 H_{\Omega})\vartheta(a(z) - a(z_0) - \mathcal{K})} \mathrm{e}^{-F_1[J - A(z)]}, \\ & \check{Q}_{21}^{\text{out}}(z) := f^{\text{OD}}(z) \frac{\vartheta(a(\infty) + a(z_0) + \mathcal{K})\vartheta(a(z) - a(z_0) - \mathcal{K} - F_1 H_{\Omega})}{\vartheta(a(\infty) + a(z_0) + \mathcal{K} + F_1 H_{\Omega})\vartheta(a(z) - a(z_0) - \mathcal{K})} \mathrm{e}^{F_1[J - A(z)]}, \\ & \check{Q}_{22}^{\text{out}}(z) := f^{\text{D}}(z) \frac{\vartheta(a(\infty) + a(z_0) + \mathcal{K})\vartheta(a(z) + a(z_0) + \mathcal{K} + F_1 H_{\Omega})}{\vartheta(a(\infty) + a(z_0) + \mathcal{K})\vartheta(a(z) + a(z_0) + \mathcal{K} + F_1 H_{\Omega})} \mathrm{e}^{F_1[J + A(z)]}. \end{split}$$

From (7.12) and (7.25), we then obtain a formula for the solution $\check{\mathbf{P}}^{\text{out}}(z)$ of Riemann–Hilbert Problem 2. Note that the quantity F_1H_{Ω} appearing in the arguments of the theta functions can be expressed via (7.18)–(7.19) as

$$F_1 H_{\Omega} = i\Psi, \quad \Psi := -\frac{2\pi\zeta}{c} - \xi, \quad \xi := C_B - C_G \frac{H_{\omega}}{2\pi i}.$$
 (7.26)

The assumption that $f^{\rm D}(z)$ is nonvanishing while $f^{\rm OD}(z)=0$ only vanishes at $z=z_0$ to first order implies that $\vartheta(a(z)+a(z_0)+\mathcal{K})$ is nonvanishing (even in the limit $z\to\infty$) and that the unique simple zero of $\vartheta(a(z)-a(z_0)-\mathcal{K})$, located at $z=z_0$ by Riemann's Theorem, is cancelled by that of $f^{\rm OD}(z)$. Therefore, it is obvious that $\check{\mathbf{P}}^{\rm out}(z)$ exists if and only if

$$\vartheta(a(\infty) + a(z_0) + \mathcal{K} - i\Psi)\vartheta(a(\infty) + a(z_0) + \mathcal{K} + i\Psi) \neq 0. \tag{7.27}$$

Lemma 10 By deforming the arc B_1 in the jump contour for $\check{\mathbf{P}}^{out}(z)$ if necessary it can be arranged that $\vartheta(a(\infty) + a(z_0) + \mathcal{K} - i\Psi) = 0$ if and only if $\vartheta(a(\infty) + a(z_0) + \mathcal{K} + i\Psi) = 0$.

Proof Since $\vartheta(-z) = \vartheta(z)$, $\vartheta(\mathcal{K}) = 0$, and $2\mathcal{K}$ is a (quasi-)period, it is sufficient to prove that there are integers N_a and N_b such that $2a(\infty) + 2a(z_0) = 2\pi i N_a + H_\omega N_b$. Introducing a second auxiliary copy of the complex z-plane on which the Abel mapping a(z) is defined with the opposite sign compared to the principal z-plane, we obtain a two-sheeted model for the Riemann surface \mathcal{R} . Denoting by $Q^+(z)$ (resp., $Q^-(z)$) the point $Q \in \mathcal{R}$ over $z \in \mathbb{C}$ on the principal (resp., auxiliary) sheet, we have therefore extended the Abel mapping to \mathcal{R} by the definition $\widetilde{a}(Q^{\pm}(z)) = \pm a(z)$ (modulo periods). With this notation, we want to show that $\widetilde{a}(Q^+(\infty)) + \widetilde{a}(Q^+(z_0)) - \overline{a}(Q^+(z_0)) = 0$



 $\widetilde{a}(Q^-(\infty)) - \widetilde{a}(Q^-(z_0)) = 2\pi i N_{\mathfrak{a}} + H_{\omega} N_{\mathfrak{b}}$. But by the Abel-Jacobi Theorem, this identity will hold for some integers $N_{\mathfrak{a}}$ and $N_{\mathfrak{b}}$ if there exists a nonzero meromorphic function k(Q) defined on \mathcal{R} with simple poles at the points $Q^-(\infty)$ and $Q^-(z_0)$ only and vanishing at the points $Q^+(\infty)$ and $Q^+(z_0)$. Similarly extending the square root branch r(z) underlying the definition of a(z) to the Riemann surface \mathcal{R} by $\widetilde{r}(Q^{\pm}(z)) = \pm r(z)$, we can exhibit this function k(Q) explicitly in the form

$$k(Q) = \frac{[z(Q)^2 - z_0^2] - \frac{1}{2}(\alpha + \beta + \gamma + \delta)[z(Q) - z_0] - [\widetilde{r}(Q) - \widetilde{r}(Q^+(z_0))]}{z(Q) - z_0},$$

where z(Q) is the coordinate (sheet projection) function satisfying $z(Q^{\pm}(z)) = z$ for all $z \in \mathbb{C}$. It is easy to verify from this formula that k(Q) has simple poles only at the points $Q = Q^{-}(\infty)$ and $Q = Q^{-}(z_0)$, and that k(Q) has a simple zero at $Q = Q^{+}(\infty)$. The fact that $k(Q^{+}(z_0)) = 0$ as well amounts to the condition that the derivative of the numerator vanishes at $Q = Q^{+}(z_0)$, which reads

$$2z_0 - \frac{1}{2}(\alpha + \beta + \gamma + \delta) = r'(z_0).$$

The *squares* of both sides of this equation are equal, as can be verified easily using the definition (7.21) of z_0 . Since the sign of $r'(z_0)$ can be changed by making a suitable deformation of the arc B_1 in the jump contour for $\check{\mathbf{P}}^{\text{out}}(z)$, the proof is finished. As a side-note, it is not possible that both of the integers N_a and N_b are even, as that would mean that $a(\infty) + a(z_0)$ is an integer linear combination of periods, which by Abel-Jacobi would imply the existence of a nonzero meromorphic function with just one simple pole at $Q = Q^-(z_0)$ that vanishes at $Q = Q^+(\infty)$. But having at most one simple pole on \mathcal{R} , the function is a constant, and vanishing at any point forces it to vanish identically.

If a deformation of B_1 is necessary for the result to hold, the original arc B_1 can be easily restored by using the constant jump matrix $\mathbf{T}(-1)$ to swap the columns of $\check{\mathbf{Q}}^{\text{out}}(z)$ in between the deformed and original arcs. In light of this result, Riemann–Hilbert Problem 2 is solvable if d>0 holds, where (considering the first factor in (7.27) and using (7.24) and (7.26))

$$d := \inf_{(N_{\mathfrak{a}}, N_{\mathfrak{b}}) \in \mathbb{Z}^2} \left| a(\infty) + a(z_0) + \frac{2\pi i \zeta}{c} + \left[N_{\mathfrak{a}} + \frac{C_{B}}{2\pi} \right] 2\pi i + \left[N_{\mathfrak{b}} - \frac{C_{G}}{2\pi} \right] H_{\omega} \right|. \tag{7.28}$$

Here the value of the Abel map $a(z_0)$ has to be interpreted relative to the contour arc B_1 deformed as necessary. The quantity d measures the distance to the (common, by Lemma 10) theta divisor for the two factors in (7.27). It depends on the data (distinct roots α , β , γ , δ of the quartic P(z), complex constant ζ , and real constants C_G and C_B modulo 2π) in the formulation of Riemann–Hilbert Problem 2. For given data, the infimum in (7.28) is clearly attained, as the absolute value grows with (N_{α}, N_{b}) because $Re(H_{\omega}) < 0$, so it is really a minimum over finitely many lattice points. Recalling the interpretation of the parameters of Riemann–Hilbert Problem 2 in terms of the outer parametrix $\check{\mathbf{O}}^{\text{out}}(z)$, we see that for given $\kappa \in (-1, 1)$ and $s = \pm 1$, d is a



function of μ in the Boutroux domain \mathcal{B} of interest (which determines $a(\infty) + a(z_0)$, c, H_{ω} , and the constants R_1 and R_2 appearing in C_G and C_B , via the roots of P(z)), $\zeta \in \mathbb{C}$, and T > 0. In this context, given $\epsilon > 0$ we set

$$S(\epsilon) := \{ \mu \in \mathcal{B}, \zeta \in \mathbb{C}, T > 0 : d \ge \epsilon \}. \tag{7.29}$$

Since C_G and C_B are affine linear in T, which does not otherwise appear in the data for Riemann–Hilbert Problem 2, the set $S(\epsilon)$ contains arbitrarily large values of T. Expressing $\check{\mathbf{O}}^{\text{out}}(z)$ in terms of $\check{\mathbf{P}}^{\text{out}}(z)$ using Table 5 we have the following result.

Proposition 12 The outer parametrix $\check{\mathbf{O}}^{\text{out}}(z)$ exists with $\det(\check{\mathbf{O}}^{\text{out}}(z)) = 1$ if d > 0 holds, in which case for every $\rho > 0$,

$$\mathcal{M}(\rho) := \sup_{\substack{|z-p| > \rho \\ p = \alpha, \beta, \gamma, \delta}} \| \check{\mathbf{O}}^{\text{out}}(z) \|$$
(7.30)

is finite, where $\|\cdot\|$ denotes any matrix norm. If ζ is bounded, μ lies in a compact subset of the relevant Boutroux domain, and for some $\epsilon > 0$, $(\mu, \zeta, T) \in S(\epsilon)$, then for every $\rho > 0$, $\mathcal{M}(\rho)$ is uniformly bounded even as $T \to +\infty$.

Proof It suffices to replace $\check{\mathbf{O}}^{\mathrm{out}}(z)$ with $\check{\mathbf{P}}^{\mathrm{out}}(z)$, because the transformation relating them given in Table 5 always exists, preserves determinants, and is uniformly bounded. It is easy to check from the conditions of Riemann–Hilbert Problem 2 that if $\check{\mathbf{P}}^{\mathrm{out}}(z)$ exists, it must have unit determinant, and the fact that existence is guaranteed by the condition d>0 has already been proven above. That $\mathcal{M}(\rho)<\infty$ for $\rho>0$ then follows by the maximum modulus principle. Existence of a uniform bound of $\mathcal{M}(\rho)$ depending only on the compact set containing μ , the bound for ζ , and the value of $\epsilon>0$ is not obvious from the explicit construction of the solution, because the arguments of the theta functions have real parts proportional to the large parameter T. However the existence of such a bound can be seen easily from the conditions of Riemann–Hilbert Problem 2, in which the dependence on T entering through the real phases C_G and C_B linear in T is controlled because only the bounded exponentials e^{iC_G} and e^{iC_B} appear in the problem.

We conclude this discussion of the outer parametrix by giving some formulæ for the quantities extracted from $\check{\mathbf{O}}^{\text{out}}(z)$ needed to write approximate formulæ for u(x) and u(x) in Sect. 7.7. Expanding for large z we obtain the convergent Laurent expansion

$$\check{\mathbf{O}}^{\text{out}}(z) = \mathbb{I} + \sum_{k=1}^{\infty} z^{-k} \check{\mathbf{O}}_{k}^{\text{out}}, \tag{7.31}$$

in which

$$\check{O}_{1,12}^{\text{out}} = \eta \check{P}_{1,12}^{\text{out}}, \quad \check{P}_{1,12}^{\text{out}} := \lim_{z \to \infty} z \check{P}_{12}^{\text{out}}(z)$$
(7.32)



where η is determined from the diagonal z-independent conjugation relating $\mathbf{\check{O}}^{\text{out}}(z)$ and $\mathbf{\check{P}}^{\text{out}}(z)$ for large z given in Table 5:

$$\eta := \begin{cases} \frac{1}{2} \mathrm{e}^{-5\mathrm{i}\pi/6} \mathrm{e}^{-\mathrm{i}TR_1}, & \mu \in \mathcal{B}_{\square}, \quad \text{gO case}, \quad s = 1 \\ -\mathrm{e}^{-\mathrm{i}TR_1}, & \mu \in \mathcal{B}_{\square}, \quad \text{gH case}, \quad s = 1 \\ \frac{1}{2} \mathrm{e}^{-\mathrm{i}\pi/6} \mathrm{e}^{-\mathrm{i}TR_1}, & \mu \in \mathcal{B}_{\square}, \quad \text{gO case}, \quad s = -1 \\ \frac{1}{2} \mathrm{e}^{-\mathrm{i}\pi/2} \mathrm{e}^{2\pi\mathrm{i}\Theta_{\infty}} \mathrm{e}^{-\mathrm{i}TR_2}, & \mu \in \mathcal{B}_{\square}, \quad \text{gO case}, \quad s = \pm 1 \\ \frac{1}{2} \mathrm{e}^{-\mathrm{i}\pi/2} \mathrm{e}^{-2\pi\mathrm{i}\Theta_{\infty}} \mathrm{e}^{-\mathrm{i}TR_2}, & \mu \in \mathcal{B}_{\triangle}, \quad \text{gO case}, \quad s = \pm 1. \end{cases}$$

Also, evaluation at z = 0 gives

$$\check{O}_{11}^{\text{out}}(0)\check{O}_{12}^{\text{out}}(0) = \nu \eta \check{P}_{11}^{\text{out}}(0) \check{P}_{12}^{\text{out}}(0)$$
(7.33)

and

$$\frac{\breve{O}_{21}^{\text{out}}(0)}{\breve{O}_{11}^{\text{out}}(0)} = \frac{1}{\eta} \begin{cases} \frac{\breve{P}_{21}^{\text{out}}(0)}{\breve{P}_{11}^{\text{out}}(0)}, & \nu = 1\\ \frac{\breve{P}_{22}^{\text{out}}(0)}{\breve{P}_{12}^{\text{out}}(0)}, & \nu = -1, \end{cases}$$

where the sign $\nu = \pm 1$ is as given in Table 6. Using the explicit solution of Riemann–Hilbert Problem 2, we have

$$\check{P}_{1,12}^{\text{out}} = \mathcal{N}(\mu) \frac{\vartheta(a(\infty) - a(z_0) - \mathcal{K} + i\Psi)}{\vartheta(a(\infty) + a(z_0) + \mathcal{K} - i\Psi)} e^{-2F_1 J}$$
(7.34)

and

$$\check{P}_{11}^{\text{out}}(0) = \mathcal{N}_{11}(\mu) \frac{\vartheta(a(0) + a(z_0) + \mathcal{K} - i\Psi)}{\vartheta(a(\infty) + a(z_0) + \mathcal{K} - i\Psi)} e^{-F_1[J + A(0)]},
\check{P}_{12}^{\text{out}}(0) = \mathcal{N}_{12}(\mu) \frac{\vartheta(a(0) - a(z_0) - \mathcal{K} + i\Psi)}{\vartheta(a(\infty) + a(z_0) + \mathcal{K} - i\Psi)} e^{-F_1[J - A(0)]},
\check{P}_{21}^{\text{out}}(0) = \mathcal{N}_{21}(\mu) \frac{\vartheta(a(0) - a(z_0) - \mathcal{K} - i\Psi)}{\vartheta(a(\infty) + a(z_0) + \mathcal{K} + i\Psi)} e^{F_1[J - A(0)]},
\check{P}_{22}^{\text{out}}(0) = \mathcal{N}_{22}(\mu) \frac{\vartheta(a(0) + a(z_0) + \mathcal{K} + i\Psi)}{\vartheta(a(\infty) + a(z_0) + \mathcal{K} + i\Psi)} e^{F_1[J + A(0)]},$$
(7.35)

in which

$$\mathcal{N}(\mu) := \frac{\alpha - \beta + \gamma - \delta}{4i} \frac{\vartheta(a(\infty) + a(z_0) + \mathcal{K})}{\vartheta(a(\infty) - a(z_0) - \mathcal{K})} e^{-2F_0}, \tag{7.36}$$



and

$$\mathcal{N}_{11}(\mu) := f^{D}(0) \frac{\vartheta(a(\infty) + a(z_{0}) + \mathcal{K})}{\vartheta(a(0) + a(z_{0}) + \mathcal{K})} e^{F(0) - F_{0}},
\mathcal{N}_{12}(\mu) := -f^{OD}(0) \frac{\vartheta(a(\infty) + a(z_{0}) + \mathcal{K})}{\vartheta(a(0) - a(z_{0}) - \mathcal{K})} e^{-F(0) - F_{0}},
\mathcal{N}_{21}(\mu) := f^{OD}(0) \frac{\vartheta(a(\infty) + a(z_{0}) + \mathcal{K})}{\vartheta(a(0) - a(z_{0}) - \mathcal{K})} e^{F(0) + F_{0}},
\mathcal{N}_{22}(\mu) := f^{D}(0) \frac{\vartheta(a(\infty) + a(z_{0}) + \mathcal{K})}{\vartheta(a(0) + a(z_{0}) + \mathcal{K})} e^{-F(0) + F_{0}},$$
(7.37)

are all finite and nonzero (all apparent singularities on the parameter space are removable).

7.6.2 Inner Parametrices

The approximation of the jump matrices for O(z) by those of its outer parametrix $\check{O}^{\text{out}}(z)$ fails to be uniformly accurate when z is near the four points $z = \alpha, \beta, \gamma, \delta$. To deal with this nonuniformity and also to avoid the problematic divergence of $\check{O}^{\text{out}}(z)$ at these four points, we define instead four inner parametrices.

Let D_p , $p \in \{\alpha, \beta, \gamma, \delta\}$ be fixed small disks in the z-plane with center z = p. Within each disk we define a conformal map $W: D_p \to \mathbb{C}$ such that W(p) = 0, as indicated in Tables 7–13 in Appendix E. It is assumed that certain contour arcs are first "fused" as indicated in these tables with the "&" notation, and the fact that W(z) is conformal follows from the explicit formula $h'(z)^2 = P(z)/(16z^2)$ and the fact that z = p is in each case a simple root of the polynomial P(z). Then, for $z \in D_p$, we define a matrix $\mathbf{P}^p(z)$ by the formula

$$\mathbf{P}^{p}(z) := \mathbf{O}(z) \exp((-Th(z) + \frac{1}{2}\zeta z)\sigma_{3})\mathbf{C}(z) \exp(-\frac{1}{2}TW(z)^{3/2}\sigma_{3}), \quad z \in D_{p},$$
(7.38)

where C(z) is a different piecewise-constant matrix function on each disk as indicated in the same series of tables. It is easy to check that $\mathbf{P}^p(z)$ satisfies exactly the same jump and analyticity conditions as does the matrix $\mathbf{A}(T^{2/3}W(z))$, where $\mathbf{A}(\xi)$ is defined in Sect. 5.3. If we replace $\mathbf{O}(z)$ with $\check{\mathbf{O}}^{\text{out}}(z)$ in (7.38), then we get instead a matrix function analytic in D_p except where $\xi = T^{2/3}W(z) < 0$, across which are the jump condition (5.32) is satisfied. It follows that the function

$$\mathbf{H}^{p}(z) := \check{\mathbf{O}}^{\text{out}}(z) \exp((-Th(z) + \frac{1}{2}\zeta z)\sigma_{3})\mathbf{C}(z) \exp(-\frac{1}{2}TW(z)^{3/2}\sigma_{3}) \frac{1}{\sqrt{2}} \begin{pmatrix} 1 & -1 \\ 1 & 1 \end{pmatrix} W(z)^{-\sigma_{3}/4},$$

$$z \in D_{p}$$
(7.39)

can be extended to W(z) < 0 from both sides so as to become an analytic function on D_p (any apparent singularity at z = p is easily seen to be removable due to the allowed growth condition on $\check{\mathbf{O}}^{\text{out}}(z)$ as $z \to p$). From Tables 7–13 in Appendix E one can check that the matrix product $\exp(-Th(z)\sigma_3)\mathbf{C}(z)\exp(-\frac{1}{2}TW(z)^{3/2}\sigma_3)$ is independent of z on each subdomain of D_p on which $\mathbf{C}(z)$ itself is constant, and that this matrix product is oscillatory and uniformly bounded in T since $p \in \{\alpha, \beta, \gamma, \delta\}$



lies on the Stokes graph so $\operatorname{Re}(h(p))=0$ unambiguously. Therefore, if $\zeta\in\mathbb{C}$ is bounded, μ lies in a given compact subset of the relevant Boutroux domain, and the parameters satisfy $(\mu, \zeta, T) \in \mathcal{S}(\epsilon)$ for some $\epsilon > 0$ (see (7.29)), then it follows from Proposition 12 in Sect. 7.6.1 that $\mathbf{H}^p(z)$ is uniformly bounded on D_p independently of T>0. We define an inner parametrix for $\mathbf{O}(z)$ on D_p by setting

$$\check{\mathbf{O}}^{\text{in},p}(z) := \mathbf{H}^{p}(z) T^{-\sigma_{3}/6} \mathbf{A}(T^{2/3} W(z)) \exp(\frac{1}{2} T W(z)^{3/2} \sigma_{3}) \mathbf{C}(z)^{-1}
\cdot \exp((T h(z) - \frac{1}{2} \zeta z) \sigma_{3}), \quad z \in D_{p}.$$

This function satisfies exactly the same analyticity and jump conditions within D_p as does $\mathbf{O}(z)$ itself. Moreover, by using (7.39) to express $\mathbf{O}^{\text{out}}(z)$ in terms of $\mathbf{H}^p(z)$, from (5.33) we see that

$$\check{\mathbf{O}}^{\text{in},p}(z)\check{\mathbf{O}}^{\text{out}}(z)^{-1} = \mathbf{H}^{p}(z)T^{-\sigma_{3}/6}\mathbf{A}(T^{2/3}W(z))\frac{1}{\sqrt{2}}\begin{pmatrix} 1 & -1\\ 1 & 1 \end{pmatrix}(TW(z))^{-\sigma_{3}/4}T^{\sigma_{3}/6}\mathbf{H}^{p}(z)^{-1}
= \mathbf{H}^{p}(z)\begin{pmatrix} 1 + \mathcal{O}(T^{-2}) & \mathcal{O}(T^{-1})\\ \mathcal{O}(T^{-1}) & 1 + \mathcal{O}(T^{-2}) \end{pmatrix}\mathbf{H}^{p}(z)^{-1}
= \mathbb{I} + \mathcal{O}(T^{-1}), \quad z \in \partial D_{p},$$
(7.40)

since W(z) is independent of T and is bounded away from zero on ∂D_p .

7.6.3 Global Parametrix and Error Estimation

The *global parametrix* for O(z) is defined in terms of the outer and inner parametrices as

$$\check{\mathbf{O}}(z) := \begin{cases} \check{\mathbf{O}}^{\mathrm{in},p}(z), & z \in D_p, \quad p \in \{\alpha,\beta,\gamma,\delta\}, \\ \check{\mathbf{O}}^{\mathrm{out}}(z), & \text{elsewhere that} \quad \check{\mathbf{O}}^{\mathrm{out}}(z) \quad \text{is analytic,} \end{cases}$$

which is just the direct analogue of (5.37) in the case of four simple roots of the quartic P(z). The error matrix $\mathbf{E}(z)$ is then defined in terms of $\mathbf{O}(z)$ and $\mathbf{O}(z)$ by (5.38), exactly as in the simpler setting considered in Sect. 5.3.3. The analysis of the error described in Sect. 5.3.3 applies nearly verbatim, with only the additional hypothesis that the parameters admit a uniform bound for $\check{\mathbf{O}}^{\text{out}}(z)$ when $z \in \mathbb{C} \setminus (D_{\alpha} \cup D_{\beta} \cup D_{\gamma} \cup D_{\delta})$. However, according to Proposition 12 in Sect. 7.6.1, such a bound is guaranteed by a uniform upper bound on $|\zeta|$, confinement of μ to a fixed compact subset of the Boutroux domain of interest, and the condition $(\mu, \zeta, T) \in \mathcal{S}(\epsilon)$ for some $\epsilon > 0$. Therefore, under these conditions the expansion (5.39) holds with $\mathbf{E}_1 = \mathcal{O}(T^{-1})$ and $\mathbf{E}(0) = \mathbb{I} + \mathcal{O}(T^{-1})$.



7.7 Asymptotic Formulæ for the Rational Solutions of Painlevé-IV on Boutroux Domains

Unraveling the explicit transformations relating $\mathbf{Y}(\lambda)$ and $\mathbf{O}(z) = \mathbf{E}(z)\check{\mathbf{O}}(z)$ and recalling the definition (3.2) of u(x) gives, for both families F = gH and F = gO,

$$\begin{split} u_{\mathrm{F}}^{[3]}(x;m,n) &= u(x) = T^{1/2} U_{\mathrm{F}}^{[3]}, \quad U_{\mathrm{F}}^{[3]} = -4s \frac{(\mathbf{E}(0) \breve{\mathbf{O}}^{\mathrm{out}}(0))_{11} (\mathbf{E}(0) \breve{\mathbf{O}}^{\mathrm{out}}(0))_{12}}{E_{1,12} + \breve{O}_{1,12}^{\mathrm{out}}}, \\ x &= T^{1/2} \mu + T^{-1/2} \zeta. \end{split}$$

Neglecting the small error terms, we therefore define an approximation for $U_{\rm F}^{[3]}$ by the formula

$$\begin{split} \check{U}_{\mathrm{F}}^{[3]} &= \check{U}_{\mathrm{F}}^{[3]}(\zeta;\mu) := -4s \frac{\check{O}_{11}^{\mathrm{out}}(0) \, \check{O}_{12}^{\mathrm{out}}(0)}{\check{O}_{1,12}^{\mathrm{out}}} \\ &= -4s v \frac{\check{P}_{11}^{\mathrm{out}}(0) \, \check{P}_{12}^{\mathrm{out}}(0)}{\check{P}_{1.12}^{\mathrm{out}}}, \end{split}$$

where in the second line we have used (7.32) and (7.33). Defining complex phase shifts by

$$\mathfrak{z}_{1}^{[3]} := -ia(0) - ia(z_{0}),
\mathfrak{z}_{2}^{[3]} := ia(0) - ia(z_{0}),
\mathfrak{p}_{1}^{[3]} := -ia(\infty) - ia(z_{0}),
\mathfrak{p}_{2}^{[3]} := ia(\infty) - ia(z_{0}),$$
(7.41)

we use (7.34)–(7.35) and $\vartheta(-z) = \vartheta(z)$ to write $\check{U}_F^{[3]}(\zeta; \mu)$ in the form

$$\begin{split} \check{U}_{F}^{[3]}(\zeta;\mu) &= \psi_{F}^{[3]}(\mu) \frac{\vartheta(a(0) + a(z_{0}) + \mathcal{K} - i\Psi)\vartheta(a(0) - a(z_{0}) - \mathcal{K} + i\Psi)}{\vartheta(a(\infty) + a(z_{0}) + \mathcal{K} - i\Psi)\vartheta(a(\infty) - a(z_{0}) - \mathcal{K} + i\Psi)} \\ &= \psi_{F}^{[3]}(\mu) \frac{\vartheta(\mathcal{K} - i(\Psi - \mathfrak{z}_{1}^{[3]}))\vartheta(\mathcal{K} - i(\Psi - \mathfrak{z}_{2}^{[3]}))}{\vartheta(\mathcal{K} - i(\Psi - \mathfrak{p}_{1}^{[3]}))\vartheta(\mathcal{K} - i(\Psi - \mathfrak{p}_{2}^{[3]}))}, \end{split}$$
(7.42)

which has the form (1.31) after using (7.26), where

$$\psi_{\rm F}^{[3]}(\mu) := -4s\nu \frac{\mathcal{N}_{11}(\mu)\mathcal{N}_{12}(\mu)}{\mathcal{N}(\mu)}.$$

Note that using (7.8), (7.21), (7.36)–(7.37), and the fact that R(0) = 4s, the factor $\psi_F^{[3]}(\mu)$ can be simplified to

$$\psi_{\rm F}^{[3]}(\mu) = z_0 \frac{\vartheta(a(\infty) + a(z_0) + \mathcal{K})\vartheta(a(\infty) - a(z_0) - \mathcal{K})}{\vartheta(a(0) + a(z_0) + \mathcal{K})\vartheta(a(0) - a(z_0) - \mathcal{K})}.$$
 (7.43)



It will be shown in Sect. 7.8 that $\check{U}_F^{[3]}(\zeta;\mu)$ is an elliptic function of ζ . We will have $U_F^{[3]} = \check{U}_F^{[3]} + \mathcal{O}(T^{-1})$ where $\check{U}_F^{[3]}$ is bounded and $1/U_F^{[3]} = 1/\check{U}_F^{[3]} + \mathcal{O}(T^{-1})$ where $1/\check{U}_F^{[3]}$ is bounded provided that $(\mu, \zeta, T) \in \mathcal{S}(\epsilon)$ with μ in a compact subset of the relevant Boutroux domain \mathcal{B} , and that ζ is bounded (conditions guaranteeing the error estimates on $\mathbf{E}(z)$ according to Proposition 12 of Sect. 7.6.1).

Similarly, for the rational function $u_{\mathbb{T}}(x)$ we find that

$$\begin{split} u_{\mathrm{F}}^{[1]}(x;m,n) &= u_{\updownarrow}(x) = |\Theta_{0,\updownarrow}|^{1/2} U_{\mathrm{F}}^{[1]}, \\ U_{\mathrm{F}}^{[1]} &= -\frac{T^{1/2}}{|\Theta_{0,\updownarrow}|^{1/2}} \frac{(\mathbf{E}(0)\check{\mathbf{O}}^{\mathrm{out}}(0))_{21}(E_{1,12} + \check{O}_{1,12}^{\mathrm{out}})}{(\mathbf{E}(0)\check{\mathbf{O}}^{\mathrm{out}}(0))_{11}}. \end{split}$$

To introduce the appropriate analogue of $\check{U}_{\rm F}^{[3]}$ for this case, recall that $T=|\Theta_0|$ and that, according to (2.4), $|\Theta_{0, \uparrow}|=\frac{1}{2}|\Theta_0|(1-s\kappa)$ with $1-s\kappa\neq 0$ for $\kappa\in (-1,1)$. Therefore, we define

$$\check{U}_{F}^{[1]} := -\sqrt{\frac{2}{1 - s\kappa}} \frac{\check{O}_{21}^{\text{out}}(0) \, \check{O}_{1,12}^{\text{out}}}{\check{O}_{11}^{\text{out}}(0)}, \tag{7.44}$$

which takes different forms depending on the sign $v = \pm 1$ in Table 6 in Sect. 7.6.1:

$$\begin{split} \check{U}_{\mathrm{F}}^{[1]} &= -\sqrt{\frac{2}{1-s\kappa}} \frac{\check{P}_{21}^{\mathrm{out}}(0) \check{P}_{1,12}^{\mathrm{out}}}{\check{P}_{11}^{\mathrm{out}}(0)} \\ &= -\sqrt{\frac{2}{1-s\kappa}} \\ &\quad \cdot \frac{\mathcal{N}_{21}(\mu)\mathcal{N}(\mu)}{\mathcal{N}_{11}(\mu)} \frac{\vartheta\left(a(0)-a(z_{0})-\mathcal{K}-\mathrm{i}\Psi\right)\vartheta\left(a(\infty)-a(z_{0})-\mathcal{K}+\mathrm{i}\Psi\right)}{\vartheta\left(a(0)+a(z_{0})+\mathcal{K}-\mathrm{i}\Psi\right)\vartheta\left(a(\infty)+a(z_{0})+\mathcal{K}+\mathrm{i}\Psi\right)}, \\ \nu &= 1; \\ \check{U}_{\mathrm{F}}^{[1]} &= -\sqrt{\frac{2}{1-s\kappa}} \frac{\check{P}_{22}^{\mathrm{out}}(0) \check{P}_{1,12}^{\mathrm{out}}}{\check{P}_{12}^{\mathrm{out}}(0)} \\ &= -\sqrt{\frac{2}{1-s\kappa}} \\ &\quad \cdot \frac{\mathcal{N}_{22}(\mu)\mathcal{N}(\mu)}{\mathcal{N}_{12}(\mu)} \frac{\vartheta\left(a(0)+a(z_{0})+\mathcal{K}+\mathrm{i}\Psi\right)\vartheta\left(a(\infty)-a(z_{0})-\mathcal{K}+\mathrm{i}\Psi\right)}{\vartheta\left(a(0)-a(z_{0})-\mathcal{K}+\mathrm{i}\Psi\right)\vartheta\left(a(\infty)+a(z_{0})+\mathcal{K}+\mathrm{i}\Psi\right)}, \\ \nu &= -1. \end{split}$$

In both cases, by similar arguments as used above to approximate $U_{\rm F}^{[3]}$ by $\check{U}_{\rm F}^{[3]}$, we will have $U_{\rm F}^{[1]}=\check{U}_{\rm F}^{[1]}+\mathcal{O}(T^{-1})$ where $\check{U}_{\rm F}^{[1]}$ is bounded and $1/U_{\rm F}^{[1]}=1/\check{U}_{\rm F}^{[1]}+\mathcal{O}(T^{-1})$ where $1/\check{U}_{\rm F}^{[1]}$ is bounded, provided that μ lies in a compact subset of \mathcal{B} , that ζ is bounded, and that $(\mu,\zeta,T)\in\mathcal{S}(\epsilon)$. The formulæ (7.45)–(7.46) can be simplified and



put into a universal form as follows. Defining complex phase shifts by

$$\mathfrak{z}_{1}^{[1]} := -i\nu a(0) + ia(z_{0}),
\mathfrak{z}_{2}^{[1]} := ia(\infty) - ia(z_{0}),
\mathfrak{p}_{1}^{[1]} := -i\nu a(0) - ia(z_{0}),
\mathfrak{p}_{2}^{[1]} := ia(\infty) + ia(z_{0}),$$
(7.47)

using $\vartheta(-z) = \vartheta(z)$ we can write

$$\begin{split} \check{U}_{\mathrm{F}}^{[1]} &= M \frac{\vartheta \left(\nu a(0) - a(z_0) - \mathcal{K} - \mathrm{i} \Psi \right) \vartheta \left(a(\infty) - a(z_0) - \mathcal{K} + \mathrm{i} \Psi \right)}{\vartheta \left(\nu a(0) + a(z_0) + \mathcal{K} - \mathrm{i} \Psi \right) \vartheta \left(a(\infty) + a(z_0) + \mathcal{K} + \mathrm{i} \Psi \right)} \\ &= M \frac{\vartheta \left(\mathcal{K} + \mathrm{i} \left(\Psi - \mathfrak{z}_1^{[1]} \right) \right) \vartheta \left(\mathcal{K} - \mathrm{i} \left(\Psi - \mathfrak{z}_2^{[1]} \right) \right)}{\vartheta \left(\mathcal{K} - \mathrm{i} \left(\Psi - \mathfrak{p}_1^{[1]} \right) \right) \vartheta \left(\mathcal{K} + \mathrm{i} \left(\Psi - \mathfrak{p}_2^{[1]} \right) \right)}, \end{split}$$

where, using (7.36)–(7.37),

$$\begin{split} M := -\sqrt{\frac{2}{1-s\kappa}} \frac{\alpha-\beta+\gamma-\delta}{4\mathrm{i}} \frac{\vartheta\left(a(\infty)+a(z_0)+\mathcal{K}\right)}{\vartheta\left(a(\infty)-a(z_0)-\mathcal{K}\right)} \\ \cdot \begin{cases} \frac{f^{\mathrm{OD}}(0)}{f^{\mathrm{D}}(0)} \frac{\vartheta\left(a(0)+a(z_0)+\mathcal{K}\right)}{\vartheta\left(a(0)-a(z_0)-\mathcal{K}\right)}, & \nu=1 \\ -\frac{f^{\mathrm{D}}(0)}{f^{\mathrm{OD}}(0)} \frac{\vartheta\left(a(0)-a(z_0)-\mathcal{K}\right)}{\vartheta\left(a(0)+a(z_0)+\mathcal{K}\right)}, & \nu=-1. \end{cases} \end{split}$$

It is straightforward to use the definitions (7.20) and $j(z)^2(z-\beta)(z-\delta)=r(z)$ to confirm the identities

$$\frac{f^{\mathrm{OD}}(z)}{f^{\mathrm{D}}(z)} = \mathrm{i} \frac{2r(z) - (z - \alpha)(z - \gamma) - (z - \beta)(z - \delta)}{(z - \alpha)(z - \gamma) - (z - \beta)(z - \delta)} \quad \text{and}$$

$$\frac{f^{\mathrm{D}}(z)}{f^{\mathrm{OD}}(z)} = \mathrm{i} \frac{2r(z) + (z - \alpha)(z - \gamma) + (z - \beta)(z - \delta)}{(z - \alpha)(z - \gamma) - (z - \beta)(z - \delta)}.$$

Therefore, setting z = 0, recalling (7.21) and using r(0) = 4sv we put M in the universal form

$$M = -\sqrt{\frac{2}{1 - s\kappa}} \frac{8s - (\alpha\gamma + \beta\delta)}{4z_0} \frac{\vartheta(a(\infty) + a(z_0) + \mathcal{K})\vartheta(va(0) + a(z_0) + \mathcal{K})}{\vartheta(a(\infty) - a(z_0) - \mathcal{K})\vartheta(va(0) - a(z_0) - \mathcal{K})}.$$
(7.48)

Finally, using the identities in (7.23) and $2\mathcal{K} = 2\pi i + H_{\omega}$ we have

$$\check{U}_{F}^{[1]} = \psi_{F}^{[1]} \frac{\vartheta(\mathcal{K} - i(\Psi - \mathfrak{z}_{1}^{[1]}))\vartheta(\mathcal{K} - i(\Psi - \mathfrak{z}_{2}^{[1]}))}{\vartheta(\mathcal{K} - i(\Psi - \mathfrak{p}_{1}^{[1]}))\vartheta(\mathcal{K} - i(\Psi - \mathfrak{p}_{2}^{[1]}))}, \quad \psi_{F}^{[1]} := e^{i(\mathfrak{z}_{1}^{[1]} - \mathfrak{p}_{2}^{[1]})}M. \tag{7.49}$$



This also has the form (1.31) except that the theta function has the same parameter as in the approximation of the type-3 rational solutions of Painlevé-IV whereas we instead expect to see the theta function for a different elliptic curve associated to the type-1 parameters. This final point will be clarified in Sect. 7.8.3; see (7.66). To use $\check{U}_F^{[1]}$ as an approximation of $U_F^{[1]} = |\Theta_{0,\uparrow}|^{-1/2} u_F^{[1]}(x;m,n) = |\Theta_{0,F}^{[1]}(m,n)|^{-1/2} u_F^{[1]}(x;m,n)$ for the type-1 function in the family F = gH or F = gO, the variables and parameters in $\check{U}_F^{[1]}$ need to be carefully interpreted. Here we recall Remark 11 of Sect. 4.1, which specifies that the parameters T, s, and s should be expressed in terms of the indices (m,n) by (4.6) or (4.8) for the gH and gO families respectively. Also, the variables s and s should be rescaled by making the replacements (4.9)–(4.10). Then finally we have a well-defined function $\check{U}_F^{[1]} = \check{U}_F^{[1]}(\xi; \mu)$ where the arguments s and s and s are fer to the variables after the indicated replacements have been made, and $\check{U}_F^{[1]}(s; \mu)$ is an accurate approximation of $|\Theta_{0,F}^{[1]}(m,n)|^{-1/2}u_F^{[1]}(x;m,n)$ when s is an accurate approximation of s in s in

The original variable μ lies in a Boutroux domain \mathcal{B} for $\kappa \in (-1,1)$, but after replacing the variables μ and ζ by their rescaled versions the approximation $U_{\rm F}^{[1]} = \check{U}_{\rm F}^{[1]}(\zeta;\mu) + \mathcal{O}(T^{-1})$ holds for μ in a homothetic dilation of \mathcal{B} . Moreover, the rescaled domain should properly be associated to the leading term (see (1.23)) $I^{-s}(\kappa) = -(\kappa+3s)/(1-s\kappa)$ of $\kappa_{\Sigma} = -\Theta_{\infty,\Sigma}/|\Theta_{0,\Sigma}| = -\Theta_{\infty,F}^{[1]}(m,n)/|\Theta_{0,F}^{[1]}(m,n)|$, as the latter is the natural value of κ associated to the rational solution $u_{\rm F}^{[1]}(x;m,n)$ according to the scalings in (1.13). Note that $\kappa \in (-1,1)$ implies that $|I^{-s}(\kappa)| > 1$. Once the Boutroux domains \mathcal{B}_{\square} , $\mathcal{B}_{\triangleright}$, and \mathcal{B}_{\triangle} have been properly defined for $\kappa \in (-1,1)$ (see Sects. 8.6 and 8.9), it will therefore be natural to extend the definition to $|\kappa| > 1$ by suitable dilations in the μ -plane. A synthesized description of these domains is given in Definition 9 in Sect. 8.9.

7.8 Differential Equations Satisfied by the Approximations

7.8.1 Derivation of the Differential Equation for $\breve{U}_{\rm F}^{[3]}(\zeta;\mu)$

We now show that the function $\check{U}(\zeta) = \check{U}_F^{[3]}(\zeta;\mu)$ defined by (7.42) satisfies exactly the differential equation (1.18) in which E depends on μ via the Boutroux conditions (4.23). Evaluating $\check{\mathbf{O}}^{\text{out}}(z)$ at z=0 yields a matrix function of ζ that we will write as $\check{\mathbf{O}}^{\text{out}}(0) = \mathbf{Z}(\zeta)$ in this section. Likewise, to emphasize the dependence on ζ in the expansion coefficients in (7.31) we will write $\check{\mathbf{O}}_k^{\text{out}} = \check{\mathbf{O}}_k^{\text{out}}(\zeta)$.

Fixing $\mu \in \mathcal{B}_{\square} \cup \mathcal{B}_{\triangleright} \cup \mathcal{B}_{\triangle}$, we observe that the matrix $\mathbf{F}(\zeta;z) := \check{\mathbf{O}}^{\text{out}}(z) \mathrm{e}^{\zeta z \sigma_3/2}$ has jump matrices that are independent of ζ , so since $\det(\mathbf{F}(\zeta;z)) = 1$, $\mathbf{F}'(\zeta;z)\mathbf{F}(\zeta;z)^{-1}$ is an entire function of z. Using the convergent Laurent expansion (7.31) and its termby-term derivative with respect to ζ shows that in fact this entire function is linear in z: $\mathbf{F}'(\zeta;z)\mathbf{F}(\zeta;z)^{-1} = \frac{1}{2}z\sigma_3 + \frac{1}{2}[\check{\mathbf{O}}_1^{\text{out}}(\zeta),\sigma_3]$. Equivalently, for each z not on the



jump contour, the outer parametrix satisfies the differential equation

$$\frac{d\mathbf{\check{O}}^{\text{out}}}{d\zeta} = \frac{1}{2}z[\sigma_3, \mathbf{\check{O}}^{\text{out}}] + \frac{1}{2}[\mathbf{\check{O}}_1^{\text{out}}(\zeta), \sigma_3]\mathbf{\check{O}}^{\text{out}}.$$
 (7.50)

In particular, upon setting z=0, $\check{\mathbf{O}}^{\text{out}}$ becomes $\mathbf{Z}(\zeta)$, and we deduce that (7.50) implies that

$$\frac{\mathrm{d}}{\mathrm{d}\zeta}(Z_{11}(\zeta)Z_{12}(\zeta)) = -\check{O}_{1,12}^{\mathrm{out}}(\zeta)(Z_{11}(\zeta)Z_{22}(\zeta) + Z_{12}(\zeta)Z_{21}(\zeta)). \tag{7.51}$$

Similarly, using again the Laurent expansion (7.31) and taking the terms in (7.50) proportional to z^{-1} we find that

$$\frac{d\check{O}_{1,12}^{\text{out}}(\zeta)}{d\zeta} = \check{O}_{2,12}^{\text{out}}(\zeta) - \check{O}_{1,12}^{\text{out}}(\zeta)\check{O}_{1,22}^{\text{out}}(\zeta). \tag{7.52}$$

Next, we make the following observation: if $\mathbf{V}(z)$ is the jump matrix for the outer parametrix $\check{\mathbf{O}}^{\text{out}}(z)$, then on arcs of the jump contour where R(z) is continuous we have the form $\mathbf{V}(z) = \mathbf{D}(a)$ for some constant $a \neq 0$ and therefore $\mathbf{V}(z)\sigma_3\mathbf{V}(z)^{-1} = \sigma_3$, while on arcs of the jump contour across which R(z) changes sign we have instead that $\mathbf{V}(z) = \mathbf{T}(ae^{-\zeta z})$ for some constant $a \neq 0$ and therefore $\mathbf{V}(z)\sigma_3\mathbf{V}(z)^{-1} = -\sigma_3$. It follows that the matrix function

$$\mathbf{G}(z) := R(z)\check{\mathbf{O}}^{\text{out}}(z)\sigma_3\check{\mathbf{O}}^{\text{out}}(z)^{-1}$$
(7.53)

is analytic except possibly on the jump contour, on which it is continuous except possibly for the endpoints of each maximal arc. Those endpoints are the roots of the quartic polynomial $P(z) = R(z)^2$, and since $\check{\mathbf{O}}^{\text{out}}(z)$ blows up at these points like a negative one-fourth power while $\det(\check{\mathbf{O}}^{\text{out}}(z)) = 1$, it follows by Morera's Theorem that $\mathbf{G}(z)$ is an entire function of z. From the asymptotic behavior of the factors (see (7.31)), it is clear that $\mathbf{G}(z)$ is in fact a quadratic matrix-valued polynomial in z. Using (7.31) and the expansion $R(z) = z^2 + 2\mu z + 4\kappa + \mathcal{O}(z^{-1})$ as $z \to \infty$ to calculate the polynomial part of the right-hand side of (7.53) gives the representation

$$\mathbf{G}(z) = \sigma_3 z^2 + (2\mu \sigma_3 + [\mathbf{\breve{O}}_1^{\text{out}}(\zeta), \sigma_3])z + \mathbf{G}(0), \tag{7.54}$$

where

$$\mathbf{G}(0) := 4\kappa\sigma_3 + 2\mu[\check{\mathbf{O}}_1^{\text{out}}(\zeta), \sigma_3] + [\sigma_3, \check{\mathbf{O}}_1^{\text{out}}(\zeta)]\check{\mathbf{O}}_1^{\text{out}}(\zeta) + [\check{\mathbf{O}}_2^{\text{out}}(\zeta), \sigma_3]. \quad (7.55)$$

On the other hand, setting z = 0 on the right-hand side of (7.53) and using R(0) = 4s gives an equivalent representation for G(0):

$$\mathbf{G}(0) = 4s\mathbf{Z}(\zeta)\sigma_3\mathbf{Z}(\zeta)^{-1}.$$
 (7.56)



Comparing the (1, 2)-entry in the equivalent representations (7.55)–(7.56) gives the identity

$$\check{O}_{2,12}^{\text{out}}(\zeta) - \check{O}_{1,12}^{\text{out}}(\zeta) \check{O}_{1,22}^{\text{out}}(\zeta) = 4s Z_{11}(\zeta) Z_{12}(\zeta) - 2\mu \check{O}_{1,12}^{\text{out}}(\zeta).$$

Using this identity and combining (7.51)–(7.52) with the definition (7.42) shows that

where on the second line we used the (1, 1)-entry of (7.56). Therefore also

$$\check{U}'(\zeta)^{2} = \check{U}(\zeta)^{4} + 4\mu \check{U}(\zeta)^{3} + (4\mu^{2} + 2G_{11}(0))\check{U}(\zeta)^{2}
+ 4\mu G_{11}(0)\check{U}(\zeta) + G_{11}(0)^{2}
= \check{U}(\zeta)^{4} + 4\mu \check{U}(\zeta)^{3} + (4\mu^{2} + 2G_{11}(0))\check{U}(\zeta)^{2}
+ 4\mu G_{11}(0)\check{U}(\zeta) + 16 - G_{12}(0)G_{21}(0),$$
(7.57)

where in the second equality we used that $tr(\mathbf{G}(0)) = 0$ and $det(\mathbf{G}(0)) = -16$, both of which follow from (7.56).

Now, since $\sigma_3^2 = \mathbb{I}$ the definition (7.53) shows that $\mathbf{G}(z)^2$ is a *scalar* polynomial, namely $\mathbf{G}(z)^2 = R(z)^2 \mathbb{I} = P(z) \mathbb{I}$. Squaring (7.54) and taking (without loss of generality) the (1, 1)-entry gives

$$P(z) = z^4 + 4\mu z^3 + (4\mu^2 + 2G_{11}(0) - 4\breve{O}_{1,12}^{\text{out}}(\zeta)\breve{O}_{1,21}^{\text{out}}(\zeta))z^2 + (4\mu G_{11}(0) + 2\breve{O}_{1,21}^{\text{out}}(\zeta)G_{12}(0) - 2\breve{O}_{1,12}^{\text{out}}(\zeta)G_{21}(0))z + 16.$$

Substituting $z = \check{U}(\zeta)$ and subtracting from (7.57) gives

Recalling the definition (7.42) of $\check{U}(\zeta)$ and using the matrix elements of (7.56) then shows that the right-hand side vanishes identically in ζ , which completes the proof of the claim. Hence $\check{U}(\zeta) = \check{U}_F^{[3]}(\zeta; \mu)$ can be written in the form $f(\zeta - \zeta_0)$ for some ζ_0 independent of ζ , where $f(\zeta)$ is the unique solution of the differential equation (1.18) satisfying f(0) = 0 and f'(0) = 4.

7.8.2 Derivation of the Differential Equation for $\check{U}_{\rm F}^{[1]}(\zeta;\mu)$

For convenience, let us relabel the arguments of $\check{U}_{\rm F}^{[1]}$ as ζ_{\updownarrow} and μ_{\updownarrow} . We now show that $\check{U}_{\updownarrow}(\zeta_{\updownarrow}) = \check{U}_{\rm F}^{[1]}(\zeta_{\updownarrow}; \mu_{\updownarrow})$ is also an elliptic function of its argument ζ_{\updownarrow} , solving



a closely related differential equation. To see this, we start from the definition (7.42) of $\check{U}(\zeta) = \check{U}_F^{[3]}(\zeta; \mu)$ and use (7.51) (with $\det(\mathbf{Z}(\zeta)) = 1$ on the right-hand side to eliminate $Z_{11}(\zeta)Z_{22}(\zeta)$) and (7.52) to find the differential identity

$$\frac{1}{2\check{U}(\zeta)}\frac{\mathrm{d}\check{U}}{\mathrm{d}\zeta}(\zeta) - \frac{2s}{\check{U}(\zeta)} - \mu - \frac{1}{2}\check{U}(\zeta) = -\frac{Z_{21}(\zeta)\check{O}_{1,12}^{\mathrm{out}}(\zeta)}{Z_{11}(\zeta)} = \sqrt{\frac{1-s\kappa}{2}}\check{U}_{\uparrow\downarrow}(\zeta_{\uparrow\downarrow}), \tag{7.58}$$

where in the second equality we used the definition (7.44). Now, using the fact shown above that $\check{U}(\zeta)$ satisfies the first-order equation (1.18) and hence (by isolating the constant E and taking a derivative) the second-order equation (1.2), it is straightforward to check that \check{U}_{\uparrow} also satisfies a related second-order equation:

$$\frac{\mathrm{d}^2 \check{U}_{\uparrow\uparrow}}{\mathrm{d}\zeta^2} = \frac{1}{2\check{U}_{\uparrow\downarrow}} \left(\frac{\mathrm{d}\check{U}_{\uparrow\downarrow}}{\mathrm{d}\zeta} \right)^2 + \frac{3}{4} (1 - s\kappa) \check{U}_{\uparrow\downarrow}^3 + 4\mu \sqrt{\frac{1 - s\kappa}{2}} \check{U}_{\uparrow\downarrow}^2 + (2\mu^2 - 6s - 2\kappa) \check{U}_{\uparrow\downarrow}$$
$$-\frac{4(1 - s\kappa)}{\check{U}_{\uparrow\downarrow}}.$$

But now recall that \check{U}_{\uparrow} should be considered as a function of $\zeta_{\uparrow} = \sqrt{\frac{1}{2}(1 - s\kappa)}\zeta$, so by the chain rule,

$$\frac{\mathrm{d}^{2} \check{U}_{\updownarrow}}{\mathrm{d} \xi_{\updownarrow}^{2}} = \frac{1}{2 \check{U}_{\updownarrow}} \left(\frac{\mathrm{d} \check{U}_{\updownarrow}}{\mathrm{d} \xi_{\updownarrow}} \right)^{2} + \frac{3}{2} \check{U}_{\gimel}^{3} + 4\mu \sqrt{\frac{2}{1 - s\kappa}} \check{U}_{\gimel}^{2} + \left(2\mu^{2} \frac{2}{1 - s\kappa} + 4 \left[-\frac{\kappa + 3s}{1 - s\kappa} \right] \right) \check{U}_{\updownarrow} - \frac{8}{\check{U}_{\updownarrow}}.$$
(7.59)

The differential equation (7.59) matches exactly the form of (1.2) in which only μ is replaced with μ_{\uparrow} determined by the relation $\mu = \sqrt{\frac{1}{2}(1 - s\kappa)}\mu_{\uparrow}$ and κ is replaced with $I^{-s}(\kappa) = -(\kappa + 3s)/(1 - s\kappa)$ defined in (1.23). Therefore, as in Sect. 1.3, this equation can be integrated up to the form

$$\left(\frac{\mathrm{d}\check{U}_{\updownarrow}}{\mathrm{d}\zeta_{\updownarrow}}\right)^{2} = P_{\updownarrow}(\check{U}_{\updownarrow}) := \check{U}_{\updownarrow}^{4} + 4\mu_{\updownarrow}\check{U}_{\updownarrow}^{3} + 2(2\mu_{\updownarrow}^{2} + 4I^{-s}(\kappa))\check{U}_{\updownarrow}^{2} + 2E_{\updownarrow}\check{U}_{\updownarrow} + 16,$$
(7.60)

which should be compared with (1.18). Here E_{\uparrow} is a constant of integration. Solving for E_{\uparrow} , eliminating \check{U}_{\uparrow} and its derivative in favor of derivatives of $\check{U}(\zeta)$ using (7.58), and finally using the differential equations (1.2) and (1.18) satisfied by $\check{U}(\zeta)$ (and the chain rule again) one finds the explicit relation between E_{\uparrow} and E:

$$E_{\uparrow} = \left(\frac{2}{1 - s\kappa}\right)^{3/2} \left[E - 4\mu(\kappa + s)\right]. \tag{7.61}$$



Remark 14 Observe that the relation (7.58) expressing \check{U}_{\uparrow} explicitly in terms of \check{U} is a limiting form of the non-isomonodromic Bäcklund transformation (2.4) expressing $u_{\uparrow}(x)$ explicitly in terms of u(x).

7.8.3 Relation Between the Corresponding Spectral Curves

If we use the differential equation (1.18) to eliminate the derivative in (7.58), we obtain a non-differential relation between \check{U} and \check{U}_{5} :

$$\check{U}_{\uparrow} = -\sqrt{\frac{2}{1 - s\kappa}} \left(\frac{1}{2} \check{U} + \mu + \frac{2s}{\check{U}} + \frac{1}{2} \frac{w}{\check{U}} \right), \quad w^2 = P(\check{U}). \tag{7.62}$$

Isolating w and squaring leads to the bi-quadratic relation

$$\begin{split} &2\sqrt{\frac{1-s\kappa}{2}}\breve{U}_{\circlearrowright}\breve{U}^2 + \left[4s(1-s\kappa) + 4\mu\sqrt{\frac{1-s\kappa}{2}}\breve{U}_{\circlearrowright} + (1-s\kappa)\breve{U}_{\circlearrowleft}^2\right]\breve{U} \\ &+ \left[8s\sqrt{\frac{1-s\kappa}{2}}\breve{U}_{\circlearrowleft} + 8s\mu - E\right] = 0, \end{split}$$

where we used the fact that \check{U} does not vanish identically to cancel a common factor. Solving now instead for \check{U} and using (7.61) and $\mu = \sqrt{\frac{1}{2}(1 - s\kappa)}\mu_{\updownarrow}$, we obtain

$$\check{U} = -\sqrt{\frac{1 - s\kappa}{2}} \left(\frac{1}{2} \check{U}_{\uparrow} + \mu_{\uparrow} + \frac{2s}{\check{U}_{\uparrow}} + \frac{1}{2} \frac{w_{\uparrow}}{\check{U}_{\uparrow}} \right), \quad w_{\uparrow}^2 = P_{\uparrow}(\check{U}_{\uparrow}). \tag{7.63}$$

Solving (7.63) for w_{\uparrow} , eliminating \check{U}_{\uparrow} using (7.62) and expressing μ_{\uparrow} in terms of μ gives

$$w_{\uparrow} = -\frac{1}{2(1 - s\kappa)\check{U}^2} \left[w^2 - 3\check{U}^4 - 2w\check{U}^2 - 8\mu\check{U}^3 + 8sw - 4(\mu^2 + 2\kappa)\check{U}^2 + 16 \right]. \tag{7.64}$$

Likewise, solving (7.62) for w, eliminating \check{U} using (7.63) and expressing μ in terms of μ_{\circlearrowright} gives

$$w = -\frac{1 - s\kappa}{8\check{U}_{\zeta}^{2}} \left[w_{\zeta}^{2} - 3\check{U}_{\zeta}^{4} - 2w_{\zeta}\check{U}_{\zeta}^{2} - 8\mu_{\zeta}\check{U}_{\zeta}^{3} + 8sw_{\zeta} - 4(\mu_{\zeta}^{2} + 2I^{-s}(\kappa))\check{U}_{\zeta}^{2} + 16 \right].$$
(7.65)

Using $s=\pm 1$, it is straightforward to check that the equations (7.62) and (7.64) constitute a birational transformation $\mathcal{T}:\mathbb{C}^2\to\mathbb{C}^2$ with action $(\check{U}_{\mathbb{C}}^+,w_{\mathbb{C}}^+)=\mathcal{T}(\check{U},w)$ and with explicit inverse given by (7.63) and (7.65). Restricting to the Riemann surface \mathcal{R} shows that $\mathcal{T}:\mathcal{R}\to\mathcal{R}_{\mathbb{C}}$ and that $\mathcal{T}^{-1}:\mathcal{R}_{\mathbb{C}}\to\mathcal{R}$. Therefore the Riemann surfaces \mathcal{R} and $\mathcal{R}_{\mathbb{C}}$ are conformally equivalent. In particular, the pull-back



under \mathcal{T} of the holomorphic differential $w_{\mathbb{Q}}^{-1}\mathrm{d}\check{U}_{\mathbb{Q}}$ on $\mathcal{R}_{\mathbb{Q}}$ is a holomorphic differential on \mathcal{R} : taking the differential of (7.62) and using $2w\,\mathrm{d}w=P'(\check{U})\,\mathrm{d}\check{U}$ and $\check{U}P'(\check{U})=w^2+3\check{U}^4+8\mu\check{U}^3+4(\mu^2+2\kappa)\check{U}^2-16$ gives

$$\begin{split} \mathcal{T}^* \frac{\mathrm{d} \check{U}_{\circlearrowright}}{w_{\circlearrowright}} &= -\sqrt{\frac{2}{1-s\kappa}} \left(\frac{1}{2} - \frac{2s}{\check{U}^2} - \frac{w}{2\check{U}^2} + \frac{P'(\check{U})}{4w\check{U}} \right) \frac{\mathrm{d} \check{U}}{w_{\circlearrowright}} \\ &= \sqrt{\frac{2}{1-s\kappa}} \frac{w^2 - 3\check{U}^4 - 2w\check{U}^2 - 8\mu\check{U}^3 + 8sw - 4(\mu^2 + 2\kappa)\check{U}^2 + 16}{4ww_{\circlearrowright}\check{U}^2} \, \mathrm{d} \check{U} \\ &= -\sqrt{\frac{1-s\kappa}{2}} \frac{\mathrm{d} \check{U}}{w} \end{split}$$

after comparing with (7.64). (Here the superscript * denotes pull-back instead of complex conjugation.) Therefore, if $(\mathfrak{a},\mathfrak{b})$ is a canonical homology basis on \mathcal{R} , then $(\mathfrak{a}_{\mathbb{Q}},\mathfrak{b}_{\mathbb{Q}})=(\mathcal{T}\mathfrak{a},\mathcal{T}\mathfrak{b})$ is a canonical homology basis on $\mathcal{R}_{\mathbb{Q}}$, and the corresponding theta function parameters are equal:

$$H_{\omega, \uparrow} = 2\pi i \frac{\oint_{\mathfrak{b} \uparrow} \frac{d\check{U}_{\uparrow}}{w_{\uparrow}}}{\oint_{\mathfrak{a} \uparrow} \frac{d\check{U}_{\uparrow}}{w_{\uparrow}}} = 2\pi i \frac{\oint_{\mathfrak{b}} \frac{d\check{U}}{w}}{\oint_{\mathfrak{a}} \frac{d\check{U}}{w}} = H_{\omega}. \tag{7.66}$$

Likewise, if C denotes any cycle on the Riemann surface \mathcal{R} of the equation $w^2 = P(\check{U})$, then by integration by parts

$$\oint_C \check{U}_{\mathbb{Q}} \, \mathrm{d} \check{U} = - \oint_{C_{\mathbb{Q}}} \check{U} \, \mathrm{d} \check{U}_{\mathbb{Q}},$$

where C_{\uparrow} is the corresponding cycle on the Riemann surface \mathcal{R}_{\uparrow} of $w_{\uparrow}^2 = P_{\uparrow}(\check{U}_{\uparrow})$. Therefore, using (7.62) and (7.63) we get

$$\begin{split} &-\sqrt{\frac{2}{1-s\kappa}}\oint_{C}\left(\frac{1}{2}\check{U}+\mu+\frac{2s}{\check{U}}+\frac{1}{2}\frac{w}{\check{U}}\right)\mathrm{d}\check{U}\\ &=\sqrt{\frac{1-s\kappa}{2}}\oint_{C^{\uparrow}_{C}}\left(\frac{1}{2}\check{U}_{\updownarrow}+\mu_{\updownarrow}+\frac{2s}{\check{U}_{\updownarrow}}+\frac{1}{2}\frac{w_{\updownarrow}}{\check{U}_{\Lsh}}\right)\mathrm{d}\check{U}_{\updownarrow}. \end{split}$$

The first two terms in the integrand on each side of this equation contribute nothing by Cauchy's Theorem. The third term on each side can only contribute a purely imaginary quantity as the residue of the pole is real in each case. Therefore, taking the real part we obtain

$$\sqrt{\frac{2}{1-s\kappa}}\operatorname{Re}\left(\oint_{C}\frac{w}{\check{U}}\,\mathrm{d}\check{U}\right) = -\sqrt{\frac{1-s\kappa}{2}}\operatorname{Re}\left(\oint_{C_{\uparrow}^{\uparrow}}\frac{w_{\uparrow}}{\check{U}_{\uparrow}}\,\mathrm{d}\check{U}_{\uparrow}\right). \tag{7.67}$$



It follows that \mathcal{R} with parameter E is a Boutroux curve if and only if \mathcal{R}_{\searrow} with parameter E_{\searrow} is a Boutroux curve. This observation motivates the definition of the parameter E for $|\kappa| > 1$ in terms of that for $\kappa \in (-1, 1)$ using (7.61); see Definition 10 in Sect. 8.9.

Finally, we have shown that, like $\check{U}_F^{[3]}(\zeta;\mu)$, $\check{U}_F^{[1]}(\zeta;\mu)$ satisfies the differential equation (1.18) for a value of κ very close (see Remark 15) to its "native" value of $-\Theta_{0,F}^{[1]}(m,n)/|\Theta_{0,F}^{[1]}(m,n)|$ with corresponding parameter $E=E(\mu;\kappa)$ chosen so that the underlying Riemann surface is a Boutroux curve. Hence it can be written in the form $f(\zeta-\zeta_0)$ for ζ_0 independent of ζ , where again $f(\zeta)$ is the unique solution of (1.18) with f(0)=0 and f'(0)=4. Note that in the gO case, the approximations defined above for $\mu\in\mathcal{B}_{\triangleright}(\kappa)$ or $\mu\in\mathcal{B}_{\triangle}(\kappa)$ are easily extended to $-\mu\in\mathcal{B}_{\triangleright}(\kappa)$ and $-\mu\in\mathcal{B}_{\triangle}(\kappa)$ by odd reflection: $(\check{U},\mu,\zeta)\mapsto (-\check{U},-\mu,-\zeta)$, which is consistent with the exact symmetry of the rational solutions as indicated in Proposition 4 in Sect. 2. To get an approximation in the only remaining case of type j=2, we use the symmetry (2.2) to express $u_F^{[2]}(\cdot;m,n)$ in terms of $u_F^{[1]}(\cdot;n,m)$, rotating both μ and ζ by a quarter turn in the complex plane: $\check{U}_F^{[2]}(\zeta;\mu):=i\check{U}_F^{[1]}(-i\zeta;-i\mu)$. Note that the approximating differential equation (1.18) is invariant under $(f,\zeta,\mu,\kappa)\mapsto (-if,-i\zeta,-i\mu,-\kappa)$ given the symmetry (1.28) in Proposition 3 in Sect. 1.4. Hence the type j=2 approximation is also an elliptic function of the form $f(\zeta-\zeta_0)$.

Remark 15 A subtle point is that when κ and s are defined by (4.6) or (4.8) as necessary to study $u_{\rm gH}^{[1]}(x;m,n)$ or $u_{\rm gO}^{[1]}(x;m,n)$ respectively according to Remark 11 in Sect. 4.1, then the parameter $I^{-s}(\kappa)$ appearing in the differential equation (7.60) satisfied by the approximation $\check{U}_{\rm F}^{[1]}(\zeta;\mu)$ is not exactly equal to the value of κ for which an elliptic function solution of the differential equation (1.18) is asserted in Theorems 3 and 4 in Sect. 1.4 as a valid approximation. The latter value is the ratio $-\Theta_{0,{\rm F}}^{[1]}(m,n)/|\Theta_{0,{\rm F}}^{[1]}(m,n)|$. In fact for the gH case we have s=1 and taking κ in terms of m, n from (4.6),

$$-\frac{\Theta_{\infty,\text{gH}}^{[1]}(m,n)}{|\Theta_{0,\text{gH}}^{[1]}(m,n)|} = I^{-s}(\kappa) - \frac{2}{n}$$

while for the gO case we may take either sign for s and taking κ from (4.8),

$$-\frac{\Theta_{\infty,gO}^{[1]}(m,n)}{|\Theta_{0,gO}^{[1]}(m,n)|} = I^{-s}(\kappa) - \frac{2s}{n - \frac{1}{3}}.$$

Arriving at the precise statements in Theorems 3 and 4 respectively therefore involves an additional approximation in which one elliptic function is exchanged for another with periods differing by $\mathcal{O}(n^{-1})$ which is equivalent to $\mathcal{O}(T^{-1})$. Since ζ is bounded, this perturbation can be absorbed into the error terms, although the phase ζ_0 generally needs to be shifted by an amount that does not tend to zero in the limit $T \to \infty$ because it involves terms proportional to T. Note however that the statements of these two theorems do not precisely specify the value of ζ_0 . A similar minor discrepancy arises in the approximation of $u_F^{[2]}(x;m,n)$ because the symmetry $\kappa \mapsto -\kappa$ does not



exactly correspond to the Boiti-Pempinelli symmetry (see (2.2)). Indeed, the latter is a reflection through the horizontal line $\Theta_{\infty} = \frac{1}{2}$ instead of through $\Theta_{\infty} = 0$. This discrepancy is dealt with in exactly the same way.

To complete the proof of Theorems 3 and 4 formulated in Sect. 1.4 assuming the existence of the hypothetical Boutroux domains $\mathcal{B}_{\triangleright}$ and \mathcal{B}_{\triangle} and under the assertion that all three domains $\mathcal{B}_{\triangleright}$, $\mathcal{B}_{\triangleright}$, and \mathcal{B}_{\triangle} have the indicated boundaries, it only remains to note that suitable uniformity of the error estimates follows from similar arguments as given in Sect. 5.6 and then to explain why the condition that $(\mu, \zeta, T) \in \mathcal{S}(\epsilon)$ for some $\epsilon > 0$ can be dropped. This second point will be justified in Sect. 7.10.3.

7.9 Zeros and Poles of the Approximations

The approximations $\check{U}_F^{[j]}(\zeta; \mu)$ of the rational solutions of type j=1,3 in the family F=gH or F=gO vanish whenever

$$i(\Psi - \mathfrak{z}_{1}^{[j]}) = 2\pi i N_{\mathfrak{a}} + H_{\omega} N_{\mathfrak{b}} \text{ or } i(\Psi - \mathfrak{z}_{2}^{[j]}) = 2\pi i N_{\mathfrak{a}} + H_{\omega} N_{\mathfrak{b}}$$
 (7.68)

and blow up whenever

$$i(\Psi - \mathfrak{p}_1^{[j]}) = 2\pi i N_{\mathfrak{a}} + H_{\omega} N_{\mathfrak{b}} \quad \text{or} \quad i(\Psi - \mathfrak{p}_2^{[j]}) = 2\pi i N_{\mathfrak{a}} + H_{\omega} N_{\mathfrak{b}}, \tag{7.69}$$

where $N_{\mathfrak{a}}$ and $N_{\mathfrak{b}}$ are arbitrary integers.

Lemma 11 For the approximations $\check{U}_F^{[j]}(\zeta; \mu)$, j = 1, 3, no two of the four conditions in (7.68)–(7.69) can hold simultaneously.

Proof As in the proof of Lemma 10 in Sect. 7.6.1, we use the Abel-Jacobi Theorem. For i = 3, we notice that taking i times the differences of any two of the phase shifts in (7.41) gives a difference of Abel maps evaluated at two distinct points of \mathcal{R} . The corresponding conditions will hold simultaneously if and only if there is a nonzero meromorphic function on \mathcal{R} with a simple pole at one of these points and vanishing at the other point. But having only one simple pole on \mathcal{R} , this function must be a constant, and hence to vanish anywhere it must vanish identically. For i = 1, taking into account that z_0 cannot equal any of the four roots α , β , γ , δ so that $2a(z_0)$ can be written as a difference of Abel maps of distinct points of \mathcal{R} over z_0 , the same argument applies to any of the four differences $i(\mathfrak{z}_k^{[1]} - \mathfrak{p}_\ell^{[1]})$ for phase shifts defined in (7.47). For the remaining two differences $i(\mathfrak{z}_1^{[1]} - \mathfrak{z}_2^{[1]}) = va(0) - 2a(z_0) + a(\infty)$ and $i(\mathfrak{p}_1^{[1]} - \mathfrak{p}_2^{[1]}) = va(0) + 2a(z_0) + a(\infty)$, we note that the proof of Lemma 10 showed that $2a(\infty) + 2a(z_0) = 2\pi i N_a + H_\omega N_b$ for some integers N_a and N_b . Therefore, it suffices to prove that neither $va(0) + 3a(\infty)$ nor $va(0) - a(\infty)$ can be an integer linear combination of $2\pi i$ and H_{ω} . For $\nu a(0) - a(\infty)$, the same argument as above applies. For $va(0) + 3a(\infty)$ we move two of the factors of $a(\infty)$ "onto the other sheet" by using the Abel mapping on the Riemann surface \mathcal{R} defined in the proof of Lemma 10 to write $va(0) + 3a(\infty) = \tilde{a}(Q^{\nu}(0)) + \tilde{a}(Q^{+}(\infty)) - 2\tilde{a}(Q^{-}(\infty))$. Thus applying the Abel-Jacobi Theorem it is sufficient to prove that there can be no



meromorphic function k(Q) on $\mathcal R$ that does not vanish identically and has only one double pole at $Q^-(\infty)$ and simple zeros at $Q^{\nu}(0)$ and $Q^+(\infty)$. Using the "coordinate" meromorphic functions z(Q) and $\widetilde{r}(Q)$ defined on $\mathcal R$ as in the proof of Lemma 10, every nonzero function with a double pole at $Q^-(\infty)$ and at worst a simple pole at $Q^+(\infty)$ is necessarily a nonzero multiple of

$$k(Q) = z(Q)^{2} - \widetilde{r}(Q) + c_{1}z(Q) + c_{2}$$

for constants c_1 and c_2 . Since $z(Q^{\nu}(0)) = 0$ and $\widetilde{r}(Q^{\nu}(0)) = \nu r(0) = R(0) = 4s$, enforcing the condition $k(Q^{\nu}(0)) = 0$ requires taking $c_2 = 4s = \pm 4$. Now, the expansion $r(z) = R(z) = z^2 + 2\mu z + 4\kappa + \mathcal{O}(z^{-1})$ as $z \to \infty$ implies also that $\widetilde{r}(Q) = z(Q)^2 + 2\mu z(Q) + 4\kappa + \mathcal{O}(z(Q)^{-1})$ as $Q \to Q^+(\infty)$. Therefore, enforcing the condition that k(Q) be analytic at $Q = Q^+(\infty)$ requires taking $c_1 = 2\mu$, and then demanding further that $k(Q^+(\infty)) = 0$ requires taking $c_2 = 4\kappa$. But since $\kappa \neq \pm 1$, this is a contradiction with $c_2 = 4s = \pm 4$. Hence no such function k(Q) exists, and the proof is finished. An alternative indirect proof can be based on the differential equation (1.18) and the results of Sect. 7.8.

Using the fact that $\operatorname{Re}(H_{\omega}) < 0$ (implying that $2\pi i$ and H_{ω} are linearly independent over \mathbb{R}), we can solve for $N_{\mathfrak{a}}$ and $N_{\mathfrak{b}}$ and hence express these conditions as "quantization rules". Thus, $\check{U}_{\mathrm{F}}^{[j]}(\zeta;\mu)$ vanishes if and only if

$$\left(\mathfrak{Z}_{1,\mathfrak{a}}^{[j]}=N_{\mathfrak{a}}\in\mathbb{Z}\text{ and }\mathfrak{Z}_{1,\mathfrak{b}}^{[j]}=N_{\mathfrak{b}}\in\mathbb{Z}\right)\quad\text{or}\quad\left(\mathfrak{Z}_{2,\mathfrak{a}}^{[j]}=N_{\mathfrak{a}}\in\mathbb{Z}\text{ and }\mathfrak{Z}_{2,\mathfrak{b}}^{[j]}=N_{\mathfrak{b}}\in\mathbb{Z}\right)$$
(7.70)

and blows up if and only if

$$\left(\mathfrak{P}_{1,\mathfrak{a}}^{[j]} = N_{\mathfrak{a}} \in \mathbb{Z} \text{ and } \mathfrak{P}_{1,\mathfrak{b}}^{[j]} = N_{\mathfrak{b}} \in \mathbb{Z}\right) \text{ or } \left(\mathfrak{P}_{2,\mathfrak{a}}^{[j]} = N_{\mathfrak{a}} \in \mathbb{Z} \text{ and } \mathfrak{P}_{2,\mathfrak{b}}^{[j]} = N_{\mathfrak{b}} \in \mathbb{Z}\right)$$

$$(7.71)$$

where

$$\mathfrak{Z}_{k,\mathfrak{a}}^{[j]} := \frac{\operatorname{Re}(H_{\omega}^*(\Psi - \mathfrak{z}_k^{[j]}))}{2\pi\operatorname{Re}(H_{\omega})} \quad \text{and} \quad \mathfrak{Z}_{k,\mathfrak{b}}^{[j]} := -\frac{\operatorname{Im}(\Psi - \mathfrak{z}_k^{[j]})}{\operatorname{Re}(H_{\omega})},$$

$$\mathfrak{P}_{k,\mathfrak{a}}^{[j]} := \frac{\operatorname{Re}(H_{\omega}^*(\Psi - \mathfrak{p}_k^{[j]}))}{2\pi\operatorname{Re}(H_{\omega})} \quad \text{and} \quad \mathfrak{P}_{k,\mathfrak{b}}^{[j]} := -\frac{\operatorname{Im}(\Psi - \mathfrak{p}_k^{[j]})}{\operatorname{Re}(H_{\omega})}.$$

Using (7.26) and expressing c and H_{ω} in terms of the elliptic periods $Z_{\mathfrak{a},\mathfrak{b}}$ by $c = Z_{\mathfrak{a}}$ and $H_{\omega} = 2\pi i Z_{\mathfrak{b}}/Z_{\mathfrak{a}}$, these expressions are exactly the left-hand sides in (1.32)–(1.33).

7.10 Residues of the Approximations at the Malgrange Divisor

The goal of this section is explain what happens to the approximations of the rational functions near points in the parameter space where the approximations fail to exist. On one hand, this will allow us to explain how Bäcklund transformations can be used



to circumvent the non-existence issue. On the other hand, we will then be able to identify zeros of a particular theta-function factor with approximations of zeros of the gH and gO polynomials themselves and thus prove Corollary 3 of Sect. 1.4 subject to the hypotheses in Sect. 7.2.

The *Malgrange divisor* of Riemann–Hilbert Problem 2 in Sect. 7.6.1 is the set of parameter values for which there is no solution of that problem. By Lemma 10 of the same section, it is equivalently characterized by either of the conditions $\vartheta(a(\infty) + a(z_0) + \mathcal{K} \mp i\Psi) = 0$. According to the formulæ (7.42) and (7.49) and Lemma 11 in Sect. 7.9, the Malgrange divisor gives rise to exactly one simple pole per period parallelogram in the ζ -plane of each of the elliptic functions $\check{U}_F^{[3]}(\zeta;\mu)$ and $\check{U}_F^{[1]}(\zeta;\mu)$. Each of these functions has one additional simple pole (of opposite residue) and two simple zeros in each parallelogram. From the differential equations (1.18) and (7.60) satisfied by $\check{U}_F^{[3]}(\zeta;\mu)$ and $\check{U}_F^{[1]}(\zeta;\mu)$ respectively, it is easy to see that each simple pole has residue ± 1 .

7.10.1 Malgrange Residues of $\check{U}_{\rm E}^{[3]}$

We now calculate the sign of the residue for the pole of $\check{U}_{\rm F}^{[3]}(\zeta;\mu)$ at the Malgrange divisor. We do this by applying a homotopy argument: the desired residue is a continuous function of the parameters in the formula for $\check{U}_{\rm F}^{[3]}(\zeta;\mu)$ such as μ , provided the spectral curve remains nondegenerate, i.e., of class {1111}. In fact, the formula for $\check{U}_{\rm F}^{[3]}(\zeta;\mu)$ depends on these parameters through (i) the phase ξ (see (7.26)) and (ii) the distinct roots α , β , γ , and δ . If the latter parameters are given instead, then $\check{U}_{\rm F}^{[3]}(\zeta;\mu)$ is determined as an elliptic function of ζ . In other words, neither the explicit formula for $\check{U}_{\rm F}^{[3]}(\zeta;\mu)$ nor the argument that it satisfies the differential equation (1.18) with P(z) taken in the form $P(z) = (z - \alpha)(z - \beta)(z - \gamma)(z - \delta)$ requires the specific relation between E, μ , and κ determined by the Boutroux conditions (4.23). Indeed, the latter relation is needed only to control the approximation of the matrix O(z) by its parametrix $\check{\mathbf{O}}(z)$. Therefore, we will write $\check{U}_{\mathrm{F}}^{[3]}(\zeta)$ for $\check{U}_{\mathrm{F}}^{[3]}(\zeta;\mu)$ and compute the desired residue as a continuous function of the parameters ξ , α , β , γ , and δ by a suitable (generally artificial) homotopy that need not be consistent with varying μ and solving (4.23) for E. That said, since the residue is either 1 or -1, it will remain constant along such a homotopy. The homotopy we select is to fix ξ and to deform the given roots $(\alpha, \beta, \gamma, \delta)$ to the points $(2e^{i\pi/4}, 2e^{3i\pi/4}, 2e^{5i\pi/4}, 2e^{7i\pi/4})$ without allowing any intermediate degeneration. (Note that the target configuration is the actual root configuration for $\mu = 0$ and $\kappa = 0$, which also yields E = 0; hence it is reachable by homotopy in μ if initially $\mu \in \mathcal{B}_{\square}$. It is not clear whether it can be reached by such a homotopy if initially $\mu \in \mathcal{B}_{\triangleright} \cup \mathcal{B}_{\triangle}$, but it is not necessary either.) In the final configuration we have, from (7.21), that $z_0 = \infty$. By expanding the Abel map $a(z_0)$ for large z_0 , one sees that as the target configuration is approached in the parameter space,

$$z_0 \vartheta(a(\infty) - a(z_0) - \mathcal{K}) \to -\frac{2\pi i}{c} \vartheta'(\mathcal{K})$$



where the constants c and K are determined from the target configuration. Therefore, from (7.42) and (7.43) we have, in the target configuration

$$\begin{split} \check{U}_{\mathrm{F}}^{[3]}(\zeta) &= -\frac{2\pi \mathrm{i}}{c} \frac{\vartheta\left(2a(\infty) + \mathcal{K}\right)\vartheta'(\mathcal{K})}{\vartheta\left(a(0) + a(\infty) + \mathcal{K}\right)\vartheta\left(a(0) - a(\infty) - \mathcal{K}\right)} \\ &\cdot \frac{\vartheta\left(a(0) + a(\infty) + \mathcal{K} - \mathrm{i}\Psi\right)\vartheta\left(a(0) - a(\infty) - \mathcal{K} + \mathrm{i}\Psi\right)}{\vartheta\left(2a(\infty) + \mathcal{K} - \mathrm{i}\Psi\right)\vartheta\left(\mathrm{i}\Psi - \mathcal{K}\right)}. \end{split}$$

Now we compute the residue at a zero of the factor $\vartheta(2a(\infty) + \mathcal{K} - i\Psi)$. Taking into account (7.26) for the ζ -dependence of Ψ , and evaluating the residue at $i\Psi = 2a(\infty)$ gives

$$\begin{split} \underset{\zeta: \mathrm{i}\Psi = 2a(\infty)}{\operatorname{Res}} \check{U}_{\mathrm{F}}^{[3]}(\zeta) &= -\frac{\vartheta(2a(\infty) + \mathcal{K})}{\vartheta(a(0) + a(\infty) + \mathcal{K})\vartheta(a(0) - a(\infty) - \mathcal{K})} \\ &\cdot \frac{\vartheta(a(0) - a(\infty) + \mathcal{K})\vartheta(a(0) + a(\infty) - \mathcal{K})}{\vartheta(2a(\infty) - \mathcal{K})}. \end{split}$$

Finally, using (7.23) and $\mathcal{K} = -\mathcal{K} + 2\pi i + H_{\omega}$ we get

$$\operatorname{Res}_{\zeta: i\Psi = 2a(\infty)} \breve{U}_{F}^{[3]}(\zeta) = -e^{-H_{\omega}/2}e^{\mathcal{K}} = 1$$

in the target configuration. Applying the homotopy argument then shows that the residue is also +1 in the arbitrary initial configuration.

7.10.2 Malgrange Residues of $\breve{U}_{\rm F}^{[1]}$ and $\breve{U}_{\rm F}^{[2]}$

With this result established, we now use the differential relation (7.58) where $\check{U}(\zeta) = \check{U}_{\rm F}^{[3]}(\zeta)$ and $\check{U}_{\mathbb{Q}}(\zeta_{\mathbb{Q}}) = \check{U}_{\rm F}^{[1]}(\zeta_{\mathbb{Q}})$ with $\zeta_{\mathbb{Q}} = \sqrt{\frac{1}{2}(1-s\kappa)}\zeta$ to find that at the simple poles corresponding to the Malgrange divisor,

$$\operatorname{Res} \breve{U}_{\mathrm{F}}^{[1]}(\zeta;\mu) = -1.$$

Finally, it follows directly that the residue of $\check{U}_F^{[2]}(\zeta;\mu)=\mathrm{i} \check{U}_F^{[1]}(-\mathrm{i} \zeta;-\mathrm{i} \mu)$ at the Malgrange divisor is

Res
$$\check{U}_{F}^{[2]}(\zeta; \mu) = 1$$
.

7.10.3 Removal of the Condition $(\mu, \zeta, T) \in \mathcal{S}(\epsilon)$

The final step in the proof of Theorems 3 and 4 of Sect. 1.4 under the hypotheses in Sect. 7.2 is to remove the condition that $(\mu, \zeta, T) \in \mathcal{S}(\epsilon)$, which bounds ζ away from the Malgrange divisor. For each (μ, T) , the Malgrange divisor is a uniform lattice $\Lambda_{\rm M}$ in the ζ -plane with lattice vectors determined from μ and κ and an offset involving T. The lattice $\Lambda_{\rm M}$ consists of all poles of the elliptic function $\check{U}_{\rm F}^{[1]}(\zeta)$ of



residue -1 (equivalently all poles of the elliptic function $\check{U}_{\rm F}^{[3]}(\zeta)$ of residue 1). The poles of $\check{U}_{\rm F}^{[1]}(\zeta)$ of residue 1 form a lattice $\Lambda_+^{[1]}$ congruent to $\Lambda_{\rm M}$ but, by Lemma 11 of Sect. 7.9, having a different offset. Likewise, the poles of $\check{U}_{\rm F}^{[3]}(\zeta)$ of residue -1form another congruent lattice $\Lambda_{-}^{[3]}$ disjoint from Λ_{M} . Let $\delta > 0$ be sufficiently small given $\epsilon>0$ that a δ -neighborhood of $\Lambda_+^{[1]}$ and $\Lambda_-^{[3]}$ is contained within $\mathcal{S}(\epsilon)$. Then $u_{\rm F}^{[1]}(T^{1/2}\mu+T^{-1/2}\zeta;m,n)^{-1}=T^{-1/2}(\check{U}_{\rm F}^{[1]}(\zeta)^{-1}+\mathcal{O}(T^{-1}))$ holds uniformly for bounded ζ in a δ -neighborhood of $\Lambda_+^{[1]}$ and $u_{\rm F}^{[3]}(T^{1/2}\mu+T^{-1/2}\zeta;m,n)^{-1}=T^{-1/2}(\xi)$ $T^{-1/2}(\check{U}_{\mathbb{F}}^{[3]}(\zeta)^{-1} + \mathcal{O}(T^{-1}))$ holds uniformly for bounded ζ in a δ -neighborhood of $\Lambda_{-}^{[3]}$. Applying a standard perturbation argument based on the Analytic Implicit Function Theorem, one sees that each point of $\Lambda_+^{[1]}$ attracts exactly one simple pole of $u_F^{[1]}(T^{1/2}\mu + T^{-1/2}\zeta; m, n)$ and each point of $\Lambda_-^{[3]}$ attracts one simple pole of $u_{\rm F}^{[3]}(T^{1/2}\mu + T^{-1/2}\zeta; m, n)$, of positive and negative residue, respectively. The attracted poles lie within a distance of $\mathcal{O}(T^{-1})$ from the corresponding attracting lattice points in any given bounded region of the ζ -plane. Every pole of the opposite residue is necessarily attracted to a point of the Malgrange divisor lattice $\Lambda_{\rm M}$, but since the error terms cannot be controlled near this lattice we cannot say for sure whether there might be clusters of additional poles attracted to these lattice points as well. We may calculate the winding number index of the rational solution about a circle of radius ϵ centered at a point of $\Lambda_{\rm M}$, but this only shows that any excess poles must be paired with an equal number of zeros; computing the integral of the rational solution around this circle and applying the Residue Theorem shows that further there must be an equal number of excess poles of opposite residues.

Recall that the Boiti-Pempinelli symmetry S_{\updownarrow} discussed in Sect. 2 yields the identity $u_{\rm F}^{[3]}(x; m, n) = i u_{\rm F}^{[3]}(-ix; n, m)$ (cf. (2.2)). It follows easily that poles of residue ± 1 of $u_{\rm F}^{[3]}(\cdot; m, n)$ correspond under rotation of the argument by $\frac{\pi}{2}$ to poles of residue ∓ 1 of $u_{\rm F}^{[3]}(\cdot;n,m)$. The poles of $u^{[3]}(\cdot;m,n)$ of residue -1 whose isolated images in the ζ -plane lie close to the lattice $\Lambda_{-}^{[3]}$ are now poles of residue 1 of $u_{\rm F}^{[3]}(\cdot; n, m)$. Being as those poles are isolated in the (rotated) ζ -plane, a residue integral calculation shows that each one must lie close to a lattice point at which the elliptic function approximation of $u_{\rm F}^{[3]}(\cdot;n,m)$ has a pole of residue 1. That approximation can be obtained by a different case of the asymptotic analysis of $u_F^{[3]}(\cdot; m, n)$ in which the indices (m, n) are permuted, corresponding in the limit to a change of sign of κ_{∞} . But in the approximation of any rational solution of type 3, poles of the approximating function of residue 1 form the Malgrange divisor of the corresponding instance of Riemann–Hilbert Problem 2 from Sect. 7.6.1. This is an indirect proof that in fact each such pole attracts exactly one pole of the same residue, even though the error has not been controlled directly near the Malgrange divisor. However, to provide this control is now easy, since $u_{\rm F}^{[3]}(T^{1/2}\mu + T^{-1/2}\zeta; m, n)^{-1}$ and its elliptic function approximation are both analytic in an ϵ -neighborhood of Λ_M . Indeed, it follows that the error term is also analytic on this neighborhood, so applying the maximum modulus principle on each ϵ -disk centered at a point of $\Lambda_{\rm M}$ proves that the error term is uniformly small on the disk since it is small on the boundary by the primary estimate valid on $S(\epsilon)$.



To deal with the function $u_{\rm F}^{[1]}(x;m,n)$, we compose $\mathcal{S}_{\updownarrow}$ with the symmetry $\mathcal{S}_{\updownarrow}$ also discussed in Sect. 2, which maps rational solutions of type 1 to solutions of type 3 (cf. (2.5)). It is easy to check that the composite transformation $\mathcal{S}_{\updownarrow} \circ \mathcal{S}_{\updownarrow} \circ \mathcal{S}_{\updownarrow}^{-1}$ maps $u_{\rm F}^{[1]}(x;m,n)$ to another function of type 1 with different (large) indices, and again the transformation has the effect of rotation in the complex x-plane that swaps the signs of the residues without introducing any new poles or removing any preexisting ones. So the same argument applies again to show that $u_{\rm F}^{[1]}(T^{1/2}\mu + T^{-1/2}\zeta;m,n)^{-1} = T^{-1/2}(\breve{U}_{\rm F}^{[1]}(\zeta) + \mathcal{O}(T^{-1}))$ holds uniformly near all poles for ζ bounded, whether they lie near the Malgrange divisor or not.

At last this completes the proof of Theorems 3 and 4 from Sect. 1.4 conditioned on the proper identification of the Boutroux domains \mathcal{B}_{\square} , $\mathcal{B}_{\triangleright}$, and \mathcal{B}_{\triangle} hypothesized in Sect. 7.2.

7.10.4 Accurate Approximation of Poles and Zeros of Rational Painlevé-IV Solutions. Zeros of the gH and gO Polynomials.

We are now also in a position to give the proof of Corollary 2 from Sect. 1.4 under the hypotheses in Sect. 7.2.

Proof of Corollary 2 Setting $\zeta=0$, let μ be a value satisfying one of the conditions in (7.70) or (7.71). Fixing this value of μ , and letting ζ be free, either $f(\zeta-\zeta_0)$ in the former case or $f(\zeta-\zeta_0)^{-1}$ in the latter case has a simple zero at $\zeta=0$. Putting an artificial coefficient $\delta\in[0,1]$ on the $\mathcal{O}(T^{-1})$ perturbing term in Theorem 3 or 4 of Sect. 1.4, it then follows from the Analytic Implicit Function Theorem that there is a unique simple zero of either u(x) or its reciprocal that depends on δ and persists up to $\delta=1$ when (m,n) are sufficiently large and hence T^{-1} is sufficiently small. As an analytic function of δ , this zero obviously satisfies $\zeta=\mathcal{O}(T^{-1})$, which under $x=T^{1/2}\mu+T^{-1/2}\zeta$ can also be interpreted as a perturbation of μ of order $\mathcal{O}(T^{-2})$ for $\zeta=0$.

Note that we actually cannot fix a value μ , because the possible values of μ for $\zeta = 0$ depend strongly on (m, n). But we can always select a sequence of values of μ depending on (m, n) large and lying within the fixed compact set C and perform the computation separately for each (m, n). Since by Theorems 3 and 4 the size of the $\mathcal{O}(T^{-1})$ error term is uniform given C, the proof is complete.

The proof of Corollary 3 (also from Sect. 1.4) under the same hypotheses then follows easily.

Proof of Corollary 3 According to the logarithmic derivative formulæ (1.5) and (1.10) and the expressions for the type-1 tau functions $\tau_F^{[1]}(x;m,n)$ given for families F=gH and F=gO in Tables 1 and 2 respectively (see Sect. 1.2), the roots of the polynomials $H_{m,n}(x)$ and $Q_{m,n}(x)$ are precisely the poles of residue -1 of $u_F^{[1]}(x;m,n)$. According to Corollary 2, these are approximated by the points in the Malgrange divisor for Riemann–Hilbert Problem 2 of Sect. 7.6.1, which one can check satisfy (7.71) for k=2.



8 Boundary Curves and Maximal Boutroux Domains

In this section, we complete the proofs of the theorems stated in Sect. 1.4 by identifying for each family of rational solutions the boundaries of the different zero/pole regions and the exterior region (and showing that they coincide along some arcs).

8.1 Universal Condition for Phase Transitions

Recall from Sects. 5.5 and 6.5 that all possible generic obstructions to the continuation of asymptotic formulæ for the Painlevé-IV rational solutions from a neighborhood of $\mu = \infty$ into the finite μ -plane are the generic bifurcation points (see Definition 4 in Sect. 5.5) captured by conditions of the form $Re(h(\gamma)) = 0$, where γ is the double root of a polynomial P(z) for a spectral curve of class {211}; nongeneric bifurcations occur at points (μ, γ) that are branch points of the quartic equation (4.19). Likewise, the elliptic approximations developed in Sect. 7.7 are valid on Boutroux domains with certain fixed abstract Stokes graphs, and in Sect. 4.4 it was shown that all boundary points of any Boutroux domain correspond to degenerate Boutroux curves. Letting $\mu \in$ \mathcal{B} approach the boundary, the generic (i.e., corresponding to case $\{211\}$) mechanism of degeneration is that a pair of simple roots of P coalesces into a double root γ and there remain two distinct simple roots α and β ; nongeneric degenerations to case {31} again correspond to branch points of (4.19). If \mathfrak{a} is the cycle that encloses the roots that coalesce into γ , then it is obvious that $\oint_{\sigma} v \, dz \to 0$ in the limit, so the only nontrivial Boutroux condition is the limiting form of $Re(\oint_b v dz) = 0$, which can also be written in the form $Re(h(\gamma)) = 0$ where h corresponds to the class {211} spectral curve at the boundary point. It follows that both types of phase transitions are captured by conditions of the same universal form:

$$\operatorname{Re}\left(\int_{\alpha}^{\gamma} \sqrt{(z-\alpha)(z-\beta)} \frac{z-\gamma}{z} \, \mathrm{d}z\right) = 0 \tag{8.1}$$

in which α , β , and γ depend on μ by (4.18). In particular (μ , γ) is a point on the Riemann surface Γ of Definition 1 from Sect. 5. In this section, we determine all relevant solutions of (8.1), which are curves in the μ -plane.

8.2 Curves in an Auxiliary Coordinate Plane

We first find a parametrization of *all* solutions of (8.1), and later we will determine which solutions are relevant. For given $\kappa \in (-1,1)$ we therefore consider (μ,γ) to lie on any sheet of $\Gamma = \Gamma(\kappa)$. Recall that at the beginning of Sect. 5.1 it was shown that the function $z \mapsto \operatorname{Re}(h(z))$ is single valued on a two-sheeted Riemann surface $\mathcal R$ over the z-plane. Upon evaluating at $z = \gamma$ we obtain a single-valued function on a two-sheeted covering, denoted $\mathcal Y$, of the Riemann surface Γ .



8.2.1 Rational Parametrization of Γ

In fact, \mathcal{Y} can be identified as a two-sheeted covering of the Riemann sphere, because the quartic (4.19) defining Γ can be rationally parametrized, as we will now show. Noting the symmetry $Q(-\gamma, -\mu; \kappa) = Q(\gamma, \mu; \kappa)$ of the polynomial in (4.19), we introduce the invariant quantities $p := \mu \gamma$ and $q := \gamma^2$ and hence (4.19) becomes a bi-quadratic equation in (p, q) that can be written in the form

$$\left(\frac{1}{2}q - 2\kappa\right)^2 - (p+q)^2 = -4(1-\kappa^2) < 0.$$
 (8.2)

Noting the sign of the right-hand side for $\kappa \in (-1, 1)$, we use a rational parametrization based on stereographic projection via the identity $(at - at^{-1})^2 - (at + at^{-1})^2 = -4a^2$ with $a = \sqrt{1 - \kappa^2} > 0$. Hence we can identify $a = \sqrt{1 - \kappa^2} > 0$.

$$p = p(t) = -\sqrt{1 - \kappa^2}(t - 3t^{-1}) - 4\kappa$$
 and $q = q(t) = 2\sqrt{1 - \kappa^2}(t - t^{-1}) + 4\kappa$. (8.3)

In particular, $\mu^2 = p^2/q$ is explicitly given by

$$\mu^2 = \mu^2(t) = \frac{\sqrt{1 - \kappa^2}}{2} \cdot \frac{(t^2 + 4wt - 3)^2}{t(t^2 + 2wt - 1)}, \quad w := \frac{\kappa}{\sqrt{1 - \kappa^2}}.$$
 (8.4)

Given t, if $\mu^2 \neq 0$ then from each choice of the square root to determine μ we obtain a unique corresponding value of γ from $\gamma = p/\mu$. Therefore each $t \in \mathbb{C}$ generates a symmetric pair of points (μ, γ) and $(-\mu, -\gamma)$ on the Riemann surface Γ of Definition 1. Conversely, given a point $(\mu, \gamma) \in \Gamma$, we can project to the t-sphere by the explicit mapping

$$(\mu, \gamma) \mapsto (p = \mu \gamma, q = \gamma^2) \mapsto t = \frac{2p + 3q - 4\kappa}{4\sqrt{1 - \kappa^2}}.$$
 (8.5)

Note that $\kappa \mapsto w$ is a strictly increasing function of (-1,1) onto \mathbb{R} . Also representing κ with the parametrization (4.28) by $\varphi \in (-\pi,\pi)$ we have simply $w = \tan(\frac{1}{2}\varphi)$.

8.2.2 Relating the Condition $\operatorname{Re}(h(\gamma))=0$ to the v-Trajectories of a Rational Ouadratic Differential

Now, $\Phi(t) := -4(h(\gamma) - h(\alpha))$ is a multivalued function on \mathcal{Y} due to purely real residues at its poles and the ambiguity of integration contour, but locally it can be written as

$$\Phi(t) = \int_{\alpha(t)}^{\gamma(t)} \sqrt{(z - \alpha(t))(z - \beta(t))} \frac{z - \gamma(t)}{z} dz$$
 (8.6)

for some branch of the square root that is continuous along the unspecified path of integration, and in which α and β are determined up to permutation symmetry in terms of (μ, γ) from (4.18), and (μ, γ) are in turn related by (4.19). Thus after rational



parametrization and choice of square roots in obtaining (μ, γ) from $(p = \mu \gamma, q = \gamma^2)$, α , β , and γ become functions of t. Differentiation with respect to t using the fact that the integrand vanishes at $z = \alpha$ and $z = \gamma$ gives

$$\Phi'(t) = -\frac{1}{2} \int_{\alpha(t)}^{\gamma(t)} \frac{P_2(z;t) \, \mathrm{d}z}{z\sqrt{(z-\alpha(t))(z-\beta(t))}},\tag{8.7}$$

where $P_2(\cdot; t)$ is the quadratic polynomial

$$P_2(z;t) := \left[2\gamma'(t) + \Sigma'(t)\right]z^2 - \left[\Pi'(t) + \gamma(t)\Sigma'(t) + 2\Sigma(t)\gamma'(t)\right]z$$
$$+\gamma(t)\Pi'(t) + 2\Pi(t)\gamma'(t),$$

in which $\Sigma(t) := \alpha(t) + \beta(t)$ and $\Pi(t) := \alpha(t)\beta(t)$. Implicit differentiation of the identity $\Pi = 16\gamma^{-2}$ (cf. (4.20)) proves that $P_2(0; t)$ vanishes identically, so $P_2(z; t)/z$ is the linear function

$$P_1(z;t) := \frac{P_2(z;t)}{z} = \left[2\gamma'(t) + \Sigma'(t)\right]z - \left[\Pi'(t) + \gamma(t)\Sigma'(t) + 2\Sigma(t)\gamma'(t)\right].$$

Now, the derivative with respect to z of $(z - \alpha(t))(z - \beta(t))$ is also a linear function of z, namely $2z - \Sigma(t)$. It turns out that $P_1(z;t)$ is proportional to the latter linear function, and this makes the integrand in (8.7) the z-derivative of an algebraic function, allowing the integral to be evaluated explicitly. For this, it is sufficient to check that the root of $P_1(z;t)$ agrees with that of $2z - \Sigma(t)$, i.e., that $Z(t) \equiv 0$, where

$$Z(t) := 2(\Pi'(t) + \gamma(t)\Sigma'(t) + 2\Sigma(t)\gamma'(t)) - \Sigma(t)(2\gamma'(t) + \Sigma'(t)).$$

Eliminating $\Pi'(t)$, $\Sigma(t)$, and $\Sigma'(t)$ in favor of $\gamma(t)$ and $\mu(t)$ and their derivatives using (4.20) and implicit differentiation yields

$$Z(t) = -64\gamma(t)^{-3}\gamma'(t) - 16\gamma(t)\mu'(t) - 16\mu(t)\gamma'(t) - 12\gamma(t)\gamma'(t) - 16\mu(t)\mu'(t)$$

so Z(t) = F'(t) where F(t) may be taken to be

$$F(t) := 32\gamma(t)^{-2} - 16\mu(t)\gamma(t) - 6\gamma(t)^{2} - 8\mu(t)^{2}$$

$$= -\frac{6}{\gamma(t)^{2}} \left[\gamma(t)^{4} + \frac{8}{3}\mu(t)\gamma(t)^{3} + \frac{4}{3}\mu(t)^{2}\gamma(t)^{2} - \frac{16}{3} \right].$$

Therefore, using (4.19) we find that in fact $F(t) = 16\kappa$, so indeed Z(t) = F'(t) = 0 holds. Therefore

$$P_1(z;t) = \frac{P_2(z;t)}{z} = \left(\gamma'(t) + \frac{1}{2}\Sigma'(t)\right)(2z - \Sigma(t)) = -2\mu'(t)(2z - \Sigma(t)),$$



where in the last equality we have again used implicit differentiation in (4.20). Using this in (8.7) gives

$$\Phi'(t) = \mu'(t) \int_{\alpha(t)}^{\gamma(t)} \frac{2z - \Sigma(t)}{\sqrt{(z - \alpha(t))(z - \beta(t))}} dz$$

$$= 2\mu'(t) \int_{\alpha(t)}^{\gamma(t)} \frac{d}{dz} \sqrt{(z - \alpha(t))(z - \beta(t))} dz$$

$$= 2\mu'(t) \sqrt{(\gamma(t) - \alpha(t))(\gamma(t) - \beta(t))}.$$

Therefore, $\Phi'(t)^2$ is well defined in terms of $\mu'(t)^2$, $\mu(t)$, and $\gamma(t)$ by

$$\Phi'(t)^{2} = 4\mu'(t)^{2}(\gamma(t) - \alpha(t))(\gamma(t) - \beta(t))$$

$$= 4\mu'(t)^{2}(\gamma(t)^{2} - \Sigma(t)\gamma(t) + \Pi(t))$$

$$= 4\mu'(t)^{2}(\gamma(t)^{2} + (4\mu(t) + 2\gamma(t))\gamma(t) + 16\gamma(t)^{-2})$$

$$= 4\mu'(t)^{2}(3\gamma(t)^{2} + 4\mu(t)\gamma(t) + 16\gamma(t)^{-2}),$$

where on the penultimate line we used (4.20) to eliminate $\Sigma(t)$ and $\Pi(t)$. It happens that $\Phi'(t)^2$ is actually a rational function of t. To this end, we first express it as a rational function of $p(t) := \mu(t)\gamma(t)$ and $q(t) := \gamma(t)^2$:

$$\begin{split} \Phi'(t)^2 &= 4\mu'(t)^2 (3q(t) + 4p(t) + 16q(t)^{-1}) \\ &= (2\mu(t)\mu'(t))^2 \mu(t)^{-2} (3q(t) + 4p(t) + 16q(t)^{-1}) \\ &= \left(\frac{\mathrm{d}}{\mathrm{d}t}\mu(t)^2\right)^2 \mu(t)^{-2} (3q(t) + 4p(t) + 16q(t)^{-1}) \\ &= \left(\frac{\mathrm{d}}{\mathrm{d}t}\frac{p(t)^2}{q(t)}\right)^2 \frac{q(t)}{p(t)^2} (3q(t) + 4p(t) + 16q(t)^{-1}) \\ &= \frac{\left(2q(t)p'(t) - p(t)q'(t)\right)^2 (3q(t)^2 + 4p(t)q(t) + 16)}{q(t)^4}. \end{split}$$

Finally, we introduce the rational expressions (8.3) for p and q in terms of t, which yields

$$\Phi'(t)^2 = (1 - \kappa^2) \frac{(t^4 + 6t^2 + 8wt - 3)^3}{t^4(t^2 + 2wt - 1)^4}, \quad w = \frac{\kappa}{\sqrt{1 - \kappa^2}}.$$
 (8.8)

We therefore conclude that, since $Re(h(\alpha)) = 0$, the curves on the *t*-sphere along which $Re(h(\gamma)) = 0$ for any branch γ of the quartic (4.19) are v-trajectories of a rational quadratic differential $\Phi'(t)^2 dt^2$ (i.e., curves in the *t*-sphere along which $\Phi'(t)^2 dt^2 < 0$ holds, cf. Definition 2 in Sect. 5.1).



8.2.3 Critical Points of $\Phi'(t)^2 dt^2$ and the Role of the Critical v-Trajectories

At this juncture we once again remind the reader of the material introduced in Sect. 5.1 and of Definitions 2 and 3 in particular. To study the level curves of $Re(\Phi) = 0$ on the t-sphere, we recall the fact that $Re(\Phi)$ is a single-valued function on \mathcal{Y} that is non-constant and takes opposite values on the two sheets of \mathcal{Y} . Moreover $Re(\Phi)$ is harmonic on \mathcal{Y} except at finitely many isolated singular points; hence by the same argument as immediately follows Definition 2 in Sect. 5.1 there can be no divergent v-trajectories on either \mathcal{Y} or on the t-sphere (the latter being the projections of the former), and by the Basic Structure Theorem [39, pg. 37] the closure K_t of the union of v-trajectories emanating from the zeros of $\Phi'(t)^2$ divides the t-sphere into a finite union of end domains, circle domains, ring domains, and strip domains. The immediate goal is to show that K_t is exactly the zero-level set on the t-sphere of $Re(\Phi(t))$.

First consider the zeros of $\Phi'(t)^2 dt^2$, i.e., the roots of the polynomial $\mathcal{Z}(t) :=$ $t^4 + 6t^2 + 8wt - 3$ that do not coincide with any zeros of the denominator. For real w, $\mathcal{Z}(t)$ has real coefficients and its discriminant is proportional to $(w^2+1)^2$ which cannot vanish for any $w \in \mathbb{R}$. For w = 0, the roots are an opposite real pair $t = \pm \sqrt{2\sqrt{3} - 3}$ and a (purely imaginary) complex conjugate pair $t = \pm i\sqrt{2\sqrt{3} + 3}$. Since the roots must retain Schwarz symmetry and remain distinct as $w \in \mathbb{R}$ varies, and since no root can vanish for any w because $\mathcal{Z}(0) < 0$, this basic structure persists for all $w \in \mathbb{R}$. We label the real roots as a(w) < 0 < b(w) and the complex conjugate roots as $\tau(w)$ and $\tau(w)^*$ with $\text{Im}(\tau(w)) > 0$. Next consider the finite poles of $\Phi'(t)^2 dt^2$, i.e., t = 0 and the roots of $\mathcal{P}(t) := t^2 + 2wt - 1$ (since $\Phi'(t)^2$ has a finite nonzero limit as $t \to \infty$ there is also a pole at $t = \infty$ in the local coordinate 1/t). The roots of $\mathcal{P}(t)$ are $t = t_{\infty}^{\pm}(w) :=$ $-w \pm \sqrt{w^2 + 1}$, and we compute that $\mathcal{Z}(t_{\infty}^{\pm}(w)) = 1 + 2w^2 \pm 2w\sqrt{1 + w^2}$. Since $(1+2w^2)^2 = (2w\sqrt{1+w^2})^2 + 1$ we have $\mathcal{Z}(t_{\infty}^{\pm}(w)) > 0$, so the poles $t = t_{\infty}^{\pm}(w)$ therefore lie outside the interval [a(w), b(w)]. Moreover $t_{\infty}^+(w)t_{\infty}^-(w) = -1$, so we have the strict ordering $t_{\infty}^{-}(w) < a(w) < 0 < b(w) < t_{\infty}^{+}(w)$. Since this shows that none of the four distinct roots of $\mathcal{Z}(t)$ coincides with a zero of the denominator of $\Phi'(t)^2$, these are all third-order zeros of $\Phi'(t)^2 dt^2$. Likewise, the four poles of $\Phi'(t)^2 dt^2$ on the t-sphere are all fourth-order poles.

Upon taking a square root, we see that the four zeros and the four poles of $\Phi'(t)^2 dt^2$ on the t-sphere are the only points of nonanalyticity of $\Phi'(t)$ and hence of any branch of $\Phi(t)$. The four poles are clearly mapped out of the finite μ -plane by (8.4), while the four zeros are taken to finite values of μ . We claim that these finite values of μ are necessarily solutions of the branch point equation $B(\mu; \kappa) = 0$ (cf. (1.17) in Sect. 1.3). Indeed, if t corresponds to a point on Γ that is not a branch point (i.e., $\gamma(t)$ is not a double root of (4.19) for $\mu = \mu(t)$), then the integral formula (8.6) for $\Phi(t)$ obviously has an analytic t-derivative determined up to a sign (because $\gamma(t)$ is distinct from $\alpha(t)$ and $\beta(t)$ and the latter are analytic functions of t). Therefore, if $\mathcal{Z}(t) = 0$ making $\Phi'(t)$ nonanalytic, then $(\mu(t), \gamma(t))$ is a branch point of Γ and hence $B(\mu(t); \kappa) = 0$ for $\mu(t) = \pm \sqrt{\mu^2(t)}$ as $B(\mu; \kappa)$ is the discriminant of (4.19).

The condition $\mathcal{Z}(t) = 0$ therefore implies that $\gamma(t)$ is a double root of (4.19) for $\mu = \mu(t)$, and furthermore $\gamma(t)$ coincides with either $\alpha(t)$ or $\beta(t)$. From the formula (8.6) we obtain that $\mathcal{Z}(t) = 0$ implies that $\text{Re}(\Phi(t)) = 0$. Therefore the four



third-order zeros of $\Phi'(t)^2 dt^2$ are all points on the zero-level set of $\text{Re}(\Phi(t))$, as are all points on the v-trajectories emanating from these points. Since $\Phi'(t)^2 dt^2$ has no simple poles to generate any further critical v-trajectories, the closure K_t of the union of critical v-trajectories is contained within the zero-level set of $\text{Re}(\Phi(t))$.

The complement in the t-sphere of the closure of the union of critical v-trajectories generally consists of finitely many disjoint end, strip, circle, and ring domains (cf. Definition 3 in Sect. 5.1). However there cannot be any strip or ring domains because by definition each such domain supports a single-valued branch of $Re(\Phi(t))$ taking distinct values on disjoint components of its boundary, in contradiction to the assertion that $Re(\Phi(t)) = 0$ holds unambiguously on all critical v-trajectories. There are no circle domains either, because $\Phi'(t)^2 dt^2$ has no double poles. So all domains are end domains. By definition, each end domain is mapped by a single-valued analytic branch of $\Phi(t)$ onto the open right or left half-plane. Therefore there can be no interior points of any end domain with $Re(\Phi(t)) = 0$, i.e., there are no components of the zero-level set of $Re(\Phi(t))$ not already contained in K_t .

8.2.4 Local Structure of the Critical v-Trajectories

Since the (two real and two complex conjugate) zeros of $\Phi'(t)^2 dt^2$ are triple roots, there are five critical v-trajectories emanating from each at equal angles of $\frac{2\pi}{5}$. For the real zeros we can say more: by Schwarz symmetry there is exactly one of the five v-trajectories from each of t=a(w) and t=b(w) that is contained in the real line. Since each of the four poles of $\Phi'(t) dt^2$ on the t-sphere is of order 4, and since there are no strip domains in this problem, each pole has a neighborhood that is covered by the closure of the union of two disjoint end domains, and there are exactly two critical v-trajectories tending to each pole in opposite directions. Since all four poles lie on the real equator of the t-sphere, by Schwarz symmetry these two critical v-trajectories are either contained in the equator or have tangents at the pole that are perpendicular to the equator.

8.2.5 Global Structure of the Critical v-Trajectories

Since exactly five critical v-trajectories emanate from each of four zeros of $\Phi'(t)^2$ dt², the union of these consists of finitely many (≤ 20) analytic arcs. Since there are no divergent v-trajectories, each arc emanating from a zero terminates at a zero (the same one in a different direction, or another one) or at one of the poles (either from within the real t-axis/equator or perpendicular to it). This system of arcs is symmetric under Schwarz reflection through the real t-axis/equator. Note that $\Phi'(t)^2 > 0$ for t < a(w) and t > b(w) while $\Phi'(t)^2 < 0$ for a(w) < t < b(w). Therefore, the real intervals (a(w), 0) and (0, b(w)) are both critical v-trajectories and no other critical v-trajectories can terminate at the pole t = 0. Also, the critical v-trajectories that terminate at each of the three nonzero poles on the equator have tangents perpendicular to the equator. Moreover, fixing the positive square root of $\Phi'(t)^2$ in the interval $b(w) < t < t_{\infty}^+(w)$ and integrating from t = b(w) one can easily see that no critical v-trajectory can cross the real axis in this interval because $\Phi(t) - \Phi(b(w)) > 0$. Continuing $\Phi(t)$ around the pole at $t = t_{\infty}^+(w)$ one can find a point in the interval



 $t_{\infty}^+(w) < t < +\infty$ at which $\operatorname{Re}(\Phi(t))$ is finite; then by integration along the real line from this point one sees that $\operatorname{Re}(\Phi(t))$ is strictly monotone with range $\mathbb R$ on $t_{\infty}^+(w) < t < +\infty$ and therefore there is exactly one point $t_0^+(w)$ in this interval at which $\operatorname{Re}(\Phi(t)) = 0$ and hence a critical v-trajectory crosses the real axis exactly at this point and nowhere else in the interval. Similarly, no critical v-trajectory can cross the real axis in the interval $t_{\infty}^-(w) < t < a(w)$ but there is a unique point $t_0^-(w) < t_{\infty}^-(w)$ such that a critical v-trajectory crosses the interval $t < t_{\infty}^-(w)$ at $t = t_0^-(w)$ and nowhere else.

Now consider the critical v-trajectories emanating from zeros of $\Phi'(t)^2 dt^2$ into the open upper half-plane/hemisphere. There are two such v-trajectories emanating from each of the real zeros t = a(w) and t = b(w) (their Schwarz reflections enter the lower half-plane, and the remaining v-trajectory from each is real), and five emanating from $t = \tau(w)$ which lies in the open upper half-plane, for a grand total of nine arcs. Exactly one of these arcs terminates on the boundary of the upper hemisphere at each of the three nonzero poles $t = t_{\infty}^{-}(w)$, $t = t_{\infty}^{+}(w)$, and $t = \infty$ lying on the equator. Exactly two more arcs exit the upper hemisphere by crossing the equator at the points $t = t_0^-(w)$ and $t = t_0^+(w)$. Therefore, there remain 9 - 5 = 4 critical v-trajectory arcs that emanate into the upper hemisphere from one zero and terminate at the same or another zero of $\Phi'(t)^2 dt^2$. An application of Lemma 4 from Sect. 5.1 shows that such an arc cannot originate from and return to the same zero without encircling a pole, hence without exiting the upper hemisphere since the poles lie on the equator. Therefore the four arcs in question connect the three zeros of $\Phi'(t)^2 dt^2$ in the closed upper hemisphere in pairs, i.e., there are really just two such critical v-trajectories, each with two distinct endpoints. It is easy to see that the only possibilities are:

- t = a(w) connected to both $t = \tau(w)$ and t = b(w) with different v-trajectories;
- t = b(w) connected to both t = a(w) and $t = \tau(w)$ with different v-trajectories;
- $t = \tau(w)$ connected to both t = a(w) and t = b(w) with different v-trajectories.

Each of these gives rise to a Jordan curve composed of v-trajectories and their endpoints, but unfortunately applying Lemma 4 to this curve does not rule out any of these options.

Consider then the special case w=0. If w=0, then $\Phi'(t)^2$ is an even function of t and this implies that the global structure of the critical v-trajectories is symmetric with respect to reflection through the origin $t\mapsto -t$ in addition to the Schwarz reflection through the real t-axis. One then has a(0)=-b(0), $t_0^-(0)=-t_0^+(0)$, and $t_\infty^-(0)=-t_\infty^+(0)$, and the existence of a v-trajectory connecting $t=\tau(0)$ with t=a(0) implies the existence of a v-trajectory connecting $t=\tau(0)$ with t=b(0) and vice-versa. Hence only the third option is possible. Lemma 4 then shows that the interior angles at the vertices t=a(0), $t=\tau(0)$, and t=b(0) of the critical v-trajectory "triangle" with real leg $(a(0),0)\cup(0,b(0))$ are all $\frac{2\pi}{5}$. Since v-trajectories cannot cross at regular points, it is easy to see that the remaining v-trajectory entering the upper hemisphere from t=b(0) terminates at the pole $t=t_\infty^+(0)$, the remaining v-trajectory entering the upper hemisphere from t=a(0) terminates at the pole $t=t_\infty^-(0)$ (by symmetry), and two of the three remaining v-trajectories entering the upper hemisphere from $t=\tau(0)$ exit the hemisphere at the points $t=t_0^\pm(0)$ while the third terminates at the pole $t=\infty$ on the equator. Applying Schwarz reflection



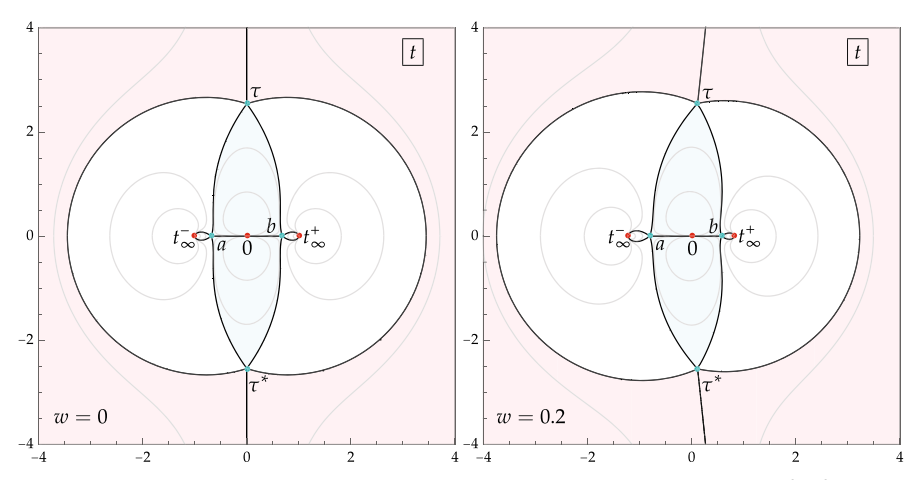


Fig. 29 The critical v-trajectories (black) and some noncritical v-trajectories (gray) of $\Phi'(t)^2$ d t^2 (numerically generated) for w=0 (left panel) and w=0.2 (right panel). Also shown are the zeros (cyan) and finite poles (red) of $\Phi'(t)^2$, which together with the black curves form K_t . The pink and blue shaded regions are $S_{\infty}=S_{\rm gH}$ and $S_0=S_{\rm gO}$ respectively defined in Sect. 8.4 (Color figure online)

to obtain the v-trajectories in the lower hemisphere, the global critical v-trajectory structure is therefore determined for the special case w=0.

We next show that the third option persists for all $w \in \mathbb{R}$. To do this, we first observe that the condition that there is no critical v-trajectory connecting a given pair of zeros of $\Phi'(t)^2 dt^2$, say $t = t_1(w)$ and $t = t_2(w)$ is open with respect to $w \in \mathbb{R}$. Indeed, let $C \subset \mathbb{C}$ be a circle in the finite t-plane with $t_1(w)$ in its interior and $t_2(w)$ in its exterior, and assume that C consists entirely of points t with $\Phi'(t)^2$ finite and nonzero. Let $A_i(w)$ denote the finite set of points on C that lie on v-trajectories emanating from $t = t_i(w)$, j = 1, 2. A v-trajectory connects $t_1(w)$ and $t_2(w)$ if and only if $A_1(w) \cap A_2(w) \neq \emptyset$. Defining d(w) as the minimum arc length distance along C between points of $A_1(w)$ and $A_2(w)$ (and taking $d(w) = +\infty$ if either $A_1(w)$ or $A_2(w)$ is empty), we can see that $d(w) \ge 0$ and d(w) = 0 if and only if $A_1(w) \cap A_2(w) \neq \emptyset$. One can also show that d(w) is lower semicontinuous on \mathbb{R} , and therefore the inverse image of d > 0 is open, which proves the observation. Now consider the open set $w \in G \subset \mathbb{R}$ for which a(w) and b(w) are not connected by a v-trajectory of $\Phi'(t)^2 dt^2$. Consider also the closed set $w \in F \subset \mathbb{R}$ for which there is a v-trajectory connecting a(w) with $\tau(w)$ and another v-trajectory connecting b(w) with $\tau(w)$. An examination of the three options above shows that F = G, as both conditions correspond to the third option. Moreover w = 0 obviously belongs to F = G, so the latter is nonempty. Since \mathbb{R} is connected, it then follows that $F = G = \mathbb{R}$.

The global structure of critical v-trajectories for $\Phi'(t)^2 dt^2$ is illustrated for two values of $w \in \mathbb{R}$ in Fig. 29.

This completes the characterization of all solutions of (8.1) as the locus K_t in the auxiliary t-sphere.



8.3 Abstract Stokes Graphs for Degenerate Boutroux Curves

The Stokes graph of a degenerate Boutroux curve \mathcal{R} is still defined as the closure K_z of the union of critical v-trajectories of $\varrho(z)\,\mathrm{d}z^2$ with $\varrho(z):=\frac{1}{16}z^{-2}P(z)$ (see Sect. 7.1) but now the quartic P(z) has fewer than four roots, being in case {31} (two roots, one being simple) or {211} (three roots, two being simple). In the latter case (of smaller codimension), K_z connects the double zero $z=\gamma$ of $\varrho(z)\,\mathrm{d}z^2$ to either the simple zero $z=\alpha$ or the simple zero $z=\beta$ (or both). The corresponding abstract Stokes graph has two vertices of degree 3 (the simple zeros), one vertex of degree 4 (the double zero), and the four special vertices of degree 1 for the four directions at $z=\infty$. It is planar, and has 5 faces just like in the nondegenerate case. By Euler's formula there are exactly 7 edges.

Since the degenerate Boutroux curves of class $\{211\}$ correspond to points on open critical v-trajectories of $\Phi'(t)^2 dt^2$ in the t-plane, the abstract Stokes graph is an invariant on each of the two image arcs in the μ -plane of a given critical v-trajectory. Similarly, the abstract Stokes graph on each image arc is independent of $\kappa \in (-1,1)$. Each critical v-trajectory of $\Phi'(t)^2 dt^2$ therefore carries a pair of abstract Stokes graphs for degenerate Boutroux curves of class $\{211\}$. These two abstract Stokes graphs are related by reflection through the origin (this is the symmetry relating (μ, γ) and $(-\mu, -\gamma)$ both of which correspond to the same value of t). We now systematically determine the abstract Stokes graphs for all critical v-trajectories of $\Phi'(t)^2 dt^2$ in the t-plane.

We begin by labeling these trajectories as follows: we denote by (t_1,t_2) the v-trajectory in the upper half t-plane with endpoints t_j , j=1,2, and we denote by $(\tau,\tau^*)_{\pm}$ the v-trajectory joining the indicated points that intersects \mathbb{R}_{\pm} . It is sufficient to study these trajectories alone because the set of critical v-trajectories of $\Phi'(t)^2 dt^2$ is Schwarz-symmetric and since $t\mapsto t^*$ implies that either $(\mu,\gamma)\mapsto (\mu^*,\gamma^*)$ or $(\mu,\gamma)\mapsto (-\mu^*,-\gamma^*)$, the quadratic differential $\varrho(z)\,dz^2$ has reflection symmetry in either the real or imaginary axis, so the Stokes graphs for t^* are just the reflections in the real and imaginary axes of those for t. In particular, if $t\in\mathbb{R}$ is in the closure of a critical v-trajectory, then one of its pair of abstract Stokes graphs has to admit a realization invariant under reflection in the real z-axis. Similarly, since the abstract Stokes graphs do not depend on $\kappa\in(-1,1)$, it is sufficient to assume that $\kappa=0$, in which case the set of critical v-trajectories of $\Phi'(t)^2\,dt^2$ is additionally symmetric in reflection through the imaginary t-axis, as shown in the left-hand panel of Fig. 29. Therefore, when $\kappa=0$, each Stokes graph for a point $-t^*$ in the closure of a v-trajectory is the reflection through the diagonal $\mathrm{Im}(z)=\mathrm{Re}(z)$ of a Stokes graph for t.

Assuming $\kappa=0$, the v-trajectory (∞,τ) lies on the positive imaginary axis in the t-plane, and furthermore from (8.3)–(8.4) we see that positive imaginary t of sufficiently large modulus corresponds to positive imaginary values of both μ^2 and $q=\gamma^2$ but negative imaginary values of the product $p=\mu\gamma$; moreover as $t=\mathrm{i}|t|\to\infty$ we have $\mu^2=\frac12\mathrm{i}|t|+\mathcal{O}(1), \,\gamma^2=2\mathrm{i}|t|+\mathcal{O}(1), \,\mathrm{and}\,\mu\gamma=-\mathrm{i}|t|+\mathcal{O}(1).$ From (4.20) we can then deduce that the simple roots of P(z) are $\alpha,\beta=\pm2\sqrt{2}\mathrm{e}^{\mathrm{i}\pi/4}|t|^{-1/2}(1+\mathcal{O}(t^{-2}))$ where the error terms are real and different for each root. Since all roots of P(z) lie



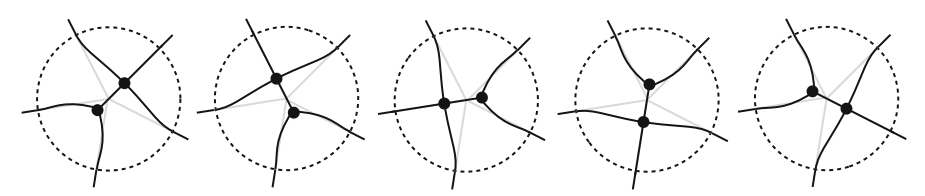


Fig. 30 The 5 orientations of the "dimer" that unfold a vertex of degree 5. These occur with their reflections through the origin on the v-trajectories in counterclockwise order around each zero of $\Phi'(t)$

exactly on the diagonal and t is imaginary, both opposite Stokes graphs are symmetric through the diagonal. Using Lemma 4 of Sect. 5.1, one shows that α and β only lie on the boundary of \mathcal{D}_{\circ} . It follows that the abstract Stokes graphs for $t \in (\infty, \tau)$ are exactly the diagram at the top of Fig. 31 and its opposite.

Moving down the v-trajectory (∞, τ) we retain symmetry in the diagonal. Upon arriving at the endpoint $t = \tau(w)$ the double root $z = \gamma$ must collide with exactly one of the simple roots, so the abstract Stokes graphs for the endpoint $t = \tau(w)$ must be the diagram in the center of the second row in Fig. 31 and its opposite. These graphs have a vertex of degree 5, which can split into a "dimer molecule" consisting of a pair of vertices of degrees 3 and 4 joined by one edge. Local analysis shows that near any zero t of $\Phi'(t)$, there are 5 possible orientations of the dimer that retain connectivity of the graph, each of which occurs along precisely one of the 5 v-trajectories that meet at t. Moreover, rotation about the critical point by an integer multiple of $\frac{2\pi}{5}$ induces a rotation of the dimer by the same angle; see Fig. 30.

The v-trajectory $(\tau, \tau^*)_+$ crosses the positive real axis at a point $t > t_\infty^+$ which implies via (8.4) that $\mu^2 > 0$. It follows that at this point the function $\varrho(z)$ is Schwarzsymmetric, so the Stokes graphs have to be symmetric with respect to reflection in the real z-axis. This selects exactly one of the dimer orientations and its reflection in the origin and therefore the abstract Stokes graphs for the v-trajectory $(\tau, \tau^*)_+$ are the right-most diagram in the second row of Fig. 31 and its opposite.

Likewise, since $\mu^2 < 0$ when t = b(w), the Stokes graphs for this point have to be symmetric with respect to reflection in the imaginary axis, and exactly one of the dimer orientations and its reflection in the origin produce abstract Stokes graphs admitting a degeneration from class $\{211\}$ to class $\{31\}$ that are consistent with this symmetry. Therefore, these graphs are the second diagram from the right in the third row of Fig. 31 and its opposite. The degeneration belonging to the point t = b(w) itself yields the right-most graph in the fourth row of the same figure and its opposite.

Since the graphs for the v-trajectories (τ,b) , (t_{∞}^+,b) , and (0,b) all degenerate into the {31} graphs for t=b(w), we can obtain the graphs for (t_{∞}^+,b) and for (0,b) by rotating the degenerating dimers in the graphs for (τ,b) through an angle of $-\frac{2\pi}{5}$ and $\frac{2\pi}{5}$ respectively. The abstract Stokes graphs for the v-trajectory (0,b) that arise are consistent with reflection symmetry in the imaginary axis for the actual Stokes graphs, as must be so because $\mu^2 < 0$ holds for 0 < t < b(w).

Reflecting the abstract Stokes graphs for $(\tau, \tau^*)_+$, (τ, b) , (t_{∞}^+, b) , (0, b), and b in the diagonal Im(z) = Re(z) then produces the abstract Stokes graphs for $(\tau, \tau^*)_-$, (τ, a) , (t_{∞}^-, a) , (a, 0), and a, respectively. This information is summarized in Fig. 31.



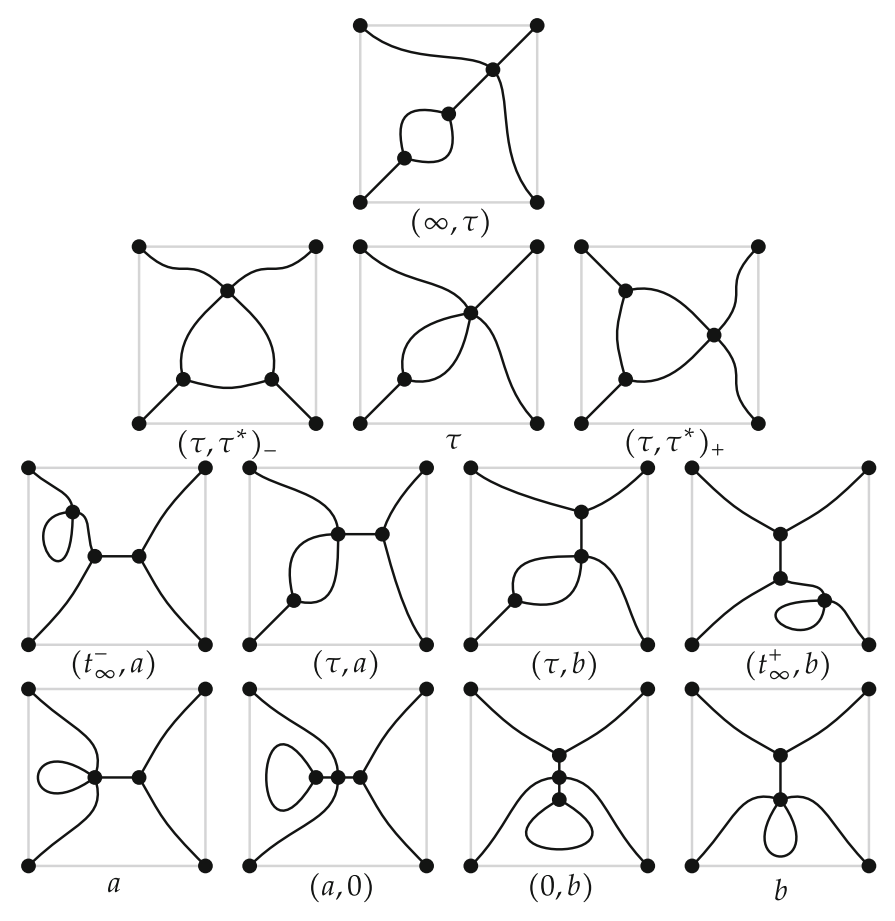


Fig. 31 Abstract Stokes graphs for the critical v-trajectories of $\Phi'(t)^2 dt^2$ in the closed upper-half t-plane. Also shown are the abstract Stokes graphs for the critical points t = a(w), t = b(w), and $t = \tau(w)$. The reflection through the origin of each graph also belongs to the same arc or critical point

8.4 The Domains S_0 , S_{∞} , and S_{\pm} in the Auxiliary Plane

Recall that under (8.4) the points on the Riemann surface Γ of Definition 1 in Sect. 5 that are mapped to $\mu=\infty$ correspond exactly to $t=t_\infty^\pm(w)$, t=0, and $t=\infty$. It is easy to see by expanding μ^2 and $q=\gamma^2$ for small t that it is the point t=0 that is mapped to the point at $\mu=\infty$ on the branch $\gamma=U_{0,gO}(\mu;\kappa)$ of (4.19) for which $\gamma=-\frac{2}{3}\mu+\mathcal{O}(\mu^{-1})$ as $\mu\to\infty$. Every neighborhood of t=0 contains parts of the two critical v-trajectories coinciding with the real intervals a(w)< t<0 and 0< t< b(w), and if the neighborhood is sufficiently small these are the only critical v-trajectories contained. Recall that $t_\infty^-(w)< a(w)<0< b(w)< t_\infty^+(w)$ and that a(w) and b(w) are mapped by $\mu=\pm\sqrt{\mu^2(t)}$ to solutions of $B(\mu;\kappa)=0$ none of which can vanish. Then, from (8.4) one sees that the real v-trajectory a(w)< t<0 is mapped bijectively onto $0<\mu^2(a(w))<\mu^2<+\infty$ while the real v-trajectory



0 < t < b(w) is mapped bijectively onto $-\infty < \mu^2 < \mu^2(b(w)) < 0$. Upon taking square roots and recalling the interpretation of critical v-trajectories, we find that $\operatorname{Re}(h(U_{0,\mathrm{gO}}(\mu;\kappa)))=0$ holds on the four coordinate axes in the μ -plane outside of the four purely real and purely imaginary solutions of $B(\mu;\kappa)=0$. Similarly, by expanding μ^2 and $q=\gamma^2$ for large t one sees that $t=\infty$ is mapped to $\mu=\infty$ on the branch $\gamma=U_{0,\mathrm{gH}}^{[3]}(\mu;\kappa)$ of (4.19) for which $\gamma=-2\mu+\mathcal{O}(\mu^{-1})$ as $\mu\to\infty$, and that the images of the two critical v-trajectories tending to $t=\infty$ parallel to the direction $\arg(t)=\pm\frac{\pi}{2}$ are four unbounded curves in the μ -plane with asymptotic arguments $\arg(\mu)=\pm\frac{\pi}{4},\pm\frac{3\pi}{4}$ along each of which $\operatorname{Re}(h(U_{0,\mathrm{gH}}^{[3]}(\mu;\kappa)))=0$. Let us refer to the interior of the closure of the union of the two end domains

Let us refer to the interior of the closure of the union of the two end domains abutting the pole at t=0 (resp., $t=t_{\infty}^{\pm}$, $t=\infty$) as S_0 (resp., S_{\pm} , S_{∞}). If we denote by ∂S the closure in $\overline{\mathbb{C}}$ of the union of critical v-trajectories both of whose endpoints are zeros of $\Phi'(t)^2$, then the t-sphere is the disjoint union $S_0 \sqcup S_+ \sqcup S_- \sqcup S_{\infty} \sqcup \partial S$. Each of the S_j is a domain containing precisely one point that is mapped to $\mu^2 = \infty$, and it is easy to see from (8.4) that

$$\frac{\mathrm{d}}{\mathrm{d}t}\mu^{2}(t) = \frac{\sqrt{1-\kappa^{2}}}{2} \cdot \frac{(t^{4} + 6t^{2} + 8wt - 3)(t^{2} + 4wt - 3)}{t^{2}(t^{2} + 2wt - 1)^{2}},\tag{8.9}$$

and hence the mapping $t \mapsto \mu^2$ is locally univalent near each of these singularities. Clearly, the only critical points of $t \mapsto \mu^2$ are the four zeros of $\Phi'(t)^2$ and the double roots satisfying $t^2 + 4wt - 3 = 0$, all of which are simple critical points. The domains S_{∞} and S_0 play a distinguished role and are illustrated with red and blue shading respectively in Fig. 29.

8.5 The Exterior Domain $\mathcal{E}_{\mathsf{qH}}(\kappa)$ as the Image of S_{∞}

We begin with the following result.

Lemma 12 Let $\kappa \in (-1, 1)$. Then the mapping $t \mapsto \mu^2$ is univalent on $\overline{S_{\infty}}$.

Proof Suppose that $t_1 \neq t_2$ are points in $\overline{S_\infty} \setminus \{\tau(w), \tau(w)^*\}$ such that $\mu^2(t_1) = \mu^2(t_2) =: \hat{\mu}^2$. Let Π_j denote a path in S_∞ from $t = \infty$ to t_j , for j = 1, 2. Then, the image paths under $t \mapsto \mu^2$ in the μ^2 -plane both begin at $\mu^2 = \infty$ and terminate at the same point $\hat{\mu}^2$. Let $\hat{\mu}$ denote a concrete choice of square root. Assuming without loss of generality that neither path Π_j passes through either of the double roots of $t \mapsto \mu^2$ except perhaps at the terminal endpoint, there are well-defined paths P_j on the Riemann surface Γ terminating at respective endpoints $(\hat{\mu}, \gamma_j)$ that project to Π_j under (8.5). Both paths P_j originate at $\mu = \infty$ on the sheet of Γ where $\gamma = -2\mu + \mathcal{O}(1)$ as $\mu \to \infty$ (because the paths Π_j start at $t = \infty$). However, they terminate at distinct points of Γ , i.e., $\gamma_1 \neq \gamma_2$ although both endpoints correspond to the same value of $\mu = \hat{\mu}$, because otherwise we obtain $(p(t_1), q(t_1)) = (p(t_2), q(t_2))$ from (8.3) which contradicts the assumption $t_1 \neq t_2$. Now let

$$L_{m,n} := \Theta_{0,\mathrm{gH}}^{[3]}(m,n)^{-1/2} u_{\mathrm{gH}}^{[3]}(\Theta_{0,\mathrm{gH}}^{[3]}(m,n)^{1/2} \hat{\mu};m,n)$$



be defined in terms of the gH rational solution $u_{\text{gH}}^{[3]}(x; m, n)$ of Painlevé-IV and the point $\hat{\mu} \in \mathbb{C}$.

We claim that P_1 and P_2 are gH paths (see Definition 6 in Sect. 6.5). To show this, first note that since Π_i , j = 1, 2, lie in the interior of S_{∞} and the terminal endpoints are not $\tau(w)$ or $\tau(w)^*$, there are no branch points on P_i . Then, we use the fact that by construction, K_t contains the projections in the t-plane of all possible bifurcation points on Γ . So, it suffices to consider intersection points of the projections Π_1 and Π_2 with K_t . Recall that all points of Π_i , j = 1, 2, except possibly the terminal endpoints lie in the interior S_{∞} whose intersection with K_t consists of exactly the critical v-trajectories denoted (∞, τ) and (∞, τ^*) . Comparing the abstract Stokes graphs worked out in Sect. 8.3 and summarized in Fig. 31 with the discussion in Sect. 6.5, we see that any bifurcation points on P_i before the terminal endpoint are necessarily of the harmless variety. Therefore, by Lemma 8 from Sect. 6.5, regardless of whether or not the endpoint of P_i is a catastrophic bifurcation point (occurring exactly when Π_i terminates on either $(\tau, \tau^*)_+$ or $(\tau, \tau^*)_-$), we deduce that in the limit $m, n \to +\infty$ with $n/m \to (1 - \kappa)/(1 + \kappa)$, $L_{m,n}$ converges to γ_i . Since $\gamma_1 \neq \gamma_2$, this is a contradiction with the assumption that $t_1 \neq t_2$. Hence $t \mapsto \mu^2$ is univalent on $\overline{S_{\infty}} \setminus \{\tau(w), \tau(w)^*\}.$

To extend the univalence to the points $\tau(w)$, $\tau(w)^*$, first we observe that since $\operatorname{Im}(\tau(w)) > 0$, it is impossible to have $\mu^2(\tau(w)) = \mu^2(\tau(w)^*)$. Indeed, since $t \mapsto \mu^2$ is Schwarz-symmetric, any common image point of $t = \tau(w), \tau(w)^*$ would have to be real, and since $t \mapsto \mu^2$ has degree 4 and $t = \tau(w)$, $\tau(w)^*$ are simple critical points of this mapping, no other solutions t of $\mu^2(t) = \mu^2(\tau(w)) = \mu^2(\tau(w)^*) \in \mathbb{R}$ than the non-real conjugate pair $t = \tau(w)$, $\tau(w)^*$ should be possible. However it is easy to see that any given real number μ^2 has at least two real preimages under $t \mapsto \mu^2$. Therefore $\mu^2(\tau(w)) \neq \mu^2(\tau(w)^*)$, and these values form a non-real conjugate pair. So, if $t_1 = \tau(w)$ or $t_1 = \tau(w)^*$, then to have the same image point in the μ^2 -plane we must have $t_2 \neq t_1$ with $t_2 \in \overline{S_{\infty}} \setminus \{\tau(w), \tau(w)^*\}$. Since we have already shown that $t \mapsto \mu^2$ is univalent on the latter set, the map is conformal at t_2 , so if N_2 is a small neighborhood of t_2 in the relative topology of $\overline{S_{\infty}}$ then its image in the μ^2 -plane is either a full neighborhood of $\mu^2(t_2)$ or it has a boundary curve passing through $\mu^2(t_2)$ with a well-defined tangent (the latter if and only if t_2 is on a smooth boundary arc of S_{∞}). However, since $\tau(w)$, $\tau(w)^*$ are simple critical points of $t \mapsto \mu^2$ and since the interior angle of ∂S_{∞} is $\frac{4\pi}{5}$ at $t = \tau(w)$, $\tau(w)^*$, so the image of a similar relative neighborhood N_1 of t_1 is locally a sector about $\mu^2(t_1) = \mu^2(t_2)$ of opening angle $\frac{8\pi}{5} > \pi$. The fact that these images necessarily overlap at points other than $\mu^2(t_1) = \mu^2(t_2)$ implies the existence of two points $t_1' \neq t_2'$ both in $\overline{S_{\infty}} \setminus \{\tau(w), \tau(w)^*\}$ with the same image under $t \mapsto \mu^2$, which contradicts the already-established univalence on that region.

Remark 16 According to (8.9), aside from the four zeros of $\Phi'(t)^2$, the remaining critical points of the mapping $t \mapsto \mu^2$ are the two roots of $\mu^2(t)$, which are simple critical points and as solutions of $t^2 + 4wt - 3 = 0$ are clearly real for all $w \in \mathbb{R}$. Since the resultant of $t^2 + 4wt - 3$ and $t^2 + 2wt - 1$ is proportional by a nonzero constant to $w^2 + 1$ which cannot vanish for any $w \in \mathbb{R}$, the double roots of $\mu^2(t)$ cannot coincide with the poles $t_{\infty}^{\pm}(w)$ for any $w \in \mathbb{R}$. By explicit calculation for w = 0 one sees that the roots of $\mu^2(t)$ lie one on either side of the interval $[t_{\infty}^-(w), t_{\infty}^+(w)]$, and hence the



same is true for all $w \in \mathbb{R}$. Since $t_{\infty}^-(w) < a(w) < 0 < b(w) < t_{\infty}^+(w)$, the double roots of $\mu^2(t)$ do not lie in $\overline{S_0}$. By Lemma 12 they also cannot lie in $\overline{S_\infty}$. Therefore the only critical points of $t \mapsto \mu^2$ that are not in ∂S are one each within S_{\pm} . Hence it is impossible for $t \mapsto \mu^2$ to be univalent on S_+ or S_- . It is also impossible for $\mu^2(t)$ to vanish at any point t of $\overline{S_0}$ or $\overline{S_\infty}$.

Lemma 12 implies in particular that the image of the boundary ∂S_{∞} in the μ -plane is a Jordan curve consisting of four arcs connecting the four branch points solving $B(\mu;\kappa)=0$ (see (1.17)) that do not lie on the real or imaginary axes, the latter being the images of $t=\tau(w), \tau(w)^*$ under $t\mapsto \mu^2$ and taking a double-valued square root. The domain S_{∞} is mapped onto the exterior of this Jordan curve, on which a function $\gamma=U_{0,\mathrm{eff}}^{[3]}(\mu;\kappa)$ is well defined by the composition

$$\mu \mapsto \mu^2 \mapsto t \mapsto p = \mu \gamma \mapsto \gamma = \mu^{-1} p,$$
 (8.10)

where univalence is used to define the second map, and p = p(t) is defined in (8.3). Note that $U_{0,\mathrm{gH}}^{[3]}(\mu;\kappa)$ has a continuous extension to the boundary. Again referring to Definition 6 we can now prove the following.

Lemma 13 Let $\kappa \in (-1, 1)$. If μ^2 is in the image of S_{∞} then there exists $\gamma \in \mathbb{C}$ and a gH path on Γ with terminal endpoint $(\mu, \gamma) \in \Gamma$ that is not a catastrophic bifurcation point.

Proof By univalence and (8.10) we obtain from μ^2 a unique point $t' \in S_{\infty}$. Letting Π denote any path in S_{∞} from $t = \infty$ to t = t' the fact that $\mu^2(t) \neq 0$ for all points of Π by Remark 16 implies that Π determines a unique image path P on the Riemann surface Γ of Definition 1 from Sect. 5 with terminal endpoint $(\mu, U_{0,gH}^{[3]}(\mu; \kappa)) \in \Gamma$. That P is a gH path that does not terminate at a catastrophic bifurcation point follows from the fact that Π lies within S_{∞} , which contains no points t mapping to any branch points or catastrophic bifurcation points of Γ (these occur only on ∂S_{∞}).

Combining Lemma 8 from Sect. 6.5 with Lemma 13, the conditional asymptotic results obtained for the gH rational solutions in Sect. 6 are valid for μ in the image of S_{∞} . We therefore will relabel S_{∞} as $S_{\rm gH}$. This motivates the following definition, which takes into account the rescaling of μ and transformation of κ needed to write the asymptotic formula (6.6).

Definition 7 (Exterior domain for the Painlevé-IV gH rationals) If $\kappa \in (-1, 1)$, $\mathcal{E}_{gH}(\kappa)$ is the image in the μ -plane, under (8.4) followed by a double-valued square root, of the domain $S_{\infty} = S_{gH}$. If instead $\pm \kappa > 1$, then $\mathcal{E}_{gH}(\kappa)$ is defined by homothetic dilation of the definition on (-1, 1):

$$\mathcal{E}_{gH}(\kappa) := \sqrt{\frac{1 \pm \kappa}{2}} \mathcal{E}_{gH}(I^{\pm}(\kappa)), \quad \pm \kappa > 1,$$

where the Möbius transformations $I^+:(1,+\infty)\to (-1,1)$ and $I^-:(-\infty,-1)\to (-1,1)$ defined in (1.23) are both involutions ($I^\pm(I^\pm(\kappa))=\kappa$). Note that by Remark 16, $\mathcal{E}_{gH}(\kappa)$ does not contain the origin for any $\kappa\in\mathbb{R}\setminus\{-1,1\}$.



8.6 The Boutroux Domain $\mathcal{B}_{\square}(\kappa)$

Recall from Sect. 4.4 that the origin $\mu=0$ is contained in a Boutroux domain \mathcal{B}_{\square} on which E=0 at $\mu=0$. It follows by the symmetry (4.30) that $E(\mu; -\kappa)=\mathrm{i} E(\mathrm{i} \mu; \kappa)$ holds for the family of functions $\mu\mapsto E$ defined by continuation on $\mathcal{B}_{\square}=\mathcal{B}_{\square}(\kappa)$ for all $\kappa\in(-1,1)$. Being a topological invariant, the abstract Stokes graph matches the lower-left panel of Fig. 27 in Sect. 7.2 for all $\kappa\in(-1,1)$ and all $\mu\in\mathcal{B}_{\square}(\kappa)$.

Lemma 14 Let $\kappa \in (-1, 1)$. The maximal Boutroux domain $\mathcal{B}_{\square}(\kappa)$ is precisely $\mathcal{B}_{\square}(\kappa) = \mathbb{C} \setminus \overline{\mathcal{E}_{gH}(\kappa)}$.

Proof Recall that the boundary of any maximal Boutroux domain \mathcal{B} consists of arcs that are the images in the μ -plane of critical v-trajectories of $\Phi'(t)^2 dt^2$ described in Sect. 8.2. The relevant arcs that bound $\mathcal{B}_{\square}(\kappa)$ are the images of arcs of K_t carrying abstract Stokes graphs that are $\{1111\} \to \{211\}$ degenerations of the abstract Stokes graph of $\mathcal{B}_{\square}(\kappa)$. From Fig. 31 we identify the boundary arcs of $\mathcal{B}_{\square}(\kappa)$ as the images of $(\tau, \tau^*)\pm$, which by Lemma 12 form together with their endpoints the Jordan curve $\partial \mathcal{E}_{gH}(\kappa)$.

Thus, for each $\kappa \in (-1, 1)$, $\partial \mathcal{B}_{\square}(\kappa) = \partial \mathcal{E}_{gH}(\kappa)$ is a curvilinear rectangle in the μ -plane. Although the unbounded region $\mathcal{E}_{gH}(\kappa)$ is the image of the unbounded exterior of the Jordan curve ∂S_{gH} in the t-plane and $\mathcal{B}_{\square}(\kappa) = \mathbb{C} \setminus \overline{\mathcal{E}_{gH}(\kappa)}$, $\mathcal{B}_{\square}(\kappa)$ is not the image of the bounded interior $\mathbb{C} \setminus \overline{S_{gH}}$ because $t \mapsto \mu^2$ is not univalent there according to Remark 16.

8.7 Aside: Asymptotic Analysis of gO Rationals at Points of $\partial \mathcal{E}_{\mathsf{qH}}(\kappa)$

Let $\kappa \in (-1,1)$ and suppose that $\mu \in \partial \mathcal{B}_{\square}(\kappa) = \partial \mathcal{E}_{gH}(\kappa)$ is not one of the four vertices (solutions μ of $B(\mu;\kappa) = 0$ that are not on the real or imaginary axes). The asymptotic behavior of $u_{gO}^{[3]}(x;m,n)$ can be rigorously analyzed for such μ as follows. We start by mimicking the setup in Sects. 7.3–7.5 for the gO case when $\mu \in \mathcal{B}_{\square}$ and for simplicity we assume that s = +1 and set $\zeta = 0$. However, to study μ on the boundary, we allow two adjacent vertices of the Stokes graph to fuse into a double root $z = \gamma$ of P(z). Being as $\mu \in \partial \mathcal{E}_{gH}(\kappa)$, it follows from Lemma 12 that this double root is the function $\gamma = U_{0,gH}^{[3]}(\mu;\kappa)$, which is well defined on $\overline{\mathcal{E}_{gH}(\kappa)}$. Mutatis mutandis, we can still use a subset of the same matrix factorizations, lens deformations, as well as the diagrams in Appendix E.1 to describe the matrix $\mathbf{O}(z)$.

However, the construction of a parametrix for $\mathbf{O}(z)$ in this situation is simpler than that described in Sect. 7.6. We give some details for the case that it is the roots $z = \gamma$, δ shown in the figures in Appendix E.1 that have fused into a double root, also denoted $z = \gamma$. First consider the outer parametrix $\mathbf{O}^{\text{out}}(z)$. After making the transformation to $\mathbf{P}^{\text{out}}(z)$ indicated in the first two lines of Table 5 in Sect. 7.6 we find that $\mathbf{P}^{\text{out}}(z)$ has jumps across just the single band B_1 from α to β and the gap G from β to γ (the second band B_2 disappears in the degeneration). As we are taking $\zeta = 0$, the jump across B_1 given generally in (7.5) reads simply $\mathbf{P}^{\text{out}}_+(z) = \mathbf{P}^{\text{out}}_-(z)\mathbf{T}(-1)$. The jump condition across G simplifies to read simply $\mathbf{P}^{\text{out}}_+(z) = \mathbf{P}^{\text{out}}_-(z)\mathbf{D}(e^{\mathrm{i}\pi/3})$. To see this, one first



takes the jump condition in the form (7.6) with the real constant C_G as given in the first line of Table 6 in Sect. 7.6, and then observes that in the {211} degeneration at hand, the integral R_2 given by (7.1) can be evaluated explicitly by residues at z = 0, ∞ :

$$R_2 = \frac{\pi}{32} \left[32 - 4(\alpha + \beta)\gamma + (\alpha + \beta)^2 - 4\alpha\beta \right].$$

Then, since the spectral curve is of class $\{211\}$ we use (4.18) and the implied quartic equation (4.19) on γ to obtain simply $R_2 = (1 - \kappa)\pi$. Because s = 1, we have $T = \Theta_0 = \Theta_{0,gO}^{[3]}(m,n) = \frac{1}{6} + \frac{1}{2}(m+n)$ and $-\kappa T = \Theta_\infty = \Theta_{\infty,gO}^{[3]}(m,n) = \frac{1}{2} + \frac{1}{2}(n-m)$, where we refer to the third line of Table 2 from Sect. 1.2 for the values of Θ_0 and Θ_∞ . Therefore using $n \in \mathbb{Z}$ we get $e^{-2iTR_2}e^{-i\pi/3} = e^{i\pi/3}$.

To solve for $\check{\mathbf{P}}^{\text{out}}(z)$, we first use a diagonal conjugation to replace the jump matrix on G with the identity and that on B_1 with $\mathbf{T}(1)$ without changing the domain of analyticity or normalization at $z = \infty$. To this end, we transform $\check{\mathbf{P}}^{\text{out}}(z)$ into $\check{\mathbf{Q}}^{\text{out}}(z)$ via a substitution of the form (7.12) in which we take

$$F(z) := \frac{1}{2}\mathrm{i}\pi - \frac{1}{6}\pi\,R_0(z)\int_G \frac{\mathrm{d}y}{R_0(y)(y-z)}, \quad F_0 := \frac{1}{2}\mathrm{i}\pi - \frac{1}{6}\pi\int_G \frac{\mathrm{d}y}{R_0(y)},$$

where $R_0(z)$ denotes the function analytic for $z \in \mathbb{C} \setminus B_1$ with $R_0(z)^2 = (z-\alpha)(z-\beta)$ and $R_0(z) = z + \mathcal{O}(1)$ as $z \to \infty$. Since F(z) is analytic and uniformly bounded for $z \in \mathbb{C} \setminus (B_1 \cup G)$, across which $\Delta F = -\frac{1}{3}i\pi$ for $z \in G$ and $\langle F \rangle = \frac{1}{2}i\pi$ for $z \in B_1$, and since $F(z) \to F_0$ as $z \to \infty$, it follows that $\check{\mathbf{Q}}^{\text{out}}(z)$ satisfies exactly the desired conditions. Moreover, comparing with Sect. 6.3 shows that $\check{\mathbf{Q}}^{\text{out}}(z)$ agrees with the outer parametrix for the gH rationals on the exterior domain as defined explicitly in (6.4). Unlike in the situation that we consider μ in the interior of $\mathcal{B}_{\square}(\kappa)$, the outer parametrix we have just constructed always exists.

For inner parametrices, we may follow exactly the construction described in Section 7.6 with the help of the data in the first two major rows of Table 7 in Appendix E.1 to install Airy parametrices near the simple roots $z=\alpha$, β of P(z). These have exactly the same matching properties onto the new outer parametrix as indicated in (7.40), and the mismatches on the disk boundaries near $z=\alpha$, β contribute terms of order $\mathcal{O}(T^{-1})$ to the error at the end. However, we have to install a different type of parametrix near the double root $z=\gamma$. Since this root lies on the level curve Re(h(z))=0, we can start by following the procedure described in Sect. 5.5 and introduce a conformal map near $z=\gamma$ to a quadratic exponent by setting $W(z)^2=2(h(z)-h(\gamma))$, taking an analytic square root so that W(z)>0 corresponds to the arc $\Sigma_{4,1}\subset\Sigma$ that originates at ∞ in the direction $\text{arg}(z)=-\frac{\pi}{2}$ and terminates at $z=\gamma$. We then introduce the rescaled coordinate $\xi:=T^{1/2}e^{-i\pi/4}W(z)$, and after a substitution $\mathbf{B}(\xi)=\mathbf{O}(z)\mathbf{D}$, where \mathbf{D} is a suitable piecewise-constant unit determinant matrix, we end up with the



following exact jump conditions near $z = \gamma$ or $\xi = 0$:

$$\begin{split} \boldsymbol{B}_{+}(\xi) &= \boldsymbol{B}_{-}(\xi) \begin{cases} \boldsymbol{L}(e^{i\pi/3}e^{i\xi^2}), & \text{arg}(\xi) = \frac{\pi}{4}, \\ \boldsymbol{U}(e^{i\pi/3}e^{-i\xi^2}), & \text{arg}(\xi) = -\frac{\pi}{4}, \\ \boldsymbol{U}(e^{-i\xi^2}), & \text{arg}(\xi) = \frac{3\pi}{4}, \\ \boldsymbol{L}(e^{i\xi^2}), & \text{arg}(\xi) = -\frac{3\pi}{4}, \\ \boldsymbol{D}(e^{i\pi/3}), & \text{arg}(-\xi) = 0, \end{cases} \end{split}$$

in which all five rays are taken to be oriented in the direction of increasing $Re(\xi)$. These jump conditions are solved by the parabolic cylinder function parametrix originally introduced by Its [38]. Indeed, defining parameters $p := \frac{1}{6}i$ and $\tau := e^{i\pi/3}$, they match exactly the form of Riemann–Hilbert Problem A.1 in [49, Appendix A]. Adjoining the normalization condition $\mathbf{B}(\xi)\xi^{\mathrm{i}\rho\sigma_3}\to\mathbb{I}$ as $\xi\to\infty$ and multiplying on the left by a holomorphic matrix function designed to give an optimal match with the outer parametrix (similarly to the construction of Airy parametrices) one obtains an inner parametrix that solves the jump conditions for O(z) exactly near $z = \gamma$ and that matches the outer parametrix on a circle around $z = \gamma$ with accuracy $\mathcal{O}(T^{-1/2})$, exactly as in the case of the Hermite polynomial parametrix used in Sect. 5.5 (which is obviously closely related, having also a quadratic local exponent). In addition to standard large-variable asymptotic expansions of parabolic cylinder functions, this estimate relies on the fact that $Re(h(\gamma)) = 0$, which holds because the degenerate spectral curve is Boutroux.

Simple modifications of these steps apply if different pairs of adjacent simple roots on the Stokes graph for the $\{1111\}$ spectral curve on $\mathcal{B}_{\square}(\kappa)$ fuse into a double root $z = \gamma$, but the fact that the outer parametrix is related by a diagonal factor to that defined in (6.4) is the same in all cases. The mismatch on the boundary of the disk centered at $z = \gamma$ dominates the asymptotic expansion of the error, and by using the fact that the matrix $\mathbf{\check{Q}}^{\text{out}}(z)$ is precisely the outer parametrix for the gH rational solutions on the exterior domain given by (6.4), we arrive at the following result.

Lemma 15 Fix $\kappa \in (-1,1)$. Suppose that $\Theta_{0,gO}^{[3]}(m,n) > 0$ and that $\hat{\mu}$ is a given point on $\partial \mathcal{B}_{\square}(\kappa) = \partial \mathcal{E}_{gH}(\kappa)$ that is not one of the four corner points. Then

$$u_{gO}^{[3]}(\Theta_{0,gO}^{[3]}(m,n)^{1/2}\hat{\mu};m,n) = \Theta_{0,gO}^{[3]}(m,n)^{1/2}(\gamma(\hat{\mu}) + \mathcal{O}(\Theta_{0,gO}^{[3]}(m,n)^{-1/2}))$$

$$(8.11)$$

$$\pi(m,n) \to \infty \text{ with } n/m \to (1-\kappa)/(1+\kappa), \text{ where } \gamma(\mu) := U_{0,gH}^{[3]}(\mu;\kappa) \text{ is the}$$

as $m, n \to \infty$ with $n/m \to (1 - \kappa)/(1 + \kappa)$, where $\gamma(\mu) := U_{0,gH}^{[3]}(\mu; \kappa)$ is the function defined on $\mathcal{E}_{gH}(\kappa)$ by (8.10) and extended to $\partial \mathcal{E}_{gH}(\kappa)$ by continuity.

This result is interesting in its own right; it basically says that the gO and gH rational solutions behave the same along the boundary $\partial \mathcal{E}_{gH}(\kappa) = \partial \mathcal{B}_{\square}(\kappa)$ even though they behave quite differently for large $|\mu|$.

8.8 The Exterior Domain $\mathcal{E}_{g0}(\kappa)$ as the Image of S_0

Using Lemma 15 we can prove the following analogue of Lemma 12.



Lemma 16 Let $\kappa \in (-1, 1)$. Then the mapping $t \mapsto \mu^2$ is univalent on $\overline{S_0}$.

Proof Univalence on $\overline{S_0} \setminus \{a(w), b(w), \tau(w), \tau(w)^*\}$ is established similarly to the univalence of the same map on $\overline{S_\infty} \setminus \{\tau(w), \tau(w)^*\}$ in the proof of Lemma 16. Here we begin with paths Π_j in S_0 from t=0 to $t_j \in \overline{S_0} \setminus \{a(w), b(w), \tau(w), \tau(w)^*\}$ for which $t_1 \neq t_2$ but $\mu^2(t_1) = \mu^2(t_2) = \hat{\mu}^2$, and we lift these t_0 to paths t_0 on the Riemann surface t_0 of Definition 1 from Sect. 5, the endpoints of which have the form $(\hat{\mu}, \gamma_j)$. The paths t_0 originate on t_0 at t_0 on the gO sheet where t_0 is t_0 or t_0 decomposite of t_0 are distinct, i.e., t_0 because the paths t_0 is start at t_0 . However the endpoints of t_0 are distinct, i.e., t_0 because t_0 because t_1 is the transfer of t_0 . We then replace t_0 with

$$L_{m,n} := \Theta_{0,\mathrm{gO}}^{[3]}(m,n)^{-1/2} u_{\mathrm{gO}}^{[3]}(\Theta_{0,\mathrm{gO}}^{[3]}(m,n)^{1/2} \hat{\mu};m,n)$$

and we notice that P_j are gO paths (cf. Definition 5 in Sect. 5.5). Indeed, one can easily verify that the v-trajectories denoted (a,0) and (0,b) are the only components of K_t within S_0 and these correspond to harmless bifurcation points only for the gO case. Therefore, by Lemma 6 in Sect. 5.5, $L_{m,n}$ converges to both $\gamma_1 \neq \gamma_2$ as $m, n \to \infty$ with $\Theta_{0,\mathrm{gO}}^{[3]}(m,n) > 0$ and the ratio n/m converging to $(1-\kappa)/(1+\kappa)$. Hence we arrive at a contradiction with the assertion $t_1 = t_2$.

Since $\mu^2(b(w)) < 0 < \mu^2(a(w))$ are real and distinct while $\mu^2(\tau(w)) \neq \mu^2(\tau(w)^*)$ form a conjugate pair, extending the univalence to the points t = a(w), b(w) follows the same line of reasoning as the extension to $t = \tau(w), \tau(w)^*$ in the proof of Lemma 12 because the interior angles of ∂S_0 at t = a(w), b(w) are the same as the interior angles of ∂S_∞ at $t = \tau(w), \tau(w)^*$, all four of which are simple critical points of $t \mapsto \mu^2$.

So the remaining possibility is that $t_1 = \tau(w)$ or $t_1 = \tau(w)^*$, that $t_2 \in \overline{S_0} \setminus \{a(w), b(w), \tau(w), \tau(w)^*\}$, and that $\mu^2(t_1) = \mu^2(t_2) = \hat{\mu}^2$. By Remark 16, the map $t \mapsto \mu^2$ is conformal at t_2 . Since the interior angle of ∂S_0 at $t = t_1$ is $\frac{2\pi}{5}$ and t_1 is a simple critical point of $t \mapsto \mu^2$, the image of a relative neighborhood N_1 in S_0 of t_1 is locally an open sector with vertex $\hat{\mu}^2$ and opening angle $\frac{4\pi}{5} < \pi$. If $t_2 \in S_0$, then the image of a small neighborhood N_2 of t_2 in S_0 is a full neighborhood of $\hat{\mu}$ in \mathbb{C} , and there are points $t_1' \neq t_2'$ in S_0 close to t_1 and t_2 respectively with $\mu^2(t_1') = \mu^2(t_2')$ in contradiction to the established univalence on S_0 . However, if $t_2 \in \partial S_0 \setminus \{a(w), b(w), \tau(w), \tau(w)^*\}$, then it lies on a smooth boundary arc of S_0 so the image of a small neighborhood N_2 of t_2 in S_0 is locally an open half-plane at $\hat{\mu}^2$, which need not intersect the image of N_1 at all.

If in fact $\mu^2(N_2) \cap \mu^2(N_1) \neq \emptyset$ then the same argument gives a contradiction. Otherwise, local analysis near $t = t_1$ shows that $\mu^2(N_2) \cap (\partial \mathcal{E}_{gH}(\kappa)^2 \setminus \{\hat{\mu}^2\}) \neq 0$, i.e., there is a point $\hat{\mu}' \in \mathbb{C}$ with $\hat{\mu}'^2 \in \mu^2(N_2)$ that also lies on a smooth boundary arc of $\mathcal{E}_{gH}(\kappa)$, and hence there is a preimage $t_1' \in \partial S_{\infty} \setminus \{\tau(w), \tau(w)^*\}$ of $\hat{\mu}'^2$. Let t_2' denote the unique preimage in N_2 of $\hat{\mu}'^2$, so that $t_2' \in \overline{S_0} \setminus \{a(w), b(w), \tau(w), \tau(w)^*\}$; in particular $t_1' \neq t_2'$. We choose a path Π in S_0 from t = 0 to $t = t_2'$ and lift it to a

¹⁰ Due to Remark 16 we no longer have to worry about Π_j passing through the roots of $t \mapsto \mu^2$ since these lie in S_- and S_+ .



gO path P on Γ with endpoint $(\hat{\mu}', \gamma_2')$. Then Lemma 6 implies that $L_{m,n} \to \gamma_2'$ as $m, n \to \infty$ with $\Theta_{0,gO}^{[3]}(m,n) > 0$ and $n/m \to (1-\kappa)/(1+\kappa)$. On the other hand, we may apply Lemma 15 to deduce that in the same limit $L_{m,n} \to \gamma_1' = U_{0,gH}^{[3]}(\hat{\mu}'; \kappa)$, and since $t_1' \neq t_2'$ while $\mu^2(t_1') = \mu^2(t_2') = \hat{\mu}'^2$, we obtain $\gamma_1' \neq \gamma_2'$, a contradiction. \square

In particular, the image of ∂S_0 in the μ -plane is a Jordan curve consisting of eight arcs connecting all eight of the solutions of $B(\mu;\kappa)=0$, which are the images of $t=a(w),b(w),\tau(w),\tau(w)^*$ under $t\mapsto \mu^2$ after taking square roots. S_0 is mapped onto the exterior of this Jordan curve, a domain on which $\mu\mapsto \gamma=U_{0,\mathrm{gO}}(\mu;\kappa)$ is well defined by the composition (8.10) (extending continuously to the boundary). Recalling again Definition 5, by analogy with Lemma 13, we have the following.

Lemma 17 Let $\kappa \in (-1, 1)$. If μ^2 is in the image of S_0 then there exists $\gamma \in \mathbb{C}$ and a gO path on Γ with terminal endpoint $(\mu, \gamma) \in \Gamma$ that is not a catastrophic bifurcation point.

Proof The proof is very similar to that of Lemma 13.

Combining Lemma 6 from Sect. 5.5 with Lemma 13 from Sect. 8.5 shows that the conditional asymptotic analysis of the gO rational solutions described in Sect. 5 is valid on the image in the μ -plane of S_0 . We therefore will relabel S_0 as S_{gO} . By analogy with Definition 7 we make the following definition.

Definition 8 (Exterior domain for the Painlevé-IV gO rationals) If $\kappa \in (-1, 1)$, $\mathcal{E}_{gO}(\kappa)$ is the image in the μ -plane, under (8.4) followed by a double-valued square root, of the domain $S_0 = S_{gO}$. If instead $\pm \kappa > 1$, then $\mathcal{E}_{gO}(\kappa)$ is defined by homothetic dilation of the definition on (-1, 1):

$$\mathcal{E}_{gO}(\kappa) := \sqrt{\frac{1 \pm \kappa}{2}} \mathcal{E}_{gO}(I^{\pm}(\kappa)), \qquad \pm \kappa > 1,$$

where the Möbius transformations $I^+:(1,+\infty)\to (-1,1)$ and $I^-:(-\infty,-1)\to (-1,1)$ defined in (1.23) are both involutions ($I^\pm(I^\pm(\kappa))=\kappa$). Note that by Remark 16, $\mathcal{E}_{gO}(\kappa)$ does not contain the origin for any $\kappa\in\mathbb{R}\setminus\{-1,1\}$.

The Jordan curves $\partial \mathcal{E}_{gH}(\kappa)$ and $\partial \mathcal{E}_{gO}(\kappa)$ have the four vertices of $\partial \mathcal{E}_{gH}(\kappa)$ in common. However, these are the only points of intersection. More precisely:

Lemma 18 For each $\kappa \in (-1, 1)$, all points of $\partial \mathcal{E}_{gO}(\kappa)$ except the four vertices of $\partial \mathcal{E}_{gH}(\kappa) = \partial \mathcal{B}_{\square}(\kappa)$ lie in $\mathcal{E}_{gH}(\kappa)$.

Proof Locally near the four vertices the conclusion follows from the fact that $t\mapsto \mu^2$ has simple critical points at the points $t=\tau(w), \tau(w)^*$ common to both $\overline{S_{gH}}$ and $\overline{S_{gO}}$ (which are mapped to the squares of the four vertices). Therefore, it is sufficient to show that no point μ on a smooth arc of $\partial \mathcal{E}_{gH}(\kappa) = \partial \mathcal{B}_{\square}(\kappa)$ can lie on any smooth arc of $\partial \mathcal{E}_{gO}(\kappa)$ or coincide with an image of either t=a(w) or t=b(w) (that are mapped to the remaining four vertices of $\partial \mathcal{E}_{gO}(\kappa)$).



If $\mu = \hat{\mu}$ is common to smooth arcs of both $\partial \mathcal{E}_{gH}(\kappa)$ and $\partial \mathcal{E}_{gO}(\kappa)$, then the argument in the final paragraph of the proof of Lemma 16 applies to yield a contradiction.

On the other hand, if $\mu = \hat{\mu}$ is a point on a smooth arc of $\partial \mathcal{E}_{gH}(\kappa)$ that is also a vertex of $\partial \mathcal{E}_{gO}(\kappa)$ corresponding to either t = a(w) or t = b(w), then because the exterior domain $\mathcal{E}_{gO}(\kappa)$ is locally a sector at $\hat{\mu}$ of opening angle $\frac{8\pi}{5} > \pi$, there is another nearby point $\hat{\mu}'$ on the same smooth arc of $\partial \mathcal{E}_{gH}(\kappa)$ that also lies within the exterior domain $\mathcal{E}_{gO}(\kappa)$. So, we can once again apply the argument from the last paragraph of the proof of Lemma 16 to the point $\hat{\mu}'$ to yield a contradiction.

Another observation relates the values of the equilibrium branches $\gamma=\gamma(\mu)$ defined on the closures of the exterior domains $\mathcal{E}_{gH}(\kappa)$ and $\mathcal{E}_{gO}(\kappa)$ by (8.10) and Lemmas 12 and 16 respectively.

Lemma 19 Let $\kappa \in (-1,1)$. If μ is one of the four vertices of $\partial \mathcal{E}_{gH}(\kappa)$ then $U_{0,gH}^{[3]}(\mu;\kappa) = U_{0,gO}(\mu;\kappa)$. If μ is not such a vertex but $\mu \in \overline{\mathcal{E}_{gH}(\kappa)} \cap \overline{\mathcal{E}_{gO}(\kappa)}$ then $U_{0,gH}^{[3]}(\mu;\kappa) \neq U_{0,gO}(\mu;\kappa)$.

Proof This follows directly from the definition of these two functions. Using the univalence of $t\mapsto \mu^2$ on $\overline{S_{gH}}$ and $\overline{S_{gO}}$ established by Lemmas 12 and 16 respectively, the point μ can be traced back to one point $t=t_{gH}\in \overline{S_{gH}}$ and one point $t=t_{gO}\in \overline{S_{gO}}$. We have $t_{gH}=t_{gO}$ if and only if both points are either $t=\tau(w)$ or $t=\tau(w)^*$, in which case μ is one of the four vertices and the equal values of $p(t_{gH})=p(t_{gO})$ defined in (8.3) imply that the corresponding values of γ are equal: $\gamma_{gH}=\gamma_{gO}$. Of course if $t_{gH}\neq t_{gO}$ but the value of μ is the same, the same argument shows that $\gamma_{gH}\neq \gamma_{gO}$.

8.9 The Boutroux Domains $\mathcal{B}_{\triangleright}(\kappa)$ and $\mathcal{B}_{\triangle}(\kappa)$

Lemma 18 shows that the region in between $\partial \mathcal{B}_{\square}(\kappa)$ and $\partial \mathcal{E}_{gO}(\kappa)$ is the disjoint union of four simply connected domains whose boundaries are curvilinear triangles. Each of these triangles consists of three arcs that are images in the μ -plane of the boundary arcs of S_+ (the triangles having a vertex on the real axis) and S_- (the triangles having a vertex on the imaginary axis). However, it is not accurate to view these domains as images of S_{\pm} because $t \mapsto \mu^2$ is not univalent (see Remark 16).

Let $\mathcal{B}_{\triangleright} = \mathcal{B}_{\triangleright}(\kappa)$ (resp., $\mathcal{B}_{\triangle} = \mathcal{B}_{\triangle}(\kappa)$) denote the maximal connected component of $\mathbb{C} \setminus \overline{\mathcal{B}_{\square}(\kappa)} \cup \mathcal{E}_{gO}(\kappa)$ that is entirely contained within the right half (resp., upper half) μ -plane, a simply connected domain whose boundary is a curvilinear triangle with vertices agreeing with those of an equilateral triangle (cf. Proposition 1 in Sect. 1.3), one vertex of which lies on the positive real (resp., imaginary) axis. See the upper right-hand panel of Fig. 5 in Sect. 1.4.

Recall from Sect. 4.4 that there is a unique real (resp., imaginary) value of E defined on the real (resp., imaginary) axis in the μ -plane for which the elliptic Riemann surface \mathcal{R} of the quartic polynomial $P(\cdot)$ defined by (1.18) is a Boutroux curve satisfying the conditions (4.23). Recall also that each point $\hat{\mu} \in \mathcal{B}_{\triangleright}(\kappa) \cap \mathbb{R}$ (resp., $\hat{\mu} \in \mathcal{B}_{\triangle}(\kappa) \cap i\mathbb{R}$) for which the Boutroux curve \mathcal{R} specified above is of class {1111} is contained within a Boutroux domain $\hat{\mathcal{B}}$. The domain $\hat{\mathcal{B}}$ is a complex neighborhood of $\hat{\mu}$ on which



 $E = E(\mu; \kappa)$ is defined as a smooth function of μ such that $E(\hat{\mu}; \kappa)$ is real (resp., imaginary) and at each point of which \mathcal{R} defined from μ and $E(\mu; \kappa)$ is a Boutroux curve of class {1111}. Finally, recall from Sect. 7.1 that each such Boutroux domain carries a well-defined abstract Stokes graph.

Lemma 20 Let $\kappa \in (-1, 1)$. Then $\mathcal{B}_{\triangleright}(\kappa)$ and $\mathcal{B}_{\triangle}(\kappa)$ are Boutroux domains with the abstract Stokes graphs depicted on the right and top panels respectively of Fig. 27 in Sect. 7.2.

Proof We prove the statement for $\mathcal{B}_{\triangleright}(\kappa)$, as the proof for $\mathcal{B}_{\triangle}(\kappa)$ is the same replacing reflection symmetry in the real axis with reflection symmetry in the imaginary axis.

Regardless of whether the Boutroux curve \mathcal{R} for a given $\mu \in \mathcal{B}_{\triangleright}(\kappa) \cap \mathbb{R}$ is of class {1111}, since E is real the polynomial $P(\cdot)$ is Schwarz-symmetric, so the Stokes graph of \mathcal{R} is also symmetric through the real axis. If \mathcal{R} is a degenerate Boutroux curve, then μ lies on an image arc of one of the v-trajectories in K_t . Clearly it cannot be any of the v-trajectories forming the boundary of S_{gH} or S_{gO} because those are mapped to points on $\partial \mathcal{E}_{\mathrm{gH}}(\kappa)$ and $\partial \mathcal{E}_{\mathrm{gO}}(\kappa)$ respectively. Nor can it be either of the v-trajectories (a,0) or (0,b) in the interior of S_{gO} because they are mapped into the exterior of $\partial \mathcal{E}_{\mathrm{gO}}(\kappa)$. So μ would have to be on the image of one of the v-trajectories labeled (∞,τ) or (t_{∞}^-,a) or (t_{∞}^+,b) or their Schwarz reflections in the real t-axis. However, from Fig. 31 explained in Sect. 8.3, we see that none of the abstract Stokes graphs for any of these arcs is consistent with an actual Stokes graph having reflection symmetry in the real axis. Therefore the unique Boutroux curve \mathcal{R} with E real associated with each point $\mu \in \mathcal{B}_{\triangleright}(\kappa) \cap \mathbb{R}$ has class {1111}. This implies that there is a well-defined abstract Stokes graph that is the same for all of these Boutroux curves.

This abstract Stokes graph has to be consistent with an actual Stokes graph having Schwarz symmetry in the real axis, and it has to be nondegenerate. However, it has to admit degeneration to one of the opposite abstract Stokes graphs for one of the arcs $(\tau, \tau^*)_{\pm}$ (class {211}) and to one of the opposite abstract Stokes graphs for the point t=a (class {31}), because an image of either $(\tau, \tau^*)_{+}$ or $(\tau, \tau^*)_{-}$ forms the arc of $\partial \mathcal{E}_{gH}(\kappa)$ containing the left endpoint of $\mathcal{B}_{\triangleright}(\kappa) \cap \mathbb{R}$ and an image of t=a is the right endpoint of $\mathcal{B}_{\triangleright}(\kappa) \cap \mathbb{R}$. Using the abstract Stokes graphs for $(\tau, \tau^*)_{\pm}$ and for t=a shown in Fig. 31 then determines the abstract Stokes graph for every point of $\mathcal{B}_{\triangleright}(\kappa) \cap \mathbb{R}$, as either the diagram on the right in Fig. 27 from Sect. 7.2 or its reflection through the origin. The parity is then resolved by the observation that when μ is the right endpoint of $\mathcal{B}_{\triangleright}(\kappa) \cap \mathbb{R}$, the spectral curve is of class {31} so all coefficients of $P(\cdot)$ are determined uniquely by the value of μ from which one can easily show that the triple root of $P(\cdot)$ lies to the right of the simple root; this means that it is the reflection through the origin of the abstract Stokes graph for t=a shown in Fig. 31 that actually appears at the right endpoint of $\mathcal{B}_{\triangleright}(\kappa) \cap \mathbb{R}$.

It remains to show that the Boutroux domain containing $\mathcal{B}_{\triangleright}(\kappa) \cap \mathbb{R}$ with the indicated abstract Stokes graph can be extended to all of $\mathcal{B}_{\triangleright}(\kappa)$. All boundary points of the Boutroux domain correspond to degenerate Boutroux curves, moreover, to continuous degenerations of class {1111} curves within the domain. There are four abstract Stokes graphs corresponding to class {211} degenerations of the abstract Stokes graph for the Boutroux domain containing $\mathcal{B}_{\triangleright}(\kappa) \cap \mathbb{R}$ obtained by fusing pairs of vertices joined by a common edge, shown in Fig. 32.



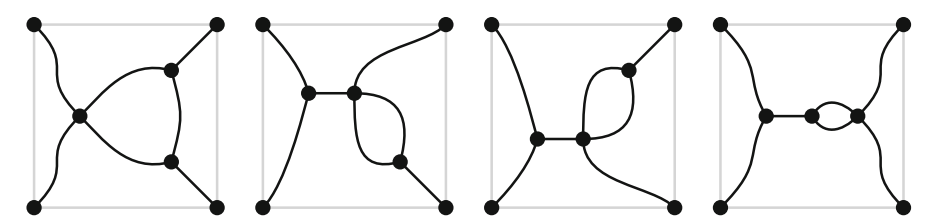


Fig. 32 The four class $\{211\}$ degenerations of the abstract Stokes graph for the Boutroux domain containing $\mathcal{B}_{\triangleright}(\kappa) \cap \mathbb{R}$

Only the degeneration shown in the right-most diagram has no representative (either under reflection through the origin or through the real axis) in Fig. 31 so this cannot occur. The other three degenerations, in the order left-to-right in Fig. 32, match

- the reflection through the origin of the abstract Stokes graph shown in Fig. 31 for $(\tau, \tau^*)_+$,
- the reflection through the real axis of the abstract Stokes graph shown in Fig. 31 for (τ, a) , and
- the reflection through the origin of the abstract Stokes graph shown in Fig. 31 for (τ, a) .

The indicated arcs are mapped precisely to the three boundary arcs of $\mathcal{B}_{\triangleright}(\kappa)$, which completes the proof.

By definition, when $\kappa \in (-1,1)$ the Boutroux domains $\mathcal{B}_{\square}(\kappa)$, $\mathcal{B}_{\triangleright}(\kappa)$, and $\mathcal{B}_{\triangle}(\kappa)$ are determined by the curves $\partial \mathcal{E}_{gH}(\kappa)$ and $\partial \mathcal{E}_{gO}(\kappa)$. According to Definitions 7 and 8 the latter curves are also defined for $|\kappa| > 1$ by dilations in the μ -plane of the same curves for $\kappa \in (-1,1)$. In light of this, and motivated also by the discussion at the end of Sect. 7.7, we extend the definitions of $\mathcal{B}_{\square}(\kappa)$, $\mathcal{B}_{\triangleright}(\kappa)$, and $\mathcal{B}_{\triangle}(\kappa)$ to all $\kappa \in \mathbb{R} \setminus \{-1,1\}$ in the natural way.

Definition 9 Given $\kappa \in \mathbb{R} \setminus \{-1, 1\}$, let $\mathcal{E}_{gH}(\kappa)$ and $\mathcal{E}_{gO}(\kappa)$ be defined by Definition 7 and 8 respectively. Then $\mathcal{B}_{\square}(\kappa) := \mathbb{C} \setminus \overline{\mathcal{E}}_{gH}(\kappa)$, and $\mathcal{B}_{\triangleright}(\kappa)$ and $\mathcal{B}_{\triangle}(\kappa)$ are the maximal connected components of $(\mathbb{C} \setminus \overline{\mathcal{E}}_{gO}(\kappa)) \cap \mathcal{E}_{gH}(\kappa)$ that intersect the positive real and imaginary axes respectively.

Referring to (7.61) finally motivates the following definition of $E = E(\mu; \kappa)$ for all $\kappa \in \mathbb{R} \setminus \{-1, 1\}$.

Definition 10 (Parameter $E = E(\mu; \kappa)$ for Boutroux curves) If $\kappa \in (-1, 1)$, $E = E(\mu; \kappa)$ is defined on $\mathcal{B}_{\square}(\kappa) \cup \mathcal{B}_{\triangleright}(\kappa) \cup \mathcal{B}_{\triangle}(\kappa)$ by obtaining E on the real and imaginary axes and continuing the solution of (4.23) to the three domains as explained in Sect. 4.4. The definition is then extended to $\mu \in (-\mathcal{B}_{\triangleright}(\kappa)) \cup (-\mathcal{B}_{\triangle}(\kappa))$ by odd reflection. If instead $\pm \kappa > 1$, then $E(\mu; \kappa)$ is defined by

$$E(\mu;\kappa) := \left(\frac{2}{1\pm\kappa}\right)^{3/2} \left[E\left(\sqrt{\frac{1}{2}(1\pm\kappa)}\mu; I^{\pm}(\kappa)\right) - 4(\kappa\mp1)\sqrt{\frac{1}{2}(1\pm\kappa)}\mu \right],$$

$$\pm\kappa > 1,$$



where the Möbius transformations $I^+:(1,+\infty)\to (-1,1)$ and $I^-:(-\infty,-1)\to (-1,1)$ defined in (1.23) are both involutions ($I^\pm(I^\pm(\kappa))=\kappa$).

The fact that this definition makes sense for $\kappa \in (-1, 1)$ was proved for $\mu \in \mathcal{B}_{\square}(\kappa)$ in Sect. 8.6 and just above for $\mu \in \mathcal{B}_{\triangleright}(\kappa) \cup \mathcal{B}_{\triangle}(\kappa)$.

8.10 Proofs of Proposition 2 and Theorems 1 and 2

The most important qualitative properties of $\partial \mathcal{E}_{gH}(\kappa)$ and $\partial \mathcal{E}_{gO}(\kappa)$ are given in Proposition 2 from Sect. 1.4, whose proof we now give.

Proof of Proposition 2 To prove item (1a) in the case $\kappa \in (-1,1)$, we observe that according to Definitions 7 and 8 from Sects. 8.5 and 8.8 respectively, $\partial \mathcal{E}_{gH}(\kappa)$ and $\partial \mathcal{E}_{gO}(\kappa)$ are Jordan curves by the fact that ∂S_{gO} and ∂S_{gH} are Jordan curves in the t-plane and the univalence of the map $t \mapsto \mu^2$ defined by (8.4) established in Lemmas 12 and 16 in Sects. 8.5 and 8.8 respectively. Schwarz reflection symmetry of the preimage curves ∂S_{gH} and ∂S_{gO} is preserved under $t \mapsto \mu^2$; then the double-valued square root map $\mu^2 \mapsto \mu$ yields Schwarz symmetry in both real and imaginary axes for $\partial \mathcal{E}_{gO}(\kappa)$ and $\partial \mathcal{E}_{vH}(\kappa)$.

Since the images of t=a,b are the four solutions of $B(\mu;\kappa)=0$ (cf. (1.17)) on the real and imaginary axes while the images of $t=\tau,\tau^*$ are the four remaining solutions, and since the image under $t\mapsto \mu^2\mapsto \mu$ of every v-trajectory in K_t of the rational quadratic differential $\Phi'(t)^2\,\mathrm{d}t^2$ is an analytic arc, items (1b) and (1c) are proved for $\kappa\in(-1,1)$ as well. Finally, item (1d) is proved for $\kappa\in(-1,1)$ by Lemma 18 in Sect. 8.8. To prove items (1a)–(1d) for $\kappa>1$ or $\kappa<-1$, we just use Definitions 7 and 8 to relate $\partial\mathcal{E}_{\mathrm{gH}}(\kappa)$ and $\partial\mathcal{E}_{\mathrm{gO}}(\kappa)$ respectively to corresponding curves with $\kappa\in(-1,1)$ by homothetic dilation (and use an easily verified dilation symmetry of the branch point equation $B(\mu;\kappa)=0$).

To prove item (2), we observe that if $\kappa \in (-1,1)$, the identities $\partial \mathcal{E}_{gH}(-\kappa) = i\partial \mathcal{E}_{gH}(\kappa)$ and $\partial \mathcal{E}_{gO}(-\kappa) = i\partial \mathcal{E}_{gO}(\kappa)$ on the first line of (1.23) follow from Definitions 7 and 8 respectively, because $\kappa \mapsto -\kappa$ is equivalent to $w \mapsto -w$. Thus one sees from (8.8) that the union of v-trajectories of $\Phi'(t)^2 dt^2$ is invariant under $(\kappa,t)\mapsto (-\kappa,-t)$, so S_{gO} and S_{gH} are reflected through the origin in the t-plane by $\kappa\mapsto -\kappa$. But (8.4) shows that $(\kappa,t)\mapsto (-\kappa,-t)$ implies $\mu^2\mapsto -\mu^2$, which proves the identities. The identities on the second line of (1.23) relate curves $\partial \mathcal{E}_{gH}(\kappa)$ and $\partial \mathcal{E}_{gO}(\kappa)$ for $\pm \kappa > 0$ to the same objects for $\kappa \in (-1,1)$; they are nothing but the definitions of $\partial \mathcal{E}_{gH}(\kappa)$ and $\partial \mathcal{E}_{gO}(\kappa)$ for $\pm \kappa > 1$ given in Definition 7 and 8 respectively, rewritten using the involutive property $I^\pm(I^\pm(\kappa)) = \kappa$. A description of other nontrivial elements of the symmetry group obtained by composing the identities in (1.23) is given in Sect. 1.4 immediately following the statement of Proposition 2. The statement that the curves $\partial \mathcal{E}_{gH}(\kappa)$ and $\partial \mathcal{E}_{gO}(\kappa)$ are invariant under rotation by $\frac{\pi}{2}$ for $\kappa = -3$, 0, 3 then follows from the identities on the first line of (1.23) for $\kappa = 0$ and the fact that $I^\pm(0) = \pm 3$.

Finally, items (3c) and (3d) for $\kappa \in (-1, 1)$ follow from the composition of maps written in (8.10) using the univalence asserted by Lemmas 12 and 16 respectively, and from Lemma 19 in Sect. 8.8. Then, items (3a), (3b), and (3d) for $\pm \kappa > 0$ follow from items (3c) and (3d) for $\kappa \in (-1, 1)$ using Lemma 5 in Sect. 5.4.



At last, we can complete the proofs of Theorems 1 and 2 stated in Sect. 1.4.

Proof of Theorem 1 Combining Lemma 8 from Sect. 6.5 with Lemma 13 and Definition 7 from Sect. 8.5 and using $\Theta_0 = \Theta_{0,\mathrm{gH}}^{[3]}(m,n)$, $\Theta_{0,\updownarrow} = \Theta_{0,\mathrm{gH}}^{[1]}(m,n)$, $\Theta_{\infty} = \Theta_{\infty,\mathrm{gH}}^{[3]}(m,n)$, and $\Theta_{\infty,\updownarrow} = \Theta_{\infty,\mathrm{gH}}^{[1]}(m,n)$ proves (1.24) for types 1 and 3 in the sense of pointwise convergence. Then since the hypotheses of Lemma 8 hold at every point of $\mathcal{E}_{\mathrm{gH}}(\kappa)$, Lemma 9 from Sect. 6.5 provides uniformity of the estimates on closed subsets of $\mathcal{E}_{\mathrm{gH}}(\kappa)$. The corresponding formula for type 2 follows from (2.2) and (2.3).

Proof of Theorem 2 In a similar way, combining Lemma 6 from Sect. 5.5 with Lemma 17 and Definition 8 from Sect. 8.8 proves (1.25) for types 1 and 3 in the pointwise sense for each point $\mu \in \mathcal{E}_{gO}(\kappa)$, in which $\Theta_0 = \Theta_{0,gO}^{[3]}(m,n)$, $\Theta_{0,\uparrow} = \Theta_{0,gO}^{[1]}(m,n)$, $\Theta_{\infty} = \Theta_{\infty,gO}^{[3]}(m,n)$, and $\Theta_{\infty,\uparrow} = \Theta_{\infty,gO}^{[1]}(m,n)$. Then uniformity on closed subsets of $\mathcal{E}_{gO}(\kappa)$ follows from Lemma 7 in Sect. 5.5, and the formula for type 2 follows from (2.2) and (2.3).

8.11 Proofs of Proposition 3 and Theorems 3 and 4

The most important properties of the function $E(\mu; \kappa)$ (see Definition 10 in Sect. 8.9) are summarized in Proposition 3 from Sect. 1.4, whose proof we now give.

Proof of Proposition 3 That $E(\mu; \kappa)$ satisfies the Boutroux equations (1.26) if $\kappa \in (-1, 1)$ is a direct consequence of the definition. Combining (7.61) with the identity (7.67) then shows that when the definition of E is extended to $\pm \kappa > 1$ as indicated in Definition 10 the same holds for $|\kappa| > 1$. For $\kappa \in (-1, 1)$, smoothness on each open component follows from the Implicit Function Theorem used as described in Sect. 4.4, and the fact that E extends continuously to the boundary of each component follows from the fact that the boundaries correspond to degenerate Boutroux curves for which E is well defined. These properties then directly extend to $|\kappa| > 1$ by the definition. The symmetry (1.27) is just a direct consequence of Definition 10, while (1.28) holds for $\kappa \in (-1, 1)$ according to (4.30) and then extends to $|\kappa| > 1$ again just from the definition.

Now we can give the proof of Theorems 3 and 4 formulated in Sect. 1.4.

Proof of Theorems 3 and 4 Since the Boutroux domains and the function $E(\mu; \kappa)$ defined on them have been properly specified, the hypotheses formulated in Sect. 7.2 are now rigorously established by independent arguments. Hence the results of Sect. 7 conditioned on those hypotheses all hold on well-defined Boutroux domains.

In particular, the approximations (1.29) and (1.30) with $f(\zeta - \zeta_0)$ written in the form (1.31) are proved in Sect. 7.7 under a technical condition that is ultimately removed in Sect. 7.10. The fact that $f(\zeta - \zeta_0)$ is an elliptic function of ζ solving the differential equation (1.18) is then proved in Sect. 7.8.

Acknowledgements The authors thank Davide Masoero and Pieter Roffelsen for useful discussions and Guilherme Silva for information about trajectories of rational quadratic differentials and for suggesting the



possibility of representing the arcs of the curves $\partial \mathcal{E}_{gH}(\kappa)$ and $\partial \mathcal{E}_{gO}(\kappa)$ in the μ -plane in terms of such trajectories. Two anonymous referees also made valuable suggestions that improved the manuscript. R. J. Buckingham was supported by National Science Foundation (grants DMS-1615718 and DMS-2108019). P. D. Miller was supported by the National Science Foundation (grants DMS-1513054 and DMS-1812625).

Appendix A. Selected Plots of Poles and Zeros

For the reader's convenience, in this appendix we present larger versions of certain subplots from Figs. 33 and 34.

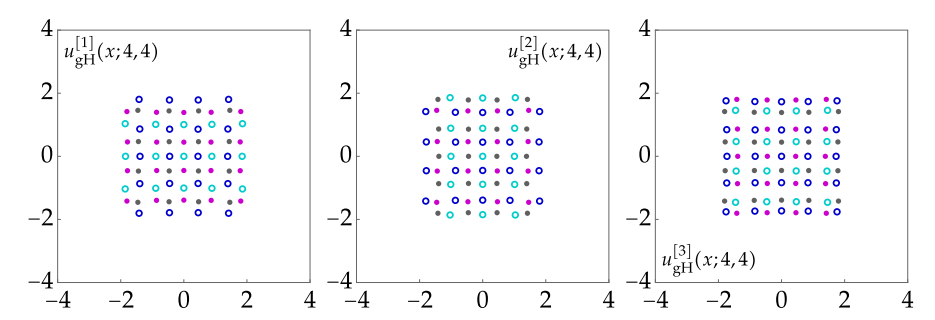


Fig. 33 Representative plots of poles (dots; magenta for residue +1 and gray for residue -1) and zeros (circles; cyan for positive derivative and blue for negative derivative) of the three types of rational solutions in the gH family. See also Fig. 3 (Color figure online)

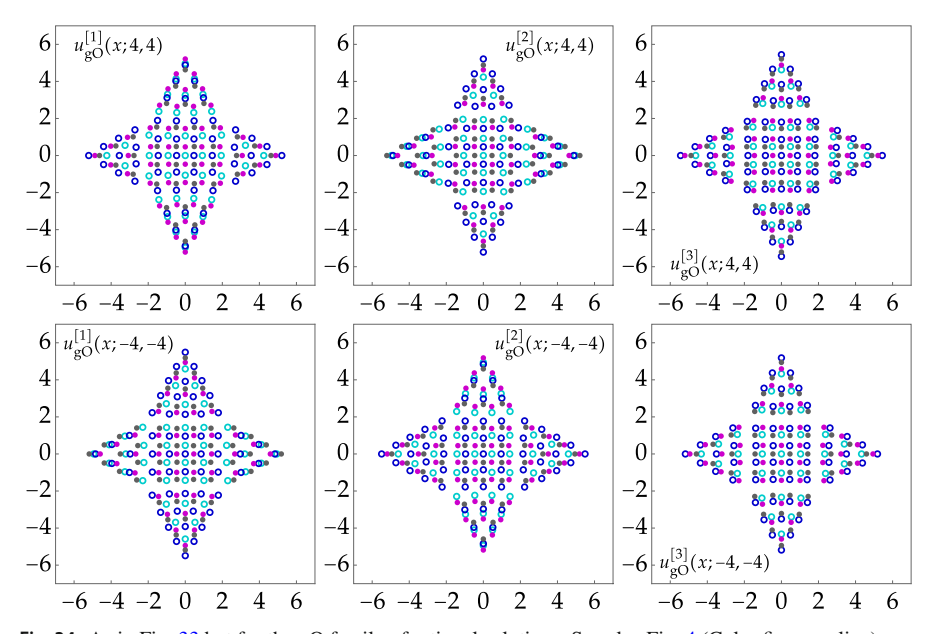


Fig. 34 As in Fig. 33 but for the gO family of rational solutions. See also Fig. 4 (Color figure online)



Appendix B. Branch Points of Equilibria

Recall that Proposition 1 formulated in Sect. 1.3 describes several properties of the branch points μ satisfying the eighth-degree polynomial equation $B(\mu; \kappa) = 0$ (see (1.17)). We now prove this proposition.

Proof of Proposition 1 Since for all $\kappa \in \mathbb{R}$ we have $B(\mu; \kappa) = B(\mu^*; \kappa)^* = B(-\mu; \kappa)$ it is obvious that the set of roots is symmetric in reflection through both the real and imaginary μ -axes, which proves (i).

The discriminant, i.e., the polynomial resultant of $B(\cdot; \kappa)$ and $B'(\cdot; \kappa)$, whose vanishing is equivalent to the existence of non-simple roots of $B(\cdot; \kappa)$, is proportional to $(\kappa^2 - 1)^8(\kappa^2 + 3)^2$. Hence the condition $\kappa \in \mathbb{R} \setminus \{-1, 1\}$ implies that all eight roots of $B(\mu; \kappa) = 0$ are simple, which proves (ii).

To prove (iii), first observe that $B(\mu; 1) = (\mu^2 - 4)^3(\mu^2 + 12)$, which has a conjugate pair of simple purely imaginary roots at $\mu = \pm i\sqrt{12}$ and two triple real roots at $\mu = \pm 2$. If we consider $\kappa = 1 + \epsilon$ for small positive ϵ , then by symmetry there will be again a pair of purely imaginary simple roots of $B(\mu; 1 + \epsilon)$, and by appropriate rescaling of $\mu \mp 2$ with ϵ one finds that each triple root splits a triad of three nearby simple roots of the form $\mu = \pm 2(1 + e^{2\pi i k/3} \epsilon^{2/3} (864)^{1/3} + \mathcal{O}(\epsilon))$ as $\epsilon \downarrow 0$, where $k = 0, \pm 1$. In particular, this shows that for κ just greater than 1, $B(\mu; \kappa)$ has eight simple roots comprising two opposite purely real and purely imaginary pairs in addition to a complex quartet of roots symmetric with respect to reflection through the real and imaginary axes. Since non-simple roots of $B(\cdot; \kappa)$ can only occur for real $\kappa = \pm 1$, there can be no collisions of roots of $B(\cdot; \kappa)$ as κ increases from 1, and together with the reflection symmetry of the roots in the real and imaginary axes this implies that for all $\kappa > 1$ the roots of $B(\cdot; \kappa)$ are all simple, with opposite real and imaginary pairs in addition to a symmetric complex quartet of roots, just as for $\kappa = 1 + \epsilon$ with $\epsilon > 0$ small. If instead we consider $-1 < \kappa < 1$, a very similar argument goes through; now one should replace ϵ with $-\epsilon < 0$ small and negative to perturb from $\kappa = 1$ in the negative direction, and the perturbation analysis produces an extra factor of $e^{2\pi i/3}$ on the subleading term $\mu \approx \pm 2$ which of course just means re-indexing k. So we again have the same triads of nearby roots, and since there can be no non-simple roots of $B(\cdot; \kappa)$ for $-1 < \kappa < 1$ the same picture persists throughout this interval as well. Finally, we observe that $B(\mu; \kappa) = B(i\mu; -\kappa)$, so the branch point configuration for $\kappa < -1$ follows immediately from that for $-\kappa > 1$ by rotation in the complex μ -plane by $\frac{\pi}{2}$.

It follows in particular that for all $\kappa \in \mathbb{R} \setminus \{-1, 1\}$, in each of the four open half-planes $\pm \operatorname{Re}(\mu) > 0$, $\pm \operatorname{Im}(\mu) > 0$, there is a triad of simple roots of $B(\cdot; \kappa)$ symmetric with respect to reflection through the real or imaginary axis bisecting the half-plane in question, and further characterized by the following additional remarkable property.

Now we show that each of the triads form the vertices of an equilateral triangle. Any configuration of eight points symmetric with respect to the real and imaginary axes and consisting of the vertices of two opposite equilateral triangles in the open right and left half-planes together with a conjugate pair of purely imaginary points



must be the roots of a polynomial $b(\mu; c, d, e)$ of the form

$$b(\mu; c, d, e) := ((\mu - c)^3 - d^3)((\mu + c)^3 + d^3)(\mu^2 + e^2)$$
 (B.1)

for real parameters c (the centers of the triangles of vertices in the open right and left half-planes are $\mu=\pm c$), d (the distance from the center of each triangle to any of its vertices is |d|), and e (the purely imaginary conjugate pair of roots is $\mu=\pm ie$). Equating the coefficients of powers of μ between $B(\mu;\kappa)$ given by (1.17) and $b(\mu;c,d,e)$ given by (B.1), we see that $B(\mu;\kappa)$ can be written in the form $b(\mu;c,d,e)$ provided that $e^2=3c^2$ (matching the coefficients of μ^6) and that after eliminating e^2 ,

$$c^4 + cd^3 = 4(\kappa^2 + 3)$$
 (matching the coefficients of μ^4), (B.2)

$$8c^6 - 20c^3d^3 - d^6 = -64\kappa(\kappa^2 - 9)$$
 (matching the coefficients of μ^2), and (B.3)

$$c^{8} + 2c^{5}d^{3} + c^{2}d^{6} = 16(\kappa^{2} + 3)^{2}$$
 (matching the constant terms). (B.4)

Obviously (B.2) implies (B.4), so there are only two conditions: (B.2) and (B.3), which amount to two equations on the two remaining unknowns c and d. We can eliminate d^3 explicitly using (B.2):

$$d^3 = \frac{4(\kappa^2 + 3) - c^4}{c}. ag{B.5}$$

Using this in (B.3) one arrives at an eighth-degree polynomial equation for c. Comparing with (1.17), it is easy to see that the equation on c is exactly $B(\sqrt{3}ic;\kappa)=0$. For all $\kappa\in\mathbb{R}\setminus\{-1,1\}$ we can therefore determine a unique positive solution $c=c(\kappa)>0$ that corresponds to the unique positive imaginary root of $B(\cdot;\kappa)$. Therefore, with d^3 determined from $c(\kappa)>0$ by (B.5) and with $e^2=3c(\kappa)^2$, we have the identity $B(\mu;\kappa)=b(\mu;c,d,e)$ which proves that $B(\cdot;\kappa)$ has two opposite triads of roots forming the vertices of equilateral triangles with centers $\pm c(\kappa)\neq 0$, along with the purely imaginary pair $\mu=\pm ie=\pm\sqrt{3}ic(\kappa)$.

We next check that d>0 (which ensures that the real vertex of each triangle is further from the origin than the center) and that d<2c (which ensures that all three vertices of each triangle lie in the same right or left half-plane as the center). But these inequalities hold for $\kappa=1\pm\epsilon$ and $\epsilon>0$ sufficiently small by the perturbation theory described above, which in particular localizes the triangles near $\mu=\pm 2$. Putting d=0 into (B.2)–(B.3) and eliminating c yields $\kappa=\pm 1$, so d>0 for $\kappa=1\pm\epsilon$ with $\epsilon>0$ small implies that d>0 for all $\kappa\in(-1,1)$ and all $\kappa>1$. Likewise, putting d=2c into (B.2)–(B.3) and eliminating c yields again $\kappa=\pm 1$, so d<2c for $\kappa=1\pm\epsilon$ with $\epsilon>0$ small implies that d<2c holds for all $\kappa\in(-1,1)$ and all $\kappa>1$. This finally shows that if $\kappa\in(-1,1)$ or $\kappa>1$, the roots of $B(\mu;\kappa)$ in the open right (left) half-plane form the vertices of an equilateral triangle symmetric with respect to reflection in the real axis and with its real vertex lying to the right (left) of its center. By $B(\mu;\kappa)=B(i\mu;-\kappa)$ a similar statement governs the roots of $B(\mu;\kappa)$ in the open upper/lower half-planes for $\kappa<-1$.



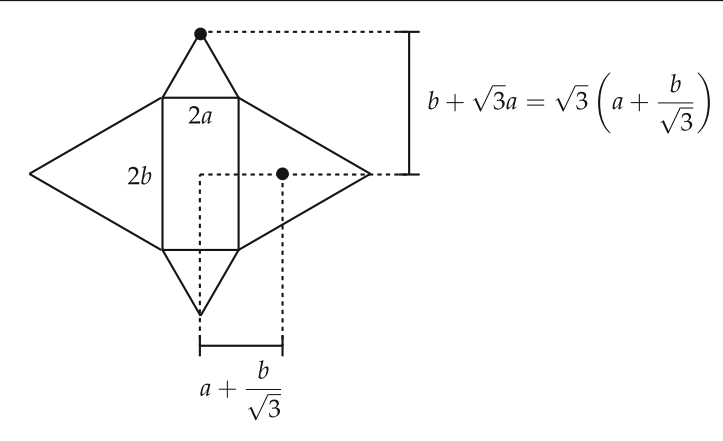


Fig. 35 For any configuration of equilateral triangles attached to the edges of a rectangle centered at the origin, the distance of the extremal vertex of any triangle from the origin is proportional by $\sqrt{3}$ to the distance of the center of either neighboring triangle to the origin (Color figure online)

For $\kappa \in (-1,1)$ or $\kappa > 1$, the remaining two roots form a purely imaginary pair $\mu = \pm \sqrt{3} \mathrm{i} c(\kappa)$ following from the identity $e^2 = 3c^2$. Some simple trigonometry illustrated in Fig. 35 then shows that the triads of roots in the open upper and lower half-planes also form the vertices of opposite equilateral triangles with their imaginary vertices further from the origin than their centers. (Alternatively, the whole argument of equating $B(\mu;\kappa)$ with $b(\mu;c,d,e)$ can be repeated replacing $b(\mu;c,d,e)$ with a polynomial of the form $((\mu-\mathrm{i}c)+\mathrm{i}d^3)((\mu+\mathrm{i}c)-\mathrm{i}d^3)(\mu^2-e^2)$ for real c,d, and e, modeling a pair of opposite real roots and two opposite equilateral triangles of roots in the upper and lower half-planes.) For $\kappa < -1$ the rotation symmetry $B(\mu;\kappa) = B(\mathrm{i}\mu;-\kappa)$ shows that the triads of roots in the right/left half-planes form the vertices of equilateral triangles. This finally proves (iii) and completes the proof of the proposition.

Appendix C. Formal Painlevé-I Approximation Near Branch Points

Suppose that μ is one of the eight branch points solving (1.17), and that U_0 is a corresponding double root of the equilibrium problem (1.15). We wish to examine solutions of the Painlevé-IV equation (1.1) that are in a sense close to $T^{1/2}U_0$ for x close to $T^{1/2}\mu$, where we recall that the parameters are large in the sense that (1.13) holds with $T\gg 1$ and $\kappa\in\mathbb{R}\setminus\{-1,1\}$. It turns out that the correct scaling is to write

$$u = T^{1/2}(U_0 + T^{-2/5}h)$$
 and $x = T^{1/2}\mu + T^{-3/10}z$

for new dependent and independent variables h and z, respectively. We substitute these into (1.1) and use the assumption that U_0 is a double root of the equilibrium equation (1.15) to remove two suites of terms from the resulting equation. The result is the



formal asymptotic (assuming h and z bounded)

$$\frac{\mathrm{d}^2 h}{\mathrm{d}z^2} = 6(U_0 + \mu)h^2 + 4U_0(U_0 + \mu)z + 2T^{-1/5}U_0 + \mathcal{O}(T^{-2/5}), \quad T \to \infty.$$

This is essentially a perturbation of the Painlevé-I equation. Indeed, if we rescale the variables by

$$w = d\left(z + \frac{T^{-1/5}}{2(U_0 + \mu)}\right) \quad \text{and} \quad h = cH,$$

then if c and d are chosen so that

$$d^5 = 4U_0(U_0 + \mu)^2$$
 and $c = 4U_0(U_0 + \mu)d^{-3}$,

we obtain

$$H''(w) = 6H(w)^2 + w + \mathcal{O}(T^{-2/5})$$

which puts the Painlevé-I approximating equation into canonical form. Note that c and d are well defined modulo the symmetry $(c,d)\mapsto (\mathrm{e}^{-6\pi\mathrm{i}/5}c,\mathrm{e}^{2\pi\mathrm{i}/5}d)$, for which it suffices to show that $U_0\neq 0$ and $U_0+\mu\neq 0$. But $U_0\neq 0$ follows easily from the fact that (1.15) has a nonzero constant term. Writing $U_0=(U_0+\mu)-\mu$, we can rewrite (1.15) as a quartic in $U_0+\mu$ with constant term $-\frac{1}{2}(\mu^4-8\kappa\mu^2+16)$. Setting the latter constant term to zero and eliminating μ between this condition and the branch point condition $B(\mu;\kappa)=0$ (cf. (1.17)) yields the condition that κ should satisfy either $\kappa=\pm 1$ or $375\kappa^2+3721=0$, neither of which are possible for $\kappa\in\mathbb{R}\setminus\{-1,1\}$. Hence it also follows that $U_0+\mu\neq 0$.

This formal analysis suggests that solutions u(x) of Painlevé-IV for large $T = |\Theta_0|$ and fixed $\kappa = -\Theta_{\infty}/T \in \mathbb{R} \setminus \{-1, 1\}$ can behave like solutions of the Painlevé-I equation when $xT^{-1/2}$ is close to one of the eight branch points satisfying (1.17), provided that also $u \approx T^{1/2}U_0$ for a branching equilibrium U_0 in some overlap domain. The particular solution(s) of Painlevé-I that would be relevant is not clear from this formal analysis. However, in [47] one finds the conjecture that for the gH family of rational solutions one should select a tritronquée solution of Painlevé-I, and in light of the result of [15] that any poles or zeros of u should be confined to a region that forms a sector with vertex at a complex branch point μ and opening angle $\frac{2\pi}{5}$ this is a very reasonable hypothesis. Based on Theorem 2, one should also expect Painlevé-I tritronquée asymptotics near the branch points on the real and imaginary axes for the gO family of rational solutions. While the proofs of these tritronquée convergence results have yet to be given, a similar result has been proven rigorously for rational solutions of the Painlevé-II equation in [19]. Near the remaining branch points the pole-free sector of the gO rational solutions is smaller, and one can only reasonably anticipate the appearance of a tronquée solution of Painlevé-I. Such solutions form a one-parameter family containing the tritronquée solutions as finitely many special cases, so just to



formulate a precise conjecture one would need to single out a particular tronquée solution of Painlevé-I. We note that the formal connection between Painlevé-IV and Painlevé-I is apparently not a direct link in the "coalescence cascade" of Painlevé equations reported in [53, §32.2(vi)]; in the latter, solutions of Painlevé-IV degenerate to solutions of the Painlevé-II equation, which in turn can degenerate into solutions of Painlevé-I. We also note there is a connection between Bäcklund transformations for the Painlevé-IV equation and the discrete Painlevé-I equation [32, 34].

Appendix D. Rational Painlevé-IV Solutions Near the Origin

By substituting appropriate Taylor or Laurent series into (1.1) one easily sees that for any solution u(x), all poles must be simple with residue ± 1 and for $\Theta_0 \neq 0$ all zeros $x = x_0$ must be simple with $u'(x_0) = \pm 4\Theta_0$. It follows from Proposition 4 in Sect. 2 that only odd powers of x appear in the power series expansion of any rational solution u(x) about x = 0. This allows one to determine sufficiently many terms from the four possible leading terms $\pm x^{-1}$ and $\pm 4\Theta_0 x$ for given $(\Theta_0, \Theta_\infty)$ admitting a rational solution to apply the four elementary isomonodromic Bäcklund transformations $u(x) \mapsto u_\nearrow(x)$, $u(x) \mapsto u_\nearrow(x)$, $u(x) \mapsto u_\nearrow(x)$, and $u(x) \mapsto u_\nearrow(x)$ (see (3.48), (3.49), (3.50), and (3.51) respectively in Sect. 3.3) and deduce the leading term of the expansion at x = 0 of the image function, also a rational solution of (1.1) for a nearest-neighbor point in the same parameter lattice (depending on the family). Therefore, starting from any one point in $\Lambda_{\rm gH} \sqcup \Lambda_{\rm gO}$, one can prove the following by induction.

Proposition 13 In the limit $x \to 0$, the leading terms of $u_F^{[j]}(x; m, n)$, F = gH or F = gO and j = 1, 2, 3, depend only on the type j and the parity of the indices (m, n) as follows:

$u_{\mathrm{F}}^{[1]}(x;m,n)$	m even	m odd	
n even	$-4\Theta_{0,F}^{[1]}(m,n)x + \mathcal{O}(x^3)$	$4\Theta_{0,\mathrm{F}}^{[1]}(m,n)x + \mathcal{O}(x^3)$	(D.1)
n odd	$x^{-1} + \mathcal{O}(x)$	$-x^{-1} + \mathcal{O}(x)$	

$u_{\mathrm{F}}^{[2]}(x;m,n)$	m even	m odd	
n even	$-4\Theta_{0,F}^{[2]}(m,n)x + \mathcal{O}(x^3)$	$-x^{-1} + \mathcal{O}(x)$	(D.2)
n odd	$4\Theta_{0,F}^{[2]}(m,n)x + \mathcal{O}(x^3)$	$x^{-1} + \mathcal{O}(x)$	

$u_{\mathrm{F}}^{[3]}(x;m,n)$	m even	m odd	
n even	$-4\Theta_{0,F}^{[3]}(m,n)x + \mathcal{O}(x^3)$	$x^{-1} + \mathcal{O}(x)$	(D.3)
n odd	$-x^{-1} + \mathcal{O}(x)$	$4\Theta_{0,F}^{[1]}(m,n)x + \mathcal{O}(x^3)$	

Theorems 3 and 4 formulated in Sect. 1.4 assert the accuracy of the approximation of $u_F^{[j]}(x; m, n)$ by an elliptic function $f(\zeta - \zeta_0)$ solving the autonomous model equation (1.18); in particular this applies in the special case that $\mu = 0$, which always lies in



 $\mathcal{B}_{\square}(\kappa)$ for all parameter values, and that ζ is bounded. In this case, by Proposition 3 in Sect. 1.4, we also have E=0. Furthermore, taking into account the identities (7.3) and (7.4) from Sect. 7.5, both of which hold if and only if $\mu=0$, as well as the condition that $(\Theta_0,\Theta_\infty)\in\Lambda_{\rm gH}\sqcup\Lambda_{\rm gO}$, one can show that the prediction of Corollary 2 formulated in Sect. 1.4 is exact in this special case. In other words, the pole or zero of $u_{\rm F}^{[j]}(x;m,n)$ that must lie at the origin according to Proposition 4 is captured exactly by the approximation formulæ of Theorems 3–4. Therefore, in this case we can determine the phase shift ζ_0 explicitly by enforcing the property that $f(\zeta-\zeta_0)$ have a zero with the same sign of derivative or a pole with the same residue at $\zeta=0$ as does the actual rational solution, as described in Proposition 13.

To do this, we first solve (1.18) with $\mu=0$ and E=0 subject to f(0)=0 and f'(0)=4 to obtain $f(\zeta)$ explicitly in terms of Jacobi elliptic functions (comparing with the notation of [53, Chapter 22] we prefer to write, e.g., $\operatorname{sn}(z|\mathfrak{m})$ in place of $\operatorname{sn}(z,k)$ where $\mathfrak{m}=k^2$), and express its pole and zero lattices in terms of the complete elliptic integrals of the first kind

$$\mathbb{K}(\mathfrak{m}) := \int_0^{\frac{1}{2}\pi} \frac{\mathrm{d}\theta}{\sqrt{1 - \mathfrak{m}\sin(\theta)}}, \quad \mathbb{K}'(\mathfrak{m}) := \mathbb{K}(1 - \mathfrak{m}).$$

This calculation depends only on whether $\kappa < -1, \kappa \in (-1, 1)$, or $\kappa > 1$ holds, and yields the following results.

 $\bullet \ \ If \ \kappa \ < -1 \ (i.e., for \ (\Theta_0, \Theta_\infty) \in \Lambda_{gH}^{[1]-} \sqcup \Lambda_{gO}^{[1]-} \sqcup \Lambda_{gO}^{[2]+}), \ then$

$$f(\zeta) = 2\mathfrak{m}^{1/4} \operatorname{sn} \left(2\mathfrak{m}^{-1/4} \zeta | \mathfrak{m} \right), \quad \mathfrak{m} := -1 + 2\kappa^2 + 2\kappa \sqrt{\kappa^2 - 1} \in (0, 1).$$
 (D.4)

It is known that $\operatorname{sn}(x|\mathfrak{m})$ has zeros at $x=2j\mathbb{K}(\mathfrak{m})+2ki\mathbb{K}'(\mathfrak{m})$ and poles at $x=2j\mathbb{K}(\mathfrak{m})+(2k+1)i\mathbb{K}'(\mathfrak{m})$ ($j,k\in\mathbb{Z}$). Since $\mathbb{K}(\mathfrak{m})$ and $\mathbb{K}'(\mathfrak{m})$ are both purely real, as is the scaling factor $2\mathfrak{m}^{-1/4}$, $f(\zeta)$ has rows of zeros alternating with rows of poles parallel to the real axis.

• If $\kappa > 1$ (i.e., for $(\Theta_0, \Theta_\infty) \in \Lambda_{gH}^{[2]-} \sqcup \Lambda_{gO}^{[1]+} \sqcup \Lambda_{gO}^{[2]-}$), then

$$f(\zeta) = 2(1-\mathfrak{m})^{1/4} \mathrm{sc} \left(2(1-\mathfrak{m})^{-1/4} \zeta \left| \mathfrak{m} \right|, \quad \mathfrak{m} := 2 - 2\kappa^2 + 2\kappa \sqrt{\kappa^2 - 1} \in (0, 1). \right) \tag{D.5}$$

The function $\mathrm{sc}(x|\mathfrak{m})$ has zeros at $x=2j\mathbb{K}(\mathfrak{m})+2ki\mathbb{K}'(\mathfrak{m})$ and poles at $x=(2j+1)\mathbb{K}(\mathfrak{m})+2ki\mathbb{K}'(\mathfrak{m})$ ($j,k\in\mathbb{Z}$). Since $\mathbb{K}(\mathfrak{m})$, $\mathbb{K}'(\mathfrak{m})$, and the scaling factor $2(1-\mathfrak{m})^{-1/4}$ are all purely real, $f(\zeta)$ has columns of zeros alternating with columns of poles parallel to the imaginary axis.

columns of poles parallel to the imaginary axis. • If $\kappa \in (-1,1)$ (i.e., for $(\Theta_0,\Theta_\infty) \in \Lambda_{gH}^{[3]+} \sqcup \Lambda_{gO}^{[3]+} \sqcup \Lambda_{gO}^{[3]-}$), then

$$f(\zeta) = 2e^{-i\pi/4} ((1-\mathfrak{m})\mathfrak{m})^{1/4} \operatorname{sd} \left(2e^{i\pi/4} ((1-\mathfrak{m})\mathfrak{m})^{-1/4} \zeta \, \Big| \mathfrak{m} \right),$$

$$\mathfrak{m} := \frac{1}{2} - \frac{i\kappa}{2\sqrt{1-\kappa^2}} = 1 - \mathfrak{m}^*.$$
(D.6)



This is the only case in which the elliptic modulus \mathfrak{m} is complex, in which case we use the principal branch square roots to interpret $\mathbb{K}(\mathfrak{m})$ and $\mathbb{K}'(\mathfrak{m})$; therefore as $\mathfrak{m}^* = 1 - \mathfrak{m}$ we also have $\mathbb{K}'(\mathfrak{m}) = \mathbb{K}(\mathfrak{m})^*$. The elliptic function $\mathrm{sd}(x|\mathfrak{m})$ has zeros at $x = 2j\mathbb{K}(\mathfrak{m}) + 2ki\mathbb{K}'(\mathfrak{m})$ and poles at $x = (2j+1)\mathbb{K}(\mathfrak{m}) + (2k+1)i\mathbb{K}'(\mathfrak{m})$ $(j,k\in\mathbb{Z})$. Since $\mathrm{arg}(\mathbb{K}(\mathfrak{m})+i\mathbb{K}'(\mathfrak{m})) = \frac{\pi}{4}$ and $\mathrm{arg}(-\mathbb{K}(\mathfrak{m})+i\mathbb{K}'(\mathfrak{m})) = \frac{3\pi}{4}$, the zeros and poles of $f(\zeta)$ form a "checkerboard" pattern with respective lattices spanned by basis vectors parallel to the coordinate axes and shifted by a half-period in each direction with respect to one another.

In all three cases, the theoretically predicted pattern qualitatively matches what one sees near the origin in the respective plots shown in Figs. 3 and 4 discussed in Sect. 1.2.

It remains to determine the phase shift ζ_0 by ensuring that the correct "sign" of pole or zero of $f(\zeta - \zeta_0)$ lies at $\zeta = 0$. Here the results depend not only on the sector of the parameter space shown in Fig. 1 but also on the parity of the indices (m, n) used to parametrize the allowed values of $(\Theta_0, \Theta_\infty)$. The results are as follows.

• Let $\kappa < -1$ and take $\mathfrak{m} \in (0,1)$ as in (D.4). If $(\Theta_{0,F}^{[1]}(m,n), \Theta_{\infty,F}^{[1]}(m,n)) \in \Lambda_F^{[1]-}$ (for either family F = gH or F = gO), then ζ_0 is given by

ζ0	m even	m odd
n even	0	$\frac{2\mathbb{K}(\mathfrak{m})}{2\mathfrak{m}^{-1/4}}$
n odd	$\frac{\mathrm{i}\mathbb{K}'(\mathfrak{m})}{2\mathfrak{m}^{-1/4}}$	$\frac{2\mathbb{K}(\mathfrak{m}) + i\mathbb{K}'(\mathfrak{m})}{2\mathfrak{m}^{-1/4}}$

If instead $(\Theta_{0,\mathrm{gO}}^{[2]}(m,n),\,\Theta_{\infty,\mathrm{gO}}^{[2]}(m,n))\in\Lambda_{\mathrm{gO}}^{[2]+}$, then ζ_0 is given by

ζ0	m even	m odd
n even	$\frac{2\mathbb{K}(\mathfrak{m})}{2\mathfrak{m}^{-1/4}}$	$\frac{2\mathbb{K}(\mathfrak{m}) + i\mathbb{K}'(\mathfrak{m})}{2\mathfrak{m}^{-1/4}}$
n odd	0	$\frac{\mathrm{i}\mathbb{K}'(\mathfrak{m})}{2\mathfrak{m}^{-1/4}}$

• Let $\kappa > 1$ and take $\mathfrak{m} \in (0, 1)$ as in (D.5). If $(\Theta_{0,gO}^{[1]}(m, n), \Theta_{\infty,gO}^{[1]}(m, n)) \in \Lambda_{gO}^{[1]+}$, then ζ_0 is given by

ζ0	m even	m odd
n even	$\frac{2i\mathbb{K}'(\mathfrak{m})}{2(1-\mathfrak{m})^{-1/4}}$	0
n odd	$\frac{\mathbb{K}(\mathfrak{m}) + 2i\mathbb{K}'(\mathfrak{m})}{2(1-\mathfrak{m})^{-1/4}}$	$\frac{\mathbb{K}(\mathfrak{m})}{2(1-\mathfrak{m})^{-1/4}}$



If instead $(\Theta_{0,F}^{[2]}(m,n), \Theta_{\infty,F}^{[2]}(m,n)) \in \Lambda_F^{[2]-}$ (for either family F = gH or F = gO), then ζ_0 is given by

ζ_0 m even		m odd
n even	0	$\frac{\mathbb{K}(\mathfrak{m})}{2(1-\mathfrak{m})^{-1/4}}$
n odd	$\frac{2i\mathbb{K}'(\mathfrak{m})}{2(1-\mathfrak{m})^{-1/4}}$	$\frac{\mathbb{K}(\mathfrak{m}) + 2i\mathbb{K}'(\mathfrak{m})}{2(1-\mathfrak{m})^{-1/4}}$

• Let $\kappa \in (-1, 1)$ and take $\kappa \in \mathbb{C}$ as in (D.6). If $(\Theta_{0,F}^{[3]}(m, n), \Theta_{\infty,F}^{[3]}(m, n)) \in \Lambda_F^{[3]+}$ (for either family F = gH or F = gO), then ζ_0 is given by

ζ_0 m even		m odd
n even	$\frac{2\mathbb{K}(\mathfrak{m})}{2\mathrm{e}^{\mathrm{i}\pi/4}((1-\mathfrak{m})\mathfrak{m})^{-1/4}}$	$\frac{-\mathbb{K}(\mathfrak{m}) + i\mathbb{K}'(\mathfrak{m})}{2e^{i\pi/4}((1-\mathfrak{m})\mathfrak{m})^{-1/4}}$
n odd	$\frac{\mathbb{K}(\mathfrak{m}) + i\mathbb{K}'(\mathfrak{m})}{2e^{i\pi/4}((1-\mathfrak{m})\mathfrak{m})^{-1/4}}$	0

If instead $(\Theta_{0,gO}^{[3]}(m,n), \Theta_{\infty,gO}^{[3]}(m,n)) \in \Lambda_{gO}^{[3]-}$, then ζ_0 is given by

ζ0	m even	m odd
n even	0	$\frac{-\mathbb{K}(\mathfrak{m}) + i\mathbb{K}'(\mathfrak{m})}{2e^{i\pi/4}((1-\mathfrak{m})\mathfrak{m})^{-1/4}}$
n odd	$\frac{\mathbb{K}(\mathfrak{m}) + i\mathbb{K}'(\mathfrak{m})}{2e^{i\pi/4}((1-\mathfrak{m})\mathfrak{m})^{-1/4}}$	$\frac{2\mathbb{K}(\mathfrak{m})}{2\mathrm{e}^{\mathrm{i}\pi/4}((1-\mathfrak{m})\mathfrak{m})^{-1/4}}$

These results are consistent in the gH case with [46, Corollary 1], a rigorous result describing the zeros of $H_{m,n}(x)$ near the origin as a locally regular lattice with spacings determined from complete elliptic integrals.

If we use the approach (ii) described in Sect. 1.4 in the discussion following Remark 4 in which a rational solution of Painlevé-IV is approximated locally near a given point μ by an exact elliptic function of ζ with a uniform lattice of poles and zeros, then we can easily use the knowledge of ζ_0 detailed above to illustrate the attraction of the actual poles and zeros to the uniform lattice for the case $\mu = 0$. This is shown for some gH rational solutions of types 1–3 in Figs. 36, 37, and 38.

These plots show the characteristic feature that since μ is fixed, the approximation for given ζ improves as the indices (m, n) increase, while for given (m, n) large it becomes less accurate as $|\zeta|$ grows. This is to be expected whether or not the approximation is exact at $\zeta = 0$.



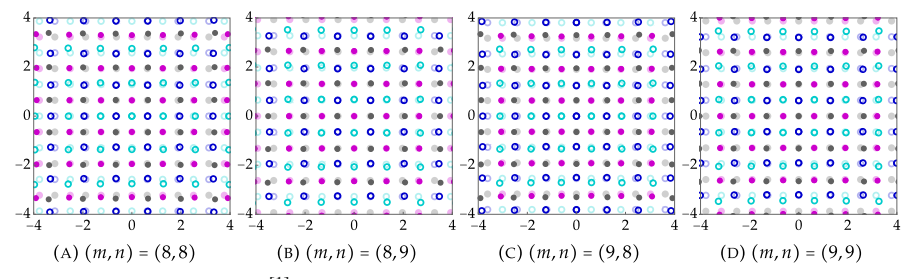


Fig. 36 Zeros and poles of $u_{\rm gH}^{[1]}(T^{-1/2}\zeta; m, n)$ in the ζ-plane (bold colors) and their large-T elliptic function approximations (faded colors). Cyan circles: zeros with positive derivative. Blue circles: zeros with negative derivative. Magenta dots: poles with positive residue. Grey dots: poles with negative residue. For the point at $\zeta = 0$ which corresponds to x = 0, these match the theoretical predictions of Proposition 13 (Color figure online)

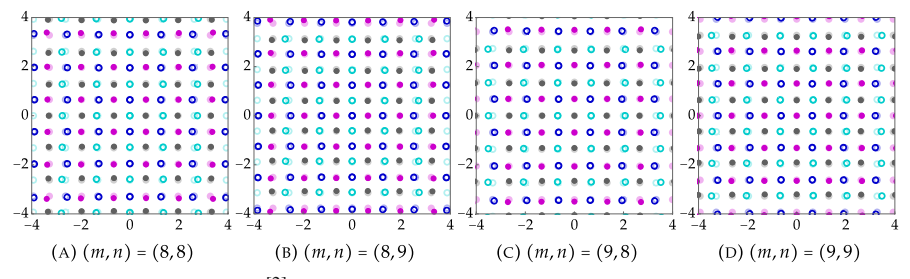


Fig. 37 As in Fig. 36 but for $u_{\text{gH}}^{[2]}(T^{-1/2}\zeta; m, n)$ (Color figure online)

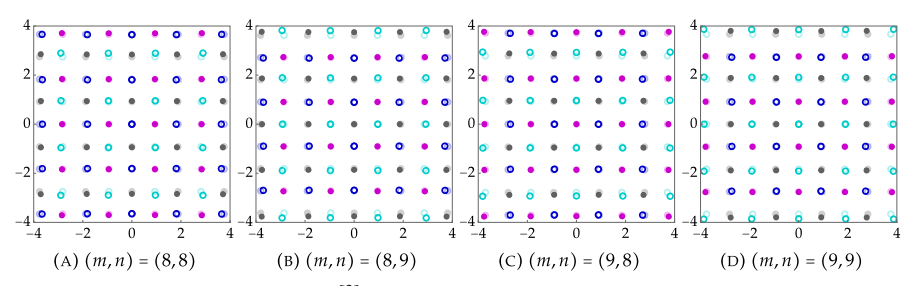


Fig. 38 As in Figs. 36 and 37 but for $u_{\rm gH}^{[3]}(T^{-1/2}\zeta;m,n)$ (Color figure online)

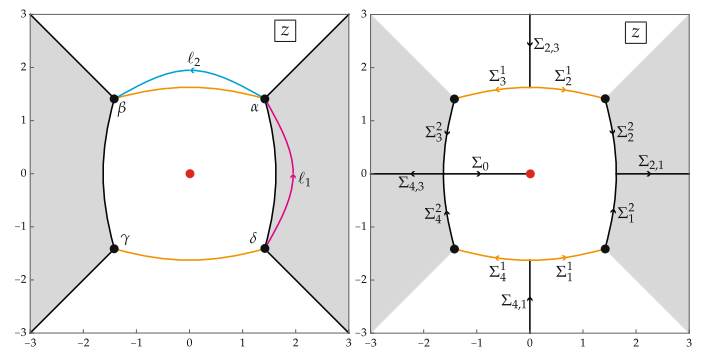
Appendix E. Diagrams and Tables for Steepest-Descent Analysis on Boutroux Domains

Here we gather *z*-plane diagrams and tables referred to in Sect. 7. In all plots gray shading means Re(h(z)) < 0 and white background means Re(h(z)) > 0.

E.1. The gO Case with $\mu \in \mathcal{B}_{\square}(\kappa)$ and s=1

Here we use representative values of $\mu = 0$ and $\kappa = 0$ (Fig. 39, Table 7).





(A) Left: Stokes graph including branch cuts (orange) for h'(z) and contours ℓ_1 and ℓ_2 appearing in (7.1). Right: arcs of the jump contour Σ for $\mathbf{M}(z)$; note that the arcs Σ_j^k , $j=1,\ldots,4$ and k=1,2, lie on the Stokes graph.

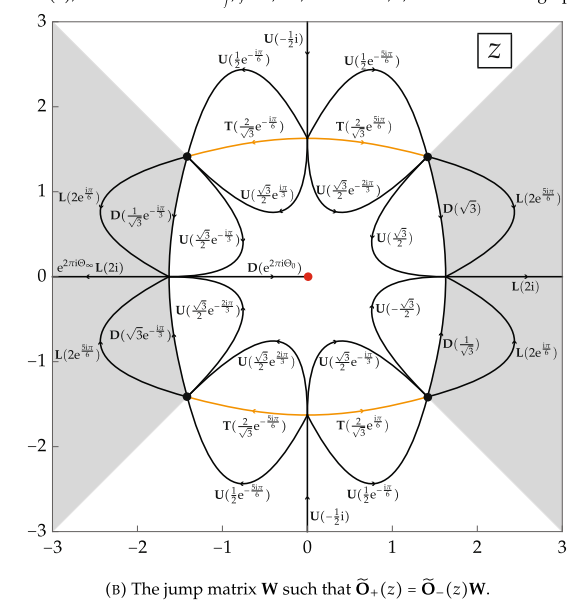


Fig. 39 Diagrams for the gO case with $\mu \in \mathcal{B}_{\square}(\kappa)$ and s=1 (Color figure online)



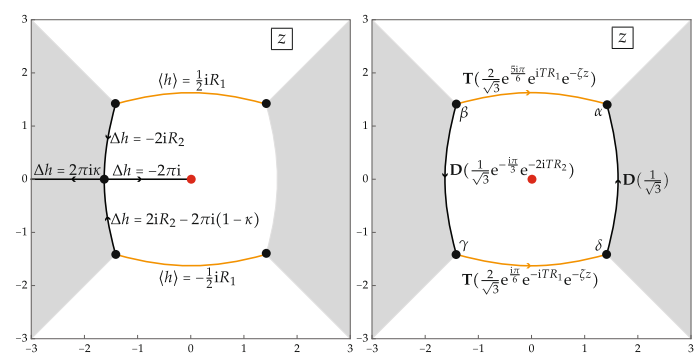


Fig. 39 continued

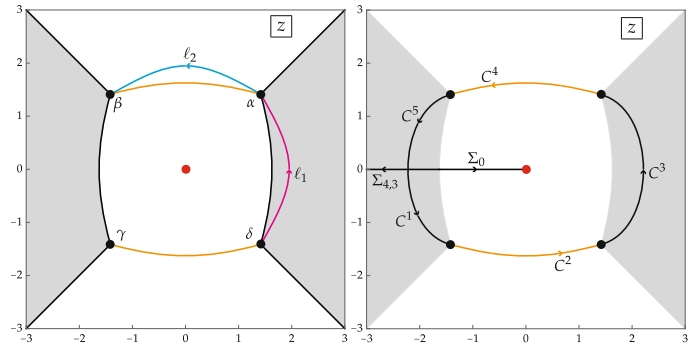
Table 7 Inner parametrix data for the gO case with $\mu \in \mathcal{B}_{\square}(\kappa)$ and s=1

p	Conformal map $W:D_p\to\mathbb{C}$	Ray Preimages in D_p		$\mathbf{C}(z)$ in D_p	
		arg(W)	Preimage	Value C	Subdomain of D_p
α	$(2h(z) - 2h(\alpha))^{2/3}$, continued from Σ_2^{1+}	0	Σ_2^{1+}	$\textbf{D}(\sqrt{\tfrac{3}{2}}e^{5i\pi/6})$	$D_{lpha}\cap\mathcal{D}_{\circ}$
	-	$\frac{2\pi}{3}$	$\Sigma_2^{1-}~\&~\Sigma_2^{2-}$		
		$-\frac{2\pi}{3}$	Σ_2^{2+}	$T(\sqrt{2}e^{2i\pi/3})$	$D_{lpha}\setminus \mathcal{D}_{\circ}$
		$\pm\pi$	Σ_2^2		
β	$(2h(z) - 2h(\beta))^{2/3}$, continued from Σ_3^{1-} ; $h(\beta)$ defined by limit along Σ_2^{1-}	0	Σ_3^{1-}	$\mathbf{D}(\sqrt{\frac{3}{2}}\mathbf{i})$	$D_eta\cap\mathcal{D}_{o}$
	23	$\frac{2\pi}{3}$	Σ_{2}^{2-}		
			-	$T(\sqrt{2}e^{i\pi/3})$	$D_eta \setminus \mathcal{D}_\circ$
		$\pm\pi$	Σ_3^2		
γ	$(2h(z) - 2h(\gamma))^{2/3}$, continued from Σ_4^{1+} ; $h(\gamma)$ defined by limit along Σ_4^{1+}	0	Σ_4^{1+}	$\mathbf{D}(\sqrt{\frac{3}{2}}\mathbf{i})$	$D_{\gamma}\cap\mathcal{D}_{\circ}$
	4	$\frac{2\pi}{3}$	$\Sigma_4^{1-}~\&~\Sigma_4^{2-}$		
		-		$\mathbf{T}(\sqrt{2}e^{2i\pi/3})$	$D_{\gamma}\setminus\mathcal{D}_{\circ}$
		$\pm\pi$	Σ_4^2		
8	$(2h(z) - 2h(\delta))^{2/3}$, continued from Σ_1^{1-}	0	Σ_1^{1-}	$\mathbf{D}(\sqrt{\frac{3}{2}}e^{i\pi/6})$	$D_\delta\cap\mathcal{D}_\circ$
	-	$\frac{2\pi}{3}$	Σ_1^{2-}		
		$-\frac{2\pi}{3}$	$\Sigma_1^{1+} \& \Sigma_1^{2+}$	$T(\sqrt{2}e^{i\pi/3})$	$D_\delta \setminus \mathcal{D}_\circ$
		$\pm\pi$	Σ_1^2		



E.2. The gH Case with $\mu \in \mathcal{B}_{\square}(\kappa)$ and s=1

Here we use representative values of $\mu = 0$ and $\kappa = 0$ (Fig. 40, Table 8).



(A) Left: Stokes graph including branch cuts (orange) for h'(z) and contours ℓ_1 and ℓ_2 appearing in (7.1). Right: arcs of the jump contour Σ for $\mathbf{M}(z)$; note that the arcs \mathbf{C}^2 and \mathbf{C}^4 lie on the Stokes graph.

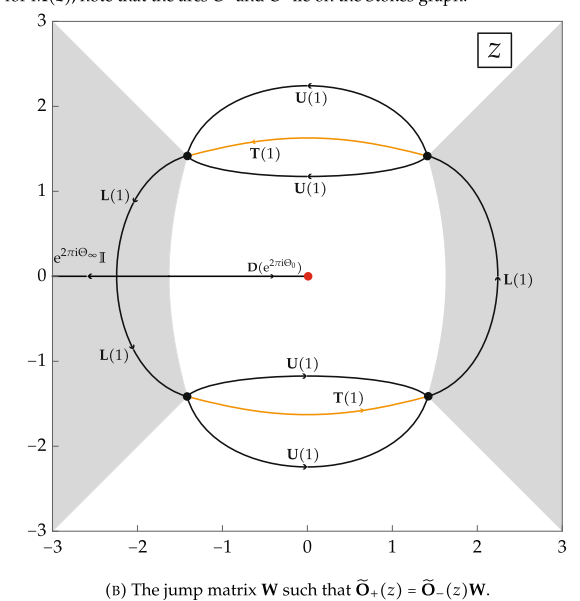


Fig. 40 Diagrams for the (only) gH case with $\mu \in \mathcal{B}_{\square}(\kappa)$ and s=1 (Color figure online)



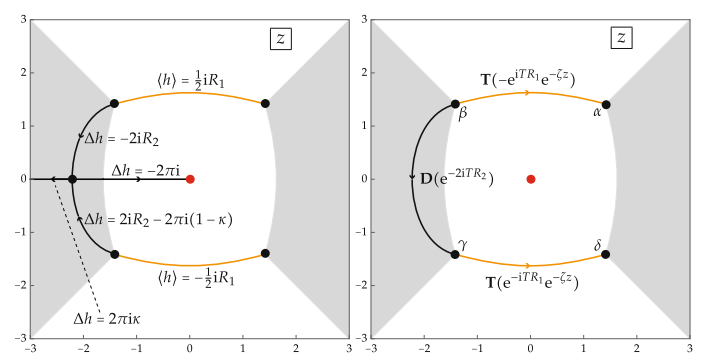


Fig. 40 continued

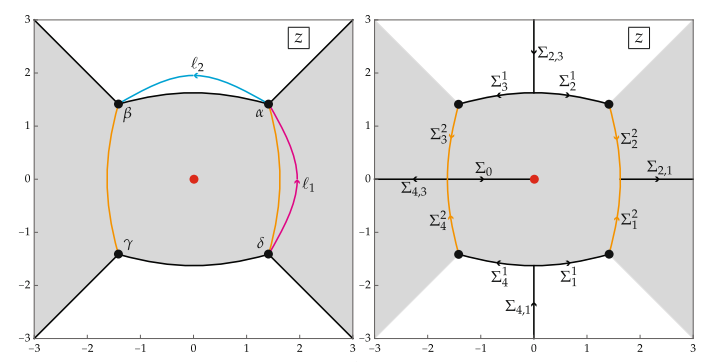
Table 8 Inner parametrix data for the (only) gH case with $\mu \in \mathcal{B}_{\square}(\kappa)$ and s=1

D	Conformal map $W:D_p o\mathbb{C}$	Ray Prei	mages in D_p	$\mathbf{C}(z)$ in D_p	
			Preimage	Value C	Subdomain of D_p
γ	$(2h(\alpha) - 2h(z))^{2/3}$, continued from C^3	0	C^3	$\mathbf{D}(e^{-i\pi/4})$	D_{lpha}
		$\frac{2\pi}{3} \\ -\frac{2\pi}{3} \\ \pm \pi$	C^{4-}		
		$-\frac{2\pi}{3}$	C^{4+}		
		$\pm\pi$	C^4		
3	$(2\langle h\rangle(\beta) - 2\langle h\rangle(z))^{2/3}$, continued from C^5	0	C ⁵	$\mathbf{D}(e^{\mathrm{i}\pi/4})$	D_{eta}
		$\frac{2\pi}{3}$	C^{4+}		
		$ \frac{2\pi}{3} \\ -\frac{2\pi}{3} \\ \pm \pi $	C^{4-}		
		$\pm \pi$	C^4		
,	$(2\langle h\rangle(\gamma) - 2\langle h\rangle(z))^{2/3}$, continued from C^1	0	C^1	$\mathbf{D}(\mathrm{e}^{-\mathrm{i}\pi/4})$	D_{γ}
		$\frac{2\pi}{3}$	C^{2-}		
		$ \frac{2\pi}{3} \\ -\frac{2\pi}{3} \\ \pm \pi $	C^{2+}		
		$\pm \pi$	C^2		
	$(2h(\delta) - 2h(z))^{2/3}$, continued from C^3	0	C^3	$\mathbf{D}(e^{\mathrm{i}\pi/4})$	$D_\delta\cap\mathcal{D}_\circ$
		$\frac{2\pi}{3}$	C^{2+}		
		$\frac{2\pi}{3} - \frac{2\pi}{3}$	C^{2-}		
		$\pm\pi$	C^2		



E.3. The gO Case with $\mu \in \mathcal{B}_{\square}(\kappa)$ and s = -1

Here we use representative values of $\mu = 0$ and $\kappa = 0$ (Fig. 41, Table 9).



(A) Left: Stokes graph including branch cuts (orange) for h'(z) and contours ℓ_1 and ℓ_2 appearing in (7.1). Right: arcs of the jump contour Σ for $\mathbf{M}(z)$; note that the arcs Σ_i^k , $j=1,\ldots,4$ and k=1,2, lie on the Stokes graph.

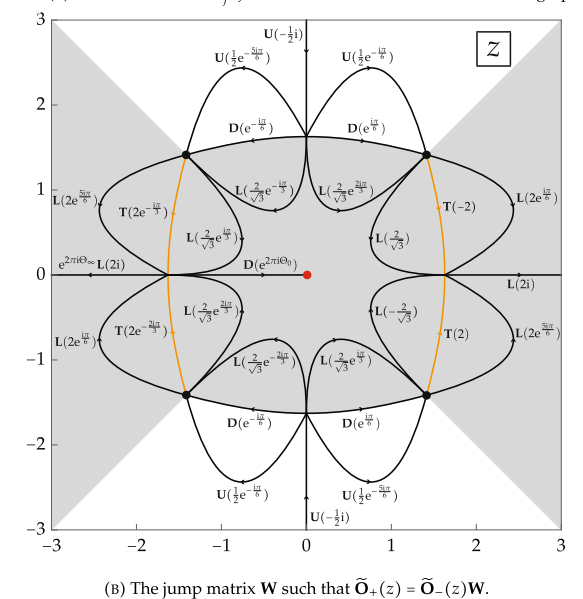


Fig. 41 Diagrams for the gO case with $\mu \in \mathcal{B}_{\square}(\kappa)$ and s=-1 (Color figure online)



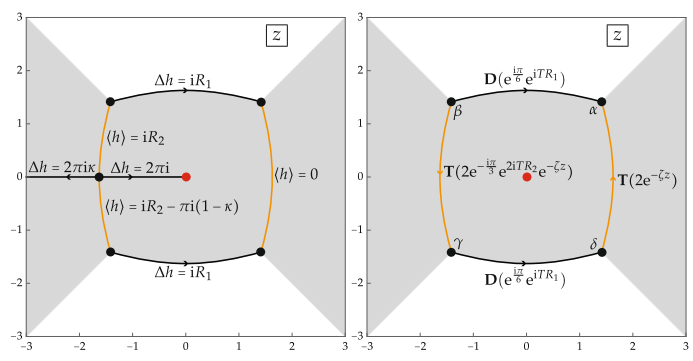


Fig. 41 continued

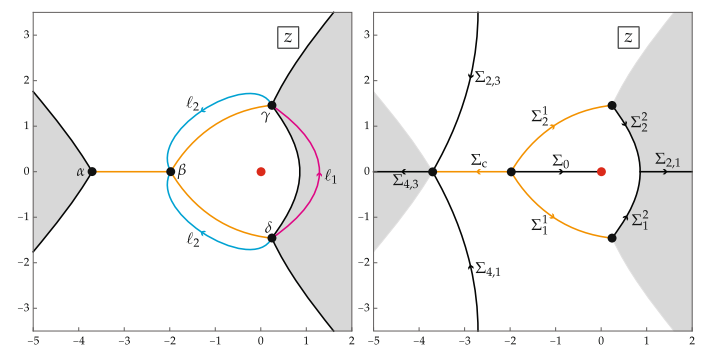
Table 9 Inner parametrix data for the gO case with $\mu \in \mathcal{B}_{\square}(\kappa)$ and s=-1

\overline{p}	Conformal map $W:D_p\to\mathbb{C}$	Ray Prei	mages in D_p	$\mathbf{C}(z)$ in D_p	$\mathbf{C}(z)$ in D_p	
		arg(W)	Preimage	Value C	Subdomain of D_p	
α	$(2h(z) - 2h(\alpha))^{2/3}$, continued from Σ_2^{1+} ; $h(\alpha)$ defined by limit along Σ_2^{1+}	0	Σ_2^{1+}	$\mathbf{T}(\sqrt{2}e^{\mathrm{i}\pi/6})$	$D_{lpha}\cap \mathcal{D}_{\circ}$	
	2	$\frac{2\pi}{3}$	$\Sigma_2^{1-}~\&~\Sigma_2^{2-}$			
		$-\frac{2\pi}{3}$	Σ_2^{2+}	$\mathbf{T}(\sqrt{2}e^{i\pi/3})$	$D_{lpha}\setminus \mathcal{D}_{\circ}$	
		$\pm\pi$	_	_		
β	$(2h(z) - 2h(\beta))^{2/3}$, continued from Σ_3^{1-} ; $h(\beta)$ defined by limit along Σ_3^{1-}	0	Σ_3^{1-}	$T(\sqrt{2}i)$	$D_eta\cap\mathcal{D}_{\circ}$	
	3	$\frac{2\pi}{3}$	Σ_2^{2-}			
		$-\frac{2\pi}{3}$	$\Sigma_3^{1+} \& \Sigma_3^{2+}$	$T(\sqrt{2}e^{2i\pi/3})$	$D_eta \setminus \mathcal{D}_\circ$	
		$\pm\pi$				
γ	$(2h(z) - 2h(\gamma))^{2/3}$, continued from Σ_4^{1+} ; $h(\gamma)$ defined by limit along Σ_4^{1+}	0	Σ_4^{1+}	$T(\sqrt{2}i)$	$D_{\gamma}\cap\mathcal{D}_{\circ}$	
	·	$\frac{2\pi}{3}$	$\Sigma_4^{1-}~\&~\Sigma_4^{2-}$			
		$-\frac{2\pi}{3}$	Σ_4^{2+}	$T(\sqrt{2}e^{i\pi/3})$	$D_{\gamma}\setminus \mathcal{D}_{\circ}$	
		$\pm\pi$				
δ	$(2h(z) - 2h(\delta))^{2/3}$, continued from Σ_1^{1-} ; $h(\delta)$ defined by limit along Σ_1^{1-}	0	Σ_1^{1-}	$\mathbf{T}(\sqrt{2}\mathrm{e}^{5\mathrm{i}\pi/6})$	$D_\delta\cap\mathcal{D}_\diamond$	
		$\frac{2}{3}\pi$	Σ_1^{2-}			
		$-\frac{2}{3}\pi$	$\Sigma_{1}^{1+} \& \Sigma_{1}^{2+}$	$T(\sqrt{2}e^{2i\pi/3})$	$D_\delta \setminus \mathcal{D}_\circ$	
		$\pm \pi$	Σ_1^2		•	



E.4. The gO Case with $\mu \in \mathcal{B}_{\triangleright}(\kappa)$ and s=1

Here we use representative values of $\mu = 1.3$ and $\kappa = 0$ (Fig. 42, Table 10).



(A) Left: Stokes graph including branch cuts (orange) for h'(z) and contours ℓ_1 and ℓ_2 appearing in (7.1). Right: arcs of the jump contour Σ for $\mathbf{M}(z)$; note that the arcs Σ_i^k , j=1,2 and k=1,2, and Σ_c lie on the Stokes graph.

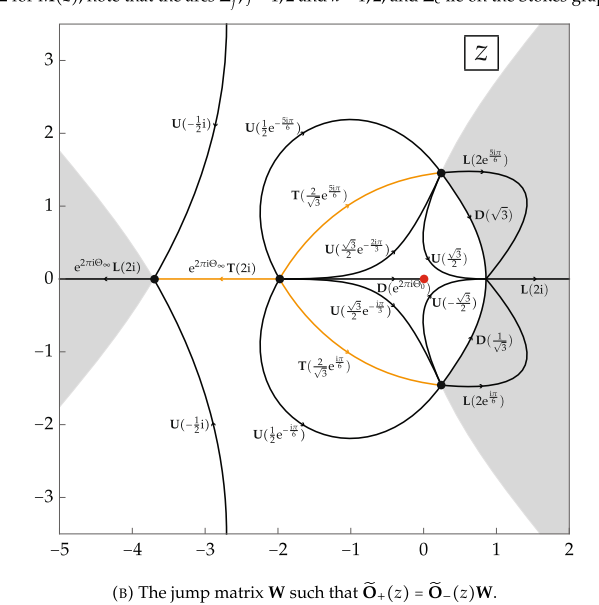


Fig. 42 Diagrams for the gO case with $\mu \in \mathcal{B}_{\triangleright}(\kappa)$ and s=1 (Color figure online)



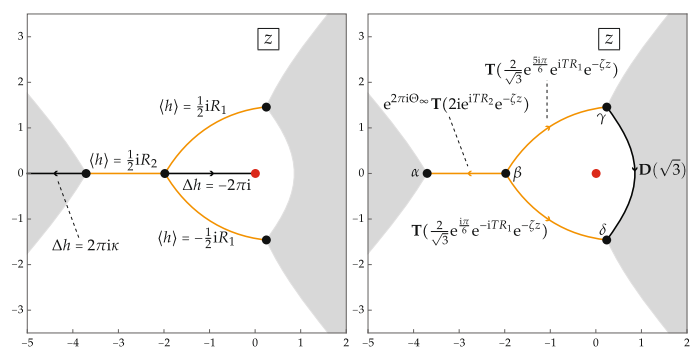


Fig. 42 continued

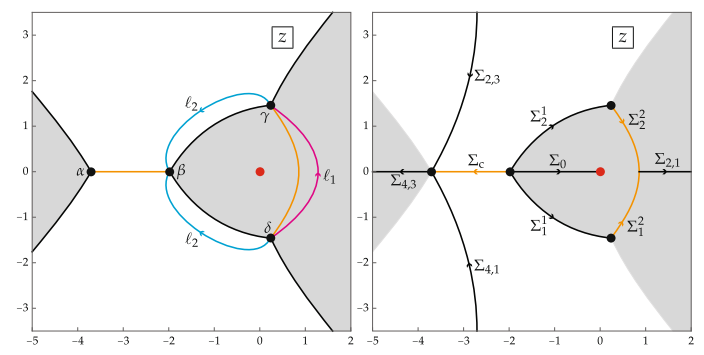
Table 10 Inner parametrix data for the gO case with $\mu \in \mathcal{B}_{\triangleright}(\kappa)$ and s=1

p	Conformal map $W: D_p \to \mathbb{C}$	Ray Preimages in D_p		$\mathbf{C}(z)$ in D_p		
		arg(W)	Preimage	Value C	Subdomain of D_p	
α	$(2\langle h\rangle(\alpha) - 2\langle h\rangle(z))^{2/3}$, continued from $\Sigma_{4,3}$	0	$\Sigma_{4,3}$	$\mathbf{D}(\frac{1}{\sqrt{2}})$	D_{α} , left of $\Sigma_{4,3}$ & Σ_{c}	
		$\frac{2\pi}{3}$	$\Sigma_{4,1}$			
		$-\frac{2\pi}{3}$	$\Sigma_{2,3}$	$e^{2\pi i\Theta} \infty \mathbf{D}(\frac{1}{\sqrt{2}})$	D_{α} , right of $\Sigma_{4,3}$ & Σ_{6}	
		$\pm \pi$	$\Sigma_{ m c}$	V 2		
β	$(2\langle h\rangle(z) - 2\langle h\rangle(\beta))^{2/3}$, continued from Σ_0 ; $\langle h\rangle(\beta)$ defined by limit along Σ_0	0	$\Sigma_1^{1+}, \Sigma_0, \& \Sigma_2^{1-}$	$T(\sqrt{\frac{2}{3}}e^{-5i\pi/6})$	$D_eta\cap\mathcal{D}_\circ$, left of Σ_0	
	2 0	$\frac{2\pi}{3}$	Σ_2^{1+}	$T(\sqrt{\frac{2}{3}}e^{-2\pi i\Theta_0-5i\pi/6})$	$D_{\beta} \cap \mathcal{D}_{\circ}$, right of Σ_{0}	
		$-\frac{2\pi}{3}$	-	1 2 :0	$D_{eta}\setminus\mathcal{D}_{\circ}$, left of Σ_{c}	
		$\pm\pi$	$\Sigma_{ m c}$	$\mathbf{D}(\frac{1}{\sqrt{2}}e^{\mathrm{i}\pi/3})$	$D_{eta}\setminus\mathcal{D}_{\circ},$ right of Σ_{c}	
γ	$(2h(z) - 2h(\gamma))^{2/3}$, continued from Σ_2^{1+}	0	Σ_2^{1+}	$\mathbf{D}(\sqrt{\frac{3}{2}}\mathrm{e}^{5\mathrm{i}\pi/6})$	$D_{\gamma}\cap\mathcal{D}_{\circ}$	
	2	$\frac{2\pi}{3}$	$\Sigma_2^{1-} \& \Sigma_2^{2-}$			
		$-\frac{2\pi}{3}$		$T(\sqrt{2}e^{2i\pi/3})$	$D_{\gamma}\setminus\mathcal{D}_{\circ}$	
		$\pm \pi$	Σ_2^2			
S	$(2h(z) - 2h(\delta))^{2/3}$, continued from Σ_1^{1-}	0	Σ_1^{1-}	$\mathbf{D}(\sqrt{\frac{3}{2}}e^{\mathrm{i}\pi/6})$	$D_\delta\cap\mathcal{D}_\circ$	
		$\frac{2\pi}{3}$	Σ_1^{2-}			
		$-\frac{2\pi}{3}$	$\Sigma_1^{1+} \& \Sigma_1^{2+}$	$T(\sqrt{2}e^{i\pi/3})$	$D_\delta \setminus \mathcal{D}_\circ$	
		$\pm\pi$	Σ_1^2			



E.5. The gO Case with $\mu \in \mathcal{B}_{\triangleright}(\kappa)$ and s = -1

Here we use representative values of $\mu = 1.3$ and $\kappa = 0$ (Fig. 43, Table 11).



(A) Left: Stokes graph including branch cuts (orange) for h'(z) and contours ℓ_1 and ℓ_2 appearing in (7.1). Right: arcs of the jump contour Σ for $\mathbf{M}(z)$; note that the arcs Σ_i^k , j=1,2 and k=1,2, and Σ_c lie on the Stokes graph.

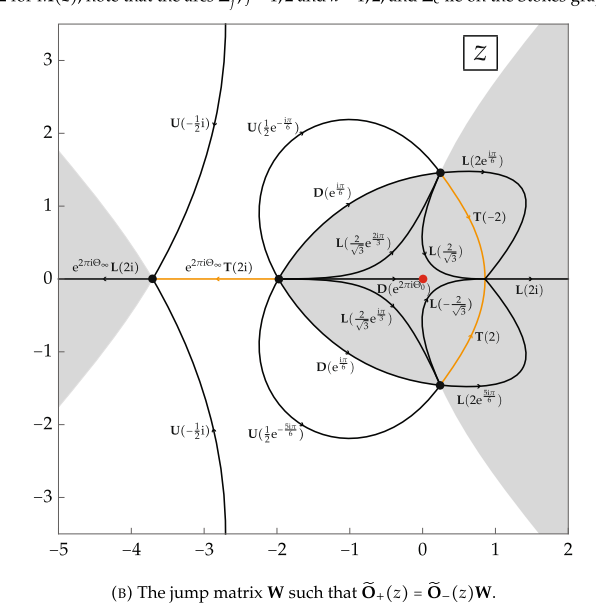


Fig. 43 Diagrams for the gO case with $\mu \in \mathcal{B}_{\triangleright}(\kappa)$ and s=-1 (Color figure online)



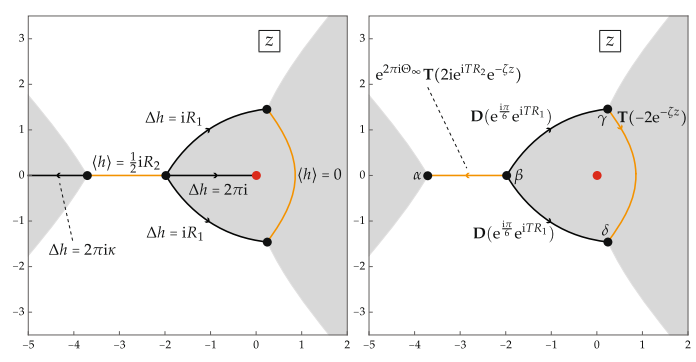


Fig. 43 continued

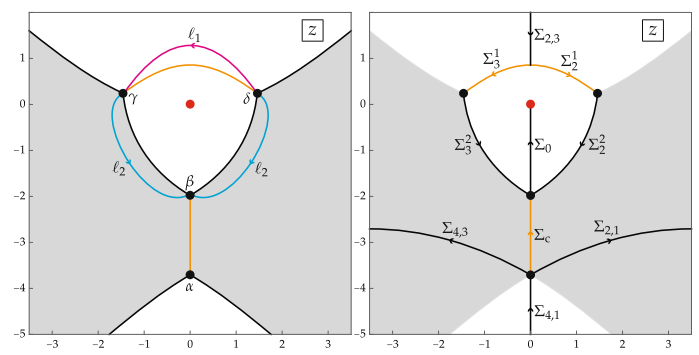
Table 11 Inner parametrix data for the gO case with $\mu \in \mathcal{B}_{\triangleright}(\kappa)$ and s=-1

p	Conformal map $W: D_p \to \mathbb{C}$	Ray Preimages in D_p		$\mathbf{C}(z)$ in D_p	
		arg(W)	Preimage	Value C	Subdomain of D_p
α	$(2\langle h\rangle(\alpha) - 2\langle h\rangle(z))^{2/3}$, continued from $\Sigma_{4,3}$	0	$\Sigma_{4,3}$	$\mathbf{D}(\frac{1}{\sqrt{2}})$	D_{α} , left of $\Sigma_{4,3}$ & Σ_{c}
		$\frac{2\pi}{3}$	$\Sigma_{4,1}$		
		$-\frac{2\pi}{3}$	$\Sigma_{2,3}$	$e^{2\pi i\Theta} \propto \mathbf{D}(\frac{1}{\sqrt{2}})$	D_{α} , right of $\Sigma_{4,3}$ & Σ_{c}
		$\pm\pi$	$\Sigma_{ m c}$,-	
β	$(2\langle h\rangle(\beta) - 2\langle h\rangle(z))^{2/3}$, continued from Σ_0 ; $\langle h\rangle(\beta)$ defined by limit along Σ_0	0	$\Sigma_1^{1+}, \Sigma_0, \& \Sigma_2^{1-}$	$\mathbf{D}(\frac{1}{\sqrt{2}}\mathrm{e}^{-\mathrm{i}\pi/6})$	$D_eta\cap\mathcal{D}_\circ$, left of Σ_0
		$\frac{2\pi}{3}$	Σ_2^{1+}	$\mathbf{D}(\frac{1}{\sqrt{2}}e^{2\pi i\Theta_0 - i\pi/6})$	$D_{eta} \cap \mathcal{D}_{\circ}$, right of Σ_0
		$-\frac{2\pi}{3}$	Σ_1^{1-}	$\mathbf{D}(\frac{1}{\sqrt{2}}e^{2\pi i\Theta_0})$	$D_{eta}\setminus\mathcal{D}_{\circ},$ left of $\Sigma_{ ext{c}}$
		$\pm\pi$	Σ_{c}	$\mathbf{D}(\frac{1}{\sqrt{2}}e^{-i\pi/3})$	$D_{\beta} \setminus \mathcal{D}_{\circ}$, right of Σ_{c}
γ	$(2h(z) - 2h(\gamma))^{2/3}$, continued from Σ_2^{1+} ; $h(\gamma)$ defined by limit along Σ_2^{1+}	0	Σ_2^{1+}	$T(\sqrt{2}e^{i\pi/6})$	$D_{\gamma}\cap\mathcal{D}_{\circ}$
	- 2	$\frac{2\pi}{3}$	$\Sigma_2^{1-} \& \Sigma_2^{2-}$		
		$-\frac{2\pi}{3}$	Σ_2^{2+}	$T(\sqrt{2}e^{i\pi/3})$	$D_{\gamma}\setminus \mathcal{D}_{\circ}$
	2./2		Σ_2^2	- 5: 16	
δ	$(2h(z) - 2h(\delta))^{2/3}$, continued from Σ_1^{1-} ; $h(\delta)$ defined by limit along Σ_1^{1-}	0	Σ_1^{1-}	$T(\sqrt{2}e^{5i\pi/6})$	$D_\delta\cap\mathcal{D}_\circ$
		$\frac{2\pi}{3}$	Σ_1^{2-}		
		$-\frac{2\pi}{3}$	$\Sigma_1^{1+}~\&~\Sigma_1^{2+}$	$T(\sqrt{2}e^{2i\pi/3})$	$D_\delta \setminus \mathcal{D}_\circ$
		$\pm\pi$	Σ_1^2		



E.6. The gO Case with $\mu \in \mathcal{B}_{\triangle}(\kappa)$ and s=1

Here we use representative values of $\mu = 1.3i$ and $\kappa = 0$ (Fig. 44, Table 12).



(A) Left: Stokes graph including branch cuts (orange) for h'(z) and contours ℓ_1 and ℓ_2 appearing in (7.1). Right: arcs of the jump contour Σ for $\mathbf{M}(z)$; note that the arcs Σ_j^k , j=2,3 and k=1,2, and Σ_c lie on the Stokes graph.

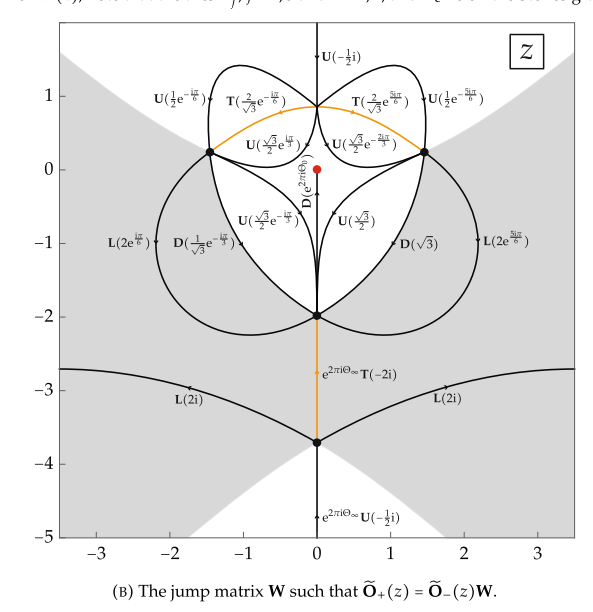


Fig. 44 Diagrams for the gO case with $\mu \in \mathcal{B}_{\Delta}(\kappa)$ and s=1 (Color figure online)



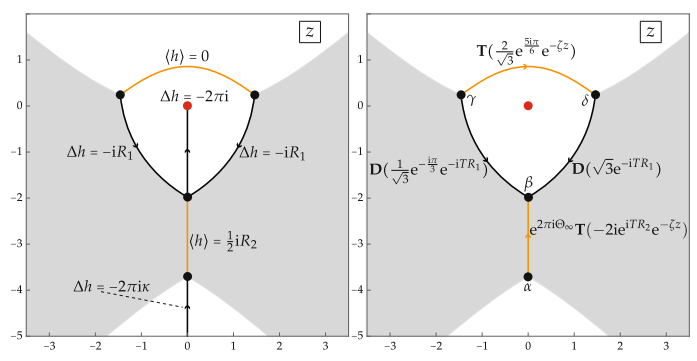


Fig. 44 continued

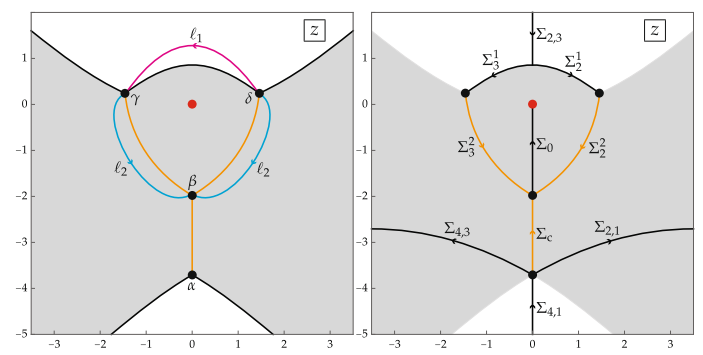
Table 12 Inner parametrix data for the gO case with $\mu \in \mathcal{B}_{\triangle}(\kappa)$ and s=1

p	Conformal map $W: D_p \to \mathbb{C}$	Ray Preimages in D_p		$\mathbf{C}(z)$ in D_p	
		arg(W)	Preimage	Value C	Subdomain of D_p
α	$(2\langle h\rangle(z) - 2\langle h\rangle(\alpha))^{2/3}$, continued from $\Sigma_{4,1}$	0	$\Sigma_{4,1}$	$T(\sqrt{2}i)$	D_{α} , left of $\Sigma_{4,1}$ & Σ_{c}
		$\frac{2\pi}{3}$	$\Sigma_{2,1}$		
		$-\frac{2\pi}{3}$	$\Sigma_{4,3}$	$e^{2\pii\Theta_\infty} T(\sqrt{2}i)$	D_{α} , right of $\Sigma_{4,1}$ & Σ_{c}
		$\pm\pi$	$\Sigma_{ m c}$		
β	$ \begin{array}{l} (2\langle h\rangle(z)-2\langle h\rangle(\beta))^{2/3},\\ \text{continued from }\Sigma_0;\\ \langle h\rangle(\beta) \text{ defined by limit}\\ \text{along }\Sigma_0 \end{array} $	0	$\Sigma_2^{2-}, \Sigma_0, \& \Sigma_3^{2+}$	$T(\sqrt{\frac{2}{3}}i)$	$D_{eta} \cap \mathcal{D}_{\circ}$, left of Σ_0
		$\frac{2\pi}{3}$	Σ_3^{2-}	$\mathbf{T}(\sqrt{\frac{2}{3}}ie^{-2\pi i\Theta_0})$	$D_{\beta} \cap \mathcal{D}_{\circ}$, right of Σ_0
		$-\frac{2\pi}{3}$		Y 5	$D_{eta}\setminus\mathcal{D}_{\circ}$, left of Σ_{c}
		$\pm \pi$	$\Sigma_{ m c}$		$D_{\beta} \setminus \mathcal{D}_{\circ}$, right of Σ_{c}
γ	$(2h(z) - 2h(\gamma))^{2/3}$, continued from Σ_3^{1-} ; $h(\gamma)$ defined by limit along Σ_3^{1-}	0	Σ_3^{1-}	$\mathbf{D}(\sqrt{\frac{3}{2}}i)$	$D_{\gamma}\cap\mathcal{D}_{\circ}$
	- 3	$\frac{2\pi}{3}$	Σ_3^{2-}		
		5	$\Sigma_3^{1+} \& \Sigma_3^{2+}$	$T(\sqrt{2}e^{i\pi/3})$	$D_{\mathcal{V}}\setminus\mathcal{D}_{\circ}$
		$\pm\pi$	Σ_3^2		,
δ	$(2h(z) - 2h(\delta))^{2/3}$, continued from Σ_2^{1+} ; $h(\delta)$ defined by limit along Σ_2^{1+}	0	Σ_2^{1+}	$\mathbf{D}(\sqrt{\frac{3}{2}}\mathrm{e}^{5\mathrm{i}\pi/6})$	$D_\delta\cap\mathcal{D}_\circ$
		$\frac{2\pi}{3}$	$\Sigma_2^{1-}~\&~\Sigma_2^{2-}$		
		$-\frac{2\pi}{3}$	Σ_2^{2+}	$T(\sqrt{2}e^{2i\pi/3})$	$D_\delta \setminus \mathcal{D}_\circ$
		$\pm\pi$	Σ_2^2		



E.7. The gO Case with $\mu \in \mathcal{B}_{\triangle}(\kappa)$ and s=-1

Here we use representative values of $\mu = 1.3i$ and $\kappa = 0$ (Fig. 45 and Table 13).



(A) Left: Stokes graph including branch cuts (orange) for h'(z) and contours ℓ_1 and ℓ_2 appearing in (7.1). Right: arcs of the jump contour Σ for $\mathbf{M}(z)$; note that the arcs Σ_i^k , j=2,3 and k=1,2, and Σ_c lie on the Stokes graph.

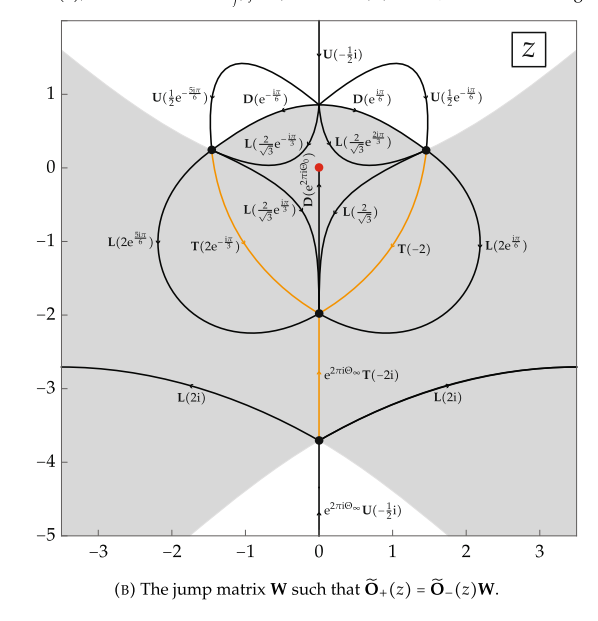


Fig. 45 Diagrams for the gO case with $\mu \in \mathcal{B}_{\triangle}(\kappa)$ and s = -1 (Color figure online)



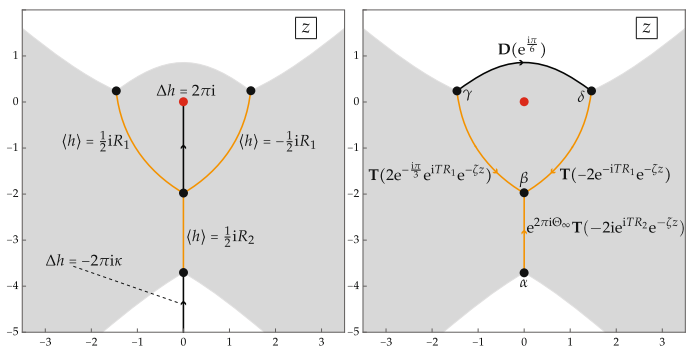


Fig. 45 continued

Table 13 Inner parametrix data for the gO case with $\mu \in \mathcal{B}_{\triangle}(\kappa)$ and s=-1

p	Conformal map $W: D_p \to \mathbb{C}$	Ray Preimages in D_p		$\mathbf{C}(z)$ in D_p	
		arg(W)	Preimage	Value C	Subdomain of D_p
α	$(2\langle h\rangle(z) - 2\langle h\rangle(\alpha))^{2/3}$, continued from $\Sigma_{4,1}$	0	$\Sigma_{4,1}$	$T(\sqrt{2}i)$	D_{α} , left of $\Sigma_{4,1}$ & Σ_{c}
		$\frac{2\pi}{3}$	$\Sigma_{2,1}$		
		$-\frac{2\pi}{3}$	$\Sigma_{4,3}$	$e^{2\pii\Theta_\infty}T(\sqrt{2}i)$	D_{α} , right of $\Sigma_{4,1}$ & $\Sigma_{4,1}$
		$\pm\pi$	$\Sigma_{ m c}$		
β	$(2\langle h\rangle(\beta) - 2\langle h\rangle(z))^{2/3}$, continued from Σ_0 ; $\langle h\rangle(\beta)$ defined by limit along Σ_0	0	Σ_2^{2-} , Σ_0 , & Σ_3^{2+}	$\mathbf{D}(\frac{1}{\sqrt{2}}i)$	$D_eta\cap\mathcal{D}_\circ$, left of Σ_0
		$\frac{2\pi}{3}$	Σ_3^{2-}	$\mathbf{D}(\frac{1}{\sqrt{2}}ie^{2\pi i\Theta_0})$	$D_{eta} \cap \mathcal{D}_{\circ}$, right of Σ_0
		$-\frac{2\pi}{3}$	Σ_2^{2+}	$T(\sqrt{2}e^{i\pi/6})$	$D_{\beta} \setminus \mathcal{D}_{\circ}$, left of Σ_{c}
		$\pm\pi$	$\Sigma_{ m c}$	$\mathbf{T}(\sqrt{2}\mathrm{i}\mathrm{e}^{2\pi\mathrm{i}\Theta_0})$	$D_{\beta} \setminus \mathcal{D}_{\circ}$, right of Σ_{c}
γ	$(2h(z) - 2h(\gamma))^{2/3}$, continued from Σ_3^{1-}	0	Σ_3^{1-}	$T(\sqrt{2}i)$	$D_{\gamma}\cap\mathcal{D}_{\circ}$
	3	$\frac{2\pi}{3}$	Σ_3^{2-}		
			$\Sigma_3^{1+} \& \Sigma_3^{2+}$	$\mathbf{T}(\sqrt{2}e^{2i\pi/3})$	$D_{\gamma}\setminus\mathcal{D}_{\circ}$
		$\pm\pi$	Σ_3^2		
δ	$(2h(z) - 2h(\delta))^{2/3}$, continued from Σ_2^{1+}	0	Σ_2^{1+}	$T(\sqrt{2}e^{i\pi/6})$	$D_\delta\cap\mathcal{D}_\circ$
	_	$\frac{2\pi}{3}$	$\Sigma_2^{1-} \& \Sigma_2^{2-}$		
		$-\frac{2\pi}{3}$	Σ_2^{2+}	$T(\sqrt{2}e^{i\pi/3})$	$D_\delta \setminus \mathcal{D}_\circ$
		$\pm\pi$	Σ_2^2		



Appendix F. User's Guide: Approximating Rational Solutions on Boutroux Domains

The approximation most directly adapted to our analysis of Riemann–Hilbert Problem 1 in Sect. 3.1 is that of the rational functions $u_{\rm gO}^{[3]}(x;m,n)$ and $u_{\rm gH}^{[3]}(x;m,n)$. The basic approximation formula for these functions reads:

$$\begin{split} u_{\mathrm{F}}^{[3]} \left(|\Theta_{0,\mathrm{F}}^{[3]}(m,n)|^{1/2} \mu + |\Theta_{0,\mathrm{F}}^{[3]}(m,n)|^{-1/2} \zeta; m,n \right) \\ &= |\Theta_{0,\mathrm{F}}^{[3]}(m,n)|^{1/2} \left(f(\zeta-\zeta_0)^{\chi} + \mathcal{O}\left(|\Theta_{0,\mathrm{F}}^{[3]}(m,n)|^{-1} \right) \right)^{\chi}, \\ f(\zeta-\zeta_0) &= \breve{U}_{\mathrm{F}}^{[3]}(\zeta;\mu) := \psi_{\mathrm{F}}^{[3]}(\mu) \frac{\vartheta(\mathcal{K}-\mathrm{i}(\Psi-\mathfrak{z}_1^{[3]}))\vartheta(\mathcal{K}-\mathrm{i}(\Psi-\mathfrak{z}_2^{[3]}))}{\vartheta(\mathcal{K}-\mathrm{i}(\Psi-\mathfrak{p}_1^{[3]}))\vartheta(\mathcal{K}-\mathrm{i}(\Psi-\mathfrak{p}_2^{[3]}))}. \end{split}$$
(F.1)

Assuming that $\chi = -\operatorname{sgn}(\ln |f(\zeta - \zeta_0)|)$, the error term is uniform for bounded ζ and for μ in a compact subset of the selected Boutroux domain \mathcal{B} . Computing the leading term consists of the following steps.

- (1) Define the parameters T > 0, $s = \pm 1$, and $\kappa \in (-1, 1)$ in terms of (m, n) by (4.3) (resp., by (4.4)) for the gH family (resp., for the gO family).
- (2) Select a Boutroux domain $\mathcal{B} = \mathcal{B}_{\triangleright}(\kappa)$, $\mathcal{B} = \mathcal{B}_{\triangle}(\kappa)$ (both for the gO family only), or $\mathcal{B} = \mathcal{B}_{\square}(\kappa)$, and ensure that $\mu \in \mathcal{B}$ (the boundaries of the domains can be numerically computed given κ using (1.22); see also Appendix G.
- (3) Using numerical root finding and continuation methods informed by the discussion in Sect. 4.4, determine the value of $E = E(\mu; \kappa)$ for which the Boutroux equations (4.23) hold.
- (4) With E determined, the polynomial P(z) given by (1.18) is now known. Find its roots α , β , γ , and δ and order them according to the Stokes graph as illustrated in Figs. 39a–45a from Appendix E relevant for the family, Boutroux domain, and sign s under consideration (recall that while these figures are for special cases of the parameters, the abstract Stokes graph depends only on the selected Boutroux domain). Then using the contours ℓ_1 and ℓ_2 and branch cuts for R(z) illustrated in the same plots, numerically compute the real constants R_1 and R_2 given by (7.1) (one can use this computation as an opportunity to verify the accuracy of the determination of E, which should force the imaginary parts of R_1 and R_2 to vanish to machine precision).
- (5) Matching the topological representation of $\mathfrak a$ and $\mathfrak b$ cycles shown in Fig. 28 of Sect. 7.6 with the actual ordering of the points obtained in the previous step, and using the relationship (7.8), numerically calculate the constant c given in (7.13) and the constant H_{ω} given in (7.15). Then taking into account the value of z_0 given in terms of the well-defined branch points α , β , γ , δ by (7.21), numerically evaluate the integrals a(0), $a(\infty)$, and $a(z_0)$ (see (7.17)). Using these, define the phase shifts $\mathfrak{z}_1^{[3]}$ and $\mathfrak{p}_3^{[3]}$, j=1,2, by (7.41).
- (6) Using Table 6 from Sect. 7.6 to determine the phases $C_{\rm G}$ and $C_{\rm B}$ relevant to the case at hand (noting also $\Theta_{\infty} = -\kappa T$), define the aggregate phase Ψ by (7.26).



(7) Recalling the definition (7.22) of $\vartheta(z)$ given H_{ω} (possibly implementing this definition using built-in function calls to Jacobi theta functions) and using $\mathcal{K} = i\pi + \frac{1}{2}H_{\omega}$, calculate the complex amplitude factor $\psi_{\rm F}^{[3]}(\mu)$ from (7.43). Then bring in Ψ and the four phase shifts to finish the rest of the calculation using (F.1).

The other approximation proved by analyzing the same Riemann–Hilbert Problem applies to the rational functions $u_{gO}^{[1]}(x; m, n)$ and $u_{gH}^{[1]}(x; m, n)$, and it reads

$$\begin{split} u_{\mathrm{F}}^{[1]} \left(|\Theta_{0,\mathrm{F}}^{[1]}(m,n)|^{1/2} \widehat{\mu} + |\Theta_{0,\mathrm{F}}^{[1]}(m,n)|^{-1/2} \widehat{\zeta}; m, n \right) \\ &= |\Theta_{0,\mathrm{F}}^{[1]}(m,n)|^{1/2} \left(f(\zeta - \zeta_0)^{\chi} + \mathcal{O}\left(|\Theta_{0,\mathrm{F}}^{[1]}(m,n)|^{-1} \right) \right)^{\chi}, \\ f(\widehat{\zeta} - \widehat{\zeta_0}) &= \widecheck{U}_{\mathrm{F}}^{[1]}(\widehat{\zeta}; \widehat{\mu}) := \psi_{\mathrm{F}}^{[1]}(\widehat{\mu}) \frac{\vartheta(\mathcal{K} - \mathrm{i}(\Psi - \mathfrak{z}_1^{[1]}))\vartheta(\mathcal{K} - \mathrm{i}(\Psi - \mathfrak{z}_2^{[1]}))}{\vartheta(\mathcal{K} - \mathrm{i}(\Psi - \mathfrak{p}_1^{[1]}))\vartheta(\mathcal{K} - \mathrm{i}(\Psi - \mathfrak{p}_2^{[1]}))}. \end{split}$$
(F.2

Again taking $\chi = -\text{sgn}(\ln |f(\widehat{\zeta} - \widehat{\zeta_0})|)$, the error term is uniform for bounded $\widehat{\zeta}$ and for $\widehat{\mu}$ in a compact subset of the chosen Boutroux domain \mathcal{B} . To compute the leading term, we modify the above steps as follows.

(1) Define the parameters T>0, $s=\pm 1$, and $\kappa\in(-1,1)$ in terms of (m,n) by (4.6) (resp., by (4.8)) for the gH family (resp., for the gO family). These are not directly related to the "native" parameters $\Theta_{0,F}^{[1]}(m,n)$ and $\Theta_{\infty,F}^{[1]}(m,n)$, but they are the correct values to use for the remaining steps of the calculation. From the given values of the variables $\widehat{\zeta}$ and $\widehat{\mu}$, define scaled versions needed for the subsequent steps by setting

$$\zeta := \sqrt{\frac{2}{1 - s\kappa}} \widehat{\zeta}$$
 and $\mu := \sqrt{\frac{1 - s\kappa}{2}} \widehat{\mu}$.

- (2) As above.
- (3) As above.
- (4) As above.
- (5) As above, but instead calculate the phase shifts $\mathfrak{z}_{i}^{[1]}$ and $\mathfrak{p}_{i}^{[1]}$ from (7.47).
- (6) As above for the indicated parameters.
- (7) As above for the indicated parameters, but now define the complex amplitude $\psi_F^{[1]}(\widehat{\mu}) = e^{i(\mathfrak{z}_1^{[1]} \mathfrak{p}_2^{[1]})} M$ in terms of M given in (7.48), and finish the calculation using (F.2).

We do not obtain any approximations for the rational solutions $u_{gO}^{[2]}(x; m, n)$ or $u_{gH}^{[2]}(x; m, n)$ directly from analysis of Riemann–Hilbert Problem 1, but we can apply the exact symmetry (2.2) to obtain the following result.

$$\begin{split} u_{\mathrm{F}}^{[2]} \left(|\Theta_{0,\mathrm{F}}^{[2]}(m,n)|^{1/2} \mu + |\Theta_{0,\mathrm{F}}^{[2]}(m,n)|^{-1/2} \zeta; m, n \right) \\ &= |\Theta_{0,\mathrm{F}}^{[2]}(m,n)|^{1/2} \left(f(\zeta - \zeta_0)^{\chi} + \mathcal{O}\left(|\Theta_{0,\mathrm{F}}^{[2]}(m,n)|^{-1} \right) \right)^{\chi}, \\ f(\zeta - \zeta_0) &= \check{U}_{\mathrm{F}}^{[2]}(\zeta; \mu) := \mathrm{i} \check{U}_{\mathrm{F}}^{[1]}(-\mathrm{i} \zeta; -\mathrm{i} \mu). \end{split}$$



Taking $\chi = -\text{sgn}(\ln |f(\zeta - \zeta_0)|)$, this formula is also uniformly valid for bounded ζ and μ in a compact subset of the chosen Boutroux domain \mathcal{B} . The leading term can obviously be computed by adapting the above procedure to variables rotated by -i in the complex plane.

Appendix G. User's Guide: Practical Computation of Boundary Curves

In this appendix, we provide further details about how (1.22) can be used practically to compute the boundary curves. An antiderivative of the integrand in (1.22) is

$$\int (f - \gamma)\sqrt{(f - \alpha)(f - \beta)} \frac{\mathrm{d}f}{f} = \frac{1}{4}\sqrt{(f - \alpha)(f - \beta)}(2f - \alpha - \beta - 4\gamma)$$
$$- \frac{1}{8}((\alpha + \beta)^2 - 4(\alpha + \beta)\gamma - 4\alpha\beta)\log\left(\frac{f - \alpha + \sqrt{(f - \alpha)(f - \beta)}}{f - \alpha - \sqrt{(f - \alpha)(f - \beta)}}\right)$$
$$- \sqrt{\alpha}\sqrt{\beta}\gamma\log\left(\frac{\sqrt{\beta}(f - \alpha) + \sqrt{\alpha}\sqrt{(f - \alpha)(f - \beta)}}{\sqrt{\beta}(f - \alpha) - \sqrt{\alpha}\sqrt{(f - \alpha)(f - \beta)}}\right).$$

Since α and β are the roots of the quadratic (1.21), the identities $\alpha\beta\gamma^2=16$ and $\alpha+\beta=-4\mu-2\gamma$ both hold. Using these as well as the quartic equation (1.15) satisfied by $\gamma=U_0$, the coefficient of the first logarithm is simply

$$-\frac{1}{8}((\alpha+\beta)^2 - 4(\alpha+\beta)\gamma - 4\alpha\beta) = 4\kappa \in \mathbb{R}.$$

Likewise, the coefficient of the second logarithm is $-\sqrt{\alpha}\sqrt{\beta}\gamma = \pm 4 \in \mathbb{R}$. Furthermore, evaluating at the limits of integration $f = \gamma$ and (by taking a limit) $f = \alpha$ and taking the real part gives

$$\operatorname{Re}\left(\int_{\alpha}^{\gamma} (f-\gamma)\sqrt{(f-\alpha)(f-\beta)} \, \frac{\mathrm{d}f}{f}\right) = -\frac{1}{4}\operatorname{Re}\left(\sqrt{(\gamma-\alpha)(\gamma-\beta)}(\alpha+\beta+2\gamma)\right) \\ + 4\kappa \log\left|\frac{\gamma-\alpha+\sqrt{(\gamma-\alpha)(\gamma-\beta)}}{\gamma-\alpha-\sqrt{(\gamma-\alpha)(\gamma-\beta)}}\right| \\ - \sqrt{\alpha}\sqrt{\beta}\gamma \log\left|\frac{\sqrt{\beta}(\gamma-\alpha)+\sqrt{\alpha}\sqrt{(\gamma-\alpha)(\gamma-\beta)}}{\sqrt{\beta}(\gamma-\alpha)-\sqrt{\alpha}\sqrt{(\gamma-\alpha)(\gamma-\beta)}}\right|.$$

This formula is invariant under permutation of (α, β) , and the last term does not depend on the choice of signs in the square roots $\sqrt{\alpha}$ and $\sqrt{\beta}$. Although the whole formula changes sign if $\sqrt{(\gamma - \alpha)(\gamma - \beta)}$ changes sign, this is irrelevant in identifying the zero set as required in the condition (1.22). At this point, we can use the fact that $\gamma = U_0$ is a root of the quartic equation (1.15), so it becomes locally one of four functions of μ parametrized by κ , and then α and β are in turn determined (up to permutation) as functions of μ with parameter κ via the quadratic equation (1.21). Thus on each of the four sheets of the solution of (1.15) over a given domain in the μ -plane, the



condition (1.22) defines a system of arcs that are the zeros of a harmonic function of μ . By combining the above explicit formula with the well-known explicit solution of the quartic equation (1.15) for $\gamma = U_0$ in terms of radicals and the subsequent use of the quadratic formula to solve (1.21) for α and β one converts (1.22) into an explicit harmonic function of μ whose zero locus can be found using standard computational software.

Appendix H. Alternate Approach to Rational Solutions of Types 1 and 2

The basic approach we have followed in this paper is to use the fact that the Painlevé-IV rational solutions of type 1, which correspond to values of κ outside of the basic interval (-1, 1), can be extracted via the formula (3.2) for $u_{\mathbb{Q}}(x)$ from Riemann–Hilbert Problem 1 in Sect. 3.1 formulated for the rational solutions of type 3, which correspond instead to $\kappa \in (-1, 1)$. Of course another approach to the rational solutions of type 1 (and also type 2) is to represent these solutions as u(x) instead of $u_{\mathbb{Q}}(x)$ in (3.2) and solve Riemann–Hilbert Problem 1 for parameters covering all lattice points far from the origin in Fig. 1. The latter approach avoids the complication of the changes of variables associated with the Bäcklund transformation $u(x) \mapsto u_{\mathbb{Q}}(x)$, but it leads to many additional cases for matrix factorizations and parametrix constructions, as one must consider spectral curves for $\kappa < -1$ and $\kappa > 1$, as well as for $\kappa \in (-1, 1)$.

H.1. Monodromy Data for gH Rational Solutions of Types 1 and 2

One further difficulty of this alternate approach in the gH case is that the rational solutions for $(\Theta_0, \Theta_\infty) \in \Lambda_{\rm gH}^{[1]-} \cup \Lambda_{\rm gH}^{[2]-}$ cannot be obtained from those for $(\Theta_0, \Theta_\infty) \in \Lambda_{\rm gH}^{[3]+}$ by means of isomonodromic transformations, so to treat these rational solutions as functions u(x) in Riemann–Hilbert Problem 1 it is necessary to repeat the procedure of Sect. 3.6 for a seed solution with parameters in $\Lambda_{\rm gH}^{[1]-}$. Note that this issue does not arise for the gO solutions as the entire lattice $\Lambda_{\rm gO}$ is spanned by isomonodromic transformations.

Applying the transformation $S_{\mathbb{Q}}$ to the seed solution u(x) = -2x for $(\Theta_0, \Theta_\infty) = (\frac{1}{2}, \frac{1}{2}) \in \Lambda_{\mathrm{gH}}^{[3]+}$, we obtain the solution $u(x) = x^{-1}$ for parameters $(\Theta_0, \Theta_\infty) = (-\frac{1}{2}, \frac{3}{2}) \in \Lambda_{\mathrm{gH}}^{[1]-}$. Without loss of generality taking the corresponding solution of (3.7) to be $y(x) = x^{-1} \exp(-x^2)$, and noting that from (3.8) we get $z(x) = 1 + \frac{1}{2}x^{-2}$, the Lax pair matrix coefficients $\Lambda_0(x)$, $\Lambda_1(x)$, and $X_0(x)$ defined in (3.10)–(3.11)



become

$$\Lambda_0(x) = \begin{pmatrix} x & x^{-1}e^{-x^2} \\ e^{x^2}(x^{-1} - 2x) & -x \end{pmatrix},
\Lambda_1(x) = \begin{pmatrix} -\frac{1}{2}(1 + x^{-2}) & -\frac{1}{2}x^{-2}e^{-x^2} \\ e^{x^2}(1 + \frac{1}{2}x^{-2}) & \frac{1}{2}(1 + x^{-2}) \end{pmatrix},
\mathbf{X}_0(x) = \mathbf{\Lambda}_0(x) - x\sigma_3.$$

Following the same strategy we have used twice before, we look first for solutions of $\Psi_x = \mathbf{X}\Psi$, and some experimentation shows that a particular solution is given in closed form by $\Psi_{1j} = x^{-1} \exp(-x^2 - x\lambda)$ and $\Psi_{2j} = -(2x + 2\lambda + x^{-1}) \exp(-x\lambda)$. Applying reduction of order to obtain the general solution, and then determining the dependence of constants of integration on λ so that the other Lax equation $\Psi_{\lambda} = \Lambda \Psi$ holds, we obtain the following analogue of Lemma 2 and Lemma 3.

Lemma 21 Fix a simply connected domain $D \subset \mathbb{C} \setminus \{0\}$ and a branch of $\lambda^{1/2}$ analytic on D. Let $\Theta_0 = -\frac{1}{2}$ and $\Theta_\infty = \frac{3}{2}$, and consider the exact solution $u(x) = x^{-1}$ of the corresponding Painlevé-IV equation (1.1). If $y(x) = x^{-1} \exp(-x^2)$, then the Lax pair equations (3.9) are simultaneously solvable for all $(\lambda, x) \in D \times (\mathbb{C} \setminus \{0\})$, and every simultaneous solution matrix has the form

$$\Psi(\lambda, x) = \frac{\lambda^{1/2}}{x} \begin{pmatrix} e^{-x^2} & \frac{1}{2}\lambda^{-1} - F(x+\lambda) \\ -(2x^2 + 2x\lambda + 1) \left[-(x + \frac{1}{2}\lambda^{-1}) + (2x^2 + 2x\lambda + 1)F(x+\lambda) \right] e^{x^2} \end{pmatrix}
\cdot \exp(-(\frac{1}{2}\lambda^2 + x\lambda)\sigma_3) \mathbf{C}, \tag{H.1}$$

where $F(z) := \exp(-z^2) \int_0^z \exp(t^2) dt$ denotes Dawson's integral [53, §7.2(ii)] and \mathbb{C} is a matrix independent of both x and λ .

Absence of logarithms again indicates that although the Fuchsian singularity of $\Psi_{\lambda} = \Lambda \Psi$ is resonant, it is also apparent, so it is possible to choose $\mathbf{C} = \mathbf{C}^{(0)}$ to define a solution for $|\lambda| < 1$ to satisfy (3.13). For solutions defined to satisfy (3.12) in the four Stokes sectors we determine $\mathbf{C} = \mathbf{C}_{j}^{(\infty)}$, $j = 1, \ldots, 4$ by asymptotic analysis of the general solution given in Lemma 21 for large λ . The results are

$$\mathbf{C}_2^{(\infty)} = \mathbf{C}_3^{(\infty)} = \begin{pmatrix} i\sqrt{\pi} \ -\frac{1}{2} \\ 2 \ 0 \end{pmatrix} \quad \text{and} \quad \mathbf{C}_1^{(\infty)} = \mathbf{C}_4^{(\infty)} = \begin{pmatrix} -i\sqrt{\pi} \ -\frac{1}{2} \\ 2 \ 0 \end{pmatrix}.$$

Therefore, there is no Stokes phenomenon between sectors S_2 and S_3 or between S_4 and S_1 (i.e., upon crossing the imaginary Stokes rays), and the corresponding Stokes matrices $V_{2,3} = V_{4,1} = \mathbb{I}$ defined in (3.15) and (3.17) respectively are trivial. On the other hand, from (3.14) and (3.16) we get

$$\mathbf{V}_{2,1} = \begin{pmatrix} 1 & 0 \\ -4i\sqrt{\pi} & 1 \end{pmatrix}$$
 and $\mathbf{V}_{4,3} = \begin{pmatrix} -1 & 0 \\ -4i\sqrt{\pi} & -1 \end{pmatrix}$.



Therefore, unlike the gH rationals in the parameter lattice $\Lambda_{gH}^{[3]+}$, the rationals in the parameter lattice $\Lambda_{gH}^{[1]-}$ have nontrivial Stokes matrices on the real rays. Similar analysis shows that gH rational solutions in the parameter lattice $\Lambda_{gH}^{[2]-}$ have instead nontrivial Stokes phenomenon (only) across the imaginary rays.

H.2. Critical v-Trajectories of $h'(z)^2 dz^2$ for $|\kappa| > 1$

The main idea of the asymptotic analysis of Riemann–Hilbert Problem 1 in all cases is to use the landscape of Re(h(z)) in the *z*-plane, where as explained in Sect. 4.3 h(z) is associated to the spectral curve for the polynomial $P(z) = P(z; \mu, \kappa, E)$ defined in (1.18). The type-1 solutions correspond to values of κ outside of the interval (-1, 1).

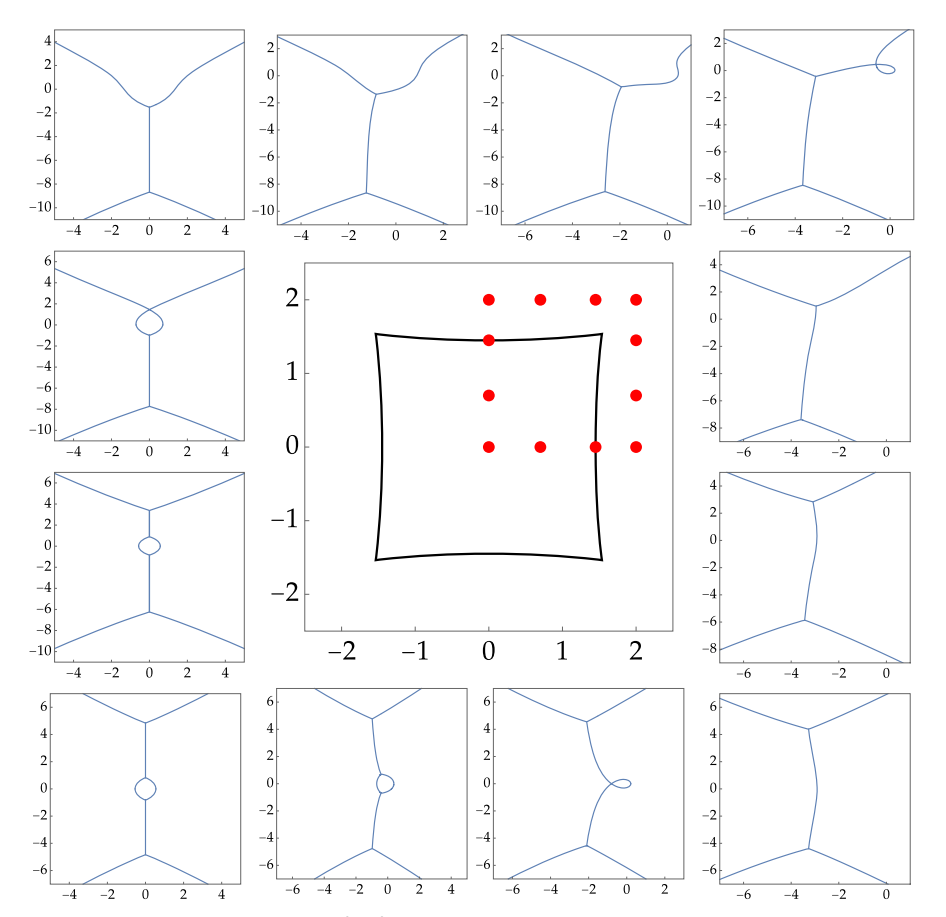


Fig. 46 Critical v-trajectories of $h'(z)^2$ d z^2 emanating from (for generic μ) simple roots of P(z) for $\kappa=3$ for the gH family. The same topological structure holds for $\kappa>1$. Counterclockwise from top left: $\mu=2$ i, $\mu\approx1.45$ i, $\mu=0.7$ i, $\mu=0$, $\mu=0.7$, $\mu\approx1.45$, $\mu=2$, $\mu=2+0.7$ i, $\mu=2+1.45$ i, $\mu=2+2$ i, $\mu=1.45+2$ i, $\mu=0.7+2$ i. Inset: Boundary of $\mathcal{B}_{\square}(3)$ in the μ -plane. The μ -values corresponding to different trajectory plots are indicated by red dots (Color figure online)



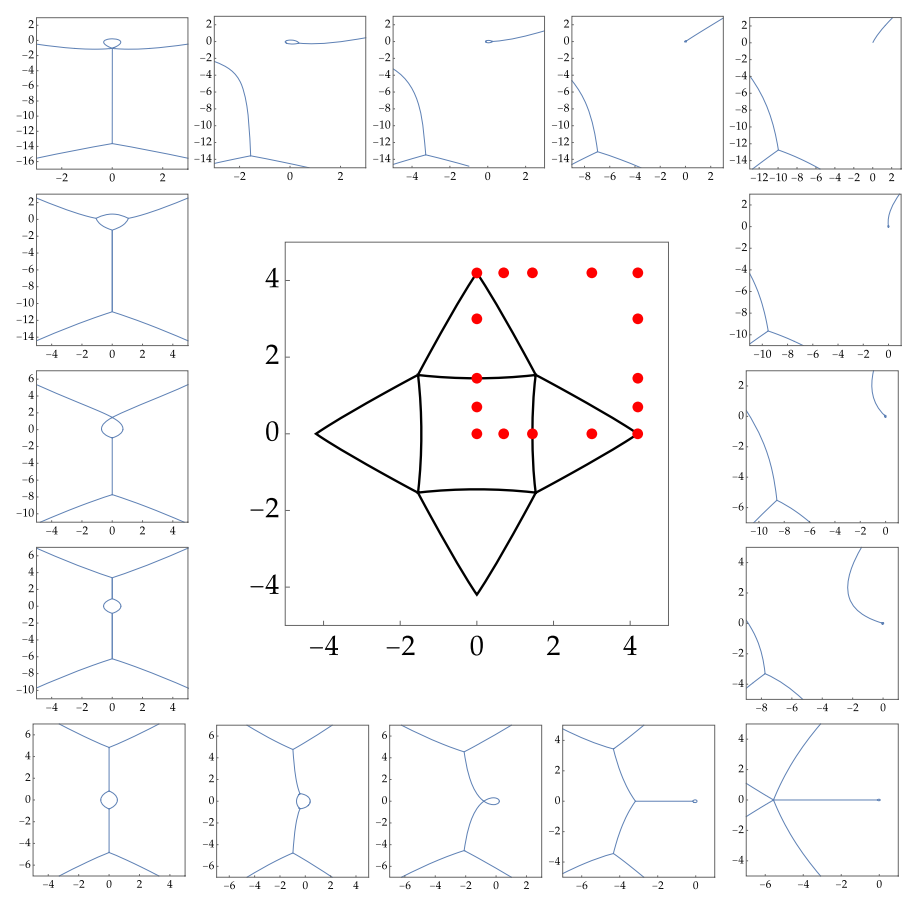


Fig. 47 Critical v-trajectories of $h'(z)^2$ dz² emanating from simple roots of P(z) for $\kappa=3$ for the gO family (for nongeneric values of μ on boundary curves we show all critical trajectories). The same topological structure holds for $\kappa>1$. Counterclockwise from top left: $\mu\approx4.19698$ i, $\mu=3$ i, $\mu\approx1.45$ i, $\mu=0.7$ i, $\mu=0,\,\mu=0.7,\,\mu\approx1.45$, $\mu=3,\,\mu\approx4.19698$, $\mu=4.2+0.7$ i, $\mu=4.2+1.45$ i, $\mu=4.2+3$ i, $\mu=4.2+4.2$ i, $\mu=3+4.2$ i, $\mu=1.45+4.2$ i, $\mu=0.7+4.2$ i. Inset: Boundaries of the regions $\mathcal{B}_{\square}(3)$, $\pm\mathcal{B}_{\triangleright}(3)$, and $\pm\mathcal{B}_{\triangle}(3)$ in the μ -plane. The μ -values corresponding to different trajectory plots are indicated by red dots

Just to give a flavor of the differences that can arise for $|\kappa| > 1$, in Figs. 46 and 47 we present the analogues of Figs. 16 and 17 in Sect. 4.3 in which we display the critical v-trajectories of the quadratic differential $h'(z)^2 dz^2$ emanating from (generically) simple roots of the quartic P(z).

References

- 1. Adler, V.É.: Nonlinear chains and Painlevé equations. Phys. D 73, 335–351 (1994)
- 2. Airault, H.: Rational solutions of Painlevé equations. Stud. Appl. Math. 61, 31–53 (1979)



- Aratyn, H., Gomes, J.F., Zimmerman, A.H.: Darboux-Bäcklund transformations and rational solutions of the Painlevé IV equation. AIP Conf. Proc. 1212, 146–153 (2010)
- Balogh, F., Bertola, M., Bothner, T.: Hankel determinant approach to generalized Vorob'ev-Yablonski polynomials and their roots. Constr. Approx. 44, 417–453 (2016)
- Bassom, A.P., Clarkson, P.A., Hicks, A.C.: Bäcklund transformations and solution hierarchies for the fourth Painlevé equation. Stud. Appl. Math. 95, 1–71 (1995)
- Bassom, A.P., Clarkson, P.A., Hicks, A.C.: On the application of solutions of the fourth Painlevé equation to various physically motivated nonlinear partial differential equations. Adv. Differ. Equ. 1, 175–198 (1996)
- Bertola, M., Bothner, T.: Zeros of large degree Vorob'ev-Yablonski polynomials via a Hankel determinant identity. Int. Math. Res. Not. 2015, 9330–9399 (2015)
- 8. Bertola, M., Lee, S.: First colonization of a spectral outpost in random matrix theory. Constr. Approx. **30**, 225–263 (2009)
- Bertola, M., Tovbis, A.: Universality in the profile of the semiclassical limit solutions to the focusing nonlinear Schrödinger equation at the first breaking curve. Int. Math. Res. Not. 2010, 2119–2167 (2010)
- Bilman, D., Buckingham, R., Wang, D.: Far-field asymptotics for multiple-pole solitons in the largeorder limit. J. Differ. Equ. 297, 320–369 (2021)
- Boiti, M., Pempinelli, F.: Nonlinear Schrödinger equation, Bäcklund transformations and Painlevé transcendents. Nuovo Cim. 59B, 40–58 (1980)
- 12. Bothner, T., Miller, P.D.: Rational solutions of the Painlevé-III equation: large parameter asymptotics. Constr. Approx. **51**, 123–224 (2020)
- 13. Bothner, T., Miller, P.D., Sheng, Y.: Rational solutions of the Painlevé-III equation. Stud. Appl. Math. 141, 626–679 (2018)
- Boutroux, P.: Recherches sur les transcendantes de M. Painlevé et l'étude asymptotique des équations différentielles du second ordre. Ann. Sci. École Norm. Sup. 30, 255–375 (1913). (In French)
- Buckingham, R.: Large-degree asymptotics of rational Painlevé-IV functions associated to generalized Hermite polynomials. Int. Math. Res. Not. IMRN 2018, rny172 (2018)
- Buckingham, R., Miller, P.D.: The sine-Gordon equation in the semiclassical limit: critical behavior near a separatrix. J. Anal. Math. 118, 397–492 (2012)
- 17. Buckingham, R., Miller, P.D.: The sine-Gordon equation in the semiclassical limit: dynamics of fluxon condensates. Memoirs Amer. Math. Soc. 225, 1–136 (2013)
- Buckingham, R., Miller, P.D.: Large-degree asymptotics of rational Painlevé-II functions: noncritical behaviour. Nonlinearity 27, 2489–2577 (2014)
- Buckingham, R., Miller, P.D.: Large-degree asymptotics of rational Painlevé-II functions: critical behaviour. Nonlinearity 28, 1539–1596 (2015)
- Chen, Y., Feigin, M.: Painlevé IV and degenerate Gaussian unitary ensembles. J. Phys. A 39, 12381– 12393 (2006)
- Clarkson, P.A.: The fourth Painlevé equation and associated special polynomials. J. Math. Phys. 44, 5350–5374 (2003)
- 22. Clarkson, P.A.: Special polynomials associated with rational solutions of the defocusing nonlinear Schrödinger equation and the fourth Painlevé equation. Eur. J. Appl. Math. 17, 293–322 (2006)
- Clarkson, P.A.: Special polynomials associated with rational solutions of the Painlevé equations and applications to soliton equations. Comp. Meth. Func. Theory 6, 329–401 (2006)
- 24. Clarkson, P.A.: Rational solutions of the Boussinesq equation. Anal. Appl. (Singap.) 6, 349–369 (2008)
- Clarkson, P.A.: Rational solutions of the classical Boussinesq system. Nonlinear Anal. Real World Appl. 10, 3360–3371 (2009)
- 26. Clarkson, P.A.: Vortices and polynomials. Stud. Appl. Math. 123, 37–62 (2009)
- Clarkson, P.A., Thomas, B.: Special polynomials and exact solutions of the dispersive water wave and modified Boussinesq equations. In: Proceedings of Group Analysis of Differential Equations and Integrable Systems IV, pp. 62–76 (2009)
- Dai, D., Kuijlaars, A.: Painlevé IV asymptotics for orthogonal polynomials with respect to a modified Laguerre weight. Stud. Appl. Math. 122, 29–83 (2009)
- 29. Deift, P., Venakides, S., Zhou, X.: The collisionless shock region for the long-time behavior of solutions of the KdV equation. Comm. Pure Appl. Math. 47, 199–206 (1994)
- 30. Deift, P., Zhou, X.: A steepest descent method for oscillatory Riemann–Hilbert problems: asymptotics for the mKdV equation. Ann. Math. 137, 295–368 (1993)



- 31. Dubrovin, B.A.: Theta functions and non-linear equations. Russian Math. Surveys 36, 11–92 (1981)
- 32. Fokas, A.S., Grammaticos, B., Ramani, A.: From continuous to discrete Painlevé equations. J. Math. Anal. Appl. **180**, 342–360 (1993)
- Fokas, A.S., Its, A.R., Kapaev, A.A., Yu, V.: Novokshenov, Painlevé Transcendents. The Riemann–Hilbert Approach, AMS Mathematical Surveys and Mongraphs 128, Amer. Math. Soc., Providence (2006)
- 34. Fokas, A.S., Its, A.R., Kitaev, A.V.: Discrete Painlevé equations and their appearance in quantum gravity. Comm. Math. Phys. **142**, 313–344 (1991)
- Fokas, A.S., Muğan, U., Ablowitz, M.J.: A method of linearization for Painlevé equations: Painlevé IV, V. Physica D 30, 247–283 (1988)
- 36. Forrester, P., Witte, N.: Application of the τ-function theory of Painlevé equations to random matrices: PIV, PII and the GUE. Comm. Math. Phys. **219**, 357–398 (2001)
- 37. Gromak, V.: On the theory of the fourth Painlevé equation. Differentsialnye Uravneniya 23, 760–768 (1987). (In Russian)
- 38. Its, A.R.: Asymptotic behavior of the solutions to the nonlinear Schrödinger equation, and isomonodromic deformations of systems of linear differential equations. Dokl. Akad. Nauk SSSR **261**, 14–18 (1981). (**In Russian**)
- 39. Jenkins, J.A.: Univalent Functions and Conformal Mapping. Springer, Berlin (1958)
- 40. Jimbo, M., Miwa, T.: Monodromy preserving deformation of linear ordinary differential equations with rational coefficients. II. Physica D 2, 407–448 (1981)
- Joshi, N., Liu, E.: Asymptotic behaviours given by elliptic functions in P_I-P_V. Nonlinearity 31, 3626–3747 (2018)
- 42. Kajiwara, K., Ohta, Y.: Determinant structure of the rational solutions for the Painlevé-IV equation. J. Phys. A 31, 2431–2446 (1998)
- 43. Lukashevich, N.: The theory of Painlevé's fourth equation. Differensialnye Uravnenija 3, 771–780 (1967). (In Russian)
- Marikhin, V., Shabat, A., Boiti, M., Pempinelli, F.: Self-similar solutions of equations of the nonlinear Schrödinger type. J. Exp. Theor. Phys. 90, 553–561: Translation of Zh. Eksper. Teoret. Fiz. 117, 634–643 (2000). (In Russian)
- 45. Marquette, I., Quesne, C.: Connection between quantum systems involving the fourth Painlevé transcendent and *k*-step rational extensions of the harmonic oscillator related to Hermite exceptional orthogonal polynomial. J. Math. Phys. **57**, 052101 (2006)
- Masoero, D., Roffelsen, P.: Poles of Painlevé IV rationals and their distribution. SIGMA Symmetry Integrability Geom. Methods Appl. 14, paper no 002 (2018)
- 47. Masoero, D., Roffelsen, P.: Roots of generalised Hermite polynomials when both parameters are large. Nonlinearity **34**, 1663–1732 (2021)
- 48. Masoero, D., Roffelsen, P.: Private communication (2020)
- Miller, P.D.: On the increasing tritronquée solutions of the Painlevé-II equation. SIGMA Symmetry Integrability Geom. Methods Appl. 14, paper no. 125 (2018)
- Miller, P.D., Sheng, Y.: Rational solutions of the Painlevé-II equation revisited. SIGMA Symmetry Integrability Geom. Methods Appl. 13, paper no. 065 (2017)
- Muğan, U., Fokas, A.S.: Schlesinger transformations of Painlevé II-V. J. Math. Phys. 33, 2031–2045 (1992)
- Murata, Y.: Rational solutions of the second and the fourth Painlevé equations. Funkcial. Ekvac. 28, 1–32 (1985)
- 53. NIST Digital Library of Mathematical Functions. http://dlmf.nist.gov/, Release 1.0.27 of 2020-06-15. Online companion to [58]
- Noumi, M., Yamada, Y.: Symmetries in the fourth Painlevé equation and Okamoto polynomials. Nagoya Math. J. 153, 53–86 (1999)
- 55. Yu, V., Novokshenov and A. A. Shchelkonogov,: Double scaling limit in the Painlevé IV equation and asymptotics of the Okamoto polynomials. Amer. Math. Soc. Trans. 233, 199–210 (2014)
- Yu, V., Novokshenov and A. A. Shchelkonogov,: Distribution of zeroes to generalized Hermite polynomials. Ufa Math. J. 7, 54–66 (2015)
- 57. Okamoto, K.: Studies on the Painlevé equations III. Second and fourth Painlevé equations, P_{II} and P_{IV} . Math. Ann. 275, 221–255 (1986)
- 58. Olver, F.W.J., Lozier, D.W., Boisvert, R.F., Clark, C.W. (Eds.) NIST Handbook of Mathematical Functions, Cambridge University Press, New York. Print companion to [53] (2010)



- Osipov, V., Sommers, H., Zyczkowski, K.: Random Bures mixed states and the distribution of their purity. J. Phys. A 43, 055302 (2010)
- 60. Strebel, K.: Quadratic Differentials. Springer Verlag, Berlin (1984)
- Van Assche, W.: Orthogonal Polynomials and Painlevé Equations, Australian Mathematical Society Lecture Series, vol. 27. Cambridge University Press, Cambridge (2018)

Publisher's Note Springer Nature remains neutral with regard to jurisdictional claims in published maps and institutional affiliations.

